PHYSICS OF ENERGY TRANSPORT IN EXTRAGALACTIC RADIO SOURCES

Proceedings of NRAO Workshop No. 9
held at Green Bank, West Virginia
on July 30 to August 3, 1984

Edited by Alan H. Bridle and Jean A. Eilek

Cover illustration. **Composite of three VLA maps of the radio galaxy Cygnus A.**

Center, **a gradient enhanced display of the total intensity distribution over the whole source, from an original map with 0.4 arcsec resolution at 6cm wavelength** *(courtesy of J. W. Dreher and R. A. Perley).*

Upper right and lower left, **displays of the total intensity distributions over the regions containing the hot spots, from maps with 0.1 arcsec resolution at 2cm wavelength** *(courtesy of R. A. Laing, R. A. Perley and P. A. G. Scheuer).*

For further details, see the paper by J.W.Dreher, R.A.Perley and J.N.Cowan on page 57 of these *Proceedings.*

PHYSICS OF ENERGY TRANSPORT IN EXTRAGALACTIC RADIO SOURCES

Proceedings of NRAO Workshop No. 9 held at Green Bank, West Virginia on July 30 to August 3, 1984

Edited by Alan H. Bridle and Jean A. Eilek

Distributed by:
National Radio Astronomy Observatory
P.O. Box 2
Green Bank, WV 24944-0002 USA

The National Radio Astronomy Observatory is operated by Associated Universities, Inc., under contract with the National Science Foundation.

TABLE OF CONTENTS

(Titles of review papers are given in capital letters)

Preface iii
List of Participants v

PHENOMENOLOGY OF EXTRAGALACTIC RADIO JETS
A. H. Bridle 1

3C120: A continuous link between moving features and a large scale radio jet
R. C. Walker 20

Radio jets in strong core classical doubles
J. O. Burns 25

Observations of large scale jets in quasars and the sidedness problem
J. F. C. Wardle and R. I. Potash 30

Pieces of jets and other thoughts on flip-flops
L. Rudnick 35

The radio jets of 3C449
T. J. Cornwell and R. A. Perley 39

Polarization structure of the jets in NGC1265
C. P. O'Dea and F. N. Owen 47

Multiconfiguration VLA maps of Cygnus A
J. W. Dreher, R. A. Perley and J. N. Cowan 57

Jet turn-on and confinement – indications from IC4296 (ABSTRACT)
G. V. Bicknell 63

CONSTRAINTS ON THE PROPERTIES OF BENT BEAMS
C. P. O'Dea 64

Bending in the first few hundred parsecs
P. N. Wilkinson, T. J. Cornwell, A. J. Kus, A. C. S. Readhead and T. J. Pearson . . 76

Distorted quasars: can sharp bends in radio structures be attributed to localized collisions ?
W. A. Christiansen, J. O. Burns and J. T. Stocke 83

Wide angle tail radio galaxies (ABSTRACT)
F. N. Owen 89

INTERPRETATION OF RADIO POLARIZATION DATA
R.A.Laing 90

VLBI polarimetry – first results (ABSTRACT)
J. F. C. Wardle and D. H. Roberts 99

ENERGY TRANSPORT IN RADIO SOURCES: EFFICIENT OR NOT ?
D. S. De Young 100

An argument for jet velocities $> 0.1c$ in powerful doubles
J. W. Dreher 109

Jet speed
L. Rudnick 114

Jet asymmetries in radio galaxies with dust lanes (ABSTRACT)
R.A.Laing 119

Evolution of superluminal radio components in 3C345 (ABSTRACT)
J. A. Biretta 120

Semi-dynamical models of superluminal radio sources (ABSTRACT)
K. R. Lind and R. D. Blandford 121

Cloud-beam interactions: bends, lobes and superluminals
R. N. Henriksen 122

Symmetries of jets and hot spots (ABSTRACT)
R.A.Laing 128

Beam inefficiencies and extended source morphologies
W. A. Christiansen 129

The Jolly Green Jet (EVENING DEMONSTRATION)
L. Rudnick 133
Menu for an all-purpose source model (EVENING DISCUSSION)
A. H. Bridle 135

LINEAR ANALYSIS OF JET STABILITY
P. E. Hardee 144
Knot production and disruption via nonlinear Kelvin-Helmholtz pinch instabilities
M. L. Norman, K.-H. A. Winkler and L. L. Smarr 150
Why dominant cluster jets are different
D. M. Sumi and L. L. Smarr 168
Vortex rings in extended doubles
L. Rudnick 182

CURRENT-CARRYING JETS
G. Benford 185
Formation and propagation of magnetized radio jets
J. Siah and P. J. Wiita 193
Force-free equilibria of magnetized jets (ABSTRACT)
A. Königl 200

TURBULENCE, ENTRAINMENT AND MAGNETIC FIELDS
D. S. De Young 202
Collimation of intermediate scale motion entrained by nuclear jets
R. N. Henriksen 211

THE PHYSICS OF PARTICLE ACCELERATION IN RADIO GALAXIES
J. A. Eilek 216
The relationship between laboratory and astrophysical jets
G. V. Bicknell 229
Global invariants of a mean fluid flow and local turbulent substructure
R. N. Henriksen 245
Sidewise shocks in the Centaurus A radio jet
J. O. Burns, D. Clarke, E. D. Feigelson and E. J. Schreier 255
Magnetic energy dissipation as the main source of synchrotron emission in jets
A. Königl 260
Laboratory electron beam simulation of cosmic radio jets
R. G. Spulak Jr. and J. O. Burns 265

AN OBSERVER'S PERSPECTIVE – I
P. N. Wilkinson 272
AN OBSERVER'S PERSPECTIVE – II
R. A. Laing 276
Discussion after observers' reviews 280

A THEORIST'S PERSPECTIVE – I
P. J. Wiita 285
A THEORIST'S PERSPECTIVE – II
A. Königl 292
Discussion after theorists' reviews 297

Quotes without comment 309

Author Index 310
Subject Index 311
Object Index 315

PREFACE

This volume contains the Proceedings of a Workshop on "Physics of Energy Transport in Extragalactic Radio Sources" held at Green Bank, West Virginia from 30 July to August 3, 1984 under the auspices of the National Radio Astronomy Observatory.

The Workshop spun off from I.A.U. Symposium No. 107 on "Unstable Current Systems and Plasma Instabilities in Astrophysics", held almost a year earlier at the University of Maryland. At that Symposium it became clear to us that the explosive growth of the radio astronomy data base on jets, hot spots and other lobe fine structure since 1982 was opening up a wide range of questions about collimation, stability and particle acceleration in jets, whose proper treatment required long-term investments in hydrodynamic and magnetohydrodynamic modeling. We therefore planned to bring together a small group of theorists and observers for an interactive Workshop to discuss the crucial phenomena. As we had both noted that the best discussions at scientific meetings often occur in the bar, we decided to hold the Workshop in the Lounge of the Residence Hall at Green Bank. We are indebted to Wally Oref and the Green Bank staff for reorganising this room to accommodate a meeting – the Lounge's small size and informal atmosphere contributed greatly to our interactions.

Each of the first four days of the Workshop contained one or two "focusing" reviews and a related group of contributed talks. Day 1 (Jet Correlations and Observational Constraints) was planned by Alan Bridle; Day 2 (Jet Sidedness, Velocity and Unification) by Dave De Young; Day 3 (Confinement and Stability) by Greg Benford; and Day 4 (Particle Acceleration, Entrainment and Turbulence) by Jean Eilek. We originally intended to leave the afternoons free for discussion in large or small groups, but a tidal wave of new results and the enthusiasm of the Workshop participants soon overwhelmed this plan. Many "talks" became an analog of transonic jet propagation in a confining medium. An initially well-collimated presentation soon entrained vigorous discussion, decelerating the speaker's flow. The resulting strongly turbulent interaction with his or her surroundings generated much heat, and significant amounts of light. We did not try to record all of the discussion for these *Proceedings*, but its outcome is represented here in several ways.

First, the deadline for manuscripts was set at one month after the meeting; many papers in this volume now emphasize the issues which became controversial at the Workshop, each author having the clarity of hindsight from the spontaneous "peer review". Second, we used written "question and answer" sheets, IAU-style, so that participants could record "sanitized" versions of discussions they considered to be particularly significant. These discussions appear after the individual papers throughout these *Proceedings*. Third, we devoted most of the morning of Day 5 to an overview session centered around *post hoc* reviews of the Workshop by two observers and two theorists – we are very grateful to Peter Wilkinson, Robert Laing, Paul Wiita and Arieh Königl for preparing these reviews while the Workshop progressed. The four *post hoc* reviews, and the extensive discussions following them (chaired with great *panache* by Larry Rudnick), were tape recorded. The transcripts of these tapes, edited by Drs. Wilkinson, Wiita and Königl (for their own reviews) and by the organizers (for Dr. Laing's review and for the general discussion), form pages 272 to 308 of these *Proceedings*. Finally, to help readers to explore the range of discussion about particular topics or sources, we have compiled a subject (topic) index and an object (source) index (pages 311 to 316 of these *Proceedings*). The indexing was done without keywords supplied by the authors, so doubtless reflects the Editors' prejudices about energy transport phenomena to some extent. We hope that these ingredients allow the *Proceedings* to convey the sense of the discussion at the Workshop fairly and accurately.

Verbatim transcripts in a lighter vein, some disguised to protect the perpetrators, are included on page 309.

Two less formal activities at the Workshop are also represented here by papers. On the second evening, Larry Rudnick set up a "laboratory" (bar-room) jet which illustrated phenomena such as the transition from laminar to turbulent flow, helical and pinch instabilities, velocity variations, vortex shedding, etc. Although drawn from a different sector of parameter space than we normally envisage

for extragalactic jets, Larry's "Jolly Green Jet" focused discussion and challenged jet modelers to demonstrate their versatility by describing its phenomena. We thank Larry for bringing this down-to-earth example of jet physics to the meeting, and for describing it briefly here (p.133). We also thank Peter Wilkinson for providing Figure 2 of Larry's "paper". On the third evening, Alan Bridle sketched an "Observers' Dream Model" which summarized what consensus had emerged from discussions of the observational constraints on energy transport, and also suggested a direction in which the models might evolve to satisfy (or escape !) these constraints. The "Observers' Dream" provoked a vigorous after-dinner discussion session at which several groups tried to rough in a physical framework for it. As it was referenced by several contributed papers, we include a formal (and somewhat expanded) version of it here (p.135).

The Workshop achieved its goal of promoting interaction amongst observers and theorists. This was due in part to the tenacity and stamina of those who attended and in part to its very small size. We owe many apologies to colleagues with strong interests in extragalactic sources who we were unable to invite in order that the meeting *be* small and interactive. We hope that these *Proceedings* adequately convey to them the main results discussed at this meeting.

We were enormously assisted in our task, and the meeting was greatly improved, by the fine support we received from the NRAO staff in Green Bank and in Charlottesville. Becky Warner coordinated the catering and room arrangements; Phyllis Jackson looked after travel arrangements and registration; Berdeen O'Brien and Beaty Sheets saw to the logistics in the meeting room; Ron Monk took a fine group photograph; the Green Bank cafeteria staff fed us well and cheerfully; Rick Fisher and Bob Vance conducted a tour of the Green Bank telescopes for single-dish neophytes; Richard Fleming administered the business arrangements. And by no means least, Wally Oref managed our projection facilities, taped our arguments, and found rapid solutions to all the problems the organizers hadn't anticipated but should have. To all of these people, without whom the Workshop could not possibly have run so smoothly, our sincerest thanks. We also thank George Kessler and Pat Smiley for their work on graphics for the *Proceedings*.

Alan H. Bridle
National Radio Astronomy Observatory
Charlottesville, Virginia

Jean A. Eilek
New Mexico Institute of Mining and Technology
Socorro, New Mexico

11th December 1984

LIST OF PARTICIPANTS

G. Benford,	*University of California, Irvine, USA*
G.V. Bicknell,	*Mt. Stromlo and Siding Spring Observatories, AUSTRALIA*
J.A. Biretta,	*California Institute of Technology, USA*
A.H. Bridle,	*National Radio Astronomy Observatory, USA*
J.O. Burns,	*University of New Mexico, USA*
W.A. Christiansen,	*University of North Carolina, USA*
T.J. Cornwell,	*National Radio Astronomy Observatory, USA*
D.S. De Young,	*Kitt Peak National Observatory, USA*
J.W. Dreher,	*Massachusetts Institute of Technology, USA*
J.A. Eilek,	*New Mexico Institute of Mining and Technology, USA*
F. Eulderink,	*Sterrewacht Leiden, NETHERLANDS*
P.E. Hardee,	*University of Alabama, USA*
R.N. Henriksen,	*Canadian Institute for Theoretical Astrophysics, CANADA*
A. Königl,	*University of Chicago, USA*
R.A. Laing,	*Royal Greenwich Observatory, UK*
K.R. Lind,	*California Institute of Technology, USA*
M.L. Norman,	*Max-Planck-Institut fur Physik und Astrophysik, W.GERMANY*
C.P. O'Dea,	*National Radio Astronomy Observatory, USA*
F.N. Owen,	*National Radio Astronomy Observatory, USA*
L. Rudnick,	*University of Minnesota, USA*
G.A. Seielstad,	*National Radio Astronomy Observatory, USA*
D.M. Sumi,	*University of Illinois, USA*
R.C. Walker,	*National Radio Astronomy Observatory, USA*
J.F.C. Wardle,	*Brandeis University, USA*
P.J. Wiita,	*University of Pennsylvania, USA*
A. Wilkinson,	*University of Manchester, UK*
P.N. Wilkinson,	*Nuffield Radio Astronomy Laboratories, Jodrell Bank, UK*

PHENOMENOLOGY OF EXTRAGALACTIC RADIO JETS

ALAN H. BRIDLE

National Radio Astronomy Observatory[a], Charlottesville, Virginia 22903

ABSTRACT. The use of the term "jet" is critically reviewed. "Jets" occur often, in a wide variety of extragalactic radio sources, and with properties well correlated both with the total luminosities of the sources and with the relative prominence of their compact radio cores. The one sided jets in powerful sources with symmetrical double lobes pose some acute problems. We need to understand why they break the symmetry of the lobes. Also, though these jets appear not to be free, it is not clear what confines them. The evidence bearing on particle acceleration and on the 3-D magnetic field structures in radio jets is briefly summarized.

1. INTRODUCTION

The observations which tell us about energy transport in extragalactic radio sources are in an exciting phase. Advances in image processing and improvements in array hardware are providing radio images of complex sources with unprecedented combinations of sub-arcsecond resolution, good sensitivity and high dynamic range. Sources we thought we knew well, such as Cygnus A, M87, NGC1265, 3C219 and 3C449, are showing new internal complexity (wisps, rings, sharp-edged jet knots and hot spots, cocoons, and hitherto undetected segments of jets). From 140 to 220 extragalactic "jets" have now been detected, depending on the rigor of your definition of a "jet". This talk updates what we know of the systematic properties of extragalactic jets – most trends suggested by early observations (e.g., Fomalont 1981, Willis 1981, Bridle 1982) have been confirmed, and several new ones have emerged. To counteract the impression that all jets are well-behaved conformists, I mention some "maverick" sources which fight the main trends.

2. WHY "JETS" ?

We left the word "jet" out of the title of this Workshop to show that heretical views of energy transport are welcome here ! But as extragalactic astronomers have described elongated luminous features as "jets" for 30 years now, and "jet language" permeates the optical, radio and X-ray literature, I expect that much of our discussion will simply *assume* that these elongated radio features map the paths of fluid outflows from active nuclei to extended radio lobes. The evidence supporting this assumption is indirect, and flimsier than we might wish, however.

The large sizes of powerful extragalactic sources show that active galaxies and QSRs eject *something* that can supply energy to relativistic particles and magnetic fields. The optical and radio cores also remain active long after the initial ejection has taken place, though we cannot prove that the activity has been continuous. VLBI shows radio emission that has been collimated on parsec scales. But we lack direct evidence that

[a] The National Radio Astronomy Observatory (NRAO) is operated by Associated Universities, Inc., under contract with the National Science Foundation.

the link between the parsec and many-kiloparsec scales is a "jet" in the fluid mechanical sense, i.e., a continuous, forced (momentum-dominated) collimated outflow. Why then do we use the word so liberally ?

The term "jet" appeared on a hunch by Baade and Minkowski (1954) that there is outflow through the optical knots in M87. This hunch has still not been directly verified. There are no emission lines from the knots – the evidence for outflow in M87 is the velocity profile of [OII] lines *in the nucleus.* The radio nucleus has yet to reveal significant proper motions – this is not evidence *against* outflow in it (radio features may, for example, mark a slowly moving shock pattern in a rapidly moving flow), but the radio data give no direct evidence *for* flow.

In the early 1970's, the existence of elongated kiloparsec-scale optical and radio features in a few bright sources encouraged continuous flow, or "beam", models of energy transport. These models have attractive aspects which have ensured their longevity. The bulk kinetic energy in a beam exerts no pressure, so is not lost adiabatically. Supersonic beams terminate at shocks near their interface with ambient gas. Shocks can transform beamed kinetic energy into relativistic particle and field energy, thus providing a framework for explaining the locations, brightness distributions, and short radiative timescales of hot spots in radio lobes. These attractions of the "beam" models have rolled the "jet" bandwagon in reverse – observers now use the word "jet" as a synonym for "elongated feature" mainly because they find such features in places where beam models postulate continuous collimated outflow, not because they have direct evidence for the outflow itself.

Stellar jets, or "bipolar flows", have a much better pedigree than this, as outflow velocities have been directly measured in many cases. In SS433, the radio proper motions and optical spectroscopic data both show a mean velocity of $0.26c$, and the flow geometry is known in detail. The ~ 100 light-day scale and typical 1.4 GHz luminosity of SS433 ($P_{tot}^{1.4} = 10^{15.8}$ W/Hz) are much less than those of extragalactic jets, however. There is also good evidence for collimated outflow from recently formed stars – velocities of tens to hundreds of km/s are known from Doppler shifted molecular emission lines at mm wavelengths, from optical spectroscopy of nearby Herbig-Haro objects (some of which are linked to the stars by sinuous filaments), and from the 2.12 μm line of H_2. It is not clear, however, that the processes which produce these galactic jets scale to the extragalactic case[1]. They nevertheless add to the momentum of the extragalactic jet bandwagon, by showing that supersonic jets can arise in astrophysical situations where accretion flows and disk geometries may be relevant.

As we have now reached a stage where most extragalactic observers automatically use "jet language" when presenting their primary data, we must be careful to distinguish evidence from prejudice when discussing energy transport. Are we sure that there is steady outflow, rather than intermittent ejection ? Could some "jets" be inflow (splashbacks, backflow ?), or a mixture of inflow and outflow ? Could some be radiation

[1] They may however allow us to study the propagation and stability of supersonic jets in a background medium with measurable properties, thus becoming a "laboratory test" of models of jet dynamics (though possibly not in the same regimes of Mach number, density contrast, or Reynolds number as in the extragalactic case).

from static, or slowly-moving, dissipative sheaths around faster primary flows, i.e. does the energy transport occur throughout the radio emitting volume ? Finally, *where's the beef ?* – can we find *hard evidence* for continuous outflow on kiloparsec scales ?

3. EVIDENCE SUGGESTING OUTFLOW

Two lines of evidence would have suggested that there is outflow in extragalactic radio sources, independent of our reasoning about the origin of radio lobes and their hot spots.

(a) Extranuclear Optical Emission Lines.

When Hα, Hβ, [OII], [OIII], [NII], [SII] and other emission lines were first found near radio jets in galaxies (see the references in Bridle and Perley 1984), there were hopes that their peculiar velocities might indicate jet velocities directly. These hopes have faded.

The extranuclear line emission is generally found *beside* the jets, particularly on the outer edges of bends. The lines are often brightest near, but not at, bright knots or hot spots. The line widths (typically 300 to 500 km/s) increase towards the radio features. The line emitting gas typically has densities $\approx 10^2$ to 10^3 cm^{-3}, and temperatures $\approx$ 20,000 K, so its pressure is near the lower limits to the pressures of radiating particles and fields in adjacent radio features. Typical peculiar velocities are a few hundred km/s.[2] These data suggest that the lines are formed when radio jets interact with ambient ISM, but the spatial displacements between the line emission and the radio features argue that the peculiar line velocities are not those of gas that is now entrained in the flow. The gas may instead be clouds which have been heated, ionized and accelerated by encountering the jets, perhaps deflecting them in the process. The detailed dynamics of the cloud/jet encounters are uncertain, however, so that while the emission line data are *consistent* with outflow along radio jets, they do not measure the flow velocities directly. They may however give lower limits to the flow velocities, similar to those obtained by saying that jets must be able to escape from their galaxies.

In some sources, e.g. 3C277.3 (Miley 1983), extranuclear line emission shares the side-to-side brightness asymmetry of a one-sided radio jet, showing that the radio asymmetry is not due primarily to Doppler favoritism in a relativistic flow. The radio asymmetries in such sources must be due either to differential dissipation in a two sided flow (e.g., by obliquely shocking and deflecting the flow at an encounter with an interstellar cloud on one side of the source but not on the other), or to intrinsic one-sidedness of the flow.

(b) Proper motions.

There is evidence for outflow in the first few parsecs of some extragalactic radio "jets" from VLBI proper motion studies of knots on these scales. In all but 4C39.25

[2] An optical continuum and emission line feature in the radio galaxy DA240 has been described as an "optical jet" blueshifted relative to the galactic nucleus by 3400 km/s (Burbidge *et al.* 1975, 1978) and the velocity discrepancy has been invoked as direct evidence for a jet velocity of 3400 km/s (Burbidge *et al.* 1978; Strom and Willis 1981). The feature has not been detected at the VLA, however, and there is now circumstantial evidence (van Breugel *et al.* 1983) that it is a foreground galaxy. Its nature is still not completely clear, but it is certainly premature to use its peculiar optical velocity as a constraint on the flow velocity in an extragalactic radio source.

(Shaffer 1984), the knots separate with time, but only in 3C345 has it been shown in an external reference frame ("NRAO 512 = fixed", Bartel *et al.* 1984) that the compact flat-spectrum "core" is stationary while a "jet knot" feature moves outward. Equally careful VLBI astrometry of knots in other sources with compact neighbors (to act as references) could reinforce the case for outflow.

To study proper motions by VLBI we must recognise patterns of knots at several epochs – we cannot track motions in continuous elongated emission. The proper motion studies must therefore relate to patterns of *dis*continuity (shocks, or turbulent "bursts") in the flow. Shock pattern speeds and flow velocities need not be the same (or even have the same sign !), but the preponderance of expansions among the knot proper motions makes it very likely that there *is* outflow, at least on the 1 to 10 parsec scales over which the motions can presently be tracked by VLBI.

Composites of VLBI, MERLIN and VLA data can "propagate the guilt" of outflow to larger scales if they demonstrate *continuity* of emission between moving parsec-scale 'jets" and the larger-scale features. The study of 3C120 by Craig Walker and colleagues (this Workshop) is an excellent example, tracing a radio connection from a superluminally expanding parsec-scale pattern to a kiloparsec-scale jet in a larger lobe-like structure. 3C179 may be the best available example combining superluminal motion, a kiloparsec-scale jet and *symmetrical* double lobes, but the continuity of the connections is less obvious in this source. Such data do not prove there is outflow in the large-scale features, but they add transverse velocities and directional alignments to the justification used by Baade and Minkowski for invoking outflow in M87 !

4. Defining a "Radio Jet"

The useful but prejudicial term "radio jet" should be employed like a useful but hazardous chemical – sparingly and carefully. If form and location will guide our view of energy transport physics, we need clear morphological criteria for jethood. I use here three criteria I have employed before (Bridle 1982; Bridle and Perley 1984), namely that be termed a "jet" a radio feature must be:

(a) at least four times as long as it is wide (after deconvolving the instrumental beam from the data),

(b) separable at high resolution from other extended structure (if any) either by brightness contrast or spatially (e.g. it should be a narrow ridge running through more diffuse emission, or a narrow feature in the inner part of a source entering more extended emission in the outer part),

(c) aligned with the radio core where it is closest to it. This is to distinguish *jets* from misaligned ridges near the hot spots in radio lobes.[3]

Even these three seemingly simple criteria are not always easy to apply. For example, if observed with lower sensitivity to smooth emission, the jet in NGC6251 (Perley *et al.* 1984a) would be a train of discrete knots, not all of which are elongated along it. I call such trains of knots *jets* only if some knots are elongated along the length of

[3] These lobe features may be closely related to jets if there is redirected outflow beyond, or backflow from, the hot spots (e.g., Robert Laing, this Workshop), but no interpretation of misaligned ridges in the lobes is yet obligatory and it is still useful to make empirical distinctions based on their alignment.

the train, or if it comprises more than two knots, as in 3C219 (Figure 1). This may exclude some real blobby jets, but rather than use prejudicial language too liberally, I prefer to hold some jet candidates in abeyance until better data convince me they are legitimate. Criterion (b) can be ambiguous in edge-darkened sources such as 3C31 or 3C449. The outer structures of such sources can equally plausibly be termed "broad jets" or "elongated lobes", as they fade away without clear terminations or hot spots. They resemble the meanderings of *subsonic* laboratory jets. I doubt that total intensity imaging alone can distinguish forced *jets* from buoyant *plumes* in the outer parts of such sources, but I ask that a bright "spine" of emission meets criterion (b) at some resolution before saying that such sources contain a *jet*.

There is a further complication in sources like M84 and 3C341 (Figure 2) which have faint emission "cocoons" around their jets. Other examples are NGC1265 (O'Dea and Owen, this Workshop), 3C147, 0938+39, 1321+31, 4C32.69 and 2354+47. Should we distinguish faint "cocoons" from brighter "jets" when discussing jet properties ? The collimation properties of the cocoons in M84 and 3C341 are quite different from those of the jets, so the distinction is not merely semantic. We need to diagnose the relationship of cocoons to the brighter structure[4] – are they faint "outer jets", static sheaths, leakage from the jets or emission from the backflows predicted by numerical simulations of hypersonic jet propagation in confining media ?

5. Rates of Detection of Extragalactic Radio Jets

Bridle and Perley (1984, BP) listed data on 125 sources with jets satisfying the above three criteria. Although the BP list is not statistically complete, the statistics of jets in several complete samples can be derived from it. It exhibits several trends that are unlikely to reflect statistical incompletenesses or biases.

Jets occur in extragalactic sources of all luminosities, sizes and structure types, justifying the assumption that they are associated with processes common to all extragalactic radio sources. Every jet in the BP list is accompanied by a detectable radio "core" in the inner kpc of the parent object, though in a some sources the cores are fainter than the brightest parts of the jet at cm wavelengths by factors ~ 2 to 4. This broadens the case for relating jets to continuing activity in the parent objects, supported further in some sources by the presence of VLBI jets. The fact that jets are neither rare nor confined to any one type of extragalactic source is strong support for the now-conventional assumption that they result from inefficiencies in the basic process of energy transport from the cores to the lobes. This conclusion is independent of whether the dissipation occurs in the primary flow itself, or in a static sheath or backflow around it.

As BP relate in some detail, jets or possible jets are detected in 65 to 80% of nearby (weak) radio galaxies, and in 40 to 70% of the extended QSRs mapped at the VLA with good dynamic range. It is much harder to detect jets in distant radio galaxies with similar powers, flux densities, and angular sizes to these QSRs – only 5% of a sample of powerful 3CR[2] galaxies mapped at the VLA have definite jets, and only $< 10\%$

[4] The cocoons may not all be the same class of phenomenon; for example, the cocoon in 3C341 has a very different brightness distribution from that in M84.

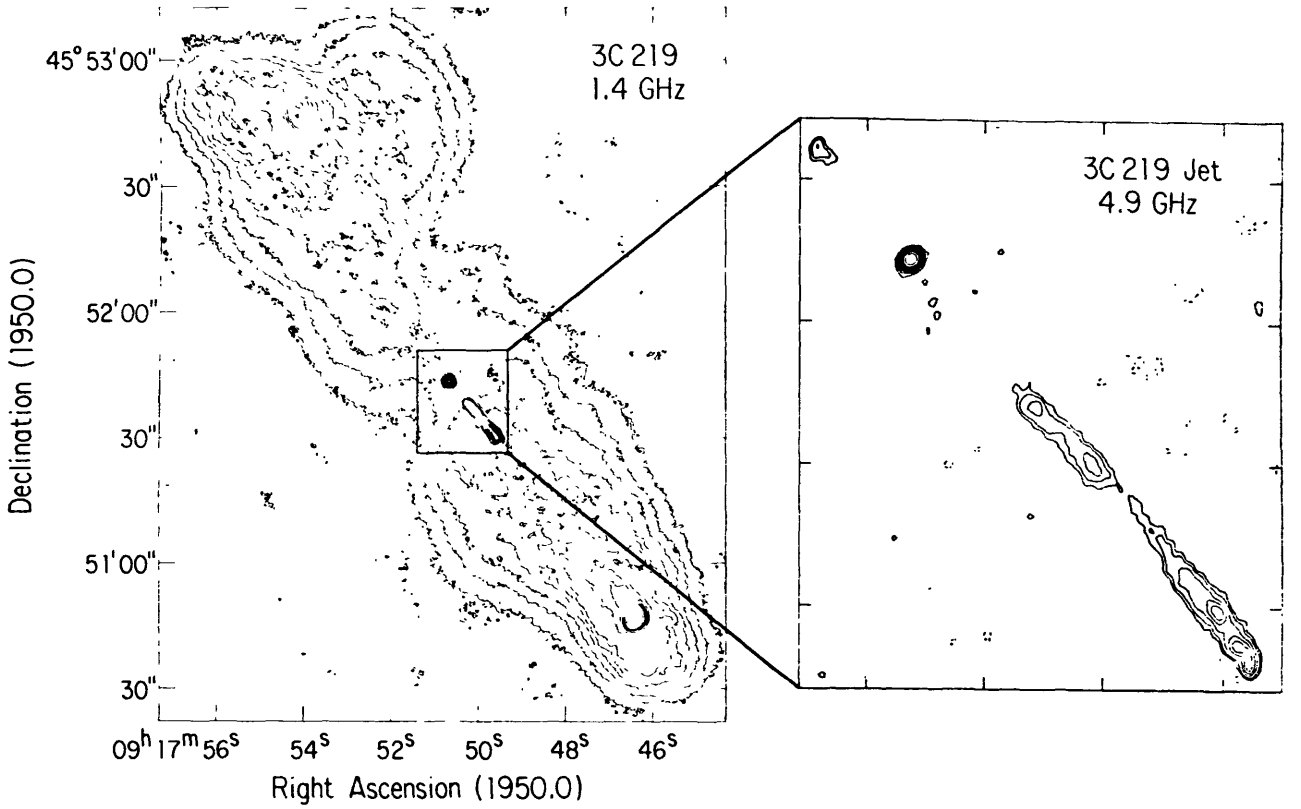

Figure 1.
(Left panel) VLA 1465 MHz map of 3C219 with 1.7 arcsec resolution (circular Gaussian restoring beam). Contours are plotted at -1, 1, 2, 3, 4, 5, 6, 8, 10, 12, 14, 16, 20, 30, 40 and 50 times 2 mJy per beam.
(Right panel) VLA 4885 MHz map of a $\sim$ 20 arcsec region near the nucleus of 3C219 (box in left panel) at $\sim$ 0.35 arcsec resolution. The brightest feature is the radio core. The contours on the jet are plotted at -1, 1, 2, 4, 6 and 8 times 0.2 mJy per beam. Note the elongated knot to the north-east of the core – presumably the brightest part of the counterjet, as it is elongated along the jet axis. Note also that this knot is opposite the end of the initial "gap" in the main jet.

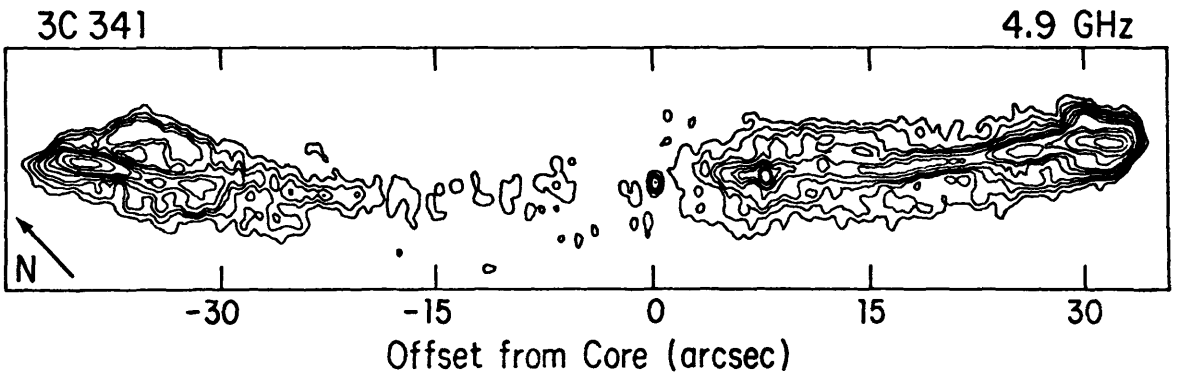

Figure 2. VLA 4885 MHz map of 3C341 with 1.0 by 0.6 arcsec resolution. The contours are plotted at -1, 1, 2, 3, 4, 6, 8, 10, 15, 20, 30, 40 and 50 times 0.237 mJy per beam. Note the cocoon around the jet(s).

have structure resembling jets. This relative faintness of jets in powerful radio galaxies is not an instrumental bias. The powerful 3CR[2] galaxies were observed at the VLA with roughly similar sensitivities, dynamic ranges and numbers of beamwidths across their lobe structures as the extended 3CR[2] QSRs. The jets in luminous radio galaxies must typically emit a smaller fraction of the total flux density than those in weak radio galaxies or extended QSRs[5].

These statistics pose an intriguing question for jet models – what is it that varies with radio luminosity among galaxies, and with the prominence of the optical nucleus among powerful radio sources generally, that affects the relative luminosities of the jets and the lobes ?

The detectability of the jets in the powerful sources may be related to the relative prominence of their cores – among the extended 3CR[2] QSRs mapped at the VLA, the detection rate of jets increases with the relative prominence $f_C = S^5_{core}/S^{1.4}_{tot}$ of the radio core, apparently regardless of redshift. All six extended 3CR[2] QSRs with $f_C > 0.03$, but only two of the six with $f_C < 0.005$, have jets or features resembling the brightest parts of jets. Saikia (1984) finds a similar correlation in a sample of 59 QSRs observed at the VLA. The lack of detectable jets in distant 3CR[2] galaxies may therefore be connected with the faintness of their radio cores relative to those of the QSRs (the median value of f_C in the distant 3CR[2] galaxy sample is only 0.0005).

Jack Burns (this Workshop) suggests a direct correlation between core and jet powers over a wide range of powers, which is consistent with these correlations between jet and core prominence and with the lack of totally "coreless" jets referred to above. A false power-power correlation might arise from z^2 bias in flux-limited samples, but the effect should clearly be tested for in volume-limited samples.

6. Trends with Luminosity

(a) Sidedness.

The symmetry of the lobes of the powerful doubles is strongly broken by their jets. Most of the powerful extended sources have lobes of roughly similar powers and sizes on each side of the parent object, but only in the weaker sources ($P^5_{core} \leq 10^{23.2}$ W/Hz or $P^{1.4}_{tot} \leq 10^{24.5}$ W/Hz) do the kiloparsec scale jets have counterjets with more than 1/4 their brightness per unit length.

Most *straight* kiloparsec scale jets are one-sided (by more than a 4:1 intensity ratio) close to their parent object, but those in weak radio galaxies become two-sided after a few kiloparsecs. The one-sided bases of the jets in these weak sources typically occupy $< 10\%$ of their length, and the jet with the one-sided base is generally somewhat brighter on the large scale.[6] Most kiloparsec-scale jets in powerful sources, whether radio galaxies or QSRs, are one-sided (more than 4:1 in brightness) for their entire lengths. All the

[5] The recent detection of a large-scale jet in Cygnus A (Perley *et al.* 1984b) is consistent with this, as this jet contains only about 0.25% of the total luminosity of the source at 1.4 GHz, and became apparent only in VLA maps of much higher quality than those available for most other powerful sources.

[6] Frazer Owen and Chris O'Dea tell me that the initial one sided regime is rare in the C-shaped trails, though some (e.g., IC708 – Vallée *et al.* 1981; 3C129 – Burns 1983) show it clearly. It will be interesting to examine this difference quantitatively in sources of different luminosities, as it might be a hint of extrinsic (environmentally induced) sidedness relationships.

large scale QSR jets are one-sided, but radio galaxy jets may be either one- or two-sided, depending on the radio power – there are 14 radio galaxies in the BP list with one-sided jets > 10 kpc long. The range $P_{tot}^{1.4} = 10^{24.5-25}$ W/Hz which marks the transition between large-scale two-sidedness and large-scale one-sidedness (at the 4:1 brightness ratio level) also marks the transition between morphological classes I (edge darkened) and II (edge brightened) of Fanaroff and Riley (1974 – FR). There is a clear trend for the jets in weak, edge darkened sources to be much more symmetric on the large scale than those in powerful, edge brightened sources.

Further details on these trends are given in Bridle (1984); now for some sources which buck them. 3C438, an FR II radio galaxy with $P_{tot}^{1.4} = 10^{26.86}$ W/Hz, has a relatively weak ($P_{core}^{5} = 10^{23.99}$ W/Hz) core and a two-sided jet. Its total radio power exceeds that of many extended double QSRs, all of which have stronger cores and one-sided jets. This could indicate that core power, rather than total power, is better correlated with jet sidedness, but this should be tested with further examples. The two weakest cores associated with clear one-sided jets are those in Cen A ($P_{core}^{5} = 10^{22.20}$ W/Hz) and M87 ($P_{core}^{5} = 10^{22.92}$ W/Hz). Both jets are short (M87 – 1.8 kpc; Cen A – 5.2 kpc); their lengths are comparable to, or shorter than, those of the one-sided bases of two-sided jets in other sources with similar total powers. The "unusual" feature of the M87 and Cen A jets may therefore not be their brightness asymmetry, but the fact that they end in two-sided "inner lobes" rather than two-sided "outer jets" extending 10 to 50 kpc beyond them. NGC3078 and NGC6146 (Wrobel and Heeschen 1984) may be further examples of this effect in nearby weak sources, so the effect might be common in *volume-limited* samples of extragalactic sources.

3C219 (Figure 1), NGC1265 (O'Dea and Owen, this Workshop) and 3C445 (Wil van Breugel, private communication) have features with >4:1 brightness asymmetries on *both* sides of their cores. 3C219 and 3C445 both have isolated knots on one side of the core opposite *gaps* in the jets on the other side. Although these knots do not by themselves meet my criteria for being termed "counterjets", they *are* elongated along the axes of the main jets. The sidedness of such discontinuous "pieces of jets" is difficult to quantify; but, at least with present resolutions, there are not enough of them to cast the overall trend into doubt. They do, however, prompt questions about the origin of "avoidance" effects, and about intermittent or "flip-flop" outflow (Rudnick and Edgar 1984; Bridle, this Workshop).

(b) 2-D Magnetic Configuration.

Three configurations of the "apparent magnetic field" $\mathbf{B_a}$ (Laing 1981) are common:

1. $B_{\parallel}$, i.e. $\mathbf{B_a}$ is predominantly parallel to the jet axis all across the jet.
2. $B_{\perp}$, i.e. $\mathbf{B_a}$ is predominantly perpendicular to the jet axis all across it.
3. $B_{\perp-\parallel}$, i.e. $\mathbf{B_a}$ is predominantly perpendicular to the jet axis at the center of the jet, but becomes parallel to the axis near one or both of its edges.

Most two-sided regions of straight jets have either the $B_{\perp}$ or the $B_{\perp-\parallel}$ configuration, while most one-sided regions of jets have the $B_{\parallel}$ configuration. In straight jets emanating from weak cores, $\mathbf{B_a}$ usually turns from $B_{\parallel}$ to $B_{\perp}$ or $B_{\perp-\parallel}$ in the first 10% of their lengths, while jets associated with powerful cores are generally $B_{\parallel}$–dominated for their entire length (Bridle 1984). This transition in magnetic properties occurs at

$P^5_{core} = 10^{23-24}$ W/Hz (roughly corresponding to $P^{1.4}_{tot} = 10^{24-25}$ W/Hz). Combining this with the sidedness trend, the FR effect, and the occurrence of hot spots, we can identify two primary types of (straight) radio jet – two-sided, $B_\perp$– or $B_{\perp-\parallel}$–dominated jets (with short one-sided bases) in weak sources with edge-darkened structures and no hot spots (FR I sources), and one-sided $B_\parallel$–dominated jets in powerful sources with edge-brightened structures and strong hot spots (FR II).

Two departures from these basic trends may be traceable to perturbations of the jet flows:

(a) Two-sided jets often have the $B_{\perp-\parallel}$ configuration where they bend. The $B_\parallel$ edge is often deeper (and more strongly polarized) on the outside of the bend (3C31, NGC6251, M84) as if $B_\parallel$ is amplified there by stretching and shearing. The bent jets in the C–shaped head-tail source NGC1265 are $B_\parallel$–dominated even though they are two-sided (O'Dea and Owen, this Workshop). The fields in such sources may be extreme examples of the $B_{\perp-\parallel}$ type resulting from viscous interaction with ambient gas.

(b) Some knots in one-sided jets have $B_\perp$, or oblique, apparent fields although fainter emission near them is $B_\parallel$–dominated – e.g. Knot A in M87, the knot 50″ from the core in NGC6251 and Knot A2 in Cen A. These "magnetic anomalies" at bright knots may be due to oblique shocks which accelerate relativistic particles and amplify the component of B_j parallel to the shock. $B_\perp$ fields also appear where one-sided $B_\parallel$ jets terminate at bright hot spots, and the physics there may be similar.

(c) Size, Curvature and Misalignments.

Jets in weak radio galaxies and in strong core-dominated sources are generally short – < 10% of all jets in BP sources with $P^5_{core} < 10^{22.5}$ W/Hz, and only 13% of those in BP sources with $P^5_{core} > 10^{26.5}$ W/Hz, are longer than 40 kpc but ≈50% of those in sources of intermediate powers exceed this length. The jets in core-dominated sources may be shortened by projection effects if cores are Doppler boosted small-scale jets, but the jets in weak radio galaxies are mainly two-sided, so are probably short intrinsically. Strong jet curvature is also common in two distinct regimes – (a) the C-shaped two-sided jets in weak "head-tail" cluster galaxies and (b) the one-sided jets in core-dominated sources. Curvature may be due to bending of a confined jet by an external pressure (as in models for head-tail sources) or to wandering of the central collimator.

The misalignments between parsec and kiloparsec-scale jets increase with increasing core prominence. Several lobe-dominated double radio galaxies with kiloparsec-scale jets have cores with one-sided parsec-scale jetlike extensions on the same side as the large jets and aligning with them to $\leq 10°$. In powerful core-dominated sources however, the misalignments between parsec and kiloparsec-scale structures are often $> 20°$, and in 3C345 (John Biretta, this Workshop) and 3C418 they exceed 90°. These trends are consistent with the short jets in core-dominated sources being close to the line of sight.

(d) Collimation.

The jets in over a dozen radio galaxies, but in few QSRs, have been resolved transversely well enough to show their lateral expansion (spreading) directly. The transverse brightness profiles are generally center brightened, so their FWHMs Φ (corrected for the instrumental resolution) can be used to characterise how the synchrotron emission

widens with angle Θ from the radio core. Bridle (1984) shows that the resolved jets in powerful sources tend to expand more slowly than those in weak radio galaxies. The jets in the powerful sources have been observed with about as many beamwidths along their lengths as those in the weaker sources, so this trend is unlikely to be merely a resolution effect. The small median angle ($< 1°$) subtended at the radio cores by hot spots in powerful doubles is consistent with the trend, if the sizes of the hot spots indicate (roughly) the diameters of the (still to be detected) jets at these distances from the cores.

7. Freedom and Confinement

The fact that radio jets are generally center brightened supports the view that they are radiative losses in the energy transport region itself, not from a static cocoon around it. $\Phi(\Theta)$ may therefore show, at least qualitatively, how the flow radius R_j varies with distance z from the core. If the jet magnetic fields $\mathbf{B_j}$ are dominated by large scale organised components whose configuration changes with distance down the jet, some features of the $\Phi(\Theta)$ evolution may also reflect changes in field organization. Except in a few very highly polarized jets, there is not much evidence for this so far (an observation which may itself constrain the 3-D form of $\mathbf{B_j}$, see §9).

If we suppose that the observable parameter $d\Phi/d\Theta \propto 2\,(dR_j/dz)\sec i$, where i is the angle of the jet to the plane of the sky, then *decreases* in $d\Phi/d\Theta$ signify that the jet pressure p_j is being balanced by a *slowly* decreasing external pressure $p_e(z)$. The $\Phi(\Theta)$ data for many well resolved jets indeed show collimation "shoulders" at which $d\Phi/d\Theta \rightarrow 0$, at projected distances $z \approx 10$ kpc. This implies that they are not free jets whose spreading rates were decided forever on parsec scales, even though VLBI data show that many jets are *first* collimated on such small scales. This property of the resolved jets raises a major question for models of energy transport – what process recollimates the jets on the kpc, or 10 kpc, scales ?

(a) Weak Radio Galaxies ($P_{tot}^{1.4} < 10^{25}$ W/Hz).

Both sides of the jets in the radio galaxies 3C449, NGC315 and 1321+31 recollimate at similar distances from their cores. Those in 2354+47 decollimate as they descend intensity gradients in its soft X-ray halo. The synchrotron properties of the jets set lower limits p_{min} to the jet pressure that typically range from $\approx 10^{-10}$ dyne/cm^2 in the inner few kpc to $\approx 10^{-13}$ dyne/cm^2 $\sim$ 100 kpc from the galactic nuclei, scaling with jet radius R_j roughly as R_j^{-1} to R_j^{-2}. These data suggest, but by no means insist, that low-power jets can be collimated by the thermal pressures in the X-ray halos, which typically decline with z as z^{-1} to z^{-2} over the appropriate ($\sim$ 10 kpc) scales.

The *average* run of $p_{min}(z)$ from the jet synchrotron calculations sets a lower limit to the required $n_e(z)T$ in a halo if the jet is thermally confined – local overpressures at knots of order M_j^2 times the mean may be tolerable (Norman *et al.* 1984). Assuming a value for T, we can estimate the minimum X-ray luminosity of a hypothetical isothermal confining halo between energies E_1 and E_2 as:

$$L_X(E_1,E_2) = 1.995\times10^{-34}\bar{g}_{E_1,E_2}\sqrt{T}\left(\exp\left(\frac{-E_1}{kT}\right)-\exp\left(\frac{-E_2}{kT}\right)\right)\int n_e^2 dV \text{ W}$$

where $\bar{g}$ is the mean Gaunt factor in the appropriate energy range. The emission measure integral $\int n_e^2 dV$ can be evaluated from $n_e(z)$ by assuming the gas distribution to have spherical symmetry. For a fixed $p_{min}(z)$, the predicted $L_X \propto T^{-1.5}$, apart from the variation of the exponential factor. The minimum L_X required if a jet *of given flux density, angular size and redshift* is confined at a given temperature is also quite sensitive to the assumed $H_0 - L_X \propto H_0^{-13/7}$ with these constraints.

For NGC315, 3C66B, IC4296, Cen A and NGC6251, such calculations show that confinement by gas at $T \approx 1$ to 3×10^7 K (c.f. the M87 halo) is (just) compatible with the *Einstein* IPC detections or upper limits for extended soft X-ray sources around the galaxies. Confinement by intracluster gas at $T \approx 7 \times 10^7$ K is even more compatible with the X-ray data. The contribution of compact nuclear X-ray sources to the IPC data is unclear in some cases, however, so sensitive X-ray imaging and temperature determinations of the regions 1-50 kpc from the galactic nuclei are needed to clarify the situation. For M87, the *Einstein* and VLA data show that p_{min} in the knots (in this case a few times 10^{-9} dyne/cm^2) exceeds the thermal pressure in the X-ray halo at their projected distances by factors > 10 (Biretta *et al.* 1983). Nevertheless, although the first kiloparsec of this jet expands at a constant rate, the lateral expansion slows after Knot A, suggesting that the outer parts of the jet are not free. Whether these discordancies in M87 should be interpreted as local shock-related overpressures in a jet with Mach number $M_j > 3$, or as a problem requiring nonthermal (magnetic ?) collimation is not completely clear.

If the longer, rapidly-expanding segments of these recollimating jets are free, then the observed $d\Phi/d\Theta \ll 1$ implies that they are supersonic. The data suggest the jets are collimated initially, and become transonic, < 1 kpc from the nuclei then escape into regions where the external pressure p_e drops rapidly. If $p_e \propto z^{-n}$ and $p_j \propto \rho_j^x$, the sound speed in the jet $c_S = \sqrt{\Gamma p_j/\rho_j} \propto p_j^{(x-1)/2x}$. If the jet stays *confined*, $p_e = p_j \propto z^{-n}$, so $c_S \propto z^{(n/2x)-n/2}$ while $v_r = v_j(dR_j/dz) \propto z^{(n/2x)-1}$. Comparing the exponents of the z dependence of these two velocities shows that continued confinement of a supersonic jet eventually requires $v_r > c_S$ if $n > 2$. If the external pressure falls faster than z^{-2}, the jet must then "detach" from p_e, i.e. become free. If p_e begins to fall slower than z^{-2} (as in the X-ray halo of M87) after a jet has become free, the jet may be reconfined. Conical shocks would propagate into it from its surface (where it first "feels" the declining gradient of p_e (Sanders 1983), reheating the jet and possibly (re)accelerating relativistic particles in it (Jean Eilek, this Workshop). The shock structure downstream from the reconfinement may be quasi-periodic, leading (a) to oscillations in the jet's expansion rate and (b) to regularly spaced bright knots along it. These phenomena may have been observed in NGC315 (Willis *et al.* 1981) and particularly in NGC6251 (Bridle and Perley 1983, PBW) whose jet is limb-brightened near its first reconfinement (consistent with particle acceleration in the conical shocks). Sanders (1983) argued that jets which stay bright enough to be observed may be just those which do oscillate between freedom and confinement in this way.

(b) Powerful Radio Galaxies and QSRs ($P_{tot}^{1.4} > 10^{25}$ W/Hz).

The narrower collimation of the jets in stronger sources, coupled with their greater

distances, means that the expansion properties $\Phi(\Theta)$ of many of them are but crudely known. The data (Bridle 1984) are adequate to show however that jets in some powerful sources must be:

(a) free with Mach numbers $M_j \geq 50$,

(b) confined by much larger $p_e(z)$ than that in nearby radio galaxies, or

(c) the approaching sides of relativistic twin jets, whose minimum p_j is overestimated by the conventional calculation due to Doppler boosting.

Several of the jets in powerful sources show little or no systematic expansion with increasing distance from their cores (e.g. 3C33.1, 3C111, 3C219), though they are resolved at all distances. This suggests that the jets in these powerful sources "flare" on small scales, then recollimate some tens of kiloparsecs from the cores. As in the weaker radio galaxies, this is evidence that the powerful jets are not free at all distances, and, in particular, are confined by a mechanism that takes effect tens of kiloparsecs from the central engine.

Potash and Wardle (1980) have argued that freedom for these jets is also inconsistent with thrust balance. The thrust of a nonrelativistic jet is given by $T_j = \rho_j v_j^2 A_j$ where ρ_j is its density, v_j its velocity and A_j its cross-sectional area. But $v_j^2 = M_j^2 c_S^2$ and $c_S^2 = \Gamma p_j/\rho_j$, so we can write $T_j = M_j^2 \Gamma p_j A_j \geq M_j^2 \Gamma p_{min} A_j$ where p_{min} follows from the synchrotron calculations. If the jets in powerful extended QSRs have the high Mach numbers M_j derived by presuming them to be free, T_j so estimated becomes so large that the jets could not be stopped or deflected by the IGM. In these cases, either M_j or p_{min} must have been over-estimated.

Thermal confinement of the pc-scale jets in several powerful radio galaxies (but not in Cygnus A) is compatible with the X-ray data but for several large-scale QSR jets, the *Einstein* data rule out pure thermal confinement at temperatures $\approx 1-3\times10^7$ K unless the jets are Doppler-boosted. Boosting with a Doppler factor $\mathcal{D} = \gamma_j^{-1}(1-\beta_j \sin i)^{-1}$ could mean that p_{min} is over-estimated by a factor $\mathcal{D}^{(8+4\alpha)/7}(\sec i)^{4/7}$, which can be larger than the relativistic correction γ_j^2 to the thrust, (thus relieving the thrust balance problem) if the flow comes close to the line of sight. Reducing p_{min} also reduces the external pressure required to confine the jet thermally. Although all the jets which have these thrust balance and/or confinement problems are one-sided, as expected if Doppler boosting is occurring, the Doppler solution has unpalatable aspects. Both the thrust balance problem and the X-ray luminosity required for thermal confinement respond only very slowly to the Doppler fix. In the thermal confinement case, the projection required for the Doppler boosting increases the *linear scale* of the radio source by sec i, and thus increases the volume to be filled with the confining gas by $\sec^3 i$. This increase must be more than compensated by the reduction in n_e^2 attending the reduction in p_{et} for the confinement problem to be solved at all. Unless the beaming cone is much wider than $1/\gamma_j$, very small angles to the line of sight are required to cope with both the thrust and confinement problems, and would make it difficult to account for the high fraction of jets now being detected in the extended 3CR[2] QSRs.

For these reasons, magnetic confinement is frequently, and increasingly, invoked for jets in the powerful sources. There is no direct evidence for the required toroidal

magnetic fields but neither is magnetic collimation excluded by the available polarimetry (see §9). Another possibility would be that some jets in powerful sources *are* thermally confined, but at temperatures $\geq 10^8$ K. A new generation of measurements of the X-ray temperatures and scale sizes around the powerful jet sources is required to test this possibility observationally, but even in clusters there are theoretical difficulties with heating and confining such hot gas.

It therefore appears that the jets in the powerful sources are not free, yet we do not know of a convincing way to confine them. In this sense the question "what collimates the energy transport in the most powerful sources ?" is no better answered in 1984 than it was in 1954, though the question can be *posed* with greater sophistication now than then !

(c) Complications at Knots and Cocoons.

The interpretation of jet collimation is also complicated by knots in the jets and by the sources with faint cocoons around brighter jets. For example, Φ decreases at each of the outer knots in NGC6251 while the lower contours of the jet expand smoothly (Perley *et al.* 1984a). The collimation properties of cocoons can differ from those of their jet "spines" – the cocoon in M84 expands much faster than the jets $> 5''$ from the core. At what level of brightness (if any) in such sources does the synchrotron expansion rate $d\Phi/d\Theta$ indicate the spreading rate of an underlying flow ? Are these sources a warning that we may be misleading ourselves about the collimation properties of jets whose radio emission happens to look simpler ?

8. Intensity Evolution and Dissipation

This Section reviews aspects of jet data relating to particle acceleration in the flows.

(a) Spectral Indices.

The most common spectral index near 1.4 GHz in extragalactic jets is $\alpha \approx 0.65$ ($S_\nu \propto \nu^{-\alpha}$), but some jets, and some knots in jets, have indices >0.8. Spectral gradients in jets are difficult to measure, as jets may be confused with the lobes at low resolution, and maps with unscaled arrays at different frequencies may not be equally sensitive to all scales. Spectral gradients along most jets are small. Those which do exist are mainly in the sense of α increasing with distance from the cores (e.g. 3C31, For A, M87, 3C279, Cen A, 4C32.69), consistent with depletion of the higher energy particles by synchrotron losses in the outer parts of these jets. Jets also generally have slightly flatter spectra than the lobes they feed (Cen A may be an exception).

Possible exceptions to this trend occur where the the brighter jets in NGC315 (Bridle, Fomalont and Henriksen, in preparation), and IC 4296 (Bicknell *et al.*, this Workshop) initially "turn on". The weak emission between the cores and the bright bases of these jets (i.e. in the regions formerly called the "gaps") has $\alpha \geq 0.8$ near 1.4 GHz, while the jets have $\alpha \approx 0.6$ to 0.65. This suggests that local flattening of the electron energy spectrum (relatively more high-energy particles) accompanies the initial increase in jet emissivity at the ends of such "gaps".

Optical continuum emission coincides with bright knots in the radio jets of 3C31, 3C66B, M87, 3C273, 3C277.3, and Cen A. The 4500Å to 6 cm spectral index is generally within 0.1 of 0.7. The optical continuum is up to 20% linearly polarized in M87 and

$\approx$ 14% linearly polarized in 3C277.3. This polarization, the positional coincidence with the radio knots, and the connected optical-radio spectrum in M87, provide evidence that the optical continuum emission is synchrotron radiation from the same region as the radio. If the magnetic field strengths are near the equipartition values (inferred from the optical-radio spectrum and the radio knot sizes), the knots are several synchrotron lifetimes from the radio cores, showing that the knots are sites of relativistic particle reacceleration (or possibly of pitch angle scattering). Imaging of the optical continuum knots in jets with the *Space Telescope* should determine how discrete, or continuous, the conversion regimes are.

The region near the M87 jet has a luminosity $\approx 10^{41}$ erg/s in the *Einstein* HRI band. Individual knots are not resolved, but this integrated X-ray luminosity is consistent with extrapolating the steep spectrum of the knots above 6000Åto the X-ray regime. Schreier *et al.* (1982) conclude that the entire spectrum is probably synchrotron emission – too much gas is required for thermal emission, and drastic departures from equipartition are required for inverse Compton emission. If the synchrotron interpretation is correct, electrons with Lorentz factors $\sim 10^{7.3}$ are required to produce the observed X-rays in the equipartition magnetic field of the knots, providing a severe test for particle acceleration models. The radiative lifetimes of such particles would be $\leq$200 yr, comparable to the light crossing time in the knots, but much less than the light travel time to the knots from the nucleus of M87. The X-ray and radio structures of the jet in Cen A are also very similar, suggesting that this is also synchrotron emission, and raising similar demands for local particle acceleration.

(b) "Adiabats" for circular and elliptical jets.

Both the magnetic field strengths B_j and the relativistic particle energies E will decrease along an expanding laminar jet in which there is no magnetic flux amplification or particle reacceleration. If magnetic flux is conserved, $B_{\|} \propto A_j^{-1}$ and $B_{\perp} \propto (\ell_j v_j)^{-1}$, where A_j is the cross-sectional area of the jet and ℓ_j is the depth of the jet in the line of sight. Assuming relativistic particle conservation and adiabatic expansion then gives the synchrotron emissivity ϵ_ν as a function of jet area A_j and velocity v_j. For $B_{\|}$-dominated fields:

$$\epsilon_\nu \propto A_j^{-(5\gamma+7)/6} v_j^{-(\gamma+2)/3} \qquad (B_{\|})$$

From this, the luminosity per unit length (the quantity most readily measured for a jet that is *unresolved* transverse to its width) is $\mathcal{L}_\nu \propto \epsilon_\nu A_j$, i.e.:

$$\mathcal{L}_\nu \propto A_j^{-(5\gamma+1)/6} v_j^{-(\gamma+2)/3} \qquad (B_{\|})$$

For well resolved jets we can also determine the variation of central intensity I_ν with FWHM (Φ) along the jet ridge line. In an optically thin jet, this will be related to the adiabat for $I_\nu \propto \epsilon_\nu \ell_j$:

$$I_\nu \propto A_j^{-(5\gamma+7)/6} \ell_j v_j^{-(\gamma+2)/3}. \qquad (B_{\|})$$

For $B_{\perp}$-dominated fields, these adiabats become:

$$\epsilon_\nu \propto A_j^{-(\gamma+2)/3} \ell_j^{-(\gamma+1)/2} v_j^{-(5\gamma+7)/6}, \qquad (B_{\perp})$$

$$\mathcal{L}_\nu \propto A_j^{-(\gamma-1)/3} \ell_j^{-(\gamma+1)/2} v_j^{-(5\gamma+7)/6}, \qquad (B_\perp)$$

and

$$I_\nu \propto A_j^{-(\gamma+2)/3} \ell_j^{-(\gamma-1)/2} v_j^{-(5\gamma+7)/6}. \qquad (B_\perp)$$

The results for the circular jet (Fanti *et al.* 1982; Perley *et al.* 1984a) follow by putting $A_j = \pi R_j^2$ and $\ell_j = R_j$ in these general forms, whereon

$$I_\nu \propto R_j^{-(5\gamma+4)/3} v_j^{-(\gamma+2)/3} \quad (B_\parallel) \text{ or } \quad I_\nu \propto R_j^{-(7\gamma+5)/6} v_j^{-(5\gamma+7)/6} \quad (B_\perp)$$

In a laminar circular jet with the typical $\gamma = 2.3$, $I_\nu \propto R_j^{-5.2} v_j^{-1.4}$ if $B_\parallel$ dominates, or $I_\nu \propto R_j^{-3.5} v_j^{-3.1}$ if $B_\perp$ dominates.

For the more general case of an elliptical jet with $A_j = \pi a_j b_j$, the adiabats for $\mathcal{L}_\nu$ and I_ν depend on the orientation of the jet cross-section relative to the observer. For a pressure matched jet with $p_e \propto z^{-n}$ and $p_j \propto \rho_j^x$ with $n < 2x$, the circular cross section is unstable, and the major axis $a_j \propto z$ and the minor axis $b_j \propto z^{(n/x)-1}$ (Smith and Norman 1981). If the jet is viewed from a direction near the minor axis of its cross section (the most probable case),

$$\mathcal{L}_\nu \propto R_j^{-(5n\gamma+n)/6x} v_j^{-(\gamma+2)/3} \quad \text{and} \quad I_\nu \propto R_j^{-(5n\gamma+n+6x)/6x)} v_j^{-(\gamma+2)/3} \quad (B_\parallel)$$

or

$$\mathcal{L}_\nu \propto R_j^{(3x+3x\gamma-5n\gamma-n)/6x} v_j^{-(5\gamma+7)/6} \quad \text{and} \quad I_\nu \propto R_j^{(n+7n\gamma+3x-3x\gamma)/6x} v_j^{-(5\gamma+7)/6} \qquad (B_\perp)$$

These adiabats are sensitive to n and x, as these determine how the ***shape*** of the jet varies with distance z from the core. As $R_j \propto a_j \propto z$ for this viewing direction, the jet would appear to be "free" but would dim at rate generally quite different from that of the circular jet. For example, if we set $\gamma = 2.3, n = 1.5$ and $x = 5/3$ to represent a cold (nonrelativistic) jet propagating in a typical X-ray halo, $I_\nu \propto R_j^{-2.9} v_j^{-1.4}$ for $B_\parallel$ dominant, or $\propto R_j^{-2.2} v_j^{-3.1}$ for $B_\perp$ dominant. As Smith (1984) has emphasized, a laminar elliptical jet viewed along its minor axis *may* dim less rapidly than a circular jet with the same apparent radius, due to its slow expansion in the hidden direction.

(c) The $I_\nu(\Phi)$ data.

The actual variations of I_ν with jet FWHM Φ (assumed proportional to R_j) are slower than most of these "adiabats" over long regions of many jets. Nearest to the core, I_ν often increases with increasing Φ – the jets "turn on" following regions of diminished emission, or "gaps". The "turn-on" is often followed by regimes many kpc long in which I_ν typically declines as Φ^{-n} with $n = 1.2$ to 1.6. In 3C31, NGC315 and NGC6251, the value of n reaches ≈ 4 far from the core, as expected for the adiabatic $B_\perp$-dominated circular jet, but in NGC6251 (PBW) the "adiabatic" decline ≥ 100 kpc from the core is repeatedly interrupted by the "turning on" of bright knots.

Dissipation and particle acceleration in jets are extensively explored later in this Workshop (see the papers by Jean Eilek, Geoff Bicknell and Dick Henriksen), so suffice

it here to note that the highly subadiabatic $I_\nu(\Phi)$ behavior of $B_{||}$-dominated jets makes it likely that some of their bulk kinetic energy (which is not lost by adiabatic expansion) is dissipated to magnetic flux and relativistic particles through shocks or turbulence. If B_j is near equipartition on the kiloparsec scales, $B_{||}$ must be amplified locally (instead of falling as R_j^{-2}) or else long $B_{||}$-dominated jets would have unreasonably high fields on parsec scales.

These mechanisms for particle reacceleration may also be effective in $B_\perp$-dominated regions, but another process can also work well there – deceleration of the jet by entraining surrounding material. The "typical" $I_\nu \propto R_j^{-1.4}$ dimming law can be reached by adiabatic compression with $v_j \propto R_j^{-0.68}$ in a circular jet with electron energy index $\gamma = 2.3$, or $v_j \propto R_j^{-0.26}$ in an elliptical jet with $\gamma = 2.3$ and $x = 5/3$ propagating in an atmosphere with $n = 1.5$. The hypothesis that adiabatic deceleration is solely responsible for the slow dimming of such jets can be tested quite simply at low frequencies. The Faraday depth through a jet is roughly proportional to $\rho_j B_j R_j$, which in a circular $B_\perp$-dominated jet entraining at constant thrust T_j is proportional to $R_j^{-2} v_j^{-3}$. The Faraday depth in such a jet would therefore be nearly constant if it decelerated with $v_j \propto R_j^{-0.68}$, whereas it would decrease as R_j^{-2} in a constant-velocity flow. The low-frequency Faraday depth variations of resolved jets in weak radio galaxies should therefore be a good diagnostic of whether their slow dimming is due to adiabatic deceleration by entrainment[7].

Detailed understanding of what keeps large scale jets lit up requires self-consistent modeling of their collimation $\Phi(\Theta)$, intensity evolution, and apparent magnetic field configurations. Abrupt changes in $\mathbf{B_a}$ from $B_{||}$ to $B_\perp$ at bright knots may indicate particle acceleration at oblique shocks, particularly if the knots have their sharpest brightness gradients on their coreward sides, as in M87 and NGC6251. The degrees of linear polarization in, and the depths of, the $B_{||}$ edges on $B_\perp$–dominated jets may indicate the extent of viscous interactions with the surrounding ISM/IGM. The observations provide copious constraints for the models – jet spreading rates $d\Phi/d\Theta$, "turn-on" heights, transverse intensity profiles, field orderliness and orientation, as well as in the $I_\nu(\Phi)$ evolution. Models of jet propagation are not yet sufficiently versatile to confront the data at all of these points self-consistently, however, but the prospects for the future are discussed elsewhere in this Workshop.

9. 3-D Magnetic Field Configurations

The jet magnetic fields $\mathbf{B_j}$ must be at least partially ordered, (a) because of the high degrees of linear polarization in the jets and (b) because of the organization seen on the available well resolved maps of the "apparent" magnetic fields. The 3-D configuration of the ordered fields is important for models of the jet dynamics, but cannot yet be

[7] It was the *appearance* of constant Faraday depth in NGC315 (Willis *et al.* 1981) and NGC5127 (Fanti *et al.* 1982) that first made me aware of the possible significance of adiabatic slowdown for keeping jets lit up. The depolarizations observed in these two jets are only marginally different from unity, however, so the published Faraday depth estimates for them should probably be treated as upper limits rather than secure measurements. Multifrequency polarimetry at arc-second resolution below 1 GHz is required to carry out this test properly.

found unambiguously from the radio data.

The intrinsic degree of polarization $p_i(\gamma) = (3\gamma+3)/(3\gamma+7)$ would be about 71% for particles with $\gamma = 2.3$ moving in a uniform field. Observed polarizations up to 40% are common in radio jets at 6 cm and shorter and local values > 50% are known. Such high polarizations imply significant spatial ordering through the jet of $\mathbf{k} \times (\mathbf{k} \times \mathbf{B_j})$, where $\mathbf{k}$ is the unit vector towards the observer. This ordering need not imply full 3-D ordering of $\mathbf{B_j}$, however, as emphasized by Laing (1981). Suppression of one spatial component of $\mathbf{B_j}$, leaving the others randomized is sufficient to explain the high polarizations, though not to explain the variation of p_ν *across* a jet. Jets with < 5% linear polarization at short wavelengths (e.g. 3C277.3, 3C388) are exceptional.

Relating the distribution of $\mathbf{B_a}(\alpha, \delta)$ over the face of a jet to that of $\mathbf{B_j}(r, \phi, z)$ throughout it is non-trivial. $\mathbf{B_a}$ lies along the dominant ordered component of $\mathbf{B_j}$ perpendicular to the line of sight $\mathbf{k}$, in a synchrotron emissivity weighted vector average. If $\mathbf{B_j}, N_0$ and γ are *axisymmetric* functions of radius r in the jet and distance z along it, and the divergence of the jet is small, $\mathbf{B_a}$ must be either parallel to, or perpendicular to, the jet axis. All three of the common configurations, $B_{||}$, $B_\perp$ and $B_{\perp-||}$, can thus be synthesized from axisymmetric $\mathbf{B_j}$ distributions. The fact that these three configurations are common probably indicates that the organized components of $\mathbf{B_j}$ are axisymmetrically distributed.

To get further, we need the information provided by the distribution of the degree of linear polarization p_ν transverse to the jet. p_ν is generally highest at the edges of the jet in $B_{||}$ regions, but near the center of the jet in $B_\perp$ regions. $B_{\perp-||}$ regions have polarization minima at each of the field transitions across the jet. Ideally, we could combine observed transverse profiles of I_ν and p_ν with the distribution of the apparent field $\mathbf{B_a}$ to infer the 3-D field configurations $\mathbf{B_j}(r, \phi, z)$. The relation of the data to $\mathbf{B_j}$ is not unique, however, especially if the data do not extend to the Faraday thick (long-wavelength) regime.

Laing (1981) gives analytic expressions and graphs of transverse profiles of I and p for several axisymmetric $\mathbf{B_j}$ distributions, assuming $\gamma = 3$ (for which many of the integrals have analytic forms) and $n_e = 0$, to eliminate Faraday effects. It is clear from Laing's results, and from more general cases that I have examined numerically, that two broad classes of 3-D field configurations generally fit the distributions of p_ν at high frequencies for which the Faraday depths should be negligible. These are (a) tangled field loops confined to a plane perpendicular to the jet axis near the center of the jet but stretched along the axis towards its edges or (b) "flux ropes" with organized helical fields of variable pitch, i.e. with ϕ and z components $B_\phi = B_0(r/R_j)\cos\psi_R$, $\quad B_z = B_0 \sin\psi_R$ (where ψ_R is the pitch angle of the field at the jet boundary $r = R_j$, Chan and Henriksen 1980) *plus* a random field component B_{rand}. Such calculations also show that $B_{||}$ can dominate $\mathbf{B_a}$ across much of the transverse profile of a jet with a helically-wound field if the jet is not in the plane of the sky (e.g. Laing 1981); thus merely searching for $B_\perp$ is inadequate as test for helical field geometries.

Observations of jets in their Faraday thick regime are required to distinguish these alternative 3-D field configurations, which have very different implications for the possible influence of the fields on jet dynamics and collimation. At frequencies where the jet

Faraday depth is finite but typically < 1 radian, the flux rope fields produce transverse Faraday rotation gradients across a jet. At these wavelengths the degree of polarization at a given location and resolution will also decrease with frequency on one side of the jet but increase on the other, until the Faraday depth becomes large. The "sheared tangled" fields would not produce such systematic transverse asymmetries in the apparent Faraday rotation or depolarization. Several beamwidths are needed across the jet to detect and distinguish these cases. As the Faraday thick regime appears to be below 1.3 GHz in most jets, this will require polarimetry with MERLIN or a composite VLA/VLBA array. Note from §8 that such observations would also test adiabatic deceleration as the prime mechanism for keeping a $B_\perp$-dominated jet lit up.

I am particularly grateful to Geoff Bicknell, Dick Henriksen, Robert Laing, Rick Perley, John Wardle and Peter Wilkinson for stimulating discussions of these topics.

REFERENCES

Baade,W., Minkowski,R. (1954). Ap.J. **119**, 215.

Bartel,N., Ratner,W.I., Shapiro,I.I., Herring,T.A. and Corey,B.E. (1984). *Proc. IAU Symp. 110, VLBI and Compact Radio Sources* (ed. R.Fanti, K.I. Kellermann and G.Setti), Dordrecht:Reidel, 113.

Biretta,J.A., Owen,F.N., Hardee,P.E. (1983). Ap.J.Lett. **274**, L27.

Bridle,A.H. (1982). *Proc. IAU Symp. 97, Extragalactic Radio Sources* (ed. D.S.Heeschen and C.M.Wade), Dordrecht: Reidel, 121.

Bridle,A.H. (1984). A.J. **89**, 979.

Bridle,A.H., Perley,R.A. (1983). *Proc. Turin Workshop, Astrophysical Jets* (ed. A. Ferrari and A.G. Pacholczyk), Dordrecht: Reidel, 57.

Bridle,A.H., Perley,R.A. (1984). Ann.Rev.Astron.Ap. **22**, 319 **(BP)**.

Burbidge,E.M., Smith,H.E., Burbidge.G.R. (1975). Ap.J.Lett. **199**, L137.

Burbidge,E.M., Smith,H.E., Burbidge.G.R. (1978). Ap.J. **219**, 400.

Burns,J.O. (1983). *Proc. Turin Workshop, Astrophysical Jets* (ed. A. Ferrari and A.G. Pacholczyk), Dordrecht: Reidel, 67.

Chan,K.L., Henriksen,R.N. (1980). Ap.J. **241**, 534.

Fanaroff,B.L., Riley,J.M. (1974). M.N.R.A.S. **167**, 31P **(FR)**.

Fanti,R., Lari,C., Parma,P., Bridle,A.H., Ekers,R.D., Fomalont,E.B. (1982). Astron. Astrophys. **110**, 169.

Fomalont,E.B. (1981). *Proc. IAU Symp. 94, Origin of Cosmic Rays* (ed. G.Setti, G.Spada and A.W. Wolfendale), Dordrecht: Reidel, 111.

Laing,R.A. (1981). Ap.J. **248**, 87.

Miley,G.K. (1983). *Proc. Turin Workshop, Astrophysical Jets* (ed. A. Ferrari and A.G. Pacholczyk), Dordrecht: Reidel, 99.

Norman,M.L., Smarr,L., Winkler,K.-H. (1984). *"Fluid dynamical mechanisms for knots in astrophysical jets"*, to appear in *Numerical Astrophysics: A Festschrift in Honor of James R. Wilson* (ed. J.Centrella).

Perley,R.A., Bridle,A.H., Willis,A.G. (1984a). Ap.J.Suppl. **54**, 292 **(PBW)**.

Perley,R.A., Dreher,J.W., Cowan,J. (1984b). *"The jet and filaments in Cygnus A"*, Ap.J.Lett., in press.

Potash,R.I., Wardle,J.F.C. (1980). Ap.J. **239**, 42.

Rudnick,L., Edgar,B.K. (1984). Ap.J. **279**, 74.

Saikia,D.J. (1984). M.N.R.A.S. **208**, 231.

Sanders,R.H. (1983). Ap.J. **266**, 73.

Schreier,E.J., Gorenstein,P., Feigelson,E.D. (1982). Ap.J. **261**, 42.

Shaffer,D.B. (1984). *Proc. IAU Symp. 110, VLBI and Compact Radio Sources* (ed. R.Fanti, K.I.Kellermann and G.Setti) Dordrecht: Reidel, 135.

Smith,M.D. (1984). M.N.R.A.S. **207**, 41P.
Smith,M.D., Norman,C.A. (1981). M.N.R.A.S. **194**, 785.
Strom,R.G., Willis,A.G. (1981). *Proc. 2nd ESO/ESA Workshop, Optical Jets in Galaxies* (ed. B.Battrick and J.Mort) ESA SP-162, 83.
Vallée,J.P., Bridle,A.H., Wilson A.S. (1981). Ap.J. **250**, 66.
van Breugel,W.J.M., Heckman,T.M., Bridle,A.H., Butcher,H.R., Strom,R.G., Balick,B. (1983). Ap.J. **275**, 61.
Willis,A.G. (1981). *Proc. 2nd ESO/ESA Workshop, Optical Jets in Galaxies* (ed. B.Battrick and J.Mort) ESA SP-162, 71.
Willis,A.G., Strom,R.G., Bridle,A.H., Fomalont,E.B. (1981). Astron.Astrophys. **95**, 250.
Wrobel,J.M., Heeschen,D.S. (1984). *"Compact-core-dominated radio emission from bright E/S0 galaxies"*, NRAO preprint.

3C120: A CONTINUOUS LINK BETWEEN MOVING FEATURES AND A LARGE SCALE RADIO JET

R. Craig Walker
National Radio Astronomy Observatory, Edgemont Road,
Charlottesville, VA 22901

ABSTRACT. VLBI monitoring observations at 6 cm show features in the parsec-scale radio core of the galaxy 3C 120 that are moving at apparent velocities of a few times the speed of light. Lower resolution VLBI observations at 18 cm and VLA observations with with resolutions between 0".1 and 12" show a continuous connection between these moving features and 100-kpc scale jet and lobe structures. These data provide the best evidence available, although still indirect, that the large scale, linear structures usually refered to as jets actually contain moving material.

1. THE GALAXY

The radio source 3C 120 is associated with a galaxy at a redshift of 0.033. The optical image of the galaxy is about 1' in extent, with an extensive network of HII regions thought to be photoionized by the nucleus (Baldwin et al. 1980). It is usually classified as a Seyfert but its spiral nature is not clearly established. The nucleus is a strong and variable source of radiation at all observed wavelengths from radio to X-ray. In many ways, 3C 120 resembles a low luminosity quasar.[1]

II. SUPERLUMINAL MOTIONS

3C 120 is one of the first sources in which apparent superluminal motions were found. Two convincing epochs of superluminal motions were seen during the 1970's, one from 1972.5 to 1974.4 and the other in 1979 (Seielstad et al. 1979, Walker et al. 1982). At other times, rapid structural variations were seen but the observations were too infrequent to reveal the motions.

In 1981, J. Benson, S. Unwin, G. Seielstad, and I began to observe 3C 120 every 4 months at 6 cm with VLBI arrays consisting of between 6 and 11 stations. With the more frequent observations, the rapid motions in 3C 120 became apparent. During the period from 1980 to the end of 1983, four new superluminal components were observed, all moving at angular

---

[1] If the type of this galaxy is uncertain, how reliable are the determinations of the types of galaxies seen as fuzz around QSO's?

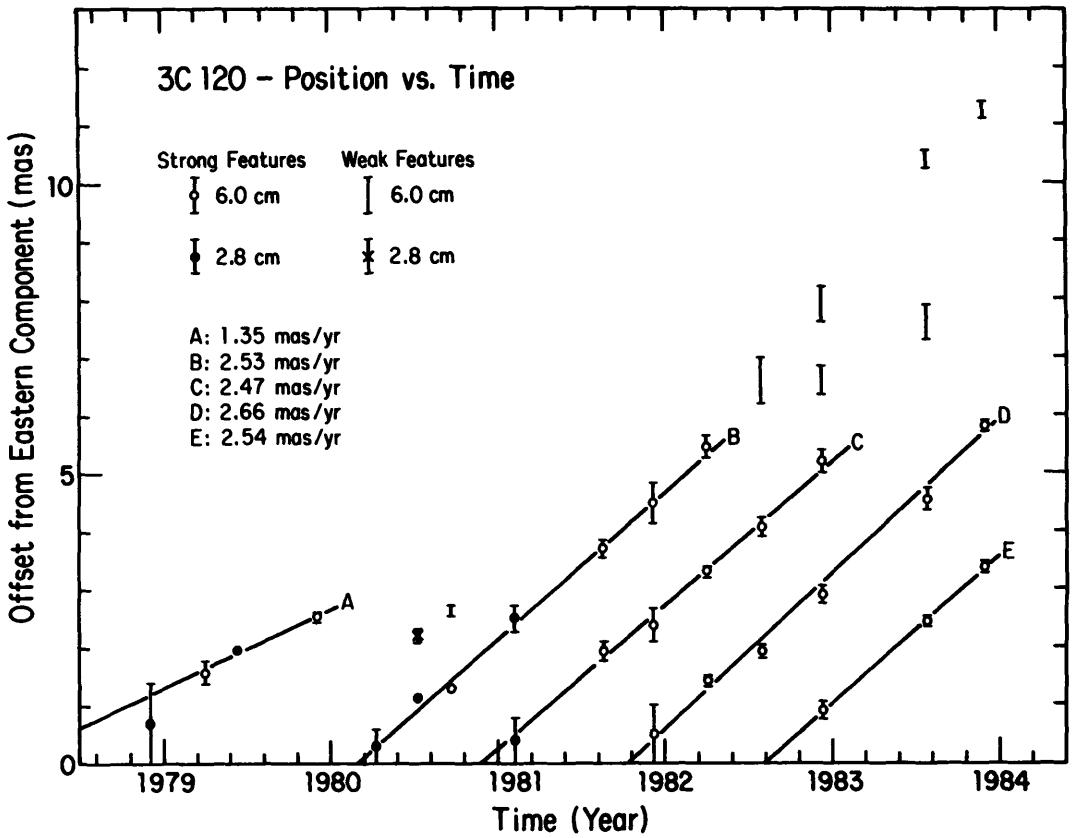

Figure 1. The positions of the features seen in VLBI maps of 3C120 since 1978 are shown relative to the eastern feature. The lines and rates represent fits to the positions of the strong features. The weak features are less reliable and caution must be used in the interpretation of their positions.

---

rates of about 2.5 mas yr^{-1} (1 mas = 0".001), or about 4c (H_o=100). This rate is about twice that of the 2 superluminal components observed during the 1970's. The results are summarized in Figure 1, which shows the positions of the various components seen in the VLBI maps relative to the position of the eastern feature. The eastern feature is assumed to be stationary although this assumption has not been checked observationally. One of the best maps from the sequence is shown as the highest resolution map in Figure 2. The labels of the features in this map correspond to the labels of the lines in Figure 1.

The standard model for superluminal motions involves relativistic motions in a jet pointed nearly along the line-of-sight (cf. Blandford and Konigl 1979). Therefore the observation of superluminal motions can be taken as good evidence for the presence of moving material in the jet on parsec scales.

III. LARGER SCALE STRUCTURES

Figure 2 shows the radio structure of 3C 120 on all scales from about 0.5 pc to over 100 kpc. Each map shows a box indicating the region covered by the next higher resolution map to emphasize the range of scales covered. These maps are from a much larger collection to be published by Walker, Benson, and Unwin (in preparation). The highest resolution map is from the 6 cm VLBI project discussed above. The next highest resolution map is from tapered data from a 14 station, 18 cm VLBI experiment done in Oct. 1982. The other maps are all from VLA observations.

The 18 cm VLBI experiment was an effort to study structures on scales of tens of milli-arcseconds whose presence was indicated by the 6 cm VLBI data. The map in Figure 2 shows that the jet bends from the position angle of the superluminal features ($\sim -102^\circ$) to nearly east-west. The jet has a variety of knots and wiggles and is seen for about 0".25 from the core before the brightness drops below the noise.

Figure 2. (Fold Out) The radio structure of 3C 120 on scales ranging from 0.5 pc to 100 kpc. The instrument and observing frequency are noted on each map along with a line showing the scale in parsecs (H_0=100). The contour levels above the third level are logarithmic with 7 contours per decade. For the VLA maps, the highest contour is at one half of the peak brightness and is a good representation of the beam. The VLBI beams are 5.1 x 9.8 mas, PA -11° for the 18 cm map and 0.84 x 6.1 mas, PA -10° for the 6 cm map. Note that the north-south elongation of features in the VLBI maps is a manifestation of the elongated beams. Maps made from tapered data were used in two cases (marked) to provide a smoother sequence of resolutions. In general, weak features seen adjacent to the very bright core (eg. the 'ears' in the 2 cm, A array map) are not real. Also the dynamic range to the north and south of the core is somewhat lower than elsewhere in the maps, so features such as the connection between the core and the southeast lobe in the 18 cm, C array map are questionable.

Contour levels: (mJy per beam - Preliminary calibration)

C array 18cm: -1.8, -0.9, 0.9, 1.8, 2.7, 3.7, 5.2, 7.2, 10, 14, 19, 27, 37, 52, 72, 100, 139, 193, 1143

C array 6cm: -0.6, -0.3, 0.3, 0.6, 1.0, 1.4, 1.9, 2.7, 3.7, 5.2, 7.2, 10, 14, 19, 27, 37, 52, 72, 1013

A array 6cm: -0.8, -0.4, 0.4, 0.8, 1.3, 1.9, 2.7, 3.7, 5.2, 7.2, 10, 14, 19, 27, 37, 52, 72, 100, 986

A array 2cm: -0.8, -0.4, 0.4, 0.8, 1.3, 1.9, 2.7, 3.7, 5.2, 7.2, 10, 14, 19, 27, 37, 52, 72, 100, 643

(The 2cm flux density scale may be low by up to 30%)

VLBI 18 cm: -4.0, -2.0, 2.0, 4.0, 6.6, 10, 14, 19, 27, 37, 52, 72, 100, 139, 193, 268, 373, 518, 720

VLBI 6 cm: -8.0, -4.0, 4.0, 8.0, 13, 19, 27, 37, 52, 72, 100, 139, 193, 268, 373, 518, 720

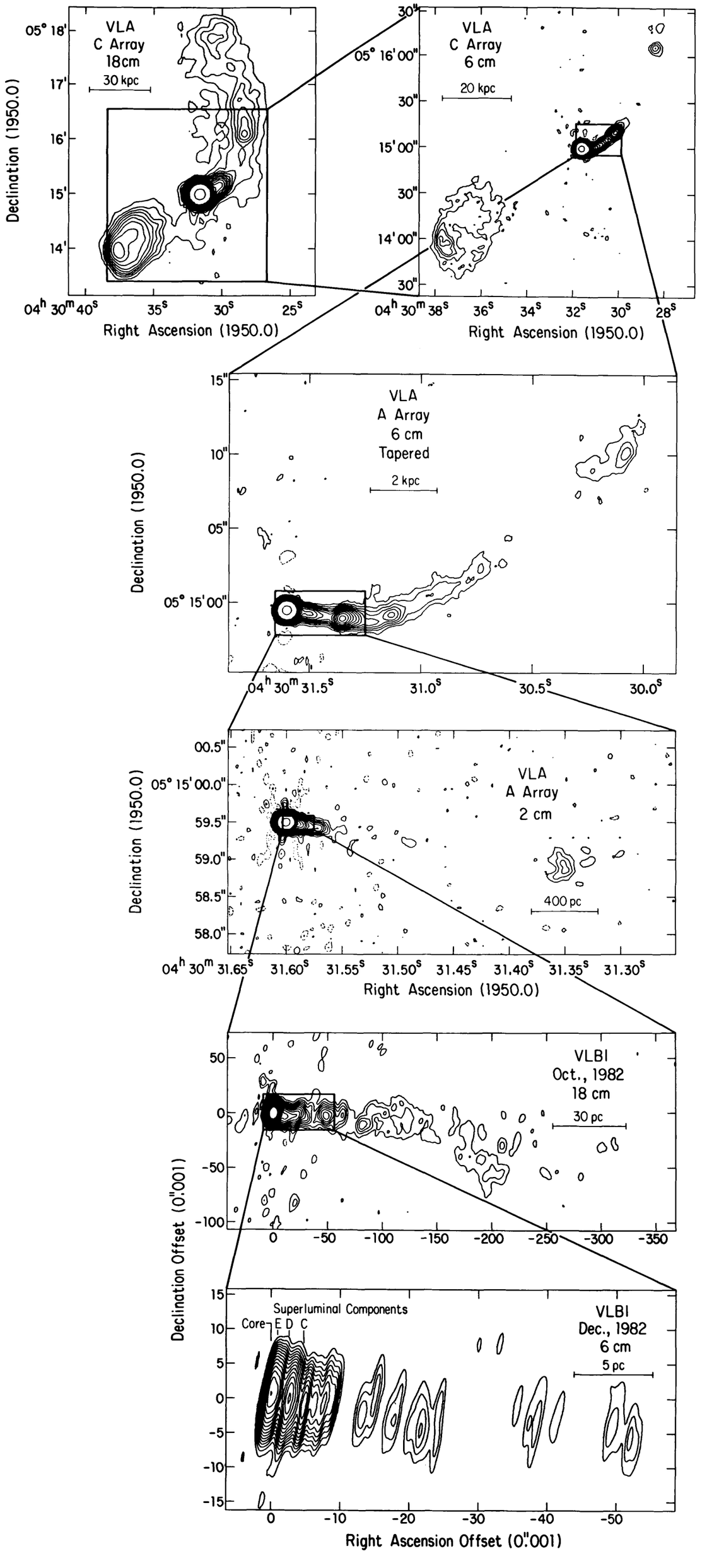
VLA
C Array
18cm
30 kpc
VLA
C Array
6 cm
20 kpc
VLA
A Array
6 cm
Tapered
2 kpc
VLA
A Array
2 cm
400 pc
VLBI
Oct., 1982
18 cm
30 pc
VLBI
Dec., 1982
6 cm
5 pc
Superluminal Components
Core
E
D
C
Declination (1950.0)
Right Ascension (1950.0)
Declination Offset (0".001)
Right Ascension Offset (0".001)

The arcsecond and larger scale structures in 3C 120 are very weak relative to the core. Previous observations showed that such structures exist (cf. Balick et al. 1982, de Bruyn and Schilizzi 1984, Soboleva et al. 1982), but very long integrations on the VLA plus corrections for closure errors (Walker, VLA Scientific Memorandum No. 152) were required to reveal the full details shown in Figure 2 and in the other maps that will be published elsewhere. The maps show that the jet is continuous from the scales seen in the 18 cm VLBI map to at least 3', although the low resolution required to see the jet above the noise at some positions could hide gaps smaller than about 20 percent of the distance to the core. The jet is initially oriented east-west, but slowly bends around until, at 3', it is nearly due north of the core. Polarization data show that the magnetic fields are parallel to the jet at nearly all positions observed by the VLA. At 2' from the core, opposite the jet, there is a lobe with a hot spot. The magnetic field in the lobe is circumferential, as in the lobes of many other sources. The spectral index is about $\alpha = -0.7$ ($S \propto \nu^{\alpha}$) throughout most of the large scale structure.

IV. CONCLUSION

The large scale radio morphology and magnetic field structure of 3C 120 are much like those seen in other extragalactic radio sources. Therefore the continuity of the radio structure of 3C 120 from parsec scales, where motions are observed, to 100-kpc scales is good, although indirect, evidence that the large scale, linear features seen in many extragalactic sources, and generally refered to as jets, actually contain moving material. Motions on small scales are seen in other sources with large scale jets but only in 3C 120 is a direct link observed.

REFERENCES:

Baldwin, J. A., Carswell, R. F., Wampler, E. J., Burbidge, E. M., and Boksenberg, A. 1980, Ap. J., 236, 388.

Balick, B., Heckman, T. M., and Crane, P. C. 1982, Ap. J., 254, 483.

Blandford, R. D., and Konigl, A. 1979, Ap. J., 232, 34.

de Bruyn, A. G., and Schilizzi, R. T., 1984, in VLBI and Compact Radio Sources, ed. R. Fanti, K. Kellermann, and G. Setti (Dordrecht: Reidel), 165.

Seielstad, G. A., Cohen, M. H., Linfield, R. P., Moffet, A. T., Romney, J. D., Schilizzi, R. T., and Shaffer, D. B. 1979, Ap.J., 229, 53.

Soboleva, N. S., Berlin, A. A., Nizhel'skii, N. A., and Spangenberg, I. I. 1982, Sov. Astron. Lett, 8, 110.

Walker, R. C., Seielstad, G. A., Simon, R. S., Unwin, S. C., Cohen, M. H., Pearson, T. J., and Linfield, R. P. 1982, Ap. J., 257, 56.

RADIO JETS IN STRONG CORE CLASSICAL DOUBLES

JACK O. BURNS

Department of Physics and Astronomy, University of New Mexico, Albuquerque, NM 87131

ABSTRACT. The properties of radio jets in classical double sources are described. Particular attention is paid to jet statistics, clumpiness, efficiencies, and confinement.

1. INTRODUCTION

Early on in the study of extragalactic radio jets, it became apparent that jets in low luminosity sources were relatively easy to detect. Current statistics (e.g., Bridle and Perley 1984) indicate that 80 – 90% of low luminosity sources have jets. This contrasts markedly with the classical double, high luminosity sources which have jets < 20% of the time (as a group including radio galaxies and quasars) on maps with <500:1 dynamic range. Is this low detection percentage in classical doubles an observational artifact due to the limited dynamic range on earlier maps ? Alternatively, is there a real physical difference in energy transport between the low and high luminosity sources ?

In an effort to address these questions and to study the general properties of jets in classical doubles, several observational programs on the VLA were undertaken. In the first, a sample of 15 classical doubles with strong cores (core flux > 10% of peak flux on previous maps) were observed at 6 cm with high resolution (0.″3 to 1″) and high dynamic range (>2000:1, generally thermal noise limited) in a search for jets. Although the present sample is not statistically complete, it should be representative of classical doubles with strong cores. About half of the sample are radio galaxies and half are quasars. All have measured redshifts. A more complete report of these observations can be found in Burns *et al.* (1984). The second project involves a much deeper search for radio jets not seen on the maps of classical doubles described above. Complete 8 – 12 hr synthesis observations are under way to lower map noise levels. Preliminary results described here are from Basart, Burns and De Young (in preparation). The third project is to search for radio cocoons around previously detected jets in luminous doubles. These jets are all good candidates for for magnetic field self-confinement since the internal jet pressures exceed 10^{-10} dyn cm^{-2}. Preliminary results described here are from Burns, Owen, Cioffi and Begelman (in preparation).

I will attempt to cull together the major results of these observations to present my view of the properties of radio jets in classical doubles.

2. OBSERVATIONAL RESULTS

2.1 Jet Detection Statistics

More than 50% of classical double radio sources with strong cores have detectable radio jets on maps with dynamic ranges of 2000:1. This detection percentage is the same for both radio galaxies and quasars. It is interesting to note that this detection rate is the same as that for other samples of quasars (e.g., Owen and Puschell 1984)

but distinctly higher than that for a general sample of radio galaxies (which have jets $< 5\%$ of the time; R.A.Laing, private communication). The obvious difference is the strength of the nuclear core. Quasars have strong cores much more often than typical radio galaxies. However, if one preselects a sample of classical doubles with strong cores, there is no difference between radio galaxies and quasars. It appears then that the strength of the radio core is an important parameter in determining the brightness of a radio jet.

It is also worth mentioning that the 50% detection rate is likely to be a lower limit. In Figure 1, a new map of the quasar 0110+297 made from 8 hrs of integration with the VLA clearly shows a one-sided jet. This was one of the sources observed by Burns *et al.* (1984) which did not have a jet on a map with 40 min integration. Further progress on this difficult question of jets in classical doubles (especially those with weak cores) will require long VLA observations (possibly in excess of 24 hrs for some sources) to achieve adequate (u, v) coverage and sensitivity necessary to detect low level jet emission.

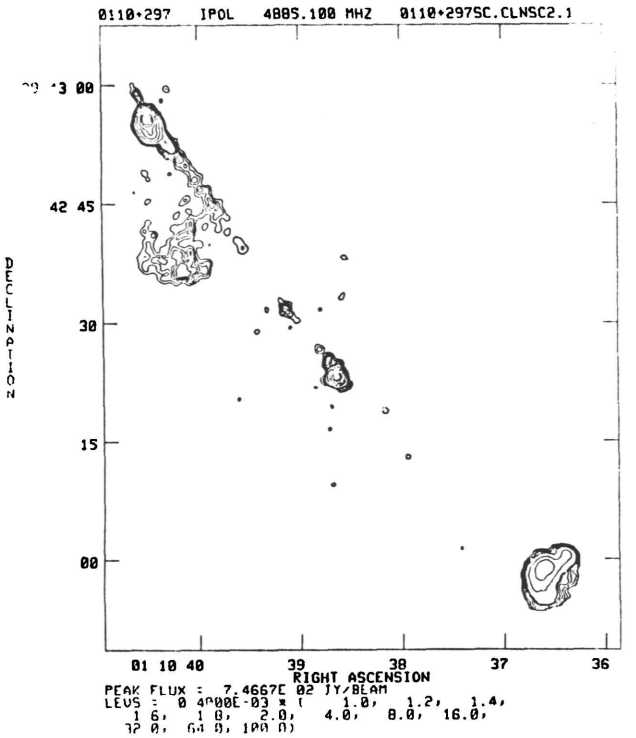

Figure 1. VLA map of the quasar 0110+297 at 6 cm. Note the clumpy, one-sided jet emission and the relatively compact northern lobe.

2.2 Jets are Clumpy

In Figure 2, a selection of radio jets from the Burns *et al.* (1984) sample is shown. Note that the continuous, smooth jet in 3C200 is unusual. Most of the jets are clumpy, resembling more a string of knots than the continuous emission seen in lower luminosity jets. The classical double jets average $S_K/S_I > 11$ where this ratio is the peak knot flux in the jet divided by the average interknot flux; three of eight jets have $S_K/S_I > 30$.

This contrasts with lower luminosity sources such as 3C449 which have $S_K / S_I < 5$.

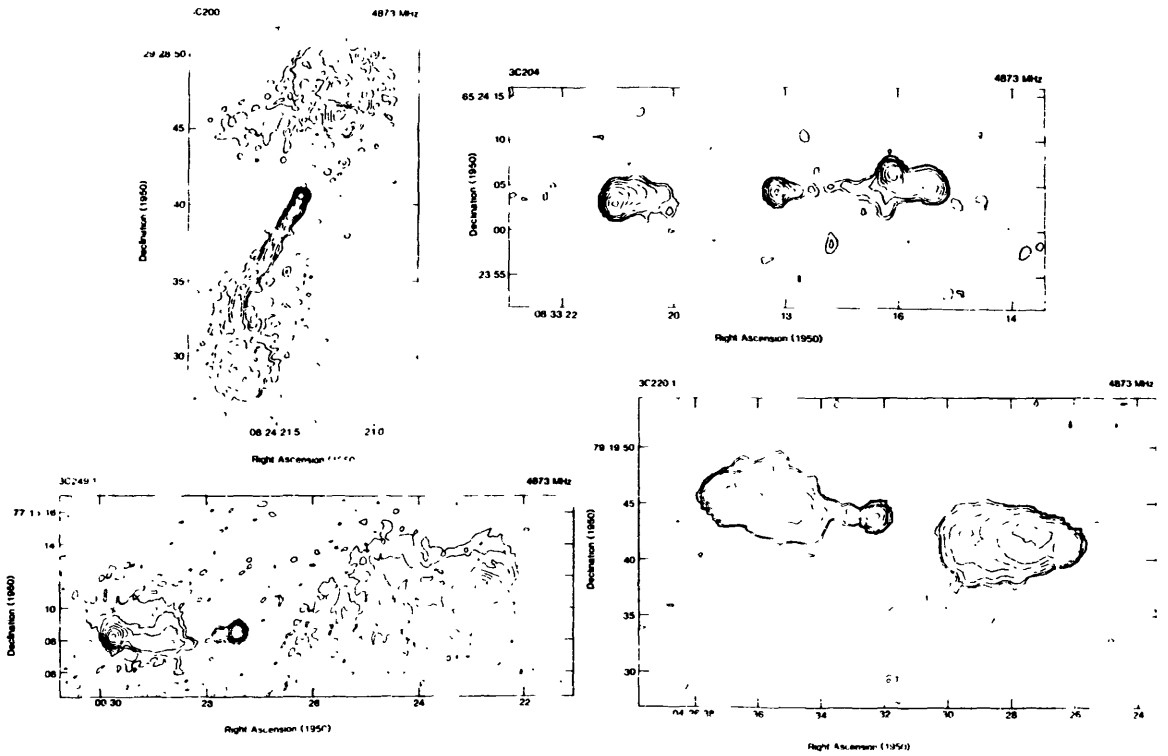

Figure 2. A sample of jets in classical doubles with strong cores from Burns *et al.* (1984).

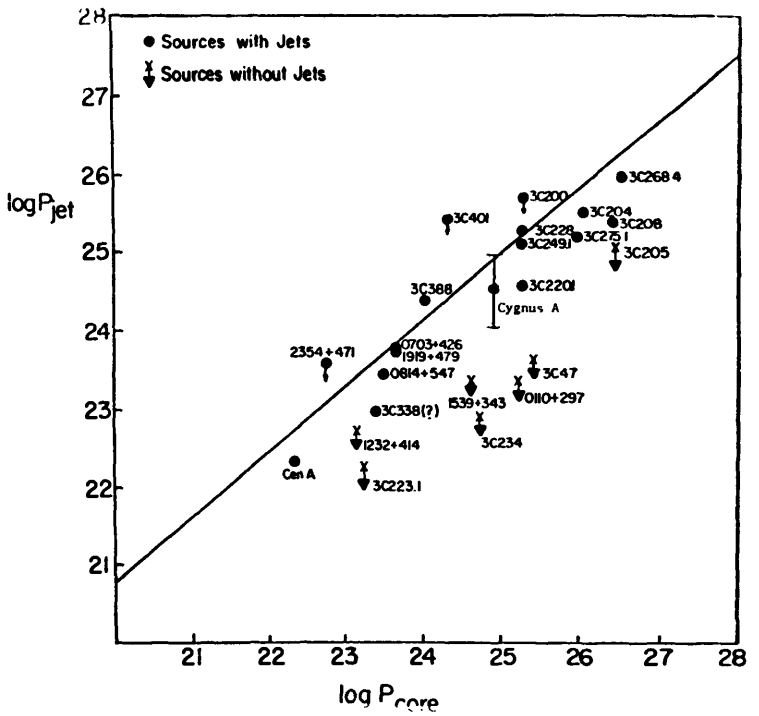

Figure 3. The integrated power in a radio jet at 6 cm plotted against 6-cm core power. The line is for reference only. Both low and high luminosity jets are shown.

2.3 Jets are One-Sided

100% of the sources in our samples have one-sided jets with side to side ratios ranging from 4:1 to $> 900 : 1$ (integrated fluxes). We have yet to find a good example of a two-sided jet in a classical double.

2.4 Possible Relationship Between Core and Jet Power

Figure 3 shows a plot of the integrated 6-cm power in a jet against the 6-cm core power. The plot includes both classical doubles and lower luminosity sources which were accessible to me. There is an interesting possible trend relating the core power to the total energy radiated by a jet. Including the upper limits for nondetections in the classical double sample, a Cox regression suggests that there is a 98% probability of a correlation (E.D.Feigelson, private communication). It is at least clear that the upper left quadrant is relatively empty, since there are few if any sources with strong jets and weak cores. However, it remains to be seen how extended the lower right quadrant will become when better dynamic range maps of classical doubles become available. I encourage observers to quote the integrated flux densities in their jets so that we will be able to see if this proposed relationship is valid.

2.5 Jet Efficiencies

As a measure of the radiative efficiency of a jet, we have computed the ratio of $P_{\rm jet}/P_{\rm total}$. A larger value for this ratio suggests an inefficient jet in the sense that a large part of the bulk kinetic energy in the flow is converted into radiation before reaching the lobes. Caution must be used here, however, in this observationally defined efficiency since it may not match theoretical definitions.

For the Burns *et al.* sample, we find that most of the classical doubles with strong cores and detected jets have $P_{\rm jet}/P_{\rm core} \sim 1$. This is similar to the relatively poor efficiencies of the lower luminosity sources. However, there is a sample of classical doubles with ratios < 0.001, such as Cygnus A, suggesting high degrees of radiative efficiency. It is not yet clear if there is a bimodal distribution of efficiencies or just a continuous distribution. The strength of the core seems to play a role (with stronger cores having less efficient jets), but other observational variables may be important as well.

2.6 Confinement

The average minimum internal pressure of the jets in the Burns *et al.* classical doubles sample is 2×10^{-10} dyn cm^{-2}. Five of the eight jet sources also have *Einstein* IPC X-ray observations. The inferred average external thermal pressure is 3×10^{-11} dyn cm^{-2}. Given the uncertainties in the X-ray data, it is still marginally possible to confine the jets thermally. However, in at least one case, the jet pressure exceeds 5×10^{-9} dyn cm^{-2}, making thermal confinement unlikely.

The alternative to thermal confinement is a magnetic field self-pinch generated by a current-carrying beam. We have yet to find a good example of a cocoon surrounding a jet with an azimuthal **B** field. However, such a **B** field configuration is difficult to detect, directly or via a rotation measure flip across the jet, because of the very high map dynamic range that is required. More observations are in progress.

2.7 Relativistic Beaming ?

The distributions of core power, source size, or hot spot distances from the cores on opposite sides show no support for the relativistic beaming hypothesis. See Burns *et al.* and De Young (these Proceedings) for more details.

2.8 One Side at a Time Emission ?

On the other hand, there is an interesting counter-example to the naive expectations of the "flip-flop" model in which a jet is said to be on only one side at a time (see e.g., Lonsdale and Morison 1983). Bridle and Perley (1984) have noted a trend for compact hot spots to be associated with the lobe on the jetted side of the source. 3C200 offers a marvelous counter-example in which the relatively compact hot spot is in the counterjet lobe and the jet lobe has no has no discernable hot spot when observed in the VLA "A" array at 2 cm (Burns, Owen, Cioffi and Begelman, in preparation).

REFERENCES

Bridle, A. H. and Perley, R. A. (1984). Ann. Rev. Astron. Ap. **22**, 319.
Burns, J.O., Basart, J.P., De Young, D.S. and Ghiglia, D.C. (1984). Ap. J. **283**, 515.
Lonsdale,C.J. and Morison,I. (1983). M.N.R.A.S. **203**, 833.
Owen,F.N. and Puschell,J. (1984). A. J. **89**, 932.

DISCUSSION

Larry Rudnick. In your thinking about jet/lobe ratios, which you consider as an efficiency, how do you interpret jets with little or no lobe emission, such as 3C273 ?

Jack Burns. I believe that these sources with very strong cores and no lobes fall in the same efficiency category as sources such as Cygnus A. The power in the jet is small relative to the core, so that $P_{\rm jet}/P_{\rm total}$ will be $\leq 10^{-3}$. In my terminology, these are *efficient* jets.

John Dreher. One "loophole" in the argument that the hot gas surrounding radio sources cannot provide sufficient pressure is to allow the temperature of this gas to be very high, with a consequent reduction in the X-ray emission (keeping the pressure constant). This loophole can be closed by estimating the energy contained in this hypothetical medium. To provide a confining pressure for the jet the medium must have energy density $u \geq u_{min}$ in the jet. The confining medium is, almost certainly, roughly spherical in distribution, and therefore $V_{medium} \gg V_{jet}$ and $E_{medium} \gg E_{jet}$. If we estimate R of the medium as ~ 1 Mpc and wish to confine a jet with $u_{min} \approx 10^{-9}$ dyn cm^{-2}, then $E_{thermal} \approx 10^{64}$ ergs $\approx 10^{10} M_{\odot} c^2$. It would seem to be very difficult to supply so much energy.

John Wardle. The X-ray spectra are comparatively soft, which directly rules out such high temperatures.

OBSERVATIONS OF LARGE SCALE JETS IN QUASARS AND THE SIDEDNESS PROBLEM

J. F. C. Wardle and R. I. Potash
Physics Department, Brandeis University
Waltham, Massachusetts 02254

ABSTRACT. We have found large scale jets in each of the eight largest radio sources from a complete sample of 4C quasars. In each case there is no visible counter jet. We argue that the observed limits on jet-counter jet ratios are incompatible with differential Doppler boosting, and that these jets are intrinsically one-sided.

Following the discovery of the first quasar with a large scale radio jet, 4C32.69 (Potash and Wardle, 1979), many similar sources have been found (44 quasars with arcsecond jets are listed by Bridle and Perley, 1984). In every case the jet is visible on only one side of the quasar (as is the case for high luminosity radio galaxies), but it is not clear whether the jets are intrinsically one-sided, or if the counter jet is below the dynamic range of the maps due to the Doppler effect. In the absence of direct velocity measurements for the jet material, we can appeal to statistical arguments to attempt to resolve this question.

We have used the VLA to map many quasars from the 4C catalog to search for more large scale jets. Our sample is taken from the complete sample of 4C quasars in the 20°-40° declination strip (Olsen, 1970; Schmidt, 1974). We have mapped the eight quasars in this complete sample whose largest angular sizes are > 50 arcseconds. The observational result we wish to report here is that all eight of these sources exhibit one-sided large scale jets.

The observations were all made with the VLA at 6 cm wavelength in the A or B configuration. The eight sources are listed in Table 1, together with some of their properties.

Table 1

Source	Redshift	LAS [arcsec]	ℓ^* [kpc]	S_j/S_{cj}
0007+33	.743	77	775	>2
0110+29	.363	76	526	>3
0130+24	.457	53	421	>20
0938+39	.617	54	500	>3
1001+22	.974	66	736	>3
1512+37	.371	51	357	>4
2325+29	1.015	50	570	>10
2349+32	.670	62	600	>64

*H_o = 50 km sec^{-1} Mpc^{-1}, q0=0

Maps of six of the sources are shown in figure 1. A map of 2349+32 has been published by Potash and Wardle (1979). The source 1512+37 was observed by us with only eight antennas of the VLA during poor observing

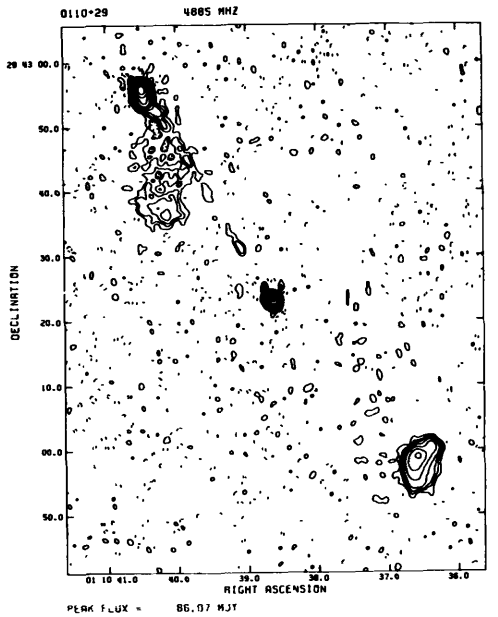

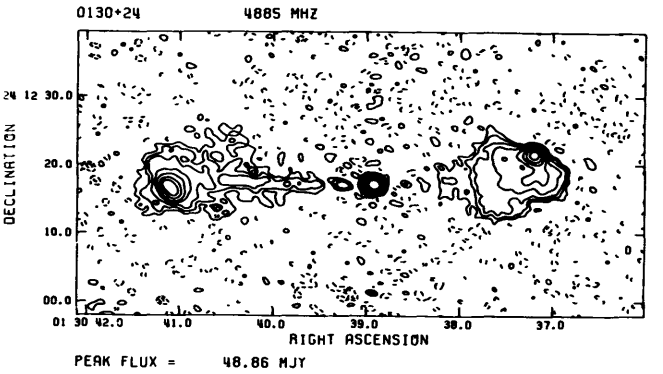

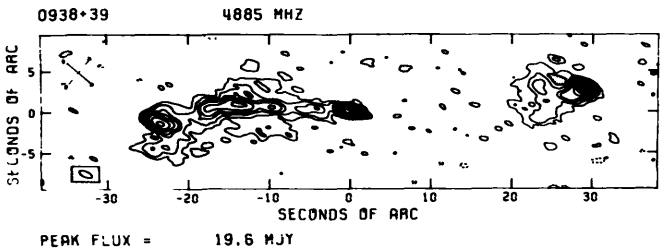

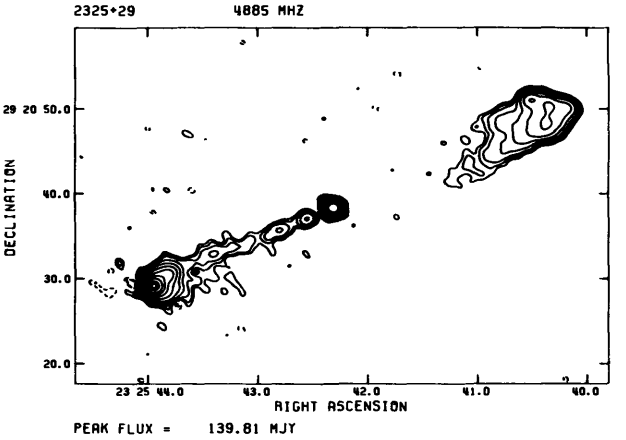

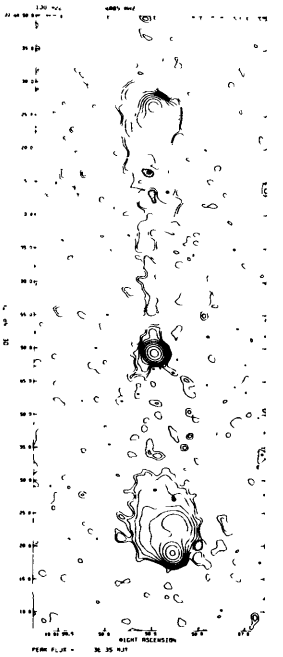

Figure 1. Maps of six sources from Table 1 made using the VLA at 5 GHz.
upper left **– 0110+29 = 4C29.02,** ***upper right*** **– 0130+24 = 4C24.02,**
center left **– 0938+39 = 4C39.27,** ***center right*** **– 2325+29 = 4C29.68,**
lower left **– 0007+33 = 4C33.01,** ***lower right*** **– 1001+22 = 4C22.26**

conditions. The resulting map had a low signal to noise ratio and the jet was not apparent. Subsequently this source was observed by Shaffer, Green and Schmidt and the jet is clearly visible. We are very grateful to Dr. Shaffer for making his map available to us in advance of publication.

The seven sources show a variety of morphologies. In six sources the jet is visible over its entire length from the central core to the outer lobe. In 0007+33 and 0110+29 the jets are faint and are only plainly visible in the vicinity of the outer lobe. These last two cases may not satisfy Bridle and Perley's (1984) conservative definition of a jet; nevertheless, we claim these are examples of intermittent jets that either turn on and off, or are cold (radio quiet) over much of their length. The statistical argument that follows is unchanged if the reader declines to consider these intermittent elongated structures as true jets.

The important point about this sample of sources is that we have observed the eight largest sources (in projected angular size) in a complete sample. Since the 4C catalog was observed at a low frequency (178 MHz), extended sources enter the catalog through their steep-spectrum extended (presumed to be unbeamed) emission, rather than through their core emission (which may be beamed). These sources should therefore be oriented at random with respect to the line of sight, and the largest sources must make the largest angle to the line of sight (i.e. be most nearly in the plane of the sky). This severely restricts the amount of Doppler boosting that can be invoked to account for the observed jet-counter jet asymmetries.

With how many intrinsically smaller or more forshortened sources should we compare the eight largest sources? Potash and Wardle (1979) observed all 51 quasars in the Olsen-Schmidt sample using the NRAO 4-element interferometer. Of these, 32 sources had a clearly resolved double or triple structure (largest angular size > 6 arcsec). Therefore we are dealing with the eight largest out of a complete sample of at least 32 sources.

If all sources have the same intrinsic linear size, then the eight sources with the largest observed angular sizes are uniformly distributed in cos θ (where θ is the angle between the major axis of the source and the line of sight) between cos θ = 1 and cos θ = 8/32, i.e. between θ = 90° and 75.5°. The median angle to the line of sight is $\cos^{-1}$ 4/32 = 82.8°. If we assume a more realistic distribution of intrinsic linear sizes, then this result is not changed significantly (except for bizarre linear size distributions). A detailed calculation will be presented elsewhere. Note that these inclination angles are anyway underestimated since the total number of double sources in the complete sample is certainly greater than 32.

The jet-counter jet ratio due to Doppler boosting is given by $((1+\beta \cos \theta)/(1-\beta \cos \theta))^{2+\alpha}$ where βc is the jet velocity and α is the spectral index. We shall assume α = .75. Inserting β = 1 and θ = 75.5°, the maximum jet-counter jet ratio we can attribute to the Doppler effect is 4.1. The maximum median value is 2.0. Looking at the lower limits on the observed ratios in table 1, column 5, we see that all eight sources have lower limits larger than the maximum median value of 2.0. Four sources have lower limits larger than the absolute maximum value of 4.1. In three cases this maximum value is exceeded by a large factor, limited only by the sensitivity and dynamic range of the map.

Note that the theoretical limit of 4.1 is overestimated, while all the observed values in table 1 are all lower limits. It is therefore clear that the Doppler effect cannot account for the one-sidedness of the jets we have found. The only assumption upon which this conclusion rests is that the quasars with extended radio structures in the 4C catalog are randomly oriented with respect to the line of sight. At present there is no compelling reason to doubt that this is the case.

We have demonstrated that, at least for large angular size quasars, the one-sidedness of the jets must be intrinsic to the source. (We have not demonstrted that they are nonrelativistic--only that the Doppler effect cannot produce a large enought jet-counter jet ratio even if $\beta = 1$.) However, the obvious symmetry between the outer radio lobes requires that both lobes are supplied with energy in at least a quasi-continuous manner.

There are two ways in which these requirements might be satisfied. First, the counter jet exists but for some reason it is radio quiet (as in the original model of Blandford and Rees (1974)). It would be necessary to invoke a specific mechanism to achieve this, since the jets are visible on one side in at least six out of eight sources. If this is due to chance, e.g. due to random environmental factors, we would expect to see jets on both sides in at least four out of the eight sources. This is clearly not the case. In the absence of a plausible mechanism for rendering one of the two jets always radio quiet, we do not favor this hypothesis.

The second possibility is that the jet is always visible, but flips from side to side, supplying energy to each radio lobe intermittently. This is the 'flip-flop' picture proposed by Rudnick (1982) and Rudnick and Edgar (1984), for which further circumstantial evidence comes from the observed hot-spot asymmetries discussed by Laing (this volume). The observed jet morphologies place rather strong constraints on the time scales involved. Since the lobe on the counter jet side is not noticibly dimmer, the cycle time for flipping must be shorter than the radiative lifetime of the lobe or the decay time for acceleration (if there is continuous reacceleration by for instance a reservoir of turbulent energy), whichever is longer. But since the jet is visible all the way from the core to the lobe in six of the eight sources, the 'on-time' on each side must be longer than the travel time from the core to the lobe. In this picture we might interpret 0007+33 and 0110+29 as jets that have recently turned off and are only visible at their ends. Since in these cases we do not see an emerging jet on the other side, we would appear to require also a significant 'off-time' while the jet changes sides. Whether these time scale restrictions can be satisfied in a consistent manner remains to be seen.

The major theoretical problem is to find a mechanism that will make the jet flip-flop. Two possibilities are the 'clam-shell' described by Icke (1983), and the multiple black hole picture discussed by Shklovsky (1982). Both of these ideas merit further investigation. Observationally, we need to observe more sources from carefully defined complete samples in order to confirm the intrinsic one-sidedness of radio jets in quasars, and to define better the timescale restrictions on the putative flip-flop mechanism.

REFERENCES

Blandford, R. D. and Rees, M. J. 1974, M.N.R.A.S., 168, 395.
Bridle, A. H. and Perley, R. A. 1984, to appear in Ann. Rev. A. and Ap.
Icke, V. 1983, Ap. J., 265, 648.
Olsen, E. T. 1970, A.J., 75, 764.
Potash, R. I. and Wardle, J. F. C. 1979, A.J., 84, 707.
Rudnick, L. 1982, in IAU Symposium 97, Extragalactic Radio Sources, ed. D. S. Heeschen and C. M. Wade (Dordrecht: Reidel), p. 211.
Rudnick, L. and Edgar, B. K. 1984, Ap. J., 279, 74.
Schmidt, M. 1974, Ap. J., 193, 505.
Shklovsky, I. S. 1982, in IAU Symposium 97, Extragalactic Radio Sources, ed. D. S. Heeschen and C. M. Wade (Dordrecht: Reidel), p. 475.

PIECES OF JETS AND OTHER THOUGHTS ON FLIP-FLOPS

L. Rudnick
University of Minnesota, Department of Astronomy
116 Church Street, SE, Minneapolis, MN 55455

ABSTRACT. I briefly discuss the status of the flip-flop model and introduce the use of isolated pieces of jets as one possible signature. Study of these jet pieces is also useful independent of the flip-flop, and may help us distinguish between discontinuous energy supplies and intermittent illumination as explanations of gaps in high surface brightness structures. Several areas are suggested for further observational and theoretical work.

(Work on 3C33.1 is in collaboration with B.K. Edgar)

The flip-flop model for extragalactic radio sources (Rudnick and Edgar, 1984, hereafter RE), postulated a nuclear demon which ejects relativistic material on only one-side of a source at a time, while maintaining a double symmetry over long time scales. This model was introduced to account for specific asymmetries commonly found among radio sources. Possible theoretical models for producing flip-flops have been proposed by Wiita and Siah (1980, who named the effect) and Icke (1983).

I think the verdict on this model is still out. One of the specific tests for the flip-flop is based on the ratio of arm lengths of doubles. RE described several samples which gave positive results, but a careful analysis of another sample by Ensman and Ulvestad (1984) shows no flip-flop evidence. I am presently working on a more comprehensive characterization of source asymmetries, through use of correlation and other functions. One of the main problems is separating the low surface brightness, symmetric structures from the high brightness, asymmetric ones, in an unbiased manner. Suggestions are welcome.

One of the predictions of the RE flip-flop is that jets should not be viewed as static structures through which material/energy flows, but that isolated pieces of jets should be found. This question is actually much broader than the flip-flop model, and can be rephrased as: "Can we find examples of collimated outflows which appear detached from their nuclear source? And if so, do these represent real switchings on-and-off of the nuclear source, or simply places where the continuous underlying outflow has been illuminated by relativistic material?" Can theorists give us more guidance to decide this issue?

A number of "pieces of jets" have been observed, including 3C401 (Laing 1981), NGC 6251 (Readhead et al., 1978), NGC 315 (Bridle et al., 1979) and 3C33.1 (van Breugel 1980), though they are not described in this way. We have obtained detailed VLA observations of 3C33.1, in order to determine whether the flow, or only the illumination, is intermittent.

Figure 1 shows a grey-scale display of the λ20cm total intensity structure, made with VLA A and D data. The nucleus is the isolated elliptical spot ~1/3 of the way from the NE hot spot, and is associated with a double galaxy at a redshift of 0.173. The gap between the core and the jet is ~90 kpc (~45") long, and was first highlighted by van Breugel (1980). Figure 2 shows brightness profiles along the jet piece, at both λ6 and λ20cm, and the derived spectral index between them.

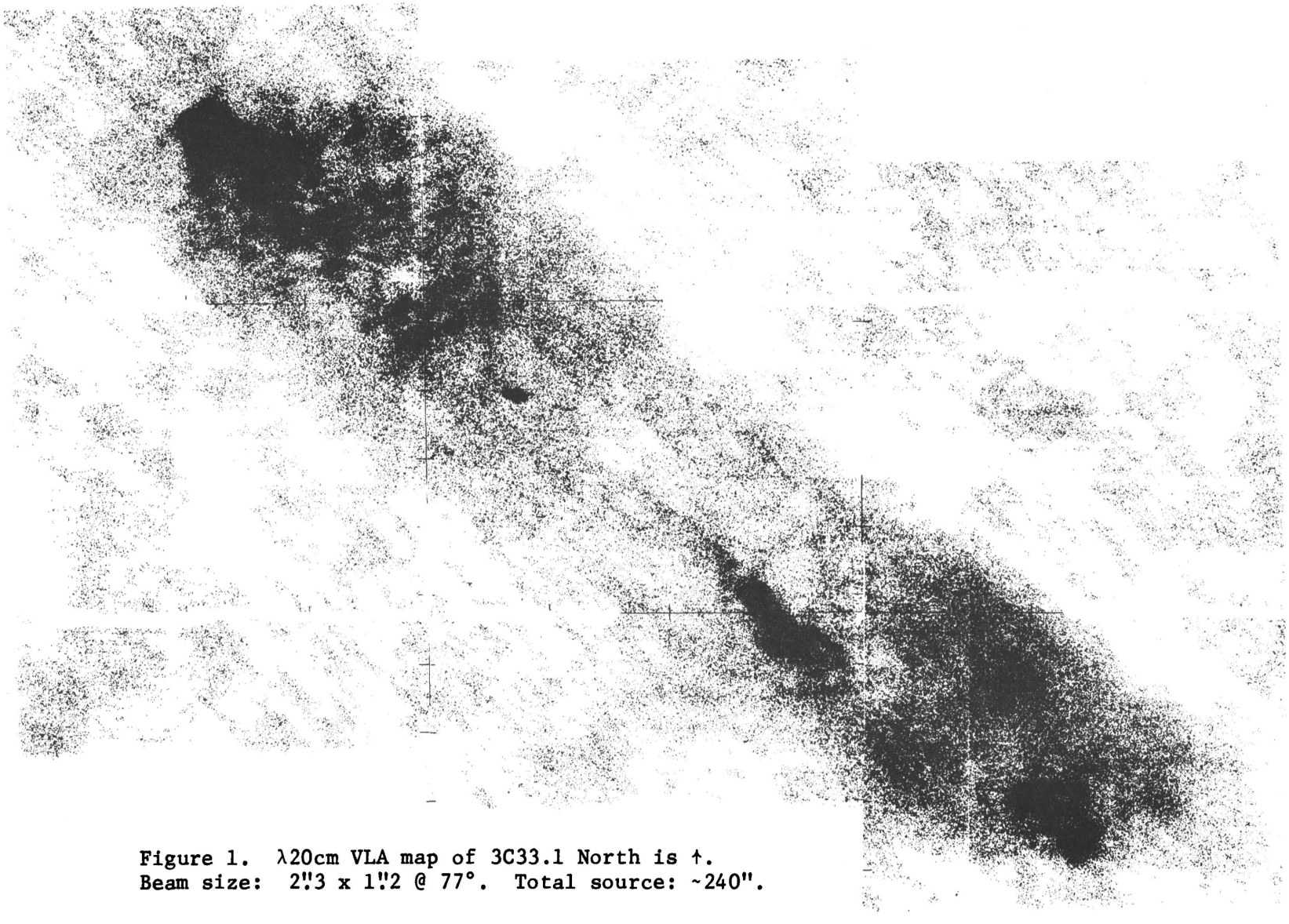

Figure 1. λ20cm VLA map of 3C33.1 North is ↑.
Beam size: 2".3 x 1".2 @ 77°. Total source: ~240".

Figure 2. Brightness and spectral index profiles along the jet piece. A typical spectral index error bar is shown.

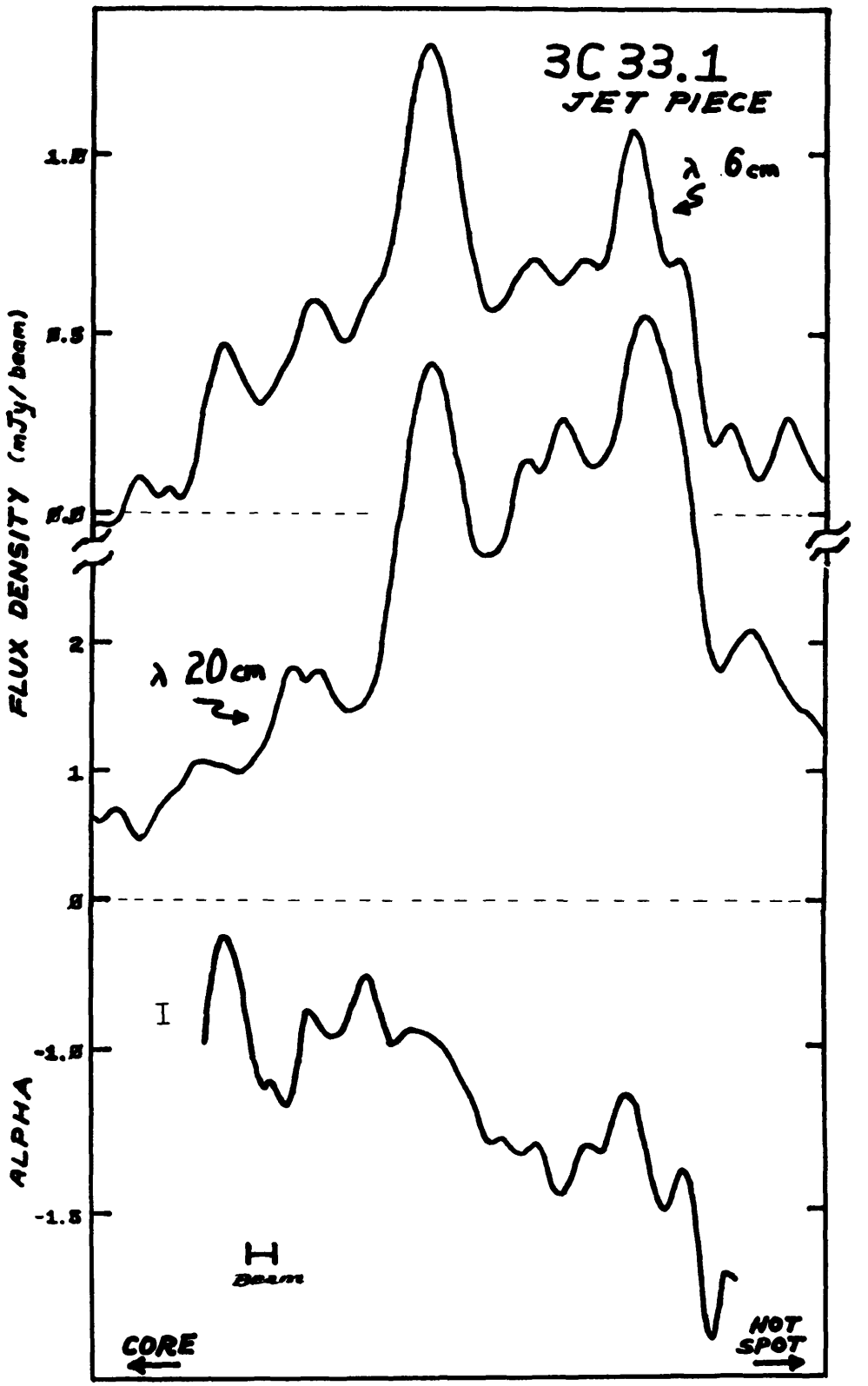

The leading edge of the jet piece (toward the southern hot spot) is characterized by two "ears", which have high polarizations (B along the ears, maps available on request). This type of morphology has been seen by V. Icke (private communication) in some analytical work on isolated pieces of moving fluid, and is also present in many of the numerical simulations of Norman and co-workers (see e.g., Zabusky 1984). In my view, then, the morphology favors a real turn-on of the fluid flow, at the the head of the jet.

However, the spectral index behavior suggests that the rear end of the jet (toward the nucleus) is not material which has been accelerated or swept back from the head: the spectral index is flatter toward the nucleus.* Similar behavior (on much smaller scales) has been seen in IC 4296 (Bicknell, this workshop). One possible explanation is that, at 90 kpc from the nucleus, the flow has reached a critical point and gone turbulent, accelerating particles (see e.g., Bicknell and Melrose 1982). For smaller nucleus-jet gaps, this critical point may be provided by a pressure drop in the confining external medium (e.g., Henriksen, Bridle and Chan 1982); for 3C33.1, deceleration below a critical Mach number may trigger the onset of turbulence, independent of the external gas (Bicknell, exclusive interview). One difficult, but potentially powerful way of examining these ideas would be to look at the properties of the very low surface brightness extensions of jets (which would show up frequently with more playing with the displays). Such an extension back toward the nucleus is just visible in Figure 1. Is there a change in width, in spectral index, in field ordering, from the low to high surface brightness jet? This is both an observational challenge, and an area in which theoretical work (e.g., origin and stability of such extensions) would be profitable.

*This conclusion is unchanged if I correct for the low surface brightness emission.

NSF grants AST81-14737 and AST83-15949 have provided partial support, for this and other contributions by L. Rudnick.

REFERENCES

Bicknell, G.V. and Melrose, D.B. (1982), Ap.J. 262, 511.
Bridle, et al. (1979), Ap.J. (Letters) 228, L9.
Ensman, L.M. and Ulvestad, J.S. (1984), preprint.
Henriksen, R.N., Bridle, A.T. and Chan, K.L. (1982), Ap.J. 257, 63.
Icke, V. (1983), Ap.J. 265, 648.
Laing, R.A. (1981), MNRAS 195, 261.
Readhead, et al. (1978), Nature 272, 131.
Rudnick, L. and Edgar, B.K.E. (1984), Ap.J. 279, 74.
van Breugel, W.J.M. (1980), Ph.D. Thesis, Leiden.
Wiita, P.J. and Siah, S.J. (1981), Ap.J. 243, 10.
Zabusky, N.J. (1984), Physics Today 37, 36.

THE RADIO JETS OF 3C449

TIM CORNWELL AND RICK PERLEY

National Radio Astronomy Observatory[a], P.O. Box O, Socorro, NM 87801

ABSTRACT. Multifrequency VLA observations of 3C449 have revealed the presence of steep gradients in rotation measure in the jets. Consequently, previous estimates of the jet thermal density and velocity from the depolarization are inaccurate. The rotation measure can be attributed to a foreground screen, probably in the galaxy itself since it is an extended X-ray source. The same X-ray emitting gas can easily confine the jets. Some estimates of the jet velocity can be made but all are subject to large uncertainties.

1. INTRODUCTION

The radio source 3C449 was one of the earliest radio galaxies studied in detail with the VLA (Perley *et al.* 1979) and, as such, has had considerable influence upon our understanding of radio jets in general. Most importantly, indirect estimates of both the jet thermal density and velocity resulted. From depolarization measurements based upon a WSRT map Perley *et al.* (1979) argued that the density of thermal matter internal to the jet was of order 0.02 cm^{-3}, and that the jet velocity was about 1200 Km sec^{-1}. Thus, the jet could be classified as slow, and heavy relative to the probable external medium. Saunders *et al.* (1981) used similar depolarization measurements to estimate the jet velocity in NGC6251 as 10,000 – 20,000 Km sec^{-1}. Unfortunately, this simple line of argument was broken by the discovery of significant rotation measure gradients in the jet in NGC6251 (Perley *et al.* 1984), consistent with a screen located somewhere exterior to the jet. Thus, estimation of the jet thermal particle density, which is important in understanding the source energetics and jet velocity, is much more difficult than previously believed.

Since 3C449 is a weak, extended X-ray source, such rotation measure gradients may also be present, and so the depolarization arguments of Perley *et al.* (1979) may be seriously in error. Subsequent 20cm VLA observations of the polarization structure in the jets of 3C449 revealed that anomalous depolarization gradients were present, so we embarked upon a detailed multi- frequency study with the goal of mapping the polarization over the wavelength range 20 to 6cm. A full presentation of the methods and results of this study will be given elsewhere, while here we present some highlights of the observations and some discussion of the implications for models of the jets.

We will use $H_0 = 100$ Km sec^{-1} Mpc^{-1}.

---

[a] The National Radio Astronomy Observatory (NRAO) is operated by Associated Universities, Inc. under contract with the National Science Foundation.

2. HIGHLIGHTS OF THE OBSERVATIONS

We made A, B, and D array observations at frequencies 1375, 1412, 1662 and 4885 MHz, giving good coverage of λ^2 space, required to untangle rotation measure effects which, if they are due to an external screen, are proportional to λ^2. The range of the u, v plane measured yields sensitivity to structures over the range 1 arcsecond to about 300 arcseconds. A greyscale plot of the jets and inner lobes at 20cm is shown in Figure 1. Properties of the jets were abstracted by fitting Gaussians to slices through the jets perpendicular to the local axis. Agreement with the Gaussian profile is suprisingly good. Figure 2 is a collection of graphs showing the variation with distance along the jet of peak brightness at 20cm, jet width, and minimum pressure compared to the external pressure due to a King model atmosphere consistent with the X-ray data (see next section). The variation of jet central brightness I_ν with width Φ is also shown in Figure 2; the upper envelope obeys a power law of the form :

$$I_\nu = I_{\nu,0}(\Phi/\Phi_0)^{-(1.5\pm0.2)}$$

The polarization data, not shown here, show considerable rotation of the position angle with wavelength. Fortunately, the variation is simply proportional to λ^2 at most positions in the jet, allowing a fit to determine the rotation measure distribution. After the rotation has been removed, the B-field vectors are predominantly perpendicular to the jet axis, with virtually no shearing at the edges except near the bends of the jets.

3. IMPLICATIONS

The presence of large rotation measure gradients in the jets of 3C449 explains the large depolarization seen in the WSRT map. The rotation measure varies from about -210 rad m^{-2} near the bases of the jets to -170 rad m^{-2} in the lobes, with strong gradients of up to about 50 rad m^{-2} across the jets. Since the position angle for the most part varies simply with λ^2, the rotation measure is almost certainly due to an external screen associated either with the hot gas producing the observed bremsstrahlung radiation, or with a thin sheath around the jet itself. Magnetic fields of about 0.25 – 0.5 μG are required in the former case, while the latter requires fields about an order of magnitude stronger. The rotation measure variations unavoidably complicate the estimation of the jet internal matter density so that we can only say that the number, 0.02 cm^{-3}, quoted by Perley *et al.* (1979) is too high by at least one, and probably by two, orders of magnitude, if one estimates the true internal rotation measure from a slab model. On the other hand turbulence could hide many orders of magnitude more thermal matter.

The collimation of the jets seems to separate into two regimes : the first, out to about 10–15 arcseconds from the core, is of relatively rapid expansion, tan(opening angle) = 0.29 North, 0.39 South, and the second, further out, is of slower expansion, tan(opening angle) = 0.15 North, and 0.14 South. Small knots are found in both jets in the first regime, but the brightness increases dramatically in the neighbourhood of the re-collimation shoulder. For comparison, the observed extended X-ray emission has a FWHM of 120 ± 30 arcseconds, for which the corresponding core radius a_c is 25 ± 8 Kpc (Miley *et al.* 1983). We can thus explain the collimation data with the picture of

L-band Image.

Resolution = 1.3 arcsecond.

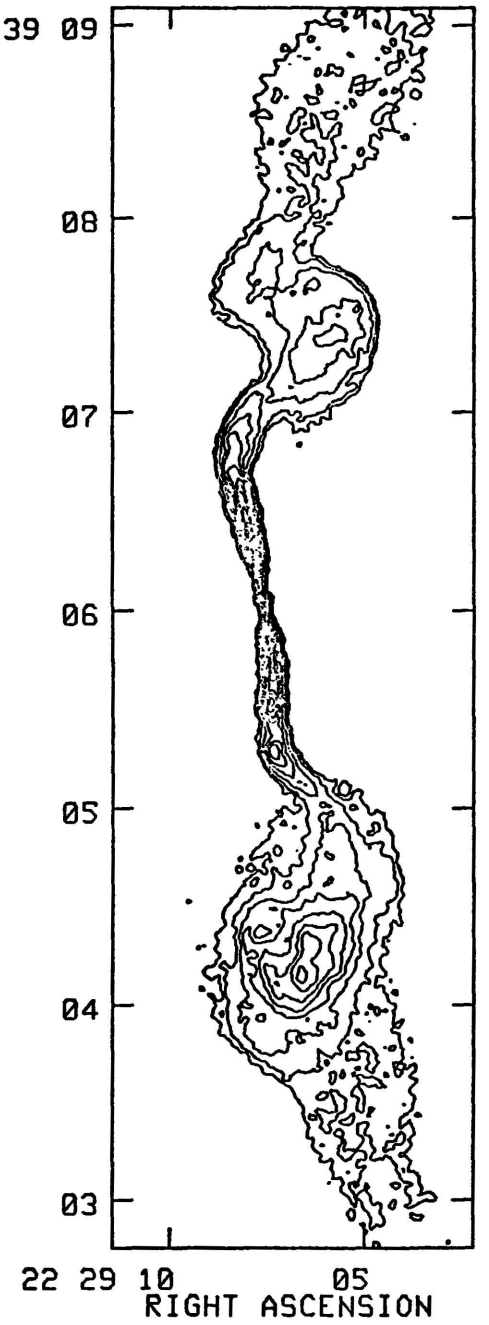

L-band image, resolution = 2.1"

Bottom contour = 3 mJy/beam, all others are even multiples.

Figure 1

Figure 2 :

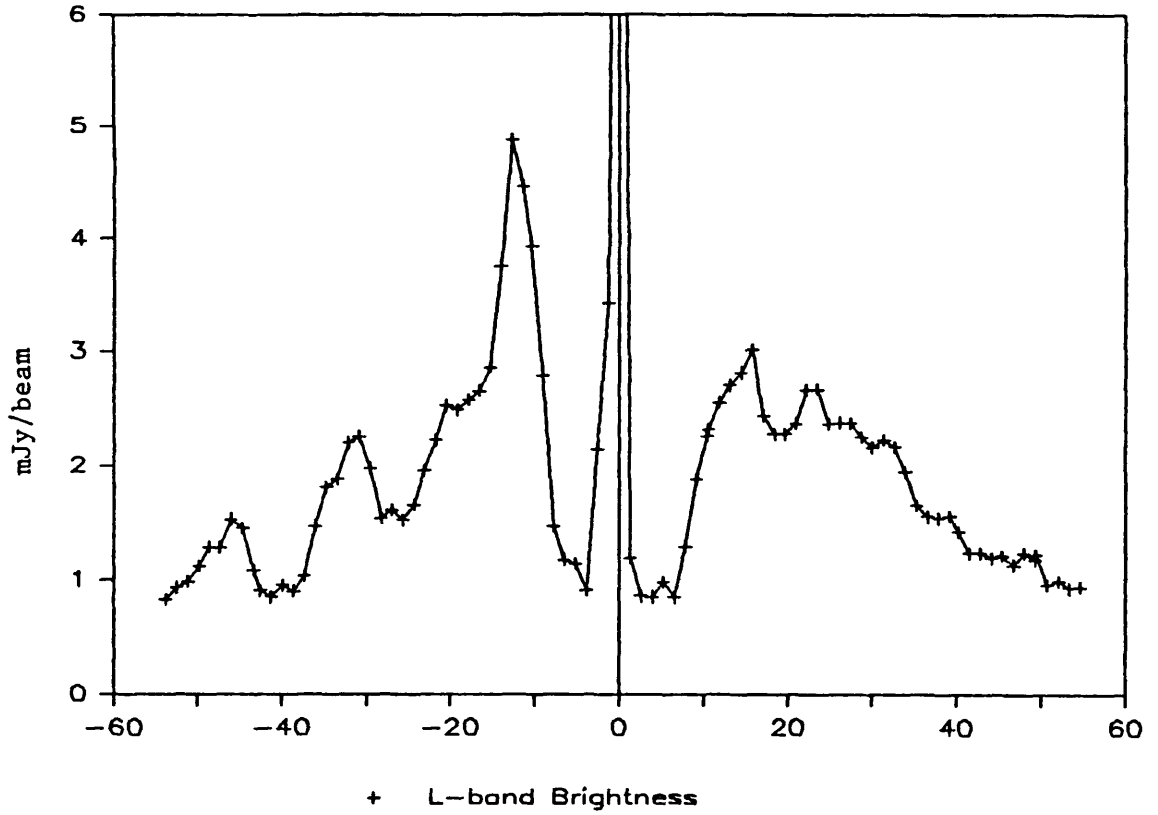
mJy/beam
6
5
4
3
2
1
0
−60
−40
−20
0
20
40
60
+ L−band Brightness

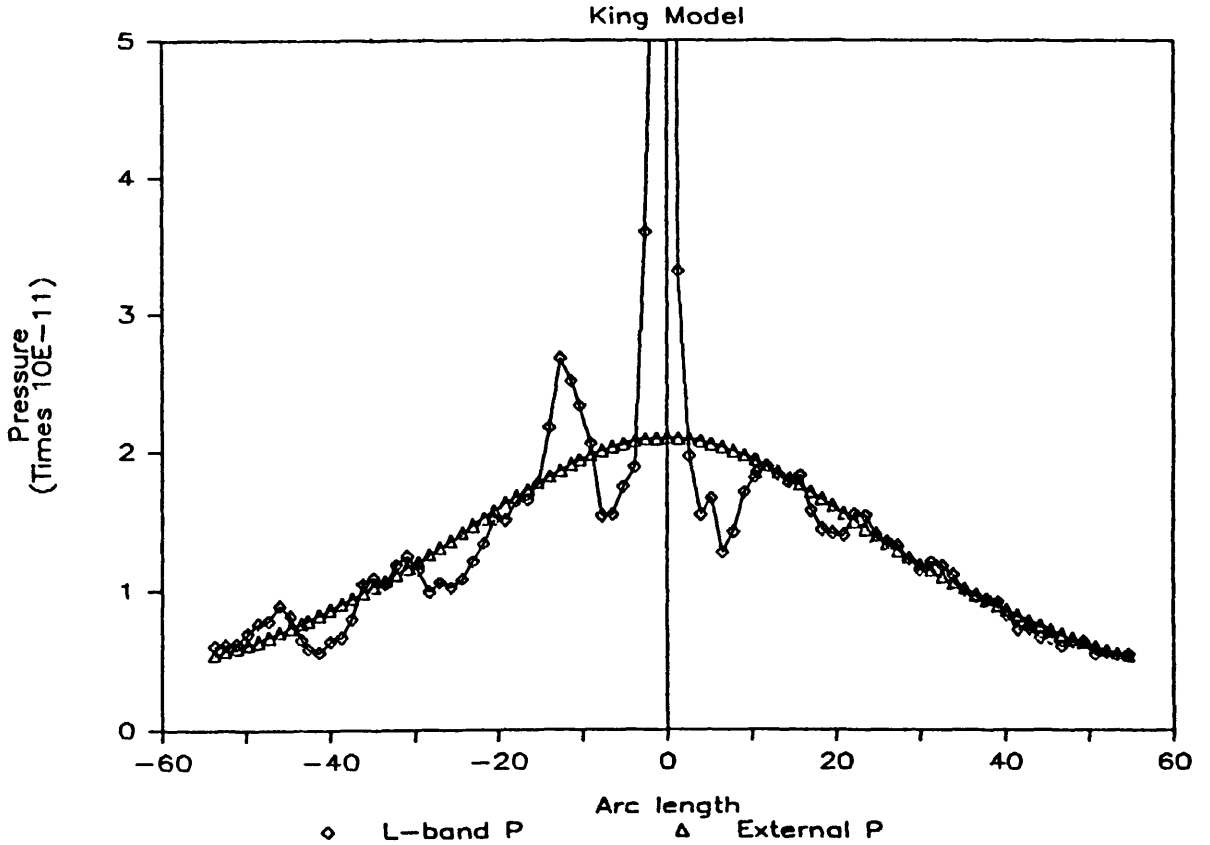
King Model
Pressure
(Times 10E−11)
5
4
3
2
1
0
−60
−40
−20
0
20
40
60
Arc length
◇ L−band P
△ External P

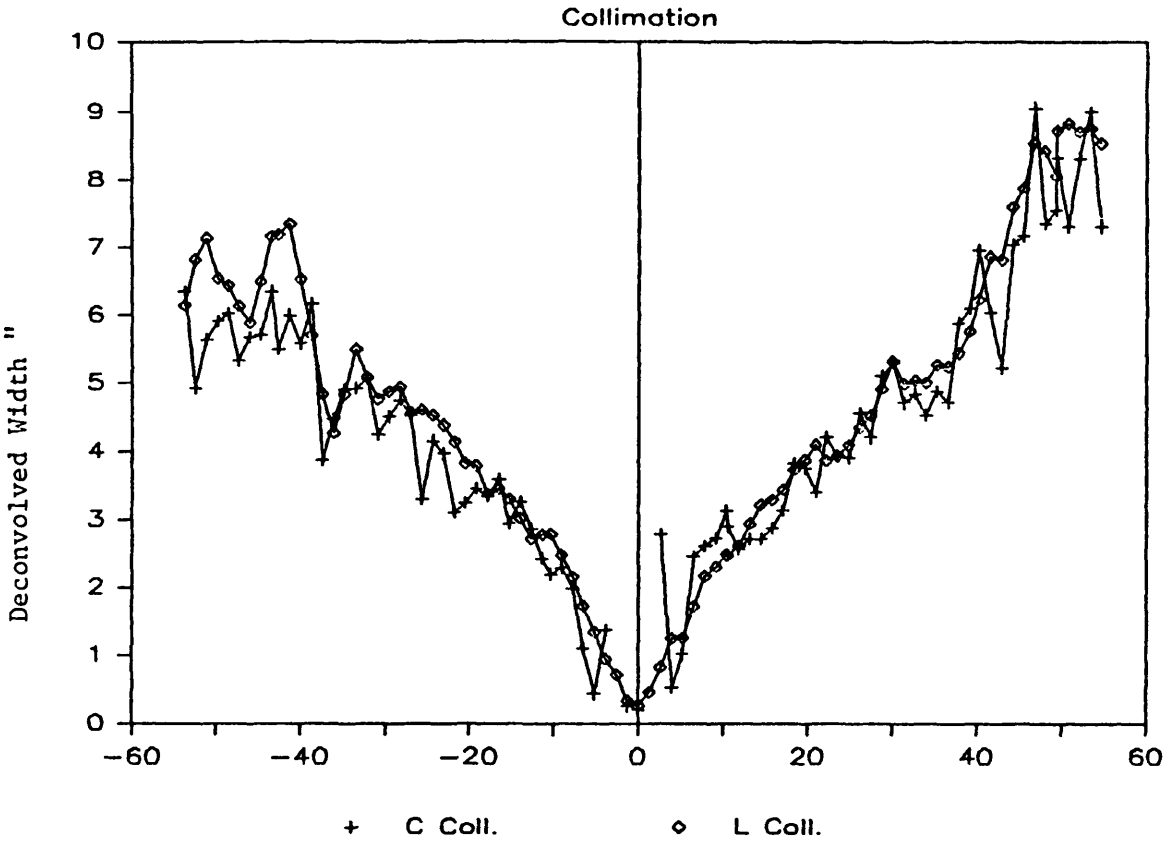
Collimation
Deconvolved Width "
10
9
8
7
6
5
4
3
2
1
0
−60
−40
−20
0
20
40
60
+ C Coll.
◇ L Coll.

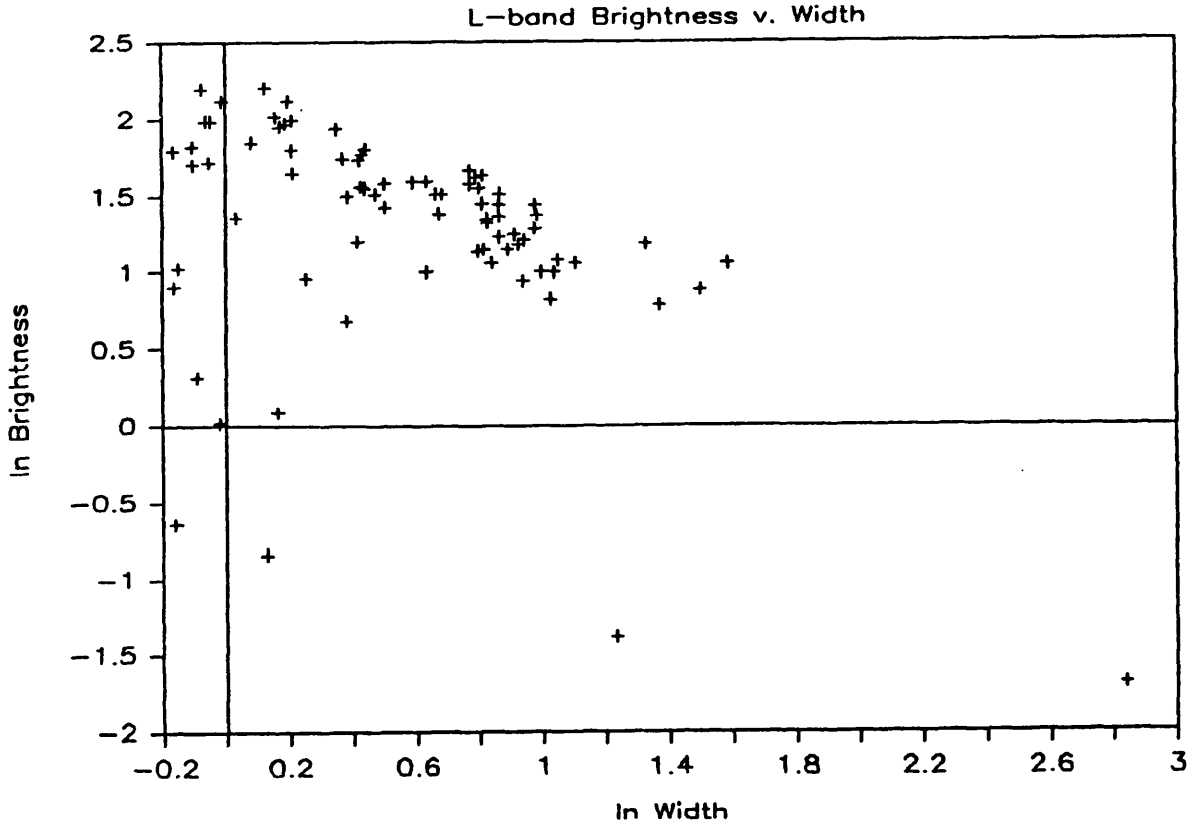
L−band Brightness v. Width
ln Brightness
2.5
2
1.5
1
0.5
0
−0.5
−1
−1.5
−2
−0.2
0.2
0.6
1
1.4
1.8
2.2
2.6
3
ln Width

an over-pressured free jet emerging into a hot, slowly declining, large scale atmosphere, with central temperature-density product $= 1.6 \times 10^5$ K cm^{-3}, and a core radius such that $a_c \sin \psi_j = 7$ Kpc, where ψ_j is the angle of the jets to the line of sight, requiring that the jets must be within about 20° of the line of sight. However, because of the limited amount of X-ray data, these numbers were derived from an analytic approximation to the King model, assuming equal virial and gas temperatures, and so should only be taken to indicate that a large scale atmosphere is probably present.

The brightness evolution of the jets is consistent with this picture of jets being confined, then becoming free, and then re-confining, all within the first 10 – 15 arc-seconds. The small knots in the regime of apparently free expansion could be shocks triggered by the detachment of the jets from an initially confining atmosphere of scale size smaller than a few hundred parsecs, while the rapid turn-on of the jets at the collimation shoulder fits the mechanism described by Sanders (1983) whereby the entry of an initially free jet into a slowly declining atmosphere produces shocks which increase the synchrotron emissivity. Subsequent shocks or entrainment could decrease the Mach number towards unity and allow the formation of large scale plumes. If the jets evolve adiabatically then the variation of central brightness with jet width should go as :

$$I_\nu = I_{\nu,0}(\Phi/\Phi_0)^{-3.5} v_j^{-3}$$

in the regime where the magnetic field is predominantly perpendicular to the jet axis (Perley *et al.* 1984). Thus to obtain agreement with the observed variation v_j must decrease as approximately the $2/3^{rd}$ power of the jet radius, or by a factor of two from the collimation shoulder to the first sharp bends. In the approximation that momentum is conserved, the jet has to entrain only its own mass in that distance. Provided that the jet is much lighter than the external medium, a moderate shear layer which is only a small fraction of the jet radius will allow such entrainment (see De Young, these Proceedings).

Bicknell (these Proceedings) has put forward a different explanation for the similar object IC4296. Optical photometry of this galaxy indicates that the core radius of the visible emission is about an order of magnitude smaller than the figure derived for 3C449 from the X-ray image. Descending the small scale pressure gradient appropriate to this core radius, the jets entrain and shock, producing the observed knots and become transonic and then subsonic in the region where the re-collimation occurs. Since the jet is now subsonic, declining pressure *slows* the jet and produces the observed sub-adiabatic decline in brightness with jet radius. The problem of reconciling the power requirements of the source with the low thermal matter density in the jets is solved since the jets are enthalpy dominated. If 3C449 has a two component atmosphere then this same model could be applied, and would allow sufficiently low jet velocities, about 1000 Km sec^{-1}, that motions in the group could trigger the curvature seen in the large scale structure (Bicknell 1984, private communication). The fluctuations in central brightness observed in the southern jet could be interpreted as due to eddies in the subsonic flow.

Other estimates of the jet velocity are available, but, as always, they are very problematical. Nevertheless, we will summarise the results:

(1) The time required for a jet to reach the very outer emission is

$$t = 1.5 \times 10^8/(v_{j,3}.\sin\psi_j) \text{ years}$$

where $v_{j,3}$ is the velocity of the jet in units of 1000 Km sec^{-1}.

Since spectral steepening is observed in the outer emission (Birkinshaw *et al.* 1981), we may equate this to the synchrotron lifetime in the outer emission to obtain an estimate for $v_j.\sin\psi_j = 2{,}500$ Km sec^{-1}.

(2) Source luminosity : The kinetic luminosity per jet is :

$$L_j = 3.5 \times 10^{40} v_{j,3}(1 + 0.16 n_{j,-3}.v_{j,3}^2) \text{ erg sec}^{-1}$$

and the total source radio power is $L_R = 2.1 \times 10^{41}$ erg sec^{-1}. If the source luminosity is powered by the jets with efficiency ϵ then we have that $L_R = 2\epsilon L_j$. The two extremes are :

$$\text{hot, fast jet : } v_j = 14{,}000.\epsilon_{0.1}^{-1} \text{ Km sec}^{-1}$$

$$\text{cold, slow jet : } v_j = 5{,}000.(\epsilon_{0.1} n_{j,-3})^{-1/3} \text{ Km sec}^{-1}$$

Any compression or decompression of the jets upon entering the lobes can change these numbers by very large amounts. For example, if the jet expands isotropically upon entering the first lobes, then the luminosity of the lobes will be decreased by a factor of about 10^4. This uncertainty is really just an extension of the problem of sub-adiabatic decline of surface brightness in the jet themselves.

(3) Ballistic models for the jet shapes require jet velocities comparable to the orbital velocity of the system causing the quasi-periodic extended emission (e.g. Blandford and Icke 1978, Lupton and Gott 1982). Thus, v_j must be in the range 300 to 2000 Km sec^{-1} depending upon whether the orbit is that of galaxies in the group, or of two nucleii about each other well within the optical envelope. The former case is difficult to reconcile with the polarization data since a huge internal thermal matter density, 10 cm^{-3}, is required. Also the dynamical age of the very extended emission would then be about an order of magnitude greater than the synchrotron lifetime.

(4) If the jet is really free in the first regime of expansion then the jet velocity is :

$$v_j = 7{,}000.n_{-3}^{-1/2} \text{ Km sec}^{-1}$$

(5) If the small wiggles in the centroid of the jets just prior to the first major bends are due to Kelvin-Helmholtz instabilities then from the equation for the fastest growing instability given by Hardee (1984) we can estimate the Mach number to be of order unity. The jet velocity must then be :

$$v_j = 1{,}200.n_{-3}^{-1/2} \text{ Km sec}^{-1}$$

which is well in excess of that required to explain the sub-adiabatic decline in surface brightness. However, we have horribly abused Hardee's stability analysis by applying it to transonic jets.

(6) If the jets are intrinsically symmetrical then the *observed* symmetry in flux from the jets, 1.05 ± 0.05, limits the Doppler boosting so that $v_j \sin \psi_j$ is not greater than about 30,000 Km $\sec^{-1}$. Again, this argument has considerable weaknesses and should not be taken too seriously.

To summarise, no one velocity estimate seems particularly trustworthy. Most depend upon estimates of the thermal matter density internal to the jet and, consequently, are of dubious reliability. The density can only be eliminated if the thrust at some part of the jet is known; unfortunately, edge-darkened sources such as 3C449 usually have no hotspots. Estimates based upon dynamical or kinematical effects are difficult since, unlike NATs, the jets are only slightly bent and the probable velocity of the galaxy in the local medium is small.

4. ONE STEP FORWARD, TWO BACK ?

By looking more carefully at 3C449 we have undermined estimates for the jet velocity and thermal matter density. We should now ask "what can be done to repair the damage ?" It is clear that the radio jets in 3C449 must be interacting with their environment to produce the following features :

- surface brightness decline
- overall source shape
- jet collimation
- rotation measure seen exterior to the jet

Examination of the jet environment depends mainly upon observations at X-ray and optical wavelengths, to map out the distributions of hot and of dark matter. Further detailed radio observations of similar type I sources would be useful to elucidate those attributes of 3C449 which are universal (and, hopefully, relevant to our understanding) and those which are merely obscuring our view.

Finally, better theoretical understanding both of the structure of magnetic fields and of turbulence in jets would help considerably the interpretation of polarization measurements.

REFERENCES

Birkinshaw, M., Laing, R.A., and Peacock, J. (1981). M.N.R.A.S. **197**, 253.
Blandford, R.D., and Icke, V. (1987). M.N.R.A.S. **185**, 527.
Hardee, P. (1984). Astrophys. J. **277**, 106.
Lupton, R.H., and Gott, J.R. (1982). Astrophys. J. **255**, 408.
Miley, G.K., Norman, C., Silk, J., and Fabbiano, G. (1983). Astron. Astrophys. **122**, 330.
Perley, R.A., Willis, A.G., and Scott, J.S. (1979). Nature **281**, 437.
Perley, R.A., Bridle, A.H., and Willis, A.G. (1984). Astrophys. J. Suppl. **54**, 291.
Sanders, R.H. (1983). Astrophys.J. **266**, 73.
Saunders, R., Baldwin, J.E., Pooley, G.G., and Warner, P.J. (1981). M.N.R.A.S. **197**, 287.

POLARIZATION STRUCTURE OF THE JETS IN NGC 1265

CHRISTOPHER P. O'DEA
National Radio Astronomy Observatory[a], Charlottesville, VA 22903
AND
FRAZER N. OWEN
National Radio Astronomy Observatory, P.O. Box O, Socorro, NM 87801

ABSTRACT. Arcsecond resolution VLA observations of the polarization structure of the jets in NGC 1265 at 21, 6, and 2 cm are presented and discussed. The fractional polarization is edge brightened and the apparent projected magnetic field is parallel to the jet axis in the inner two-thirds of the length of the jets. The polarization structure of the outer third of the jets is more complex: the apparent projected magnetic field is perpendicular to the jet axis in the east jet and is perpendicular to the jet axis in the center and parallel on the edges in the west jet. The polarization structure in the inner two-thirds of the jets is generally consistent with that expected for an initially tangled field which has been sheared tangentially to the beam surface. There is no evidence for depolarization at 21 cm. Differential rotation measure variations along the jets of ~ 30 rad m^{-2} appear to be produced in an external foreground screen which may be located in an interstellar medium in NGC 1265.

1. INTRODUCTION

NGC 1265 (3C 83.1B, 0314+416) is the prototypical Narrow Angle Tail (NAT) source and has been the subject of much observational (e.g., Ryle and Windram 1968; Miley *et al.* 1972; Wellington *et al.* 1973; Riley 1973; Miley 1973; Miley *et al.* 1975; Owen, Burns, and Rudnick 1978; Gisler and Miley 1979) and theoretical (e.g., Pacholczyk and Scott 1976; Begelman, Rees, and Blandford 1979; Jones and Owen 1979; Christiansen, Pacholczyk, and Scott 1981) attention. NATs present us with a laboratory for the study of the interaction of the radio luminous beams with their interstellar and intracluster environment and thus permit us to gain insight into the physical conditions in these three media. A summary of results on the polarization structure of the jets from detailed multifrequency VLA observations are presented and discussed briefly in this paper. Additional results and further details are presented elsewhere (O'Dea 1984, O'Dea and Owen 1984).

2. OBSERVATIONAL RESULTS

VLA observations at 21 cm (A and C configuration), 6 cm (A, B, and D configuration) and 2 cm (C configuration) were obtained of NGC 1265. (For a description of the VLA see Thompson *et al.* 1980.) The flux density scale of Baars *et al.* (1977) was used. The data were calibrated and reduced as described by O'Dea (1984). Maps

[a] The National Radio Astronomy Observatory (NRAO) is operated by Associated Universities, Inc., under contract with the National Science Foundation.

were made and CLEANed using the NRAO AIPS software (see O'Dea 1984 for details). The positive bias in the polarized flux density was removed (see Wardle and Kronberg 1974). In all the maps shown here, the fractional polarization was "blanked" (i.e., set to a null value) below a signal-to-noise ratio of 3. A scale of 0.″35 kpc/arcsecond is used throughout this paper ($z = 0.0183$, e.g., Noonan 1981, giving a distance to the Perseus cluster of ~ 72 Mpc; assuming $H_o = 75$ km sec^{-1} Mpc^{-1}).

(a) Fractional polarization structure. A black and white radiophotograph of the fractional polarization at 21 cm (1.″2 resolution) is shown in Figure 1. The fractional polarization is edge brightened over much of the inner roughly two-thirds of the jets (i.e., within ~ 10 kpc of the core). The polarization structure of the outer third of the jets is less clear due to the lower signal-to-noise ratio; however it is not symmetrically edge brightened in this region as it is closer to the core. In the last third of the jets, portions of the east jet are edge *darkened* in fractional polarization, while the west jet is asymmetrically edge brightened on the east side.

The one-dimensional profiles (at 1.″2 resolution) of the fractional polarization or three sigma upper limits along the ridge of maximum brightness in the east and west jets are shown in Figure 2 at 21 and 6 cm. These profiles show that except at a few points, the fractional polarizations at 6 and 21 cm are in good agreement within the errors. The fractional polarization is mostly in the range $\sim 10 - 25\%$, though there are significant excursions above (to $\sim 35\%$) and below (to $\sim 4\%$) this range.

(b) Projected magnetic field. The electric field vectors (i.e., polarization position angles) with length proportional to fractional polarization are shown superimposed on a total intensity map at 6 cm (1.″2 resolution) in Figure 3a. Because of the lack of depolarization at 21 cm and the small values of rotation measure (see below), the position angles at 6 cm are within a few degrees of the intrinsic (zero wavelength) values. The apparent projected magnetic field should be approximately orthogonal to the observed electric field vectors at 6 cm (for transparent synchrotron emission). The projected magnetic field is mostly parallel to the jet axis along the inner two-thirds of the length of the jets with somewhat more complex structure along the outer third of the length of the jets. In the outer portions of the east jet, the magnetic field is mostly perpendicular to the jet axis, while in the west jet the projected B field is mostly perpendicular to the jet axis in the center and parallel to the jet axis on the edges.

A blow up of a portion of the west jet (the two bright knots) is shown is Figure 3b; here the 0.″45 resolution 6 cm data have been used and the CLEAN components convolved with an elliptical beam (0.″45 × 2.″0 at a position angle of $-45°$) in order to increase the sensitivity by averaging along the jet axis. In this map the fractional polarization is clearly edge brightened, varying from $\sim 25 - 30\%$ on the edges to $\leq 5\%$ in the center. The B field is parallel to the jet axis on both sides of this portion of the jet.

(c) Rotation measure structure. There is no evidence (at 1.″2 resolution) in the two-dimensional rotation measure, RM, maps (not shown) for any significant RM structure

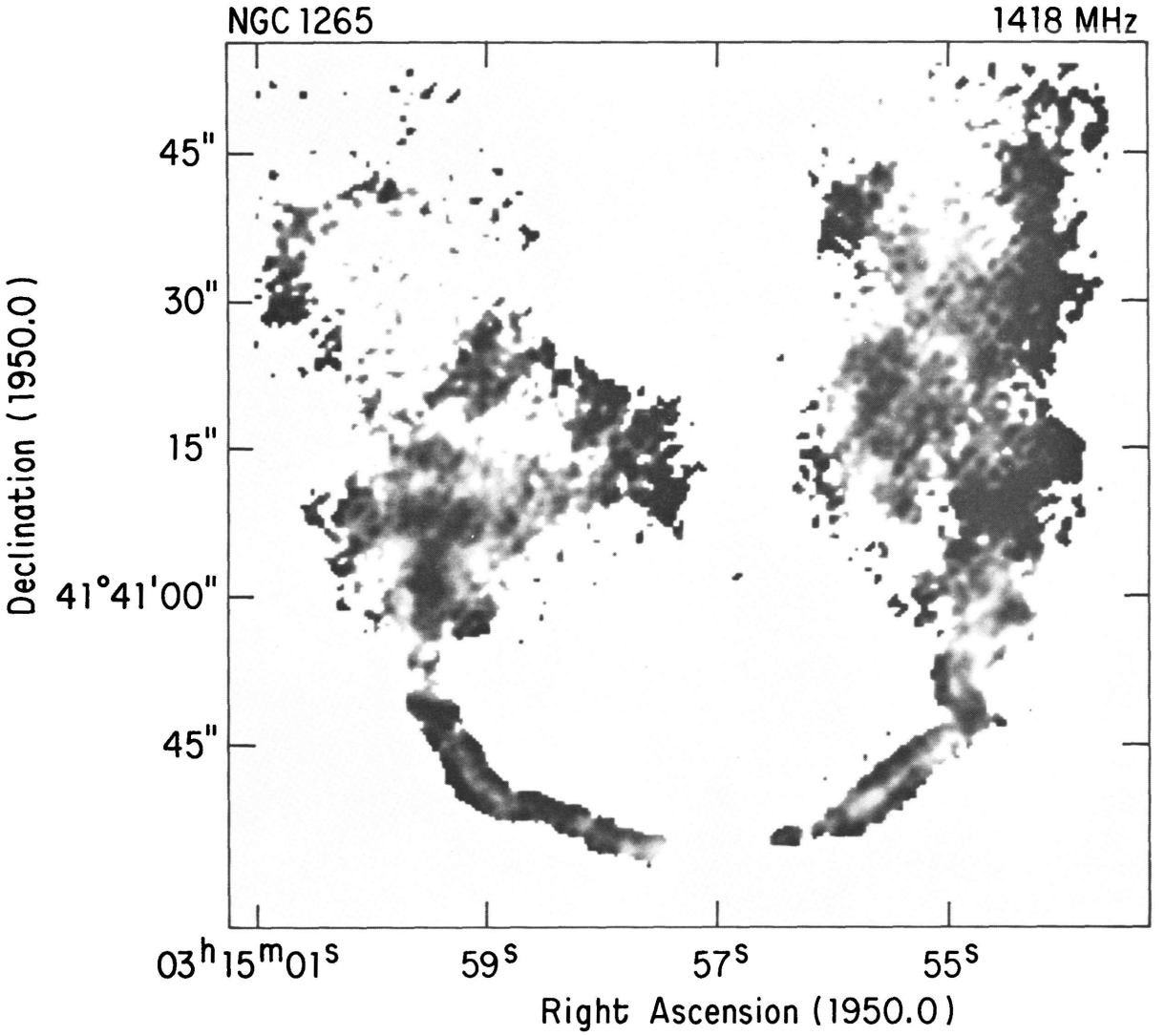

Figure 1. A black and White radiophotograph of the fractional polarization of NGC 1265 at 21 cm (A and C configuration data; 1.2" resolution). Only values with a signal-to-noise ratio greater than three are shown.

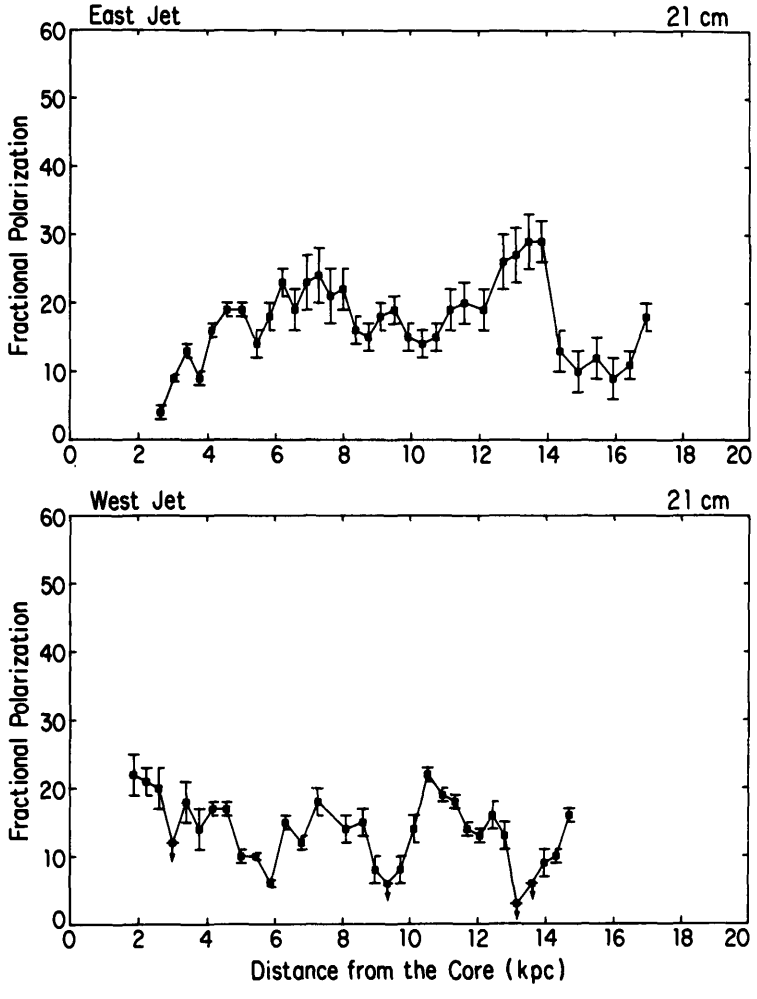

Figure 2a. The one-dimensional distribution of fractional polarization at 21 cm (A and C configuration data; 1.2" resolution) along the east and west jets in NGC 1265.

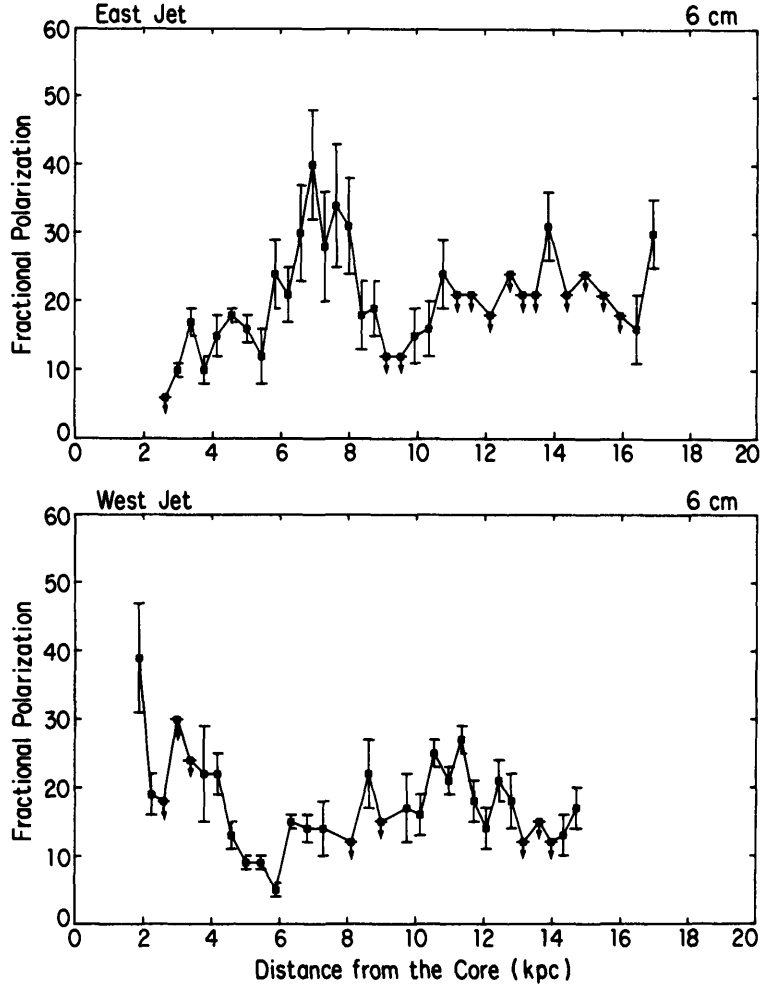

Figure 2b. The one-dimensional distribution of fractional polarization at 6 cm (B and D configuration data; 1.2" resolution) along the east and west jets in NGC 1265.

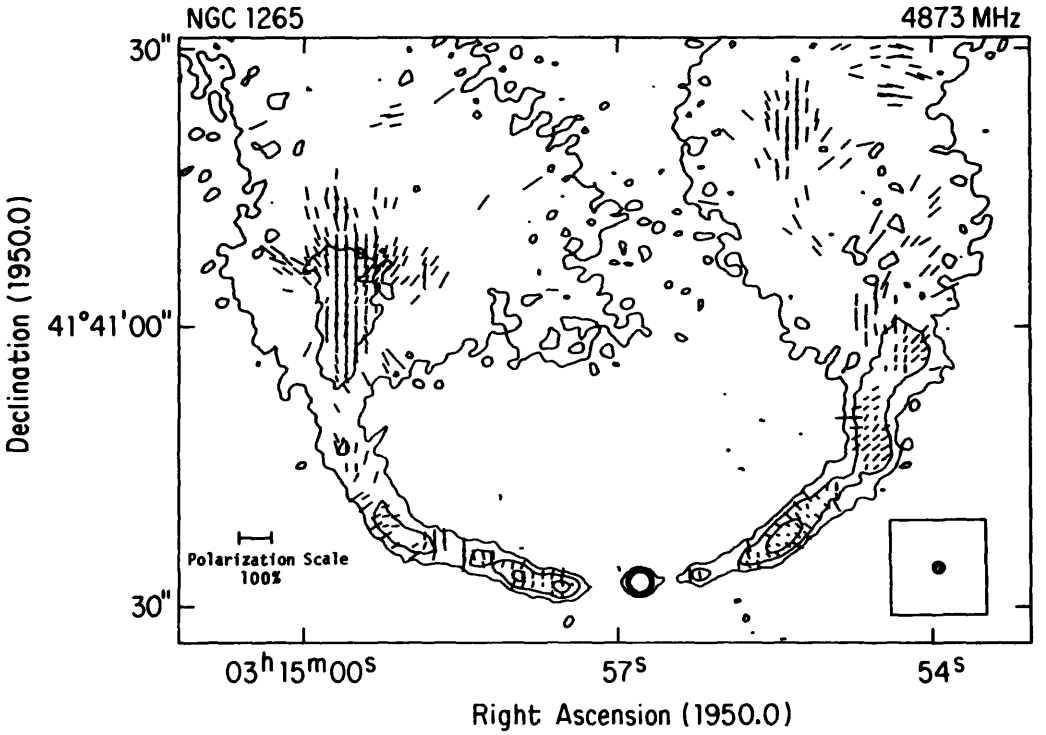

Figure 3a. A contour plot of total intensity at 6 cm (B and D configuration data; 1.2" resolution) with polarization position angle superposed (length proportional to fractional polarization). Contour levels are -0.2, 0.2, 0.8, and 3.0 mJY/beam.

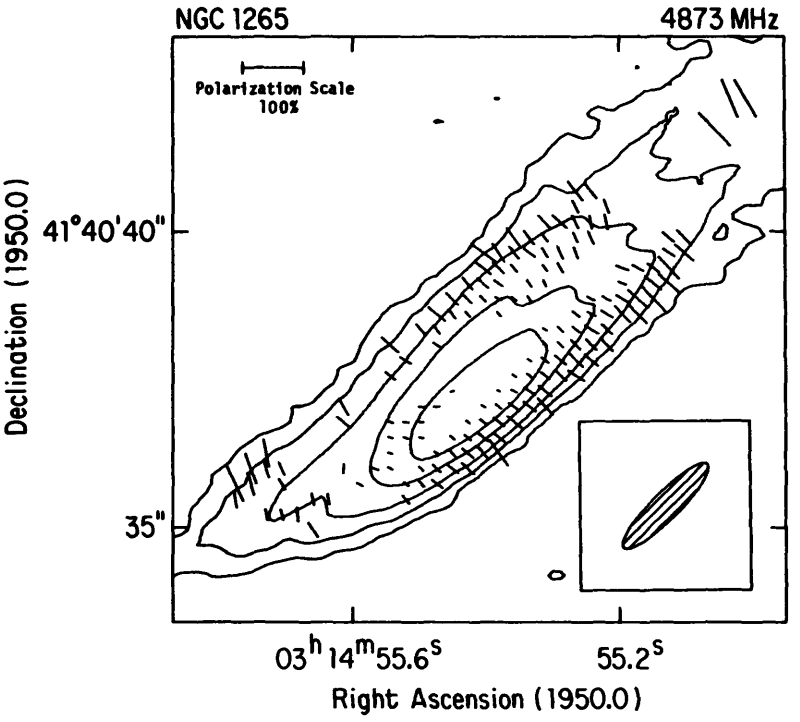

Figure 3b. A contour plot of total intensity of the W2-W3 knot region in the west jet at 6 cm (A, B, and D configuration data; 0.45" x 2.0" resolution at position angle 45 degrees) with polarization position angles superposed (length proportional to fractional polarization). Contour levels are -0.2, 0.2, 0.5, 1.0, 2.0, and 3.0 mJy/beam.

across the jets; however, there is significant RM structure *along* the jets. The one-dimensional distribution of rotation measure between 6 and 21 cm (at 1.″2 resolution) along the ridge of maximum brightness of the east and west jets is shown in Figure 4a. Note that a difference of π radians between 1418 and 4873 MHz corresponds to a rotation measure of 76.2 rad m^{-2}. This value was added to some negative values of RM in order to minimize the size of the jumps in RM. Although there are differences in the details, to first order, the trends in the RM variations are similar along both jets. Along the west jet the RM varies smoothly from $\sim$ 23 rad m^{-2} at $\sim$ 2 kpc from the core, to $\sim$ -4 rad m^{-2} at 10 kpc from the core to $\sim$ 20 rad m^{-2} at 12 $-$ 15 kpc from the core. Along the east jet the RM varies from $\sim$ 25 $-$ 35 rad m^{-2} at $\sim$ 3 kpc from the core to $\sim$ 13 rad m^{-2} at $\sim$ 7 $-$ 8 kpc from the core to $\sim$ 30 rad m^{-2} at 10 kpc from the core. The changes in RM do not appear to be associated with any particular variations in fractional polarization along the jets.

A least-squares fit was obtained to the equation $\chi = RM\lambda^2 + \chi_o$, where χ is the observed position angle, χ_o is the intrinsic (i.e., zero wavelength) position angle, and λ is the wavelength. The resulting fits at six points with especially high signal-to-noise (using data from 21, 6, and 2 cm maps tapered to 3.″2 resolution) are shown in Figure 4b. The fits are all very good and the data are consistent with $\chi \propto \lambda^2$ between 2 and 21 cm for up to $\sim$ 120° of rotation. The derived RM's are also in excellent agreement with those found earlier between 6 and 21 cm (Figure 4a).

3. DISCUSSION

(a) Magnetic field structure. The projected B field is *parallel* to the jet axis in the inner two-thirds of the jets in NGC 1265 in contrast to what is seen in most other symmetric low power jets (e.g., Bridle 1982, Bridle and Perley 1984). Generally, low power jets, such as those in NGC 1265, have apparent projected fields which are *perpendicular* to the jet axis. However, in beams which are confined by and interact very strongly with an external medium (as suggested by the bending) a velocity gradient or shear will be set up across the beam. This shear will stretch out an initially tangled field along the beam axis, resulting in a jet with a mostly parallel projected B field. The appearance of the perpendicular component of the B field further down the jets could be due to the gradual expansion of the jets and/or a decrease in velocity of the jets. If magnetic flux is conserved, the parallel component varies as $B_{||} \propto r_b^{-2}$ and the perpendicular component varies as $B_\perp \propto r_b^{-1} v_b^{-1}$, where r_b is the beam radius and v_b is the beam velocity (e.g., Blandford and Rees 1974, Bicknell and Henriksen 1980). However, it is not clear whether these simple laws will be obeyed, since there is evidence that magnetic flux is not conserved in these jets (O'Dea 1984).

Laing (1981) has calculated the expected total intensity and polarization structure due to a variety of magnetic field geometries, one of which is that of a tangled field which has been sheared tangentially to the beam surface (his model B). He finds that the observed polarization structure is a strong function of the inclination angle to the line of sight, δ. Laing's formula were used to calculate theoretical profiles for jets with radii appropriate to NGC 1265 (i.e., 0.″5, 1.″0, and 1.″5) for a variety of inclination angles.

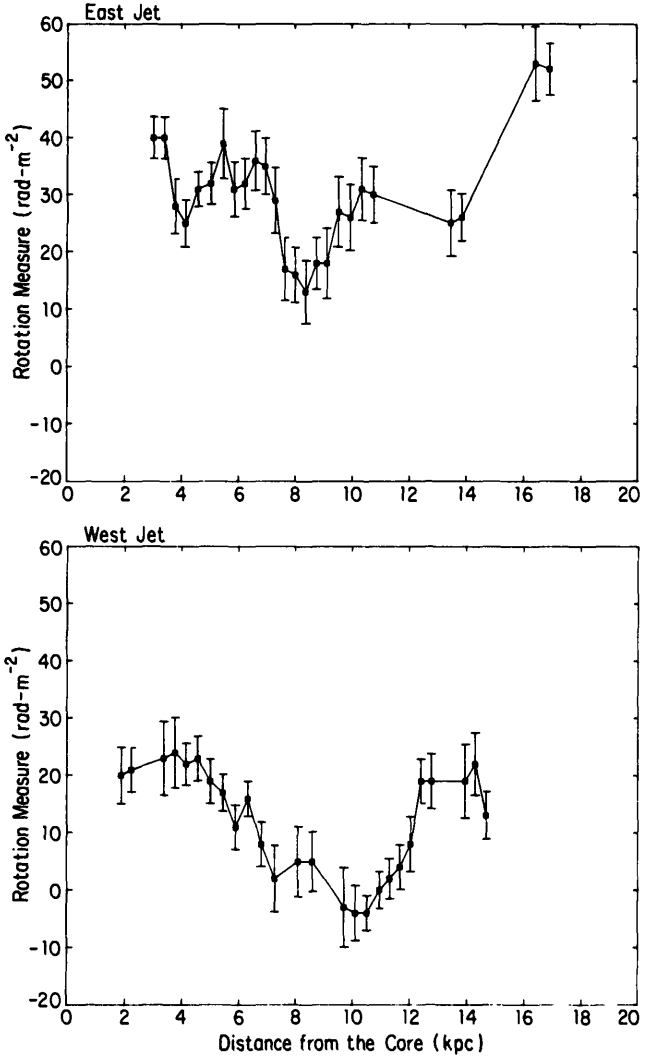

Figure 4a. The one-dimensional distribution of rotation measure between 6 and 21 cm (1.2" resolution) along the ridge of maximum brightness of the east and west jets.

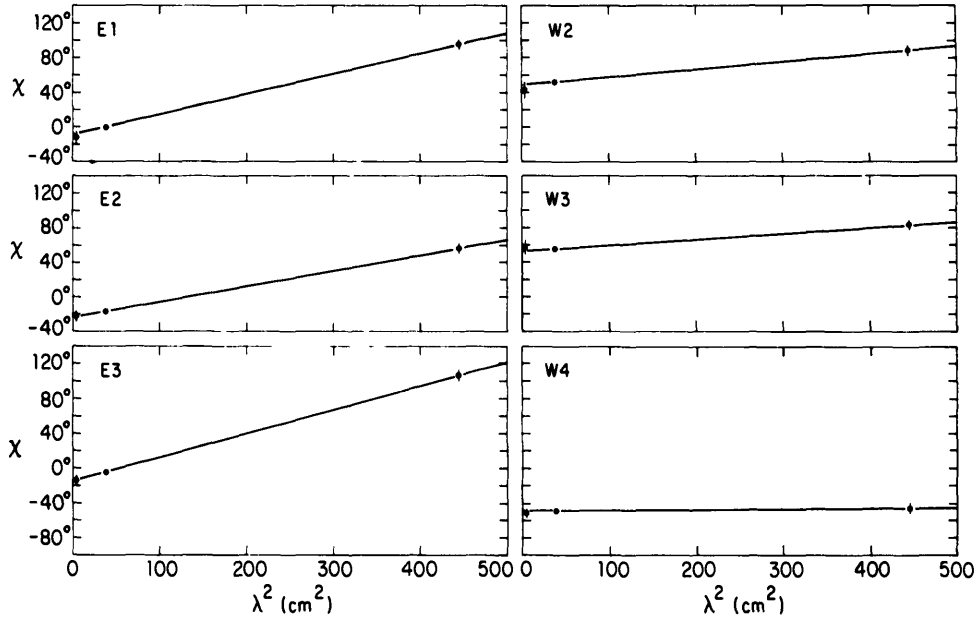

Figure 4b. Plots of the position angle at 21, 6, and 2 cm vs. wavelength squared at six points with high signal-to-noise ratios. The fit rotation measures are shown as solid lines.

The profiles were then numerically convolved to the resolution of the observations using a gaussian of FWHM 1.″2. (Note that while the theoretical profiles are calculated assuming axial symmetry, the observed total intensity profiles are edge brightened.) The effect of convolution with a gaussian beam is to increase the range of inclination angle over which the projected B field is exclusively parallel to the jet axis. For a jet of radius 1.″5, convolved with a 1.″2 gaussian beam, the projected B field is parallel to the axis for the range of inclination angle $45° \leq \delta \leq 135°$. This regime of parallel projected field is accompanied by edge brightened fractional polarization as is seen in NGC 1265. Since most of the bending of the jets occurs in this regime, the jets in NGC 1265 should be within $\sim 45°$ of the plane of the sky. Since the measured radial velocity of the galaxy NGC 1265 is ~ 2200 km sec^{-1} (Chincarini and Rood 1971) this requires the total velocity to be ≥ 3100 km sec^{-1}, which is a plausible value.

Using Laing's formula, convolved profiles were also generated for the helical field with constant pitch angle (e.g., Fomalont *et al.* 1980) and the Chan and Henriksen (1980) (CH) field with variable pitch angle. However, the *pure* helical and CH fields cannot provide a consistent description of the polarization of the jets in NGC 1265 (see O'Dea 1984 for details). This should not be too surprising given that both fluid turbulence and shearing are expected to occur within the jets. More realistic models which include random field components should be considered (see Perley, Bridle and Willis 1984).

(b) Limits to the effective Faraday depth within the jets. The lack of depolarization can be used to set an upper limit to the effective Faraday depth in the jets and thus to the amount of position angle rotation which can occur within the jets.

The central Faraday depth, F_c, is given by $F_c = 2RM\lambda^2 = 1600 n_e B_\mu L \lambda^2$ rad, where n_e is the thermal particle density in cm^{-3}, B_μ is the *net* component of the magnetic field along the line of sight in μG, L is the path length through the source in kpc, and λ is the wavelength in m (e.g., Cioffi and Jones 1980). It is assumed that the jets can be represented by barely resolved cylinders uniformly filled with thermal particles, B field, and radiating particles. A conservative estimate of the maximum permissible Faraday depth would be that required to produce a three sigma decrease in the depolarization ratio between 6 and 21 cm. This gives an upper limit to the central Faraday depth through the jets (at the positions of the bright inner knots) of $F_c < 1.9$ rad at 21 cm (Cioffi and Jones 1980). At other positions along the jets, the signal-to-noise ratio is lower, allowing a higher value for the Faraday depth. Given this value for the Faraday depth, the upper limit to the *apparent* rotation measure between 6 and 21 cm is ~ 9.5 rad m^{-2}.

A model dependent estimate of the internal thermal particle density can also be made, using $L = 0.8$ kpc, and $B_\mu \simeq B_{\rm minP} N^{-1/2}$, where $B_{\rm minP} \simeq 15$ μG, is the minimum pressure magnetic field (e.g., Burns *et al.* 1979), and N is the (unknown) number of cells of tangled magnetic field along the line of sight. This gives an upper limit to the particle number density of $n_e < 2 \times 10^{-3} N^{1/2}$ cm^{-3}.

(c) Location of the rotation measure structure. The changes in RM along the jets are at

least a factor of 3 larger than the 3 sigma upper limit to the amount of rotation measure that can be produced within the jets. In addition, the position angles at 2, 6, and 21 cm are consistent with $\chi \propto \lambda^2$ over a range of rotation of up to $\sim 120°$. Since the maximum rotation obtainable from an unresolved cylinder is $\sim 45°$ (e.g., Cioffi and Jones 1980) this suggests that the rotation occurs in a foreground screen. There are four possible locations for this screen: our Galaxy, the Perseus cluster, a sheath around the jets, and an interstellar medium (ISM) in NGC 1265. Each location will be considered in turn.

The Galaxy. The RM variations in NGC 1265 occur over a size scale of several arcseconds. Burn (1966) has considered the properties of the Galactic clouds which would be required to produce observable amounts of Faraday rotation on sufficiently small scales. He finds that implausible conditions are required. It seems that any contribution from our Galaxy to the RM of NGC 1265 is likely to be uniform over the $\sim 1'$ scale of the jets.

The Perseus cluster. If the line of sight through the cluster goes through many reversals in the cluster magnetic field, then the differential RM structure will be washed out (e.g., Burn 1966). There should be significant RM structure in the cluster only if the cell size of the tangled field is comparable to the path length. However, in that case, the RM structure would still be uniform over the relatively small scale of the RM variations in NGC 1265. Thus, although the Perseus cluster may contribute to the foreground RM, it is unlikely that the RM variations along the jets in NGC 1265 are produced in the cluster magnetic field.

A sheath around the jets. The possible origins of a sheath or cocoon around the jets are discussed elsewhere (O'Dea 1984). But, whatever its origin, because radio emission is seen, there must be a magnetic field outside the jets. The parameters of the sheath can be estimated assuming 30 rad $m^{-2} = 800 n_e B_\mu L$. Taking $L \simeq 2$ kpc (from the size of the cocoon of diffuse emission around the west jet), and $B_\mu \leq 15$ μG (assuming that the magnetic field in the cocoon is not greater than that in the jets, estimated from minimum presure) gives $n_e > 10^{-3}$ cm^{-3} which is higher than the estimated particle density in the intracluster medium. Thus, the data are roughly consistent with the hypothesis that the RM is produced in a sheath around the jets if there is an ISM of some kind.

An ISM in NGC 1265. The RM variations along the jets have a size scale which is comparable to the expected size scale of the ISM in NGC 1265 (Jones and Owen 1979). There is also evidence for RM structure due to an ISM in NGC 6251 (Perley, Bridle, and Willis 1984), M84 (Laing and Bridle 1984), and 3C 449 (Cornwell and Perley 1984, these Proceedings). If the ISM is responsible for producing the RM structure, then 30 rad $m^{-2} = 800 n_e B_\mu L$. This can be accounted for with plausible values for the parameters of the ISM; e.g., if L = 10 kpc, and $B_\mu \leq 1$ μG, then $n_e \geq 4 \times 10^{-3}$ cm^{-3}. This limit is consistent with estimates of the particle density in an ISM which has achieved an equilibrium between between stellar mass loss and ram pressure stripping (e.g., Gisler 1976; Lea and De Young 1976; Jones and Owen 1979). The large scale gradient in the RM could be due either to a change in the path length, orientation of the B field,

the density of the ISM, or various combinations of these possibilities. If there is *not* a significant ISM, i.e., the galaxy contains a significant magnetic field, but the density is that of the ICM ($n_{icm} \simeq 5 \times 10^{-4}$ cm^{-3}; e.g., Forman and Jones 1982) then the required magnetic field is $B_\mu \sim 8$ μG. This seems rather high since if the galaxy is swept free of an ISM it is hard to imagine how the galaxy could maintain such a high magnetic field.

At this point the data seem most consistent with the hypothesis that the differential RM structure along the jets is produced in an ISM in the galaxy NGC 1265.

ACKNOWLEDGEMENTS

The authors are pleased to thank J. Eilek, L. Rudnick, A. Bridle and R. Laing for helpful discussions.

REFERENCES

Baars, J. W. M., Genzel, R., Pauliny-Toth, I. I. K., and Witzel, A. (1977). Astron. Astrophys. **61**, 99.
Begelman, M. C., Rees, M. J., and Blandford, R. D. (1979). Nature **279**, 770.
Bicknell, G. V. and Henriksen, R. N. (1980). Ap. Lett. **21**, 29.
Blandford, R. D. and Rees, M. J. (1974). M.N.R.A.S. **169**, 395.
Bridle, A. H. (1982). *Proc. IAU Symp. 97, Extragalactic Radio Sources*, ed. D. S. Heeschen and C. M. Wade (Dordrecht: D. Reidel) p. 121.
Bridle, A. H. and Perley, R. A. (1984). Ann. Rev. Astron. Ap. **22**, 319.
Burn, B. J. (1966). M.N.R.A.S. **133**, 67.
Burns, J. O., Owen, F. N. and Rudnick, L. (1979). A. J. **84**, 1683.
Chan, K. L. and Henriksen, R. N. (1980). Ap. J. **241**, 534.
Chincarini, G. and Rood, H. J. (1971). Ap. J. **168**, 321.
Christiansen, W. A., Pacholczyk, A. G., and Scott, J. S. (1981). Ap. J. **251**, 518.
Cioffi, D. F. and Jones, T. W. (1980). A. J. **85**, 368.
Fomalont, E. B., Bridle, A. H., Willis, A. G., and Perley, R. A. (1980). Ap. J. **237**, 418.
Forman, W. and Jones, C. (1982). Ann. Rev. Astron. Ap. **20**, 547.
Gisler, G. R. (1976). Astron. Aatrophys. **51**, 137.
Gisler, G. R. and Miley, G. K. (1979). Astron. Astrophys. **76**, 109.
Jones, T. W. and Owen, F. N. (1979). Ap. J. **234**, 818.
Laing, R. A. (1981). Ap.J. **248**, 87.
Laing, R. A. and Bridle, A. H. (1984). In preparation.
Lea, S. M. and De Young, D. S. (1976). Ap.J. **210**, 647.
Miley, G. K. (1973). Astron. Astrophys. **26**, 413.
Miley, G. K., Perola, G. C., Van der Kruit, P. C., and van der Laan, H. (1972). Nature **237**, 269.
Miley, G. K., Wellington, K. J., and van der Laan, H. (1975). Astron. Astrophys. **38**, 381.
Noonan, T. W. (1981). Ap. J. Supp. **45**, 613.
O'Dea, C. P. (1984). Ph.D. thesis, University of Massachusetts, Amherst.
O'Dea, C. P. and Owen, F. N. (1984). In preparation.
Owen, F. N., Burns, J. O., and Rudnick, L. (1978). Ap. J. (Letters) **226**, L119.
Pacholczyk, A. G. and Scott, J. S. (1976). Ap. J. **203**, 313.
Perley, R. A., Bridle, A. H., and Willis, A. G. (1984). Ap. J. Suppl. **54**, 291.
Riley, J. M. (1973). M.N.R.A.S. **161**, 167.
Ryle, M. and Windram, M. D. (1968). M.N.R.A.S. **138**, 1.
Thompson, A. R., Clark, B. G., Wade, C. M., and Napier, P. J. (1980). Ap. J. Suppl. **44**, 151.
Wardle, J. F. C. and Kronberg, P. P. (1974). Ap. J. **194**, 249.
Wellington, K. J., Miley, G. K., and van der Laan, H. (1973). Nature **244**, 502.

Multiconfiguration VLA Maps of Cygnus A

John Dreher
Department of Physics, Room 26-315
Massachusetts Institute of Technology
Cambridge, MA 02139

Rick Perley
National Radio Astronomy Observatory
P.O. Box O, Socorro, NM 87801

John Cowan
Department of Physics and Astronomy
University of Oklahoma
Norman, OK 73019

Abstract. Maps of Cygnus A at 1.4 and 5 GHz made with multiple configurations of the VLA show a number of interesting features: a jet, a possible counterjet, complex fine structures in the lobes, and very hard edges to the lobes. The jet is very bright but contributes an unusually small fraction of the total source power. The ratio of jet to core powers is similar that of other powerful sources. An upper limit to the jet/counterjet brightness ratio is 4, a value that might be explained by beaming if the jet has $\beta \sim 0.8$. The hard edges to the lobes suggest that ram confinement may be occuring on the sides as well as the fronts of the lobes. Overall, the lobes and the hotspots both exhibit a strong "S" symmetry. A distortion of this symmetry might be explained if the lobes have $\beta \sim 0.1$.

1. Introduction

We have recently presented elsewhere a first description of our mapping project for Cygnus A (Perley, Dreher, and Cowan, 1984; Paper I), so in this talk I shall concentrate on a few points not covered in that paper[1]. The project in total includes polarization mapping at 1.4, 4.5, 5.0, and 15 GHz using multiple configurations designed to achieve the greatest possible *uv* plane coverage and scaled, so far as possible, to facilitate comparisons between the different bands. Here, only the total intensity distributions at 1.4 and 5 GHz are discussed, using a preliminary subset of the full data.

As it is not practical to reproduce the gray-scale depictions of the maps in these *Proceedings*, the reader is referred to the figures of Paper I. The first notable item on these figures is the presence of a jet extending from the core about $2/3^{rds}$ of the way to the northwest hotspot. Secondly, there is a suggestion of a counterjet visible in the best renderings of the source. The jet and possible counterjet are discussed in §2. Another feature is both new and startling: a complex system of wisps or filaments filling the lobes. Also of interest are the very hard edges of the lobes. These features

[1]My fellow authors did not have the chance to review this talk before it was given, so any errors are mine alone – JWD.

are discussed in §3. Finally, in §4, the symmetry of the source is considered and the possibility of a time-delay effect is raised.

2. Jet(s?)

The jet leads into the northeast lobe and is roughly parallel to the VLBI jet (Linfield 1981). Towards the core, the jet is quite narrow, with a width of < 500 pc. It is lost in the brighter parts of the lobe before reaching either of the hotspots. As discussed in Paper I, it does not appear likely that the jet can be confined by the pressure available from the gas responsible for the X-ray emission of the cluster.

Table 1 compares the Cygnus jet to several other well-known *narrow* jets found in other sources. The lengths of the jets do not correlate with anything in an obvious way. As the jets in the Table were selected to be narrow, it is not surprising that the opening angles are all fairly small; it is also known that luminous sources tend to have narrow jets (Bridle and Perley 1984). Of interest here is the tendency of the jet brightness (using typical values, not maxima) to increase with source luminosity. The Cygnus jet is extraordinarily bright. Why has it resisted detection for so long then? The last column gives the answer: although bright, the jet contributes a very small fraction of the total source power and has, until now, been lost in the very bright lobes. Earlier in this workshop Jack Burns discussed the correlation between jet and core powers for a sample of 15 edge-brightened doubles with prominent cores (Burns *et al.*, 1984). Figure 1 reproduces their plot of P_{jet} vs P_{core} at 5 GHz with points added for Cygnus and for four other low-redshift, edge-brightened radio galaxies (data from Linfield and Perley, 1984, for 3C111; Perley, private communication, for 3C 219; and Dreher, 1984, for 3C321 and 3C382, which are shown as lower limits in P_{jet}). The values for Cygnus agree well with those found for the other sources.

Table 1. Narrow Jets

Source	ID	P_5	Jet			B_{eq}	$\frac{P_{jet}}{P_{source}}$
			length	open. angle	5 GHz bright.		
Cyg A	G	2000	40	0.03	90	140	0.3%
4C32.69	Q	300	120	<0.06	30	50	15
3C219	G	160	35	0.07	30	60	2
3C111	G	30	80	0.04	1.4	~25	1
NGC6251	G	1.5	150	0.08	0.7	15	40
3C449	G	0.8	20	0.2	1.8	30	8
		$\times 10^{31}$ erg $s^{-1}Hz^{-1}$	kpc	rad	$\frac{mJy}{arcsec^2}$	μG	

An important issue in understanding radio sources is whether the one-sided jets typically observed in high luminosity objects are truly one-sided or, rather, two-sided with an assymmetry

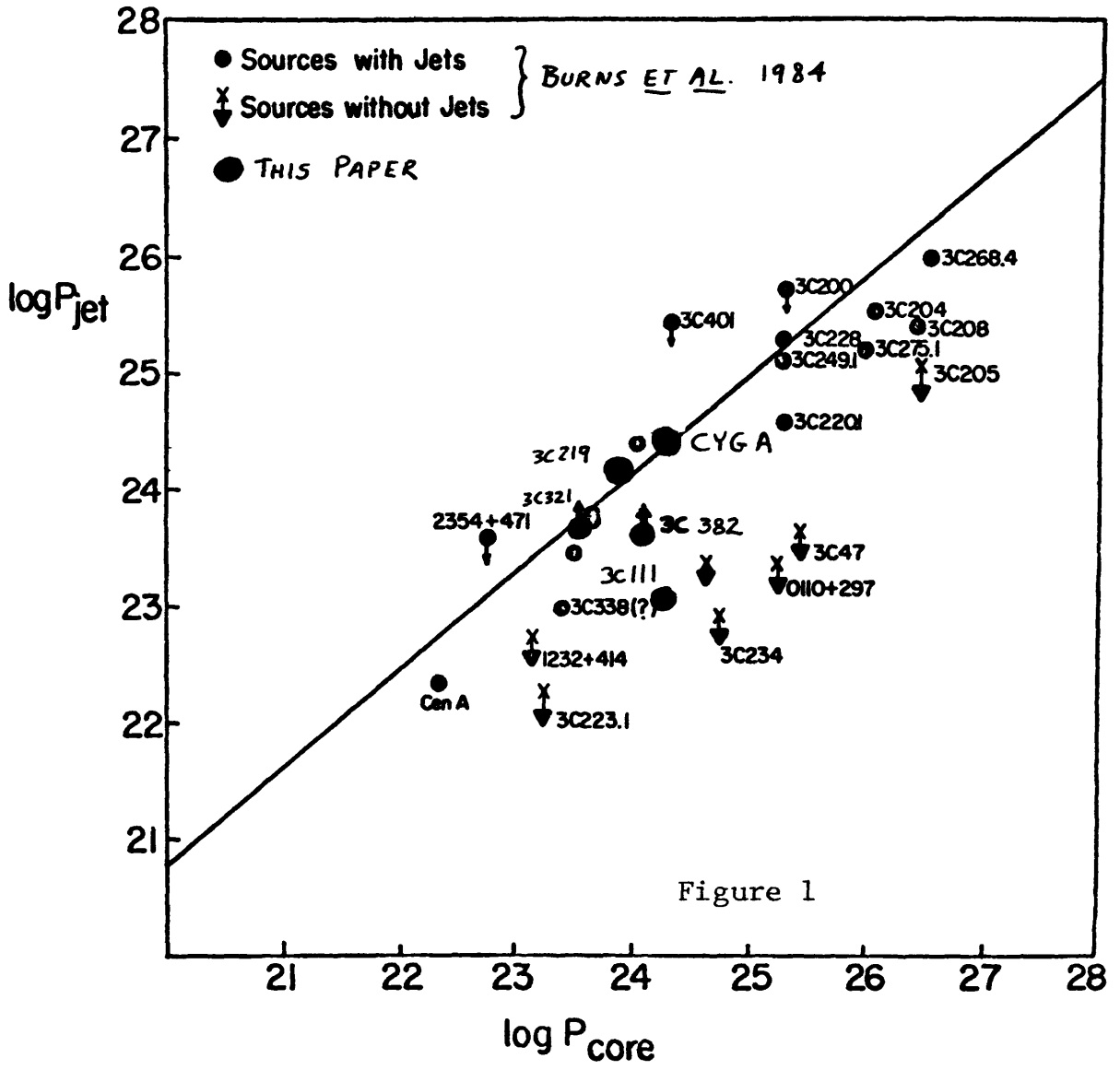

Figure 1

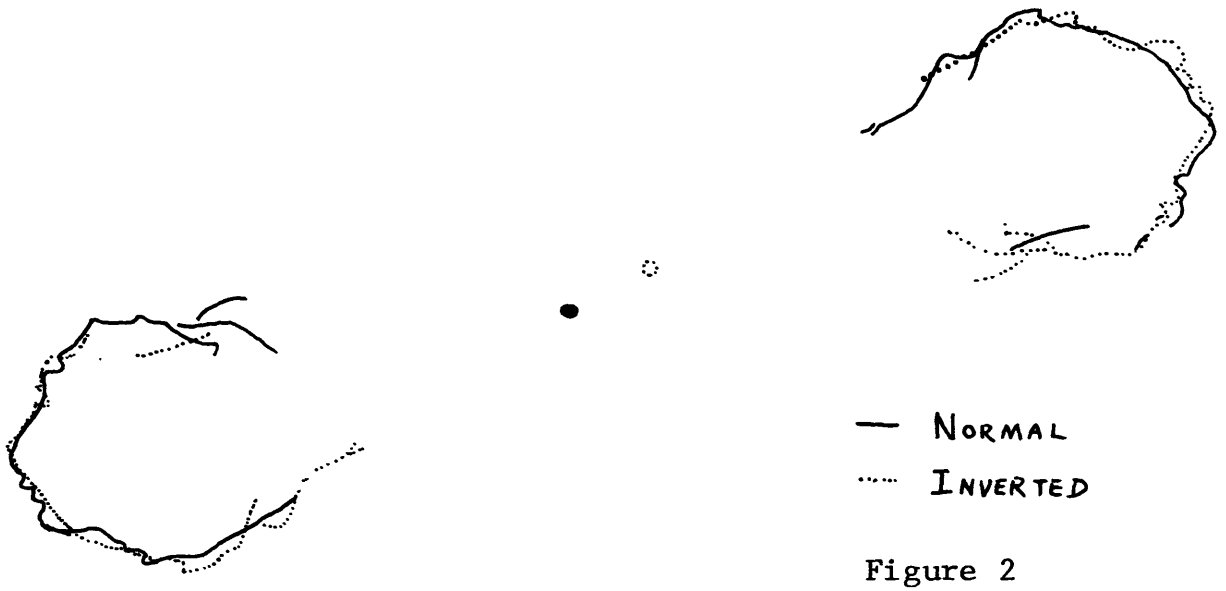

Figure 2

induced by relativistic motion. Bearing this in mind, while most people can make out what appears to be a counterjet leading from the core about halfway out into the southeast lobe, especially when presented with a high quality display of the data, caution must be used in interpreting this feature because of its possible significance. *If* it is in fact real, then the jet to counterjet brightness ratio is roughly 4. In paper I (see also the paper by Dreher elsewhere in these *Proceedings*) it is argued that the jet may well have a β of $\gtrsim$0.8, which would be sufficient to explain the brightness ratio if the inclination of Cygnus A were about 30° from the plane of the sky.

3. Lobes

The complex structure of the lobes was a surprise. The abundant wispy or filamentary structure is amorphous near the "heads" of the lobes and seems to become stretched out in the "tails." In addition, other features with a qualitatively different appearance can be seen: several thin arcs to the south and west of the northwest hotspots "A" and "B," a fuzzy ring to the east of the "A" hotspot (perhaps seen as component "C" on the map of Hargrave and Ryle, 1974), and a kidney-shaped ring on the core side of the southeast lobe. None of these structures has yet been explained.

Why haven't these features been evident before? These maps have three features previously unavailable: *i)* $\sim$1" resolution or better, *ii)* dynamic range in excess of 1000::1, and, most importantly, *iii)* much better coverage of the *uv* plane, achieved by at least 8 hours of observing in each of several configurations of the VLA. I am aware of three other sources that have been mapped in a similar fashion. Hercules A revealed a complicated system of jets and rings, very different in size and organization than those in Cygnus (Dreher and Feigelson 1984). 3C310 also showed many arcs inside its lobes, but, again, did not really resemble either of the others (van Breugel and Fomalont, 1984). 3C 219, on the other hand, seems to have smooth lobes (Perley and Bridle, private communication). Clearly, we have just scratched the surface of this new category of morphological features.

Comparison of the 1.4 and 5 GHz maps reveals a very strong spectral index gradient from the hotspots to the inner parts of the lobes, with $\Delta\alpha > 1$, as has been noted by several previous authors (*eg* Winter *et al.*, 1980, and Dreher, 1979). By comparing our maps at 20, 6 and 2 cm with maps made outside this range we eventually hope to detect unambiguous ageing effects in the lobes. The source is largely depolarized at 1.4 GHz and shows a patchy polarization distribution at 5 GHz. The large rotation measure associated with the southeast lobe is well known, but our newest data indicate similar large rotation measures occuring over the other lobe too. This complex topic cannot be dealt with until we have completed the 15 GHz mapping.

Another feature of the lobes worthy of note is the presence of very sharp edges, both on the "leading" edge of the lobes and also on the sides of the lobes in several regions. Many of these edges are unresolved at 0.4" resolution. In addition, the lobes do not appear edge darkened in the vicinity of these sharp edges, as might be expected, for example, if the lobes had uniform emissivity across their volumes. It seems possible that these hard edges may be produced by shocks where the highest energy density regions of the lobes are ram-confined against the surrounding gas. The lack of limb darkening may then indicate that the emissivity is increased in the vicinity of these shocks.

4. Symmetry

Another hotspot, here denoted "E", to the west of the bright southeast hotspot "D" and connected to it by a faint bridge can be seen on the maps. The "D"/"E" pair is now seen to be strikingly similar to the "A"/"B" pair on the opposite side, which are also connected by a faint bridge. The two pairs exhibit a rough "S" symmetry. Robert Laing will present very striking maps showing the fine structure of the "A" and "D" hotspots immediately following this paper. This fine structure also reinforces the similarity of these two hotspots.

Even more remarkably, the outer edges of the bright parts of the two lobes (in particular the hard-edged regions found in the outer half of each lobe) also exhibit an excellent "S" symmetry. Figure 2 is an attempt to illustrate this; however, it can best be appreciated by making a transparent overlay. The high degree of matching over the edges of the lobes suggests that these complex shapes are governed not by random processes (like smoke plumes) but by some systematic process common to both lobes, something like the pointing direction of the jet(s) for example. The similarity in shape also suggests to me that the lobes are basically very similar. However, when the inverted image is superimposed upon the original to match the edges, the central source is not aligned. One way to explain this is to imagine that the lobes are traveling outward with some $\beta_{\rm lobe}$ and to invoke a time-delay effect to explain the difference in the observed displacements of the lobes from the core. Let the observed distance between the two images of the core be ΔD, the source diameter be D, and the inclination from the plane of the sky be i. Then $\beta = (\Delta {\rm D}/{\rm D}\sin i)$. If $i = 30^{\rm o}$, then the observed $\Delta {\rm D}/{\rm D} = 0.07$ gives $\beta_{\rm lobe} \sim 0.1$. Such a high velocity would suffice to confine the lobes by ram pressure against even a fairly tenous surrounding medium. It may well be, of course, that some other asymmetry of the source is involved. In particular, it will be interesting to look for asymmetries in the X-ray emitting medium when those observations become available.

5. Concluding Remark

Some of the most interesting questions raised by these observations are a consequence of the large amount of data gathered. The details of the lobe edges lead to questions concerning the processes occuring at the lobe surface. The novel fine structure of the lobes in Cygnus and a few other sources suggests that radio source lobes, hitherto often regarded as fairly dull, are the sites of many interesting phenomena. Finally, the detection of jets, and, just as importantly, counterjets, is essential to understanding the basic structure of extragalactic radio sources. Clearly, observations such as those made on Cygnus A will be needed for many other sources to define and solve these probems. These observations will require far more observing time per source than the usual multiple "snapshots" and will also be a grievous load on the image processing systems. I hope that the VLA referees reading this will realize that attempts to obtain maximal amounts of data do not serve only to satisfy the observer's desire to make "perfect" maps but also can actually lead to knowledge of new phenomena. I would also apologize to the observers for the antisocial aspects of reducing the enormous data sets that will be needed, except that I am sure that by now they all have or plan to have their own gigantic data sets.

References

Burns, J.O., Basart, J.P., DeYoung, D.S., and Ghiglia, D.C. 1984, *Ap.J.*, in press.
Bridle, A.H., and Perley, R.A. 1984, *Ann.Rev.Ast.Ap.* **22**, in press.
Dreher, J.W. 1979, *Ap.J.* **230**, 687.
Dreher, J.W. 1984, preprint.
Dreher, J.W. and Feigelson, E.F. 1984, *Nature* **308**, 43.
Hargrave, P.J. and Ryle, M., 1974, *M.N.R.A.S.* **166**, 305.
Linfield, R., 1981, *Ap.J.* **224**, 436.
Linfield, R., and Perley, R. 1984, *Ap.J.* **279**, 74.
Perley, R.A., Dreher, J.W., and Cowan, J. 1984, *Ap.J.L.*, in press.
van Breugel, W. and Fomalont, E.F., preprint.
Winter, A.J.B. *et al.*, 1980, *M.N.R.A.S.* **192**, 931.

JET TURN-ON AND CONFINEMENT – INDICATIONS FROM IC4296

G. V. BICKNELL

Mount Stromlo and Siding Spring Observatories

ABSTRACT. VLA observations of IC4296 (Killeen, Bicknell and Ekers in preparation) at 6cm with a resolution of 1 arcsec show the existence of shock structures in both jets, close to the core. These shocks could be due to the jet becoming underexpanded just beyond an optical core radius (Bicknell 1984 – *Ap.J.*, in press), or may be where the (initially free) jets are coming into equilibrium with the interstellar medium (Sanders 1983 – *Ap.J.* **266**, 73). Beyond these shocks, both jets widen and the spectral index flattens from 0.9 to 0.6, indicating shock and/or turbulent acceleration of initially cool relativistic electrons.

Einstein IPC X-ray data show an unresolved X-ray source coincident with IC4296. Attributing this to thermal emission and using surface photometry and spectroscopy to model the gravititational field of IC4296, Killeen, Bicknell and Carter (*Ap.J.*, submitted) find that the pressure of the X-ray gas exceeds the minimum pressure of the jets. The X-ray emission is unresolved because there is almost no contribution to the gravitational field from the weak group of galaxies surrounding IC4296 and most of the hot gas concentrates within a few core radii of the centre of IC4296.

CONSTRAINTS ON THE PROPERTIES OF BENT BEAMS

CHRISTOPHER P. O'DEA

National Radio Astronomy Observatory[a], Charlottesville, Virginia 22903

ABSTRACT. The physics of bent radio luminous plasma beams is reviewed and constraints on the momentum and kinetic energy flux are examined. Expressions for the bulk velocity, particle density, and efficiency of conversion of bulk kinetic and internal energy into radio luminosity are given. VLA data on the intensity ratios of opposing jets in a sample of Narrow Angle Tail (NAT) sources are used to set an upper limit of $0.2c$ to the bulk velocity of the beams/plasmons. Within the context of models for NATs, order of magnitude estimates are made of the bulk velocities, particle densities, efficiencies and mass loss rates of the beams/plasmons in 19 NATs.

1. INTRODUCTION

It is currently thought that the radio luminosity of the extended structure of radio galaxies is powered by the energy (both kinetic and internal) carried by plasma beams which originate in the galactic nucleus (for reviews see e.g., Begelman *et al.* 1984; Bridle and Perley 1984). The content of these beams, their bulk velocities, particle densities, and efficiencies are not well understood. The constraints on the energy and momentum flux in bent radio luminous beams in Narrow Angle Tail sources may provide important insight into the physical conditions within the beams. The bending of the beams provides a more reliable constraint on the momentum flux than is generally available in straight beams (e.g., Burns 1983). For this reason, the physics of bent radio luminous beams is discussed here in some detail. The constraints are combined to derive order of magnitude estimates of the bulk velocity, particle density, and efficiency of conversion of bulk kinetic and internal energy into radio luminosity of quasi-continuous beams and plasmons in a channel. The three basic models for the morphology and energetics of NATs (Begelman, Rees and Blandford 1979 (BRB); Jones and Owen 1979 (JO); Christiansen, Pacholczyk and Scott 1981 (CPS)) are reviewed. The allowed parameter space is examined and a detailed comparison of the models is made. Additional details (e.g., derivations, calculations, and supplementary discussion) can be found in Chapter VII of O'Dea (1984).

In this paper, the term *jet* will refer to the observed radio structure, and the term *beam* will refer to the postulated flow (e.g., Baan 1980; Bridle 1982).

2. THE PHYSICS OF BENT BEAMS

In this section the physics which may be relevant to the bending of beams in NATs is discussed. The basic equations are given and their inherent assumptions are discussed.

Consider a beam, of radius r_b, mass density ρ_b, and bulk flow velocity v_b, composed of thermal particles, relativistic particles and magnetic fields. It will be assumed

[a] The National Radio Astronomy Observatory (NRAO) is operated by Associated Universities, Inc., under contract with the National Science Foundation.

here that the beams are composed of roughly equal numbers of protons and electrons; however, the velocity estimate is independent of the density (see below), and the estimated number densities can be scaled for other mixtures. The *net* energy flow down the beam is given by

$$L_E = \pi r_b^2 v_b \Gamma\big((\Gamma-1)c^2\rho_b + \Gamma(U_{\rm int} + P_{\rm int})\big) \tag{1}$$

(e.g., Landau and Liftshitz 1959) where $\Gamma = (1-\beta^2)^{-1/2}$ is the Lorentz factor, $\beta = v_b/c$, where c is the speed of light, $P_{\rm int}$ is the internal pressure,

$$P_{\rm int} = \frac{B^2}{8\pi} + \frac{U_{rel}}{3} + nkT, \tag{2}$$

$U_{\rm int}$ is the total internal energy density,

$$U_{\rm int} = \frac{B^2}{8\pi} + U_{rel} + \frac{3nkT}{2}, \tag{3}$$

where B is the strength of the magnetic field, U_{rel} is the energy density in relativistic particles (protons and electrons), k is the Boltzmann constant, and n and T are the density and temperature, respectively, of the nonrelativistic (thermal) particles.

The first constraint on the properties of the beams is based on the assumption that the kinetic and internal energy of the beam are tapped with an efficiency ϵ to provide the observed radio luminosity, L_{rad}. (At this point it is not important how this is done.) If the beams expand, adiabatic losses will reduce the energy of the radiating particles ($E \propto r_b^{-2/3} v_b^{-1/3}$). Taking this into account, and assuming for the moment a constant velocity beam gives

$$L_{\rm rad} \simeq \epsilon L_E \left(\frac{r_{\rm bi}}{r_{\rm bf}}\right)^{2/3} \tag{4}$$

where r_{bi} and r_{bf} are the initial and final beam radii (cf. JO). The assumption that the jet luminosity is powered by the energy carried by the beam requires *in situ* particle acceleration all along the beam. How good is this assumption? Since the jets in NATs tend to be relatively short, the usual synchrotron lifetime arguments do not suffice. In the case of NGC 1265, for example, relativistic particles which are created in or near the core can travel the entire ~ 20 kpc length of the jets within their estimated synchrotron and inverse Compton lifetime of $\sim 3 \times 10^6$ yrs (in a 15 μG field) for a beam velocity of $\sim 0.02c$, which is plausible.

However, the surface brightness of jets tends to decrease much slower with increasing radius than expected, given magnetic flux conservation and adiabatic expansion losses (e.g., Burch 1979; Fomalont *et al.* 1980; Bridle 1982; Perley, Bridle and Willis 1984; Bridle and Perley 1984). Unless the conditions in the beams are very different from the current ideas, the slow dependence of the intensity on radius strongly suggests that *in situ* particle acceleration is taking place all along the beams. However, the changes in both surface brightness and spectral index along jets suggest that the

amount and possibly the form of the particle acceleration varies along the beams. Thus, the amount of success attained in applying this constraint will depend to a large extent on how realistic it is to assume that the efficiency is roughly constant along the beams.

The second constraint on the beams is based on the assumption that the bending of the beams can be described by simple hydrodynamics. A NAT source moving with galaxy velocity v_g through an intracluster medium (ICM) of mass density ρ_{icm} experiences a ram pressure $\rho_{icm}v_g^2$. This pressure is exerted over a scale length h which can depend on the extent of the interstellar medium (ISM) in the galaxy (see JO). The relativistic time-independent Euler's equation for an ideal fluid (i.e., negligible viscosity) is given by

$$\frac{w_b\Gamma^2\beta^2}{R} \simeq \frac{\rho_{icm}v_g^2}{h} \tag{5}$$

where $w_b = \rho_b c^2 + U_{int} + P_{int}$ is the relativistic enthalpy, and R is the bending scale length or radius of curvature (e.g., Landau and Lifshitz 1959; cf. Jones and Owen 1979). The additional assumption has been made that the change in velocity of the beam over the scale length, R, is comparable to the velocity, i.e., $(v_b \bullet \nabla)v_b \simeq v_b^2/R$.

For a fluid with a nonrelativistic equation of state (i.e., dominated by thermal particles) $w_b \simeq \rho_b c^2$; while for a fluid with a relativistic equation of state (dominated by relativistic particles in rough equipartition with the magnetic fields) $w_b \simeq B^2/4\pi + (4/3)U_{rel}$. Note that if $(U_{int}+P_{int}) \simeq 10^{-11}$ ergs cm^{-3} (as is the case in the NATs; e.g., O'Dea and Owen 1984b), then $\rho_b c^2 > (U_{int}+P_{int})$ if the beam particle density is larger than $n_b = \rho_b/m_H > 9\times10^{-9}$ cm^{-3}, where m_H is the mass of the hydrogen atom. At this point the data allow only typical model dependent upper limits to the number densities in radio jets of $n_b < 10^{-3}$ cm^{-3} (e.g., Bridle and Perley 1984). However, the number densities estimated below (within the context of these models) are typically several orders of magnitude larger than 10^{-8} cm^{-3} and are consistent with the assumption made here that $w_b \sim \rho_b c^2$.

The assumption of negligible viscosity has been made in order to obtain the simplest form of Euler's equation, (5). The existence of viscosity will cause kinetic energy to be dissipated along the beam (e.g., Landau and Lifshitz 1959). Such energy dissipation is suggested by the slow dependence of the intensity and the pressure on the jet radius (e.g., Bridle 1982) and is assumed here as a constraint on the beam energy flow (equation 4). The neglect of viscosity in Euler's equation is equivalent to neglecting the effects of energy dissipation on the bending of the beam. This is a good assumption only if a very small fraction of the beam kinetic energy is dissipated. The results obtained below suggest that in general, relatively low efficiencies ($\epsilon \ll 0.01$) are required to produce the observed radio luminosities in the *jets*. An additional (possibly larger) fraction of the beam kinetic energy may be dissipated in heating of the thermal particles in the beam (e.g., Eilek 1979). This amount is harder to estimate, but even if it is a factor of ~ 10 larger than that needed to power the radio luminosity, the total fraction of the energy dissipated would only be a few percent or less. The very gradual bending of the radio jets in NATs (e.g., O'Dea and Owen 1984b) is also consistent with this estimate, since substantial energy dissipation would cause beams to be bent much faster than is

observed. Thus, the assumption of negligible viscosity is probably adequate for these order of magnitude calculations.

(a) Cold Beams. Beams in which the Mach number, M, is very large, i.e., $(\Gamma-1)c^2\rho_b \gg \Gamma(U_{int} + P_{int})$, have internal energies which are small compared to their bulk kinetic energies and are called *cold*. This is the most commonly made assumption. Combining equations (1) and (4) and ignoring the pressure term gives:

$$L_{rad} \simeq \epsilon\pi r_b^2 \rho_b v_b c^2 \Gamma(\Gamma-1)\left(\frac{r_{bi}}{r_{bf}}\right)^{2/3} \simeq \epsilon\pi r_b^2 \rho_b v_b^3 \left(\frac{\Gamma^3}{\Gamma+1}\right)\left(\frac{r_{bi}}{r_{bf}}\right)^{2/3} \tag{6}$$

(cf. Rees 1978). In the limit $M \gg 1$, $\rho_b c^2 \gg U_{int} + P_{int}$, hence $w_b \simeq \rho_b c^2$ and equation (5) becomes:

$$\frac{\rho_b v_b^2 \Gamma^2}{R} \simeq \frac{\rho_{icm} v_g^2}{h}. \tag{7}$$

Using equation (7) to substitute for $\rho_b v_b$ in equation (6) gives:

$$\frac{\beta\Gamma^2}{\Gamma(\Gamma-1)} \simeq \frac{\rho_{icm} v_g^2 \epsilon\pi r_b^2 cR}{L_{rad} h}\left(\frac{r_{bi}}{r_{bf}}\right)^{2/3} = \xi \tag{8}$$

where the constant, ξ, is composed of quantities which in principle can be observed or estimated. This gives a quadratic equation in Γ which has only one non-trivial root, i.e., $\Gamma = (\xi^2+1)/(\xi^2-1)$, where $\xi > 1$. This gives the following solution for the beam velocity

$$v_b = \frac{2c\xi}{\xi^2+1}. \tag{9}$$

The other (trivial) solution requires $\Gamma = 1$, i.e., $v_b = 0$. Note that equation (9) is correct for any velocity, and that the dependence on the beam density, ρ_b, has been eliminated. This latter point is especially important due to the current controversy over the interpretation of polarization measurements of jets (e.g., Laing 1981 and these Proceedings). The most general form for the particle number density n_b is given by

$$n_b = \frac{\rho_{icm} v_g^2 R}{h m_H c^2}\left(\frac{\xi^2+1}{\xi^2-1} - 1\right)^{-1}. \tag{10}$$

If an upper limit to the beam velocity, v_{bmax}, can be obtained, e.g., through limits on the amount of relativistic beaming allowed in the jets, then equation (8) can be rearranged to give a lower limit to the particle acceleration efficiency, i.e.,

$$\epsilon > \frac{\beta_{max}\Gamma_{max}^2 h L_{rad}}{\Gamma_{max}(\Gamma_{max}-1)\rho_{icm} v_g^2 \pi r_b^2 cR}\left(\frac{r_{bf}}{r_{bi}}\right)^{2/3}. \tag{11}$$

(b) Warm Beams. In some cases, the equations for highly supersonic beams may not be appropriate. In fact, in the Jones and Owen (1979) model, the beam must have a Mach

number ~ 1. For this reason, the more general case of a *warm* beam ($M \geq 1$) will be considered. Thus, equations (1) and (4) are combined without further assumptions at this point to give the energy flow constraint. The case of a beam with a nonrelativistic equation of state ($w_b \sim \rho_b c^2$, i.e., dominated by thermal particles) will be considered and equation (7) for the momentum flow constraint will be used. Together, these constraints give

$$L_{\rm rad} = \epsilon \pi r_{\rm b}^2 c \beta \Gamma \left(\frac{(\Gamma - 1)\rho_{\rm icm} v_{\rm g}^2 R}{h \Gamma^2 \beta^2} + \Gamma (U_{\rm int} + P_{\rm int}) \right) \left(\frac{r_{\rm bi}}{r_{\rm bf}} \right)^{2/3} . \tag{12}$$

Unfortunately, this results in a sixth order polynomial in Γ or β. Thus, simplifying assumptions are needed.

In the limit of nonrelativistic bulk velocity, equation (12) gives the following solution for $v_{\rm b}$,

$$v_{\rm b} \simeq \frac{L_{\rm rad}}{\epsilon \pi r_{\rm b}^2} \left(\frac{r_{\rm bf}}{r_{\rm bi}} \right)^{2/3} \left(\frac{\rho_{\rm icm} v_{\rm g}^2 R}{2h} + U_{\rm int} + P_{\rm int} \right)^{-1} . \tag{13}$$

Using Euler's equation, (7), the beam particle number density is then

$$n_{\rm b} \simeq \frac{\rho_{\rm icm} v_{\rm g}^2 R}{h m_{\rm H}} \left[\frac{\rho_{\rm icm} v_{\rm g}^2 R}{2h} + (U_{\rm int} + P_{\rm int}) \right] \left[\frac{L_{\rm rad}}{\epsilon \pi r_{\rm b}^2} (\frac{r_{\rm bf}}{r_{\rm bi}})^{2/3} \right]^{-2} . \tag{14}$$

Note that the beam particle density depends on higher powers of the observables than does the beam velocity, and is thus more sensitive to the uncertainties in those parameters. If an upper limit to the beam number density can be set using multifrequency polarization measurements, (and the other parameters can be estimated) an *upper* limit to $(U_{\rm int} + P_{\rm int})$, can be obtained. This is in contrast to the usual *lower* limit which is obtained from the minimum pressure calculations (e.g., Burns *et al.* 1979).

An upper limit to the efficiency, ϵ, can be obtained if an upper limit to the beam particle density, $n_{\rm bmax}$, and a lower limit to $(U_{\rm int} + P_{\rm int})$ can be determined, i.e., from equation (14),

$$\epsilon < \frac{L_{\rm rad}}{\pi r_{\rm b}^2} \left(\frac{h n_{\rm bmax} m_{\rm H}}{\rho_{\rm icm} v_{\rm g}^2 R} \right)^{1/2} \left(\frac{r_{\rm bf}}{r_{\rm bi}} \right)^{2/3} \left(\frac{\rho_{\rm icm} v_{\rm g}^2 R}{2h} + U_{\rm min} + P_{\rm min} \right)^{-1} . \tag{15}$$

If an upper limit to the beam velocity, $v_{\rm bmax}$, can be obtained, then equation (13) can be rearranged to give a lower limit to the efficiency, i.e.,

$$\epsilon > \frac{L_{\rm rad}}{v_{\rm bmax} \pi r_{\rm b}^2} \left(\frac{r_{\rm bf}}{r_{\rm bi}} \right)^{2/3} \left(\frac{\rho_{\rm icm} v_{\rm g}^2 R}{2h} + U_{\rm int} + P_{\rm int} \right)^{-1} . \tag{16}$$

At this point, the respective equations for $v_{\rm b}$, $n_{\rm b}$, and ϵ can be compared for both the warm and cold beams in the nonrelativistic limit. All other properties being equal, the warm beam will be about a factor of 2 lower in velocity and less efficient and a factor of 4 denser than the cold beam.

3. MODELS FOR NATS

In this section the three plasma beam/cloud models for the morphology and energetics of Narrow Angle Tails sources are briefly reviewed and some general comments are made.

(a) Quasi-continuous beams. The two quasi-continuous beam models differ to the extent to which the ISM of the parent galaxy is important. In the "naked" beam model the ISM is insignificant and the beam interacts directly with the ICM gas which streams freely through the galaxy (BRB; Vallée *et al.* 1981; Baan and Mckee 1983). For a galaxy velocity which is transonic in the ICM, there will be a bow shock in front of the beams. The bending of the beam is then described by Euler's equation, (7), where the scale height of the pressure gradient is simply the beam radius, $h \sim r_b$. Beams in sources like NGC 1265 must be moderately supersonic with Mach numbers of ~ 5. The beam must carry enough bulk kinetic energy to power the luminosity of the tails, i.e., $L_{rad} \sim L_{tail}$. Typically, the jets expand by a factor of ~ 10 into the diffuse tails, i.e., $(r_{bf}/r_{bi}) \sim 10$, and the radiating particles experience significant adiabatic losses.

In the Jones and Owen (1979) model, a significant ISM exists in the galaxy. This appears to be consistent with the results of numerical hydrodynamic calculations of ram pressure stripping of the ISM from galaxies moving at transonic velocity ($M \geq 1$) through the cluster gas (e.g., Gisler 1976; Lea and De Young 1976; Shaviv and Salpeter 1982). In this case, a bow shock will form in front of the galaxy, and there will be a turbulent wake behind the galaxy. The ram pressure from the ICM is then distributed across the ISM ($h \simeq r_s$, the radius of the ISM). The pressure gradient across the beam is weaker by a factor of r_b/r_s than in the case of the BRB model. Thus, for a given bending scale length, a beam embedded in an ISM will have a momentum flux which is weaker by the factor r_b/r_s than a beam exposed to the ICM. Although the weaker JO jet may be unable to power the radio luminosity of the tails, the energy in the turbulent galactic wake may be available to reaccelerate the particles if the beam can be bent on the scale r_s. The radio luminosity of the tail is then

$$L_{rad} \simeq \epsilon \pi \rho_{icm} r_s^2 v_g^3 \tag{17}$$

(JO). If the beam is only transonic, $M \sim 1$ and $R \sim h \sim r_s$ and the beam is bent back into the galactic wake; hence these warm beams need only power their own radio emission, $L_{rad} \sim L_{jet}$. Thus, since the jet expansion is generally not significant over the region in which the bending occurs (and in any case only the global parameters of the beams are estimated here), $(r_{bf}/r_{bi}) \sim 1$.

(b) Multiple Plasmons in a Channel. CPS suggested that the "multiple plasmon in a channel" model (Christiansen 1973; Christiansen *et al.* 1977) would work for the case of NGC 1265 if there were a significant ISM. CPS consider only the case of cold, $M \geq 1$, nonrelativistic plasmons. The plasmons traveling through the channel in the ISM would have smaller energetic requirements than those in the *independent* multiple plasmon model (Wellington *et al.* 1973; Jaffe and Perola 1973; Pacholczyk and Scott 1976). The energetics of this model are then similar to those of the JO model in that,

for a given transverse pressure gradient across the beam and bending scale length, the time-averaged momentum flux in the two models must be the same. Each plasmon must have a momentum flux which is higher by the factor d/r_p than a similar volume of fluid in a JO beam, where d is the distance between plasmons and r_p is the plasmon radius. In addition, CPS assume that the pressure gradient scale length is the channel/plasmon radius (CPS equation 4) instead of the ISM radius. This requires the plasmons to be supersonic and increases the estimated plasmon momentum flux by an additional factor of r_s/r_p over that of the JO beam. As in the JO model, the turbulent galactic wake is assumed to provide the energy for the radio luminosity in the tail.

The constraint on the plasmon kinetic energy flux is

$$L_{rad} \simeq \frac{\epsilon \pi r_p^3 \rho_p v_p^3}{2d} \tag{18}$$

where ρ_p and v_p are the plasmon mass density and velocity, respectively. The constraint on the momentum flux of a cold nonrelativistic plasmon is given by Euler's equation:

$$\frac{\rho_{icm} v_g^2}{h} \simeq \frac{\rho_p v_p^2 r_p}{Rd} \tag{19}$$

(CPS equation 8) and CPS take $h \sim r_p$ (CPS equation 4). Combining these two conditions gives the plasmon velocity, v_p, and number density, $n_p = \rho_p/m_H$:

$$v_p \simeq \frac{2hL_{rad}}{\pi \epsilon r_p^2 \rho_{icm} v_g^2 R} \tag{20}$$

and

$$n_p \simeq \frac{\epsilon^2 \pi^2 R^3 \rho_{icm}^3 r_p^3 v_g^6 d}{4h^3 L_{rad}^2 m_H}. \tag{21}$$

If an upper limit to the plasmon particle density, n_{pmax}, can be obtained, (and the other parameters can be estimated) an upper limit to the distance d between plasmons can be derived. The condition $d > r_p$ must be met for this model to be distinguished from the continuous beam models. If an upper limit to the plasmon velocity, v_{pmax}, is obtained, a lower limit to the particle acceleration efficiency in the plasmon can be obtained from equation (20),

$$\epsilon > \frac{2hL_{rad}}{v_{pmax} \pi r_p^2 \rho_{icm} v_g^2 R}. \tag{22}$$

If an upper limit to the plasmon particle density, n_{pmax}, can be obtained, an upper limit to the efficiency can be obtained from equation (21),

$$\epsilon < \frac{2L_{rad}(h^3 n_{pmax} m_H)^{1/2}}{\pi v_g^3 (R^3 \rho_{icm}^3 r_p^3 d)^{1/2}}. \tag{23}$$

4. Upper Limits to the Beam/Plasmon Velocity

The observed limits to the intensity ratios of two oppositely directed jets can be used to set limits to the beam or plasmon velocities. The intensity ratio due to relativistic Doppler enhancement of two beams with $\beta = v_b/c$ and inclination angle θ to the line of sight is given by

$$\frac{S_1}{S_2} = \left(\frac{1-\beta_2\cos(\theta_2)}{1-\beta_1\cos(\theta_1)}\right)^{2-\alpha} \tag{24}$$

where α is the spectral index ($S \propto \nu^{\alpha}$) (e.g., Blandford and Königl 1979; Scheuer and Readhead 1979; van Groningen *et al.* 1980). Using data from O'Dea and Owen (1984a,b), average ratios of the side-to-side intensities of the two opposing jets in 26 twin jet NATs were estimated (shown in Figure 1). These ratios are probably upper limits to the amount of intensity enhancement due to Doppler enhancement, since there are also intrinsic variations in jet intensity. For the purposes of this calculation it is assumed that $\beta_1 = \beta_2$, $\theta_2 = \theta_1 - 180°$, and $\alpha = -0.65$. The distribution of intensity ratios expected for given values of β and a random distribution of angles was determined for an artificial Monte Carlo generated sample of 10^4 sources.

The median of the observed intensity ratio distribution, 1.6, was compared to the median of the artificial distribution using a chi-square test (Conover 1980). Even moder-

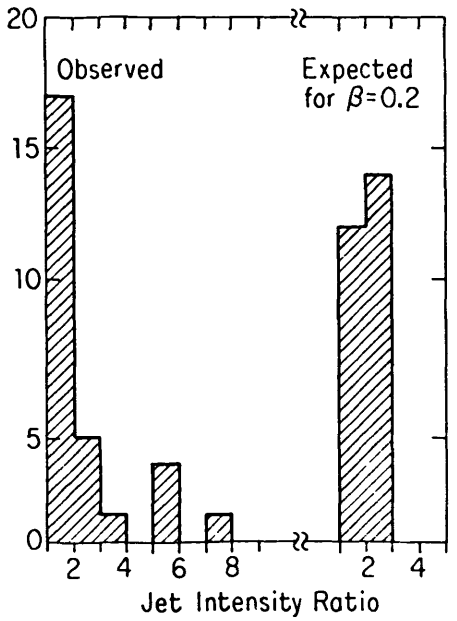

Figure 1. **The observed distribution of average intensity ratios between opposing jets in a sample of 26 twin jet NATs (data from O'Dea and Owen 1984a,b); and the predicted distribution due to relativistic Doppler enhancement (equation 24) for $\beta = 0.2c$ and a random distribution of angles to the line of sight.**

ately low values of β predict larger median ratios of intensities between the opposing jets than are observed. The median of the observed distribution is less than that expected for $\beta = 0.15$ with a 94% confidence and is less than that expected for $\beta = 0.20$ with a 99.7% confidence. The expected distribution for $\beta = 0.20$ is also shown in Figure 1. Thus, values of $\beta > 0.2$ are unlikely for these sources.

One possible problem is that the choice of twin jet NATs for this statistical comparison may discriminate against sources whose jets are at a small angle to the line of sight. Such sources might appear to be single tail sources because of the much smaller projected distance between the jets, and so would not have been included in the sample of twin jet NATs. However, these results are unchanged if angles less than 40° to the line of sight are omitted.

5. DISCUSSION

It is of interest to compare the velocities, densities and efficiencies for the three models – BRB, JO, and CPS. All three models input different values for radio luminosity, pressure gradient scale height, and beam/plasmon expansion which result in some cases in significantly different model parameters. The range of parameter space required by the nonrelativistic warm beam and plasmon models can be explored using the data on 19 NATs from O'Dea and Owen (1984a,b,c). An efficiency for the conversion of the beam kinetic energy into radio luminosity of $\epsilon = 1\%$ was assumed for the calculations of the velocities and densities. An efficiency of $\sim 1\%$ is generally required by the various theoretical models for extended sources in order to explain the observed radio luminosity (e.g., Pacholczyk and Scott 1976; Christiansen *et al.* 1977, 1979; Eilek 1979). However, it is not clear that these models *can* provide such an efficiency since very little work has been done in predicting the efficiencies of the various particle acceleration mechanisms (cf. Eilek 1979). An upper limit to the beam velocity of $v_b < 0.20c$ (based on the upper limits to the relativistic beaming enhancements) was assumed for the calculation of the lower limit to the efficiency. For unresolved jets, the velocities and efficiencies will be lower limits and the densities will be upper limits. The detailed results are given elsewhere (O'Dea 1984) and are only summarized here.

For an efficiency of 1%, both the JO and CPS models require lower limits to the velocities in the range $\sim 1 - 10(\times 10^3)$ km sec^{-1}. The BRB model requires beam velocities which are systematically higher by a factor of ~ 10. In general, these nonrelativistic beam velocities are consistent with the upper limit of $\beta < 0.2c$ (i.e., 60×10^3 km sec^{-1}) from the limits on relativistic beaming. This provides evidence that the beams in these low luminosity sources have nonrelativistic bulk velocities. There are a few exceptions, however, i.e., in the BRB model, 0039+211 and 1108+411 are required to have beam velocities $v_b \sim c$, unless $\epsilon > 1\%$.

The galaxy velocities required to power the tails through a turbulent galactic wake (at 1% efficiency) are less than or are comparable to the assumed galaxy velocities for nearly all of the sources. The required galaxy velocities for 4 sources with relatively high radio luminosities, 0039+211, 1108+411, 1132+492, and 1619+428, are a factor of ~ 2 higher than the assumed velocities. However, velocities this high (i.e., $\sim 2 - 3 \times 10^3$ km sec^{-1}) are not ruled out for these sources, and requiring the jets themselves to provide

the tail luminosity also has problems with these sources. All four of these sources require either relativistic velocities ($v_b \sim 0.5c - 1c$) or efficiencies $> 1\%$ in the BRB model. Thus, a turbulent galactic wake, as suggested by Jones and Owen, is capable of providing the radio luminosity in the tails of these sources if a 1% efficiency can be achieved.

The Mach numbers required by the BRB and CPS models are only mildly transonic ($M \sim 2 - 4$), though these numbers would be increased for smaller jet radii.

The upper limits to the particle density for the BRB and JO models are generally in the range $\sim 10^{-4} - 10^{-6}$ cm^{-3}. The densities in the CPS model are typically higher by a factor of $\sim 10^3 - 10^4$. For the current parameters, the CPS model requires densities ≥ 0.1 cm^{-3} for NGC 1265, 0907-091, 1244+699, and 1705+786. This difficulty could be relieved by using an efficiency much less than 1% or by using a much smaller plasmon radius. No more than a factor of 3 can be gained by reducing the value of the distance between plasmons. Higher resolution observations of some of these sources would be interesting.

The predicted density for NGC 1265 is $\sim 2 \times 10^{-5}$ cm^{-3} in both the BRB and JO models. This density is well below the current (model dependent) upper limit from the lack of depolarization at 21 cm of $n_b < 2 \times 10^{-3}$ cm^{-3} (O'Dea and Owen 1984a). However, the estimated density of ~ 0.3 cm^{-3} in the CPS model is grossly inconsistent with this limit. Since the jets are resolved, the only way to reduce the estimated density below the upper limit is to reduce the efficiency to $\epsilon < 8 \times 10^{-4}$. This is not inconsistent with the lower limit on ϵ from the upper limit on the plasmon velocity of 0.2c, however, it is much lower than previous estimates of the efficiency of plasmons (e.g., Christiansen *et al.* 1979; CPS) which suggest that efficiencies of at least 10^{-2} are required to account for the luminosity of extended radio sources. If the limit on the density in NGC 1265, $n_b < 2 \times 10^{-3}$ cm^{-3}, is typical of other NATs then the same situation would be encountered by the CPS model in nearly all the other NATs.

Assuming an upper limit to the beam velocity of 0.2c, lower limits to the efficiencies of $\sim 10^{-4}$ (CPS), $\sim 10^{-3}$ (JO), and $\sim 10^{-2}$ (BRB) are required. Ten sources (including NGC 1265) are required by the BRB model to have lower limits to the efficiency $\geq 1\%$. It remains to be seen whether such high efficiencies can be produced by reacceleration models. The upper limits to the efficiencies (estimated by requiring the density to be less than 2×10^{-3} cm^{-3}) in the BRB and JO models are fairly high, typically $\epsilon_{max} \sim 1$, and 0.1, respectively, and are not very useful. Lower upper limits to the particle densities are needed in order to more tightly constrain the efficiencies. Thus, the CPS model is consistent with $10^{-2} < \epsilon < 10^{-4}$, the JO model is consistent with $10^{-1} < \epsilon < 10^{-3}$, and the BRB model is consistent with $1 < \epsilon < 10^{-2}$.

In the calculations presented here, the CPS model gives an upper limit to the efficiency in NGC 1265 of $\epsilon < 8 \times 10^{-4}$; while CPS obtain a much higher estimate of $\epsilon \sim 10^{-2}$ using similar input parameters. The reason appears to be that there is a numerical error in one of their calculations (O'Dea 1984).

The mass loss rate through a continuous beam, $\dot{m}_b$, is given by $\dot{m}_b = \pi r_b^2 \rho_b v_b$, and for a stream of plasmons in a channel, $\dot{m}_p \simeq \dot{m}_b (r_p/d)$. Note that $\dot{m} \propto \epsilon$, so that these results can be scaled using different values of ϵ. The mass loss rates, assuming an

efficiency of 1%, are typically $\sim 10^{-1} - 10^{-3}$ $M_\odot$ yr^{-1} for the JO and BRB models, and $\sim 10^{1} - 10^{-1}$ $M_\odot$ yr^{-1} for the CPS model; i.e., the mass loss rate in the CPS model is much higher than in the BRB and JO models. The large dispersion in the estimates may at least partially be due to the uncertainties in the input paramaters. These numbers can be compared with estimates for sources of mass in the ISM, and the mass loss rate from the parent galaxy due to ram pressure stripping. The mass input rate from stars (stellar winds, etc.) into the ISM is estimated to be roughly $\sim 0.1 - 1$ $M_\odot$ yr^{-1} for a typical elliptical galaxy (e.g., Faber and Gallagher 1976; Gisler 1976). The mass loss rate from a galaxy due to ram pressure stripping is given by $\dot{m} \sim \pi r_s^2 f c_{ism} \rho_{icm}$, where r_s, ρ_{icm}, and c_{ism}, are the radius, density, and sound speed of the ISM, and f is a factor which takes into account the radial decrease in density ($f \sim 0.1$; JO). Using $r_s = 10$ kpc, $\rho_{icm} = 10^{-25}$ g cm^{-3}, and $c_{ism} = 2 \times 10^7$ cm sec^{-1} (for a pressure of 3×10^{-11} dynes cm^{-2}, typical values for NGC 1265, O'Dea and Owen 1984a) gives $\dot{m} \sim 10$ $M_\odot$ yr^{-1}. This suggests that the mass loss due to the beams/channels is small compared to both the mass input into the ISM from stars, and the mass loss from the galaxy due to ram pressure stripping.

Within the context of the bending models for quasi-continuous beams, the observed galaxy velocities and ICM densities are sufficient to account for both the morphology and energetic requirements of NATs. These results are entirely consistent with the idea that the tailed morphology is due to the interaction of the moving radio source with the ICM (Miley *et al.* 1972; Wellington *et al.* 1973).

At this point, all three models for the jets in NATs can be made consistent with the observations with the appropriate value for the efficiency. It is not yet clear at what level these required efficiencies become unrealistic. A choice between the models or even better estimates for the beam/plasmon velocity and density cannot be made until better constraints on the efficiency (both theoretical and observational) can be obtained.

ACKNOWLEDGEMENTS

The author is extremely grateful to F. Owen for suggesting this topic and for providing much advice and encouragement. Thanks are also extended to W. Baan, S. Baum, G. Bicknell, A. Bridle, W. Dent, J. Eilek, and T. Jones for helpful discussions, to F. Schwab for help with the manuscript preparation, and to B. Eno for inspiration.

REFERENCES

Baan, W. A. (1980). Ap. J. **239**, 433.

Baan, W. A. and Mckee, M. R. (1983). Astron. Astrophys. , submitted.

Begelman, M. C., Blandford, R. D., and Rees, M. J. (1984). Revs. Mod. Phys. **56**, 255.

Begelman, M. C., Rees, M. J., and Blandford, R. D. (1979). Nature **279**, 770. (**BRB**).

Blandford, R. D. and Königl, A. (1979). Ap. J. **232**, 34.

Bridle, A. H. (1982). *Proc. IAU Symp. 97, Extragalactic Radio Sources*, (ed. D. S. Heeschen and C. M. Wade) Dordrecht: Reidel. p. 121.

Bridle, A. H. and Perley, R. A. (1984). Ann. Rev. Astr. Ap. **22**, 319.

Burch, S. F. (1979). M.N.R.A.S. **187**, 187.

Burns, J. O. (1983). *Proc. Turin Workshop, Astrophysical Jets*, (ed. A. Ferrari and A. G. Pacholczyk) Dordrecht: Reidel. p. 67.

Burns, J. O., Owen, F. N. and Rudnick, L. (1979). A. J. **84**, 1683.
Christiansen, W. A. (1973). M.N.R.A.S. **164**, 211.
Christiansen, W. A., Pacholczyk, A. G., and Scott, J. S. (1977). Nature **266**, 593.
——————————————— (1981). Ap. J. **251**, 518. (CPS).
Christiansen, W. A., Rolison, G. G., and Scott, J. S. (1979). Ap.J. **234**, 456.
Conover, W. J. (1980). *Practical Nonparametric Statistics* (New York: John Wiley and Sons).
Eilek, J. A. (1979). Ap. J. **230**, 373.
Fomalont, E. B., Bridle, A. H., Willis, A. G., and Perley, R. A. (1980). Ap. J. **237**, 418..
Gisler, G. R. (1976). Astron. Astrophys. **51**, 137.
Jaffe, W. J. and Perola, G. C. (1973). Astron. Astrophys. **26**, 423.
Jones, T. W. and Owen, F. N. (1979). Ap. J. **234**, 818. (JO).
Laing, R. A. (1981). Ap.J. **248**, 87.
Landau, L. D. and Lifshitz, E. M. (1959). *Fluid Mechanics* (New York: Pergamon).
Lea, S. M. and De Young, D. S. (1976). Ap.J. **210**, 647.
Miley, G. K., Perola, G. C., Van der Kruit, P. C., and van der Laan, H. (1972). Nature **237**, 269.
O'Dea, C. P. (1984). Ph.D. thesis, University of Massachusetts, Amherst.
O'Dea, C. P. and Owen, F. N. (1984a). In preparation.
——————————————— (1984b). In preparation.
——————————————— (1984c). In preparation.
Pacholczyk, A. G. and Scott, J. S. (1976). Ap. J. **203**, 313.
Perley, R. A., Bridle, A. H., and Willis, A. G. (1984). Ap. J. Supp. **54**, 291.
Rees, M. J. (1978). M.N.R.A.S. **184**, 61P.
Scheuer, P. A. G. and Readhead, A. C. S. (1979). Nature **277**, 182.
Shaviv, G. and Salpeter, E. E. (1982). Astron. Astrophys. **110**, 300.
Vallée, J. P., Bridle, A. H., and Wilson, A. S. (1981). Ap. J. **250**, 66.
van Groningen, E., Miley, G. K., and Norman, C. A. (1980). Astron. Astrophys. **90**, L7.
Wellington, K. J., Miley, G. K., and van der Laan, H. (1973). Nature **244**, 502.

DISCUSSION

Geoff Bicknell. For beams of Mach number ~ 1 the most important contribution to the energy flux is the heat flux, not the kinetic energy flux as you have assumed. This changes the estimates of jet parameters. Furthermore, the most important influence on the surface brightness of a $M \approx 1$ jet is the decrease of velocity due to entrainment, not dissipation. This also has an effect on the estimation of jet parameters.

Chris O'Dea. The beam Mach numbers in the BRB model are certainly greater than one, and those in the JO model are slightly greater than one (see Jones and Owen 1979). In any case, an estimate of the internal energy density $(U + P)$ is included in the calculations of the beam parameters. The constraint on the momentum flux from Euler's equation suggests that the beam velocity *cannot* decrease sufficiently to account for the brightness-radius evolution.

Dick Henriksen. Intergalactic jets need not, in fact must not, slow down so rapidly as laboratory jets ($\propto x^{-1}$) if they are to deliver energy to the lobes. This is possible with sufficiently rapidly varying (declining) density.

BENDING IN THE FIRST FEW HUNDRED PARSECS

P.N.WILKINSON AND T.J.CORNWELL
National Radio Astronomy Observatory[a], P.O. Box O, Socorro, NM 87801
A.J.KUS
Torun Radio Observatory, Nicolaus Copernicus University,
ul. Chopina 12/18, 87-100 Torun, Poland
AND
A.C.S.READHEAD AND T.J.PEARSON
California Institute of Technology, Robinson 105-24, Pasadena, CA 91125

ABSTRACT. VLBI maps of jets in the nuclei of the quasars 3C309.1 and 3C380 show sharp apparent bends on the 100 pc scale. At present we cannot say whether these bends are greatly enhanced by projection or what their underlying cause is. However, progress can be expected on understanding this phenomenon within a few years.

1. INTRODUCTION

Partly this talk is an advertisement for the fact that in VLBI we have now reached a stage where we can unambiguously map quite complex structure on scales of tens of milliarcseconds and less; at redshifts typical of high luminosity sources, these correspond to linear dimensions of hundreds of parsecs. Some of these maps show clearly that jet bending does not only occur on the kiloparsec and larger scales – to which most of this Workshop is devoted – but also happens much closer to the nucleus.

At the present time we don't understand why this near-in bending occurs – largely because there is no 2-dimensional information to complement the high resolution radio intensity maps. Thus, for example, we have no optical emission line or X-ray data of the sort which has led us to favour different forms of dynamical interaction to explain beam-bending on the larger scales. It may be that, on the smaller scales, models involving ballistic motion and movements of the central "nozzles" are still plausible, but we are not yet in a position to distinguish definitively between these two bending hypotheses.

At first sight, therefore, one might think that the study of jets on these scales is, and is destined to remain, a rather sterile pursuit. This is not the case for at least three reasons. First, we will soon have optical data from the *Space Telescope*, at least with resolutions down to about 50 mas; secondly, detailed polarisation maps from VLBI are clearly just around the corner and we shall then be able to proceed by analogy with the extended jets; thirdly, these compact jets are strong enough for us to obtain direct velocity information, from component proper motions, with existing VLB equipment. On the larger scales, however, we shall need more patience and determination to measure proper motions and so the compact bent jets have the potential of giving us new constraints on the jet phenomenon in general.

[a] The National Radio Astronomy Observatory (NRAO) is operated by Associated Universities, Inc., under contract with the National Science Foundation.

2. Steep-spectrum Compact Cores

The jets we are studying are found in steep-spectrum compact core sources (SSCS) and we should briefly reiterate what these things are. It is now clear that there are plenty of sources with steep radio spectra but whose angular sizes are less than a few arcsecs; this usually corresponds to projected linear sizes of sub-galactic dimensions. They are found in a wide variety of objects, from Seyferts and other active galaxies to quasars, both radio loud and quiet. This heterogeneous collection share several common properties, *viz.*: low polarisation, steep radio spectra (usually with a turnover in the 0.1 – 1 GHz range), and low radio variability. In a few well-studied examples (e.g. Miley *et al.* 1981; Heckman *et al.* 1983; van Breugel *et al.* 1984) there is a clear connection between the radio morphology and the properties of the extended emission-line clouds, which leads one to the conclusion that the beams are being braked and bent by interaction with dense thermal gas.

We have been studying SSCS in bright 3C quasars and it is pertinent to note that all seven such quasars in 3CR have peculiar, bent or distorted structures (Wilkinson *et al.* 1984a). In one specific case, 3C48, there is direct optical evidence that we may be looking at an interacting galaxy system (Boroson and Oke 1982; Bothun *et al.* 1982; Balick and Heckman 1983) and there is at least some circumstantial evidence that the radio structures of these quasars might also be due to a beam/energetic gas interaction (Wilkinson *et al.* 1984a,b).

3. The Jet in 3C309.1

This quasar ($z = 0.911$) has a LAS of $\sim 2''$ corresponding to a projected linear dimension of $8.4h^{-1}$ kpc (for $H_0 = 100h$ km s^{-1} Mpc^{-1} and $q_0 = 0.5$). It has a triple structure with a central core (e.g., Wilkinson *et al.* 1982, Figure 6) which is the component we are studying with VLBI. Figure 1a is a 5 GHz MERLIN map showing the nucleus and the curving jet to the East. Figure 1b shows a 1.6 GHz VLBI map of the nucleus, while Figure 2 is an attempt to show these two maps on the same scale. Note, however, that there is another extended component to the West of the nucleus not shown in any of these Figures.

There is interesting fine detail in the VLBI jet (overall length $300h^{-1}$ pc), including wiggles and structures which one might be tempted to think of as shocks, but as yet we are not in a position to interpret these features. For the present the three important facts to note are: first, that the flat-spectrum core in this VLBI map is the weak feature right at the very top of the jet, and thus the jet is very one-sided (>100:1 in peak brightness); secondly, that the jet apparently bends through roughly a right-angle in its own diameter at a projected distance of $\sim 250h^{-1}$ pc from the core; thirdly, that the jet maintains its integrity for roughly $4h^{-1}$ kpc after this sharp apparent bend.

We also have VLBI maps at other frequencies (not shown here) and, if we take the results of standard synchrotron calculations, the strongest knot in the VLBI jet should be a strong source of X-rays because of inverse Compton scattering. However, the integrated X-ray flux is >300 times *less* than that predicted from this knot alone and the easiest way around this dilemma is to assume that the electrons in the knot are in bulk relativistic motion towards us with a Doppler factor ~ 3. These calculations

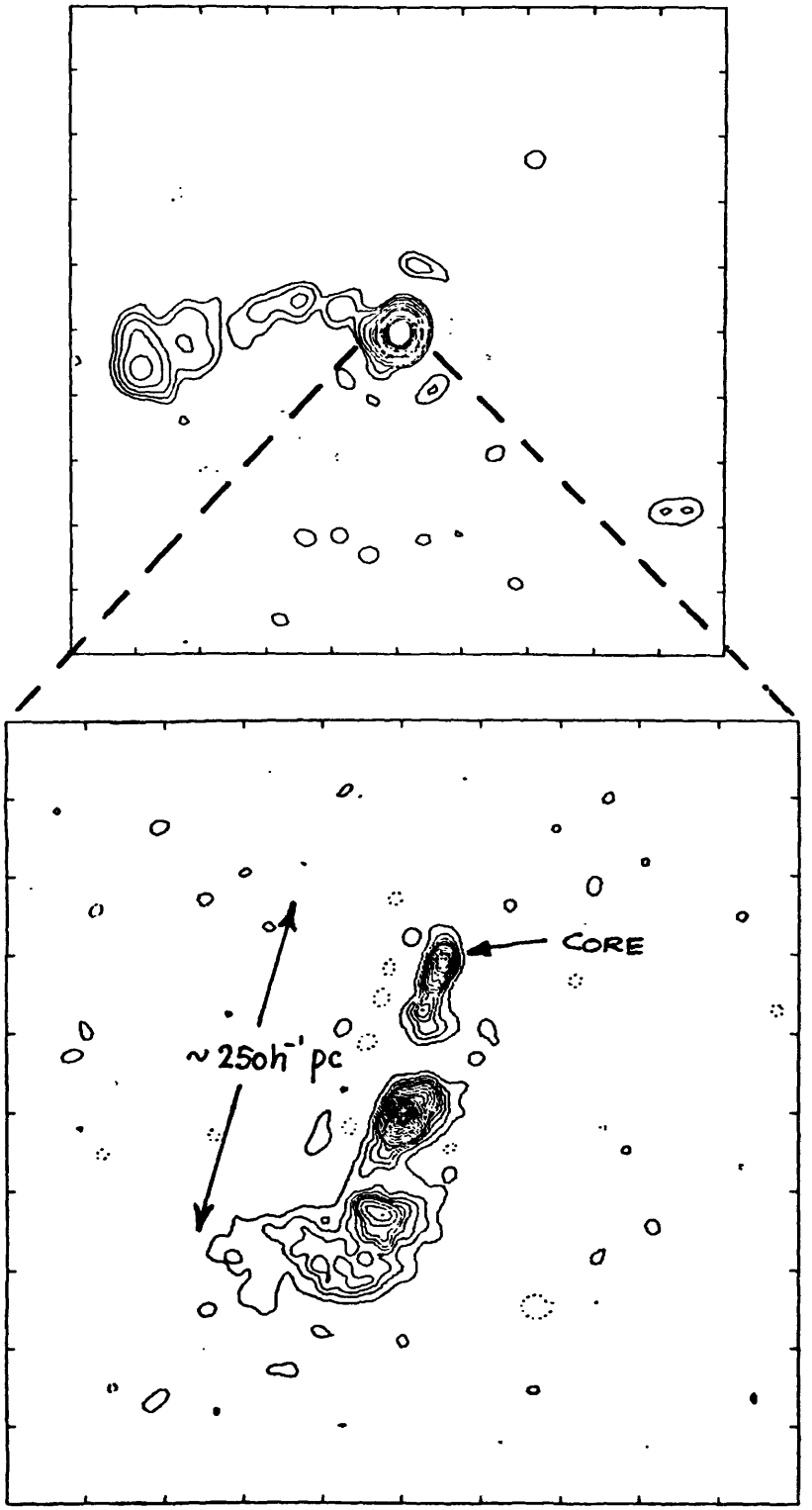

Fig. 1a : MERLIN map of the quasar 3C309.1 at 5GHz; the resolution is 60 milliarcsec and the scale is 240 milliarcsec per tick mark.

Fig. 1b : VLBI map of the nucleus at 1.6 GHz; the resolution is 2.5 milliarcsec and the scale is 12 milliarcsec per tick mark.

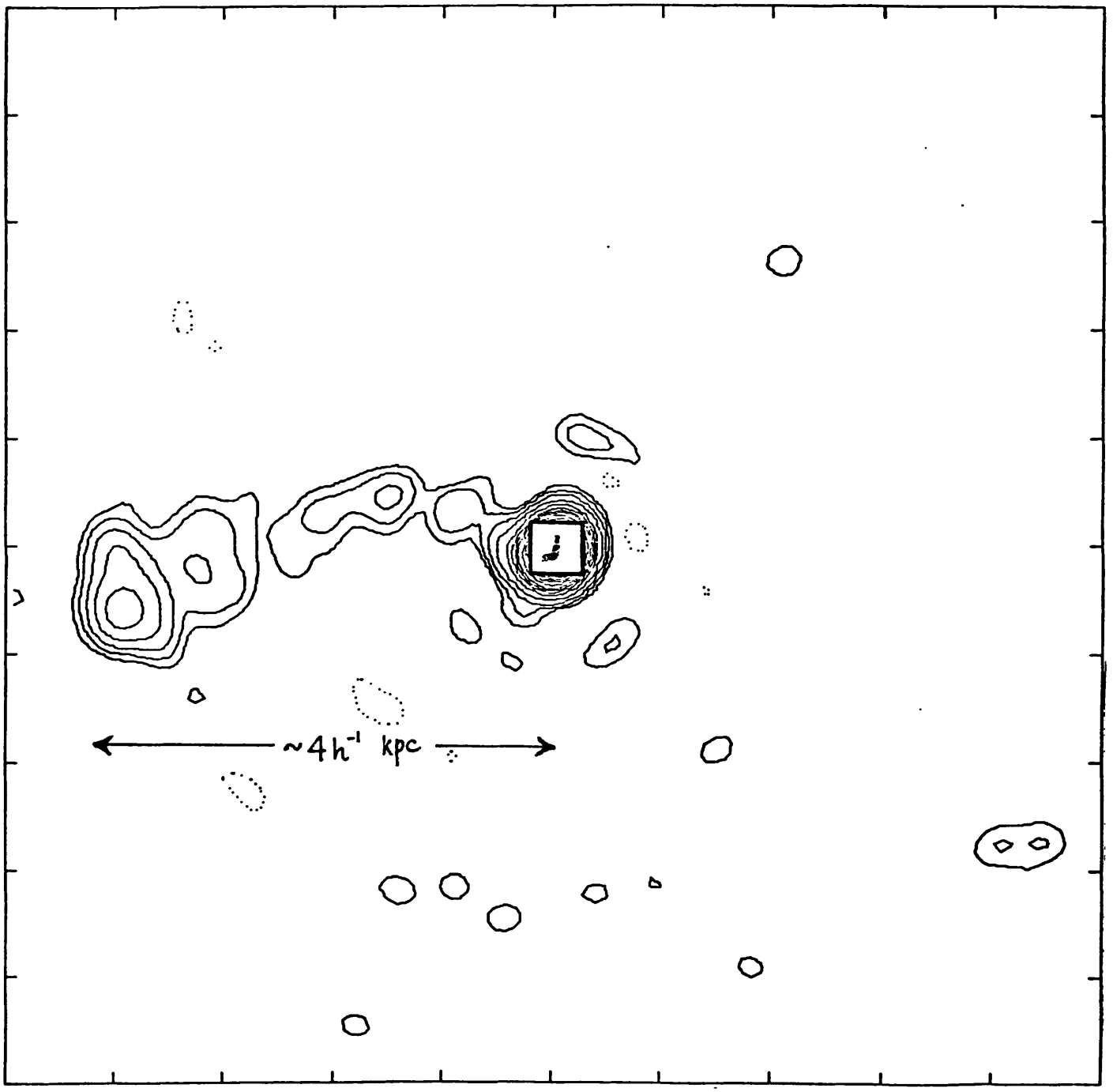

Fig. 2 : An attempt to show the overall jet in 3C309.1. Fig 1b has been reduced in size until it is on the same scale as Fig 1a.

are notoriously sensitive to the input parameters but do provide weak evidence that the beam velocity is relativistic about 150 pc from the core. This has led us first to try and interpret the overall jet shape as being a result of relativistic ballistic motion with with the "direction of fire" of the blobs changing with time. More specifically, in a precession model the cone angle of ejection must increase with time in order to fit the overall shape shown in Figure 2. This is a similar conclusion to that reached by Muxlow *et al.* (1984) to explain the rather similarly shaped jet in 3C418. On this type of explanation the sharp bend is basically an artifact of projection when the beam is close to the line of sight.

A good fit to the overall jet shape (not including the wiggles as yet) can be obtained with such a model – whose details are still under discussion and will be presented at a later date – but the number of free parameters involved in the fit means that without further information it cannot yet be regarded as a clear-cut demonstration of what is actually happening in the source.

Could instead the bend be due to the beam hitting the cosmic equivalent of a brick wall ? If so, then we must accept that the beam's hold on life is tenacious because it is not disrupted by the impact. Presumably, by analogy with the situation on larger scales, the wall is a very dense molecular cloud. The equipartition pressure in the beam (not assuming bulk relativistic motion in the calculation) is $\sim 3 \times 10^{-6}$ dyn cm^{-2}, which is two to three orders of magnitude higher than the minimum pressures in extended jets. Thus the putative cloud responsible for the bending must be made of considerably sterner stuff than those further out.

4. The Jet in the Nucleus of 3C380

The LAS of this quasar ($z = 0.691$) is $8''$ corresponding to about $32h^{-1}$ kpc. When mapped with sub-arcsec resolution with MERLIN the radio emission emerges as remarkably tangled and distorted for such a highly luminous source (Wilkinson *et al.* 1984b). The conclusion drawn from these maps was that the most likely cause of the distortions is a strong interaction between the radio-emitting plasma and its environment – and by analogy with 3C48 that the radio source may well be situated in a merging galaxy system. However the evidence for all this is only circumstantial. For this reason, two of us (PNW and TJC) have collected multi-array, multi-frequency polarisation data on the VLA to look for evidence of a large amount of dense gas in and around the radio source.

We now also have made a VLBI map of the radio nucleus which, like the VLBI map of 3C309.1, shows a jet with large apparent bends on the 100 pc scale. A preliminary version of the map, at 5 GHz and with a resolution of 1 mas, is shown in Figure 3. Note that although the brightest point is not exactly at the end of the jet, this does not necessarily mean that the jet is incipiently two-sided. Spectral effects can play tricks with the unwary observer and a second, higher frequency, map is needed to locate the flat or rising spectrum core.

The initial impression given by Figure 3 is that we are dealing with some sort of fluid flow phenomenon rather than a superposition of ballistically moving blobs – but this is a subjective opinion. Unfortunately, the structure of the entire source is so complicated

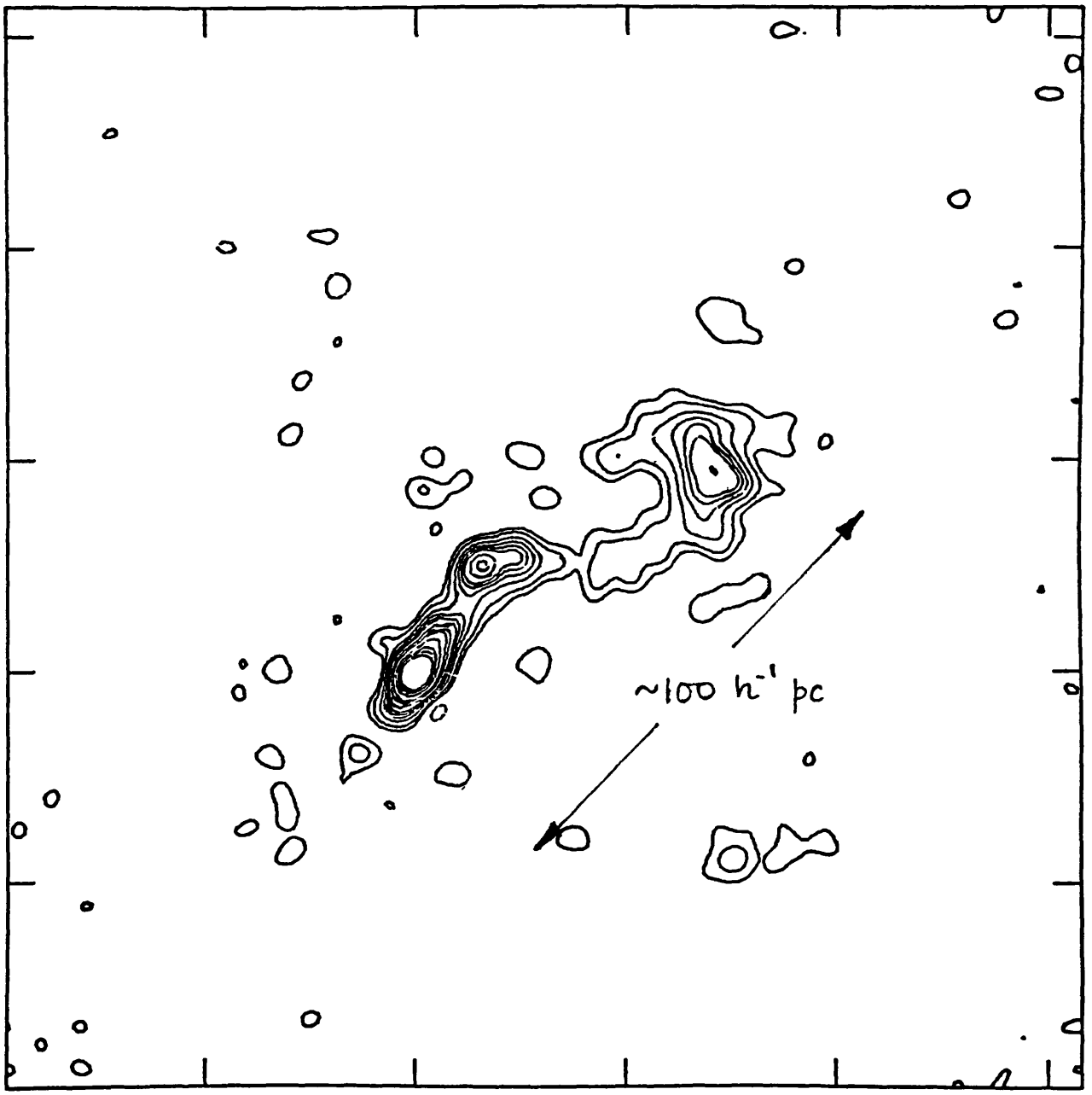

Fig. 3 : A VLBI map of the nucleus of the quasar 3C380 at 5 GHz; the resolution is 1 milliarcsec and the scale is 10 milliarcsec per tick mark.

that it is unclear where the beam goes after fading below the noise in Figure 3. About 40% of the total core flux is missing from this map and in order to reveal these lower surface brightness features we shall combine data from MERLIN with the present data; hopefully this new map might elucidate the beam's subsequent track somewhat better. For the moment, then, further interpretation of Figure 3 is premature.

5. CONCLUSIONS

If you really want to find bent, high luminosity, radio jets then SSCS in quasars are the places to find them – the two sources we have discussed here are merely examples among many. But, as we said in the introduction, radio intensity maps alone are not sufficient to tell us what is causing their peculiar shapes. Help is on the way in the form of the *Space Telescope*, and together with polarisation maps on sub-100-mas scales we should soon get a fair idea whether or not beam/cloud interactions are the underlying cause of this phenomenon. Whatever turns out, it will be fascinating to combine these data with direct velocity measurements. There is a lot to learn from these sources.

REFERENCES

Balick, B. and Heckman, T. M. (1983). Ap.J. **265**, L1.

Boroson, T. A. and Oke, J. B. (1982). Nature **296**, 397.

Bothun, G. D., Mould, J., Heckman, T., Balick, B., Schommer, R. A., and Kristian, J. (1982). A. J. **87**, 1621.

Heckman, T. M., Miley, G. K., Balick, B., van Breugel, W. J. M. and Butcher, H. R. (1982). Ap. J. **262**, 529.

Miley, G. K., Heckman, T. M., Butcher, H. R., and van Breugel, W. J. M. (1981). Ap.J.Letts. **247**, L5.

Muxlow, T. W. B., Jullian, M. and Linfield, R. (1984). *Proc. IAU Symp. 110, VLBI and Compact Radio Sources* (ed. R. Fanti, K. Kellermann and G. Setti), Dordrecht: Reidel, 141.

van Breugel, W. J. M., Heckman, T. M., Butcher, H. R. and Miley, G. K. (1984). Ap.J. **277**, 82.

Wilkinson, P. N. (1982). *Proc. IAU Symp. 97, Extragalactic Radio Sources* (ed. D. S. Heeschen and C. M. Wade), Dordrecht: Reidel, 145.

Wilkinson, P. N., Spencer, R. E., Readhead, A. C. S., Pearson, T. J. and Simon, R. S. (1984a). *Proc. IAU Symp. 110, VLBI and Compact Radio Sources* (ed. R. Fanti, K. Kellermann and G. Setti), Dordrecht: Reidel, 25.

Wilkinson, P. N., Booth, R. S., Cornwell, T. J. and Clark, R. R. (1984b). Nature **308**, 619.

DISCUSSION

Dick Henriksen. Supersonic ($M_j \gg 1$) jets can bend through $\psi \approx \sin^{-1}(1/\Gamma)$, where $\Gamma = C_p/C_v = 5/3$, or $4/3$ (relativistic), by oblique shocks without being "lobish" and decollimating.

Peter Wilkinson. I'm pleased to hear that !

DISTORTED QUASARS: CAN SHARP BENDS IN RADIO STRUCTURES BE ATTRIBUTED TO LOCALIZED COLLISIONS?

W. A. Christiansen
Department of Physics and Astronomy
University of North Carolina
Chapel Hill, N. C. 27514

J. O. Burns
Department of Physics and Astronomy
University of New Mexico
Albuquerque, N. M. 87131

J. T. Stocke
Steward Observatory
Tuson, AZ 85721

ABSTRACT

The radio structures of many distorted quasars seem to follow a distinctive pattern consisting of a "classical double" configuration with a single sharp bend. Thus, they resemble the shape of a dog's leg. We suggest that these dogleg structures are the result of collisions between the radio ejecta of the quasars and clumps of high density gas in the vicinity of the quasar. Specifically, the possibility that the "clumps" might be the ISM's or gaseous halos of companion galaxies is examined and found to plausible, although additional optical imaging and spectroscopy is needed to test this hypothesis.

INTRODUCTION

The study of distortions from the so-called linear, classical double structure of radio sources has, in the case of nearby radio galaxies, been a fruitful line of inquiry providing new insights into the nature of the local environment of the radio source. In general two major types of distortion have been identified: "S"-Type distortions, in which the source structure retains an inversion symmetric structure through the nuclear core. Such structures may most easily be attributed to "internal" causes confined to the radio galaxy itself; such as precession of the radio ejection axis or perhaps density gradients within the radio galaxy. "C"-Type distortions, in which the usual linear source structure appears to have a continuous bend. These structures may be attributed to "external" causes, such as motion of the radio galaxy through an external medium (head tail sources) or the existence of large scale density or pressure gradients external to the radio galaxy (wide angle tail sources). The "C"-type distortions seem to be associated with radio galaxies which are resident in clusters of galaxies.

Both types of distortion can be found in the structures of radio loud quasars; however, high resolution, high dynamic range VLA maps of distorted quasars indicate an interesting difference betweeen "C"-type distortions in quasars and radio galaxies. Specifically, distorted quasars usually appear to consist of two straight sections connected by an abrupt bend (resulting in a "dogleg" structure, as illustrated in Figure 1), rather than the continuous curvature usually found in "C"-type radio galaxies. In an extensive VLA

survey (in the "snapshot" mode) of 117 quasars with extended structures Hintzen et al., 1983, found that 19 sources had distortions with angles greater than 20°. Of these 19 distorted quasars, 17 appear to have the dogleg structure and only 2 appeared to have smoothly curved "C" shaped structures. In a complementary study we (c.f. Stocke et al., 1984) have used the VLA in both "A" and "B" configurations to obtain high resolution, high dynamic range (1000:1 peak flux to peak noise) maps of a small set of 4 quasars known from lower resolution observations to have distortion angles in excess of 20°. All four of these sources exhibit the dogleg structure rather than continuous curvature. Our 6 cm A-Array map of a prototype dogleg quasar, 3C 275.1 is presented in Figures 1a, 1b.

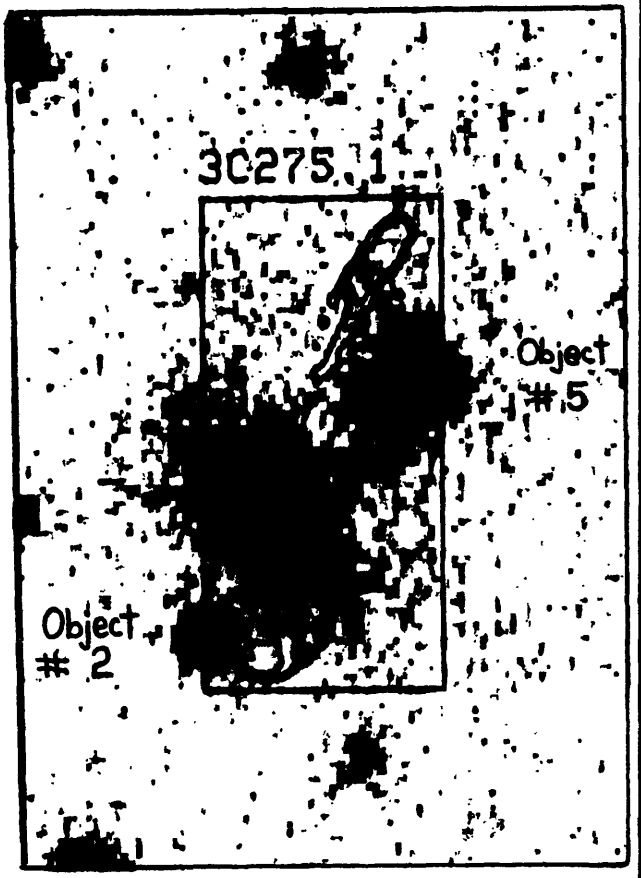

Figure 1a: The 6cm VLA A-Array map of 3C 275.1 superimposed on a 122 minute exposure through an R filter of the optical field taken with the KPNO 4m telescope and video camera by Hintzen, et al., 1981.

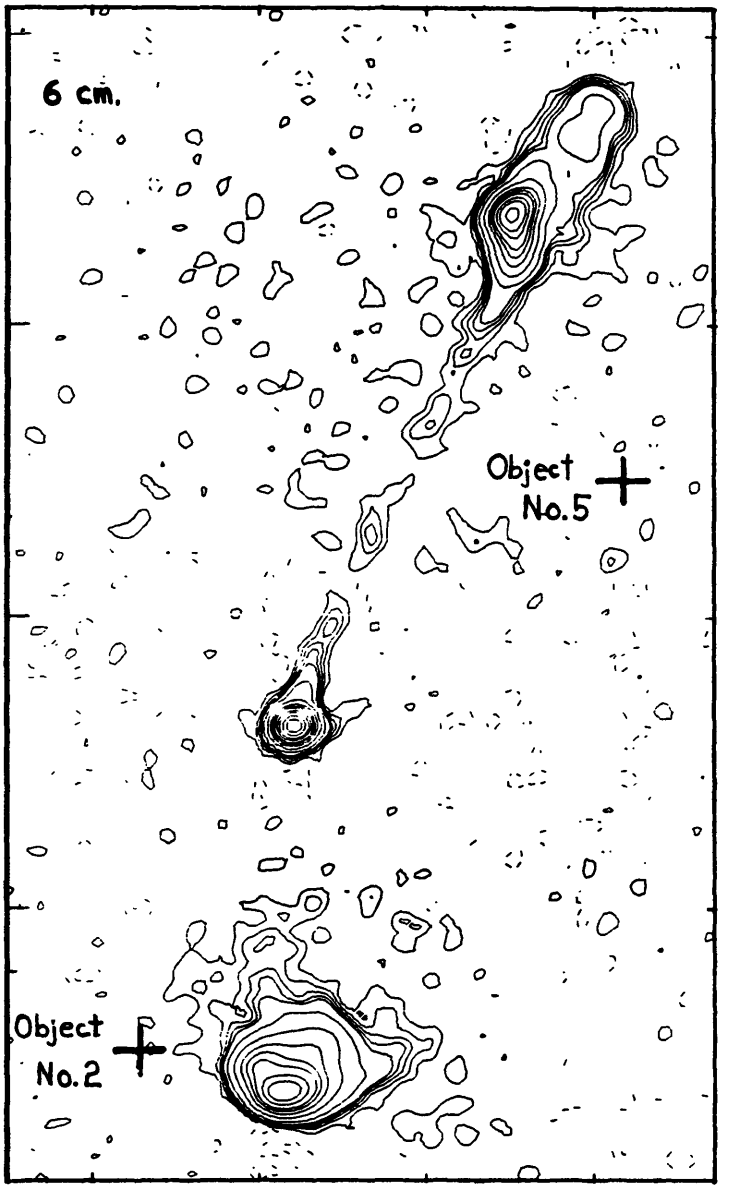

Figure 1b: The 6cm VLA A-Array full synthesis map of 3C 275.1. The contour levels are 0.17 Jylbeam*(-0.3, 0.3, 0.5, 0.8, 1.0, 2.0, 5.0, 10.0, 15.0, 20.0, 30.0, 40.0, 60.0, 80.0, 100)%.

INTERPRETATION

Because of the abrupt bending observed in the dogleg structures, we are led to hypothesize that the distortion is caused by a localized discontinuity in the environment external to the quasar. Specifically, we would like to consider the possibility that the sharp bends in dogleg quasars are caused by inelastic collisions between the quasar's radio ejecta and dense objects which might plausibly be found in the immediate vicinity of the quasar. Candidates for such intergalactic "targets" might be intergalactic clouds, such as those believed to comprise the "Ly α Forest" and/or the gaseous halos or interstellar media of galaxies themselves. For such a localized collision, which is illustrated schematically in Figure 2, we may write down a set of three kinematical constraints.

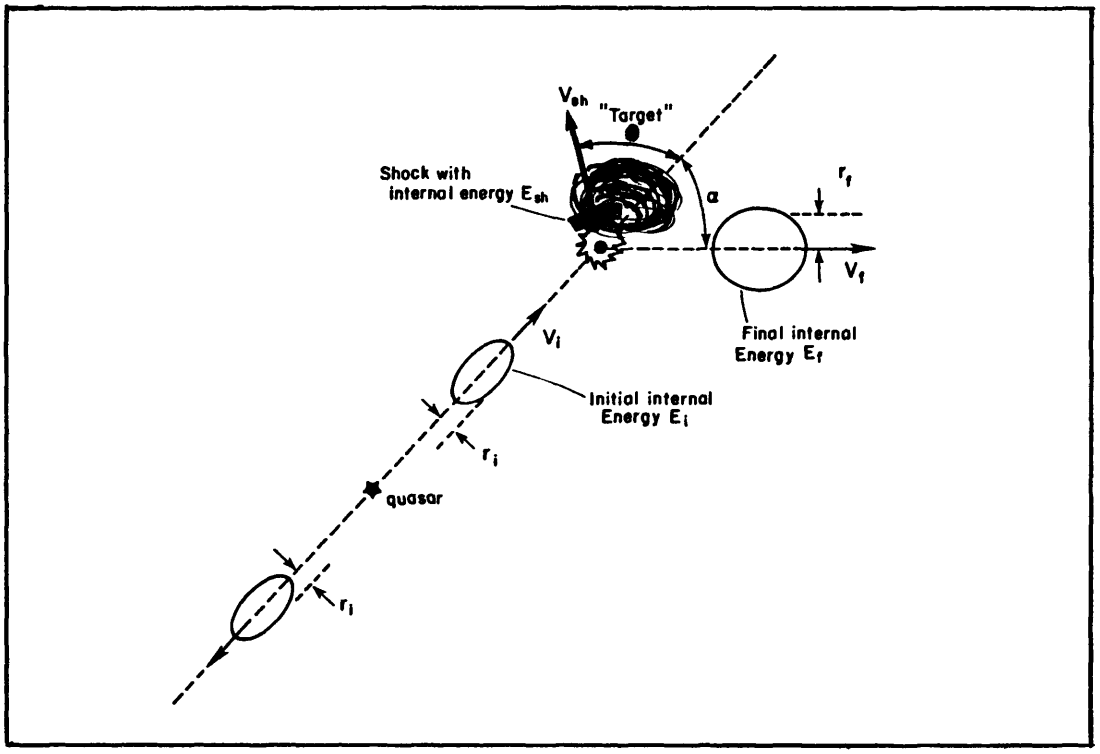

Figure 2

$$\text{Energy:} \qquad E_i + \frac{1}{2} m v_i^2 = E_{sh} + \frac{1}{2} m_{sh} v_{sh}^2 + E_f^2 + \frac{1}{2} m v_f^2 \tag{1}$$

$$\text{Momentum:} \qquad m v_f \sin\alpha = m_{sh} v_{sh} \sin\theta \tag{2}$$

$$m v_i = m v_f \cos\alpha + m_{sh} v_{sh} \cos\theta \tag{3}$$

where all of the above parameters are defined in Figure 2. There are clearly two many variables in equations (1), (2) and (3) to solve consistently so we have reduced the number of variables by making the following reasonable assumptions:

(1) Before the collision the radio lobe is "cold" i.e., $E_i \ll 1/2\ mvi^2$

(2) During the collision the outgoing lobe material is shock heated and thus the immediate post-collision internal ("thermal") energy is near equipartition with the thermal energy in the shocked halo gas,

$$E_{sh}(0) \simeq \frac{1}{2} m_{sh}(0)\ v_{sh}^2(0) \simeq E_{th} \tag{4}$$

where t = 0 at collision.

(3) Following the impact the shock-heated radio lobe expands adiabatically until ram pressure equilibrium is re-established:

$$E_f = E_{th}(r_i/r_f)^{3\eta - 3} \tag{5}$$

where η is the adiabatic index ($\eta = 5/3$ for an ideal gas).

With these assumptions the energy equation (1) becomes

$$\frac{1}{2} m(v_i^2 - v_f^2) = E_{th}\left(2 + (r_i/r_f)^{3\eta - 3}\right) \tag{6}$$

During the halo-radio lobe collision the thermal energy in the deflected radio plasma cloud must have been at least sufficient to balance the back reaction ram pressure for the galactic halo. Thus $F_\perp \leq E_{th}/r$ where $F_\perp$ is the average deflecting force during the collision. Then since the change in momentum perpendicular to the original line of flight is $\Delta P_\perp \sim F_\perp\ \Delta t$ where the collision timescale is

$$\Delta t \sim r_i/v_{sh} \sim r_i/(E_{th}/\pi r^3 \rho_c)^{1/2} = r_i(m/E_{sh})^{1/2} \tag{7}$$

$$\Delta P_\perp \sim (E_{th} m)^{1/2} \sim m\ v_f\ \sin\alpha \tag{8}$$

From equations (6) and (8) we can now derive an upper limit of v_f

$$v_f^2 \lesssim v_i^2/\left(1 + \sin^2\alpha\ (4 + 2(r_i/r_f)^{3\eta-3})\right). \tag{9}$$

Within the context of these constraints a few requirements emerge concerning the post collision structure of the radio source: (1) Because of the heating which occurred during the collision, the lobe which suffered the collision will be more expanded and closer to the quasar than the lobe which was undisturbed. (2) The ratio of the penetration distances and sizes of the two lobes is a sensitive function of the deflection angle as can be seen from equation (9) above. (3) For reasonable quasar energetics (i.e. E total $> 10^{58}$ ergs) and nonrelativistic ejection velocities ($v_i < 0.1c$) the target must absorb a lot of momentum in order to cause the observed deflection. For a deflection of $\sim 30°$ the mass of the target must exceed $\sim 10^8\ M_\odot$.

Given the above restrictions we now turn to the nature of the target. The lower limit for the target mass just overlaps with the mass range allowed for the Ly α Forest clouds and is also in the range of the "intergalactic" HI clouds which have been detected in some clusters of galaxies.

On the other hand, the gaseous component of ordinary galaxies often greatly exceeds 10^8 $M_\odot$ and the possibility that galaxies themselves are targets has the advantage that we can test this hypothesis by searching for galactic images located in the immediate vicinity of the sharp bend in the dogleg structures. We note that the probability of a radio lobe-galaxy collision is a simple convolution of the mean lobe solid angle plus the mean solid angle covered by a companion galaxy within one radio lobe stopping distance of the quasar. The mean lobe solid angle ($\Omega_\ell \sim 0.2$ STR) has been estimated from the mean size/separation ratios for classsical doubles (c.f. Stocke, et al., 1984). We do not know the extent of either ISM's or gaseous halos of galaxies during the quasar era; however, based on Perrenod's, 1978, models of the evolution of the intergalactic (or intercluster) medium which involve extensive stripping of gas from galaxies as clusters evolve, we suspect that the gas content of companion galaxies (especially ellipticals) could have been higher. To obtain an order of magnitude estimate of the collision probability we simply assume that the radius of the galactic gas distribution is of the same order of magnitude as the visible light distribution, ~ 10 kpc. The probability of a lobe galaxy collision is then

$$P_c \sim 0.07\ N_c$$

where N_c is the average number of companion galaxies within one penetration distance of the quasar. According to the survey of Hintzen et al., the incidence of the dogleg phenomenon is about 15%. Thus if $N_c \sim 2$ the galactic collision hypothesis may indeed provide a plausible explanation for the evidence of the dogleg phenomenon. This number of companions is almost an order of magnitude less than the average number of galaxies found within a core radius of rich Abell clusters ($N \sim 13$) according to Bachall, 1975.

Finally, we have carefully examined optical images of the fields of our 4 dogleg quasars. In 3 of the 4 cases (3C275.1, Figure 1a, 3C270.1, and 4C25.01) there is indeed a faint object projected at the vertex of the bend. Lacking redshift data we can say no more; however, for 3C275.1 Hintzen, 1984, has obtained a redshift for object #2 and finds it is indeed a companion of the quasar ($Z \sim 0.56$, for both objects).

CONCLUSION

While we are well aware of the dangers of post facto statistics in identifying galaxies as targets for quasar radio lobe deflections, we feel that further exploration of this hypothesis may provide new insights into both quasar radio physics and possibly the evolution of the intergalactic medium through the effects of such dramatic encounters on the gas content of the target galaxy.

Bachall, N. A., 1975, Ap. J., 198 249.

Hintzen, P., 1984, private communication.

Hintzen, P., Boeshaar, G. O. and Scott, J. S., 1981, Ap. J., 246, L1.

Hintzen, P. Ulvestad, J., and Owen, F., 1983, A. J. 88, 709.

Perrenod, S., 1978, Ap. J., 226, 566.

Stocke, J. T., Burns, J. O. And Christiansen, W. A., 1984, submitted to Ap. J.

DISCUSSION

Paul Wiita. Is there a redshift known for the companion of the second QSR ?

Wayne Christiansen. For the second QSR, which is 4C25.01, the companion doesn't have a known redshift.

Paul Wiita. In 3C275.1, most of the bending appears to occur in the northern jet, close to the QSR core. The inner part of the northern jet seems to point very nearly towards the southern lobe, implying little or no bending needed there.

Wayne Christiansen. The bending angle at the core is hard to measure because the bending at the core is on a scale only slightly greater than our own beam size, but we can estimate an upper limit of 11°. This upper limit is still considerably less than the overall bend of 23°.

Alan Bridle. I agree with Paul's concern over 3C275.1, and I am puzzled that the supposed deflector in its case is so far from any of the bright radio features of the southern lobe.

WIDE ANGLE TAIL RADIO GALAXIES

FRAZER N. OWEN

National Radio Astronomy Observatory[a], P.O. Box O, Socorro, New Mexico 87801

ABSTRACT. In the last ten years a class of radio source has been recognized in clusters of galaxies, which have been called "Wide Angle Tails". These sources resemble head tail sources like NGC1265 and 3C129 except that they have an angle of more than 90° between their twin tails. The prototype of the class is 3C465. Initially, it was thought that these sources were simply-slower moving examples of the NGC1265 class. While this still may be true, it is also clear that this type of source is always associated with central dominant galaxies in clusters, which are likely to be almost at rest in the cluster relative to the cluster gas. Simple quantitative models which are used to explain "Narrow Angle Tail" sources like NGC1265 require much larger velocities for the "Wide Angle Tail" galaxies than seems possible ($v > 1000$ km/sec). Alternative pictures are possible. These include using $\mathbf{j} \times \mathbf{B}$ forces or cool clouds to deflect the tails. Also, slowing down of the jets due to entrainment may help explain these structures. Further work is necessary, including the effects of realistic models of the structure of the cluster gas and the gravitational potential, for these sources to be understood.

[a] The National Radio Astronomy Observatory (NRAO) is operated by Associated Universities, Inc., under contract with the National Science Foundation.

INTERPRETATION OF RADIO POLARIZATION DATA

ROBERT A. LAING[1]

Royal Greenwich Observatory

The Workshop organizers asked me to review the interpretation of radio polarization data, partly because misinterpretations are evident in the current literature, and partly because we now know more about the possible Faraday-rotating and depolarizing phases around radio sources than we used to.

1. BASIC THEORY

The basic theory is all in a classic paper by Burn (1966) that is much *referenced*, but (I suspect) not often *read*. We define a *complex polarization*

$$Q + iU = P \exp(2i\chi)$$

where P (real) is the polarized intensity and χ is the position angle of the polarization. The *Faraday depth* of a point $\mathbf{r}$ with respect to an observer at the origin,

$$\phi(\mathbf{r}) = K \int_0^r n\mathbf{B} \bullet \mathbf{dl},$$

measures the integral out to r of the line-of-sight $\mathbf{B}$ times the thermal electron density n in any intervening media. K is a constant, 8.1×10^5 for ϕ in radians, n in m^{-3}, B in gauss and l in parsecs. The *Faraday dispersion function* $F(\phi)$ measures the polarized flux coming from a Faraday depth ϕ, and there is a Fourier transform relation

$$P(\lambda^2) = \int_{-\infty}^{+\infty} F(\phi) \exp(2i\phi\lambda^2) d\phi$$

between the complex polarization and the Faraday dispersion function. Unfortunately one cannot exploit the inverse transform

$$F(\phi) = \pi^{-1} \int_{-\infty}^{+\infty} P(\lambda^2) \exp(-2i\phi\lambda^2) d(\lambda^2)$$

to find $F(\phi)$ from $P(\lambda^2)$ in practice, as (a) we would need to know $P(\lambda^2)$ for $\lambda^2 < 0$ – this would be the polarization observed if all of the magnetic fields were reversed – and

[1] Reconstructed and edited from a tape recording and Dr. Laing's viewgraphs by A.H.Bridle – Eds.

(b) the data are too poorly sampled in λ^2. We therefore exploit less direct approaches using models of the distribution of Faraday depth, and these get us into trouble.

I will briefly review the relations between rotation and depolarization as a function of wavelength for different distributions of thermal material and magnetic fields relative to the radio source, and on different angular scales relative to the beam of the telescope.

2. Foreground Screens

(a) Resolved foreground screen. The simplest possible case is foreground matter that is resolved by the telescope, so the Faraday depth is effectively constant across the beam. In this case there is no depolarization, and the apparent position angle varies as

$$\chi(\lambda^2) = \alpha + R\lambda^2$$

where α is the intrinsic (zero-wavelength) position angle of the polarized emission at the source, and R is the "rotation measure" of the screen (equal to the Faraday depth ϕ at the far side of the screen).

(b) Unresolved foreground screen. The first complication, even with no thermal matter in the source at all, comes in the case of an unresolved foreground screen. The rotation measure R then varies across the beam of your telescope, so the beam vectorially adds polarized signals that have been rotated by different amounts. This generally causes depolarization. In general, the rotation of position angle $\delta\chi \not\propto \lambda^2$ in this case, its form depending entirely on the distribution of irregularities ("clouds") across the beam, and many different behaviours are possible.

A simple case would be a uniform source viewed with two clouds with equal and opposite rotations in the beam. This produces no net rotation, but either depolarization or *re*polarization may occur as the observing wavelength is varied. If the screen has a *Gaussian* distribution of irregularities, the polarization has a wavelength dependence (Burn 1966)

$$P(\lambda^2) \propto \exp -(\lambda/\lambda_0)^4.$$

It has occasionally been said that this dependence is a characteristic of a foreground screen, but it is a characteristic only of foreground screens with a well-defined *scale size* (which enters into the prescription of λ_0). A real screen will have a range of scale sizes, and will produce a smoother variation of $P(\lambda^2)$, lacking the sharp cutoff. It can be though of as superposing a collection of laws of the above form, and the resulting $P(\lambda^2)$ variation depends on the spectrum of the scale sizes in the screen. If the scale sizes of the irregularities in the screen are small compared with the beam, and if the field is stochastic, there will generally be depolarization without much net Faraday rotation. Whether or not there is net rotation depends entirely on whether or not there is a net preferred field direction in the screen.

3. Mixed Thermal and Emitting Media

(a) The uniform slab. Suppose the source contains mixed thermal and relativistic (i.e. synchrotron-emitting) electrons and a fairly uniform magnetic field. The first approximation to this case is the uniform slab, or cube, of depth L, thermal density n and

magnetic field B_z along the line of sight. Figure 1 sketches the behavior of $P(\lambda^2)$ and $\chi(\lambda^2)$ for this case, also assuming uniform radiating electron density. Here $P \propto \sin\delta/\delta$ where $\delta = KnB_zL\lambda^2$.

It is often said that the position angle χ rotates as λ^2 in a slab model. It does, but only in the range $0 \leq \chi \leq \pi/2$. At the wavelengths where $P(\lambda^2)$ goes through zero, $Q + iU$ goes through zero, so *both* Q and U must change sign. As $\chi = (1/2)\tan^{-1}(U/Q)$, χ must change by $\pi/2$ at these wavelengths, giving rise to a "sawtooth" $\chi(\lambda^2)$ variation. This is, of course, an extreme approximation to a more realistic situation, which I mention here only to point out that, contrary to a common misconception, the $\delta\chi \propto \lambda^2$ variation does not continue indefinitely with increasing wavelength.

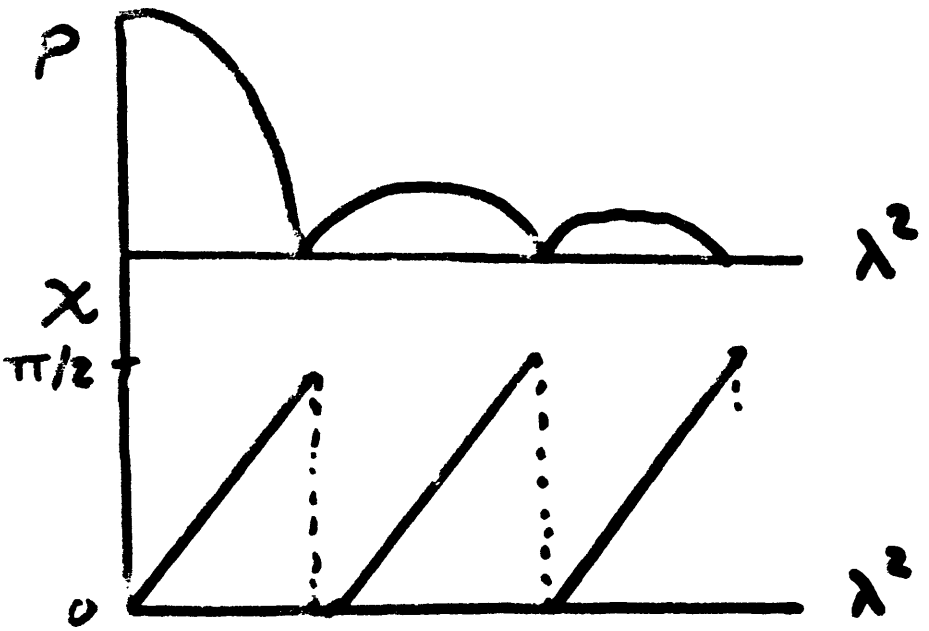

Figure 1. Sketch of P and χ as functions of λ^2 in the simple uniform slab model, after Burn (1966).

(b) More realistic mixed geometries. In most realistic cases, $P(\lambda^2)$ does not have zeroes, so $\chi(\lambda^2)$ varies continuously. Most cases with uniform fields resemble the curves sketched in Figure 2. The sphere and the cylinder are soluble analytically, and I'm sure some other cases are – again, for some explicit examples, see Burn (1966).

Basically, in all cases P falls towards zero with increasing wavelength, with possibly some wiggles, while the rotation $\delta\chi \propto \lambda^2$ until $\delta\chi \sim \pi/4$ or so, then the rotation generally falls below the extrapolation of this law. The detailed behavior depends very much on the geometry, but the main point is that $\delta\chi$ does not increase $\propto \lambda^2$ indefinitely. The fundamental distinction between this behavior and that of the foreground screen is that the foreground screen rotates all emission from the source behind it by the same amount $\delta\chi$, while thermal material mixed with the source rotates different parts of the source emission through different angles.

The condition for the λ^2 rotation law is that the Faraday dispersion function is

symmetrical about some rotation measure R, i.e. that $F(R-\phi) = F^*(R+\phi)$. This condition is fulfilled by the slab, by some other special mixed geometries, and by the foreground screen, but it is not generally fulfilled by *realistic* geometries for quasi-ordered fields and mixed-in matter. The range of λ^2 rotation that can be produced by mixed-in thermal material depends on the detailed geometry – but if λ^2 rotation persists over $\delta\chi > \pi/2$, and *certainly* if it persists over $\delta\chi > \pi$, you can be sure that you are not observing entirely mixed-in gas, but are dealing with a foreground screen to some extent.

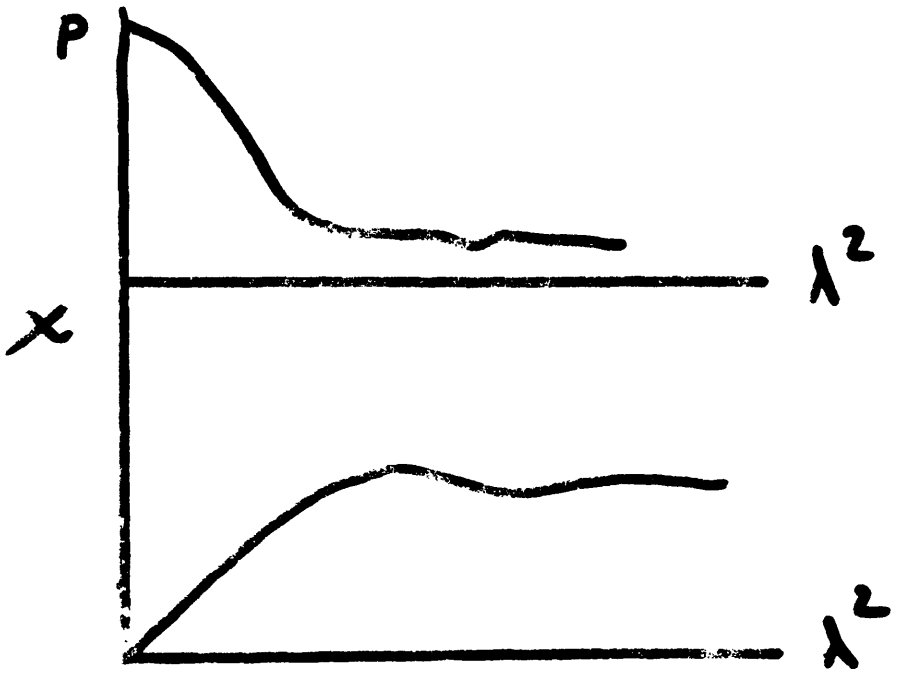

Figure 2. Sketch of P and χ as functions of λ^2 in a more realistic geometry, after Burn (1966).

4. Summary of Diagnostics

- **λ^2 rotation, no depolarization** – a foreground screen is producing the rotation.
- **λ^2 rotation, with depolarization** – rather messy, and the possibilities depend on the range of rotation observed.

If the observed rotation $\delta\chi < \pi/2$, it may be occurring either within the source, or in a foreground screen, or both. If it is entirely within the source, it should not continue as $\delta\chi \propto \lambda^2$ at longer wavelengths.

If $\delta\chi > \pi/2$ while remaining $\propto \lambda^2$ in the presence of depolarization, there is probably a foreground screen and something else as well, either inside the source or in front of it. The depolarization could be due to a two-phase foreground medium in which n and $\mathbf{B}$ vary smoothly on the large scale but there is cloud structure on the small scale (e.g. narrow line clouds in a hot medium). Alternatively, the depolarization could be occurring inside the source while some rotation occurs outside it. It may not be possible *in principle* to distinguish these alternatives unless the media involved can be seen in some other way.

• **deviations from λ^2 rotation, with depolarization** – the worst case, and very hard to sort out. Mixed geometries with quasi-uniform fields inside the source are possible, as are partially resolved foreground screens, or a mixture of the two.

• **depolarization without rotation** – this can indicate an unresolved foreground screen, or material internal to the source. *Re*polarization without rotation would signify that something is afoot in a foreground screen.

• **the best tests** of whether you understand what you're seeing are to keep decreasing the beam size at a given wavelength until nothing further happens, and to keep increasing the wavelength until you learn whether the range of the λ^2 rotation exceeds that consistent with mixed-in gas.

• **are upper limits safe ?** – unfortunately not. It is possible to get a high percentage polarization from a field with many reversals if the field is sufficiently anisotropic (Laing 1980, 1981). In this case, the rotation through the medium is a random walk which ends up with a mean close to zero, and quoting an upper limit to the thermal density n from an upper limit to Faraday rotation or depolarization is extremely dubious unless you include a factor to take account of the (unknown) number of reversals along the line of sight. This can give, in quite realistic cases, an extra factor of 10^2 or 10^3 in n. I do not wish to imply that I think that jets or screens *are* much heavier than previously thought, but the density *limits* often seen in the literature are unreliable for this reason.

5. Types of Foreground Medium

What phases of the foreground medium are likely get in our way and possibly be confused with thermal matter in the source itself ? There is an array of possibilities.

Relevant to polarization VLBI and to broad-band studies of compact sources is the optical broad line region. It is comparable in scale to the VLBI jets, and will completely depolarize any parts of the source that we happen to view through it. The probability of a broad line region covering a large fraction of a VLBI jet is also quite small however. Effects of the broad line regions have yet to be clearly detected.

Extended narrow line regions will depolarize the source, and their effects are now becoming well known through the work of Wil van Breugel, Tim Heckman, George Miley, Harvey Butcher, and their colleagues. Most of these regions probably consist of dense clouds with relatively small filling factors, incoherently rotating the polarization across the instrumental beam, producing foreground depolarization. This phenomenon must be remembered when we observe high luminosity sources in which it is difficult to map the extent of the forbidden line regions spectroscopically. I am aware of powerful sources where the polarization in the bridge disappears close to the galaxy for no apparent reason. As the forbidden line luminosities from these objects are large, we should suspect that they may have extensive forbidden line regions which will produce strong depolarization.

Another relevant phase of the ISM of the parent radio galaxies has been detected by observations of smooth rotation measure gradients across M84 by Alan Bridle and myself, and was also seen at this Workshop in the data Tim Cornwell showed for 3C449. In M84 (Figure 3) we detect coherent rotation measure patterns on a scale of several

kiloparsecs (comparable to that of the associated *Einstein* X-ray source) and aligned parallel to the major minor axis of the outer stellar distribution of the galaxy. The maximum excursions of the rotation measure are between +35 rad m^{-2} and −35 rad m^{-2}, at the 3.″9 resolution of Figure 3. The rotation measure gradients are antisymmetric with respect to the nucleus and are of both signs (so there must be large-scale field reversals in the rotating medium). M84 is near the galactic pole, and the galactic foreground rotation close to zero. This coherent large scale rotation measure structure is well resolved and occurs without any depolarization. These properties distinguish it from the media detected elsewhere by their forbidden lines. The forbidden line media heavily depolarize the sources and have no coherent large scale rotation measure structure.

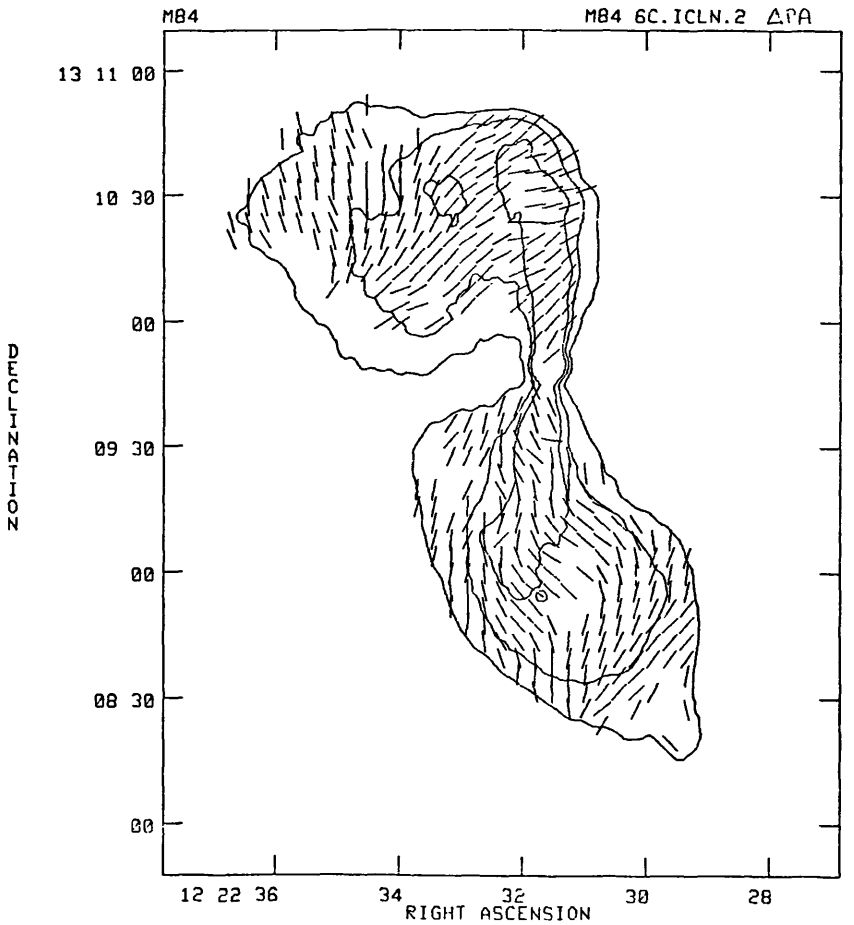

Figure 3. The distribution of $\delta\chi$ between 20cm and 6cm across M84 displayed on total intensity contours to show the outline of the radio source. The vectors are of equal length, their orientations showing the angle $\delta\chi$ (zero rotation is displayed as a vertical vector). Note the banded pattern of the rotation, and the asymmetry of the rotation pattern with respect to the central core. Data from R.A.Laing and A.H.Bridle, in preparation.

The rotation measure structure, and the X-ray source, in 3C449 both have a much larger physical scale than in M84, but many of the other characteristics are similar

– field reversals, and a reasonably ordered, well resolved rotation measure structure. Although the rotation measure structure in 3C449 is not sampled as two-dimensionally as that in M84, due to the shape of the radio jets in 3C449 (Cornwell and Perley, these Proceedings), the medium in 3C449 cannot be entirely mixed into the jets as it exhibits too much λ^2 rotation (Cornwell, private communication). I suspect that in M84 and 3C449 we are seeing rotation in large scale magnetoionic haloes of the parent galaxies. These screens may also be similar to that producing the rotation measure gradients along the jet in NGC6251 (Perley *et al.* 1984). As the jet in NGC6251 is one-sided one cannot be certain that the Faraday screen in that galaxy is not a disk, rather than being spherically distributed as appears to be the case in the two-sided sources M84 and 3C449. These screens have Faraday depth gradients which will cause apparent depolarization in low resolution observations at low frequencies; such depolarizations could be, and have been, falsely interpreted as "weighing" their jets.

We do not yet have any evidence for magnetic fields in the hot intracluster media detected at X-ray wavelengths, but they will be a further complication for polarization observations if they exist.

Finally, the inhomogeneities in our galaxy may be more of a problem than we have realised, particularly near the galactic plane and in the regions away from the plane where Phil Kronberg and colleagues have found large rotation measure anomalies. Cygnus A is a possible example; it has the largest rotation measure gradients known for an extragalactic radio source and is seen through a spiral arm region close to the plane with lots of neutral hydrogen and ionized gas. There is a large concentration of possible anomalous depolarizers and rotators in the galactic plane, and we should not forget them !

REFERENCES

Burn, B. J. (1966). M.N.R.A.S. **133**, 67.
Perley, R. A., Bridle, A. H. and Willis, A. G. (1984). Ap.J.Suppl. **54**, 291.

DISCUSSION

John Wardle. Burn is misleading on the high-λ^2 variations in the mixed geometries because he calculates an expectation value of the rotation; it really becomes undetermined, as all the different parts of the source become out of phase. There's really no reason for χ to go one way or the other in that regime. You wouldn't, for example, look for a flat rotation law at long wavelengths.

Robert Laing. I didn't mean to imply that you would. The curve I drew for $\delta\chi$ in Figure 2 is just a crude approximation to Burn's solution for a sphere. I quite agree, and it's not the detailed shape of the curves that I'm emphasising. The point is that you don't have a variation that keeps on going as λ^2 when the polarization starts getting low.

John Dreher. When you do get into that depolarized regime in practice, that's where it becomes extremely difficult to measure a rotation anyway. The fact that the flattening of the $\chi(\lambda^2)$ shape there might be used to tip you off that this was happening is theoretically nice, but I don't think it's very practically useful.

Robert Laing. I think that's a limitation of the restricted number of wavelengths. It's not out of the question with more wavelengths for observation.

George Seielstad. But that's where you're measuring very weak polarizations.

Robert Laing. Yes, but if you start off with a polarization as high as 60% you should be able to do this if you're careful.

John Wardle. The deviations from the λ^2 law start before the polarization has fallen to half of its value at short wavelengths, and that's easily observable. The corollary is that you should be very careful intepreting rotation measures if the polarization *is* below a half of the short-wavelength value.

Alan Bridle. It's also important to realise that this *is* the regime people must be getting into when they start talking about measuring thermal densities in jets, and that's why we should be careful about how to diagnose it and interpret it properly. Incorrect density estimates get fed back into the velocity quagmire as incorrect velocity limits.

Frazer Owen. I think the case for a foreground medium in M84 is very convincing, but in 3C449 it's not very convincing because the rotation measure structure there correlates with the lobes, and the jets don't show it. It could very easily be an internal pattern there.

Robert Laing. But Tim Cornwell has shown that the rotation is varying as λ^2, which is a good argument for it being in front of the jets. One can argue whether the foreground is local, or associated with the galaxy. My prejudice in this case is that it associated with the 3C449 galaxy; it has the right scale for the X-ray source and it really does oscillate up and down along the jet if you look carefully. The problem with most jet sources is that they are so one-dimensional ! That's why M84 is so nice. We need to repeat this exercise on some sources with big lobes to find out whether there are significant correlations with the radio intensity structures.

Frazer Owen. I'm bothered by attributing it *all* to the foreground screen. It's clear there must *be* a foreground screen, because of the big shift in the zero point of the rotations, but I'm not so clear that the fluctuations must be a result of a foreground screen. In M84 it's all very close to the nucleus, you're looking at a much smaller region there. In 3C449 you're really looking at something analogous to a cluster medium. It's much less convincing that it would have these fluctuations.

Robert Laing. There you need to go to lower frequencies to get more rotation.

Frazer Owen. That won't help, you'd just see the same foreground screen.

John Wardle. But if it's *resolved* it would help if you saw depolarization, as that has to be internal.

Robert Laing. If it's *well* resolved. But if you see more than 90° or 180° *in the variations* going as λ^2, then you know that *the variations* are also foreground, not just the mean.

Frazer Owen. Or some part of it.

Robert Laing. You can always attribute 30° or 45° of λ^2 rotation as an internal effect, but not a lot more. It would obviously be hard to rule out that much being internal, if you see more in the total.

Arieh Königl. In 3C449 the gradients seem to be symmetric about the nucleus, while in M84 they are less so. Is that correct ?

Robert Laing. They are antisymmetric, rather than symmetric, in M84 – the rotations immediately south of the nucleus are positive, while those immediately north are negative. As you say, in 3C449, it's mainly symmetric.

John Dreher. "Depolarization" can even be observed in the absence of *any* Faraday effects. If one has an unresolved $\Delta\alpha$, with an associated gradient in (intrinsic) position angle of the polarization, then regions of different α will "beat" against one another to produce varying *apparent* polarization. This effect is frequently seen to occur around flat spectrum cores where they are not fully resolved from steeper spectrum jets. It can also happen where hot spots or jets are seen superimposed on a steeper-spectrum bridge.

Robert Laing. Yes, I should have mentioned that – it's also in Burn (1966) !

VLBI POLARIMETRY – FIRST RESULTS

J.F.C.WARDLE AND D.H.ROBERTS

Physics Department, Brandeis University, Waltham. MA 02254

ABSTRACT. We have made successful first epoch observations of the polarization distribution in several compact radio sources, using four antennas of the U.S. VLBI Network at λ6cm with a resolution of $\approx$ 2 mas. The polarization map of the well-known superluminal quasar 3C345 shows the following features. The compact opaque core is essentially unpolarized ($<$ 1 %). Nearly all the polarized flux is associated with the jet. The inner knot in the jet (component C3 in Unwin *et al.* 1983 – *Ap.J.*, **271**, 536) is $\approx$ 21% polarized in position angle 17°, and the outer knot (C2) is $\approx$ 11% polarized in position angle 85°; the position angle of the jet is −75°. These high degrees of polarization imply that the internal Faraday rotation in the jet is small, and that the density of ultrarelativistic electrons in it greatly exceeds the density of thermal electrons.

ENERGY TRANSPORT IN RADIO SOURCES:

EFFICIENT OR NOT?

D. S. De Young
Kitt Peak National Observatory
National Optical Astronomy Observatories*
P.O. Box 26732
Tucson, Arizona 85726-6732

ABSTRACT. The question of the flow velocity of the material which powers the extended and compact radio sources is considered, as this issue is crucial to energy transport in radio sources. The various velocity indicators are reviewed and their implications examined. The principal conclusions are that there is strong evidence for non-relativistic flow on the large scales, and that there are serious problems with relativistic flow in compact sources. Thus the "standard model" of radio sources may have to undergo significant revision.

1. INTRODUCTION

Though the original title of this review was sidedness, velocity and unification, it will basically revolve around the question of velocity. However, in discussing velocity, the issues of sidedness and unification will naturally arise. First I shall list what I feel to be indications for the velocity of the radio emitting material which is flowing from the nucleus to the extended radio sources. These will be discussed to varying extent in what follows.

A. Direct and Unambiguous Indicators
   None

B. Semi-Direct Indicators
   Optical Emission Lines

C. Indirect Indicators
   Radio Morphology
   Radio Brightness Distribution
   Change in Angular Extent with Time
   X-Ray Observations
   Spectral Index Changes

*Operated by the Association of Universities for Research in Astronomy, Inc., under contract with the National Science Foundation.

The implications of these velocity indicators will be discussed in terms of what I call the "standard model" first put forward by Blandford and Rees (1974). Recall that this model begins with an unspecified source of relativistic plasma deep in the nucleus of the parent galaxy or QSO, perhaps together with some dynamically unimportant magnetic field. This extremely hot gas inflates a cavity in a surrounding cooler gas cloud, and if the cloud is rotationally flattened and axisymmetric, the hot relativistic gas may "break out" in opposite directions along the axis of rotation. (It should be mentioned that this process has never been calculated, although some work on one-sided jet formation has been done by Rayburn (1977), Wiita (1978) and Smith et al. (1983)). If the presumed de Laval nozzles can actually form, the random motion of the relativistic plasma is converted via a sonic transition to cold, collimated relativistic flow.

This "standard model" has many virtues, the principal ones being that it is the most efficient way of supplying energy to the extended radio sources and that it naturally accounts for their double nature. In addition, relativistic motion can explain some of the phenomena observed in compact radio sources, and for all of these reasons it has become generally accepted as the explanation of energy transport in extended radio sources. However, it is well known that there are some observations which cause problems with this model, and in my view they are severe. In accord with Alan Bridle's earlier remark which encouraged heretical thinking, I should like to discuss the importance of the various velocity indicators in the context of the following question: Is there relativistic velocity on any scale?

2. LARGE SCALE STRUCTURE

Morphological indicators, though very indirect, are abundant for the large scale (>10 kpc) structure of radio sources. Particular problems for relativistic motion arise when considering the morphology of the lower luminosity, "edge darkened" radio sources, a classic example of which is 3C 449 (Perley et al., 1979). These sources show curvilinear structure which can be described as "bends", "wisps", and "plumes". Such structures are not what one would associate with collimated relativistic flow with extremely high rigidity. In fact, the outer extensions of sources such as 3C 449 bring most to mind the flow associated with subsonic, turbulent plumes. Another class of source whose morphology looks non-relativistic are cluster sources such as 3C 465 and the remarkable object 1919+479 (Burns, 1981). It is not clear at all as to how these objects are distorted, though Eilek et al. (1984) have discussed several possibilities. What seems clear is that the structure is most consistent with low

velocity flow rather than a rigid relativistic beam with extremely high momentum per unit mass.

Another problem associated with this general class of distorted sources lies in their brightness distribution. The highest values of surface brightness lie in the inner regions of the radio structure in the form of bright knots. In the context of the "standard model" high surface brightness knots occur at the end of the beam when it is decelerated via a shock front due to its encounter with the surrounding medium; a picture which is directly contradicted by the observations. The standard assumption is that one somehow can produce shocks in the inner regions of the beam without disrupting it, perhaps with oblique shocks. However, this has never been calculated for a relativistic beam, nor is it clear how such shocks could be maintained, or if shocks sufficiently strong to produce the observed bright spots will also disrupt the flow. Similar problems arise with C-shaped sources such as NGC 1265. Not only do these contain bright spots near the nucleus, they are also bent, and they show wisp or plume-like structures in their low surface brightness regions.

Bending itself poses a dilemma for relativistic and even hypersonic flow. Changing the direction of such flows almost invariably results in a shock in the region of such a change unless the "ductwork" is very carefully constructed. Thus for relativistic flows one would expect a bright spot in the radio emission to occur whenever a bend occurs, and this is not seen to be the case. Attempts have been made to model the various brightness distributions seen in these sources with strictly relativistic flow (Gower et al. 1982). While fairly convincing agreement is obtained, the models require eight free parameters to achieve the desired results, and it is not clear that a strong case can be made when so many degrees of freedom are required.

3. SIDEDNESS

Many radio sources display asymmetric structure, and this often takes the form of a long filament of emission which extends from one side of the nucleus to an extended lobe but which is not present on the other side. These filaments are usually called "jets", a name which implies an assumed model for their nature, and they appear in the lower luminosity radio galaxies and also in very luminous radio quasars. Their sizes range from tens to hundreds of kiloparsecs. A more complete compilation of their properties is found in the recent paper by Bridle (1984).

One sided jet structures have been proposed as velocity indicators in the following sense. If the bulk motion away

from the nucleus is relativistic on the large scale, then one sided jets could be the result of Doppler enhancement of a weakly emitting jet which is pointed nearly at the observer. The oppositely directed jet would have its apparent emission correspondingly reduced to below the limits of detectability. It has been suggested that all one sided jets are in fact a result of this relativistic Doppler beaming (Browne, 1983).

This explanation for sidedness encounters some severe difficulties when compared with observations. There are a few one sided radio sources whose emission is aligned with the spectroscopically determined rotation axis of the parent galaxy, and this rotation axis lies nearly in the plane of the sky. Probably the best example of this is NGC 5128. There are in addition statistical arguments (Saikia and Wiita, 1982) which suggest that the distance from the nucleus to the two diffuse lobes in one sided jet sources is in the wrong sense. That is, for relativistic beaming, the nearer lobe is on the side with the jet and is seen at a later age. Assuming equal lobe velocities, it should thus appear farther from the nucleus. However, the argument is probably not compelling due to the number of assumptions involved and the lack of a truly strong correlation.

A statistical argument which is telling is the recent result reported by Wardle (1984). He has examined the largest radio QSO's in a complete sample, and has found that they all have one sided jets. Statistically one would expect these objects to be lying nearly in the plane of the sky; thus this result casts serious doubt on the relativistic beaming hypothesis. An intriguing alternative has recently been put forward by Rudnick and Edgar (1984) in which sidedness arises as a result of alternating side at a time ejection from the nucleus itself. Such a suggestion poses a real challenge to theorists who wish to construct a model for such a nuclear engine.

4. EMISSION LINES

An increasing number of the smaller radio sources are being found to have optical emission lines associated with them (Miley 1983). These lines are usually seen along the periphery of the radio emitting regions and they include emission lines of heavy elements such as oxygen and sulfur as well as hydrogen. The logical inference drawn from these observations is that we are seeing the interaction between the outward moving radio source and the interstellar medium of the parent galaxy. The nature of this interaction may be shock excitation, or entrainment, or both. The velocities of the line emitting regions relative to the galaxy range from a few hundred to a thousand kilometers per second, and the line

widths are typically a few hundred kilometers per second.

The optical observations are a direct measure of velocity, but ambiguity remains as to the relation of this velocity to the flow velocity in the radio source itself. If the emission lines arise from a turbulent boundary layer which entrains the ambient ISM, then the velocities can range from essentially the velocity of the jet itself down to nearly zero. The key question, which is as yet unanswered, is just where in such a boundary layer the line emitting regions lie. On the other hand, if the emission lines arise from a bow shock which precedes the leading edge of the jet, then the velocity of this gas would be expected to be comparable to, but always less than, the velocity in the beam. More detailed flow calculations concerning boundary layers need to be done, but in any case the emission line observations clearly place lower limits on the flow velocity, and they may be within an order of magnitude of it.

5. VELOCITY AND COMPACT SOURCES

The structure and temporal behavior of compact radio sources clearly provide the strongest evidence in support of relativistic motion. When it is possible to resolve the structure of these objects, they appear as one sided jets which are parsecs in length. If there is a large scale one sided jet also present in the radio source it usually lies on the same side as the compact jet (e.g., NGC 6251). However, this structure gives no indication of velocity per se. The strongest statement that can be made is that compact one sided jets are consistent with Doppler enhanced relativistic motion on those scales. Moreover, as more detailed VLBI maps become available, it is becoming clear that these compact jets also often have a twisting, bending structure (Walker, 1984; Muxlow, 1984). If this is generally the case, then the dilemma of how to bend (and in some cases reverse the direction of) a rigid, highly relativistic beam without disrupting it once again comes to the forefront. The problem is particularly acute because it is generally assumed that the compact jet is the base of the beam which powers the entire radio source tens to hundreds of kiloparsecs distant.

Another property of compact sources which may be used to infer a velocity is the time variation of the radio flux. About half of all compact sources vary at some level (Kellermann and Pauliny-Toth, 1981), some by only a few percent and some by factors of two or more. The more extreme examples of such objects push the "Compton Catastrophe" limit, and these difficulties can be alleviated if the variations are Doppler enhanced by relativistic motion almost along the line of sight to the observer.

While this explanation is attractive, it does pose the following dilemma. The probability that one of a pair of sources will be aligned to within an angle θ of the line of sight is $(1-\cos\theta)$. For relativistic effects to be important one must have $\sin\theta = 1/\gamma$, where γ is the Lorentz factor, and large values of γ imply the above probability in $P \sim 1/2\gamma^2$. Values of $\gamma \sim 10$ are required to explain the observations, hence $P \sim 0.01$, and not 1/2 as seen from the data. The only way out of this dilemma is to postulate a new population of radio sources with faint relativistic jets which are so dim that we really are seeing only the one percent that are nearly pointed at us. This solution is not only inelegant but may suffer from a fatal flaw; disembodied jets are not seen. Instead they always have a core with them, and since the cores, co-located with the central engine, are not Doppler boosted, where are the hundredfold more core sources without jets that we should be seeing? As will be discussed below, Doppler boosting is not the only explanation available to explain these flux variations.

A related phenomenon which may be velocity related is the level of x-ray emission seen from compact sources. One can calculate the amount of x-ray flux expected from inverse Compton scattering of the radio photons by the relativistic electrons in compact sources, and for NRAO 140 in particular this value is $\sim 10^3$ times that observed (Marscher and Broderick, 1982). Again, this situation can be resolved if the radio source is moving relativistically at a small angle to the line of sight.

Probably the most compelling arguments for relativistic motion arise from compact sources which are observed to change their structure with time (e.g., Kellermann and Pauliny-Toth, 1981). Although only a few of these sources have been observed, their apparent superluminal motion is consistent with, and most easily explained by, relativistic motion of the source nearly along the line of sight. While this is perhaps the most satisfying explanation, it is not a unique one. Several others exist for this and for flux variations with time, each with varying degrees of contrivance (Marscher and Scott, 1980). It is difficult to say whether each of these alternate explanations has truly fatal flaws, or if instead some of them could be made very viable if as much effort were expended upon them as upon the currently popular model.

There is one final, and in my view most difficult, problem with relativistic motion on the small scale in the context of present models. If the large scale (>1 kpc) motion is non-relativistic, including the large scale jets, and if in the compact jets we are seeing the base of the beam that powers the entire radio source, then relativistic motion on the compact scale implies that the flow must be decelerated to non-

relativistic velocities in the distance between the end of the compact jet and the onset of the large scale jet. This raises enormous difficulties, for it implies that in this region must be deposited the major fraction of the energy of the entire radio source. Moreover, this energy deposition must be done nearly invisibly, from radio through optical to x-ray wavelengths, since this region is not the brightest region of the source at any wavelength. In fact it is often a very faint region, even in those sources such as 3C 120 where one can see continuous emission from the superluminal region to the larger scale structure (Walker, 1984).

All of the difficulties mentioned above, but especially this last one, raise so many problems that it seems necessary that we seriously consider whether there is relativistic motion which is dynamically important on any scale in the radio sources.

6. CONCLUSIONS

It seems to me that the case for slow, non-relativistic motion in "edge-darkened" sources and in large scale jets (including QSO's) is now compelling. The situation for simple doubles such as 3C 33 is of course less clear; the observations are consistent with either fast or slow speeds. It now seems that luminosity is not a discriminant, given the new evidence about one sided jets in QSO's. Thus the efficiency and simplicity of the original relativistic beam model must be abandoned, and a more complex picture which must involve more interaction with the surrounding medium needs to be constructed.

The arguments for relativistic motion on the parsec scale are strong, but so are the problems raised by such motion. As more detailed VLBI maps become available, the intensity of these problems may increase. If one wishes to hold fast to relativistic motion to explain the superluminal effect and yet avoid the energy deposition problem, then an obvious solution is a hybrid model containing a small amount of energy in relativistic flow which is quickly damped out. In such a model the relativistic portion of the flow can never be energetically important. How a "nuclear engine" can be made to produce such a flow in a natural and uncontrived way remains to be seen.

REFERENCES

Blandford, R. J. and Rees, M. J. 1974, M.N.R.A.S., 169, 395.
Bridle, A. H. 1984, A. J., 89, 979.
Browne, I. W. 1983, M.N.R.A.S., 204, 23p.

Burns, J. O. 1981, M.N.R.A.S., 195, 523.
Eilek, J., Burns, J. O., O'Dell, C. and Owen, F. 1984, Ap. J., 278, 37.
Gower, A. C., Gregory, P. C., Hutchings, J. B. and Unruh, W. G. 1982, Ap. J., 262, 478.
Kellermann, K. I. and Pauliny-Toth, I. 1981, Ann. Rev. Astr. & Ap., 19, 373.
Marscher, A. P. and Broderick, J. J. 1982, Ap. J., 255, L11.
Marscher, A. and Scott, J. 1980, P.A.S.P., 92, 127.
Miley, G. K. 1983, in "Astrophysical Jets", ed. A. Ferrari and A. Pacholczyk, (Reidel, Boston), pp. 99-112.
Muxlow, T. 1984, private communication.
Perley, R. A., Willis, A. G. and Scott, J. S. 1979, Nature, 281, 437.
Rayburn, D. R. 1977, M.N.R.A.S., 179, 603.
Rudnick, L. and Edgar, B. K. 1984, Ap. J., 279, 74.
Saikia, D. J. and Wiita, P. J. 1982, M.N.R.A.S., 200, 83.
Smith, M. D., Smarr, L., Norman, M. L. and Wilson, J. R. 1983, Ap. J., 264, 432.
Walker, C. 1984, this volume.
Wardle, J. F. C. 1984, this volume.
Wiita, P. J. 1978, Ap. J., 221, 436.

DISCUSSION

Dick Henriksen. Bulk relativistic motion need not be converted *immediately* into waste heat. The bulk energy can be converted into internal energy of large scale circulatory eddies, which only gradually decay.

Dave De Young. To have relativistic jets on VLBI scales and nonrelativistic jets on 1-10 kpc scales requires deceleration of the relativistic flow in the region between the end of the VLBI jet and the onset of the larger, slower jet. In the context of the VLBI jet powering the entire source, it is by no means clear that the major portion of this energy can be converted quietly into essentially subsonic eddies in the required distance. I do not know the origin of your use of the word "can", since the proper calculation has yet to be done.

Alan Bridle. In a sample of 46 edge-brightened (FR class II) sources with one-sided jets from the Bridle and Perley (1984) list, I found 17 in which the jet feeds the farther hot spot, 15 in which it feeds the nearer, and 14 which are too symmetric to say which hot spot is nearer or farther (given the finite sizes of the hot spots and the finite resolution). It therefore seems that the brightness asymmetries of the jets are uncorrelated with the separation asymmetries of the hot spots, in conflict with the naive relativistic flow model.

Dave De Young. I agree.

Frazer Owen. Low frequency variability is questionable evidence for relativistic motion because the size scale of the emitting region is larger at meter wavelengths than at centimeter wavelengths where evidence of high brightness temperature is much rarer. Also, the Rickett *et al.* model using interstellar scintillations as observed in pulsars explains this frequency dependence quite well.

Chris O'Dea. High brightness temperatures, $T > 10^{12}$K, are found at centimeter wavelengths in variable sources. Thus, there is still a problem.

Larry Rudnick. We have measurements of the velocities in one highly collimated flow – SS433. What, if anything, can this help us understand about extragalactic jets ?

Dave De Young. In order for SS433 to be useful in this context you have to assume the same physical processes are at work in both objects. This is probably right for "microphysics" such as viscous effects, but by and large we don't understand these in SS433 either. For global processes, such as the central engine and the role of the large scale structure in the environment, I would be hesitant to scale upward from SS433 to extragalactic jets.

An Argument for Jet Velocities > 0.1 c in Powerful Doubles

John W. Dreher
Room 26-315, Massachusetts Institute of Technology
Cambridge, MA 02139

Abstract. The L/cT method is used to estimate the jet velocities for 12 edge-brightened doubles. Using plausible model parameters, the estimates for L/cT are all much larger than unity, which is impossible. The model parameters can be adjusted to give a conservative lower limit to L/cT. These limits are of order 0.1, leading to lower limits on the jet velocities of $\sim$0.1 c.

1. Introduction

One method of determining jet velocities is to estimate the kinetic energy delivered by the jet from the observed source properties and to estimate the jet momentum flux from the measured size and the inferred minimum pressure of the terminal hotspot (*eg* Bridle and Perley 1984). This method relies on the assumption of the "standard" source model in which the source's energy is generated in the core, converted into energy carried by a highly-collimated beam, transported to the outer parts of the radio source with (relatively) little loss, and dissipated in a shock where the beam is decelerated by an encounter with the surrounding medium, with some of the energy going into particle acceleration. Observationally, the beam is identified with the jets seen in many sources, and the terminal shock with the hotspots. For this talk, I shall also make the assumption that the beam carries its energy entirely as the bulk kinetic energy of the outflow. With this assumption, and working in the frame of the hotspot, the ratio of jet mechanical power (L, erg s^{-1}) to momentum flux (T, dynes) is equal to the ratio of kinetic energy (K) to momentum (p) for a single particle. We have

$$K \equiv E - m_0c^2 = (\gamma - 1)m_0c^2$$

From the invariance relation $E^2-(cp)^2 = -(m_0c^2)^2$,

$$p = (E^2/c^2 - m_0^2c^2)^{1/2} = (\gamma^2-1)^{1/2}m_0c$$

Hence,

$$L/T = K/p = c[(\gamma-1)/(\gamma^2-1)^{1/2}] = c[(\gamma-1)/(\gamma+1)]^{1/2}$$

The ratio L/cT, therefore, varies from 1 when $\gamma \to \infty$ to $\beta/2$ when $\gamma \to 1$.

If we knew L and T, we could thus determine v_{jet}. Of course, we do not know these quantities, but have only order of magnitude estimates of them. If $L/cT << 1$ (*ie* $v_{jet} << c$), this uncertainty is not too bad, since we will obtain an order of magnitude estimate of the velocity, which is still interesting. As I shall show in §2, however, using reasonable assumptions L/cT is not $<< 1$ for the powerful radio galaxies. In this case, a rough value for L/cT does not lead to a good determination of the jet velocity, since as L/cT varies from .1 to 1, v_{jet} varies from 0.2c to ∞. In addition, by considering jets that are very "inefficient" in the sense of converting little of their total mechanical

energy into radio emitting particles, it is possible to increase the estimated L without conflicting with observations, although at the price of increasing the total power that must be supplied by the central engine. The L/cT method cannot, therefore, yield good upper limits on v_{jet}. What can be attempted is to find a plausible *lower limit* on v_{jet} and also constraints on the source models required to keep the estimated L/cT from exceeding unity. Doing this in §3, I find both that $v_j > 0.1$ and that the particle acceleration processes in the hotspots must be very efficient.

2. A Reasonable Guess for L/cT

In order best to apply the method, sources with well resolved hotspots, from which meaningful minimum pressures can be derived, are needed. It would be nice, also, to have observed jets; however, in the cases where the jet is not seen, the argument can still be applied using the brighter hotspot. If this choice is wrong, the actual value of L/cT would be higher than that calculated, which would strengthen my conclusions. A suitable set of observations of powerful double radio galaxies, observed with a spatial resolution of better than 0.5 kpc, can be found in Dreher (1981, 1984). Table 1 lists a few properties of these sources and their hotspots. While not a complete sample in any sense, these sources should be fairly representative of nearby edge-brightened doubles. In particular, the luminosity range includes doubles with "average" luminosities as well as high luminosity objects.

Table 1

Source	L_{radio}	Brighter Hotspot			Jet	L/cT Estimates		β
		Diam	B_{min}	p_{min}	seen?	First	Lowest	
3C 98	4	2.3	40	1	no	15	0.09	0.18
2244+366	4	1.0	180	16	no	5	0.03	0.06
3C 382	6	3.2	60	2	yes	7	0.04	0.09
3C 192	7	3.7	50	1	no	10	0.06	0.11
3C 321	11	2.0	150	12	yes	5	0.03	0.05
3C 390.3	13	1.2	130	8	maybe	23	0.14	0.27
3C 111	15	1.3	190	18	yes	10	0.06	0.12
3C 33	16	1.3	220	24	no	8	0.05	0.10
3C 452	19	1.1	110	6	maybe	53	0.32	0.57
3C 234	51	1.1	270	40	no	23	0.14	0.28
3C 61.1	66	1.1	120	7	no	157	0.942	0.998
Cyg A	1080	1.4	540	150	yes	77	0.46	0.76
	$\times 10^{42}$ erg s^{-1}	kpc	μG	$\times 10^{-10}$ dyne cm^{-2}				

To determine L/cT, we first require an estimate for L, the mechanical luminosity of the jet. Let L be converted to ultra-relativistic particles with efficiency η_{acc}. These particles first serve to supply the radio luminosity of the hotspot, L_{hot}. From the hotspot, these particles flow back into the lobes, expanding in the process and suffering adiabatic losses. Although this expansion is a continous

process, a simple estimate of the losses may be made by treating the hotspot and the lobe as uniform regions and ignoring the transition. In this case, the usable energy after expansion is reduced by a factor η_{lobe}, which can be expressed in terms of the energy densities, u, in the two regions as $(u_{lobe}/u_{hot})^{1/4}$ (Hargrave and McEllin 1975). Within the lobe the remaining energy must be at least enough to supply the radio luminosity of the lobe, L_{lobe}. This energy must also account for the rate of increase in the stored energy in the lobe, dU_{lobe}/dt. This term may be estimated by its time average U_{lobe}/t where t is the source lifetime. U_{lobe} then is found from the usual minimum energy argument. Overall the jet mechanical luminosity is given by

$$L \sim \eta_{acc}^{-1}[L_{hot} + \eta_{lobe}^{-1}(L_{lobe} + U_{lobe}/t)]$$

I shall adopt values for the various parameters to provide a fairly conservative (that is *low*) value for L. η_{acc} must be less than unity and is often taken to be a few percent: $\eta_{acc} = 10^{-1}$ seems reasonable. The lobes and the hotspots have roughly equal contributions to the total source luminosity for most sources, therefore I use $L_{hot} = L_{lobe} = L_{radio}/4$ (where the last has been calculated after removing the flux of the core source). For the sources in Table 1, $(u_{lobe}/u_{hot})^{1/4}$ varies between 1/2 and 1/6, so η_{lobe} is close to 1/4. The most difficult term to estimate is t. A plausible value may be found from the distance from the core to the hotspot divided by v_{lobe}, the rate of advance of the leading edge of the lobe into the surrounding medium. This velocity can in turn be estimated by equating the value of the minimum pressure, calculated for the entire region at the tip of the lobe rather than just for the most compact part of the hotspot, to the ram pressure $\rho_{ICM}v_{lobe}^2$, where ρ_{ICM} is found using a moderately high intracluster density of 10^{-3} cm^{-3}. For the sources under consideration, this leads to typical values for v_{lobe} and t of $\sim$300 km s^{-1} and $\sim 10^8$ years respectively. Put together, one finds that for powerful doubles $L \sim 50\ L_{radio}$.

Next, the thrust T can be obtained from the requirement that the jet be stopped by the pressure of the stagnation point downstream from the terminal shock, leading to the expression $T = p(\pi/4)d_{jet}^2$ where p is the pressure and d_{jet} is the diameter of the jet at the shock. The pressure can be estimated from p_{min}, the minimum pressure of the most compact parts of the hotspot (calculated from the syncrotron emission in the normal way). If the hotspot is not well resolved, this can lead to an underestimate of the pressure and hence a high value for L/cT, but the hotspots given in the table have all been resolved well enough largely to avoid this problem. One way to find d_{jet} would be to use d_{hot}, the observed diameter of the hotspot; however, the jet diameter is very likely to be significantly smaller than that of the hotspot. In the cases of 3C 111 (Linfield and Perley 1984, Dreher 1984) and 3C 382 (Dreher, 1984) the jet can be seen entering the hotspot and $d_{jet} \sim (1/3)d_{hot}$. A similar value for the ratio of the observed width of the hotspot to the width of the beam can be found in the models of Smith *et al.* (1984). I adopt, therefore, the relation $T = p_{min}(\pi/4)(d_{hot}/3)^2$.

The column labled "first" in Table 1 presents the results of applying these relations to find what ought to be a reasonable estimate of L/cT. Surprisingly, all of the estimates are much larger than unity! The true value, of course, must be less than unity, so I am forced to two conclusions immediately: first, it will be necessary to reexamine all the assumptions with an eye to reducing L/cT as much as possible, which will constrain possible models, and, second, it is unlikely that L/cT

can be made low enough so that relativistic effects can safely be ignored.

3. Lower limits for L/cT

To reduce the estimate for L, first I let dU_{lobe}/dt be negligible with respect to L_{lobe}. The arguments in the preceeding section led to values of $dU_{lobe}/dt \sim 4L_{radio}$. This could be reduced several ways: *i)* the average value of v_{lobe} could be less than that required to confine the leading edge of the lobe, *ii)* the lobe minimum energy might be reduced, *eg* by reducing the filling factor (see Perley, Dreher, and Cowan 1984 for a possible example), and/or *iii)* another source of the lobe's energy than the hotspot and jet could be found. Second, I take $\eta_{lobe} = 1/2$. Next, I adopt the value 0.25 for η_{acc}, which is about the highest that can be found in the literature. Finally, I leave $L_{hot} = L_{lobe} = L_{radio}/4$ since this is already a conservative assumption (in many cases $L_{hot} < L_{lobe}$, which increases L). The net effect is to reduce the estimate for L from 50 L_{radio} to only 3 L_{radio}, which certainly seems to be a *very* conservative lower limit.

Now an upper limit on T is needed. The size of the jet is not very adjustable, since d_{jet} is *observed* to be $\sim d_{hot}/3$. The minimum pressure, on the other hand, can readily be increased. One way to do this is to allow the hotspot to be far from equipartition. However, while the pressure in the hotspot is, by hypothesis, balanced by the jet on one side, on the other it must be balanced by the ram pressure of the ICM. Since I am trying to establish that v_{jet} must be $> 0.1c$, I can consistently take an upper limit to the velocity of the hotspot out into the ICM as 0.1c, for if the hotspot were going faster, the jet would have to be going faster still just to catch up with it, much less dissipate energy within it. Once again, I adopt a fairly dense ICM density of 10^{-3} cm^{-3} to find p to be less than about 10^{-8} dyne cm^{-2} or roughly 10 p_{min}. Another way to increase p would be to postulate additional fine structures within the hotspots. This amounts to using a filling factor less than unity in the minimum pressure calulations. A plausible lower limit on this filling factor is 10^{-2}, which increases p_{min} by a factor of ten. In fact, considerable complex fine structure has recently been found in the hotspots of Cyg A, but the revised values for p_{min} are not changed very much (R. Laing, private communication). Thus I conclude that T can only be increased by at most a factor of ten.

Combining the lower limit on L with the upper limit on T yields the *lower limits* on L/cT given in the column marked "lowest" in the table. The last column in the table shows the corresponding lower limits on $\beta \equiv v_{jet}/c$.

4. Discussion

After pushing all of the parameters fairly hard, I still find that the lower limits on L/cT imply that all of the edge-brightened doubles considered here must have jets with velocities of at least $\sim$0.1 c. For any one source, it might be possible to escape this conclusion. In particular, if hotspots turn on and off, a source with its hotspot in the off state would have a high apparent value of L/cT. However, this seems unlikely to be true for all the sources in Table 1, especially since these were selected in a way that biases towards bright and presumably active hotspots. There also seems to be a tendency for the value of L/cT to increase with L_{radio}, which certainly does not seem unreasonable and which might help explain why the less luminous edge-darkened sources seem to have much

slower jets. With jet velocities > 0.1 c, relativistic effects will begin to be important in terms of Doppler enhancements and time-delay effects. The L/cT argument does not, however, provide any useful information about just how close to c the jet velocity must be. For example, in the case of 3C 61.1, the lower limit works out to be 0.998 c, but given the roughness of the estimate, it could just as well have worked out to be 0.7 say. Thus these calculations have no bearing on whether jets in powerful doubles are relativistic in a dynamically important sense, *ie* have η significantly different from unity.

If the true jet velocities exceed the limits given in the table, some of the parameters governing the energetics can be relaxed. In particular, if the hotspot is moving outward at a velocity comparable to the jet velocity (both exceeding ~0.1 c), not all the momentum of the jet need be stopped in the hotspot. In this case, downstream from the terminal shock the material will still be moving outward (in the frame of the core) with a significant velocity. The momentum flux of this secondary flow can then be balanced against ram pressure on the external medium acting over a much larger area than the cross-sectional area of the jet. Similar considerations apply even if the hotspot is not moving outward if the shock in the jet is very oblique. Nonetheless, the very large values of L/cT estimated in § 3 using reasonable estimates for parameters seem sufficient to make models that have low particle acceleration efficiencies (~1%) unattractive.

Finally I note that the argument presented here is just the other side of the well-known "waste energy" problem. In this problem, the point is raised that if jets are relativistic, then it is necessary to find somewhere to dissipate most of the energy in an unobserved form. I have argued that what we know of source energetics strongly suggests that the whole process must be very "inefficient" in the sense of producing radio emission from jet kinetic energy and that, as a consequence, the large mechanical luminosities associated with relativistic jets are necessary. The question of where the rest of the energy goes remains puzzling.

References

Bridle, A.H., and Perley, R.A. 1984, *Ann.Rev.Ast.Ap.* **22**, in press.
Dreher, J.W. 1981, *A.J.* **86**, 883.
Dreher, J.W. 1984, preprint.
Hargrave, P.J., and McEllin, M. 1975, *M.N.R.A.S.* **173**, 37.
Linfield, R., and Perley, R. 1984, *Ap.J.* **279**, 74.
Perley, R.A., Dreher, J.W., and Cowan, J. 1984, *Ap.J.L.*, in press.
Smith, M.D., Norman, M.L., Winkler, K.A., and Smarr, L. 1984, preprint.

JET SPEED

L. Rudnick
University of Minnesota, Department of Astronomy
116 Church Street S. E., Minneapolis, MN 55455

ABSTRACT. Line emission has been detected from the optical counterparts of the extended radio QSO 0812+02 (Wehinger et al., 1984). At the radio/optical hot spot, the velocity is measured to be 1200 km s^{-1} relative to the QSO nucleus. Spatially asymmetric line emission argues against a relativistic explanation for the one-sided radio jet. Observations such as these hold great promise for measurements of velocities and momentum fluxes in radio sources, although a better understanding of the interactions between thermal and relativistic material are needed.

(Work in collaboration with F. Ghigo and K. Johnston at long wavelengths, and P. Wehinger, S. Wyckoff, H. Spinrad, T. Gehren and A. Boksenberg at short wavelengths.)

PKS 0812+02 is a $z \sim 0.4$ QSO in a cluster of galaxies, which has optical emission coincident with its northern hot spot (Wyckoff et al., 1983, Ghigo et al., 1982). Figure 1 shows a λ20cm map of this source, in which its main features can be seen, viz., a strong nucleus, a one-sided jet terminating in a hot spot, and two, fairly symmetric low surface brightness lobes. There is also a weak, diffuse hot spot in the southern lobe which may be associated with optical emission, but that I won't discuss here.

A radio/optical overlay is shown in Figure 2, for the northern half of the source. The coincidence of the hot spot emissions is clear. Previously our optical spectral information on the hot spot was limited to a description of the continuum, which could roughly be described as an $\alpha \approx -1.1$ power-law. Now, new long-slit spectral observations of this system have shown extensive emission line material, from the QSO, the jet, and the hot spot (Wehinger et al., 1984). Figure 3 shows preliminary polaroid copies (from the analysis screen) of KPNO 4-meter Cryocam data. Over several exposures, and both [OIII] and [OII], there is an observed velocity difference of 1200 km s^{-1} between the nucleus and hot spot, with a possible gradient along the jet. The analysis and interpretation of these data are still under discussion amongst my collaborators, but I'd like to give you an idea of the issues we're looking at.

Emission line material in radio galaxies has been studied by van Breugel and collaborators (see van Breugel et al., 1984, and references therein). Their main conclusion is that the thermal material, pre-existing in the galaxies, is made visible by its interaction with the relativistic flow, as well as perturbing the flow itself. Our 0812+02 observations do not have the spatial resolution or coverage to make this kind of analysis. However, because of the much larger energies involved, it seems prudent to consider all possibilities for the thermal/relativisitic particle relationship. Other extended emission line systems have also been found (e.g., Fosbury et al., 1984).

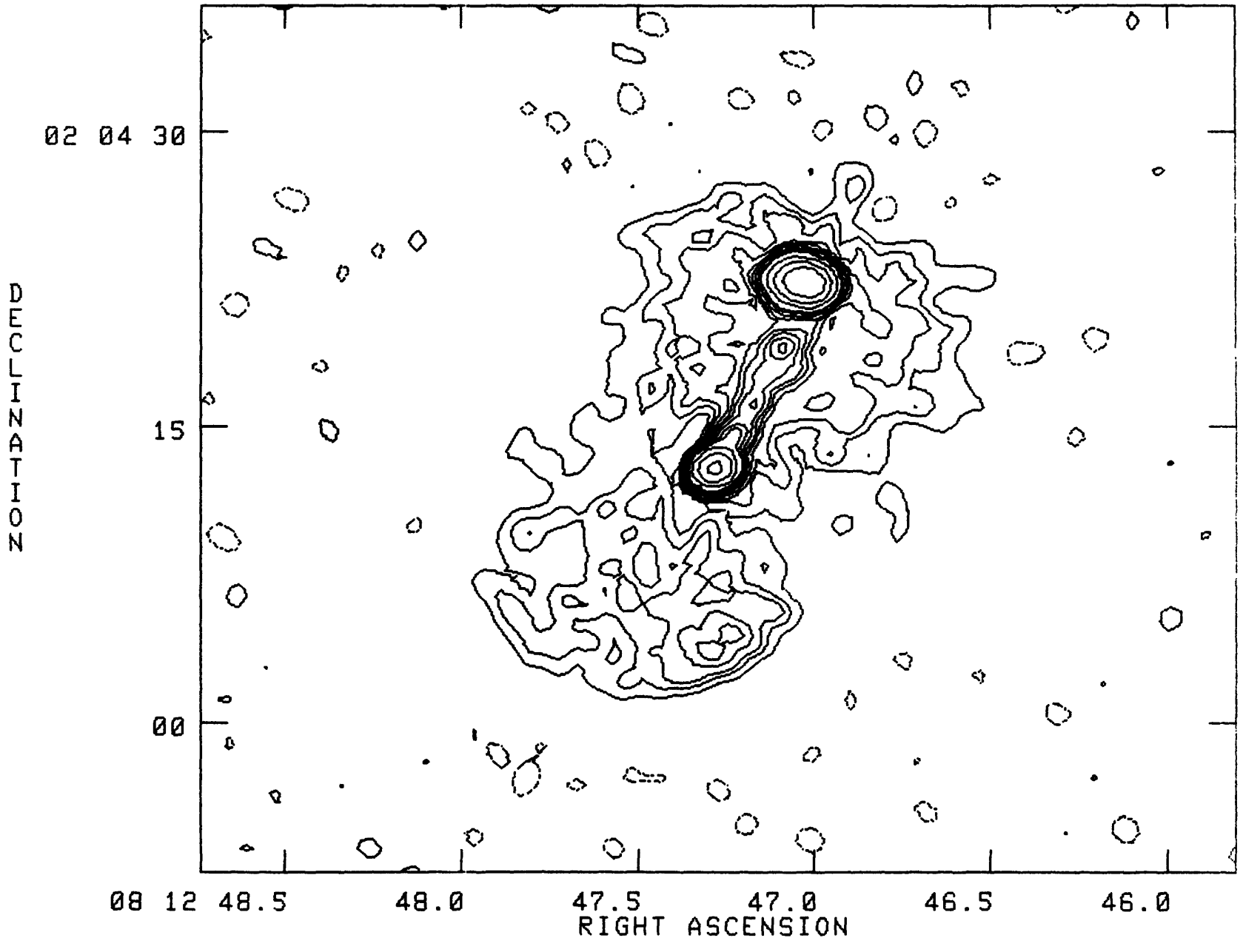

Figure 1. λ20cm map, 0812+02.

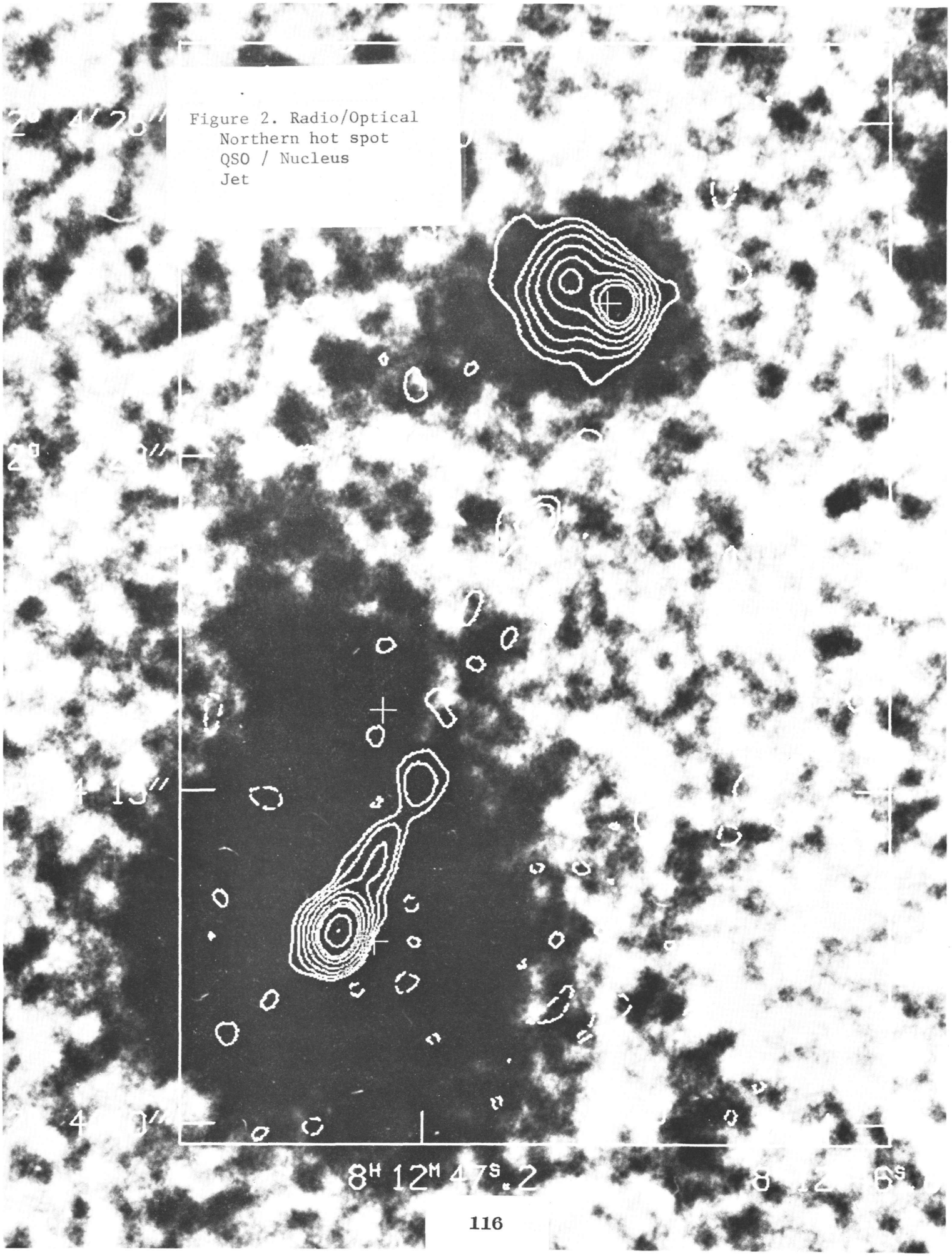

Figure 2. Radio/Optical
Northern hot spot
QSO / Nucleus
Jet

Figure 3. Preliminary analysis, Cryocam long-slit spectra.

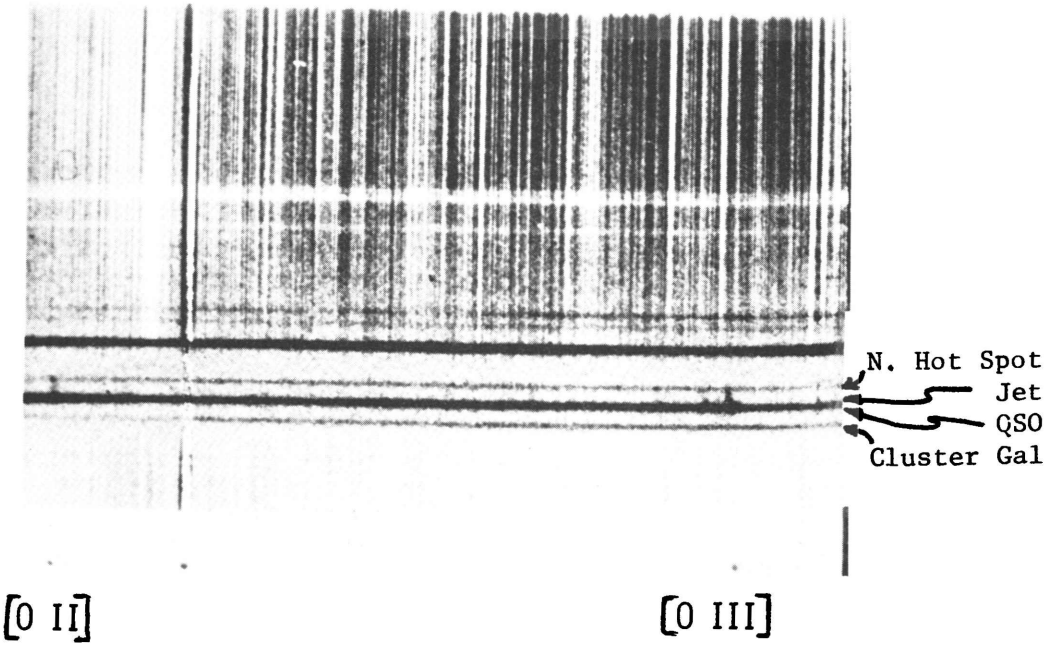

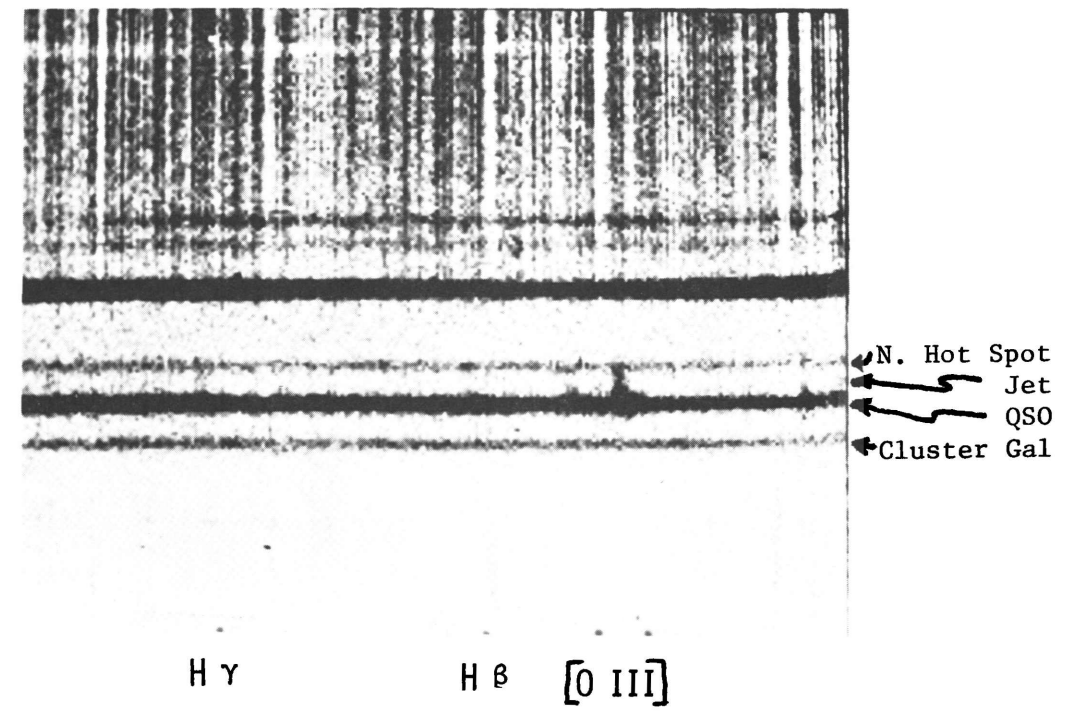

One basic issue is the origin of the thermal particles. They could be either material entrained during transport from the nucleus, or pre-existing and made visible locally. Either way, theoretical work will be needed to relate the observed emission line velocities to the relativistic particle flow velocity. Norman et al. (1983), for example, have shown that entrained material may be flowing either forwards or backwards, depending on the Mach number and beam/ambient medium density ratio. If these uncertainties can be sorted out, then we can actually measure some of the momentum transferred by the radio jet.

Another question is the excitation mechanism for the emission lines. Possibilities include photoionization from the QSO, shock heating by the relativistic plasma, and synchrotron triggered cooling of an ambient, hot ($\sim 10^7$ K) gas (Eilek and Caroff 1979). It's not clear to me how to decide amongst the possibilities, given the currently available information.

There are a host of possible new probes of jets which are introduced through line emission properties, even if the interactions are at unresolveably small scales. For example, one could look for spatial correlations between jet parameters and those of the emission lines (e.g., luminosity, velocity, line width, excitation levels).

There is one interesting argument which comes out from our preliminary analysis (with thanks to R. Ekers). The lack of emission line material from the southern half of the source cannot be due to Doppler (un-)boosting, because the northern lines are so subrelativistic. Even if the putative southern jet were relativistic, it would be missing its non-relativistic thermal counterpart. If you want to argue that the southern part of the host galaxy is just lacking in thermal material, then the effects on the observed radio structure are severe enough to call most other standard source analyses into question.

At the University of Minnesota, this work has been supported, in part, by NSF grants AST81-14737 and AST83-15949.

REFERENCES

Eilek, J.A. and Caroff, L.J. (1979), Ap.J. 233, 463.
Fosbury et al. (1984), MNRAS 208, 955.
Ghigo et al. (1982), IAU Symposium #97 (ed. Heeschen and Wade), p. 43.
Norman et al. (1983), in "Astrophysical Jets," (Dordrecht: Reidel).
van Breugel et al. (1984), Ap.J. 277, 82.
Wehinger, P.A., Wyckoff, S. and Spinrad, H. (1984), BAAS 16, 520.
Wyckoff et al. (1983), Ap.J. 265, 43.

JET ASYMMETRIES IN RADIO GALAXIES WITH DUST LANES

ROBERT A. LAING[1]

Royal Greenwich Observatory

ABSTRACT. The brightness asymmetries of jets in eight radio galaxies apparently crossed by dust lanes were discussed. The jets are generally oriented approximately perpendicular to the dust lanes in projection, so it is statistically likely that this perpendicularity holds in three dimensions. Assuming the jets in these galaxies to be outflows, their orientations can be categorized as "towards the observer", "away from the observer", or "close to the plane of the sky" from the apparent orientations of the associated dust lanes. (The dust lanes are assumed to be circular and approximately planar on the scale of the inner parts of the jets). By this criterion, the *brighter* of the two jets is oriented *away* from the observer in three cases, and close to the plane of the sky in four more. In the remaining case (Cen A) the brighter jet would be considered to be near the plane of the sky from the dust lane evidence, but HI absorption evidence suggests that it may be oriented towards us.

These data show that it is unlikely that the brightness asymmetries in most of these jets result from Doppler boosting of the approaching sides of bulk relativistic flows.

[1] Due to unforseen circumstances, Dr. Laing's original text failed to reach us in time for inclusion in these Proceedings, so this abstract was prepared by us – Eds.

EVOLUTION OF SUPERLUMINAL RADIO COMPONENTS IN 3C345

JOHN A. BIRETTA

California Institute of Technology, Pasadena, CA 91125

ABSTRACT. We present VLBI observations of 3C345 from 1978 through 1984 at 5, 11, and 22 GHz. The outer two knots show a relatively simple evolution: that of the innermost knot is much more complex.

The outer two VLBI knots move away from the core with apparent speeds of about 6 and 8c ($H_0 = 100$ km/s/Mpc). The knots are at different position angles and their motion is slightly non-radial. At high frequencies their flux decays slowly, and the spectra steepen. The flux decay is much too slow to be explained as adiabatic expansion. The apparent jet opening angle is 25°. The super-luminal motion and the weak inverse Compton X-ray flux require the jet to be within 8° of the line of sight, hence the intrinsic opening angle is probably less than 3° and typical of other quasar jets.

The innermost knot brightened rapidly as it moved away from the core, and caused the largest flux outburst ever seen from 3C345. During this time the spectrum of this knot was flat from 7 to 90 GHz. A large infrared and optical outburst occurred at the same time. The kinematics are also complex. The knot accelerated from 2c to 6c. It also changed position angle from −135° to −87° which is close to that of the two outer knots. At later epochs the core was extended at a position angle of about −90°, which argues against a simple fixed path for the knots.

DISCUSSION

Alan Bridle. Can you tell which of components D and C4 is really the core ? Is Bartel's astrometry relative to NRAO 512 good enough to distinguish them ? This is important as it tests whether the VLBI features preserve their sidedness.

John Biretta. Before the appearance of the new components, C2 and C3 moved away from the core with uniform speeds. After the appearance of the new componment, C2 and C3 moved with the same speeds as before relative to D, but at much slower speeds relative to C4. Hence it would be very surprising if D were not the core. Astrometric observations by Bartel *et al.* between 1972 and 1981 are inconclusive on this question. Since D and C4 are separating, astrometry at *current* epochs might clarify this.

Chris O'Dea. Have you considered the possibility that the initial increase in brightness with distance from the core is due to a decrease in synchrotron opacity of the components from $\tau \gg 1$ to $\tau \approx 1$?

John Biretta. The spectral index of the new component remained flat between 11 and 22 GHz while the flux doubled. This could be explained as an opacity decrease and/or expansion of an inhomogeneous synchrotron radiation source.

SEMI-DYNAMICAL MODELS OF SUPERLUMINAL RADIO SOURCES

KEVIN R. LIND AND ROGER D. BLANDFORD[1]

Theoretical Astrophysics, California Institute of Technology, Pasadena, CA 91125

ABSTRACT. VLBI observations of compact radio sources exhibit core-jet structure and apparent superluminal expansion. Both features can be produced by a relativistic jet of radio-emitting plasma beamed towards the observer. This model implies that there should be several fainter unbeamed sources for every beamed source. We calculate partial luminosity functions – the probability distribution functions for the observed flux from a source at a given distance viewed from different directions – for different source models. We emphasize kinematical models that approximate relativistic shock fronts. These differ from the kinematically simpler models which are usually invoked in that the velocity of the emitting fluid, which is responsible for the Doppler boosting, is distinct from the velocity of the pattern, which is responsible for the superluminal motion. Numerical calculations of the emission from semi-dynamical shock models demonstrate that a range of partial luminosity functions can be produced. It is concluded that source counts cannot be used as precise probes of relativistic beaming, and are of limited use in testing the beaming hypothesis.

This work was supported under National Science Foundation Grant AST 82-13001.

[1] Supported by a grant from the Alfred P. Sloan Foundation

CLOUD-BEAM INTERACTIONS: BENDS, LOBES AND SUPER LUMINALS

R.N. Henriksen
Canadian Institute for Theoretical Astrophysics
University of Toronto
Toronto, ON M5S 1A1 Canada

There is growing evidence for the interaction of the energy-momentum beams believed to power the radio 'jets' and both intra and inter galactic 'clouds'. The papers by van Breugel et al (1984), Lonsdale and Barthel (1984) make it clear that abrupt beam deflection with consequent formation of radio and thermal 'hot spots', is one possible result. This disequilibrium process should be contrasted with the more gradual 'buoyant refraction' (e.g. Henriksen, Vallée and Bridle, 1981; Fieldler and Henriksen, 1984) or 'ram pressure bending' (Jones and Owen, 1979; Begelman, Rees and Blandford, 1979; Wilson and Ulverstad, 1982) that takes place in equilibrium with an extended cloud or 'atmosphere'.

The pressure will change dramatically over distances comparable to a beam diameter at the boundary of a 'cloud' by definition, generally producing strong internal oblique shocks in the beam as it deflects. We summarize the properties of these shocks below and then clarify qualitatively the various possible types of beam-cloud interaction. Finally, we sketch how these basic interactions might produce apparent super-luminal motion.

§1 Oblique Shock Waves

We restrict our discussion here to non-relativistic beams for which Landau and Lifshitz' text on fluid mechanics is an authoritative source. Relativistic oblique shocks can be discussed in parallel with the results given here (see also Königl, 1980) but this will be done elsewhere (Henriksen, 1984, in preparation). Our notation follows that of Landau and Lifshitz and we refer to the sketch in fig.1.

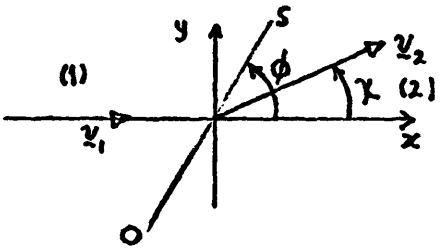

OS is the oblique shock. $\underline{v}_1$ and $\underline{v}_2$ are the pre and post shock stream lines.

Fig.1

From continuity of tangential stress, normal mass flux, normal momentum flux and normal energy flux there follows, in a frame in which the shock is stationary,

$$v_1 \cos\phi = v_2 \cos(\phi-\chi) \tag{1}$$

$$\rho_1 v_1 \sin\phi = \rho_2 v_2 \sin(\phi-\chi) \tag{2}$$

$$\rho_2/\rho_1 = \frac{(\gamma+1)M_1^2 \sin^2\phi}{2+(\gamma-1)M_1^2 \sin^2\phi} \tag{3}$$

$$p_2/p_1 = \frac{2\gamma}{\gamma+1} M_1^2 \sin^2\phi - \frac{\gamma-1}{\gamma+1}, \tag{4}$$

and, after various manipulations,

$$M_2^2 \sin^2(\phi-\chi) = \frac{2+(\gamma-1) M_1^2 \sin^2\phi}{2\gamma M_1^2 \sin^2\phi-(\gamma-1)}, \tag{5}$$

$$\tan\chi = \frac{2 \cot\phi (M_1^2 \sin^2\phi-1)}{(\gamma+1)M_1^2-2 (M_1^2 \sin^2\phi-1)} . \tag{6}$$

Moreover, $v_1 \sin\phi > c_{s_1} > c_{s_2} > v_2 \sin(\phi-\chi)$ which, together with (1), requires $\chi>0$ so that the stream line refraction always reduces the smallest angle between the stream line and the shock, as shown. Equation (6) shows that the deflection angle of the stream is zero for a normal shock ($\phi=\frac{\pi}{2}$) and for a shock of zero strength (sound wave) at the Mach angle $\phi=\sin^{-1}(1/M_1)$. There are generally two values of ϕ (two shocks) for a fixed deflection χ until the maximum deflection χ_{max} is reached. As $M_1\to\infty$ we find $\{\phi_{max} \equiv \phi(\chi_{max})\}$

$$\begin{aligned} \sin\chi_{max} &\simeq 1/\gamma \\ \sin^2\phi_{max} &\simeq (1/2)(1+1/\gamma), \end{aligned} \tag{7}$$

while as $M_1 \to 1$

$$\chi_{max} \simeq \frac{4}{\gamma+1} \left[\frac{2}{3}(M_1-1)\right]^{3/2} \tag{8}$$

$$\sin^2\phi_{max} \simeq 1/M_1^2 + 4/3 (M_1-1).$$

For $\gamma = 5/3$, (7) gives $\chi_{max} = 36.^0 9$, $\phi_{max} = 63.^0 4$, while for $\gamma = 7/5$ we have $\chi_{max} = 45.^0 6$ and $\phi_{max} = 67.^0 8$. Such intrinsic deflections are clearly of some observational interest, but note that the pressure jump required for the maximum deflection is not greatly changed from that in a normal shock (eq.4). Weakly supersonic beams execute only gentle wiggles due to oblique shocking as eq.(8) shows that for $\gamma = 5/3$, $\chi_{max} = 4.^0 2$, $\phi_{max} = 78.^0 6$ when $M_1 = 1.2$. The wave length of wiggles due to internally reflecting oblique weak shocks should not be too different from $R\sqrt{M_1^2-1}$.

§2 Possible Cloud-Beam Interactions

The basic interaction to which the equations of the preceding section should apply is the glancing collision or 'ricochet'. This geometry is sketched in fig.2 (after Norman et al. (1982), Smith et al. (1984) and Landau and Lifshitz).

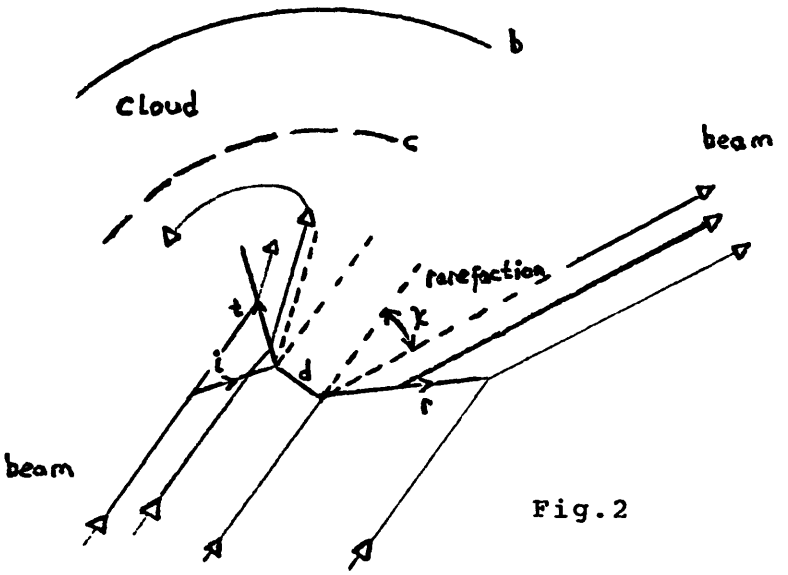

Fig.2

Ricochet Interaction:

i is an incident shock, t is transmitted to the cloud (reflected from the beam) and r is reflected from the cloud. The Mach disc d and rarefaction sectors are required in general to reconcile the 3 shocks. b is the bow shock in the the cloud and c is a contact discontinuity.

The essential point about the ricochet interaction is the time dependence of the geometry as the working surface shock complex advances and evolves (e.g. Lonsdale and Barthel, 1984). It is also worth observing that, were the cloud 'thin' compared to the beam diameter in the transverse dimension, then fig.2 might be roughly symmetric about d, leading to a bifurcation of the beam. This divergence may not persist down stream, however, because of the internal refractions (M.L. Norman, private communication), leading to subsequent intertwining and re-combining.

A distinct form of beam rebirth is called here a 'cloud rupture'. Suppose in figure 2 that the cloud is hit directly by the beam so that the structure on the left of d is also symmetrically on the right. Suppose further that somewhere on the perimeter of the bow shock b the cloud has an 'edge' characterized by $\rho_c = \rho_* e^{-z/\Delta}$, z normal to the wall. Then (Zel'dovitch + Raizer, II, pp.849,859) the breakout time for an energy release E near the wall is $\tau \simeq 24\ (\rho_* \Delta^5/E)^{1/2}$. If the working surface does not move significantly during this time then $E \simeq L_j \tau$ (L_j is the jet power) so that

$$\tau \simeq 8\ \{\rho_* \Delta^5/L_j\}^{1/3} \qquad (9)$$

$$\simeq 10^{12}\ \{\rho_*(-3)\Delta^5(100\text{pc})/L_j(42)\}^{1/3}\ \text{sec.}$$

'Rupture deflection' will only work if this time is small compared to ~ Δ/v_h, where v_h is the beam 'head' velocity. Almost any angle of deflection (i.e. approaching 180°) is possible in this picture however.

§ Super Luminal Interactions

It is likely that the VLBI radio jets and the broad (and possibly also the narrow) emission line cloud regions overlap physically (e.g. Saunders, 1984). Thus cloud-beam interactions of the sort described above are liable to occur. This can lead to two types of super luminal phase velocity. The first is a sequential 'neon sign' or 'Christmas tree' chain of hot spots.

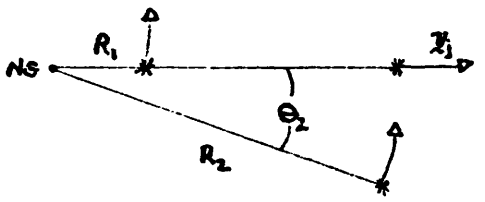

Fig. 3a

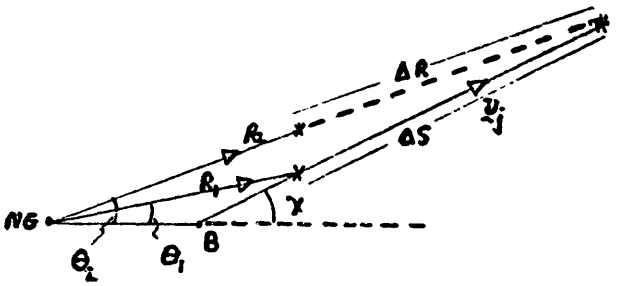

Fig. 3b

Fig.3a:

The line v_j denotes the beam from the nucleus of the galaxy (NG). R_1, R_2 are the radial distances of clouds in circular orbit (asterisks) in a plane 'containing' v_j. R_1 has just drifted into the beam and R_2 is taken to be the next to follow.

Fig.3b:

The bent line NG-B and v_j denotes a bent beam. R_1, R_2 are the radial distances of radially moving clouds in the plane of the beam. R_1 has just drifted into the beam and R_2 is about to do so.

The essential features indicated in figure 3 are (i) the assembly of rapidly-moving clouds and (ii) the pre-existing beam line. Moreover the cloud is supposed to be excited by the beam to form a radio hot spot on contact. Neither the cloud nor the jet motion need be relativistic. An observer in the galaxy and viewing the beam perpendicularly would see the chain of excitations moving with $V_{app} = (R_2\dot{\theta}_2/R_2\theta_2)\ (R_2-R_1) = (R_2\dot{\theta}_2/\theta_2)\ (1-R_1/R_2)$ in the case of (3a), and $V_{app} = (\dot{R}_2/\Delta R)\ \Delta S$ in the case of (3b). In either case V_{app} can clearly be made much larger than the physical velocities $R_2\dot{\theta}_2$ and $\dot{R}_2$, and certainly super luminal. The velocity between the next pair of excitations need not be simply related to that between the first pair. The probability of such configurations must however be examined. We must rely on an increased density of clouds near the nucleus

to explain the predominance of expanding sources over contracting ones. The apparent trajectory will curve in these models only if the beam curves.

The retarded time or Döppler transformation still applies to V_{app}, and in fact

$$V_{obs} = V_{app} \sin \psi / (1 - \frac{V_{app}}{c} \cos \psi) \qquad (10)$$

if ψ is the angle between the local beam direction and the line of sight. For small ψ and $V_{app} >> c$, apparent contraction can occur (M. Rees, private conversation).

Of course the apparent continuity of the motion will depend on the detailed structure of the cloud and on the lifetime of the radio excitation. For example, consider a cloud whose edge is really a long straight wall. Let a point on the cloud edge move radially with velocity V_R and tangentially in the beam-cloud plane with velocity V_θ. Let it moreover possess a spin $\dot{\phi}$. Then the velocity with which the point of interaction between the cloud and beam moves (for the perpendicular observer) is

$$V_{app} = V_R \cos\theta - V_\theta \sin\theta - \cot\phi \, (V_R \sin\theta + V_\theta \cos\theta) + \csc\phi \dot{\phi}^2 (R \sin\theta), \qquad (11)$$

where ϕ is the angle between the straight edge and the beam, and θ is θ_2 in fig. (3a) if R_2 locates the reference point on the cloud edge. The term $\alpha \phi^{-1}$ (ϕ small) is the 'guillotine effect' while that $\alpha \phi^{-2}$ is the 'scissors effect'. Either speed can be super luminal for small enough ϕ. The cloud structure required might be the cocoon wall of the beam's first passage (see also R. Laing regarding lobes in these proceedings). This model for continuous motion is subject to the usual objection that the motion will accelerate as ϕ decreases.

We observe in conclusion that this moving screen picture can combine with the usual Döppler or retarded time effects as in eq.(10). Thus we might only need modest boosting by the screen effect to give V_{app}/c the necessary value $\lesssim 1$. To obtain a lifetime as short as a few years as is observed (Biretta, Walker: These proceedings), requires

$B^2/8\pi \gtrsim 10^{-3}$ erg cm^{-3}. As U_{photon} (1 pc) $\simeq$ L(44) x $10^{-4.5}$, such a value may require inverse Compton losses to be dominant.

References:

Begelman, M.C., Rees, M.J., and Blandford, R.D., 1979, Nature, 279, 770.
Fiedler, R. and Henriksen, R.N., 1984, Ap. J., 281, 554.
Henriksen, R.N., Vallée, J.P., Bridle, A.H., 1981, Ap. J., 249, 40.
Jones, T.W., and Owen, F.N., 1979, Ap. J., 234, 818.
Königl, A., 1980, Physics of Fluids, 23, 1083.
Lonsdale, C.J., and Barthel, P.D., 1984, Astronomy and Astrophysics, in press.
Norman, M.L., et al., 1982, Astr. Astrophys., 113, 285.
Saunders, R., 1984, IAU Symp. #107, 193.
Smith, M.D., et al., 1984, preprint.
van Breugel, et al., 1984, NRAO preprint.
Wilson, A.S., and Ulvestad, J.S., 1982, Ap. J., 263, 576.

SYMMETRIES OF JETS AND HOT SPOTS

ROBERT A. LAING[1]

Royal Greenwich Observatory

ABSTRACT. The brightness symmetries of jets and hot spots in powerful extended radio sources were discussed. It is common for *both* sides of powerful radio galaxies to have bright, compact hot spots when observed with resolutions of a few hundred parsecs. In such sources, there is generally no jet detected on *either* side on maps with dynamic ranges of ~1000:1. In contrast, one side of a powerful extended QSR source generally contains a hot spot of significantly higher surface brightness than the other; this side also tends to be the jetted side of the source if a jet is visible. If a one-sided jet can be traced all the way from its initial turn-on to a hot spot in a lobe, then that hot spot is the most compact in the source.

Morphological, spectral and polarimetric evidence was presented that the more diffuse "secondary" hot spots in lobes with multiple hot spots are the result of deflected outflows from the more compact hot spot. If a jet is seen in a source with a "multiply spotted" lobe, it generally feeds the most compact hot spot in the multiply spotted lobe. The secondary spots are often limb-brightened on the side away from the primary spot. Their radio continuum spectra are generally steeper than that of the more compact hot spot on the same side of the source but less steep than that of the more diffuse hot spot (if any) on the other side of the source. The apparent magnetic field in the region between the compact and secondary hot spots on the same side of the source also tends to be oriented parallel to the line joining them. These properties of secondary hot spots are similar to those predicted by numerical simulations of *nonaxisymmetric* modes of jet deflection (e.g., the formation of nonaxisymmetric oblique shocks by jet instabilities or by a wandering jet impinging obliquely on the wall of a cavity in the circumgalactic medium).

[1] Due to unforseen circumstances, Dr. Laing's original text failed to reach us in time for inclusion in these Proceedings, so this abstract was prepared by us – Eds.

BEAM INEFFICIENCIES AND EXTENDED SOURCE MORPHOLOGIES

W. A. Christiansen
Department of Physics and Astronomy
University of North Carolina
Chapel Hill, N. C. 27514

ABSTRACT

One of the most striking aspects of the structural morphology of extended radio sources possessing one-sided jets is the apparent symmetry of the two radio lobes in conjunction with the strong asymmetry of the jet itself. A plausible interpretation of this peculiar morphology within the context of symmetric (i.e. two-sided), continuous beam models for radio source evolution is that the observed radio jet delineates regions where beam transport of energy is "inefficient".

An analysis of hot spot and lobe luminosity ratios indicates that, at least for sources in which the jet luminosity is within an order of magnitude of the lobe luminosity, the implied energetics of two-sided continuous beams with asymmetric transport inefficiencies are not consistant with observations.

INTRODUCTION

One inference concerning extended radio jets which can command a near unanimous concensus among theorists is that in some sense they delineate the "energy pipeline" running from the nuclear core to the outlying extended radio lobes and it is through this pipeline that the synchrotron emission of the lobes is replenished or sustained. A more controversial issue is related to the specific physical nature of this pipeline. Is the flow continuous or fluctuating; relativistic or nonrelativistic? It might be hoped that the observed morphology of jets, especially the existence of gaps and/or blobs along with the well known tendency of more luminous jets to be one-sided, could prove to be capable of narrowing the range of possibilities implied by the preceding questions.

A particularly vexing issue concerns the one-sided morphology of most of the more luminous jets in conjunction with the near symmetry (AVE luminosity ratio ~ 1.8) in the two extended lobes on opposite sides of the nuclear core. This near equality in lobe luminosities implies that the time averaged power delivered to both lobes must be nearly the same and also suggests that correlations between lobe and jet morphologies might provide useful constraints on theories of energy transport from the nucleus to the lobes.

In many respects, the simplest interpretation of both one-sidedness and the presence of large gaps in jets would seem to be that the nuclear engine fluctuates strongly in power delivered and possibly direction (as in a "flip-flop").

However, the two-sided continuous beam model continues to receive a great deal of attention. In the context of the two-sided continuous beam model, two interpretations of the observed one-sidedness of jets have been advanced: (a) the beam may be relativistic and the observed jet would then delineate the portion of the beam which is more or less approaching the observer, thus

benefitting from "Doppler favoritism" or (b) the observed jet delineates regions in a non-relativistic (two-sided) beam where inefficiencies, possibly in the form of instabilities, have rendered the beam visible. The relativistic hypothesis has received considerable attention both in the published literature and at this workshop. Many of the advantages and difficulties of the relativistic model are well known and will not be discussed further in this contribution. Rather, we shall explore some simple implications for jet-lobe morphologies which may be drawn from the inefficiency hypothesis.

ANALYSIS

In this type of model for radio jets the observed synchrotron radiation would be associated with regions where the directed motion of the beam has been partially randomized. Let $F_J < 1$ represent the fraction of the total initial hydrodynamic power in the beam (P_{Beam}) which is consumed in creating a visible jet (e.g. heating the background gas, synchrotron radiation losses, etc.). Then if $\delta_J < 1$ represents the fraction of this randomized kinetic energy loss from the beam which is coverted into synchrotron radiation, the luminosity of the jet will be

$$L_J = \delta_J F_J P_{Beam} \tag{1}$$

Thus, the amount of hydrodynamic power remaining in the beam when it emerges from the pipeline is

$$P'_{Beam} = (1-F_J)P_{Beam}. \tag{2}$$

It is this emergent power which is available for maintaining the lobe synchrotron emission. For confined beams a "hot spot" in a lobe defines the region where the beam is stopped (i.e. randomized) and relativistic particles are energized. We expect that these particles will be streaming and/or diffusing out of the hot spots to inflate and energize the lobes, but we again expect that the luminosity of either the hot spots or the lobes will scale proportionately with the impinging power, i.e.

$$P_{HS} = \delta_{HS} P'_{Beam} = \delta_{HS}(1 - F_J)P_{Beam}$$

$$P_L = \delta_L P'_{Beam} = \delta_L(1 - F_J)P_{Beam}$$

Here δ_{HS} represents the fraction of randomized beam energy converted to radiation in the hot spot and δ_L represents the total fraction of beam energy transformed in into radiation emanating from the entire lobe (including the hotspot). Thus, $\delta_L > \delta_{HS}$. In any case, we may now estimate the inefficiency coefficient for the jet in terms of δ's and the observed jet and hot spot (or lobe) luminosities, i.e.

$$F_J = \frac{\delta_{HS(or\ L)}\ L_J/\delta_J\ L_{HS(or\ L)}}{1 + (\delta_{HS(or\ L)}\ L_J/\delta_J\ L_{HS(or\ L)})} \tag{4}$$

Returning to the question of one-sidedness, if this model is applicable, we would conclude that the transport efficiency of the pipeline on the opposite (counter jet) side of the source is <u>higher</u> and, hence, the loss fraction is much smaller than F_J, i.e.,

$$F_{CJ} \ll F_J < 1 \tag{5}$$

(where F_{CJ} is the fraction of the beam power lost in this putative counter jet). Again the hydrodynamic power reaching the lobe on the counter jet side of the source is

$$P''_{Beam} = (1 - F_{CJ})\ P_{Beam}. \tag{6}$$

Therefore, if the sychrotron conversion efficiency $\delta_{HS(or\ L)}$ is the same in both hot spots (or lobes) on opposite sides of the source the ratio of steady state luminosities is,

$$\frac{L^{J}_{HS(or\ L)}}{L^{CJ}_{HS(or\ L)}} = \frac{1 - F_J}{1 - F_{CJ}} \tag{7}$$

Thus, in the steady state, the luminosity of the hot spot (or Lobe) on the same side of the source as the jet should be consistently less than the luminosity of the hot spot (or Lobe) on the side of the source which doesn't have a visible jet. Referring to equation (4) we may substitute for F_J and conclude

$$\frac{L^{J}_{HS(or\ L)}}{L^{CJ}_{HS(or\ L)}} \lesssim \frac{1}{1 + (\delta_{HS(or\ L)}L_J/\delta_J L^{J}_{HS(or\ L)})} < 1 \tag{8}$$

As far as hot spot luminosity ratios are concerned, it appears that the hot spot associated with the one-sided jet is consistently the more luminous. In their review, Bridle and Perley, 1984, report that 16 of 17 Fanoroff and Riley Type 2 radio sources with bright cores have the one-sided jet pointing toward the brighter hot spot. Furthermore, among the FR Type 2 sources with weak core emission, the jet still points to the brighter hot spot in 10 of 17 cases. In any event, actual hot spot luminosity ratios appear to run strongly counter to the expectation of the simple inefficiency hypothesis which led to equation (8) above.

A similar result emerges if lobe luminosity ratios are considered rather than hot spot ratios. To illustrate our point, we have listed in Table I the flux densities for lobes, hot spots and jets reported in the literature for several well known sources with prominent one-sided jets. Note that many of these sources possess very large (possibly steep spectrum) extended features as well as hot spots and/or intermediate structures. In any case it is clear that among the sources listed in Table I the ratios of the luminosities of jet-hot spots or jet-lobes to the opposite hot spots or lobes are not correlated and definitely do not stay below the upper limit implied by equation (8).

TABLE 1

Source	Total Jet Luminosity (ergs/sec)	Hot Spot Luminosity (Jet Side) (ergs/sec)	Lobe Luminosity (Jet Side) (ergs/sec)	Hot Spot Luminosity (Opposite Jet) (ergs/sec)	Lobe Luminosity (Opposite Jet) (ergs/sec)	Hot Spot Luminosity Ratio L^J_{HS}/L^{CJ}_{HS}	Lobe Luminosity Ratio L^J_L/L^{CJ}_L
M87	4.2×10^{40}	---	4.1×10^{41}	---	6.7×10^{41}	---	0.61
NGC315	1.56×10^{41}	---	6.4×10^{40}	---	5.2×10^{40}	---	1.23
B0844+31	1.7×10^{40}	3.6×10^{40}	2×10^{41}	2.2×10^{40}	1.9×10^{41}	1.6	1.05
3C388	10^{40}	8×10^{41}	2.7×10^{42}	4×10^{41}	3.1×10^{42}	2	0.87
3C219	2.5×10^{42}	---	3.3×10^{43}	---	3.2×10^{43}	---	1.03
4C74.17.1	2.9×10^{41}	---	3.7×10^{41}	---	4.4×10^{41}	---	0.84
NGC6251	6.6×10^{41}	2×10^{41}	1.6×10^{41}	2×10^{41}	2.2×10^{41}	1	0.73
3C66B	6.6×10^{41}	---	6.73×10^{41}	---	8.4×10^{41}	---	0.80

CONCLUSION

In conclusion, the preceeding simple, but general, model demonstrates that the inefficiency hypothesis for a symmetric two-sided beam is not easily reconciled with observations. Either a relaxation of the assumption of symmetry in the power source and/or the introduction of variability in the power supply would seem to offer the possibility of explaining jet lobe morphologies. In either of these cases, however, the assumption of differential inefficiencies in the energy pipeline then becomes irrelevent to the interpretation of source morphology.

BIBLIOGRAPHY

1. Bridle, A. and Perley, R. (1984) Ann. Rev. Astron. and Astrophys., 22, 319.

THE JOLLY GREEN JET

L. RUDNICK

Department of Astronomy, University of Minnesota, 116 Church Street S.E., Minneapolis MN 55455

ABSTRACT. A method is described whereby any observational or theoretical astrophysicist may obtain first hand experience about the development of turbulence in fluid flows. The flow is set up, and the details should be observed, with grains of salt.

For those of us who are visually oriented, I recommend the following experiment in fluid flow (Figure 1). Attentive parties at the meeting (e.g., Figure 2) estimated Reynolds numbers of ~ 10 to 10^2. Depending on the conditions of the ambient fluid, and the flow rate, one can observe laminar flow, firehose instabilities, pinching modes and vortex ring formation, and phase *vs.* group velocity effects. Variations are encouraged.

To set up the flow, prepare a saturated saline solution with a healthy dose of food coloring. Allow the saline solution to flow into clear water through a small orifice, as diagrammed in Figure 1. Sit back and enjoy.

I hereby acknowledge a long-standing debt to Don Herbert, Mr. Wizard. This work is not supported by any NSF grant.

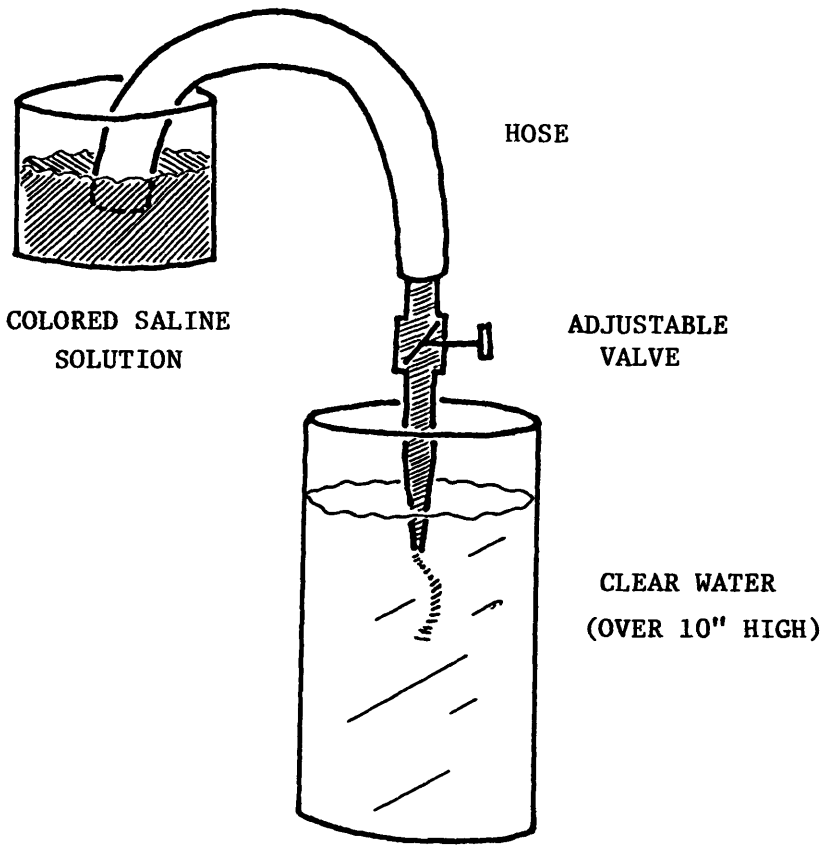

Figure 1. Apparatus required to produce the Jolly Green Jet.

Figure 2. Observations and theoretical modeling of the Jolly Green Jet in progress at the Workshop. *Top left*, Alan Bridle and Dick Henriksen; *top right*, Arieh Königl, Bridle, Henriksen; *bottom left* Königl, Bridle, Henriksen, Larry Rudnick; *bottom right*, Henriksen, Rudnick, Greg Benford. *Original photographs courtesy of Peter Wilkinson.*

MENU FOR AN ALL-PURPOSE SOURCE MODEL

ALAN H. BRIDLE

National Radio Astronomy Observatory[a], Charlottesville, Virginia 22903

1. INTRODUCTION

An "Observers' All-Singing, All-Dancing Dream Model" for energy transport in extragalactic sources was presented to the theorists after dinner on the third day of the Workshop. It summarized the observational constraints relating to energy transport in such a way as to promote debate about the physics of a model. It was based on what consensus I found regarding these constraints in discussions among the observers in the first three days of the meeting. These discussions included Jack Burns, John Dreher, Jean Eilek, Robert Laing, Larry Rudnick, Craig Walker, John Wardle and Peter Wilkinson, but the form the arguments take here is tinted (some may say tainted) with my own views, and none of the above should take any blame for this version's shortcomings. At the meeting, the "Observers' Dream" focused an evening of discussions in which several groups brainstormed the physics which might be implied by it.[1]

2. EVIDENCE FOR $\gamma_j \gg 1$ ON PARSEC SCALES

The evidence for Lorentz factors $\gamma_j \approx 5$ in some parsec-scale flows is drawn (in different sources) from the following smorgasbord (see also Dave De Young's review on "jet efficiency"):

(a) the superluminal knot separations in VLBI "core-jets" can be simply explained if $\gamma_j \approx 2.5$ to 10 (for $H_0 = 100$ km/s/Mpc), and if these jets are oriented within the beaming cone (whether or not this is $\approx 1/\gamma_j$ radians, see below) from the observer's line of sight,

(b) the same parameters entail Doppler boosting which accounts for the one-sidedness of the same VLBI core-jet structures,

(c) the same assumptions explain the low Compton X-ray fluxes from compact radio sources (e.g. Marscher and Broderick 1981),

(d) the small angles to the line of sight required by the relativistic-flow interpretation of the above effects are consistent with the large apparent bending observed in the jets of core-dominated sources, and with the misalignments between parsec- and kiloparsec-scale structures in these sources.

Similar assumptions (but with higher values of γ_j) would explain the excessive brightness temperatures implied by rapid low frequency variability, but the variations may also be due to interstellar scintillations (Rickett *et al.* 1984).

---

[a] The National Radio Astronomy Observatory (NRAO) is operated by Associated Universities, Inc., under contract with the National Science Foundation.

[1] Understandably, none of these *ad hoc* "theory groups" wished to have its midnight back-of-the-napkin "models" exposed to the daylight of these Proceedings, but the "Observers' Dream" and the rationale behind it are reproduced here in the hope that they can stimulate further discussion of the problems – Eds.

These arguments favor $\gamma_j \gg 1$ in some parsec-scale jets, and there is little evidence *against* bulk relativistic motion on this scale.[2] It is attractive to propose, as in the "unified" models, that when the line of sight lies within the beaming cone (whether or not this is larger than $1/\gamma_j$) we sample the smorgasbord of core-dominated, superluminal, etc. phenomena described above, but when it is outside the beaming cone we see only the unbeamed parts of the source. The difficulties of explaining sharp bends in relativistic jets (e.g. De Young, this Workshop) may be ameliorated if such bends are actually gradual bends in 3-D that have been amplified by projection.

If some parsec-scale emission is Doppler boosted, one might expect an inverse correlation between the relative prominence of the sub arc-second "cores" seen with connected element interferometers and the projected linear sizes of the extended emission around them – there is some evidence for this (Kapahi and Saikia 1982) in QSR samples. On the other hand, some core dominated superluminal sources have extended radio structures (e.g., Schilizzi and de Bruyn 1983) whose linear sizes would be unusually large if the entire source makes an angle $< 1/\gamma_j$ radians to the line of sight. This problem may be circumvented if the jet trajectories are curved, making the cone of directions over which superluminal motion can be observed broader than $1/\gamma_j$ however[3], so the statistics of extended source sizes around bright cores may be a weaker constraint on the parsec-scale flow parameters than the other phenomena described above. There is therefore broad agreement that:

1. The central engines can make collimated bulk relativistic ($\gamma_j \approx 5$) flows which radiate for at least a few parsecs.

3. EVIDENCE AGAINST $\gamma_j \gg 1$ ON KILOPARSEC SCALES

(a) Weak radio galaxies.

The sensitivity of Doppler boosting to $v_j \sin i$ (where v_j is the flow velocity and i is the angle of the flow out of the plane of the sky) argues against $v_j \approx c$ in the C–shaped jets in "narrow head-tail" sources. If these are bent by the ram pressure of the IGM, v_j changes direction along them by angles approaching 90°. If $v_j \approx c$, they would (a) have large side-to-side asymmetries and (b) change brightness noticeably as they bend, unless the flows are nearly all very close to the plane of the sky, which is highly improbable. This says (e.g. Chris O'Dea, this Workshop):

2. The velocities in head-tail flows are nonrelativistic.

Studies of some elliptical or S0 radio galaxies with dust lanes also show that one-sidedness at the bases of their two-sided jets is not due to Doppler favoritism – three of the one-sided jet bases in seven such galaxies studied by Robert Laing (this Workshop) are on the *receding* side (if the flow goes *out*, not *in*!), and three others lie too close to the plane of the sky for their brightness asymmetry to be due to Doppler boosting. These

[2] Although 3C147 has a complex, two-sided parsec-scale structure (Preuss *et al.* 1984), this is not yet a problem for the bulk relativistic flow model of small jets – a *small* number of apparently two-sided core-jets could arise in the 3C sample as a result of bending relativistic flows across the line of sight.

[3] Scheuer (1984) has proposed an example of such a situation, where the flows follow diverging curves, rather than straight lines. The refractive shock models described by Lind and Blandford (this Workshop, and *M.N.*, in press) give one physical basis for bent trajectories. The Doppler boosting cone may also be broadened by such effects.

data and the brightness asymmetries of some head-tail sources (e.g. 3C129) suggest that (at least in sources with total 1.4 GHz powers $P_{tot}^{1.4} < 10^{24}$ W/Hz) :

3. Some brightness asymmetries in kiloparsec-scale jets are not due to Doppler boosting.

This should make us distrust one-sidedness *alone* as evidence for bulk relativistic motion on any scale, or in sources of any power. Whatever makes non-Doppler asymmetries on kiloparsec scales in weak sources may operate elsewhere too ! Also, as there is no "Compton catastrophe" for weak radio cores, we should attempt to measure proper motions in them. If none proves to be superluminal, there would be no evidence for bulk relativistic motion in *any* weak radio galaxy jets, large or small.

(b) Powerful radio galaxies and QSRs.

The flow parameters in the jets in weak and strong sources could however be significantly different, as the jets in the weaker sources have significantly different properties from those in more powerful sources (Bridle 1984 and this Workshop). The jets in powerful sources are narrow, blobby, and tend to make hot spots, while those in the weak sources are wider, smoother, and fade away without making hot spots. The first list is more characteristic of hypersonic flows, with little entrainment and lots of internal reflecting shocks, punching their way out to classical "working surfaces". The second list is more characteristic of mildly supersonic flows, entraining ambient gas and decelerating, perhaps turning into buoyant plumes (e.g., Geoff Bicknell, this Workshop). It would therefore be attractive if the central engine made high Mach number, narrow flows in powerful sources, and lower Mach number, wide flows in weak sources.

The correlation of jet magnetic orientation with luminosity (Bridle 1984) may also be explained if the mean flow *velocity* increases with source power. The parallel magnetic field components in powerful jets must be maintained efficiently along them against $1/R_j^2$ dilution, as these jets are $B_{||}$ dominated over most of their length (except perhaps at very bright knots, where oblique fields may occur). In weak sources, $B_{||}$ need not be maintained so efficiently, as their jets generally become $B_{\perp}$-dominated, except perhaps at their edges and at bends. If $B_{||}$ maintenance is linked to shear at the edges of a jet, we need a deep, strong velocity shear around straight powerful jets but a shallow, weak shear around straight weak ones. Velocity estimates based on assuming steady energy supply to the lobes and thrust balance between jets and the brighter lobe features (e.g., Bridle and Perley 1984) also suggest that v_j increases with P_{tot}.

These ideas taken together suggest that:

4. Mean flow velocities and Mach numbers both increase with increased power output from the central engine.

But does v_j approach c in the kiloparsec-scale jets in the most powerful "classical double" sources ? The evidence on this point is ambiguous.

Some bent one-sided large-scale jets in powerful sources (e.g. 4C49.22, 4C32.69) have smooth brightness variations which are inconsistent with changing Doppler boosts in high-γ_j flows *if they bend because they are confined or deflected.* Such jets might instead be ballistic, their shapes arising from wobble (precession ?) of the primary collimator; $\mathbf{v_j}$ would not then follow the bends but the wiggle pattern would move outwards as a whole, so that changes in $v_j \sin i$ and in the Doppler boost could still

be small. We need to assess whether such jets are indeed ballistic in order to assess whether their brightness distributions argue against $v_j \approx c$. John Wardle showed us evidence that $B_{||}$ is enhanced at the outer edges of the bends in the jet in 4C32.69; this is a phenomenon seen in the jets of lower power sources, where it is attributed to real bending of the flow and to shearing of the field at the outer edges of the bends. If this interpretation is correct, the smooth brightness variation in the jet in 4C32.69 argues that its one-sidedness is not due to Doppler boosting; this may be a useful way to attack this question for other long one-sided jets.

In some radio galaxies, such as 3C277.3, bright, low-velocity extranuclear optical emission line features share the asymmetries of adjacent one-sided radio continuum jets. This requires non-Doppler interpretations of the radio jet asymmetry, as the emission lines cannot be Doppler boosted. Larry Rudnick (this Workshop) has extended this argument to the powerful QSR 0812+02, which has a one-sided optical emission line feature on the same side as its one-sided radio jet. These correlations between radio continuum and optical emission line asymmetries hint that the non-Doppler asymmetries of jets in weaker radio galaxies may indeed extend to more powerful sources.

If the brightness asymmetries in the long one-sided jets in powerful sources are due to the Doppler boost, these jets must be longer in 3-D than they appear in projection. Without detections of the counterjets, it is difficult to assess how seriously this argues against the Doppler boost as the prime cause of these jet asymmetries. We have learned that our statistics of 3CR and 4C QSR source sizes come from samples with significant numbers of one-sided jets – if some kiloparsec-scale flows are even mildly relativistic, the reference samples of lobe-dominated QSRs may be biased away from the plane of the sky to some extent, making us underestimate the intrinsic sizes. Nonetheless, it will embarrass the Doppler boost interpretation if large numbers of very one-sided jets continue to be found in samples of the *most extended* QSR radio sources, as reported here by John Wardle and by Frazer Owen. Even so, energy balance in the lobes and thrust balance at the hot spots may require *mildly* relativistic ($\beta \approx 0.5$) jets in the most powerful sources (e.g. John Dreher, this Workshop). We must carefully distinguish recessed hot spots, which may be oblique shocks in continuing flows, from genuine "beam caps" when making these calculations, however. We also need to know how to recognize, and discount, overpressures at shocks near the ends of hypersonic jets when making the thrust balance calculations for powerful sources.

Overall, it seems likely that:

5. The jets which radiate on kiloparsec scales are generally nonrelativistic, or at most mildly relativistic, flows. There is no clear evidence for flows with $\gamma_j \approx 5$ on kiloparsec scales.

4. PARSEC - KILOPARSEC CORRELATIONS

(a) Core - jet detectability.

With resolving powers ≥ 0.1 arcsec, core and jet detectabilities appear coupled. Jets are detected more often in sources with prominent cores (see the papers by Jack Burns and myself earlier in these Proceedings), and there are very few, possibly no[4],

[4] Robert Laing's evidence that the "core" of 3C351 may be a one-sided jet is my reason for equivocating

known coreless ("disembodied") large-scale jets. Either both the cores and the jets are about equally Doppler boosted, or the luminosities of intrinsically one-sided jets are coupled to those of the cores. This requires that:

6. A significant fraction of the core luminosity in most sources is no more strongly beamed than is the large-scale jet luminosity.

(b) Sidedness.

The correlation between the brightness asymmetries of resolved parsec-scale scale and kiloparsec-scale emission in the same source hands model builders their worst dilemma, so the evidence is worth relating again in some detail.

Of 20 sources in the Bridle and Perley (1984, BP) list with both parsec-scale jets (or jetlike elongations) and kiloparsec-scale jets, five exhibit superluminal expansion (3C120, 3C179, 3C273, 3C279, 3C345 – Cohen and Unwin 1984). In all five, one-sided kiloparsec- and parsec-scale jets start out *on the same side* of the unresolved core. Fifteen other sources in the BP list have jets on both scales, but the proper motions on the parsec scales are either unknown or small. In 12 of the 15 (NGC315, 3C78, 3C84, 0957+56, 3C111, M87, Cen A, NGC6251, 3C371, 3C405, 3C418 and 3C454.3) the brighter large-scale jet is on the same side as a small-scale one-sided jet. The other three are 3C147 (complex small-scale structure), M84 (no closure-phase VLBI map, so its sidedness is unknown), and 3C309.1 (complex large-scale structure, though Peter Wilkinson's results suggest that it fits the trend of the other 12). The fact that the one-sided small-scale jet points "towards" the brighter of the large-scale jets in at least 17 of these 20 sources argues that the prime cause of the jet brightness asymmetry is the same on both scales. Three possibilities may be envisaged: (a) both large and small scale jets are the approaching sides of two-sided (symmetric) bulk relativistic flows, (b) both arise from symmetric two-sided flows whose dissipation of flow energy to synchrotron radiation is greater on one side than on the other, (c) both arise from intrinsically one-sided flows.

Option (b) may be hard to arrange; what physics could maintain a purely dissipative asymmetry over a 10^5 : 1 range of linear scales, and make its range increase with the power output of the central engine ? Constraints **(1)**, **(5)** and **(6)** complicate option (a) if we place all the required ingredients in every source and rely on variations in geometrical aspect to dictate which features dominate the observed radiation. This approach would require a *two-component* ($\gamma_j \approx 5$ and $\gamma_j \approx 1$) flow on parsec scales, the latter persisting to kiloparsec scales and producing the pc-kpc sidedness correlation. This option becomes less attractive as higher fractions of one-sided jets show up in powerful sources (unless the beaming/boosting cones are much wider than $1/\gamma_j$).

Option (c) has no problem with the statistics of large-scale one-sidedness – but if the asymmetric flows were nonrelativistic, or only mildly relativistic, on *both* kiloparsec and parsec scales it would not explain superluminal motions, weak X-ray emission from bright cores, rapid variability etc. in that fraction of the sources which is favorably oriented towards the observer. We can resolve this difficulty if:

---

here; other jetted sources with "steep-spectrum cores" could enter this category if no flat spectrum compact component is found in their "core".

7. The engines normally eject material asymmetrically, with both relativistic ($\gamma_j \approx 5$) and nonrelativistic components of the flow on the same side at the same time.

This permits sources in which the flows are sufficiently close to the line of sight to exhibit bulk relativistic effects on parsec scales, but produces the *correlation* between parsec- and kiloparsec-scale sidedness via the *intrinsic* asymmetry. It can be criticised as "having our cake and eating it", but may be physically reasonable if the relativistic flow has a nonrelativistic sheath, or boundary layer. It can be distinguished from other alternatives statistically if the intrinsic asymmetry is too large to be overcome often by boosting. It allows many one-sided jets in big sources, but predicts that only a *small* fraction of the cores in sources with one-sided large-scale jets will show superluminal motions – half of the relativistic flows will be receding from us, and only a subset of the approaching ones will be oriented so as to exhibit superluminal motion. The superluminal motions should always be on the same side as the large-scale jet. Note that the sources with very prominent cores may be those in which emission from the nonrelativistic core component has been augmented by a Doppler-boosted relativistic component, so the statistics of superluminal motion in bright-core sources do not test the above prediction. Because it postulates a nonrelativistic component in the core, hypothesis (7) can satisfy constraint (6) and also pass Scheuer's (1984) "core detectability" test.

5. Old stuff – Large-scale symmetries

The size and brightness symmetries of the large-scale double structures both require that these structures are unbeamed, and that energy is transported to both sides of most sources within the typical time scale τ_{lobes} for radiative decay of the emission from the lobes. (τ_{lobes} is $\geq \tau_{syn}$, the local synchrotron decay time, the inequality depending on the physics of particle transport and reacceleration within the lobes). Energy transport from the nucleus need not be continuous, however, and *some* sources show detailed "avoidance" behavior in their brightest regions, suggesting that it is not (Rudnick and Edgar 1984; also see Ensman and Ulvestad 1984). The basic requirement is thus:

8. Energy transport is equalised on the two sides of most sources on time scales $< \tau_{lobes}$.

6. Constraints on Flip-Flop Models

Constraints (7) and (8) together nudge us in the direction of "flip-flop", or at least very asymmetric, outflow models (Willis *et al.* 1978; Wiita and Siah 1981; Robson 1981; Linfield 1982; Saikia and Wiita 1982; Rudnick 1982 and this Workshop; Icke 1983; Lonsdale and Morison 1983; Rudnick and Edgar 1984), and impose constraints on the *mean* time scale τ_{flip} for reversing the asymmetry at the central engine:

9. The asymmetry of the large-scale flow must reverse on a typical time scale τ_{flip}, where $\tau_{flip} < \tau_{jet} < \tau_{lobe}$ in the low power sources, but $\tau_{jet} < \tau_{flip} < \tau_{lobe}$ in the powerful sources.

Here τ_{jet} is the typical time scale for decay of the emission from the jet(s) in a given source – it will generally be the energy transport time scale d_j/v_j for a jet feature distant d_j from the core, but could be the local synchrotron decay time scale if this is $< d_j/v_j$ and there is no particle reacceleration. The constraints in (9) are required if flip-flop

models are to produce two-sided jets and two-sided lobes in the weak sources, but one-sided jets and two-sided lobes in the more powerful sources. Loosely speaking, they call for rapidly flipping asymmetric ejection in the weak sources and slowly flipping asymmetric ejection in the powerful ones. τ_{flip} need not be interpreted strictly as the constant period of an oscillation – it is sufficient that it represent the *mean* time between the flow from the central engine favoring one side over the other. "Pieces of jets" (Larry Rudnick, this Workshop) could be cases where the ejection is intermittent, or flips sides, on a time scale $< d_{lobe}/v_j$. The flip-flop model readily accommodates both "avoidance" behavior and "pieces of jets", but apparently smooth two-sided jets (as in the symmetric parts of 3C31 or M84) are harder to explain, unless $v_j\tau_{flip}$ is below the linear resolution of present maps. This may be possible if the flows in weak radio galaxies are decelerating due to entrainment, but seems somewhat contrived. It might be simpler if the model could provide for the average asymmetry of the flow to decrease with decreasing luminosity of the central engine.

7. Constraints from Hot Spots

Hot spots can occur on both sides, on one side only, or on neither side, of double sources – the hot spots are prominent in powerful sources and absent in weak ones. The absence of hot spots in weak sources can be interpreted as a low-Mach number effect, as in §3, but there is also an important correlation in powerful sources with strong cores (BP; Robert Laing, this Workshop) – in many of these, one hot spot has significantly higher surface brightness and flatter spectrum than any other, and this is usually the jetted hot spot if a jet is visible. (This is the main *systematic* difference between the radio structures on the jetted and unjetted sides of strong-core doubles). In powerful radio galaxies, or powerful sources with weak cores (these definitions are almost equivalent), the hot spot brightnesses are generally more equal and the jet and hot spot symmetries are less clearly related – the jets are also much harder to detect. The enhanced brightness of the jetted hot spots in strong-core doubles could be due either to intrinsic asymmetries or to the hot spots having mildly relativistic motions, but the brighter hot spots in such sources are not systematically further from the cores, as expected in naive (steady, collinear) relativistic outflow models.

A model with intrinsically asymmetric outflow can accommodate these constraints if $\tau_{flip} > \tau_{hotspot}$ in most QSRs but $\tau_{flip} < \tau_{hotspot}$ in most powerful radio galaxies. Cyg A exemplifies the powerful radio galaxy case – it has a relatively weak core, strong symmetric hot spots and a weak jet; these properties fit mildly relativistic symmetric flows easier than intrinsically asymmetric flows. The brightness fluctuations of the main jet in Cyg A may fit an *intermittent* ejection model, but the brightness symmetry of its hot spots would be explained more convincingly in an *alternating* ejection model if there was clear evidence for similar "pieces of the counterjet" among the filaments and wisps in its South-following lobe[5].

[5] Whether such evidence existed already was debated at the Workshop, based on VLA images of Cyg A employing various contrast- and gradient-enhancement techniques. The brightness, location, shape and continuity of the Cyg A counterjet, if one exists, are so important that I reserve assessment of them until the experimental evidence becomes clearer.

8. THE STUFF THE "DREAM" IS MADE OF

The "Observers' Dream" is thus a central engine that can produce intrinsically asymmetric, relativistic *and* nonrelativistic flows whose velocity, Mach number, flipping time scale, and perhaps asymmetry, all increase with total power output. To meet constraint (6), the nonrelativistic (unbeamed) flow should begin on sub-parsec scales in most sources. Whether there need be a relativistic flow on *any* scale in intrinsically weak sources depends on whether superluminal motions are found in those with weak large-scale structure[6]. The $\gamma_j \approx 5$ component specified in (7) could be an "optional extra" if superluminal motions and rapid variability prove to be sufficiently rare in complete samples selected by the flux density in their large scale structures.

Conversely, it is not (yet) essential that highly relativistic flow persists beyond $\sim$ 10 pc in any of the sources which *do* show evidence for it closer to the nucleus, but detection of superluminal motions at greater distances could extend the range required. The modelers are free to specify the fate of this component of the flow far from the core, providing it "poops out" sufficiently that its radiation rarely dominates the large-scale emission; the *radio* data do not yet tell us clearly where or even whether it is decelerated to nonrelativistic velocities.

9. PROBLEMS FOR THE OBSERVERS

(1) Find secure, direct constraints on the flow velocities, particularly in the one-sided, powerful jets.

(2) Find out *how* one-sided these jets really are by hunting for their counterjets. This will be easiest in sources with bright enough small-scale structure to permit self calibration, but which are not too core-dominated. I hope that improvements in image processing, and long VLA syntheses, will show us the counterjets in some powerful sources – this would tell us (a) by how much the asymmetries of these sources exceed the non-Doppler asymmetries at the bases of the jets in weaker sources, and (b) how bad the inclination-related problems are for these sources if their asymmetries are interpreted using the standard relativistic flow models. Such observations could also tell us more about how well the radiation is suppressed in the initial "gaps" in jets, and between "pieces of jets" further from the cores; this would help us to assess whether we are dealing with actual flip-flops, or variable asymmetry, or variable jet velocity.

(3) Use VLB arrays to study the cores in complete samples of sources with (a) one-sided and (b) two-sided, large-scale jets. How often does superluminal motion occur in each of these groups ? Do their parsec scale properties differ – is there any evidence, other than jet sidedness, for relativistic flow on parsec scales in weak sources with two-sided jets ? How often does superluminal motion occur on the large-scale jetted side of sources with one-sided jets ? Are there convincing cases of two-sided jets on parsec scales, or of a one-sided parsec-scale jet opposing a one-sided kiloparsec-scale jet ?

(4) Do we violate Faraday rotation constraints if we ask that the relativistic parsec-scale flows are surrounded by nonrelativistic flows going in the same direction ? This requires polarimetry of the superluminal components – the maps John Wardle showed

[6] 3C120 shows that this *can* happen, and the core dominated BL Lac objects with weak, edge darkened large-scale structure may be the best places to search for superluminal motions to test this point.

us here prove there is polarized signal to look at, so VLBI referees should be encouraged to allocate the time !

10. Problems for the Theorists

(1) How difficult is it to brake a relativistic jet between the parsec and kiloparsec scales without converting much of its energy into heat ? Must a jet be transonic to slow down quietly (Begelman 1982; Scheuer 1983) ? (If quiet braking is possible, the nonrelativistic or mildly relativistic flow required on kiloparsec scales in powerful sources may derive its energy and momentum fluxes by degrading an initially relativistic flow).

(2) How would a spine of "radio-quiet" relativistic flow affect the observable properties of a sheath of "radio-loud" nonrelativistic flow on kiloparsec scales ? Could it be bent without becoming visible in ways which conflict with jet data ? Could it provide ongoing particle acceleration far from the core ?

(3) Can a flip-flop jet production mechanism be made, which switches its asymmetry on time scales *long* compared with those of outflow from the primary collimator, but *short* compared with those of radiative decay in the jets of weak sources and the lobes and hot spots of strong ones ? Can the switching time, flow velocity, initial Mach number (and perhaps asymmetry) be made to increase with outflow power ?

I thank Chris O'Dea, Craig Walker and Joan Wrobel for comments on an early draft of this paper, and the other observers at Green Bank for lively discussions.

References

Begelman,M.C. (1982). *Proc. IAU Symp. 97, Extragalactic Radio Sources* (ed. D.S.Heeschen and C.M. Wade) Dordrecht:Reidel, 223.

Bridle,A.H. (1984). A.J. **89**, 979.

Bridle,A.H., Perley,R.A. (1984). Ann.Rev.Astron.Ap. **22**, 319 (**BP**).

Cohen,M.H., Unwin,S.C. (1984). *Proc. IAU Symp. 110, VLBI and Compact Radio Sources* (ed. R.Fanti, K.I.Kellermann and G.Setti) Dordrecht:Reidel, 95.

Ensman,L.M., Ulvestad,J.S. (1984). A.J. **89**, 1275.

Icke,V. (1983). Ap.J. **265**, 648.

Kapahi,V.K., Saikia,D.J. (1982). J.Astrophys.Astron. **3**, 465.

Linfield,R. (1982). Ap.J. **254**, 465.

Lonsdale,C.J., Morison,I. (1983). M.N.R.A.S. **203**, 833.

Marscher,A.P., Broderick,J.J. (1981). Ap.J.Lett. **247**, L49.

Preuss,E., Alef,W., Whyborn,N., Wilkinson,P.N., Kellermann,K.I. (1984). *Proc. IAU Symp. 110, VLBI and Compact Radio Sources* (ed. R. Fanti, K. Kellermann and G. Setti) Dordrecht:Reidel, 29.

Rickett,B.J., Coles,W.A., Bourgois,G. (1984). Astron. Astrophys. **134**, 390.

Robson,D.W. (1981). Nature **294**, 57.

Rudnick,L. (1982). *Proc. IAU Symp. 97, Extragalactic Radio Sources* (ed. D.S.Heeschen and C.M. Wade) Dordrecht:Reidel, 47.

Rudnick,L., Edgar,B.K. (1984). Ap.J. **279**, 74.

Saikia,D.J., Wiita,P.J. (1982). M.N.R.A.S. **200**, 83.

Scheuer,P.A.G. (1983). *Highlights of Astronomy, Vol.6* (ed. R.M.West) Dordrecht:Reidel, 735.

Scheuer,P.A.G. (1984). *Proc. IAU Symp. 110, VLBI and Compact Radio Sources* (ed. R. Fanti, K. Kellermann and G. Setti) Dordrecht:Reidel, 197.

Schilizzi,R.T., de Bruyn,A.G. (1983). Nature **303**, 26.

Wiita,P.J., Siah,M.J. (1981). Ap.J. **243**, 710.

Willis,A.G., Wilson,A.S., Strom.R.G. (1978). Astron.Astrophys. **66**, L1.

LINEAR ANALYSIS OF JET STABILITY

Philip E. Hardee
University of Alabama
Tuscaloosa, AL 35486

ABSTRACT. The linear stability analysis of jets with cylindrical cross section is reviewed. In a linear stability analysis perturbations to a jet are analyzed in terms of Fourier components which in cylindrical geometry split into Fourier modes with different configuration. The Fourier modes split into an OM and many RM solutions. The effect of growing OM and RM components on a jet is different and the relative importance depends on jet parameters. In general, OM and RM solutions of a Fourier mode will have a characteristic frequency and wavenumber. Higher characteristic frequency and wavenumber of a Fourier mode and its associated OM and RM solutions mean that these Fourier components grow more rapidly, are more sensitive to the effects of shear at the jet surface and become non-linear at smaller amplitudes. Lower characteristic frequency and wavenumber Fourier modes grow more slowly but are less sensitive to the effects of shear and become non-linear at larger amplitudes. Because the higher frequency and wavenumber Fourier modes can be stabilized absolutely or at small amplitude, the lower frequency and wavenumber Fourier modes are those that are most likely to be directly observable. In fact it is the pinch Fourier mode whose effects are directly observable in numerical models of axisymmetric jets and whose effects may be responsible for knots in the structure of some extragalactic jets. It also seems likely that the twisting seen in many extragalactic jets which allow non-axisymmetric Fourier modes can be described by the propagation properties of the twist Fourier mode.

I. Introduction

It has long been known that the contact surface between a flow and a stationary background is Kelvin-Helmholtz unstable to small perturbations. This instability and its development in time and space regulate the interaction between a jet and its confining medium. A complete description of this interaction requires a non-linear analysis of the evolution of the contact surface. Numerical work describing the non-linear evolution of an axisymmetric jet is discussed by Mike Norman elsewhere in this workshop proceedings and in a paper by Norman et al. (1982). An analytical approach that can be used to evaluate the initial interaction at the contact surface and dominant modes of instability is to analyze the linearized continuity and momentum equations. The general approach is to evaluate the response of the contact surface to a small perturbation in density, pressure and velocity. The overall response of the contact surface is described in terms of the evolution of the Fourier wave components needed to describe the initial perturbation. In general, the initial disturbance propagates with the group velocity of the Fourier components. The individual Fourier wave components propagate with some phase velocity and may be growing or damped.

II. Stability of Cylindrical Jets in Vortex Sheet Approximation

In cylindrical geometry the Fourier wave components used to describe a perturbation to the jet's surface are of the form

$$A = A_n \exp i\,[kz + n\phi - \omega t]$$

and may be thought of as Fourier modes with mode number n = 0, ± 1, ± 2, etc., which are pinching, helical twisting and fluting modes etc.. The equations of continuity and momentum linearized in an appropriate coordinate system provide a dispersion relation relating, the frequency ω and the wavenumber k for each Fourier mode, n. On a cylindrical supersonic jet with sharp velocity discontinuity, the vortex sheet approximation, Fourier components propagating with the jet flow are growing in amplitude. In general, both frequency, ω, and wavenumber, k, are complex but the fastest growth occurs for k real and ω complex, temporal growth, or for ω real and k complex, spatial growth (Gaster 1968). These fastest growth rates can be related by the appropriate mode velocity for the frequency and wavenumber of interest. Each Fourier mode, n, consists of an ordinary mode (OM) solution of the dispersion relation and of reflection mode (RM) solutions. The nature of the OM solutions has been investigated in some detail by Ferrai et al. (1981) and by Hardee (1983). Each Fourier mode, n, has a maximum growth rate at some real wavenumber k_n^* or real frequency ω_n^* and we might expect that wavenumbers or wave frequencies near to those of the maximum growth rate would come to dominate after sufficient time for growth has elapsed. We can think of each (OM) solution as having a characteristic wavenumber k* and frequency ω^*. Comparison between the Fourier modes reveals that $k^*_0 > k^*_1$ and that $k_n^* \sim n\, k^*_1$ when n > 1. Except for the OM pinching mode (n = 0) whose maximum growth rate is less than that of the OM twisting mode (n = 1), the the maximum growth rate is approximately proportional to k_n^* and increases as n increases (Hardee 1983).

In addition to the OM solutions to the dispersion relation each Fourier mode admits an infinite number of RM solutions, some of whose properties have been investigated by Ferrari et al. (1981), Cohn (1983) and Birkinshaw (1984). The RM solutions arise from the infinite number of zeros in the Bessel and Hankel functions which describe the response of a fluid inside and outside the jet, respectively, and the matching of these functions at the contact surface. Each RM solution has a sharply peaked maximum in the rate of growth and it has been found that $k^*_{n,RM} \geq k^*_{n,OM}$. Except for the n = 0 Fourier mode, the RM solutions have higher characteristic wavenumber than the OM solution of a particular Fourier mode. RM solutions associated with pinching have a much higher growth rate than the OM solution, comparable to the OM twisting mode solution, for high Mach number light jets and have been identified with the formation of periodic shocks seen in axisymmetric numerical simulations. The OM pinching mode grows more rapidly only on transonic heavy jets (Cohn 1983). The RM solutions associated with twisting n = 1 and fluting n > 1 Fourier modes can have growth rates comparable to the OM solutions depending on the Mach number and density of the jet. Like the RM solution associated with the n = 0 Fourier mode these solutions mostly affect the jet inside the contact surface, e.g., RM solutions associated with the n = 1 Fourier mode may twist the jet center but only minimally perturb the contact surface.

An analysis of the portion of parameter space over which the RM solutions associated with the n > 0 Fourier modes grow more rapidly than the OM solution is in progress.

For the case of an isothermal jet and external medium in which the jet radius changes linearly with distance it has been shown that frequencies and wavenumbers scale inversely proportional to the jet radius, i.e., $\omega \propto R^{-1}$ and $k \propto R^{-1}$. Provided jet expansion, or contraction is slow as is the case for observed jets and jet Mach numbers and densities relative to the external medium remain constant then the fastest growing wavenumbers or frequencies, i.e., those with the fastest spatial growth, are those whose wavelength increases and frequency decreases proportional to the jet radius, R (Hardee 1982). For example, the fastest growing twist wavelength is (Hardee 1984)

$$\lambda_1^* \geq \lambda_1^p \simeq \left[\frac{4.2}{1+\eta^{1/2}} M - 2.5 \right] R$$

where $\eta \equiv n_{jet}/n_{ext}$, $\lambda^*_1 \rightarrow \lambda^p_1$ as $n >> 1$ and λ^p_1 is the fastest temporally growing wavelength. Slower propagation of wavelengths longer than λ^p_1 on light jets account for the more rapid spatial growth at λ^*_1 in spite of slower temporal growth at the longer wavelength. All OM and RM solutions associated with the Fourier modes will behave similarly. For isothermal jets of constant radius or varying radius it is not difficult to find k^*_n for the OM and RM solutions either by performing a spatial analysis where $k = k_R + i\, k_I$ and looking for the minimum growth length where $\ell \equiv k_I^{-1}$ or by performing a temporal analysis where $\omega = \omega_R + i\, \omega_I$ and $\ell \equiv (\omega_R/k)/\omega_I$.

Recent work (Hardee in preparation) has shown that even if conditions in a jet and in the external medium are varying such as might be expected along real jets that the quantity $\omega(u/R)$, where u is the jet velocity, is an invarient for any solution of the dispersion relation. In particular, the fastest spatially growing OM twist frequency is given by

$$\omega_1^* \simeq 0.1\ (u/R)$$

Observed quantities are usually wavelengths which can be found from

$$\omega^* \lambda^* = v^*_{ph}$$

where v^*_{ph} is the phase velocity associated with the most rapid spatially growing frequency ω^* of any OM or RM Fourier mode solution. In general v^*_{ph} and λ^* must be found numerically although when $\omega >> \omega^* << \omega$ there are suitable analytic expressions for v_{ph} (see Hardee 1984).

III. Magnetic Fields, Velocity Shear and Non-linear Effects

The effect of magnetic fields inside a jet on jet stability has been investigated by Ferrari et al. (1981), Ray (1981), and by Fiedler and Jones (1984). Provided the jet is superalfvenic as well as supersonic the linearized stability analysis indicates little change in results found for strictly fluid jets. The assumption of equipartition in extragalactic jets

means that the Alfven Mach number is similar to the sonic Mach number so we expect the fluid results to be sufficiently accurate unless a jet is transonic or the magnetic energy is comparable to the flow energy. The effect of magnetic confinement on the n = 0 pinching mode has been considered by Cohn (1983) and again there appears to be little change in the results found previously which assumed thermal pressure confinement. As long as the jet remains "light" the primary instability is of the Kelvin-Helmholtz type. On the other hand, if the jet is "heavy" with little or no external medium then the n = 0 pinching mode is driven by the current and behaves like a classic theta pinch in the reference frame of the jet fluid (Hardee unpublished). While the linearized stability analysis suggests little effect of magnetic fields on jet stability, it is likely that the magnetic fields become important as the amplitude of the Fourier components becomes large. For example, the inclusion of magnetic field inside a plasma column serves to stabilize the n = 0 pinch mode at some finite amplitude and confining magnetic fields can tie additional material to a jet which increases the jet's inertia and slows wave growth (Benford 1981). While the effects of finite amplitudes on wave growth have not yet been considered except for the OM solution of the n = 1 twist mode (see Benford 1981) it is thought that amplitude growth slows and perhaps saturates when amplitudes become large. Qualitatively this means that the OM and RM solutions to the linearized dispersion relation which grow faster at higher wavenumber are also those that become non-linear at smaller amplitude. This is a simple result of the fact that motions of the fluid approach the sound speed at smaller amplitudes for higher wavenumber. If we assume that saturation occurs at amplitudes inversely proportional to k*, then the slower growing OM and relatively small k* RM solutions associated with low n Fourier modes are those that may be directly observable.

Although the effect of shear has not yet been included in cylindrical geometry the effect of a plane parallel shear layer on stability has been investigated by Ray (1982) and by Choudhury and Lovelace (1984). In this situation waves with wavenumber $k \gtrsim 1.28\ h^{-1}$, where h is the scale height of the shear layer, are stabilized. A similar conclusion is suggested by the work of Ferrari et al. (1982) in which the effect of shear on a 2-dimensional jet was considered. At the same time a new wave mode with wavenumbers $k >> h^{-1}$ are destabilized. If this result can be applied to a cylindrical jet then waves with wavelength Λ where (Hardee 1983)

$$\Lambda_n = \{(2\pi R/n)/[(2\pi R/n)^2 + \lambda_n^2]^{1/2}\}\lambda_n$$

are stabilized when $\Lambda_n < 4.91\ h$. Note that the true wavelength Λ is the wavelength between wave crests which propagate around a cylindrical jet and λ is the wavelength parallel to the jet axis. If this condition is written in terms of λ then waves are stabilized by velocity shear when

$$\lambda_n < \lambda_n^{min} = 2\pi n^{-1}\,[(1.28R/nh)^2-1]^{-1/2}R$$

with result that only those Fourier modes with sufficiently small n such that $k_n^* < k_n^{max} = 2\pi/\lambda_n^{min}$ remain unstable. Note that all Fourier modes except n = 0 and n = 1 can be stabilized if h = R. Because the characteristic wavenumber of the RM solutions $k^*_{RM} > k^*_{OM}$ for the n > 0 Fourier modes these solutions may be stabilized for h < R. However, a few RM solutions for the n = 0 Fourier mode with $k^*_{RM} \sim k^*_{OM}$ are likely to

remain unstable even in the presence of shear. To summarize, it seems likely that the presence of a shear layer might stabilize nearly all of the low n RM solutions, stabilize the high n OM and RM solutions and lead to destabilization of a new wave mode within the shear layer having high wavenumber.

IV. Conclusion

In spite of limitations imposed by the assumption of infinitesimal disturbance, the linear theory is a powerful predictive tool when coupled with laboratory and numerical experiments. Comparison between the linear stability analyses of the OM and RM solutions of the n = 0 pinching Fourier mode and axisymmetric numerical simulation have already proved informative (see Norman elsewhere in these proceedings). In a similar manner comparison between the OM solution of the n = 1 twist Fourier mode and observed twisted jets is also proving informative by providing estimates of jet Mach numbers. Perhaps more useful is the fact that a description of the propagation of helical twisting on a "light" non-ballistic jet is provided by the linear analysis which describes the wave like propagation of a small amplitude twist. The wavelength of a small amplitude twist varies as

$$\lambda^{(h)} = (v_{ph}/v_{ph,o})\,(R/R_o)\lambda_o^{(h)}$$

where the subscript "o" refers to the initial conditions. This result suggests a <u>new</u> class of twisted jet models that may prove to be more consistent with observed twisted jets.

The linear stability analysis performed to date when considered in the light of laboratory jets and numerical simulations of axisymmetric jets suggests several things in the real world. First we might expect to see the fast growing RM solution of the pinching Fourier mode affecting the behavior of supersonic jets and the OM and RM solutions of the twist Fourier mode affecting the behavior of supersonic jets. Second the higher n OM and RM solutions will be affected by the presence of a velocity shear and their importance to the behavior of jets depends on the thickness of the shear. Third the longer wavelength Kelvin-Helmholtz modes may be responsible for large scale features but not jet turbulence. The appearance of a new unstable mode within the shear layer sugests that any shear will be turbulent.

Clearly this type of analysis remains a useful research tool. Some of the things that still need to be done are to investigate the effect of magnetic confinement and internal magnetic fields on the Fourier modes and to study the effect of shear in cylindrical geometry on the Fourier modes. The linear analysis is also useful as a necessary first step in any non-linear theoretical analysis and it seems important to develop non-linear techniques to handle some of the large scale jet distortions that are predicted to arise from the linear stability analysis. This work will also provide a good basis for comparison with the future laboratory and numerical experiments.

V. References

Benford, G. 1981, Ap.J., 247, 792
Birkinshaw, M. 1984, MNRAS, 208, 887.
Choudhury, S.R. and Lovelace, R.V.E. 1984, Ap.J., (in press).
Fiedler, R. and Jones, T.W. 1984, Ap.J., (in press).
Ferrari, A., Trussoni, E. and Zaninetti, L. 1981, MNRAS, 196, 1051.
Ferrari, A., Massaglia, S. and Zaninetti, L. 1982, MNRAS, 198, 1065.
Gaster, M. 1968, Phys. Fluids, 11, 723.
Hardee, P.E. 1982, Ap.J., 257, 509.
Hardee, P.E. 1983, Ap.J., 252, 775.
Hardee, P.E. 1984, Ap.J. 277, 106.
Norman, M.L.,Smarr, L., Winkler, K.H.A. and Smith, M.D. 1982, Astr.Ap., 113, 285.
Ray, T. P. 1982, MNRAS, 196, 195.
Ray, T. P. 1982, MNRAS, 198, 617.

KNOT PRODUCTION AND JET DISRUPTION VIA NONLINEAR KELVIN-HELMHOLTZ PINCH INSTABILITIES

Michael L. Norman, Karl-Heinz A. Winkler
Max-Planck-Institut für Physik und Astrophysik
Institut für Astrophysik, Karl-Schwarzschild-Str. 1
8046 Garching b. München, West Germany

L. Smarr*
Departments of Astronomy and Physics, University of Illinois
Urbana, Illinois 60801, USA

ABSTRACT. We summarize the results of time-dependent numerical hydrodynamical simulations which investigate the behavior of pinching modes of the Kelvin-Helmholtz instability in the nonlinear regime. Ordinary mode (OM) pinch instabilities, important only at Mach numbers of order unity, are shown to be disruptive. Reflection mode (RM) pinch instabilities, important in supersonic jets with parameters of astrophysical interest, are shown to be not disruptive, but rather saturate at finite amplitude through the formation of oblique internal shockwaves. The saturated RM pinch instability consists of a near-periodic train of biconical internal shockwaves which propagates with a fraction of the mean flow velocity. Properties of the shock system are given for jets of different density ratios and Mach numbers. The effect of pinch instabilities on energy transport in extragalactic jets is discussed.

1. INTRODUCTION

A persistent worry that has existed since the original proposal of the fluid beam hypothesis (Scheuer, 1974; Blandford & Rees, 1974) to account for the structure and energetics of extragalactic radio sources is the potential disruption of the "energy-pipe" via Kelvin-Helmholtz (K-H) instabilities. Linear stability analyses performed by many authors (e.g. Ferrari et al. 1978, 1981, 1982; Hardee 1979, 1982, 1983; Ray 1981; Cohn 1983) have dealt with this issue, and have generally found that a variety of modes of the K-H instability have significant growth rates even at high Mach numbers. On the basis of linear growth rates, the ordinary mode (OM) helical instability and the reflection mode (RM) pinch instability are potentially the most important modes for flow modification and jet disruption. However, these processes cannot be addressed by a linear analysis, being fundamentally nonlinear.

In this paper we summarize the results of time-dependent numerical hydrodynamical simulations which investigate the behavior of pinching modes in the nonlinear regime. OM pinch instabilities, important only at Mach numbers of order unity, are shown to be disruptive. RM pinch instabilities,

*Visitor, Max-Planck-Institut für Astrophysik; Alfred P. Sloan Fellow

important in supersonic jets with parameters of astrophysical interest (i.e. low density ratio, high Mach number), are shown to be not disruptive, but rather saturate at finite amplitude through the formation of oblique internal shockwaves. The saturated RM pinch instability consists of a near-periodic train of biconical internal shockwaves which propagates with a fraction of the mean flow velocity. The structural and propagation properties of the shock system are given for jets of different beam density ratios and Mach numbers. Growth lengths are determined empirically.

Finally, the role of pinch instabilities in extragalactic jets is discussed. The properties of emission knots produced by the RM pinch instability are deduced using simple synchrotron theory arguments. We show how measurements of knot proper motion can be used to constrain the local flow velocity in pressure-confined supersonic jets.

2. LINEAR PINCH INSTABILITIES

Linear analyses of the K-H instability in supersonic beams distinguish between two basic types of pinch (i.e. axisymmetric) modes depending upon the number of internal nodes in the radial function of the perturbation variables (Ferrari et al. 1981, Cohn 1983). The ordinary, or fundamental, pinch mode has no internal nodes, whereas the reflection modes comprise an infinite family parameterized by the number of internal nodes. Reflection modes derive their name from the special property of a supersonic shear surface investigated by Miles (1957), which is that for certain angles of incidence, a plane linear wave will be reflected from the surface with a greater amplitude than it had upon incidence. A reflection mode instability requires the existence of two such shear surfaces in close proximity, such as in a supersonic beam, between which waves can repeatedly reflect and grow to nonlinear amplitude. In this context, the nodes of a particular reflection mode can be thought of as the point where incident and reflected waves destructively interfere. Thus, whereas the OM is a purely longitudinal mode, the RM posses an additional transverse component.

This difference in physical character is accompanied by differences in linear growth rates and phase and group velocities, which led Cohn (1983) to conclude that the OM and RM dominate in different regions of the density ratio - Mach number parameter space. Defining $\eta = \rho_{beam}/\rho_{external}$ and $M = V_{beam}/C_{beam}$, Cohn determined empirically that the RM have significantly larger growth rates in the regime $M > 2\eta^{0.3}$. This boundary is indicated in Figure 1 by the upper dashed line. The black dots indicate the cases we have studied numerically. As can be seen, we have five cases in the vicinity of this boundary: two on the OM side, and three on the RM side. We can therefore investigate whether there is a change in modal character in the nonlinear regime upon crossing this boundary, and what effect this has on bulk energy transport in supersonic jets.

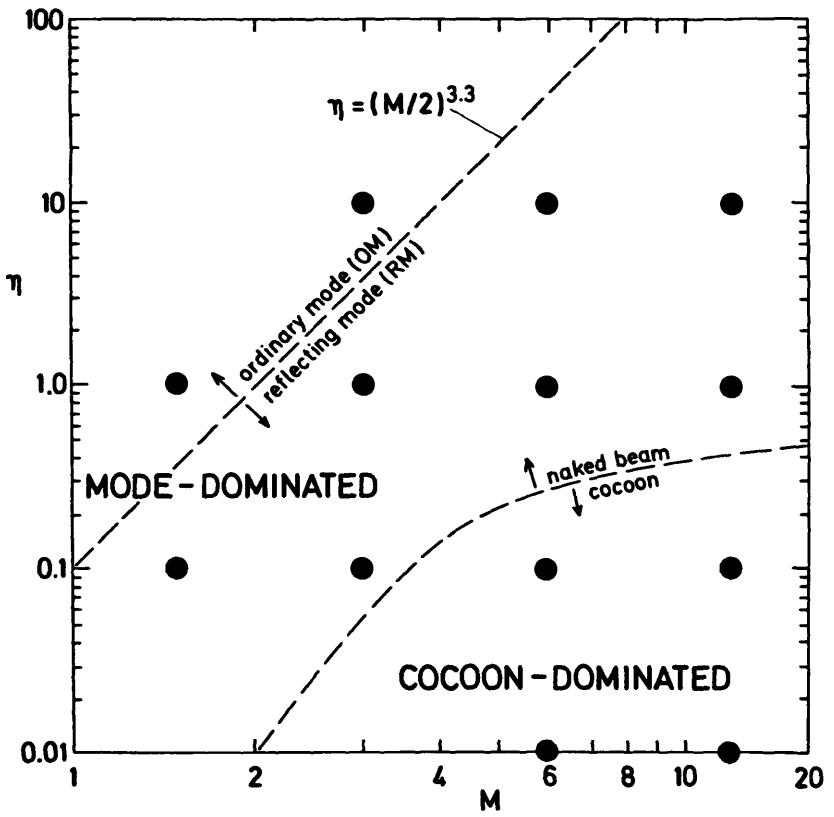

Fig. 1: Structure of parameter space, showing boundaries between ordinary mode-, reflection mode-, and cocoon-dominated regions (dashed lines), and location in parameter space of numerical experiments (black dots), from Cohn (1983), and Norman et al. (1984).

3. JET DISRUPTION

Figure 2 illustrates nonlinear pinch instabilities in the OM-dominated regime. The numerical procedure is as follows. At t = 0, the jet extends across the computational domain $0 \leq R/R_{jet} \leq 10$, $0 \leq Z/R_{jet} \leq 40$, flowing from left to right in pressure equilibrium with the surrounding gas. The initial jet radius is resolved with 20 zones. The jet parameters are $\eta = 10$, $M = 3$. Both jet gas and ambient gas are assumed to obey the ideal gas equation of state with adiabatic index $\gamma = 7/5$. The jet is continuously replenished at left, where a numerical inflow condition has been established; the jet exits the domain at right, where a numerical outflow condition has been established. A perturbation is applied to the jet by adjusting the input sound speed so that the jet flows in with a one percent pressure excess. The subsequent evolution of the jet is computed until a quasi-steady state is reached using the techniques outlined in Norman et al. 1983, and described in detail in Norman and Winkler 1984. The initial jet boundary is kept sharp through the use of the LeBlanc interface tracking technique (Norman 1980; Norman and Winkler, 1984).

In laboratory terminology, we are simulating the downstream behavior of an almost perfectly expanded Mach 3 cold air jet exhausting into a quiescent atmosphere. Experimental data exist for these parameters (Abramovich 1962) with which our numerical results can be compared.

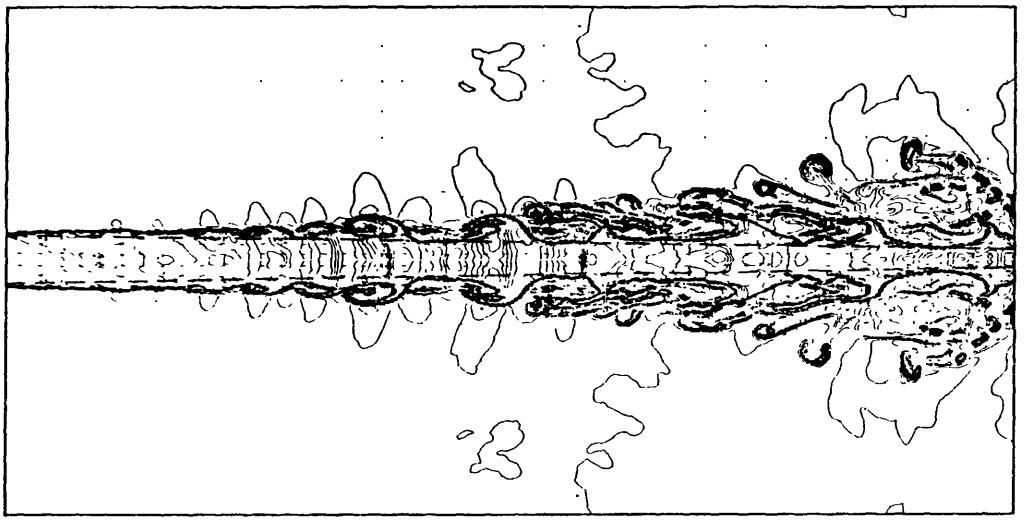

Fig. 2: Nonlinear pinch instability in the OM-dominated regime ($M=3, \eta=10$). Density contour plot. Note inward propagation of mixing layer on jet boundary (dashed lines).

Density contours of the flowfield at $\tau \equiv tC_{beam}/R_{beam} = 19$ are shown in Figure 2. The boundary of the jet appears black because of the superposition of many contour lines at the 10:1 density discontinuity. The pinch instability manifests itself as waves on the jet boundary, which reach perceptible amplitude roughly five jet diameter downstream of the inlet, and continue to grow in amplitude further downstream. The effect of the instability is to create an ever-broadening mixing layer which eats into the supersonic core of the jet and spreads the jet as a whole. Notice that the inward progress of the mixing layer is governed by long wavelength waves, $\lambda/R_{jet} \geq 1$. We measure a mixing angle for the inner edge of the mixing layer (dashed line in Fig. 2) of $\Theta = \delta/Z \approx -0.02$, where $\delta = R_{edge}-R_{jet}$. Therefore, at $Z \approx 50\ R_{jet}$, the mixing layer will reach the axis, whereupon the jet will become fully turbulent. The rate of outward spreading is more difficult to determine, but appears to be roughly three times the inward spreading rate.

Abramovich (1962) measured supersonic core lengths in various cold air jets, and found a value of $\ell_{core} = 60\ R_{jet}$ for a jet of identical parameters. Insofar as supersonic core lengths in pressure-matched jets in particular are known to be uncertain to 40 to 60% (Shirie and Seubold 1966) - due to the sensitivity of core length on level of input turbulence and precise nozzle geometry - we consider the agreement quite good. A comparison of Mach 1.5 jets is likewise good: the case $\eta = 1$, $M = 1.5$ described in Norman et al. 1984 (cf. Fig. 10) yields $\ell_{core} \approx 20\ R_{jet}$, whereas Ambramovich measured $\ell_{core} = 19\ R_{jet}$ in the laboratory. We credit the good agreement to the conclusion that the inward progress of the mixing layer is governed by long wavelength shear instabilities, which we <u>can</u> adequately model, and not by short wavelength instabilities, which we <u>cannot</u> adequately model. As the assumption of axisymmetry limits us to studying only poloidal motions, we conclude that poloidal mixing is the dominant mixing process in the first supersonic core-length of the jet.

The flow beyond the terminus of the supersonic core is fully turbulent and subsonic (Shirie and Seubold 1966), and, in effect, disrupted. Unless kept axial by buoyancy or a preferential gradient, the flow will generally not preserve its initial direction. Thus, the role of nonlinear OM pinch instabilities in jets is one of entrainment, deceleration and ultimately disruption, through the establishment of a mixing layer on the jet boundary.

4. KNOT PRODUCTION

Figure 3 illustrates nonlinear pinch instabilities in the RM-dominated regime. The numerical procedure is exactly as described in the last section, only now the jet parameters are $\eta = 1$, $M = 3$. The only change from Figure 2, therefore, is to lower the jet density by a factor of ten. However, the change in flow behavior is striking.

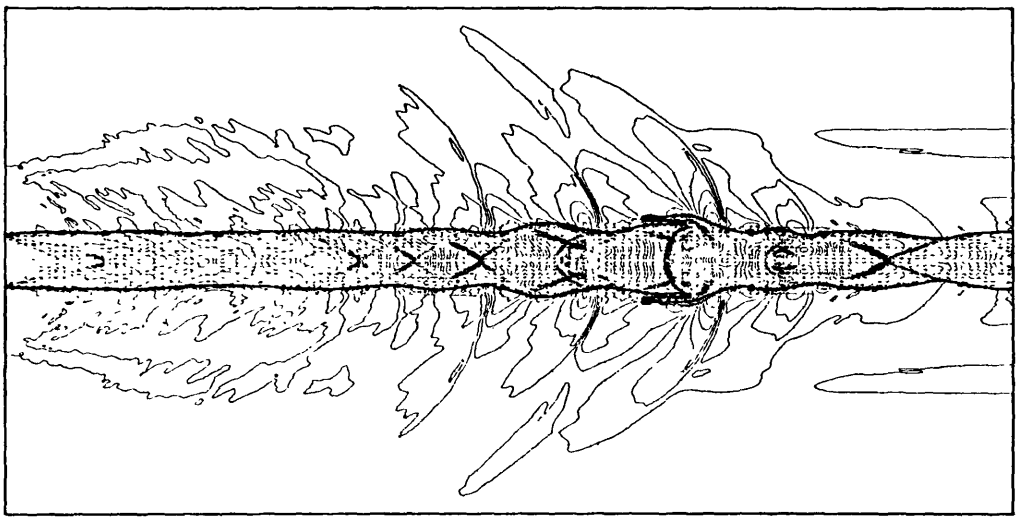

Fig. 3: Nonlinear pinch instability in the RM-dominated regime ($M=3, \eta=1$). Density contour plot. Note undulations of jet boundary (solid lines) and internal and external shockwaves.

Figure 3 shows density contours of the flow field at $\tau = 8$. As the jet and ambient gas have equal densities, the contour lines do not reveal the position of the jet boundary; this is indicated in the Figure by the solid lines. One can see that the jet boundary is no longer subject to turnover and mixing to the extent of that shown in Figure 2, but rather exhibits a finite-amplitude undulation. One can also see the development of oblique shockwaves within the jet, appearing distinctly first at $Z/R_{jet} \approx 11$, and subsequently growing in strength downstream. We observe the positions of shocks and undulations to be coupled, the entire assemblage moving downstream with a substantial fraction of the jet velocity. In the next section we quantify the pattern propagation speed. The pattern propagates supersonically with respect to the ambient medium, and hence the advancing boundary corrugations drive shocks into the surrounding gas. A schematic of the fully-developed flow structure is shown in Figure 4.

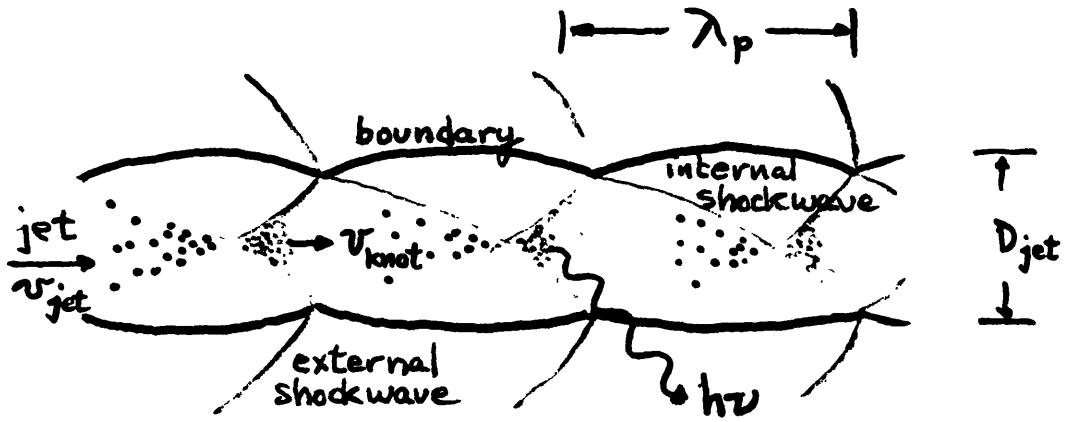

Fig. 4: Schematic of RM-induced shockwaves and high pressure knots, and definition of quantities appearing in Table 1.

The relationship of this nonlinear pinching mode to the linear reflection modes is not entirely clear, although both modes clearly involve the reflection of waves off of the jet boundary to amplify the instability. That both the linear and nonlinear pinch instabilities change character in the same region of the η-M parameter space is compelling evidence for a strong relationship. Insofar as the shockwave system propagates as a coherent unit, it may be a nonlinear superposition of reflection modes, and not a single reflection mode in the nonlinear regime. Figure 3 shows that this is convective instability, with the waveform showing considerable convective evolution. This further complicates a comparison with linear theory.

We can make the following conclusions concerning the effect of this kind of pinch instability on jet energy transport.

The small amount of mixing at the jet boundary in Figure 3 implies that jet deceleration is mediated primarily by the system of internal and external shockwaves. Since the shockwave pattern moves downstream with a substantial fraction of the mean flow velocity and the shockwaves themselves are oblique, they decelerate the mean flow relatively little. These facts point to the conclusion that pinch instabilities in the RM-dominated regime are not disruptive, as in the OM-dominated regime, but rather gradually decelerate the mean flow through the conversion of directed kinetic energy into heat via oblique internal shockwaves. Examples of supersonic jets propagating stably despite extensive arrays of internal shockwaves are given in Norman et al. 1984, Smarr et al. 1984, and in the color plates in the appendix to this paper.

As a consequence of the internal shockwaves produced in the present type of pinch instability, high pressure regions are produced immediately downstream of the points of shock intersection. The possibility that these regions may be observed as emission knots in astrophysical jets is discussed in Norman et al. 1984, and in the last section of this paper. Here we simply point out that emission knots thus produced would exhibit the characteristic spacing and propagation velocity of the underlying shock system. It is therefore important to determine how these quantities depend on jet parameters, so that observations of knot spacing and proper motion can be used as a probe of the underlying flow.

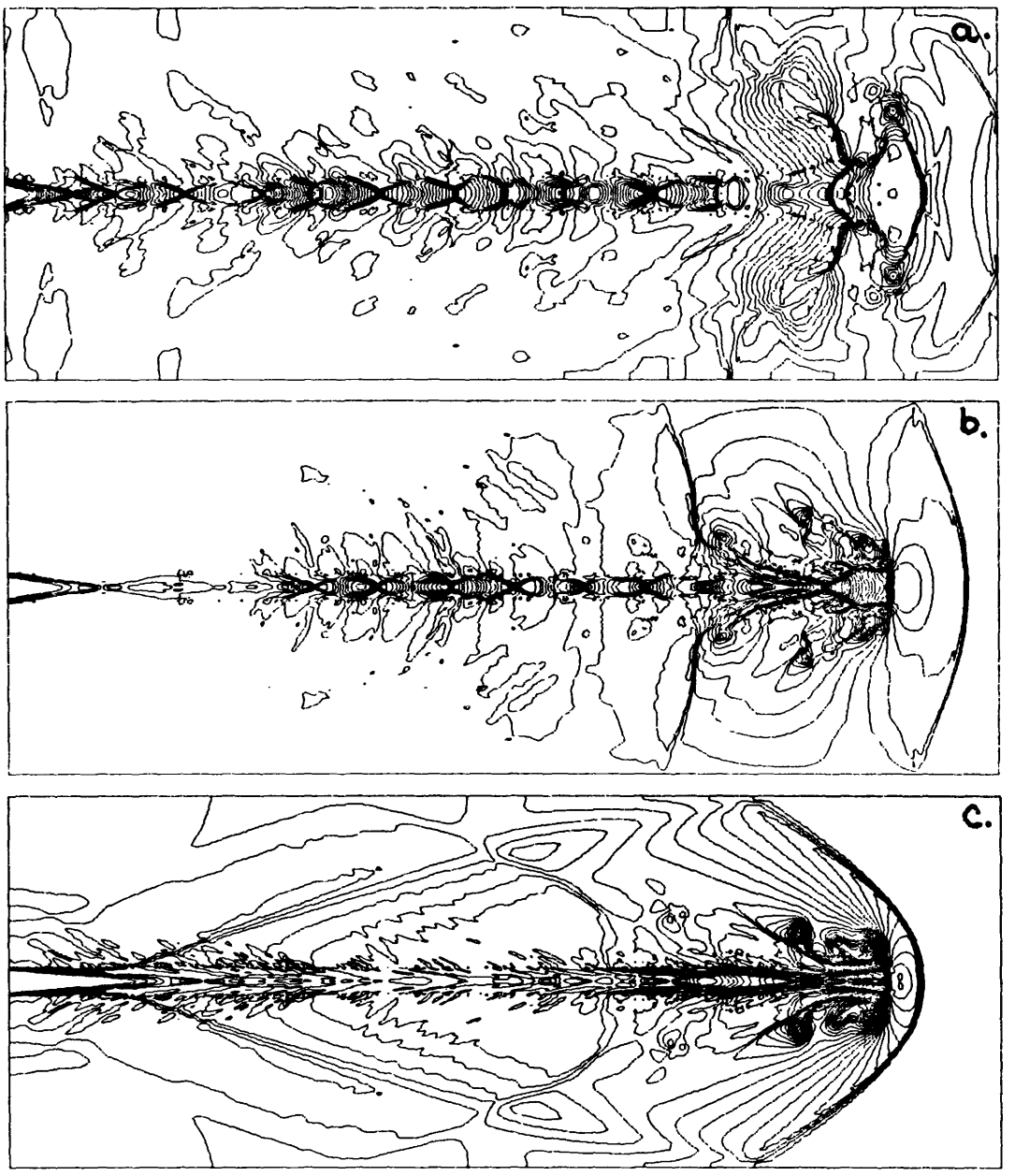

Fig. 5: Pressure contour plots showing shockwave structure in pressure-matched jets of varying Mach numbers and density ratios. a) M=3, η=1; b) M=6, η=10; c) M=12, η=10. Note Mach number dependence of distance from inlet to the first strong internal shockwave.

5. NONLINEAR PROPERTIES

Returning to Figure 1, we see that the majority of our data points lie below the line $M = 2\eta^{0.3}$, in the RM-dominated region of parameter space. This is also likely to be the region of greatest astrophysical relevance. In this section we discuss the occurrence and nonlinear properties of pinch instabilities in the RM-dominated regime in order to investigate their dependence on jet density ratio and Mach number. The calculational data base we shall use for this investigation are the set of propagating jets described and documented in Norman et al. 1983, and in the appendix to this paper.

Of the eleven cases satisfying $M > 2\eta^{0.3}$ in Figure 1, only seven are suitable for our purposes; the jets with parameters lying below the lower dashed line in Figure 1 exhibit internal shock structures that are driven by perturbations in the surrounding cocoon ("cocoon-dominated", see Norman et al. 1984). The jets of the seven remaining cases have essentially no cocoons ("naked beam"), and several exhibit shock structures which are ordered ("mode-dominated"). The parameters of the seven jets considered are listed in Table 1. Snapshots of the flowfields at advanced times are presented in the appendix.

5.1 Occurrence and Growth length

In all but Case 2 and Case 10 of Table 1, we find regular arrays of biconical shockwaves arise in the flow. At Mach 1.5 the instability is either not excited or the shockwaves are too weak to be detected. By Mach 3, the shock systems are prominent and extensive (cf. Fig. 5a). At Mach 6 we observe that the shock system develops further downstream (cf. Fig. 5b), although it is quite similar in appearance to the Mach 3 shock system once fully developed. Further increasing the Mach number to 12 shows that there is clearly a Mach number scaling of the pinch instability growth length, as internal shockwaves are largely absent in the first 24 jet diameters downstream of the inlet (cf. Fig. 5c). However, when the jet in Figure 5c is allowed to propagate to greater lengths, as in Figure 6, boundary constrictions and the accompanying shockwaves do emerge further downstream.

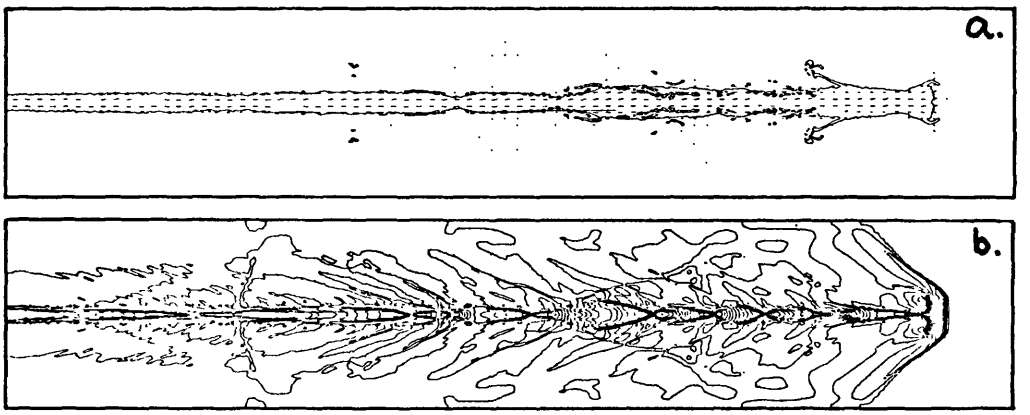

Fig. 6: Development of RM pinch instability in a high Mach number jet (M=12, η=10). a) jet boundary, showing undulations; b) pressure contour plot, showing shock structure.

TABLE 1. Shockwave pattern wavelength and propagation speed

Case*	M	η	λ_p / R_{jet}	V_p	V_p/V_{jet}	$M - \frac{V_p}{C_{jet}}$	$\frac{P_{knot}}{P_{ambient}}$	comments
2	1.5	0.1	-	-	-	-	-	no shock system
3	3.0	1.0	4.8	0.8	0.25	2.2	2.	well-developed shock system
4	3.0	0.1	4.8	1.4	0.14	2.6	3.	well-developed shock system
5	6.0	10.	5.0	1.0	0.53	2.8	3.	well-developed shock system
6	6.0	1.0	5.2	2.5	0.42	3.5	4.	boundary effects
9+	12.0	10.	≥ 9.5	≤ 2.5	≤ 0.66	≥ 4.1	5.	convective evolution
10	12.0	1.	-	-	-	-	-	no shock system-insufficient length

*Case numbers according to Table 2, Appendix
+ extended domain $0 \leq Z \leq 160$, cf. Fig. 6

Our numerical results are consistent with a linear scaling of instability growth length with Mach number $\ell_g = \alpha M D_{jet}$, with $1 \leq \alpha \leq 2$. Physically, this means that only one or two wave reflections are needed to amplify the perturbations applied to the jet at the inlet to nonlinear amplitude.

5.2 Wavelength and pattern speed

Table 1 summarizes pattern wavelength λ_p and propagation speed V_p for those cases where the shockwave system is well-developed. The wavelength assumes a typical value of $\lambda_p/R_{jet} \approx 5$ in the range $3 \leq M \leq 6$, with a weak Mach number dependence. Case 9 shows convective evolution of the shock pattern wavelength $\frac{d\lambda_p}{dZ} < 0$ (cf. Fig. 6b), and thus only a lower limit on λ_p is indicated.

Normalized pattern velocities V_p/V_{jet} show positive dependencies on density ratio and Mach number. The relative Mach number of the jet with respect to the pattern $M - V_p/C_{jet}$ is also tabulated, and accordingly shows a negative dependence on density ratio and a positive dependence on Mach number.

5.3 Knot overpressure

Typical (not peak) values of knot overpressure $P_{knot}/P_{ambient}$ are shown in Table 1, and show a positive dependence on the relative Mach number defined above. That the dependence is not quadratic could be due to shock obliquity.

Although Case 6 develops strong internal shockwaves, a spurious wave which is generated where the bow shock encounters the R = 15 boundary impinges on the jet, and perturbs it considerably. The shock system is likely to have been driven by this perturbation, or at least modified by it. Therefore, the entries in Table 1 under Case 6 are less reliable than the others.

Case 10 does not develop an extensive internal shock system, presumably because the domain was too short to allow the pinch instability to grow.

6. ASTROPHYSICAL IMPLICATIONS

Kelvin-Helmholtz instabilities couple a supersonic jet to its confining medium via mass and momentum exchange. In general, the rate of this exchange depends upon the properties of the two media and the nature of the excited mode(s), and governs the efficiency of streamwise energy transport within the jet. Pinch instabilities allow a high degree of coupling in principle because the wavefronts of all unstable modes are normal to the flow direction, thus maximizing the rate of momentum transfer from the jet to its environment.

We have confirmed the result of Cohn (1983) that pinch instabilities change character across the boundary given by $M=2\eta^{0.3}$. Jets satisfying $M<2\eta^{0.3}$ lie in the ordinary mode-dominated regime, and couple to their environment primarily via mass exchange in a mixing layer at the jet boundary. Jets satisfying $M>2\eta^{0.3}$ lie in the reflection mode-dominated regime, and couple to their environment via shockwaves, which transfer jet momentum directly without mass exchange. With regard to energy transport, OM-dominated jets are more severly effected than RM-dominated jets, the former being subject to deceleration and disruption via entrainment and mixing, while the latter propagate without disruption despite some dissipation of directed kinetic energy at internal shockwaves.

This bimodal behavior of how pinch instabilities effect jet kinetic energy transport may help explain the correlation between radio power and morphological class in extended double radio sources (Fanaroff and Riley, 1974). Assuming that the integrated radio power of a source is a measure of the kinetic power of the jet supplying it, then low power sources will have jets in the OM-dominated regime and high power sources will have jets in the RM-dominated regime, since the jet kinetic luminosity $\mathcal{L}_{jet} \propto M^3\eta^{-\frac{1}{2}}$. It is important to note that virtually all laboratory supersonic jets lie in the OM-dominated regime, as they are dense and cold ($\eta > 1$) and of low Mach number ($M \leq 3.5$). As we have seen in Section 3, such jets develop turbulent boundary layers which ultimately consume the supersonic core, and become thereafter fully turbulent. Jets powering "relaxed" doubles may therefore <u>look</u> like laboratory jets because they <u>are</u> like laboratory jets insofar as they are fully turbulent. The effects of pressure stratifications in the interstellar and intergalactic medium confining the radio jet may limit the usefulness of laboratory analogies, however.

As we have seen in Section 4, internal shockwaves are the distinguishing characteristic of jets in the RM-dominated regime, provided that

the jet length sufficiently exceeds the instability growth length. If RM pinch instabilites were the dominant energy dissipation mechanism in high power radio jets, then their distinguishing morphological feature would be moving emission knots. However, since the instability growth length scales linearly with Mach number, and jet power scales with the cube of the Mach number, the highest power jets may not produce emission knots, and may be effectively invisible.

Typical knot overpressures are less than an order of magnitude (cf. Table 1), although knot-interknot pressure ratios are considerably greater, due to the strong rarefaction zones which precede the internal shockwaves. A factor of ten pressure variation is common in RM-dominated jets (cf. Fig. 10a, Smarr et al. 1984), which would yield a factor of $\sim 10^2$ in radio brightness, assuming that the synchrotron emissivity scales with roughly the square of the particle energy density (Smith et al., 1984).

Knots propagate downstream with 10-50% of the jet speed (cf. Table 1); measurements of knot proper motion would therefore constrain the jet speed to lie within the range $2 \leq V_{jet}/V_{knot} \leq 10$.

Little experimental data exists on jets in the RM-dominated regime, where the jets which power the edge-brightened radio sources most certainly lie. L. Mach (1897) describes an experiment where he produced a supersonic jet of roughly one centimeter in diameter and one meter in length, the first thirty centimeters of which had no apparent mixing layer. The jet's parameters put it just into the RM regime, which could account for the enhanced boundary stability. Experimental verification of the reflection mode pinch instability and the propagating shock system it produces would be an extremely important test of the explanation of radio source morphology given above, as well as our emission knot mechanism. Begelman, Blandford, and Rees (1984) review the experimental prospects for exploring this low density, high Mach number regime.

Finally, a jet propagating in a non-constant and stratified atmosphere, such as exists in and around elliptical galaxies, is subject to "parameter evolution": that is, the jet's Mach number and density ratio are no longer constant parameters, but vary as a function of position down the jet. This topic is pursued by Sumi and Smarr in a paper in these proceedings. As Sumi and Smarr show, parameter evolution is relatively slow for jets in isothermal atmospheres, which means that a jet is either in the OM or the RM regime along its entire length, and therefore has the corresponding stability and energy transport properties. Jets in cooling-core accretion flows, however, are subject to rapid parameter evolution, which Sumi and Smarr show is one of increasing density ratio at approximately constant Mach number. The significance of this is that a jet with initial parameters in the RM regime will evolve into the OM regime and be disrupted. Physically, this occurs because the external sound speed is an increasing function of galactocentric distance and the jet Mach number with respect to the confining ambient gas drops below unity.

Sumi and Smarr propose that the wide-angle tail (WAT) morphology is a consequence of local jet disruption via rapid parameter evolution, with the inner collimated jet being in the RM regime and the outer plume-like

structure being in the OM regime. If this model proves correct, then observations of WAT jet morphology could provide information on the distribution of the gaseous environment in which they propagate. Conversely, a knowledge of pressure and temperature distributions around galaxies, used in conjuction with theoretical and numerical jet models, could provide useful constraints on the physical properties of the jet.

ACKNOWLEDGEMENTS

L. S. acknowledges partial financial support under NSF grants nos. PHY 80-01496 and 83-08826.

REFERENCES

Abramovich, G. N. 1962, "Theory of Turbulent Jets", (Gosudarstvennoye Izdatel'stvo Moscow, 1960); English translation by the U. S. Air Force Systems Command, Foreign Tech. Div., Technical Documents Liaison Office, MCL 3256, ASTIA AD 283, 858 (1962).

Blandford, R. D., & Rees, M. J. 1974, M. N. R. A. S., 169, 395.

Begelman, M. C., Blandford, R. D., & Rees, M. J. 1984, Rev. Mod. Phys., 26, 255.

Cohn, H. 1983, Ap. J. 266, 73.

Fanaroff, B., & Riley, J. M. 1974, M. N. R. A. S., 167, 31.

Ferrari, A., Trussoni, E., & Zaninetti, L. 1978, Astr. Ap., 64, 43.

Ferrari, A., Trussoni, E., & Zaninetti, L. 1981, M. N. R. A. S. 196, 1054.

Ferrari, A., Trussoni, E., & Zaninetti, L. 1982, M. N. R. A. S. 198, 1065.

Hardee, P. E. 1979, Ap. J., 234, 47.

Hardee, P. E. 1982, Ap. J., 257, 509.

Hardee, P. E. 1983, Ap. J., 269, 94.

Mach, L. 1897, Wien Ber., 106-II, 1025.

Miles, J. W. 1957, J. Acous. Soc. Amer., 29, 226.

Norman, M. L. 1980, Ph. D. dissertation, University of California at Davis; Lawrence Livermore Laboratory Report UCRL-52946.

Norman, M. L., Winkler, K.-H. A., & Smarr, L. L. 1983, in "Astrophysical Jets", ed. A. Ferrari & A. G. Pacholczyk, (Dordrecht: Reidel).

Norman, M. L., Smarr, L. L., & Winkler, K.-H. A. 1984, in "Numerical Astrophysics: A Festschrift in Honor of James R. Wilson", ed. R. Bowers, J. Centrella, J. LeBlanc, & M. LeBlanc, (Jones and Bartlett: Boston).

Norman, M. L., & Winkler, K.-H. A. 1984, in preparation.

Ray, T. P. 1981, M. N. R. A. S., 196, 195.

Scheuer, P. A. G. 1974, M. N. R. A. S., 166, 513.

Shirie, J. W., & Seubold, J. G. 1966, AIAA Journal, 5, 11, 2062.

Smarr, L. L., Norman, M. L., & Winkler, K.-H. A. 1984, Physica D, in press.

Smith, M. D., Norman, M. L., Winkler K.-H. A., & Smarr, L. L. 1984, submitted M. N. R. A. S.

Winkler, K.-H. A., & Norman, M. L. 1984, in preparation.

APPENDIX:

Shock structure, strength, and history in pressure-matched supersonic jets.

In this appendix, color plates*are presented which display shockwave-related phenomena in the parameter survey of jets introduced in Norman et al. 1983, and discussed in Norman et al. 1984, Smarr et al. 1984 and the present paper. These plates are intended to complete the archive begun in Norman et al. 1983 (cf. Sect. 3) displaying properties of our jet survey.

As discussed in Norman et al. 1984, shockwave behavior in pressure-matched jets is sensitive to the two input parameters of Mach number $M \equiv V_{jet}/C_{jet}$ and density ratio $\eta \equiv \rho_{jet}/\rho_{ambient}$. A key factor in this sensitivity is whether or not the jet builds a cocoon around it as it propagates, for a jet with a cocoon is a) effectively propagating in a medium with different properties than the true ambient medium, and b) shockwaves can be driven by motions within the cocoon. Plate 1 illustrates the variations in cocoon thickness and extent as density ratio is varied by three orders of magnitude in four Mach 12 jets; from top to bottom, the density ratios are η = 10., 1., 0.1, and 0.01.

The 73 colors shown in the color bar at the bottom of Plate 1 are each assigned to a particular value of the gas density such that the highest density regions are bright red, the lowest density regions are dark blue, and intermediate values of density in equal logarithmic intervals are assigned the spectral colors in between. Thus, our color bar spans the entire dynamic range of the physical quantity being plotted. Since our grid has 640 zones along the axis of symmetry, while the color image has only 512 pixels, the image slightly underresolves our solution. As the calculations are axisymmetric, the image has been mirrored about the axis of symmetry for ease of visualization.

The remaining twelve Plates each display a jet of a particular parameter pair, using three different flow visualization techniques that we find useful in studying the structure, strength and evolution of shockwaves in time-dependent jets. The format is as follows.

The top frame shows shockwaves and strong compression and rarefaction zones that develop in the flow. Operationally what is done is to assign to each computational zone a color depending on the sign and magnitude of the local divergence of the velocity field $\underline{\nabla}\cdot\underline{V}$. Large negative divergences pick out shockwaves and compression zones, which are colored red; large positive divergences pick out expansion zones, which are colored blue. Any zone that is less than 5% of the largest positive $\underline{\nabla}\cdot\underline{V}$ in the flow, and greater than 5% of the smallest negative $\underline{\nabla}\cdot\underline{V}$ in the flow is colored white. Other parts of the jet/ambient medium are assigned grey tones as follows: black-jet boundary (contact discontinuity), light grey - disturbed ambient medium, and dark grey - undisturbed ambient medium.

The middle frame is a seventy-three color representation of the gas pressure distribution in the flow, made in precisely the same way as described above for the density plots in Plate 1. The color bar is the same as shown in Plate 1.

*Reproduced here in black-and-white. For color presentation, see Report MPA 151 of the Max-Planck-Institut für Astrophysik (September 1984), available on request from the authors.

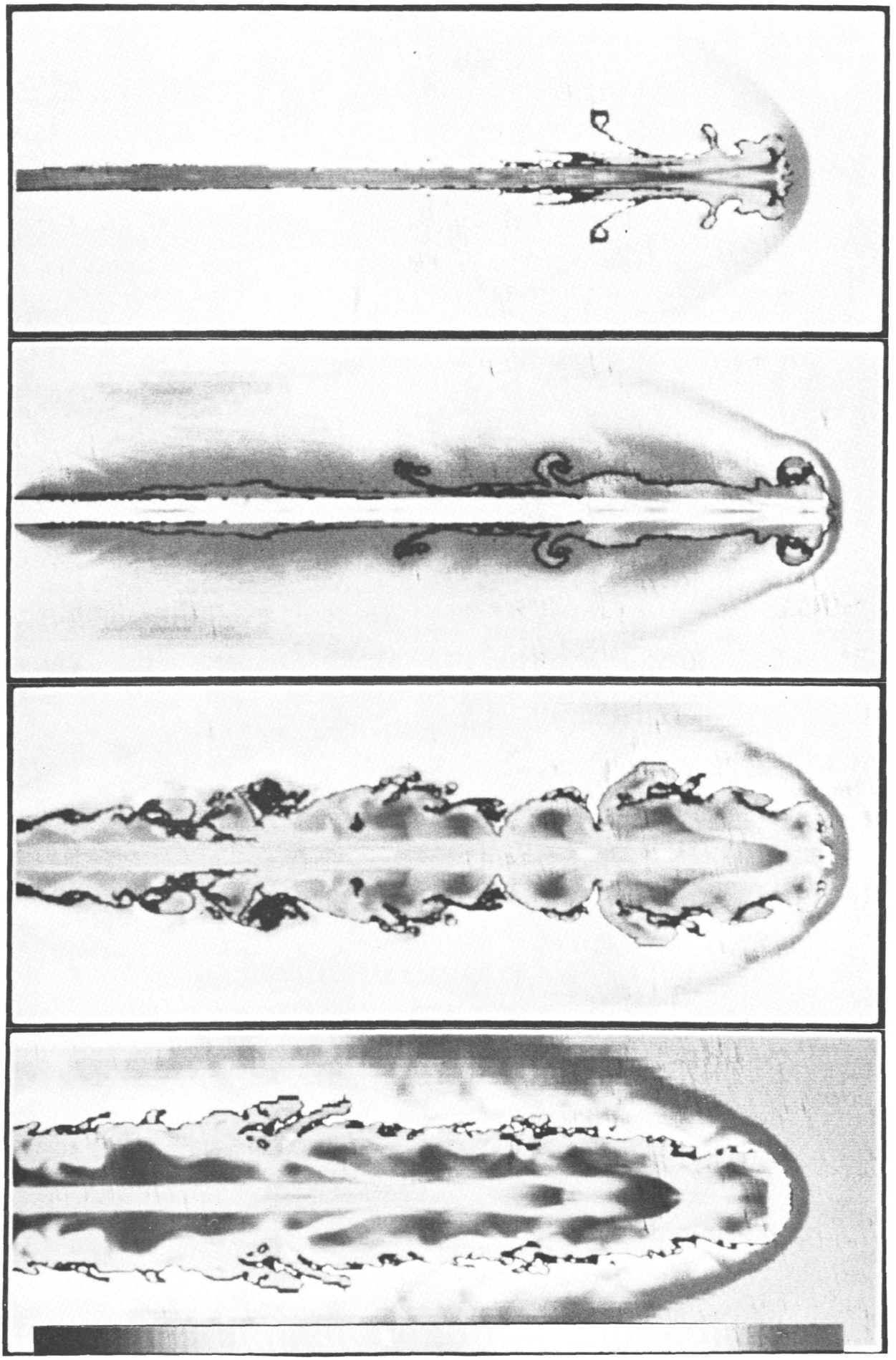

Plate 1. Dependence of cocoon thickness on beam density for four Mach 12 jets

The bottom frame shows the space-time history of the gas pressure on the axis of the jet, and indirectly records a great deal about shock dynamics in a propagating jet. The space-time "grid" consists of 640 by (typically) 300 uniform zones, with the space axis running horizontally $0 \leq Z \leq 80$, and the time axis running vertically $t_1 \leq t \leq t_2$; t_1 and t_2 are given in Table 2. Operationally, the procedure is the same as in the middle frame, however here only 15 bins are used between the minimum and maximum pressures. To further enhance the high pressure regions, all pressure bins below and including ambient pressure have been assigned the grey tones shown in the accompanying color bars. The color bars used in conjuction with the maximum and minimum pressures and pressure increments given in Table 2 allow one to derive quantitative information from the color figures, such as the mean knot overpressure discussed in Section 5, above.

Further details on how these plots are physically made, as well as an efficient algorithm for generating them are given in Winkler and Norman 1984.

CAPTION FOR PLATES 2-13:

Shock structure, strength, and history in pressure-matched supersonic jets. Top frame: composite jet structure showing shockwaves and strong compression zones (bright red), strong rarefaction zones (dark blue), jet gas (white), unshocked external gas (dark grey), shocked external gas (light grey), and contact discontinuity (black). Middle frame: false color image of the logarithm of the gas pressure, where maximum pressure is red, minimum pressure is blue, and intermediate pressures are assigned the spectral colors of the color bar in Plate 1. Bottom frame: false color image of the axial pressure as a function of space (horizontal axis) and time (vertical axis). Color bar and Table 2 define the pressure levels; pressure levels below and including ambient pressure are given in grey tones. See text for further information.

TABLE 2. Physical data for space-time axial pressure plots in Plates 2-13

Case	M	η	t_1	t_2	P^*_{min}	P^*_{max}	$P_{n+1}/P_n^\dagger$	Comments
1	1.5	1.0	10.	187.	2.3(-1)	2.8	1.19	substantial entrainment
2	1.5	0.1	5.	120.	1.4(-1)	3.2	1.25	little entrainment
3	3.0	1.0	4.	118.	1.7(-2)	4.0	1.47	propagating knots modulated by standing oscillation; $\lambda/R \approx 9.5$
4	3.0	0.1	1.	60.	1.5(-2)	7.5	1.56	complex transition to ordered knot phase: $t \geq 40$.
5	6.0	10.	2.5	80.	1.8(-2)	7.0	1.52	strong trailing shockwave; knots
6	6.0	1.0	2.5	43.5	2.0(-2)	1.1(1)	1.57	knots excited by spurious reflected shockwave
7	6.0	0.1	1.	27.	9.2(-3)	3.5(1)	1.80	cocoon-driven internal shockwaves; $\frac{dz}{dt} \approx -2$.
8	6.0	0.01	1.	28.	1.4(-2)	9.2(1)	1.90	short-timescale pressure fluctuations
9	12.0	10.	2.	38.	2.7(-2)	1.3(1)	1.55	quasi-ballistic jet; scant internal structure despite spurious impinging shockwave
10	12.0	1.0	1.25	20.	5.2(-2)	6.5(1)	1.67	thin cocoon: shear-wave induced internal shocks near jet terminus
11	12.0	0.1	0.5	14.	1.0(-2)	3.2(2)	2.10	cocoon-driven internal shockwaves
12	12.0	0.01	1.	7.6	1.8(-2)	5.0(2)	2.10	strong pressure variations near jet terminus

*normalized by the ambient pressure
†pressure ratio between color bar levels in space-time axial pressure plots

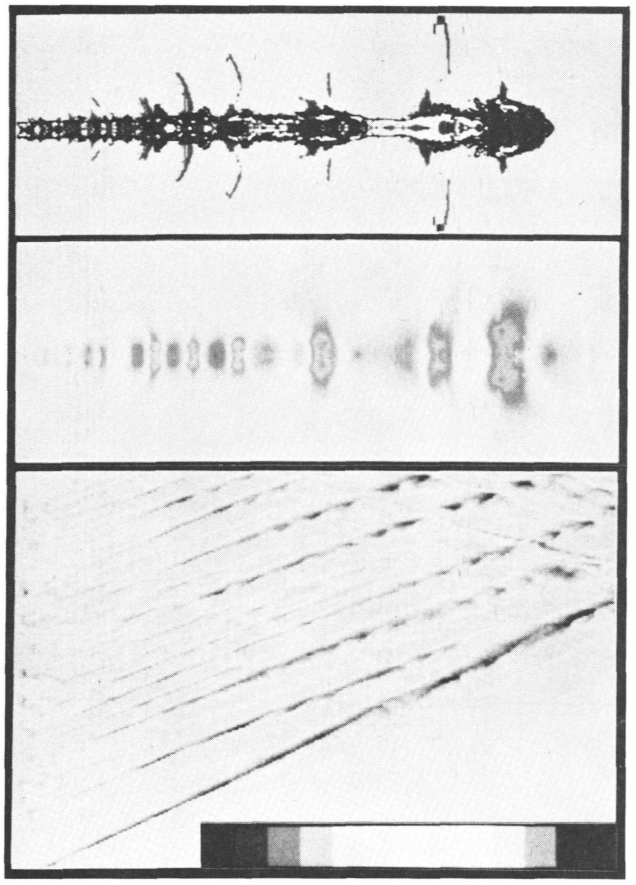

Plate 2. Density Ratio = 1, Mach Number = 1.5

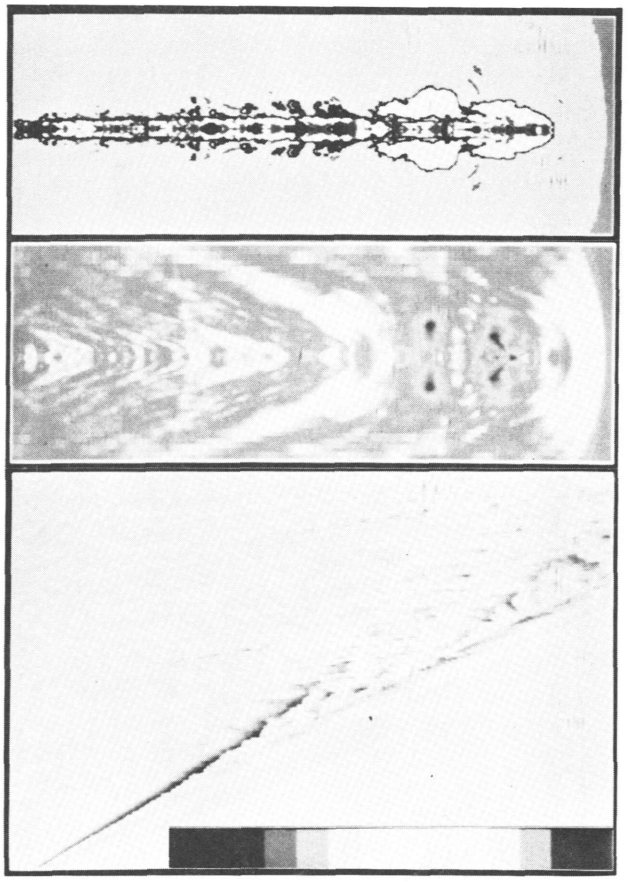

Plate 3. Density Ratio = 0.1, Mach Number = 1.5

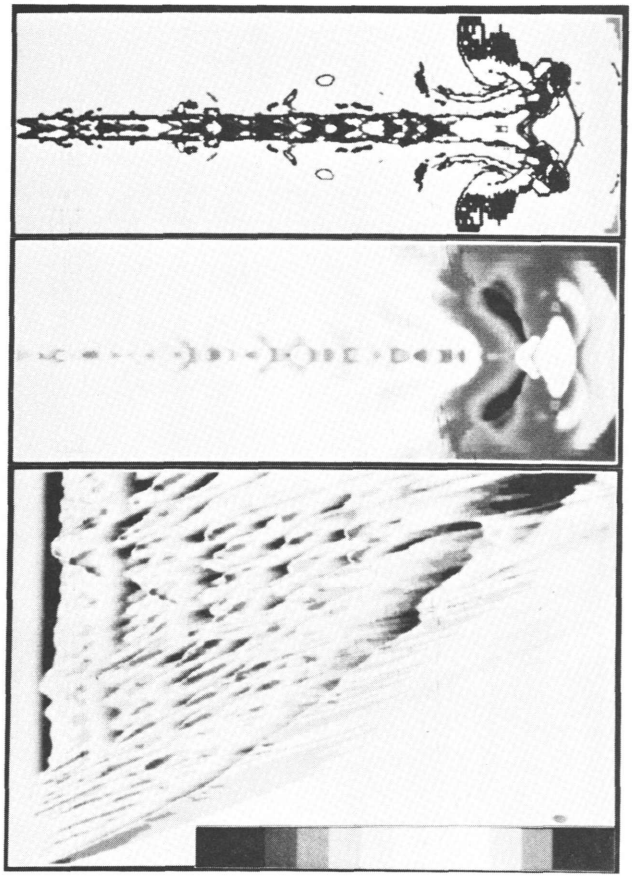

Plate 4. Density Ratio = 1, Mach Number = 3

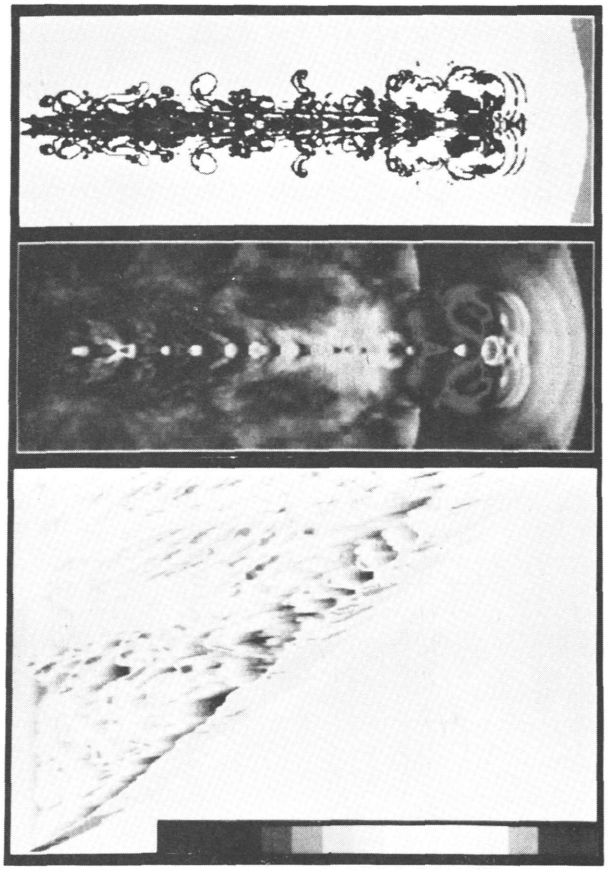

Plate 5. Density Ratio = 0.1, Mach Number = 3

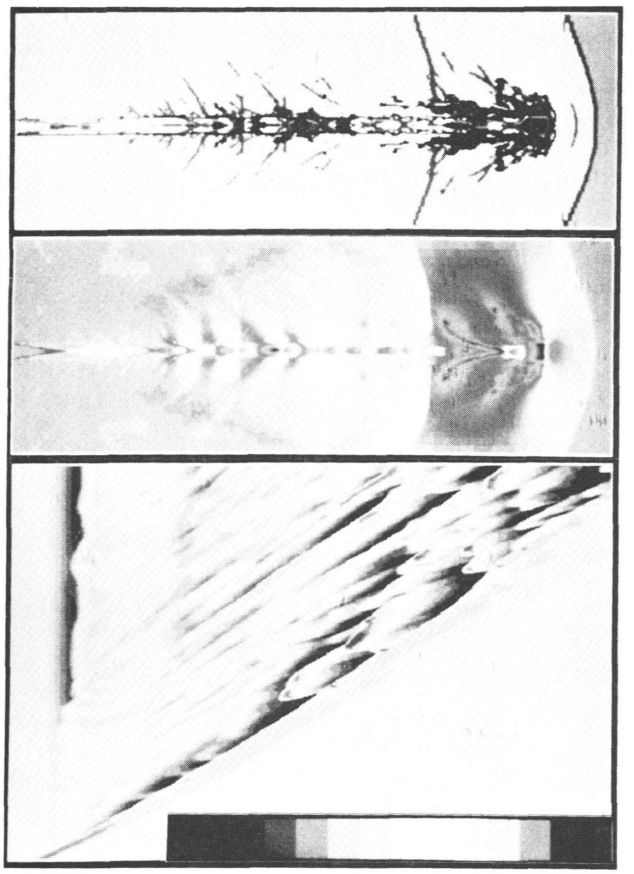

Plate 6. Density Ratio = 10, Mach Number = 6

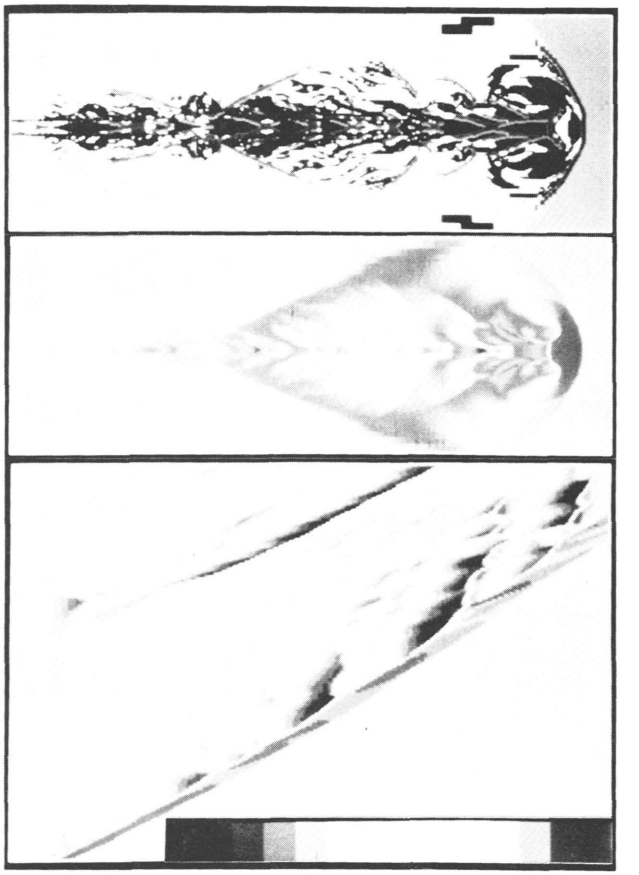

Plate 7. Density Ratio = 1, Mach Number = 6

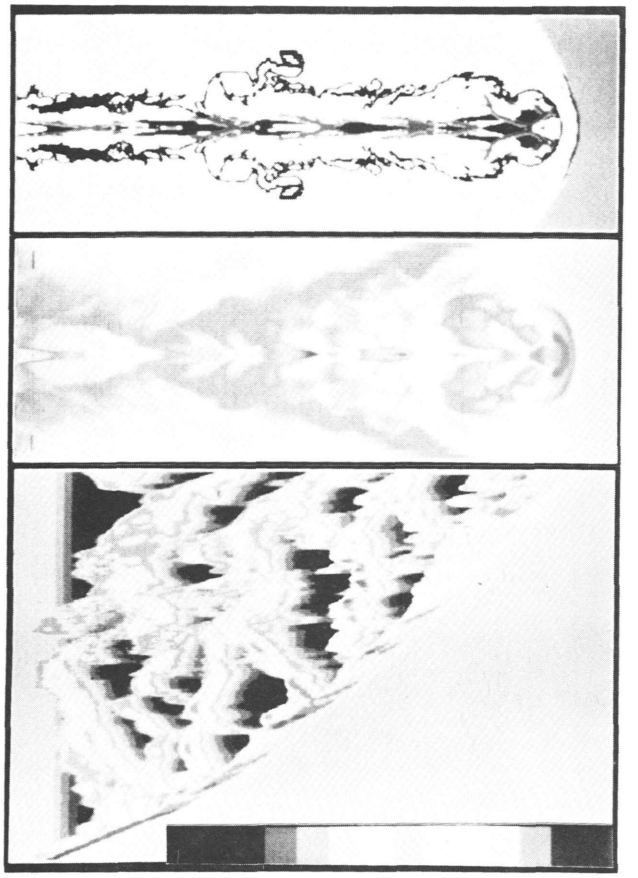

Plate 8. Density Ratio = 0.1, Mach Number = 6

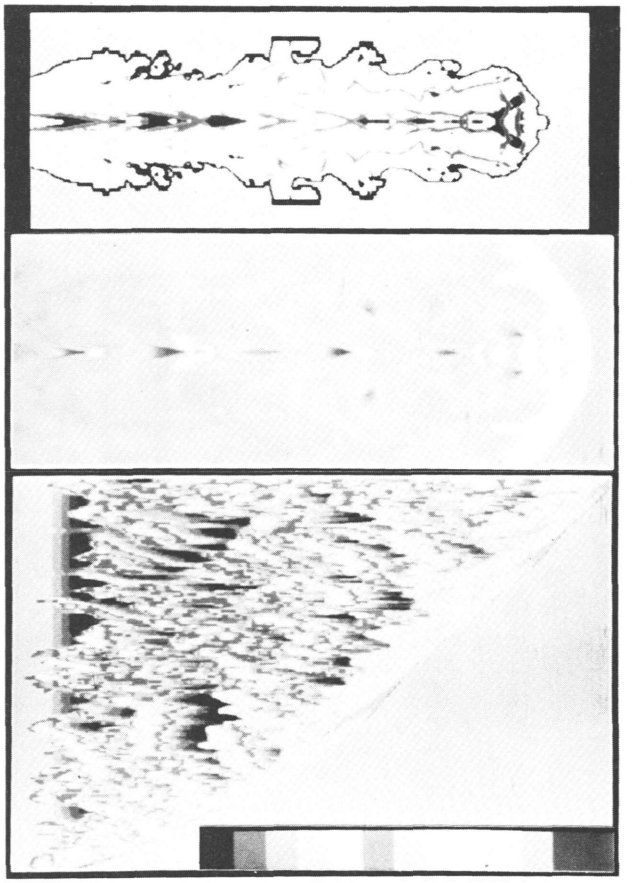

Plate 9. Density Ratio = 0.01, Mach Number = 6

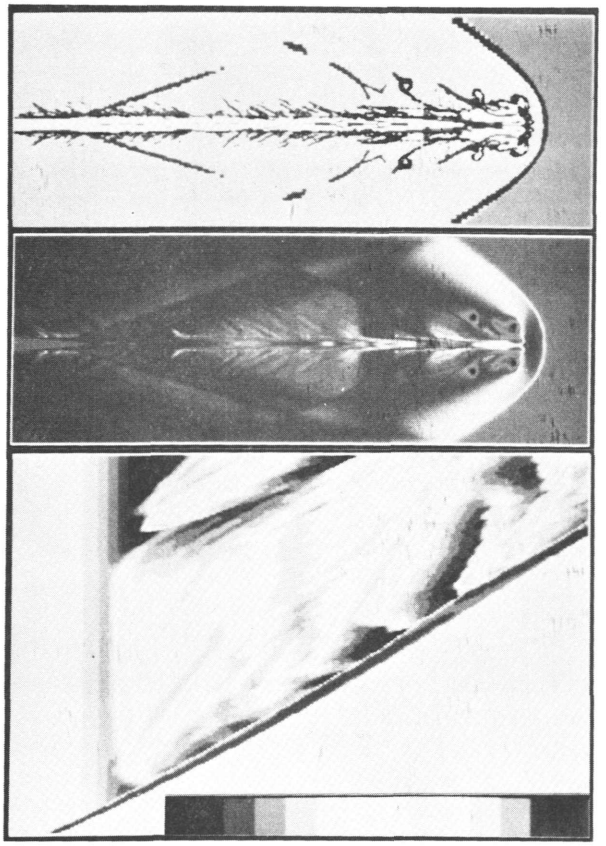

Plate 10. Density Ratio = 10, Mach Number = 12

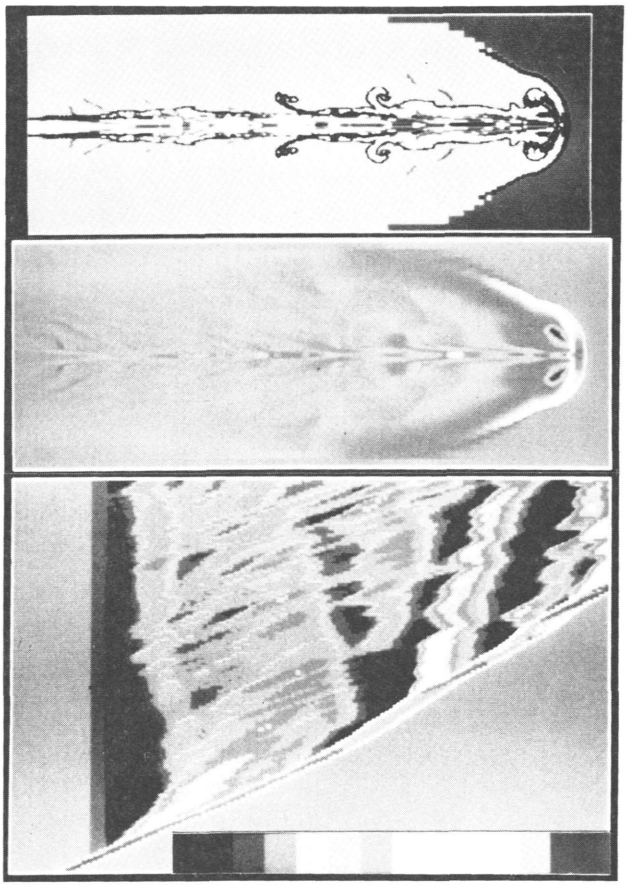

Plate 11. Density Ratio = 1, Mach Number = 12

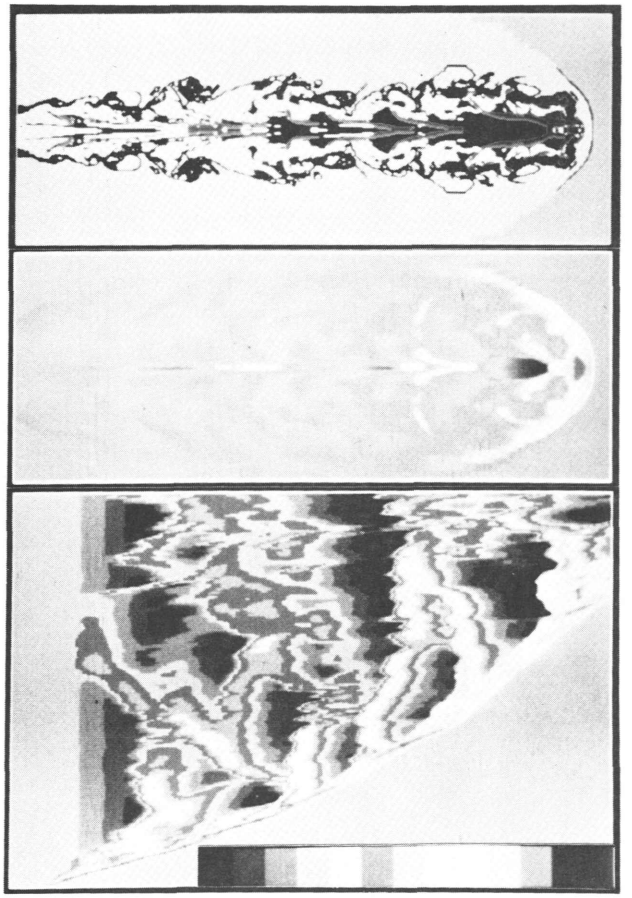

Plate 12. Density Ratio = 0.1, Mach Number = 12

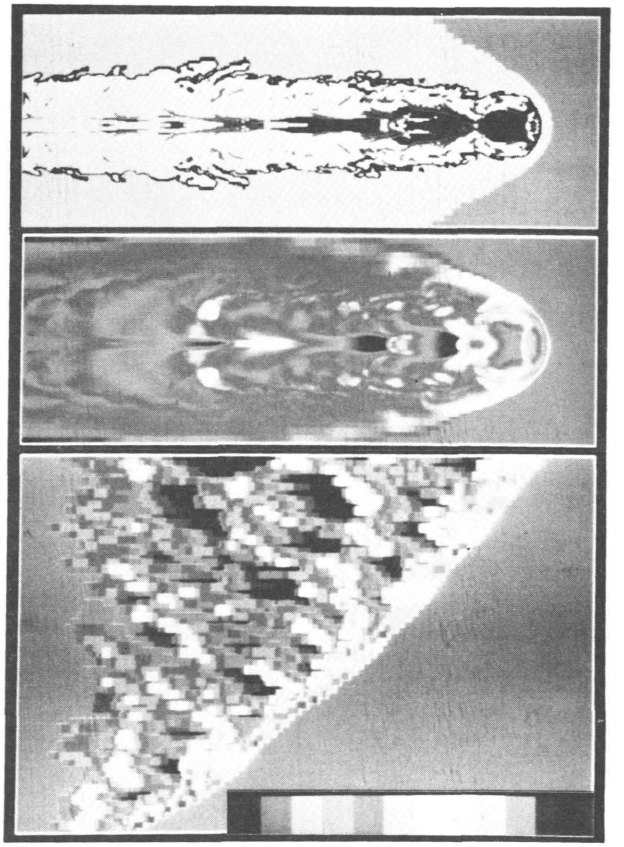

Plate 13. Density Ratio = 0.01, Mach Number = 12

Why Dominant Cluster Jets are Different.

Dean M. Sumi and Larry L. Smarr*
Department of Astronomy,
University of Illinois at Urbana-Champaign

ABSTRACT: Recent numerical simulations by Norman et al 1983 have shown that the ability of axisymmetric hydrodynamic jets stabily to propagate through a pressure confining atmosphere depends on two parameters: 1) the ratio of the internal jet density to the external atmosphere's density and 2) the jet's internal Mach number. As the pressure of the external atmosphere changes along the jet's path, these two parameters change accordingly, leading to the possibility that a stable jet can suddenly become unstable. Elliptical galaxies which are stationary with respect to any outside gas medium, can sustain two generic types of atmospheres, 1) an outflowing wind and 2) a radiatively cooling inflow. Isolated elliptical galaxies should have wind atmospheres, whereas dominant galaxies at the center of clusters of galaxies can have cooling inflow atmospheres. We find that jets emerging through wind atmospheres propagate stabily. In contrast, jets emerging through cooling inflow atmospheres rapidly evolve through parameter space, crossing over into the unstable region. The instability manifests itself as a strong planar shock which abruptly brings the jet from a supersonic to a subsonic flow. After this shock we expect a subsonic plume to continue onward. The behavior of jets in these different atmospheres may help explain the three classes of radio morphology found associated with dominant cluster galaxies: close doubles, short jets, and Wide Angle Tail (WAT) radio sources. In particular, our picture explains why these sources are often smaller in size than comparably powered radio sources from isolated elliptical galaxies.

Introduction

On the simplest level, jet morphology is determined by the interaction of the galaxy, the gas in and around the galaxy, and the jet, itself. Observations of the reconfinement shoulder in NGC 315 (Sanders 1983) and dynamic bending in narrow angle tail radio sources (Begelman et al 1979 and Jones et al 1979) demonstrates the initimate relationship between the jet and its surrounding environment. We examine a different aspect of this relationship between jet and environment, namely how Kelvin-Helmholtz instabilities (instabilities at the shear boundary between the jet and its confining medium) can affect a jet as it moves outward through a galaxy's gaseous medium. We will consider only galaxies stationary with respect to any outside gas medium and can, therefore, think of the subsequent gas configuration as an atmosphere around the galaxy. The parameters of the atmosphere will be determined by the potential well of the galaxy, and the energy balance in the atmosphere.

We will restrict ourselves to hydrodynamic jets which are pressure confined by the atmosphere. Within this scope, we look at the stability of jets, discuss the various atmospheres possible in elliptical galaxies, use the various atmospheres to trace a jet's stability through an atmosphere, and finally, look at examples of jets propagating through these atmospheres.

* Alfred P. Sloan Fellow

Jet Instabilities

Jets, by their very nature, are shear flows which are subject to Kelvin-Helmholtz instablilities. The lower order modes are the most observable, i.e. the n=0 mode (The "pinch" mode), and the n=1 mode (The "garden hose" instability or the "helical" mode). Although the helical mode is potentially the fastest growing of the two modes (Hardee 1982), we restrict ourselves to the axisymmetric pinch mode. Many jets (M87, 3C111, NGC 6251) do not appear to be strongly influenced by helical modes over a large fraction of their length, giving us some confidence that pinch modes may be dominant in the nonlinear regime.

Supercomputer simulations of axisymmetric pressure confined jets (Norman et al 1983 (NSW)) indicate that in the nonlinear regime the linear pinch instability saturates into shock fronts. The global structure of these shock fronts are of two basic types depending on the jet's location in a parameter space (see NSW, figure 6) defined by 1) the ratio of the internal jet density and the external confining atmosphere density η; 2) the internal Mach number, M (see figure 1). We will denote this space as (η, M) space. Two runs performed by NSW (our figure 2, and 3 are their figure 10) illustrate the two types of shock structure, one at η = 1, and M = 1.5 (figure 2b) and another at η = 1, and M = 3.0 (figure 3b). The jet in figure 2 has planar shock structure (shocks perpendicular to the jet flow) whereas the jet in figure 3 has biconical shock structure (shocks oblique to the jet flow).

The transition line between these two global structures was mapped out numerically by NSW and was found to correspond to the transition line between different types of pinch instability in the linear regime. From the linear analysis (see literature references in NSW) of idealized slab and cylindrical jet flows, one finds a subdivision of n = 0 pinch mode solutions; the lowest order (m = 0) is known as the ordinary mode (OM) pinch instabilities and the higher order solutions ($m \geq 1$) are known collectively as reflecting mode (RM) pinch instabilities. The relative growth rate of each mode (dependent on η, M, and wavelength) determines the dominance of the mode and, therefore the characteristic mode seen in a particular part of (η, M) space. Cohn (1983) finds a boundary between the OM dominated and RM dominated regime can be given roughly by

$$\eta \cong \left(\frac{M}{2}\right)^{3.3} \qquad (1)$$

where jets with $\eta > (M/2)^{3.3}$ are in the OM dominated regime. NSW noted that planar shock jets fall into the OM dominated regime and biconical shock jets fall into the RM dominated regime of (η, M) space. Though it is not precisely known how these linear modes develop into nonlinear shock structures, we are able to use equation (1) as a guide to the regions in (η, M) space where each shock structure is important. This line is labeled in figure 1 the planar shock / biconical shock (PS/BS) line.

NSW find that the type of shock structure has a strong influence on the jet's ability to propagate supersonically. Planar shocks will strongly decelerate the flow rendering it subsonic. Severe entrainment also occurs as the jet is "necked down" or pinched (see figure 2a). Biconical shocks, however, causes only slight decelerations of the flow and the jet remains supersonic along its entire length. There are only small undulations in the

FIGURE 1

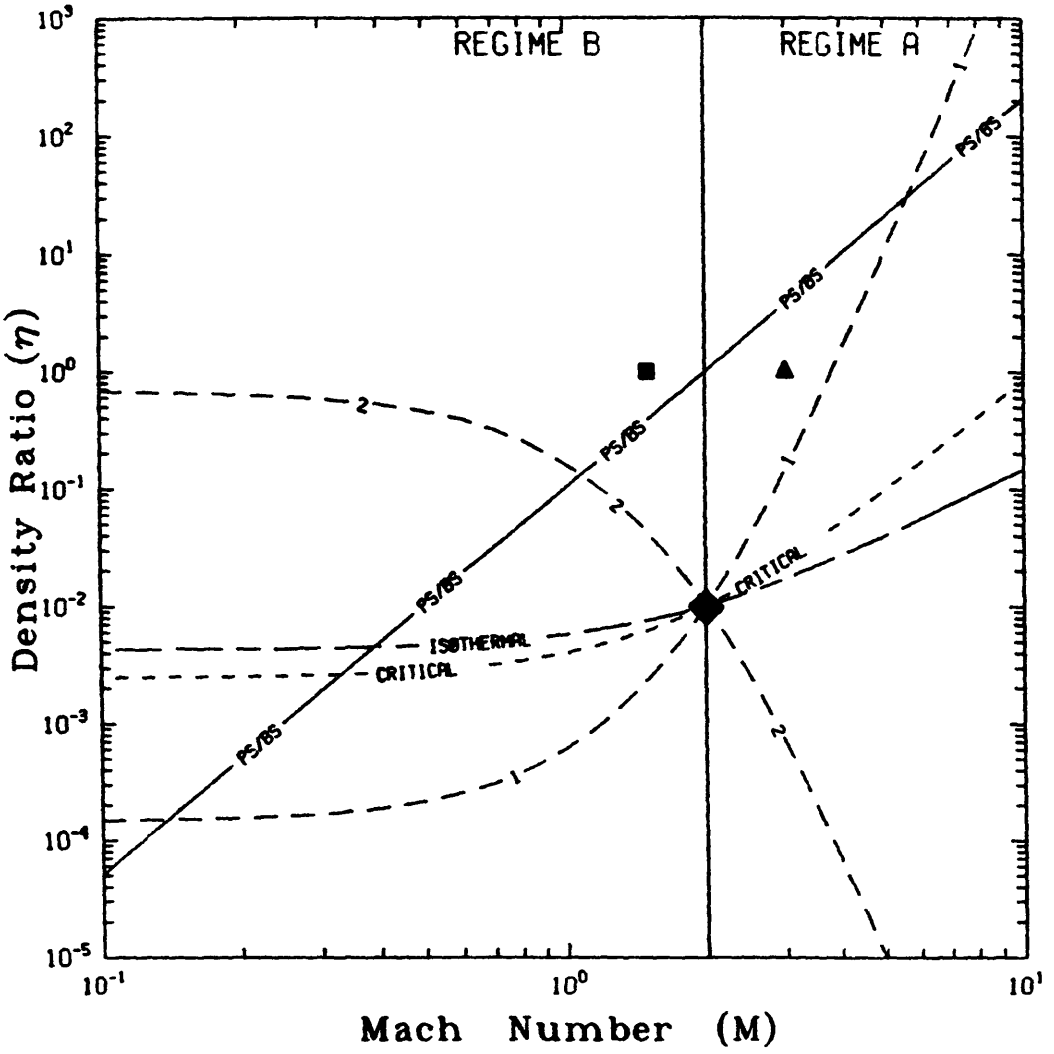

Figure 1. The (η, M) parameter space adapted from NSW figure 6. Plotted are the planar shock / biconical shock (PS/BS) line and jet parameters for the jet in figure 2 (■) and the jet in figure 3 (▲). For η = 0.01 and M = 2 (◆), the A and B regimes are labeled and are separated by regime B, the solid line. The isothermal line designates the boundary line between increasing and decreasing external temperature distribution. The critical line designates the critical jet path (ζ = 3.3) which will intersection with the PS/BS line. Lines 1 and 2 are jets paths passing through (◆) with δ = 2.5 and -2.5, respectively. These illustrate extremes of jet behavior.

FIGURE 2

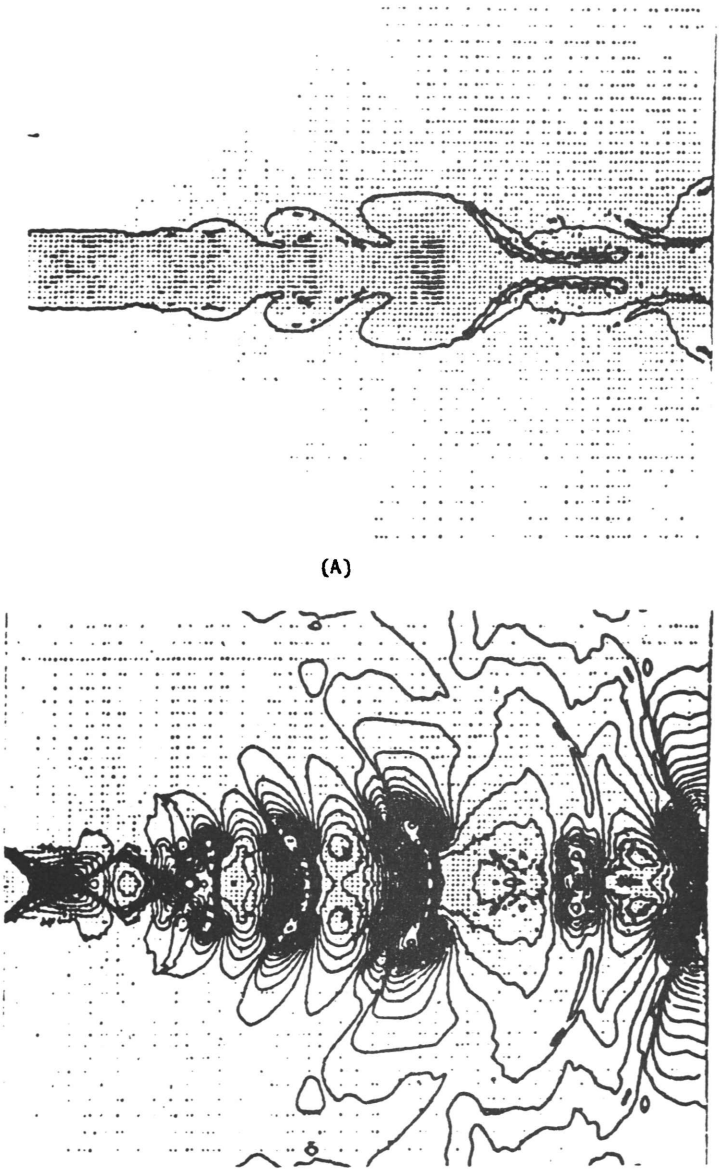

(A)

(B)

Figure 2. NSW simulation of a η = 1.0, M = 1.5 axisymmetric jet in a constant temperature and density medium. A) The jet boundary and velocity vectors. B) The pressure contours. Figure reproduced from NSW figure 10.

FIGURE 3

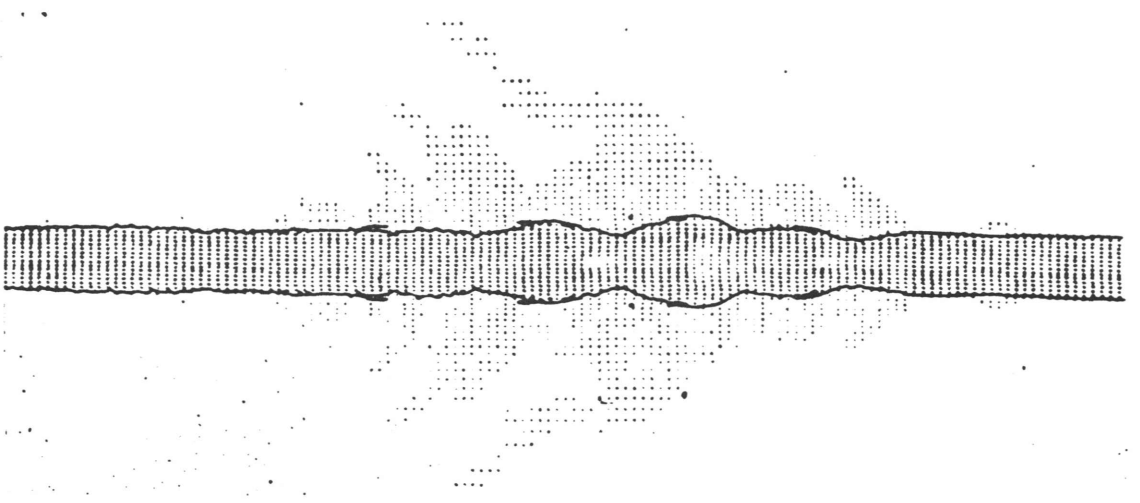

(A)

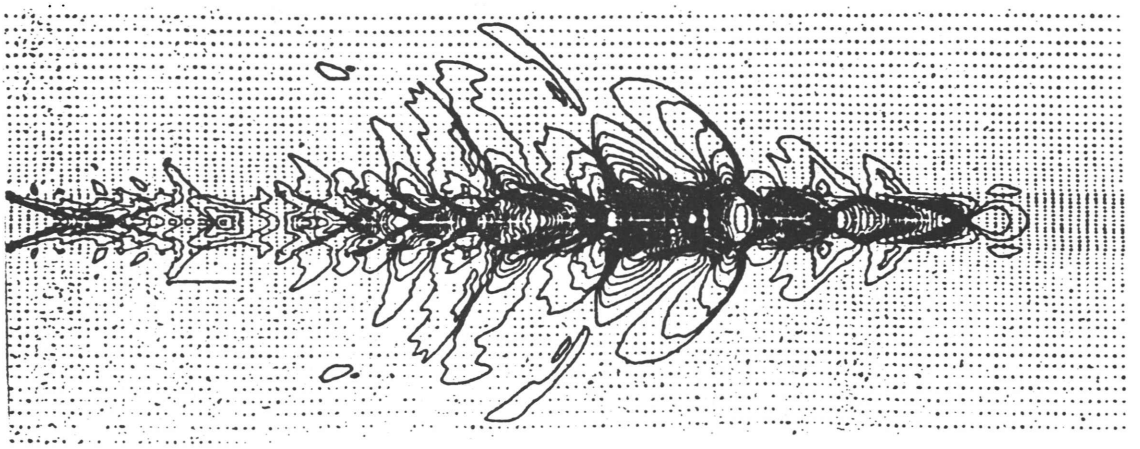

(B)

Figure 3. NSW simulation of a η = 1.0, M = 3.0 axisymmetric jet with the same confining medium. A) The jet boundary and velocity vectors. B) The pressure contours. Figure reproduced from NSW figure 10.

jet boundary and consequently no appreciable entrainment (see figure 3b). The (η, M) parameter space thus has regions separated by equation (1) where a jet when perturbed axisymmetrically will continue to propagate supersonically (the biconical shock regime) or will be decelerated down to a subsonic jet and mixed with the outside medium through entrainment (the planar shock regime).

The simulations conducted by NSW were run in a spatially uniform temperature and density confining medium. To assess the stability of pressure confined jets in a real galaxy, we need to be able to determine how the jet will react to the changing external medium and how this will in turn affect the shock structure. In this paper, we sketch out the simpliest approximation to the real world, namely that to lowest order a jet's local (η, M) is determined by the local confining medium's temperature and density through the pressure balance assumption. In general, the confining medium will have varying temperature, density, and pressure thereby changing the local (η, M) of the jet as it emerges from the galaxy. We further assume that the local (η, M) of the jet determines the shock structure, as found in the NSW calculations. Smarr et al 1983 (SNW) point out that the local (η, M) of the jet varies strongly through shocks but on average the values of (η, M) vary slowly along the jet and therefore this assumption is not inconsistent. The next step will be to perform new supercomputer simulations of jets in varying atmospheres to determine whether our "broad brush" picture given herein holds up in detail.

Given these assumptions we can follow a jet's path through (η, M) space as it moves through the confining medium and are able to use its location in this space to determine its ability to continue to propagate supersonically. It should be noted that points along the jet path through (η, M) space indicate the local (η, M) at a particular spatial location along the jet and not the jet as a whole. That is, when we observe a jet we see it at a moment in its propagation. Different points along the jet are at different points in (η, M) space.

Within the scope of our analysis, we can model a jet in terms of an equation of state for the jet given by

$$P_j \propto n_j^{\gamma} \quad , \tag{2}$$

pressure equilibrium

$$n_j T_j = n_{ext} T_{ext} , \tag{3}$$

and energy conservation

$$v_o^2 + \frac{2\gamma k T_o}{(\gamma - 1)\mu} + \phi_o = v_j^2 + \frac{2\gamma k T_j}{(\gamma - 1)\mu} + \phi \quad , \tag{4}$$

where P is pressure, n is the number density, T is temperature, v is velocity, ϕ is the gravitational potential of the host galaxy, k is the Boltzmann constant, γ is the ratio of specific heats, and μ is the mean molecular weight. The subscripts are j for jet, ext for the external medium, o for the initial jet, and * for the initial external medium. We have assumed that we can model a jet using an adiabatic equation of state, equation (2). This obviously will be violated when moving through strong shocks; we must, therefore, assume further that, at least in the biconical shock regime, the shocks are weak.

In terms of the variables of our parameter space one can easily show that

$$\eta \equiv \frac{n_j}{n_{ext}} = \eta_o \left(\frac{n_{ext}}{n_*}\right)^{\left(\frac{1}{\gamma} - 1\right)} \left(\frac{T_{ext}}{T_*}\right)^{\left(\frac{1}{\gamma}\right)} \qquad (5)$$

and

$$M^2 = \left(M_o^2 - \frac{2\mu}{\gamma k T_o}(\Phi - \Phi_o) + \frac{2}{\gamma - 1}\right)\left(\frac{P_{ext}}{P_*}\right)^{\left(\frac{1}{\gamma} - 1\right)} - \frac{2}{\gamma - 1} . \qquad (6)$$

Both these equations are dependent on only the external parameters of the confining medium.

Confining Atmospheres

We will consider atmospheres which contain an ambient medium plus mass inputs from stellar mass loss and planetary nebulae, energy inputs from supernovae explosions, and energy losses from radiation. We expect two generic types of atmospheres i) an outward flowing 'wind' model where sufficient energy is deposited by supernovae into the atmosphere so that the gas can escape, and ii) an inward flowing cooling model where the central core pressure support is removed by radiative losses causing the atmosphere to collapse (Mathews and Baker 1971). No truly static atmosphere is considered since any static atmosphere will evolve into the wind or cooling inflow regimes.

Cooling inflows can occur in a galaxy when

$$\sigma^2 > \left(\frac{2}{9}\right)\left(\frac{\alpha_{SN}}{\alpha}\right) E_{SN} \qquad (7)$$

(MacDonald and Bailey 1981), where σ is the line-of-sight velocity dispersion of the galaxy, α_{SN} is the specific mass loss rate for supernovae, E_{SN} is energy per unit mass of supernovae ejecta, and α is the total specific mass loss rate. The values for α_{SN}, α, and E_{SN}, are only poorly known, but current estimates (White, and Chevalier 1983) indicate that this dispersion limit is $\sim$ 700 km/sec, which excludes all elliptical galaxies from having cooling inflow atmospheres (The maximum velocity dispersion observed in elliptical galaxies is $\sim$ 400 km/sec, cf. Tonry and Davis 1981).

This limit, however, only pertains to single isolated galaxies. Dominant elliptical galaxies at the kinematic centers of cluster of galaxies are known to have cooling inflows, notably M87 in the Virgo cluster (e.g. Canizares et al 1979) and NGC 1275 in the Perseus cluster (e.g. Fabian and Nulsen 1977). Sumi and Smarr (1984) contend that the small core radii ($\sim$ 50 kpc) of the dark matter in some clusters of galaxies, termed pit clusters (Blandford and Smarr 1982), will naturally cause cooling inflows onto these central galaxies. This concentration of dark matter will tend to increase the effective velocity dispersion of the galaxy to cluster-like dispersions ($\sim$ 1000 km/sec). The galaxy dispersion is unchanged because the dominance of the dark matter occurs outside the optical extent of the galaxy. This higher velocity dispersion, and the relative unimportance of supernovae as energy inputs (Compared with shock heating as gas is stripped from cluster galaxies), allows the atmosphere around central galaxies in clusters of galaxies to satisfy (7), and making possible cooling inflows onto the central galaxy.

With an understanding of where the different atmospheres may be applica-

ble, we now would like to get a feel of the distribution of various important parameters of the two types of atmosphere. In the interest of brevity, we will summarize many years of work by many authors. Various simulations of wind type atmospheres indicate that the density, and pressure are declining as one moves outward from the galaxy. The temperature also declines but only much more slowly and is almost isothermal. In cooling inflow type atmospheres, the temperature strongly increases and the density strongly decreases as one moves outward, near the core of the galaxy. The pressure can also be increasing as one moves outward from the galaxy (a pressure inversion).

Stability of Jets in Galaxy Atmospheres

In this the discussion of stability, we choose simple analytic functions to represent the confining atmosphere. The analysis with more realistic atmospheres will be presented in a later paper. We represent the density, and temperature as power laws:

$$T_{ext} = T_*\left(\frac{r}{r_*}\right)^{\alpha} \tag{8}$$

and,

$$n_{ext} = n_*\left(\frac{r}{r_*}\right)^{\beta}. \tag{9}$$

The pressure of this atmosphere is given by

$$P_{ext} = P_*\left(\frac{r}{r_*}\right)^{\alpha + \beta}. \tag{10}$$

Substituting these equations into (5) and (6), we find that for (5)

$$\eta = \eta_o\left(\frac{r}{r_*}\right)^{[(1/\gamma - 1)\beta + (1/\gamma)\alpha]} \tag{11}$$

and for (6)

$$M^2 = \left(M_o^2 + \frac{2}{\gamma - 1} - \frac{2\mu}{\gamma k T_o}(\phi - \phi_o)\right)\left(\frac{r}{r_*}\right)^{[(1/\gamma - 1)(\alpha + \beta)]} - \frac{2}{\gamma - 1}. \tag{12}$$

Solving for r/r_* in (12) and replacing this into (11) we get

$$\eta = \eta_o\left(\frac{M^2 + \frac{2}{\gamma - 1}}{M_o^2 + \frac{2}{\gamma - 1} - \frac{2\mu}{\gamma k T_o}(\phi - \phi_o)}\right)^{\delta} \tag{13}$$

where

$$\delta \equiv \frac{(1 - \gamma)\beta + \alpha}{(1 - \gamma)(\alpha + \beta)}. \tag{14}$$

To discuss the behavior of the jet we consider two extreme regimes. First, we consider the case where the potential term is negligible compared to the kinetic and thermal terms in (12). Secondly, we will discuss the potential dominated case at the end of this section. This first assumption is equivalent to assuming the jet is unbound gravitationally to its host galaxy and reduces (13) to a parametric representation of the jet in (η, M) space.

Equation (13) is important in that it allows us to find the asymptotic behavior of the jet as either $M \to \infty$ or $M \to 0$. We take the limit as $M \to 0$ of (13) and find that

$$\lim_{M\to 0} \eta = \eta_o \left(\frac{\frac{2}{\gamma - 1}}{M_o^2 + \frac{2}{\gamma - 1}}\right)^{\delta} = \text{constant.} \qquad (15)$$

For a jet of decreasing Mach number, the slope of the jet path in (η, M) space will go to zero.

At the opposite limit, $M \to \infty$

$$\lim_{M\to\infty} \eta = \eta_o (M)^{\zeta} \qquad (16)$$

where $\zeta = 2\delta$. For a jet with increasing Mach number, the coefficient ζ is the asymptotic slope of jet path in (log η , log M), space. We will refer to this as the asymptotic logarithmic slope of the jet path.

To assess the stability of a jet, we use the (η, M) space (figure 1) and determine the jet path in this space using (13). Jet paths which cross into the planar shock regime are presumably thereafter subject to planar shocks and will be degraded into subsonic flows.

For any point in (η, M) space, there is a jet path leading from this point. The character of this path is determined ultimately by the external medium through δ in equation (13). In figure 1, we choose our arbitary point at $\eta = 10^{-2}$ and M = 2.0, this point is designated by (◆). The lines 1 and 2 through (◆) are jet paths from this point with δ = 2.5 and -2.5, respectively. Note that each line has two branches: one toward higher Mach numbers and another toward lower Mach numbers.

From equation (12), we find that the particular branch the jet takes as it propagates outward depends on the α, and β of the confining atmosphere. For $\gamma > 1$ in equation (12), we find that for $\alpha + \beta < 0$(regimes A), the Mach number increases with distance along the jet whereas for $\alpha + \beta > 0$ (regime B), the Mach number decreases. For $\alpha + \beta = 0$ (regime C), the Mach number is constant. In figure 1, the paths 1, and 2 leading from (◆) toward lower Mach numbers are followed by the jet as it propagates outward if the atmosphere is in regime B type; the paths 1, and 2 leading from (◆) toward higher Mach numbers are followed by the jet as it propagates outward if the atmosphere is in regime A. In general, we can separate (η, M) space around any point (η_o, M_o) into 1) $M > M_o$, which encompasses all jet paths propagating through a regime A atmosphere, 2) $M < M_o$, which encompasses all jet paths propagating through a regime B atmosphere and 3) $M = M_o$, the boundary line between regime A and B (regime C). In figure 1, we separate (η, M) space around point (◆) into regime A, and B.

From equation (10), we find that these conditions on α, and β are conditions separating special regimes of the pressure distribution. Regime A is a decreasing pressure distribution, regime B is an increasing distribution (a pressure inversion), and regime C is a constant distribution.

Another important dividing line in the (η, M) diagram separates atmospheres with temperatue distributions with 1) $\alpha > 0$, and 2) $\alpha < 0$. The boundary line where $\alpha = 0$ represents an isothermal atmosphere. Using (13) we can plot this line in figure 1 for point (◆). In regime A, the asymptotic logarithmic slope of this line, ζ, is 2.

Finally, we can delineate the regions where a jet in the biconical shock regime will cross into the planar shock regime. Jet paths into regime B asymptotically go to zero logarithmic slope and will intersect the PS/BS line. For regime A the asymptotic logarithmic slope is given by ζ. The condition for intersection with the PS/BS line is $\zeta = 3.3$ (equation (1)). Thus, there will be an intersection of the jet path with the planar shock regime if:

$$\alpha > -\frac{1.3(1-\gamma)\beta}{1.3-3.3\beta} \qquad (17)$$

Again using (13) we plot the critical PS/BS intersection jet path (the equality in equation (17)) on figure 1 for point (◆).

We now come to our conclusions about jet propagation in the two types of elliptical galaxy atmospheres. As noted in the previous section, isolated ellipticals have wind type atmospheres which are isothermal or have declining temperature distributions and will have declining pressure distributions. Therefore, all jet paths will be in regime A and will move toward higher Mach number. The largest upward logarithmic slope asymptotically can only reach the isothermal line with logarithmic slope equal to 2. A jet with initial conditions below the PS/BS boundary therefore must have a path through (η, M) space which does not intersect this boundary. Consequently such jets can propagate supersonically along its entire length and get out of the galaxy to large distances.

For cooling inflow atmospheres, we can separate the jet's response into either regimes A or B. In regime A, we can use (16) to describe the jet's asymptotic behavior. By its very nature a cooling inflow has $\alpha \geq 0$. Therefore, the smallest asymptotic logarithmic slope of a jet's path is given by the isothermal atmosphere line asymptotic slope of 2. A jet path along this line, as seen in the wind atmosphere case, will not intersect the PS/BS line. However, if a cooling inflow has temperature and density distributions such that condition (17) is satisfied, a jet in this atmosphere will make the transition into the planar shock regime. In regime B, we find that all jet paths will make this transition, since all paths have limiting slopes of zero and move toward lower Mach numbers. We, therefore, have the situation where as long as condition (17) is satisfied by the cooling inflow atmosphere a jet initially in the biconical shock regime will at some point cross into the planar shock regime. The jet then will go subsonic, if perturbed.

The above analysis must be modified to accommodate the potential term, ϕ. This term is especially important for gravitationally bound and nearly bound jets. From (12), we find that as the potential term becomes important the Mach number tends to go to zero for all jets. The density ratio, η, is unaffected by the potential (equation (11)). The jet path in (η, M) space is toward zero Mach number and the asymptotic logarithmic slope also approaches zero. The net result is for all gravitationally bound jets in the biconical shock regime to cross into planar shock regime. Example jet paths for jets which are bound are plotted in figure 4. Jet path 3 would follow the $\alpha = 0$ line if the potential were neglected. Jet path 4 is the same atmosphere parameters as jet path 2 in figure 1 only not neglecting the potential term. For convenience, we have used a linearly increasing potential term. This not meant to represent a physical galaxy potential, but rather to mathematically represent a case between a 1/r (point mass) and a log(r) (extended dark

FIGURE 4

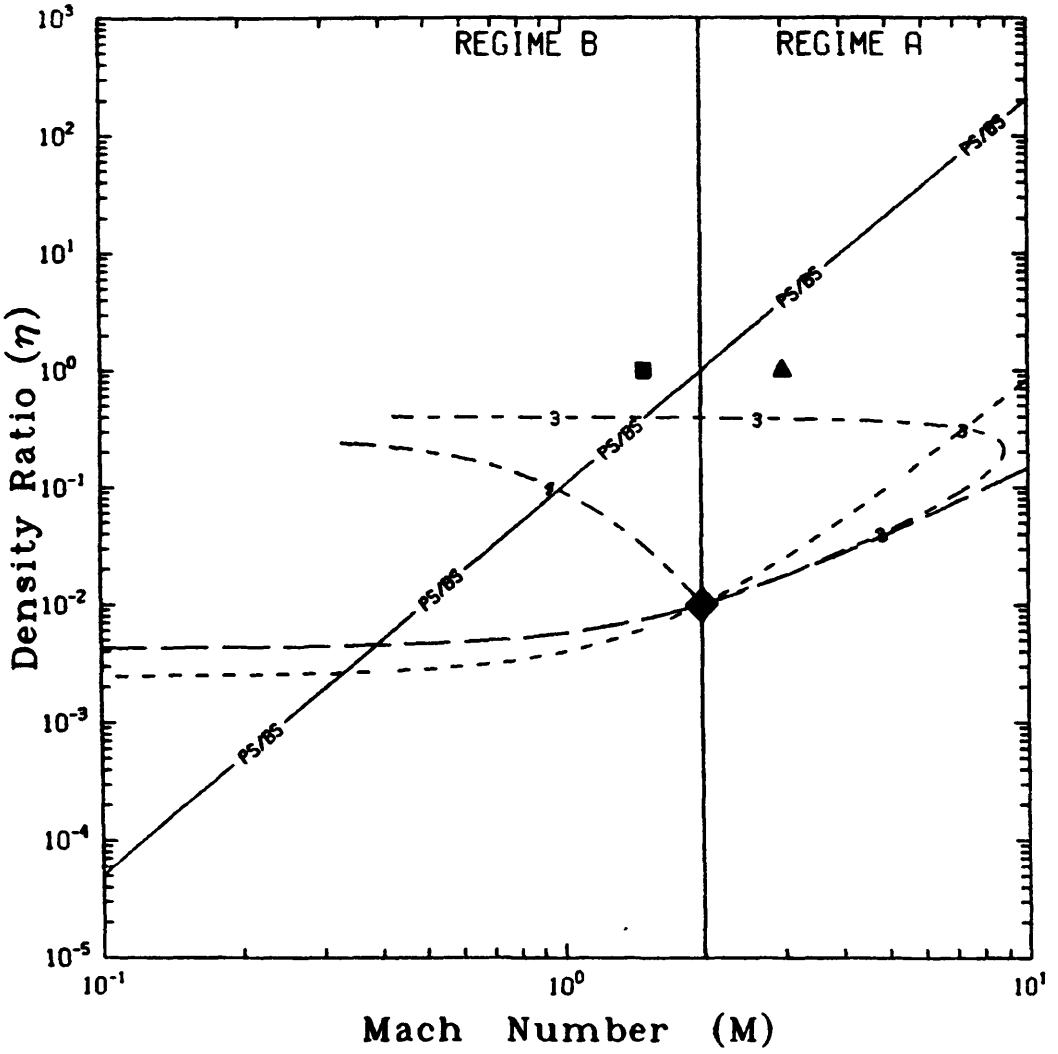

Figure 4. Jet paths for gravitationally bound jets. The potential is chosen to be a linear function of radius. Jet path 3 is initially on the isothermal jet path in figure 1 and jet 4 is initially on the same path as jet path 2 in figure 1. Both jet paths cross into the planar shock regime.

matter) potential.

We find that the type of atmosphere has a profound effect on the ability of a jet to propagate supersonically throughout its entire length. Within certain constraints (17), a cooling inflow type atmosphere can cause a supersonic pressure confined jet to be unstable to becoming subsonic. Wind atmospheres, however, allow a supersonic jet to propagate along its entire length supersonically, as long as the jet is not gravitationally bound to its host galaxy. More realistic calculations of galaxy atmospheres, using observational data, are underway (SS). Full scale numerical simulations with Norman and Winkler are planned later this year.

Discussion

Based on the analysis above, we expect a correlation between jet morphology, the atmosphere type, and, in a special sense, galaxy type. Isolated elliptical galaxies are most likely to have wind atmospheres and should have lengthy supersonic jets. Examples of this type of galaxy/jet might be NGC 315 or NGC 6251 both with long collminated jets and fairly isolated - both are outlying members of Zwicky clusters. NGC 6251 has a jet length of order 200 kpc and a large string of knots. If these knots are shocks induced by pinch instabilities, they only slightly disturb the jet flow, as might oblique shocks (See discussion in NSW and SNW)

Galaxies with known cooling inflows are all dominant galaxies at the kinematical center of their cluster or group. As an example, we speculate that the M87 jet may be showing the biconical shock to planar shock transition (See figure 1 in Biretta et al 1984 (BOH)). Prior to knot A the jet is well collminated and has four knots (D, E, F, I from the nucleus outward). At knot A the jet shocks very strongly. This shock looks like a planar shock in high resolution VLA radio maps (BOH). The post shock flow is much wider than the preshock flow and also has the distorted structure of a subsonic flow. This post shock structure is often called a plume to differentiate it from the preshock jet. In our model knot A represents the disrupting planar shock and the up stream knots represents oblique shocks with the transition after or at knot I. We regard M87's jet morphology as a prototype of "short jets" in dominant cluster members. Other examples include 4C26.42 and 3C84 (NGC 1275).

The basic M87 type morphology (Jet-hotspot-plume) is repeated in many dominant cluster galaxies as noted by Blandford and Smarr (1982). The cD galaxy in Abell cluster 1795 (van Breugel et al 1984) has a radio source, 4C26.42, with inner hotspots at ~ 1 kpc and plume structures in an inversion symmetric configuration. Wide Angle Tail radio sources (WAT) which have been associated with dominant cluster galaxies (Owen and Rudnick 1976) also have the jet-hotspot-plume morphology but on sometimes much larger scales - 4C47.51 has hotspots at ~ 100 kpc. Most of the discussion on WAT sources (e.g. Eilek et al 1984 and references therein) focus on why the subsonic plumes bend at large distances. Our model sheds no new light on this problem.

Finally, as Valentijn and Bijleveld (1983) have pointed out, most (80%) of dominant cluster galaxies with radio jets are unresolved close doubles. As Blandford and Smarr (1982) speculate, these may be examples of the same planar shock phenomena which has been resolved in the "short jets" and the WAT radio sources. We urge attention be given to obtaining high resolution VLA maps of

these sources to see if the basic morphology predicted by our model occurs here.

Summary

We have discussed possible atmospheres a jet might encounter as it emerges from an elliptical galaxy. Wind type atmospheres tend to keep a jet in its initial shock regime. Cooling inflow atmospheres (which may only be possible in galaxies at the center of a cluster of galaxies) will tend to drive a jet toward the planar shock regime and degrading it into a subsonic flow. This type of jet instability may make it possible to understand the observed association between short jet - hotspot - plume sources, in particular WAT radio sources, and dominant central galaxies. More definitive answers will require better observations of elliptical galaxy atmospheres and numerical simulations to verify our simplified model.

Acknowledgements

We wish to thank M. L Norman and K.-H. Winkler for allowing us to reproduce their simulations of jets, and for encouragment and conversations on this project. In addition, we gratefully acknowledge R. D. Blandford and J. F Hawley for clarifying remarks. We also would like to thank F. N. Owen, J. O. Burns, J. A. Eilek and T. Cornwell for interesting conversations on the problems with various radio sources. The National Science Foundation (grants PHY 80 - 01496 and PHY 83 - 08826) and the Alfred P. Sloan Foundation provided partial support for this work. Both of us thank Prof. Dr. R. Kippenhahn for his generous support in allowing us to have an extended visit at the Max Planck Institut fuer Physik und Astrophysik, Institut fuer Astrophysik, where much of the preliminary work on this project was done.

References

Begelman, M. C., Rees, M. J., and Blandford, R. D. (1979) Nature, 279, 770.

Biretta, J. A., Owen, F. N., Hardee, P. E. (1983) Astrophys. J., 274, L27.

Blandford, R. D., and Smarr, L. L. (1982) University of Illinois Astronomy Department Preprint # IAP 82-39.

Canizares, C. R., Clark, G. W., Markert, T. H., Berg, C. , Smedira, M., Bardas, D., Schnopper, H., and Kalata, K. (1979) Astrophys. J., 234, L33.

Cohn, H. (1983) Astrophys. J., 269, 500.

Eilek, J. A., Burns, J. O., O'Dea, C. P. O., and Owen, F. N., (1984) Astrophys. J., 278, 37.

Fabian, A. C., and Nulsen, P. E. J. (1977) Monthly Notices R. Astr. Soc., 180, 479.

Hardee, P. E., (1982) Astrophys. J., 257, 509.

Jones, T. W., and Owen, F. N. (1979) Astrophys. J., 234, 818.

MacDonald, J., and Bailey, M. E. (1981) Monthly Notices R. Astr. Soc., 180, 995.

Mathews, W. G., and Baker, J. C. (1971) Astrophys. J., 170, 241.

Norman, M. L., Smarr, L. L., and Winkler, K.-H. A. (1984) Max Planck Institut fuer Physik und Astrophysik Preprint MPA 115.

Owen, F. N., and Rudnick, L. (1976) Astrophys. J., 205, L1.

Sanders, R. H. (1983) Astrophys. J., 266, 73.

Smarr, L. L., Norman, M. L., and Winkler, K.-H. A. (1984) Physica D. - Proceeding of the Conference on Fronts, Interfaces, and Patterns, Los

Alamos. In press.
Sumi, D. M., and Smarr, L. L. (1984) in preparation.
Tonry, J. L., and Davis, M. (1981) Astrophys. J.,246, 666.
Valentijn, E. A., and Bijleveld, W. (1983) Astron. and Astrophys., 125, 223.
van Breugel, W., Heckman, T., Miley, G. (1984) Astrophys. J., 276, 79.
White, R. E. III, and Chevalier, R. A. (1983) Astrophys. J., 275, 69.

VORTEX-RINGS IN EXTENDED DOUBLES

L. Rudnick
University of Minnesota, Department of Astronomy
116 Church Street, SE, Minneapolis, MN 55455

ABSTRACT. Vortex rings appear to be a commonly excited mode in the fluid transport of relativistic material to radio source lobes. They may serve as both passive probes of the transport physics and as active dynamical contributors to the source evolution.

(Work in collaboration with T.W. Jones.)

One common feature of recent well-processed maps are usually referred to as "bubbles", but may in fact be vortex rings such as those seen in laboratory and everyday flows. The reader is referred to published maps of Hercules-A (Dreher and Feigelson 1984), 3C310 (van Breugel and Fomalont 1984) and Cygnus-A (Perley and Dreher 1984) for good examples. Some structures may be intrinsically spherical, but elliptical features, like the one in the eastern lobe of Cygnus, must closely resemble vortex rings.

In the laboratory, vortex rings can be formed by viscous forces at an orifice itself (the classical smoke-ring), or as what we generally refer to as a Kelvin-Holmholtz instability, further downstream. Figure 1 shows the development (without forcing) of vortex rings in a fog jet. This type of instability reaches a maximum saturated amplitude for fD/v (the Strouhal number) ~ 0.3, where f is the temporal frequency of the instability, D the jet diameter, and v the flow velocity. This relation is the same (within an order unity factor) as that described by Hardee (this workshop) for the fastest growing helical instability modes. Note also the breakup of the rings into filamentary structures, such as are now being found in radio sources.

Figure 2 shows the persistance of laboratory vortex rings, and their ability to entrain material. Turner (1960) proposed to use vortex rings to transport industrial waste to high altitudes. Could astrophysical rings carry relativistic particles out into radio lobes?

The supersonic calculations of Norman et al. (1983) also show structures which resemble detached vortex rings. By extrapolating from the laboratory results, we are looking into ring formation and stability as a function of Reynolds number, etc., in order to develop an observational probe of flow conditions.

REFERENCES

Dreher, J.W. and Feigelson, E.D. (1984), Nature 308, 43.
Crow, S.C. and Champagne, F.H. (1971), J. Fluid Mech. 48, 547.
Maxworthy, T. (1974), J. Fluid Mech. 64, 227.
Norman, M.L., Winckler, K.H. and Smarr, L. (1983), in "Astrophysical Jets," (Dordrecht: Reidel).
Perley, R.A. and Dreher, J.W. (1984), Ap.J. (Letters), in press.
Turner, J.S. (1960), Mech. Eng. Sci. 2, 356.
van Breugel, W.J.M. and Fomalont, E.B. (1984), Ap.J. (Letters) 282, L55.

Figure 1. Fog jet spark photographs, Crow and Champagne (1971) Reynolds numbers - top: 10,500, bottom: 19,500.

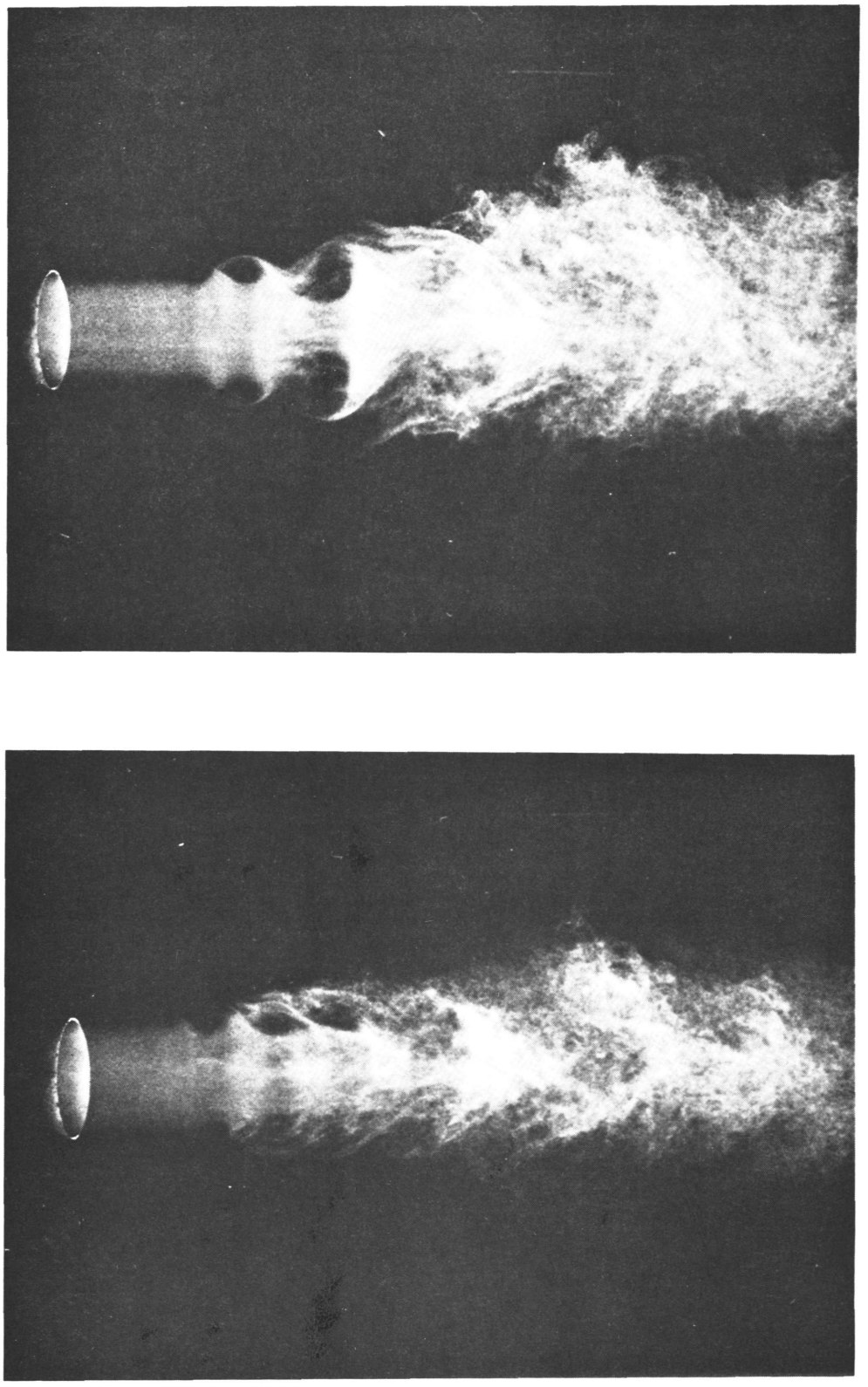

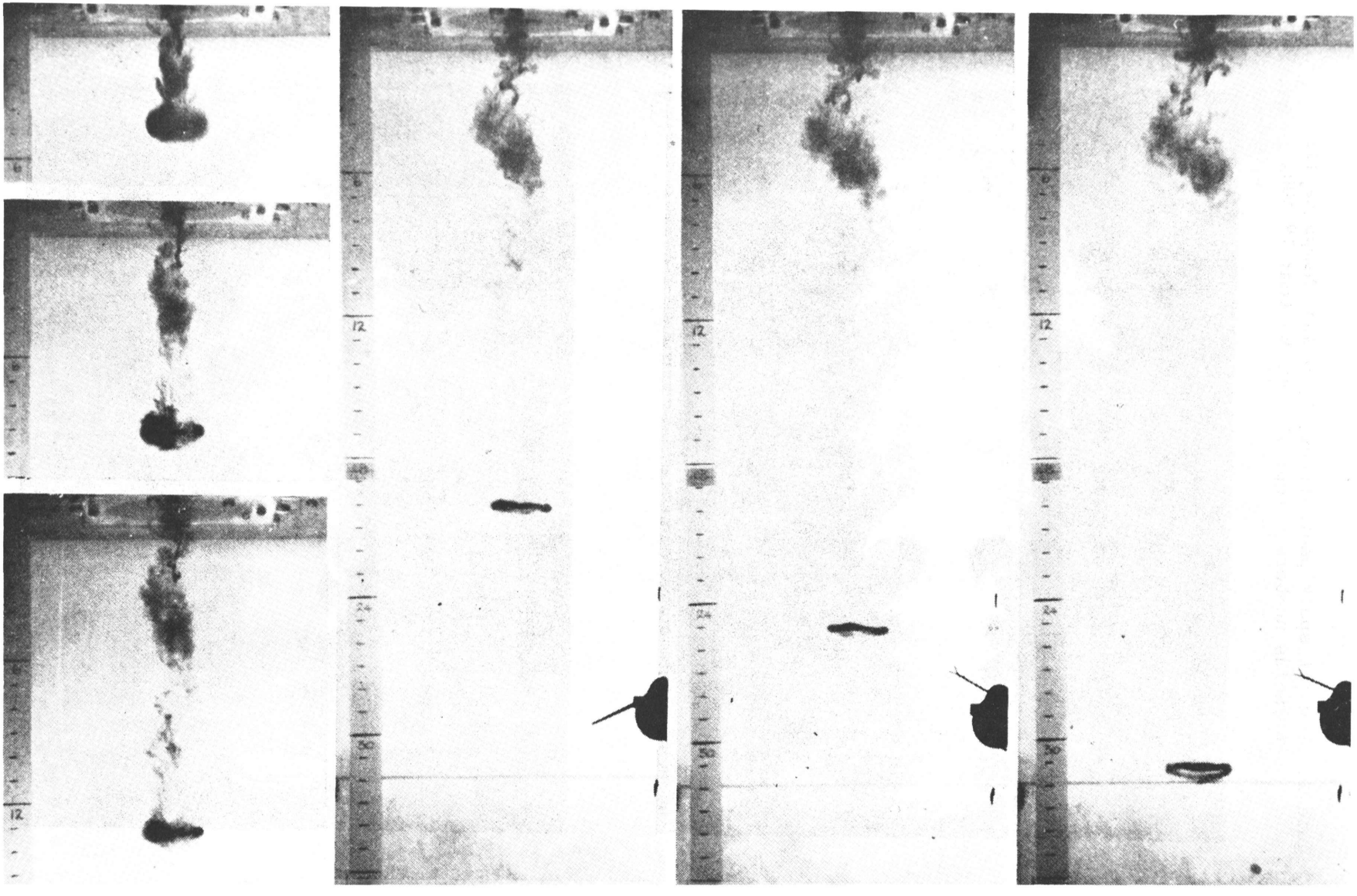

Figure 2. Vortex ring time sequence, Maxworthy (1974).

CURRENT-CARRYING JETS

Gregory Benford
Physics Department
University of California, Irvine, CA 92717

ABSTRACT

The best evidence for current-carrying jets comes from a need to invoke a B_θ to confine high-pressure jets. We can learn how such jets form by studying the electrodynamics of existing laboratory beams. In both laboratory and astrophysical jets, fields are developed during the transient rise of current at the jet head, and persist thereafter. Current is conserved, so studying B_θ at kpc can tell us about J_z near the nozzle. I propose that magnetically dominated nozzles account for Bridle's observed correlations in weak vs. strong jets. A possible escape from B_θ- dominant jets lies in abandoning the incoherent synchrotron assumption. If knots and hot spots emit through coherent plasma mechanisms, this greatly relieves the pressure problem. This radical suggestion might be testable for small, nearby lobes such as those of Sco X-1. Observations of amplitude jitter and long autocorrelation times would be clear evidence of non-synchrotron emission.

JET ELECTRODYNAMICS

For about eight years now the notion that jets emerging from magnetospheres may well carry significant currents has been gaining ground. It was at first not an appealing idea within the traditional astrophysical pictures. It demands circuits flowing over huge distances, and the first question asked was always, what stops this current from shorting out? After all, there are good conductors aplenty in the intergalactic and interstellar medium. Why should a current remain attached to an onrushing beam?

From my point of view, the answer depended more upon what I knew happened to real relativistic electron beams in the laboratory. There, a beam occurs because a large capacitor discharges across a narrow gap. The electrons reach the anode, a thin foil, and go straight through into the chamber beyond. There their electrodynamics are much like those we might expect of jets. They must find a return current path. If they are restrained from immediately snaking into the walls (either because the conducting walls are far away, or else an imposed axial magnetic field directs them), they will generate a return current in the dense background plasma which fills the chamber. Without this plasma the beam explodes radially from self-charge. The beam eventually reaches the far end of the cylindrical chamber and usually returns current through the walls. The return current pattern set up in the plasma lasts for a magnetic diffusion time, which is quite long compared to

the beam lifetime (or, in astrophysics, the jet duration).

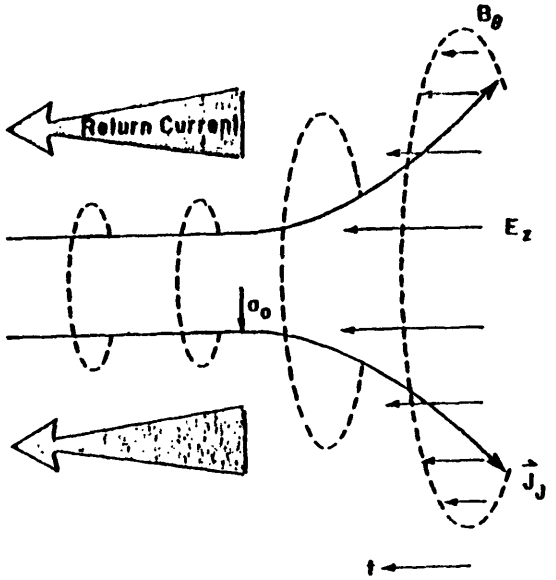

Fig. 1

The basic picture of Fig. 1 is common to both cases. An important point is that the jet is always flared at the head because of (1) scattering by the dense plasma, and (2) inadequate B_θ to restrain the transverse outward pressure. This is crucial to establishing the return current by the inductive field E_z, which arises from dI_j/dt. A simple solution for the jet radius behind the head is $a = a_o z^{-1/2}$, where z is the distance back from the head in units of $v_j\tau$, with v_j the jet velocity and τ the rise time of the current I_j. One can solve for the electrodynamics in the head region, assuming a conductivity in the dense plasma.

Keeping only E_z, B_θ and E_r,

$$\frac{1}{r}\frac{\partial}{\partial r} r E_r = -\frac{1}{v_j\tau}\frac{\partial}{\partial Z} E_z$$

$$\frac{1}{c\tau}\frac{\partial B_\theta}{\partial Z} = \frac{\partial E_z}{\partial r} - \frac{1}{v_j\tau}\frac{\partial E_r}{\partial Z}$$

$$\frac{1}{r}\frac{\partial}{\partial r} r B_\theta = \frac{4\pi}{c}(J_z + \sigma E_z) - \frac{1}{c\tau}\frac{\partial E_z}{\partial Z} .$$

The flaring of the head drives return currents with an E_z which is distributed over large volumes outside the equilibrium jet radius, a_o. This means that the return current will be driven over a large cocoon radius, R_c. In Fig. 2, $R_c/a_o = 5$, conductivity σ is constant and the time shown is halfway through the current rise. Further detailed solutions of the

electrodynamics are needed, especially including the fact that the plasma conductivity will not be constant. I expect conductivity to be good where the beam meets the plasma, but that turbulence (garden variety electrostatic microinstabilities from streaming) will degrade conductivity substantially precisely where the return currents are simultaneously building up. This essential difference is why the usual picture of perfect conductivity MHD fails for jets. Indeed, the perfect MHD picture would lead to the return current being driven only in a skin depth, $c/\nu_p \simeq 10^8$ cm within the jet radius. This means the jet will be a sheet pinch, with B_θ distributed inside the jet, growing with radius, but then dropping to zero within the skin depth. There is nothing

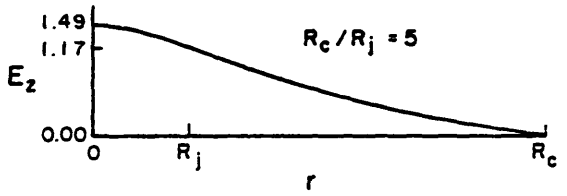

Fig. 2

inherently wrong with this picture, but it is probably unrealistic in the face of imperfect conductivity. To see how unrealistic, we need solutions with time-varying conductivity. The most obvious effect of increasing resistivity behind the beam head occurs at large radii. At the back of the flared trumpet, beam current falls as the envelope contracts. This drives an induced current in the turbulent plasma which tries to keep the net current close to zero; i.e., opposite to the return currents. This will not be as effective as the induction at the beam head, because the conductivity is not as good. Thus a net return current will persist at large radii after the envelope has contracted, leading to a thick current-carrying cocoon. Full solutions should show this behavior. Incidentally, the laboratory beam community has never, to my knowledge, done such detailed studies.

We know nature does use currents to make beams propagate. Lightning produces fields of 10^3 - 10^4G, making a major contribution to the pressure (atmosphere plus magnetic) of $\sim 10^6$ dyne/cm^2. Lightning travels about 10^4 times its radius before it strikes the ground or a cloud, which provides the conducting path for charge balance. The discharge is unstable for hose-like sidewise motions. One does not see lightning strokes wriggling in neat sinusoids because the growth time is comparable to the total stroke time, ~ 1 sec.

The Crab Nebula must return the currents emitted by the pulsar, over a scale > light year (where the "wisps" occur). The Crab current is 3×10^{14} Amp (derived from the Goldreich-Julian corotation currents); this is 10^{10} times the current in a lightning bolt. Confining such quasar jets as 4C32.69

requires a current I ~ 500 times this.

In astrophysical cases, the jet charge is taken away in a time R_j/c, and the voltage drop at the end of the jet is $\sim 10^6 (\nu/\nu_p)L$ volts where ν is the collision frequency associated with the turbulence, ν_p the plasma frequency, and L is the depth of the resistive layer (not necessarily the "working surface") in units of 10 kpc. Thus we can't expect more than an MeV/particle from this zone, and the voltage drop is less important than the collisional losses.

MAGNETIC FIELDS AS THE THEORETICIAN'S PROP

Why do some like the idea of a confining field?

1. Many strong sources now seem to require it to contain the large implied equipartition energies.
2. Helical field geometries promise to be stable, or at least tolerant of lateral perturbations from outside. A simple calculation of kinking modes implies that jets are stable up to $B_\theta/B_z \sim 6$, so B_θ can dominate. Also, a B_θ distributed far outside the jet will anchor dense plasma to the beam, effectively increasing the mass, and thus slowing lateral instabilities. Both these points help explain how the classical doubles can be so straight for so long (Benford, 1981).
3. A few cases of severely bent jets might be best explained by Lorentz forces between the jet current and an intergalactic field. Even if we eventually explain such bending by other forces, there seems a true difficulty in keeping jets intact while they are bent; magnetic fields, which act as elastic buffers, could be crucial here. (Benford, 1982; Eilek, Burns, O'Dea and Owen, 1984).

The trouble with these arguments is that they help theoreticians do their job, but not observers. We expect that a pinched jet will be most luminous where pressure is highest; i.e., the axis, where B_z dominates. Thus the confining B_θ is pushed conveniently off to the dim cocoon region, where it is hard to observe.

Still, if our aim is not to merely "study the weather" (Rees, 1982), then invoking currents necessarily tells us something about the birthing region itself. Currents make loops, and any J_z seen at 100 kpc distances must have come from the magnetosphere or nozzle. Clear evidence of B_θ thus tells us something we can use in exploring acceleration models in the core.

A valuable hint may lie in Bridle's (1982) noting that $B_\parallel$-dominated jets are bright and one-side, while $B_\perp$-dominated jets are dim and two-sided. I suggest that:

(a) the bright sources have a larger seed $B_\parallel$ to shear-amplify (and perhaps larger shear) so $I(\nu) \propto B_\parallel^2$ is higher;

(b) the seed $B_\parallel$ is close to the value which would blow open the nozzle, $\sim 10^{-4}$ G;

(c) the other side of the galaxy has a seemingly minor difference in confining gas density, or a slightly higher $B_\parallel$, which takes that nozzle beyond the blowout limit. This jet is then unconfined at small radius and spreads its energy over a region, lowering its surface luminosity below what we can see. (Further out, focusing occurs by (2), to give distant hot spots).

The B_θ-dominated jets, on the other hand, have smaller seed $B_\parallel$, do not disrupt their nozzles, and because their seed $B_\parallel$ is not close to the blowout field, can tolerate fluctuations in conditions on both sides of the core. (Fig. 3).

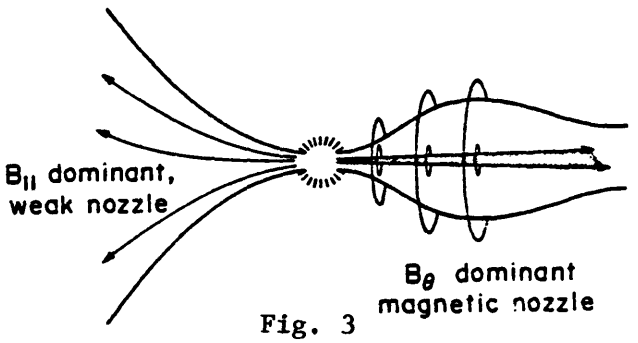

Fig. 3

This demands that asymmetry deep within the engine persist for many dynamic time scales. By relating the failure to focus to one parameter, $B_\parallel/B_\perp$, which governs confinement at small radii, this picture connects several observed systematics. The obvious way to test this idea is through VLBI polarization, if we can see a $B_\perp$-dominated region closer in than the $B_\parallel$-strong regime.

On the $B_\parallel$-dominant side, though there will be some B_θ, the expansion rate $d\theta/dt$ will be large. Recollimation can occur downstream, producing lobes. On the confined B_θ side, $d\theta/dt$ is low. Because a helical field geometry with significant B_θ can tolerate some sidewise displacement without disruption, some misalignment between jets on the pc and kpc scale is natural.

There are grave difficulties in making the original Blandford and Rees nozzle picture work. The nozzles seem to be 100 pc or so long (the scale height of the galactic gas), and yet VLBI doesn't seem to show us these features (though, of course, the story isn't fully in yet). I suggest that a way to shorten the scale length for self-built nozzles is to invoke a shorter distance -- the self-pinch length. Perhaps including a dominant B_θ in calculations such as Siah and Wiita's (these proceedings) could yield magnetic nozzles of the needed size. In such environments, synchrotron losses are probably vital. Such nozzles could not last forever. Magnetic diffusion times in geometries with ratio β = plasma pressure/magnetic pressure,

ion temperatures T in GeV and collision frequencies ν comparable to the cyclotron frequency are

$$\text{diffusion time} \approx 10^7 \text{ yr } R_{14}^2 \; B_4 \; \beta_{-2} \; \left(\frac{\nu_c}{\nu}\right)_1 T^{-1}$$

which might imply a comparable flip-flop time. The main point is that magnetic nozzles may be implied by studies of confinement at 100 kpcs away.

ARE WE ALWAYS SEEING SYNCHROTRON EMISSION?

Though I proposed current-carrying jets in both small jets near pulsars and in extragalactic jets, it is bothersome that only indirect arguments -- the need for confinement of equipartitioned plasmas -- truly require them. I thus began to question a shibboleth of our field: is the radiation from these particularly intense regions <u>always</u> synchrotron?

I have some experience with laboratory plasmas which suggests this is not a question we can lightly discard. In many experimental configurations using mildly relativistic electron beams, simple adjustment of background plasma density or magnetic field strengths can switch from predominantly synchrotron-emission regimes to those where collective radiation by plasma modes vastly overpowers synchrotron power. (In these experiments, typically $\gamma = 3$, current = 10 to 100 kAmp, pulses of 100 to 1000 nsec., $n_b = 10^{12}$/cc, $n_p = 10^{13} - 10^{14}$/cc.) Moreover, <u>there is no great change in polarization or spectrum</u>. Yet the brightness temperature can rise by six orders of magnitude.

The underlying physics for synchroton emission vs. plasmon emission is the same. An acceleration in a plasma will produce radiation, so when a relativistic electron encounters an oscillating electrostatic wave at ν_p, it can Doppler shift this up to a peak of about $\gamma^2 \nu_p$. If the acceleration comes from the cyclotron motion, the spectrum peaks at $\sim \gamma^2 \nu_c$. We can compare the two schematically:

	<u>synchrotron emission</u>	<u>plasmon emission</u>
spectral peak	$\nu \approx \gamma^2 \nu_c$	$\nu \approx \gamma^2 \nu_p$
base frequency	$\nu_c \approx 280 \; B_{-4} \; H_z$	$\nu_p \approx 90 \sqrt{n_{-4}} \; H_z$
polarization	same	
spectrum	same	
power	$\sim N B^2$	$\sim N E^2 + (N^*)^2 E^2$

Here N is the number of electrons, N* is the number cooperating in bunches of size $\approx c/\nu_p$, B is the ambient magnetic field and

$E = \langle E_k^2 \rangle^{1/2}$ is the rms average electrostatic field strength in plasma oscillations (produced by streaming instabilities). Usually one finds in weak turbulence that $E^2 << B^2$. However, intense cases abound where $E^2 > nT$, the thermal plasma energy. This need not be small compared with B^2. In any case, we have seen cases where $N^{*2}/N = 10^6$, yielding a measured brightness temperature T_b exceeding 10^{18} (Benford and Smith, 1980). For a discussion of coherently excited synchrotron emission, which has application to pulsars (Tzach and Benford, 1982). In these cases we observed the synchrotron harmonics and measured the beam pitch angle distribution from them. Again, $T_b > 10^{18}$.

Astrophysicists have long assumed synchrotron emission as the "default" choice, since no one could make a case for other, more powerful mechanisms. The essential message I bring is that this is no longer so. Plasmon emission far above ν_p can occur when $n_b/n_p > 0.01$, as experiment shows (Kato et al., 1982). Also, there is no way to distinguish plasmon emission from synchrotron through the polarization. This arises basically because both processes yield Doppler-shifted dipolar patterns. (See Fig. 4 for the measured plasmon pattern at ν_p from our laboratory.) After averaging over power law distributions for the electrons, there is no distinction between the mechanisms (Windsor and Kellogg, 1974).

I then propose that we seriously consider plasmon emission in hot spots and knots, where we suspect streaming instabilities might arise. Even mildly collective emission will greatly enhance the emissivity, lowering the energetics required, the pressures generated, and thus avoiding the necessity to invoke magnetic confinement.

Detection Polarization is no help in distinguishing plasma emission from synchrotron emission, once one makes the usual assumptions of isotropic particles having a power law distribution function. Detection of a high brightness temperature T_b is the obvious test, but if the emission is spotty (ie., the packing fraction of coherent zones is low) then the average T_b can still ape that of synchrotron emission, $\sim 10^{12}$K. In such cases the only hope is that there are a relatively small number of coherent zones, N*, so that

(a) the radiation amplitude has a fluctuation of order $(N^*)^{-1/2}$;
(b) the signal phase displays an autocorrelation time t_{ac} far greater than the $\sim 10^{-8}$ sec. typical of incoherent emission observed with a linewidth of 100 MHz.

In the laboratory (a) is all we typically see, since in such fast experiments we discard the phase information. In our experiments we often see amplitude fluctuations (lasting ~ 10 ns) in the range 0.01 to 0.1. This implies $N^* \sim 100$ and a packing fraction ~ 0.01 in our volume of $\sim 10^4$ cm^3.

Detecting coherence in extragalactic sources seems impossible, unless they prove to have high T_b, because most likely N* is very large in spatially extended sources. Thus I suspect the best place to look is in galactic sources such as the symmetric lobes around Sco X-1. If these are in fact compression points in magnetically dominated jets (Achterberg et al., 1984) then N* may be relatively small and both (a) and (b) could be used.

Looking for long t_{ac} can be done using presently digitized data. A clear indication might come from rapid swings in polarization angle in less than a second. It is difficult to estimate from the current simple theories, how many radiators there are, since there is in addition, the possibility that the collective system acts not merely like an antenna (bunching), but can become a maser, with spatial amplification. Similarly, we cannot calculate t_{ac} very well. (One crude standard is that solitons may last for about 100 ion plasma periods, which yields $\sim 10^{13} n_p^{-1/2}$ sec. Our observed fluctuations last about 30 times this long.) Galactic sources are probably the only ones which can avoid the blurring effects of dispersion, as well.

Actually, I would rather have plasmon emission go away and not bother us. Losing the synchrotron assumption knocks a valuable prop from under many of our models. As heresies go, it could cause a lot of trouble if we cannot disprove it. I do not think plasmon processes occur often, simply because the required streaming instabilities are probably rare. Still, we cannot neglect the plasmon possibility.

This work was supported by AFOSR and the taxpayers of California.

REFERENCES

Achterberg, A., Blandford, R. D. and Goldreich, P. 1983, Nature 304, 607.
Benford, G. 1981, Astrophys. J. 247, 792.
Benford, G. and Smith D. 1982, Phys. Fluids 25(8), 1450.
Bridle, A., 1982, IAU Proc. 97, Reidel Publ.
Eilek, J. A., Burns, J. O., O'Dea, C. P., and Owen, F. N. 1984, Astrophys. J. 278, 37.
Kato, K, Benford, G., and Tzach, D. 1983, Phys. Fluids 26(12), 3636.
Rees, M. 1982, IAU Proc. 97, Reidel Publ.
Tzach, D. and Benford, G. 1981, Astr. and Space Sci. 80, 307.
Windsor, R. A. and Kellogg, P. J. 1974, Astrophys. J. 190, 167.

FORMATION AND PROPAGATION OF MAGNETIZED RADIO JETS

Javad Siah and Paul J. Wiita
Department of Astronomy and Astrophysics, University of Pennsylvania (E1)
Philadelphia, PA 19104

ABSTRACT. Numerical models of the boundaries of radio jets consisting of a relativistic fluid flowing into a confining gas cloud are discussed. In these models a fixed fraction of the total energy of the jets is assumed to be in the form of ordered magnetic fields. The azimuthal component of the field at the boundary between the two fluids is determined by setting the azimuthal Alfvenic Mach number equal to unity with respect to the confining cloud. The poloidal field components are computed in two limiting cases. When all of the azimuthal field is assumed to remain within the jet the resulting jets are wider than those formed in identical potentials with no anisotropic magnetic pressure, and these jets emerge more slowly. When the azimuthal component is assumed to escape from the jet into a sheath around it, the pinching effect of this field geometry produces better collimation. But if too high a fraction ($\gtrsim$0.15) of the energy is in organized external magnetic fields the jet's stability is adversely affected.

1. INTRODUCTION

Many jets show evidence of ordered large scale magnetic fields (e.g. Bridle 1982) but not very much has been done to investigate the dynamical effects of magnetic fields on radio jets. X-ray measurements indicate that gas pressure confinement of jets is often insufficient to produce all of the observed focusing of jets. Also, if the convergence speed of an unmagnetized jet exceeds its internal sound speed it will produce shocks that can halt further compression (e.g. Norman, Smarr and Winkler 1984). If the jet is magnetized the pinching effect of a toroidal component can bring about convergence at speeds comparable to the Alfvenic velocity of the flow (Achterberg, Blandford and Goldreich 1983). Chan and Henriksen (1980) studied steady-state self-similar magnetized jet flows for super-Alfvenic non-relativistic plasma. They showed that as the beam starts to widen the azimuthal field component can grow and recollimate the beam.

The basic idea of the twin-exhaust model (Blandford and Rees 1974) is that collimated beams form as hot buoyant gas emerging from a central engine exits through a pair of de Laval nozzles in a confining flattened gas cloud. This hypothesis was supported by computations of the boundary between an internal relativistic fluid and an external non-relativistic cloud (Wiita 1978a, 1978b) and confirmed by detailed 2-D hydorcode models of one non-relatvistic fluid penetrating another (Norman *et al*. 1981, Smith *et al*. 1982). All of these calculations agree that at low source luminosities the Kelvin-Helmholtz instabilities would break the jet into bubbles, while at higher power levels continuous or quasi-continuous (Wiita 1978b) jets would form. It seems likely that at very high luminosities a global Rayleigh-Talyor instability comes into play and causes the gas to emerge in a large cloud (Smith *et al*. 1982). Unfortunately, even

the most detailed 2-D hydrodynamical computations performed to date have been forced to neglect magnetic fields.

This paper extends our previous work on relativistic fluids emerging through flattened clouds (Wiita 1978a,b, Wiita and Siah 1981, Siah and Wiita 1983, hereafter SW) to incorporate several important influences of a magnetic field upon jet propagation and collimation. We stress that this is not a full magnetohydrodynamic calculation, but just as our earlier computations yielded results that were usually in good agreement with more sophisticated numerical models (see SW), we expect that these results are qualitatively correct. A more detailed description of the theory and motivation behind this work is presented elsewhere (Siah 1984) and additional cases and further discussion will be published (Siah 1985).

2. ASSUMPTIONS AND MODEL CONSTRUCTION

These models assume that a continuous source of relativistic plasma of luminosity L is turned on at t = 0. This plasma starts out expanding with spherical symmetry and in the earliest stages moves with relativistic velocities. By the time the blob begins to react to the axisymmetry of the surrounding cloud, its expansion becomes sub-relativistic and so Newtonian dynamics can be used; from this point on axisymmetry and reflection symmetry are assumed (Wiita 1978b). The basic parameters of the confining cloud, (which is assumed to be isothermal for simplicity) are its temperature, T, central pressure, p_o, scale height $\underline{l}$, and eccentricity, $\underline{e}$ (or, more generally, its angular momentum). Improved collimation can be achieved if a more realistic "dimpled" gas potential is used (e.g. Sparke 1982, Morita 1982, SW); this requires the introduction of another parameter, $\underline{b}$, the core radius of the mass distribution that binds the gas to the galactic nucleus. Because of the relativistic equation of state taken for the interior fluid, internal pressure gradients are not important as long as the boundary velocity does not exceed ~0.2c anywhere, and a great simplification results: the interior pressure, P, can be taken as a function of time alone. Another key assumption is that the shocked and swept up external gas remains in a thin shell forming the boundary between the two fluids. At large distances, the gas density is assumed to equal a constant low value, typical of the intracluster medium ($n_\infty \cong 10^{-3}$-10^{-4}cm^{-3}). Discussion of these approximations and of the errors they may introduce can be found in Wiita (1978b) and SW.

A dimensionless luminosity is of major importance in determining whether bubbles or jets form; it is defined as: $L' = L/(p_o l^2 a)$, with $\underline{a}$ the adiabatic sound speed in the external gas. Typically the cut-off between jets and bubbles is for $L' \cong 10$-100. Unfortunately, our calculational scheme is incapable of detecting the possible onset of the global R-T instability.

The most important assumption made concerning the ordered magnetic fields is that a fixed fraction, β, of the luminosity goes into that form at all times, which is a reasonalbe Ansatz. The other basic assumption is that after the initial relativistic and spherical expansion phase is over, the torodal component of the field is such that the azimuthal velocity of the confining cloud is matched by the azimuthal Alfvenic velocity on the

boundary, i.e., $v_\phi^2 = B_\phi^2/(4\pi\rho)$, where v_ϕ is given by eqn. (4) of SW. While this choice is not too strongly motivated and was mainly made to simplify the dynamical equations (2) and (3), it is supported by other analyses (e.g. Acterberg et al. 1983).

The poloidal field strength was determined for two limiting classes of models: in Class 1 the entire field is taken to be confined within the jet, corresponding to a completely neutral beam; in Class 2 all of the azimuthal component of the field is assumed to escape from the jet and only poloidal field components remain inside the jet, an extreme case of a current carrying beam with a return current outside it.

Class 1 models assumed a dependence of the form: $B_\phi \propto (r^2+b^2)^{3/4}$ inside the jet. This azimuthal field's energy density was then subtracted from the total field energy density, and the remaining poloidal energy density was split between the radial and polar components of the magnetic field using a self-similar prescription: $B_r/B_z = r/z$. The presence of the interior field supresses pinching off near the equatorial plane and thus favors jets over bubbles. But these Class 1 magnetized jets differ little from unmagnetized jets, other than being less well collimated.

Class 2 jets allow for more interesting results. A simple power law dependence was chosen for the external azimuthal field:

$$B_\phi(r,z) = B_\phi(R,Z)\ (R/r)^n, \qquad \text{for } r > R, \tag{1}$$

where $B_\phi(R,Z)$ is the azimuthal field on the boundary, R(Z;t). To avoid adding another parameter in the form of a cut-off radius, and to effectively allow for a distributed return current (e.g. Benford 1984), we require $n > 1$; $n = 1.5$ was chosen for the work presented here. Such a field will constrict the plasma beam. The magnetic energy outside the jet is then found and subtracted from the total energy in magnetic fields, βLt, to obtain the internal magnetic field. We divide the interior of the jet into two regions at Z_*, with (Z_*,R_*) the point on the boundary where the radial distance is approximately equal to the polar distance. For $0 < z < Z_*$ the flux should be mainly radial and we again assume self-similarity holds. But for $Z_* < z < Z_f$, the field must obey tangential flux conservation. When we insert the anisotropic magnetic pressure into the equation of motion for the boundary we finally obtain (Siah 1984)

$$dU_r/dt = (dA/m)\ \{-B_rB_z/(4\pi\ \sin\theta) + [(B_\phi^2+B_z^2)/4\pi]\cos\theta + [P(t)-p(R,Z)]\cos\theta - \rho(R,Z)U_r(U_r\cos\theta + U_z\sin\theta)\}, \tag{2}$$

$$dU_z/dt = (dA/m)\ \{-B_rB_z/(4\pi\ \cos\theta) + [(B_\phi^2+B_r^2)/4\pi]\sin\theta + [P(t)-p(R,Z)]\sin\theta - \rho(R,Z)U_z(U_r\cos\theta + U_z\sin\theta)\}. \tag{3}$$

Here a segment of the boundary of surface area dA and mass m is at (R,Z), $U_r = dR/dt$, $U_z = dZ/dt$, θ is the angle between the z azis and the tangent to this boundary element, p(r,z) is given by eqn. (5) of SW, and the external density $\rho(R,Z) = \gamma p(R,Z)/a^2$.

3. RESULTS

The outcome of our numerical experiments are briefly summarized in Table 1 and in Figures 1 - 4. In the table column (1) is the run identi-

TABLE 1

Class 2 Models, With Exterior Azimuthal Field

Run	L_{46}	l_{100}	b_{100}	e	β	L′	Z_f	R_{max}	$t_{end}(10^{12}s)$	$\theta_{max}(^0)$	Outcome*
(1)	(2)	(3)	(4)	(5)	(6)	(7)	(8)	(9)	(10)	(11)	(12)
10	0.5	1.35	2.00	0.75	0.05	199.03	10.60	2.65	21.289	14.02	B;(b)
11	0.5	1.35	2.00	0.75	0.08	199.03	14.29	2.63	24.165	10.44	B;(b)
22	0.5	1.35	2.00	0.75	0.15	199.03	20.79	2.34	24.039	6.42	J,TB;(b)
12	3.0	1.35	2.00	0.2	0.05	1194.16	48.14	7.27	52.108	8.59	J,TB;(a)
15	3.0	1.35	2.00	0.2	0.15	1194.16	2.22	0.45	0.793	11.55	J,-P;(a)
13	3.0	1.35	2.00	0.75	0.05	1194.16	27.08	7.67	67.407	15.81	B;(b)
21	3.0	1.35	2.00	0.75	0.075	1194.16	41.12	6.55	63.739	9.05	J,TB;(a)
16	3.0	1.35	2.00	0.75	0.10	1194.16	47.60	5.89	61.071	7.05	J,TB;(a)
17	3.0	1.35	2.00	0.75	0.15	1194.16	2.41	0.45	0.793	10.69	J,-P;(a)
14	3.0	1.35	2.00	0.999	0.075	1194.16	23.47	6.37	61.154	15.19	B;(b)
8	1.0	0.4642	1.50	0.2	0.05	3367.09	310.31	61.91	28.876	11.28	J,TB;(a)
4	1.0	0.4642	1.50	0.7	0.05	3367.09	67.89	7.66	2.819	6.43	J,TB;(a)
18	1.0	0.4642	1.50	0.9	0.01	3367.09	34.20	9.03	22.503	16.43	J,TB;(a)
5	1.0	0.4642	1.50	0.9	0.03	3367.09	52.59	6.60	34.407	7.15	B;(c)
19	1.0	0.4642	1.50	0.9	0.08	3367.09	44.62	6.16	18.295	7.86	B;(c)
24	1.0	0.4642	1.50	0.9	0.10	3367.09	124.81	9.03	7.148	4.59	B;(b)
23	1.0	0.4642	1.50	0.9	0.15	3367.09	2.95	0.60	0.325	13.04	J,-P;(a)
6	1.0	0.4642	1.50	0.999	0.05	3367.09	100.33	7.53	6.388	4.29	B;(c)

* J indicates still a jet, B indicates a bubble has formed at t_{end}.
TB (time bound) indicates that the calculations were stopped as no major changes were occurring.
-P means that the interior gas pressure was so low that the bubble or jet is likely to dissipate.
(a) : the B_r and B_z components of the interior magnetic field survive to the end of the run.
(b) : the B_r and B_z components of the interior magnetic field fade out in the middle of the run.
(c) : the B_r and B_z components of the interior magnetic field fade out early in the run.

fying number and columns (2)-(6) contain the key input parameters: the total luminosity in units of 10^{46}erg s^{-1}, the gas scale height and stellar core radius, both in units of 100 pc, the flattening parameter of the cloud, and the fraction of the power going into the magnetic field. All of the models considered here have $T = 10^7$K and $p_o = 2.76 \times 10^{-6}$ dyne cm^{-2}, but these parameters are related through L'. Columns (8)-(11) give the most fundamental results: the maximal extent, Z_f, and thickest radius, R_{max} (both in units of 1) at the time when the computation halted, t_{end}, which is expressed in units of 10^{12}s. A characteristic collimation angle, $\theta_{max} = \arctan(R_{max}/Z_f)$, is shown in column (11); it is certainly larger than the usual definition of the opening angle, $\arctan(v_r/v_z)$. As discussed by SW the effective opening angle for such jets is expected to decrease as the jets continue to penetrate a constant density medium (cf. Norman et al. 1982). Column (12) indicates if the final configuration was a jet or if a bubble formed, and also mentions why the computation was halted. These models can run for the equivalent of over 10^6yr, yielding jets collimated to better than a few degrees out to ~10kpc.

Figure 1 plots Class 1 runs 4, 6, and 10 at the same time; they differ only in their values of β. As the fraction of energy devoted to the magnetic field increases the jets emerge at a lower pace and are relatively thicker. The completely confined magnetic field contributes a net outward transverse pressure and decreases collimation.

The Class 2 models summarized in Table 1 are more diverse. The general trends noted in our earlier papers hold, with higher L' tending to yield jets, while higer e's produce better collimation but also favor bubble formation; however, these simple trends are modified by the b dependence which is not explored in the models presented here. Small variations of the magnetic field strength make for dramatic differences in boundary evolution. As β increases the collimation at first improves and the jet's working surface expands more quickly. There is also a tendancy to prevent bubble formation. But this effect can only be exploited up to a point; comparison of runs 13, 21, 16, and 17 or runs 7, 5, 19, 24 and 23 illustrate that as β rises above ~0.10 to ~0.15 the jet is disrupted at an early stage in its growth. Figures 2, 3 and 4 illustrate the time evolution of the boundary between the relativistic fluid and the confining cloud. The results are insensitive to changes in the number of grid points, and energy is conserved to better than 2% in almost all runs. In certain runs our assumptions lead to the external B_ϕ containing all of the alloted magnetic field energy; this somewhat exaggerated outcome is noted in column (12) of the table whenever it occurs.

4. CONCLUSIONS

This work is another step towards producing more realistic models of extragalactic radio jets. Many simplifying assumptions have been employed, but they seem to allow us to reproduce many characteristics of observed jets at trivial expense when compared to large hydrocodes; thus, a much wider range of parameter space can be explored. Even though the configurations for the azimuthal field component were chosen mainly for their simplicity, other workers (Benford 1984, Cohn 1983, Acterberg et al. 1983) made similar choices that indicate that ours are reasonable. Note that our jets are destroyed if too much energy is taken to reside in the form

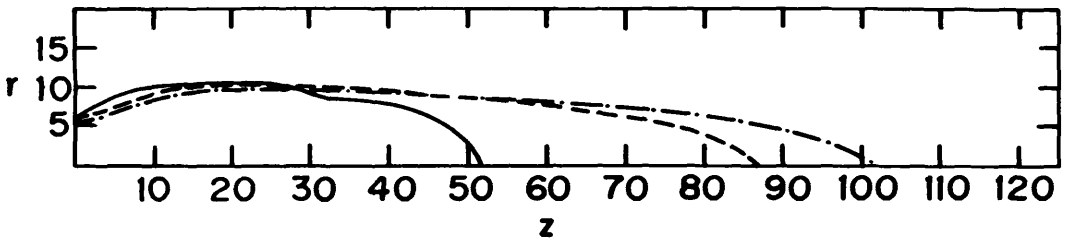

Figure 1. The boundaries of three Class 1 (interior azimuthal magnetic fields) jets at a fixed time, $t \sim 3 \times 10^5$yr. Run 5 (dot-dashed) has $\beta = 0.01$, run 1 (dashed) has $\beta = 0.1$, and run 10 (solid) has $\beta = 0.3$. Otherwise these runs are identical, with $L' = 3353$ and $e = 0.9$. In this and all subsequent figures, only one quadrant is shown since axisymmetry and mirror symmetry are assumed.

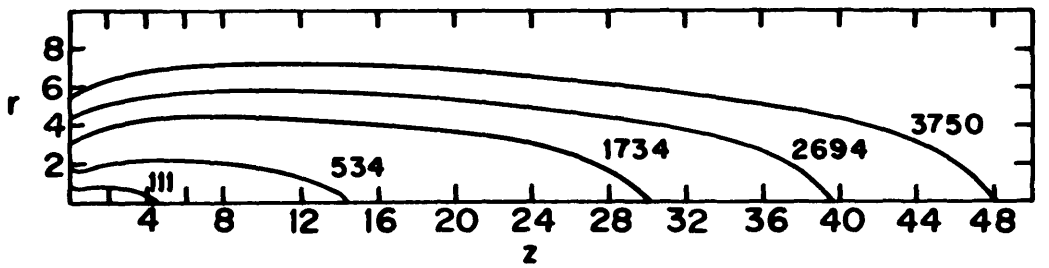

Figure 2. The evolution of the boundary of the Class 2 (exterior azimuthal magnetic field) jet No. 12, with time, in units of ~440 yr, labelling the curves. This run has $L' = 1194$, $e = 0.2$ and $\beta = 0.05$.

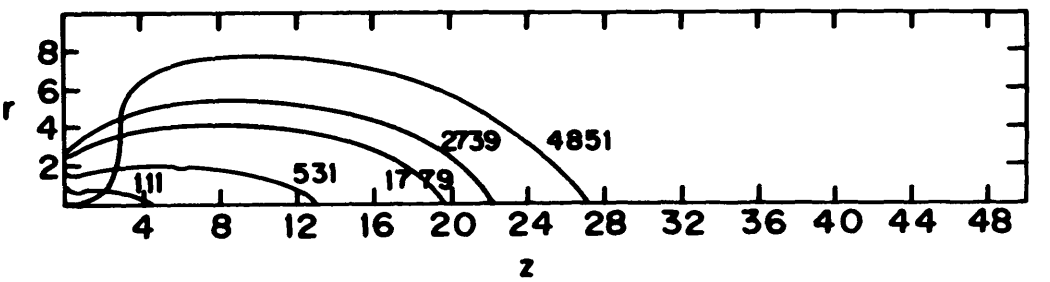

Figure 3. As in Fig. 2 for Class 2 run 13, which has $e = 0.75$, but is otherwise identical to No. 12.

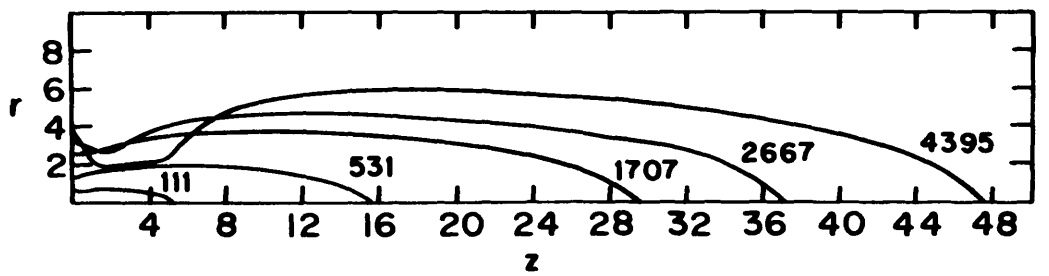

Figure 4. As in Fig. 2 for Class 2 run 16, which has $\beta = 0.10$, but is otherwise identical to No. 13.

of magnetic fields, a result that can be qualitatively compared to the analytic computations of Chan and Henriksen (1980). A more detailed discussion and comparison with other work is given elsewhere (Siah 1984, 1985).

It must be noted that the boundary equations of motion do not include terms accounting for the radiation of the plasma or the shocked gas; while they should not affect the dynamics very much, they are obviously very important and will be treated in future work. Another point that should be made clear is that while in Class 2 models we assume the azimuthal component can escape from the jet, we also assume that the flow becomes tangential to the boundary of the jet as the jet becomes more elongated; this logical simplification is compatible with observations of strong jets, but is not required by them.

Our most important new conclusions can be stated as:

1) Magnetic fields can aid collimation and jet development if the toroidal field is allowed to convect outside.
2) If the field is completely contained inside, the jet is slowed and widened.
3) Too much energy in the form of a magnetic field around the jet is very likely to disrupt the beam.

This work has been supported in part by NSF grant AST 82-11065.

REFERENCES

Achterberg, A., Blandford, R.D. and Goldreich, P. 1983, Nature, 304, 607.
Benford, G. 1984, Ap.J., 282, 154.
Blandford, R.D. and Rees, M.J. 1974, M.N.R.A.S., 176, 443.
Bridle, A.H. 1982, in Extragalactic Radio Sources, eds. D.S. Heeschen and C.M. Wade (Reidel: Dordrecht), p. 121.
Chan, K.L. and Henriksen, R.N. 1980, Ap.J., 241, 534.
Cohn, H. 1983, Ap. J., 269, 500.
Morita, K. 1982, Pub. Astr. Soc. Japan, 34, 65.
Norman, M.L., Smarr, L., Wilson, J.R. and Smith, M.D. 1981, Ap.J., 247, 52.
Norman, M.L., Smarr, L. and Winkler, K.-H. 1984, to appear in Numerical Astrophysics, ed. J. Centrella.
Norman, M.L., Smarr, L., Winkler, K.-H., and Smith, M.D. 1982, Astr. Ap., 113, 285.
Siah, J. 1984, Ph.D. thesis, University of Pennsylvania.
Siah, J. 1985, in preparation.
Siah, J. and Wiita, P.J. 1983, Ap.J., 270, 427.
Smith, M.D., Smarr, L., Norman, M.L. and Wilson, J.R. 1982, Nature, 293, 277.
Sparke, L.S. 1982, Ap.J., 254, 456.
Wiita, P.J. 1978a, Ap.J., 221, 42.
Wiita, P.J. 1978b, Ap.J., 221, 436.
Wiita, P.J. and Siah, M.J. 1981, Ap.J., 243, 710.

FORCE-FREE EQUILIBRIA OF MAGNETIZED JETS

Arieh Königl
Department of Astronomy and Astrophysics, The University of Chicago
5640 South Ellis Avenue, Chicago, IL 60637

ABSTRACT. Previous studies of magnetized jets assumed that the ratio of magnetic to thermal pressure does not in general exceed unity, and adopted an axisymmetric, self-similar model for the magnetic field configuration. However, flux-conservation arguments indicate that extended, magnetized jets should eventually become magnetic-pressure dominated. In such jets, the mean field is expected to satisfy the force-free equation $\nabla \times \boldsymbol{B} = \mu \boldsymbol{B}$, whose solution is generally neither self-similar nor axisymmetric. Here I report on a study of the magnetic equilibrium configurations of supersonic jets that are confined by a slowly varying external pressure. If the jets are somewhat dissipative, then the parameter μ will be constant across the jet, and will change only slowly along the jet. The presence of a dissipation mechanism enables the jet to settle to a minimum-energy configuration. However, if the jet material is a sufficiently good conductor, then the global topological properties of the magnetic field lines should be preserved. In particular, the magnetic helicity (which is a measure of the twist and knottedness of the field lines) should be an approximately conserved quantity. Under these conditions, the minimum-energy solution of the field equation is in general a linear superposition of an axisymmetric ($m = 0$) mode which accounts for the net flux and axial current in the jet, and a helical ($m = 1$) mode which varies along the jet with a "universal" wavelength $\lambda \approx 5R$ (where R is the local jet radius). The latter, nonaxisymmetric mode becomes energetically favorable when the confining pressure drops below a certain critical value, which depends on the magnitudes of the conserved magnetic flux and helicity. This general solution has originally been proposed in order to account for some of the characteristics of laboratory-generated toroidal pinches.

The minimum-energy force-free solution can be applied to the interpretation of the total and the polarized emission from certain resolved, extended jets. In particular, it provides a unified explanation of the various nonaxisymmetric features exhibited by the large-scale jet in NGC 6251, including the oblique orientations of projected magnetic field vectors and of Faraday rotation-measure gradients with respect to the jet axis, and the apparent transverse oscillations of the ridge line which do not involve the outer isophotes. A conceivable alternative interpretation of the latter feature might be that it represents a kink mode of the Kelvin-Helmholtz instability, but this turns out to be inconsistent with the relatively short wavelength ($\lambda \approx 5R$) of the apparent oscillations; the observed wavelength is, however, consistent with the predictions of the force-free equilibrium model. This model also explains the oscillations of the FWHM along the NGC 6251 jet, and their observed correlation with bright emission knots. However, in contrast to the customary interpretation which links these features to actual compressions of the jet, in this model they are merely apparent synchrotron-radiation effects which arise from the periodic, nonaxisymmetric geometry of the magnetic field in the emission region.

Another application of the minimum-energy force-free solution is to the interpretation of the large ($> 180°$) polarization position-angle (P.A.) swings that have been measured in a number of BL Lac objects and highly variable quasars. Such sources are often identified with relativistic jets that are observed at a small angle to the axis. In this interpretation, the swings are attributed to the propagation of shock waves along an unresolved, relativistic jet in which the relative magnitude of the nonaxisymmetric field component is sufficiently large. As the shocks move through successive transverse cross sections of the jet, they "illuminate" (by enhanced synchrotron emission) the progressively rotated magnetic field vectors associated with the $m = 1$ mode, giving rise to a systematic variation of the apparent polarization P.A. A particularly interesting example of this process is provided by the BL Lac object 0727-115, which has exhibited quasi-periodic, step-like changes in the polarization P.A., as well as oscillations of the degree of polarization (with the polarization minima coinciding with P.A. jumps). This apparently nonuniform behavior can be attributed to relativistic aberration, and is reproduced in this model even when the shock velocity is constant. This, in turn, lends additional support to the inferred association of radio polarization "rotators" with relativistic jets.

Further details of the force-free jet model and its possible applications are given in two papers, written in collaboration with Arnab Rai Choudhuri, which are scheduled for publication in the February 1, 1985 issue of the Astrophysical Journal.

DISCUSSION

Paul Wiita. Can you simply explain why you get no contribution from $m = 2$ or any higher modes ?

Arieh Königl. This has to do with the imposed boundary condition, namely, that the radial component of the magnetic field vanish at the jet surface (assuming a cylindrical geometry). When this condition is imposed on the force-free, constant-μ solution, it turns out that all the modes with $m \geq 2$ have a higher energy (for given magnetic flux and helicity) than the $m = 0$ and $m = 1$ modes. (This is discussed in more detail in the first of the two papers referred to in my abstract).

Larry Rudnick. Modelling of the "rotator" events seen by the Allers has shown that they may be interpreted as random walks in Q and U, with no physical rotation going on. Rotations are fairly common in models where a steady-state number of random, polarized components are active at any given time. One prediction of this model is that the apparent rotations should eventually appear in both directions for a given source.

Arieh Königl. If the apparent quasi-periodic behavior of the position angle in 0727-115 were, in fact, confirmed, then this would presumably argue against a "random walk" model. Simple ideas about the origin of the twisted field lines in jets suggest that they should have a fixed sense of rotation, so, *prima facie*, the presence or absence of reversals in the apparent position angle rotation could serve to distinguish between these two models. However, even in the "shock in a force free jet" interpretation it is conceivable that different events in the same source would exhibit opposite senses of rotation (for example, a shock might move either upstream or downstream in the frame of the jet).

TURBULENCE, ENTRAINMENT AND MAGNETIC FIELDS

D. S. De Young
Kitt Peak National Observatory
National Optical Astronomy Observatories*
Tucson, Arizona 85726

ABSTRACT. Evidence for the presence of turbulence in extended radio sources is reviewed, and its effects on the physics of energy transport in these objects is discussed. Turbulent entrainment of the interstellar medium in radio galaxies is suggested as the origin of the optical emission lines, and results of some numerical experiments on entrainment are given which suggest that most entrainment occurs largely near the leading edge of a radio source and that its extent decreases with increasing Mach number. Turbulent amplification of magnetic fields is also reviewed; the required field strengths and scales can be obtained by this process but at low efficiency.

I. INTRODUCTION

In considering the role that turbulence may play in energy transport in extended radio sources, it would seem logical to ask if turbulence is expected to be present at all; until rather recently little or no mention was made of turbulence in radio sources. From an observational perspective, the morphology of many "edge darkened" radio sources suggests that large scale turbulent structures are present. Prime examples include 3C 449, NGC 1265 and 1919+479. Moreover, the recent VLA map of the "classical", edge brightened source Cygnus A (Perley, 1984) shows a wealth of detailed and convoluted internal structure that is virtually identical to that of fully developed turbulence seen in Earthbound laboratories.

From a more theoretical point of view, a simple calculation of the Reynolds number to be associated with the energy flow can give an estimation of whether turbulence will be important or not. Recall that the Reynolds number R is simply an "appropriate" velocity times an "appropriate" scale length divided by the relevant viscosity ν or magnetic diffusivity λ. For a hot, thermalized hydrogen plasma, $\nu \approx 5 \times 10^4 \; n_{-4}/[T_6^{1/2} \; B_{-6}^{2}]$cgs, and $\lambda \approx 4 \times 10^5 \; T_6^{-3/2}$ emu

*Operated by the Association of Universities for Research in Astronomy, Inc., under contract with the National Science Foundation.

(eg. Spitzer 1962), where n_{-4} is the number density in units of 10^{-4} cm^{-3}, T_6 is the temperature in millions of Kelvins, and B_{-6} is the magnetic field in microgauss. This form for ν is that appropriate when the gyrofrequency is much greater than the collision frequency, and a value of 30 for the Coulomb logarithm has been used. The values for the appropriate velocities and scale size are less clear, but using the small values of 10^7 cm s^{-1} and one parsec still provide very large Reynolds numbers: $R \sim 10^{20}$. Thus one would expect fully developed turbulence on virtually all scales. The one exception to this situation could occur if magnetic fields were strong enough to dominate the energy density of the flow.

If a significant fraction of the radio source volume contains fully developed turbulence, then turbulence can have a significant effect on radio source evolution through several processes. The first involves particle acceleration. It is by now well known that re-energization of the relativistic electron population is required to occur in many sources throughout a large portion of the radio source - in some cases even along the radio jets. A consequence of turbulence is the cascade of energy in a loss free manner to ever smaller scales until the dissipation range is reached. Such a process provides a natural source of wave energy for several stochastic reacceleration mechnanisms that may resupply energy to the electrons (e.g. Eilek, 1984 and references therein). Another process which occurs in turbulent boundary layers is entrainment of the ambient medium. This process has interesting consequences and will be considered at some length in the next section. Finally, MHD turbulence can provide amplification of weak magnetic fields. Such amplification is required for many sources, as will be shown in the last section.

2. TURBULENCE AND ENTRAINMENT

A turbulent boundary layer between a jet and its surrounding medium will entrain gas from that medium. This entrainment and its accompanying momentum transfer will affect the dynamics of the jet, may explain optical emission lines seen in some sources, and may be directly pertinent to the electron re-energization problem. Before examining these consequences, it is useful to investigate the physics of entrainment in a little further detail.

Laboratory experiments have revealed the entrainment process to proceed by forming large scale eddies first, which then subsequently evolve into finer and finer structure. One of the best examples of this can be found in Brown and Roshko (1974) where this "gulping", or perhaps,

"ingestion" followed by "digestion" can clearly be seen. These experiments permit the empirical determination of the external mass entrained by a large scale eddy, and this is $\Delta M \approx \pi^2 \rho_o R_e^2 R_j$, where ρ_o is the density of the ambient medium, R_e is radius of the large scale eddy and R_j is the radius of the jet. Revelation of the "gulping" mode of entrainment implies that is does not occur all along the length of the boundary layer but only in the region where the large scale eddies first form. Thus an entrainment rate can be estimated from ΔM times the production rate of large scale eddies, or $\dot{M} \sim \Delta M \, U_c/R_e$, where U_c is convection speed. This simple formula will be converted into astrophysical parameters subsequently when comparison is made with emission line data.

Laboratory studies, while enlightening, have largely been done at subsonic flow velocities. What evidence we have for flow velocities in radio sources indicates that the velocities are probably supersonic relative to the surrounding medium (De Young, 1984), and it is essential to our understanding of the entrainment process to see if supersonic flow significantly changes things. In addition, the laboratory studies are of an essentially steady state process and thus apply to the boundary of a well established beam. One needs to know the role of the leading edge of the beam, and that of its accompanying bow shock, in the entrainment mechanism.

As an initial effort at understanding these problems, a series of numerical experiments are being made on entrainment by jets. The calculations involve use of a time dependent, fully non-linear 2-D axisymmetric hydrocode which has been described in some detail elsewhere (De Young, 1977). The object is to obtain entraimnent rates as a function of parameters such as Mach number, beam radius, internal and external densities and temperatures, and in addition to gain some understanding of where entrainment occurs and how it occurs. The empirical result that entrainment seems to occur via the formation of large scale eddies provides encouragement that the results of the calculation will not be significantly affected by the finite grid size used in the code. This series of calculations is not yet complete, but some preliminary results are emerging which may provide some help in understanding the physics of entrainment.

Entrainment is measured by following the progress of a series of LaGrangian marker particles embedded in the ambient medium. High velocity flow (the beam) is then introduced on axis at one end of the volume and the calculation followed until well past the point where a steady state flow is established within the cylindrical

volume. The criteria for entrainment are not obvious. The ones used here are a combination of velocity and trajectory; a particle is considered to be entrained if it acquires a velocity in the direction of the beam flow which is at least as great as one tenth the sound speed in the ambient medium, or if it is obvious from its spatial trajectory that it has been captured by the flow. Usually there is very good agreement between these two criteria. An example of the particle trajectories is shown in Figure 1, which is for a Mach number 5, pressure balanced beam with equal interior and exterior densities. The beam radius is 10 in scaled units, and the axis of symmetry lies at the bottom. The effects of the leading edge vortex immediately behind the bow shock are clearly seen; this vortex is also seen in the calculations by Norman et al. (1982). Near the axis of symmetry the effects of the bow shock initially sweeping particles aside is also seen.

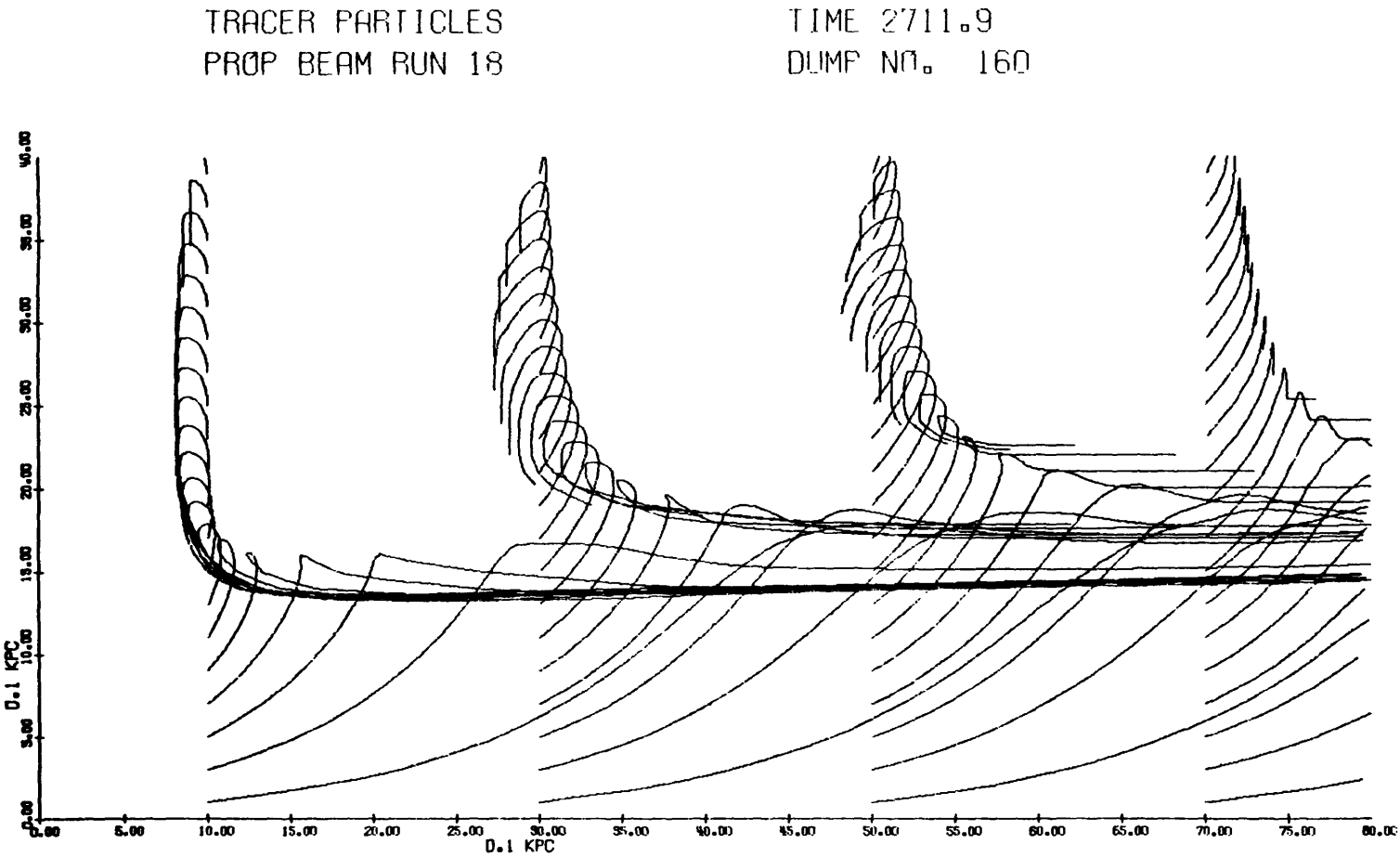

Figure 1

These two effects lead directly to two of the early conclusions from these calculations. As the Mach number grows larger and larger the initial bow shock becomes stronger and sweeps more of the ambient gas aside as it passes. This strong outward motion inhibits the trapping of ambient gas by a leading vortex just behind the shock, and hence entrainment decreases as Mach number increases. Indications are that the entrainment radius, which is the radial distance from the symmetry axis out to which gas is entrained, decreases with Mach number as roughly the one-half power. The second effect has already been alluded to, namely that the leading edge vortex plays an important role in entrainment for low Mach number flows.

Entrainment implies transfer of momentum to the surrounding medium, and the calculations show this effect on beam dynamics in a manner that would be expected. High Mach number (M = 20) flows are not perceptibly decelerated, not only because the entrainment rate is low but also because the momentum flux is high (for a fixed density). However a flow with M = 2 shows a drop in flow velocity on the symmetry axis by a factor of two. Low Mach number, high entrainment beams will clearly be significantly decelerated.

3. RELATION TO RADIO SOURCES

As mentioned earlier, evidence for a turbulent boundary layer and entrainment stems from the morphology of radio sources. Even stronger evidence may come from the discovery of optical emission lines in and around extended radio sources. These line regions are now seen in 8 radio galaxies (Miley, 1983) and are often far removed from the stellar population; in the case of 3C 277.3 the lines are seen ~80 kpc from the nucleus, 50 kpc for 4C 29.30, and 40 kpc for NGC 5128 (Cen A). Not only are hydrogen lines observed, but also lines from heavy elements such as oxygen, nitrogen, and sulfur, and the question naturally arises as to how these elements, produced by stars, have gotten so far from the site of their generation. Entrainment of the metal rich interstellar medium by the radio source on its way out from the nucleus is of course what is being suggested here, and a simple calculation can test the order of magnitude plausibility of this idea. Recasting the empirically derived entrainment rate obtained in the preceding section yields $\dot{M} \approx 60\ R_j^2\ \delta\ n_o C_8\ M_o\ yr^{-1}$ where R_j is the jet radius in kpc, the large scale eddy size R_e has been written as δR_j ($\delta<1$), n_o is the ISM number density, and C_8 is the sound speed in the boundary layer in units of 10^8 cm s^{-1}. The convection speed has been set equal to C_8; it cannot exceed this for any appreciable time and may be somewhat below it. If the jet is moving supersonically relative to the

ambient medium, the ISM in the boundary layer will have been shock heated by the bow shock to a temperature whose sound speed is comparable to that of the jet velocity, i.e., C_8 ~1. For R_j ~1, n_o = 0.1 - 0.01 and δ = 0.1 the total mass entrained in 10^8 years is 10^7 - 10^8 M_o. Estimates of the mass in emission lines in 3C 277.3 varies from 10^5-10^9 M_o, depending on the filling factor (Miley et al., 1981), and for Cen A it lies in the range 10^6-10^8 M_o (Graham and Price, 1981). After entrainment the material will travel a distance of D = 100 v_8 t_8 kpc with velocity v = $10^8 v_8$ cm s^{-1} and t = $10^8 t_8$ years.

In order to appear in emission lines the shock heated and entrained ISM must cool to ~10^4 •K by the time it travels outside the galaxy. For a gas with solar abundances the cooling time is $t_c = 3 \times 10^2 T^{1.6}/n$ seconds for 3 X 10^5 < T < 4 x 10^7 •K (McKee and Cowie, 1977). For post shock temperatures resulting from a 10^3 km s^{-1} shock, $t_c \approx 10^6/n$ yr, where n is the number density. Thus values of n from 0.01 to 0.1 place the material in the right range of positions for this velocity. Although these calculations are only order of magnitude estimates, they show that entrainment is certainly a consistent explanation for the emission lines.

Another intriguing aspect of this process is to follow the evolution of the cooling emission line regions even further. A natural consequence will be star formation, and in fact OB associations are found by Graham and Price (1981) to co-exist with the emission line filament along the edge of the radio source in Cen A. More detailed consideration of this process can be found elsewhere (De Young, 1981), but if star formation is taking place in this manner, then the stars that form will be comoving with the entrained gas. Using a "standard" initial mass function one finds that about 1.3 x 10^{-2} of all the mass formed into stars will be in stars of mass >10 M_o. If star formation proceeds at ~10% efficiency, then 10^4-10^5 stars of M>10 M_o could be formed over 10^8 yr. These objects are of interest because of their short lifetimes (~10^7yr) and because at the end of that time they become supernovae, yielding 10^{50}-10^{52} ergs per event and a remnant generating ~10^{38} ergs. s^{-1}. Thus 10^4-10^5 of these co-moving "time bombs" can play a significant role in the energy budget of a radio source.

4. TURBULENCE AND MAGNETIC FIELDS

Equipartition magnetic fields of ~10^{-5} gauss are found in the large lobes of the extended sources. If this

magnetic field were transported (i.e., convected) out to the lobe through the beam "pipeline" then a problem arises in confining the beam. An isotropic magnetic field in the beam in constrained by $B^2/8\pi \leq n_o kT_o$ for pressure confined beams. The external environment is either extragalactic ($n_o \leq 10^{-4}$ cm^{-3}, $T_o \leq 10^8$K) on interstellar ($n_o \leq 0.1$ cm^{-3}, $T_o \sim 10^4$ K);in either case the B field is restricted to values of 10^{-5}-10^{-6} gauss. A simple flux conserving calculation will show that to obtain fields of $\sim 10^{-5}$ gauss in lobes of dimension 10-100 kpc or larger from beams of radius 1-10 kpc requires fields in the beams to be high enough that pressure confinement fails by two to four orders of magnitude.

If a large fraction of the radio source volume is turbulent on some scale, then the possibility arises that the required magnetic field can be generated in situ through turbulent amplification of a dynamically unimportant seed field which can be easily convected outward with the beam flow. In order for this to work, the field that is generated must not only have the required strength, but it must also have uniform structure on the large scales that are observed. It is easy to show that large scale field structure cannot arise from dissipative field line reconnection of small scale structure or through recombination at a neutral sheet. Both of these processes require times in excess of 10^{10} yr to produce regularity on scales greater than 1 kpc. Naively one might expect that the largest scale field structure that can be produced will be comparable to the size of the largest fluid eddy that is driving the amplification. As this is presumably the beam size, very large scale structure will be hard to acquire. This turns out not to be the case when the fluid contains a special form of vorticity. Also, intuition would lead one to expect the field to be amplified until the mean energy density in the field is comparable to that in the fluid turbulence, at which point the stress forces in the field will damp the turbulence. While this must be the case, one needs to know the timescale for this process and its efficiency to see if such a concept is viable.

An effort to address some of these problems has been made by numerically solving the non-linear time dependent MHD equations (De Young, 1980). The technique uses moments of these equations, and while 3-dimensional, it does not provide spatial information because it uses Fourier transforms of the moments. Starting with a magnetic energy which is 10^{-6} of that in the fluid turbulent energy, equipartition is reached on scales up to that of the largest eddy by about 10 turnover times of that eddy. Scaled to astrophysical quantities, this means that a small seed field of 10^{-9} gauss will be amplified to 10^{-6} gauss on scales up

to 1 kpc in 10^7 yr. If, in addition, the fluid turbulence has a net helicity, $\bar{v} \cdot \bar{\nabla} \times \bar{v}$, then amplification of magnetic fields on scales larger than the longest eddy size can occur. In the optimum case, equipartition fields 10 times the largest eddy size are produced after ~ 100 turnover times, which translates into 10 kpc scale fields in 10^8 years.

The efficiency of this process is low. In general the field is generated at about 5% efficiency, and the very large scale field with about 1% efficiency. This problem is not unique to field generation but is also true of many particle acceleration processes, and it poses a general dilemma. The turbulent energy cascades to ever smaller scales until it reaches the dissipation scale, where it presumably ends up as heat, with some fraction of it being used to reaccelerate particles. This suggests that about ten times as much energy as we see in radio emission from these sources is being dissipated away. Where does it go, and why don't we see it? This problem was raised several years ago (De Young, 1980), but as yet it appears to me that no satisfactory solution is yet at hand.

5. REFERENCES

Brown, G. L. and Roshko, A. 1974, J. Fluid Mech., 64, 775.
De Young, D. S. 1977, Ap. J., 211, 329.
_____. 1980, Ap. J., 241, 81.
_____. 1981, Nature, 293, 43.
_____. 1984, this volume.
Eilek, J. 1984, this volume.
Graham, J. A. and Price, R. M. 1981, Ap. J., 247, 813.
McKee, C. F. and Cowie, L. L. 1977, Ap. J., 215, 213.
Miley, G. K. 1983, in "Astrophysical Jets", ed. A. Ferrari and A. Pacholczyk, (Reidel, Boston), pp. 99-112.
Miley, G. K., Heckman, T. M., Butcher, H. R. and van Breugel, W. 1981, Ap. J., 247, L5.
Norman, M. L., Smarr, L. L., Winkler, K. and Smith, M. D. 1982, Astr. Ap., 113, 285.
Perley, R. 1984, private communication.
Spitzer, L. 1962, The Physics of Fully Ionized Gases (New York: Wiley-Interscience).

DISCUSSION

John Dreher. Your calculations of **B** field generation by the fluid flow through the hot spot seem to show that the field energy is in scales from $\approx d_{hotspot}$ to $\approx 10\ d_{hotspot}$. What limits (if any) does this provide on the possible amounts of small-scale field reversals, the possible presence of which so complicates the interpretation of depolarization data?

Dave De Young. This calculation tells you how much field *energy* resides at different scales, and contains no vectorial information. For the kinetic forcing function used, there is considerable energy available at small scales as well as at $d_{hotspot}$ and 10 $d_{hotspot}$. This might lead one to think that significant small scale field reversals are present. This is true, but it is a function of the spectral form of the kinetic energy input. While I can argue that the flat function used is physically reasonable, it is by no means conclusive. The *minimum* small scale field energy would result from using a δ-function energy input at $d_{hotspot}$, which would result in an inertial cascade to smaller scales with $E_m(k) \propto k^{-3/2}$. One can estimate in a vague way the importance of small scale structures by taking the ratio of $E_m(k)$ at $k \leq 1$ to $E_m(k)$ at large k, $\geq 10^2$.

COLLIMATION OF INTERMEDIATE SCALE MOTION ENTRAINED BY NUCLEAR JETS

R.N. Henriksen
Canadian Institute for Theoretical Astrophysics
University of Toronto, Toronto, ON M5S 1A1, Canada

The relation between the VLBI nuclear jets and the much larger scale VLA jets remains a crucial question. We adopt the view here that the VLBI jets are the 'prime movers' for the larger scale VLA motion. They may not in fact be the 'first jets' to the VLA and single dish 'last jets', but they are sufficiently different in scale to be regarded as a major step along the causal chain.

This is not a new notion. Indeed, many people have grappled with the fate of the 'waste heat' to be expected as relativistic jets decelerate, because not much of this is seen (although it is possible that the kinetic energy of the broad (BLR) and narrow (NLR) emission line regions is related to this energy, according to our present idea). Our solution stems from a suggestion by Henriksen et al. (1982) that the VLBI jet energy is transferred by turbulent diffusion to the nuclear medium (effective Prandtl number $\simeq 1$). Essentially the jet energy is stored in the intermediate scales of the turbulent motion initiated by the prime jet. This is really the only way to store the energy 'invisibly', at least if the turbulence is not supersonic (which it may be, as it is driven - hence the possible excitation of the BLR).

The coupling between the jet and the surrounding medium in our view is by an 'inverted cascade' from the Kelvin-Helmholtz unstable scales near the jet, to the largest background eddies. We model this coupling by a turbulent kinematic viscosity, υ_T/a, in which υ_T is the inertial part and 'a' is a factor (see below) that allows for magnetic coupling. We then model the induced mean flow by using the exact Landau-Squires one-sided incompressible jet solution, as modified for the presence of a mean magnetic field (Wang, 1983). The incompressibility will not allow us to model supersonic motion, but otherwise it should not be too bad inside the galaxy. We show that the entrained flow is collimated in a jet, whose opening angle depends on the hydrodynamic power of the jet in a way consistent with the empirical result of Bridle (1984).

§ 1. Application of the Landau-Squires-Wang Solution

We model the 'prime jet' by a point momentum source (along Z) at the origin. This essentially assumes that the VLBI jet gives up its energy to the motion of the surrounding medium on small scales. Other solutions, in which an axial jet (as an axial singularity - Henriksen, 1984, in preparation) co-exists

with the entrained flow, complicate the algebra. We refer to the sketch in fig.1.

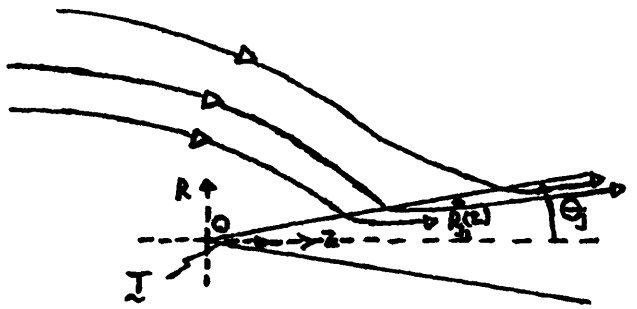

Fig.1:
The conical entrained flow produced by the momentum source T at O. The stream lines and magnetic field lines are labelled with open arrowheads. The solid lines are the conical generators of the entrained jet.

In spherical polar co-ordinates $\{r,\theta,\phi\}$ the solution for the entrained flow is given exactly by:

$$\underset{\sim}{V} = (\nu_T/a) r^{-1} \{2\,[(A^2-1)\,(\cos\theta - A)^{-2} - 1],\ 2\sin\theta(\cos\theta - A)^{-1},\ h\sin^{-1}\theta\} \tag{1}$$

$$\underset{\sim}{B} = \sqrt{4\pi\rho}\ M_A^{-1}\ \underset{\sim}{V}, \tag{2}$$

$$p = p_e + 4\rho(\nu_T/a)^2\ (A\cos\theta - 1)\ (A-\cos\theta)^{-2} r^{-2}, \tag{3}$$

$$T = 16\rho\pi(\nu_T/a)^2 A\ \left[1 + \frac{4}{3(A^2-1)} - \frac{A}{2}\ \ln\left\{\frac{A+1}{A-1}\right\}\right]. \tag{4}$$

Here, V is the velocity vector, B is the magnetic field vector, T is the jet 'thrust' (total force exerted on the surrounding fluid in the Z direction), p is the pressure, ν_T is a 'turbulent viscosity', $h(\nu_T/a)$ is the constant specific angular momentum of the flow. Moreover,

$$a \equiv 1 - M_A^{-2}, \tag{5}$$

where M_A is the Alfvénic-Mach number of the flow (V/V_A), which is taken constant. This factor allows for the contribution by the magnetic field to the total effective viscosity ν_T/a.

The constant $A \geq 1$ can be understood by noting that

$$rV_j \equiv rV_r(\theta=0) = (\nu_T/a)\ 4/(A-1), \tag{6}$$

and that the boundary of the entrained jet, defined by $V_R(\theta_j) = 0$, is given by

$$\cos\theta_j = 1/A, \qquad \text{or} \quad R_j = Z\sqrt{A^2-1} \tag{7}$$

Thus, as $A \to 1$ from above, the jet velocity becomes infinite (as does the thrust) and the entrained jet takes on a zero opening angle.

The radial mass transport inside θ_j is easily calculated to be

$$F = 4\pi\rho\ (v_T/a)A^{-1}\ r, \tag{8}$$

and the radial magnetic flux inside this same boundary is (see eq.(2))

$$\Phi = \sqrt{64\pi^3\rho}\ M_A^{-1}(v_T/a)A^{-1}\ r. \tag{9}$$

From these results we readily find the mass per unit time entrained in a radial distance Δr, as well as the entrained radial magnetic flux over this distance. It is remarkable that the entrained mean radial field varies as r^{-1} from (9). This explains why the mean magnetic flux on the VLA scale should not be extrapolated back to the VLBI scale, nor indeed should the mass transport be.

The equation of a poloidal stream line or magnetic field line is (fig.1)

$$r\ \sin^2\theta/(A-\cos\theta) = r(\theta_j)/A, \tag{10}$$

where $r(\theta_j)$ is the radius at which the given stream-field line crosses the jet boundary. This gives $r\sin\theta \equiv R \propto Z^{1/2}$ when $Z^2 >> R^2$. It is important to note that neither the pressure gradients nor the magnetic forces confine the jet as both effects act to straighten the poloidal stream lines. These are actually being confined by the viscous stresses (Wang, 1981) which increase as $A \to 1^+$ and $T \to \infty$. This is the source of the 'auto-collimation' we test below against the observations.

We observe from equations (2), (10) and (7) that the azimuthal magnetic field has a maximum on a given field line where that line enters the jet ($\cos\theta_j = 1/A$), and falls off asymptotically only as $Z^{-1/2}$ along that field line. Moreover the central stream lines which have crossed into the jet at smaller $r(\theta_j)$ will always have the larger azimuthal twist at a given Z. This is then an 'anti-CH' field which is more twisted centrally and sheared toward the edges. The 'core' stream lines of the jet will always have the transverse field dominating before the more recently entrained outer regions. (What will actually be observed of course, depends on the emissivity weighting along the line of right.) We observe finally that R_{min} (yielding $B_\phi(\max)) = r(\theta_j)\sqrt{1-1/A^2}$ so that B_ϕ increases generally only as $(A-1)^{-1/2}$ as $A \to 1^+$. This contrasts with B_r near the axis which goes as $(A-1)^{-1}$ (eq.(2)). Thus the longitudinal field will come to dominate at high power ($A \to 1^+$) as is observed (Bridle, 1984).

§2. Viscous Collimation, Magnetic Switching and Sidedness

Our principal results now follow immediately from the preceding considerations. Consider first the relation between the collimation of the entrained jet and the total power, L. From (7) and (6) as $A \to 1^+$ we have that

$$V_j = 2\,(\upsilon_T/a) r^{-1}\,(d\Phi/d\theta)^{-2}, \qquad (11)$$

where $d\Phi/d\theta \equiv R_j(Z)/Z = \sqrt{A^2-1}$. Moreover, equation (4) gives as $A \to 1^+$

$$T = (64\pi/3)\,\rho(\upsilon_T/a)^2\,(d\Phi/d\theta)^{-2}. \qquad (12)$$

The total power in the flow is strictly

$$L(r) = \int_{4\pi} r^2 d\Omega \left\{\rho v^2 (1+M_A^{-2}) v_r + \gamma/(\gamma-1)\; p v_r\right\},$$

but as $A \to 1+$ this implies

$$L(r) = V_j(r) T. \qquad (13)$$

Equations (11), (12) and (13) now yield together a testable formula

$$d\Phi/d\theta = (128\pi/3)^{1/4}\,[\rho(\upsilon_T/a)^3]^{1/4}\,(rL)^{-1/4}, \qquad (14)$$

provided we can regard the hydrodynamic power L(r) at sufficiently small r as being proportional to the observed radio power. The $L^{-1/4}$ law fits the envelope of observations (Bridle, 1984). However, this requires the viscosity to vary downward from a fixed upper limit (dependence on ρ is weak). This fixed upper limit could well be $\upsilon_T/a = (\upsilon_{T_o}/a) R_j c$ (or possibly $(\upsilon_{T_o}/a) V_A R_j$ if the turbulence is sub-Alfvénic), where V_{T_o} is a number, for the relativistic jets. Generally V_{T_o} will be a small number ($\lesssim 0.1$) to imitate a sub-grid scale viscosity.

For a field-stream line near the axis of the jet over its whole length, $B_r/B_\phi \propto Z^{-1/2}\,(A-1)^{-1/2}$ as indicated above. The axial distance over which B_r dominates should on this view satisfy $Z_{\|} \propto (A-1)^{-1} \propto (d\Phi/d\theta)^{-2}$ (Z in units of jet length). The existing data (Bridle, 1984) are rather bimodal, but at least the range in $Z_{\|}$ and $(d\Phi/d\theta)^2$ are comparable.

The sidedness question (Bridle, 1984) remains mysterious. However, Wang (1983) showed that in a two-sided jet arrangement, the more powerful jet entrained at a larger rate from a more limited volume of space. In a real situation such material may soon be wholly expelled, leaving the powerful jet loss-less and presumably invisible, while the less powerful jet is left lossy and visible. Such an effect will be more pronounced at

higher powers (i.e. as A→1+). This is the "stripped jet - unstripped jet" model for one-sidedness. The mass expulsion may eventually interfere with fueling the central engine, leading to one or both jets temporarily switching off. In this view, time dependence is essential.

References:

Bridle, A.H., 1984, Astr. J., 89, 979.
Henriksen, R.N., Bridle, A.H., Chan, K.L., 1982, Ap. J., 259, 63.
Wang, D.J., 1983, Phys. Fluids, 26, 2887.

DISCUSSION

John Biretta. In this picture, the jet opening angle depends on the viscosity ($d\Phi/d\Theta \propto \nu^{3/4}$). Would you expect all jets to have similar viscosities ?

Dick Henriksen. This viscosity must be a turbulent viscosity. This will depend only on the velocity profile (shear) which will probably give a (weak) dependence on the source *velocity* and hence power. However, if the source velocity is *c*, there will be no such dependence.

John Dreher. Dick Henriksen's model uses a "viscosity" to accelerate a sheath around a line source of energy and momentum. Does Dave De Young's calculation of the direct entrainment indicate that this "viscosity" is too low at high Mach numbers for this model to work ?

Dave De Young. As I understand Dick's model, it seems difficult to compare the two. My calculation is a direct numerical integration of the time dependent nonlinear hydrodynamic equations which include compressibility effects such as shocks. It is my understanding that the Henriksen calculation is incompressible, time independent, and for potential (i.e. laminar) flow. Thus I think we are calculating different physics problems. Viscosity generally does not play a major role in high, or even low, Mach number problems, and although this code probably has more viscosity in it than is truly realistic (for numerical reasons), there seems to be little evidence for viscous effects in the calculation.

Dick Henriksen. The viscosity involved should be clearly identified. The viscosity I'm talking about is viscosity from the sub-eddies (sub grid scale viscosity). Dave's calculations would not be expected to show these effects unless he put them in analytically. This way of dealing with turbulence, by renormalizing the viscosity in the laminar flow equations, is the *simplest* way of dealing with turbulence, known as the "zero equation" model of turbulence, e.g. Monin,A.S. and Yaglom,A.M., *"Statistical Fluid Mechanics"*, MIT Press (1971).

THE PHYSICS OF PARTICLE ACCELERATION IN RADIO GALAXIES

Jean A. Eilek
Physics Department, New Mexico Tech
Socorro, NM 87801

ABSTRACT

Particle acceleration in the diffuse plasma environment of extragalactic radio sources probably occurs through turbulence and/or shocks in the plasma. This paper reviews the basic physics of each process and attempts some discussion of the efficiency, spectral output and sites of occurence of each process.

INTRODUCTION

The relativistic electrons in the diffuse plasma of radio galaxies must be reaccelerated in situ. The need for this was initially determined from the fact that the source lengths exceed the radiative lifetimes times the outflow speed (or, indeed, lightspeed in a few cases), so that local reacceleration in the source is necessary. The spectral index in tailed sources rarely steepens smoothly going down the tail, as would be expected from synchrotron losses in an outflow or wake; rather, the spectral index is often found to remain constant or to fluctuate, again indicating local acceleration processes. More recently, detailed observations of jets have found that the surface brightness does not decline as it would in an adiabatic case; this as well as the presence of "gaps" at the start of the VLA-scale jets may be due local particle acceleration in the jets.

The particle spectrum in the extended sources is commonly observed to be a power law, $f(p) \propto p^{-s}$ with $4 \lesssim s \lesssim 5$ (note that the energy spectrum is related to this by $N(E) \propto E^{2-s}$, and that the synchrotron spectral index is given by $\alpha = (s-3)/2$).

In a diffuse plasma environment such as that of the radio jets, lobes and tails, at least two particle acceleration mechanisms are probably important: shock acceleration and stochastic acceleration in a field of MHD turbulence. An understanding of the acceleration process as applied to radio sources requires looking at the overall energy source (whether the kinetic energy of the cold outflowing gas, or some other source), the mechanism by which this energy source is coupled to the energetic particles, the efficiency of this coupling and the acceleration rate which results from the coupling (compared in particular to the radiative or adiabatic loss rates), and also the particle distribution which results from the gains and losses. In this paper I present a short review of the physics of each process. I shall try to emphasize the conditions under which each process may operate, the basic mechanism involved, the efficacy

(both acceleration rate and efficiency) and particle spectrum resulting from each process. The details of the physics can be found in the particular references.

BASICS

Generally, a charged particle in a plasma will be accelerated by a non-zero electric field (including that arising from a fluctuating magnetic field). A diffuse plasma is unlikely to carry a strong E field for any distance, due to the high conductivity; thus, stochastic processes come to mind. The acceleration game for radio galaxies consists in large part of guessing under what conditions such a process -- be it classical Fermi acceleration, involving moving magnetic mirrors which reflect particles for a net energy gain by the latter; shock acceleration, which requires turbulent scattering on either side of the shock; turbulent acceleration by a random field of MHD waves; or some other mechanism -- is likely to be relevant, efficient and to produce or maintain the observed power law particle spectrum.

One problem for understanding acceleration is the initial establishment of a "hot" component, such as the relativistic electrons which apparently coexist with the thermal gas in a radio source. This requires either injection of the hot component into the gas from some external source, or some internal process which goes against thermodynamic equilibrium to establish a superthermal component, such as the creation of a high energy power law tail on a Maxwellian distribution. A simpler problem than this is to understand how the already relativistic particles in the background of cooler, thermal gas can maintain their high energy in the face of losses. In the radio galaxy case, this latter problem has seen a good deal of progress recently. In this review I shall address only this latter problem, assuming that a relativistic component already exists in the plasma.

The plasma is believed to act as a fluid. The classical Coulomb scattering length is quite large compared to the size of the source, but the Larmor radii of the particles is much smaller than the source size. It is also possible that plasma microturbulence keeps the particle collision length small. Thus, it is likely that the gas is effectively collisional, and therefore it acts like a fluid. Further, as is discussed elsewhere in this meeting in detail, the plasma is probably turbulent. Evidence for this includes lab analogs of jet flows; the behavior of polarization, both percent and angle; and the strong impression of turbulence in total intensity maps of many sources.

The nature of the turbulence is not easily observable, but several modes are probably represented. The large scale flow will develop fluid turbulence due to its interaction with the surrounding galactic and extragalactic gas. This turbulence usually develops as a cascade from large driving scales (such as the source scale, or the Taylor length) down to small scales (the "dissipation length," $l_o/Re^{3/4}$) with a power law spectrum in the "inertial range" between these two limits. This power law

often obeys either the Kolmogorov (1941) law (for the pure fluid case), $W_f(k) \propto k^{-5/3}$, or the Kraichnan (1965) form (for a magnetohydrodynamic case), $W_f(k) \propto k^{-3/2}$. However, "young" turbulence, driven at some low wavenumber, will show steeper spectra which flatten out to the Kolmogorov/ Kraichnan form after about ten eddy times. Also, Grappin et al. (1983) have recently reported a k^{-3} spectrum in numerical simulations with asymptotic (v,b) correlations.

The plasma and magnetic field will also support MHD wave modes, Alfven (A) and magnetosonic (MS) waves, in what is probably a random situation. The MHD turbulence may be driven by edge instabilities and proceed via wave-wave interactions to form a cascade from large to small scales, as in the fluid turbulent case. It may also be driven internally by Lighthill radiation from the fluid turbulence (e.g., Eilek and Henriksen, 1984). In the latter case, each eddy of the fluid turbulence acts as an internal source for A and MS waves of period comparable with the eddy period. The wavelengths of the MHD waves can range in principle from the source size down to the cyclotron radius of the thermal gas; the wave spectrum depends on the balance of the driving and damping mechanisms at each wavelength as well as on cascade processes.

A third set of turbulent modes are the multitude of high frequency plasma waves, with wavelengths smaller than the thermal gas gyroradius. These almost certainly exist in the radio source plasma. These modes are known to lead to plasma heating and particle acceleration in other environments (e.g., Smith, 1979 on solar flare models), and may also be important in magnetic reconnection acceleration (e.g., Priest, 1982), but they have not as yet been considered in the radio source problem. Therefore, except as a possible source of collisions and anomalous transport effects, they shall not be considered explicitly here.

Observable turbulent scales are limited by interferometer resolution to no less than few kpc. Unfortunately most of the range of possible turbulent scales described above is well below this; thus, most of the theories reviewed here can be tested only by indirect means. One such is polarization transport modelling, as suggested by Spangler (1982), or by Eilek (1984, in progress).

FERMI ACCELERATION

The basic Fermi acceleration model (Fermi, 1949) invokes test particle scattering from moving clouds or magnetic mirrors (with mirror velocity v_m). If the time between collisions is t_{coll}, the rate of energy gain from this process is

$$\frac{dp}{dt} = \alpha p \qquad (1)$$

where the (energy independent) acceleration rate $\alpha = t_{coll}\, v_m/c$ for the case of approaching mirrors (first order process) or $\alpha = t_{coll}\, (v_m/c)^2$ for the case of randomly moving mirrors (second order process).

When this process is balanced against particle or energy losses which also have a loss rate, t_{loss}, which is independent of time (for instance, expansion losses with $t_{loss} \sim R/V_{exp}$, or energy independent leakage from the system), it is easy to show that an initially monoenergetic particle spectrum, or an initially steep power law, is broadened into the power law,

$$f(p) \propto p^{-s} \quad \text{with } s = 3 + 1/\alpha t_{loss} \tag{2}$$

A particle distribution which was initially a power law flatter than this is preserved by the acceleration process.

Three important caveats must be mentioned regarding this classical result. First, the particle distribution depends sensitively on the product αt_{loss}, the ratio of the acceleration rate to the loss rate. Several authors have pointed out that this ratio could have almost any value, dependent on local conditions, rather than being confined to the range 0.5 to 1.0 required by the observed distributions. Burn (1975) and Achterberg (1979) have suggested, however, that when the scattering clouds are turbulent MHD waves, that the feedback of the particle energy gain may regulate this ratio to lie in the desired range.

Second, the synchrotron energy loss rate is

$$\frac{dp}{dt} = \frac{4}{9} \frac{e^4 B^2}{m^4 c^6} p^2. \tag{3}$$

Comparison of this with the acceleration rate, equation (1), shows that there must exist a highest energy for which acceleration can beat radiative losses. This predicts a high energy (in fact, exponential) cutoff to the power law spectrum of equation (2).

Finally, this basic model is a test particle approach. In radio sources the energy density of the relativistic particles is significant compared to that in the turbulence and/or shocks. Thus, the effect of the particle acceleration on the turbulence and shocks must be included in any global model of radio sources.

ACCELERATION BY SHOCKS

Shocks almost certainly occur in radio sources at the "working surface" where the beam runs into the external medium. They have probably

been seen explicitly in a few jets, for instance M87 and Cen A (cf. Biretta et al., 1983, or Burns, in this proceedings). Numerical simulations (eg. Norman et al., 1982) suggest that internal shocks form in supersonic jet flows; internal turbulence may shock if driven supersonically. The shocks are of course the site of strong heating of the thermal plasma as well as acceleration of the energetic component, thus potentially reducing the overall efficiency.

Shock acceleration provides converging "mirrors" which act in a first order Fermi acceleration process. In particular, the shock is a site of converging flow. If an energetic particle passing through the front scatters from some scattering center moving with the fluid (or not too differently from the fluid) it will be reflected back through the shock; it will again scatter, and be reflected again, and so on until it finally escapes from the region. The energy gain per scattering is aproximately $\Delta p \approx [(4/3)(u_1-u_2)/c]p$ if u_1 and u_2 are the upstream and downstream flow speeds (let $r = u_1/u_2 \leqslant 4$ be the compression ratio). If the collision time is t_{coll}, and the probability of escape per scattering is $\eta \approx 4\, u_2/c$, the Fermi coefficients can be written,

$$t_{loss} \approx t_{coll}/\eta;\ \alpha \approx \frac{4}{3}\frac{u_1-u_2}{c}\frac{1}{t_{coll}}. \qquad (4)$$

Thus, the analysis above predicts that an initial delta function distribution will be broadened to a power law,

$$f(p)\alpha p^{-s} \text{ with } s = 3r/(r-1). \qquad (5)$$

(cf. Bell, 1978. Purists will please note that the same result can be derived in more elegant fashion, by solving the Fokker-Planck equation across the jump; cf. Blandford and Ostriker, 1978).

This result comes from an appealing and simple macroscopic argument. All that it requires is that the energetic particles be scattered by the plasma rather than diffusing through it freely, and that the scattering rate is not too energy dependent. In the radio galaxy case (as in any astrophysical plasma) the scattering is probably due to plasma waves, whether MHD waves or high frequency microturbulence. A particularly attractive possibility is that the streaming particles themselves generate A waves through the usual streaming instability (cf. Wentzel, 1969) and thus trap themselves.

The acceleration rate in the shock is

$$\frac{dp}{dt} \approx \frac{4}{3}\left(\frac{r-1}{r}\right)\frac{u_1}{c}\frac{p}{t_{coll}} \qquad (6)$$

and thus depends on t_{coll}, which depends on the particle energy as well as on the intensity and spectrum of the waves. These quantities must be determined using a particular model of the wave physics (eg. Legage and Cesarsky, 1982; another example is presented in the next section). The upper limit to the range of energies which can be accelerated reflects two factors: the energy dependence of the scattering centers (for instance, the largest wavelength present if the scattering is due to A waves, see below), and any radiative losses. In particular, synchrotron losses will lead to a high energy cutoff, above which the particle spectrum falls off exponentially.

If the energy density in the relativistic particles is dynamically important, they can no longer be treated as test particles. The back reaction of their acceleration on the shock will be important and must be considered (cf. Axford et al., 1982, and McKenzie and Volk, 1982, for work in this direction).

ACCELERATION BY MAGNETOHYDRODYNAMIC TURBULENCE

Turbulent acceleration in the context of radio galaxies has mainly addressed the two MHD modes, Alfven and magnetosonic waves. The particle interaction with each mode is quite different. The interaction with MS waves occurs through the Landau resonance.

$$\omega = k_{11} v_{11}. \tag{7}$$

If the particle pitch angle distribution is fairly isotropic, this condition allows all particles to "see" MS waves of essentially all wavelengths.

On the other hand, Alfven waves interact with particles through the cyclotron resonance,

$$p k_{11} = \Omega m/(\mu - v_A/c) \tag{8}$$

where $\Omega = eB/mc$ and μ is the cosine of the pitch angle. This relates the particle energy to a specific set of wavelengths. Because of this resonance, the particles "see" only wavelengths at or greater than their resonant wavelength, $\lambda_{res}(p) = 2\pi/k_{res}(p) \approx 2\pi p/\Omega m$. For electrons with $\gamma \sim 10^3$, this wavelength is on the order of one A. U. under radio galaxy conditions.

Thus, the details of the acceleration process depend quite strongly on the wave mode considered, and especially for A waves depend on the wave spectrum as well as intensity. The evolution of the particle spectrum is generally addressed using quasi-linear theory (which is limited to low wave amplitudes, and which may or may not be observationally verified;

e.g., Jokipii, 1979). The wave spectrum in a particular source depends on the details of the wave driving and damping mechanism therein, and should also be addressed in any self consistent model.

a) Magnetosonic Wave Turbulence.

The damping of MS waves and their acceleration of relativistic particles was addressed by Kulsrud and Ferrari (1971) and by Barnes and Scargle (1973), among many others, and has recently been investigated in the context of radio sources by Burn (1975), Achterberg (1979) and Bicknell and Melrose (1982).

The acceleration rate of a particle of energy p is given by (Eilek, 1979; Bicknell and Melrose, 1982)

$$\frac{dp}{dt} \approx a_1 \frac{V_{ms}^2}{c} \frac{p}{B^2} \int_{k_{min}}^{k_{max}} k W_m(k) dk \qquad (9)$$

where $\delta B^2 = \int W_m(k)dk$ is the energy density of the MS waves and V_{ms} is the wave speed; a_1 is an order-unity constant. This is clearly an example of the Fermi process (cf. equation 1). The rate depends on the total wave intensity, but only indirectly on the wave spectrum. The particle spectrum produced by MS wave acceleration will thus be a power law for energies below the cutoff determined by synchrotron losses.

The spectrum and amplitude of the waves depend on the driving and damping mechanisms, as well as on non-linear wave-wave interactions. MS waves suffer several damping mechanisms on the thermal gas as well as that due to Landau acceleration of the relativistic component. An important consideration for radio source physics is which of the damping mechanisms are dominant; does the MS wave energy go into accelerating the relativistic particles or into heating the thermal gas?

While the detailed analysis of each mode is complex (cf. Eilek, 1979), we can find a couple of trends, as follows. First, the competition between Landau acceleration of relativistic particles and heating of the thermal gas depends essentially on the ratio of the energy densities. Thus,

$$\frac{\gamma_{\Lambda,rel}}{\gamma_{\Lambda,th}} \approx \frac{E_{rel}}{E_{th}}$$

if γ_i describes the damping rate due to the i^{th} mechanism, so that $dW(k)/dt = -\gamma_i(k)W(k)$. Second, thermal conductive damping can be most

important at low wavenumbers (note, $\gamma_\Lambda(k) \propto k$ but $\gamma_{ther}(k)$ = constant for k above the e-e collision wavenumber). The condition to have $\gamma_{\Lambda,rel}(k) > \gamma_{ther}(k)$ is approximately

$$k > 10^{-15} \frac{n_3}{v_{ms,3} c_{s,3}^3} \frac{E_B}{E_{rel}} \text{ cm}^{-1},$$

where $n_3 = n/10^{-3}$ cm^{-3}; $(v_{ms}, c_s)_3 = (v_{ms}, c_s)/10^3$ km s^{-1}. Thus, relativistic particle acceleration dominates the MS wave spectrum in conditions of high E_{rel} and low n_g; otherwise heating of the thermal gas dominates.

Estimating the efficiency of MS wave acceleration requires knowledge of two factors. Internally, the fraction of wave energy that goes into relativistic particles rather than into heating of the background gas is determined by the relative strengths of the various damping rates, and can be as high as 10 to 100 percent if the gas density is low, or as low as 0.1% or less if the density is high. Externally, the fraction of the outflow energy (or other energy source) which is turned into MS waves must be estimated. Laboratory estimates suggest that something like 1 to 10 percent of the jet flow energy goes into fluid turbulence; in wakes and tails the factor may be larger. If the turbulent cascade is carried by MHD waves (as Bicknell and Melrose suggest), no further coupling is needed; if the cascade is a fluid effect and the MHD waves are Lighthill radiated (as Henriksen, Bridle and Chan, 1982; or Eilek and Henriksen, 1984 suggest) the fraction of fluid turbulent energy flow radiated into A or MS waves is probably less than unity.

b) Alfven Wave Turbulence

This mode has been investigated in the radio source context by Lacombe (1977, 1979), by Eilek (1979) and Eilek and Henriksen (1984). The resonant nature of the wave-particle interaction leads to an acceleration mechanism quite different from that of the MS waves. One particularly interesting result is the possibility that the particle power law distribution observed in radio sources arises as an asymptotic solution when A wave acceleration balances synchrotron losses.

The acceleration rate is

$$\frac{dp}{dt} \approx \frac{2\pi^2 e^2 v_A^2}{c^3} \frac{1}{p} \int_{k_{res(p)}}^{k_{max}} W_A(k) \frac{1}{k} \left[1 - \left(\frac{v_A}{c} + \frac{\Omega m}{pk}\right)^2\right] dk \qquad (10)$$

if $W_A(k)$ is the energy density in A waves; $k_{res(p)} \approx \Omega m/p$; v_{A_ν} the Alfven speed. For the case of a power law wave spectrum, $W_A(k) \propto k^\nu$ for $k > k_o$,

the acceleration rate becomes

$$\frac{dp}{dt} \approx a_2 \frac{v_A^2}{c} \Omega_m \frac{\delta B^2}{B^2} \left(\frac{k_o p}{\Omega_m}\right)^{\nu-1} \qquad (11)$$

where a_2 is another order-unity constant. This does not follow the usual Fermi criterion (equation 1). Thus, the spectral evolution must be investigated anew. In particular comparing the synchrotron loss rate, equation (3), suggests that a wave spectrum αk^{-3} could provide a balance against radiative losses at all energies for which resonant waves exist. Thus, both the wave spectrum and intensity are critical in determining the acceleration rate and particle spectrum.

The wave spectrum depends on the balance of driving, damping and nonlinear (including cascade) processes at each wavenumber. For A waves the dominant damping is the acceleration of the relativistic particles. The damping rate at wavenumber k is

$$\gamma_{cyc(k)} = \frac{4\pi^2 e^2 v_A^2}{c^3} \frac{1}{k} \int_{p_{res(k)}}^{p_{max}} p^2 \left[1 - \left(\frac{v_A}{c} + \frac{m\Omega}{pk}\right)^2\right] \frac{\partial f(p)}{\partial p} dp \qquad (12)$$

Other losses are cyclotron resonant heating of the thermal gas, which affects only the very highest wavenumbers, and non-linear processes such as nonlinear Landau damping (in which A + A → MS), which are important only at high wave intensities.

The fact that the Alfven waves are damped almost totally by the relativistic particle acceleration means that little or none of the wave energy will be lost to heating of the thermal gas. This fact will lead to some improvement of the efficiency arguments compared to the case of MS wave acceleration; but the macroscopic coupling arguments remain the same as discussed above.

The wave driving is harder to estimate. As discussed above, the conventional assumption for turbulence is that driving at low wavenumbers generates a cascade which driven by wave-wave interactions. This cascade terminates at some high k at which dissipation becomes important. This is the approach of Bicknell and Melrose (1982), for instance. On the other hand, Eilek and Henriksen (1984) investigated the case in which fully developed fluid turbulence generates MS waves internally via Lighthill radiation. In this case the wave spectrum in the steady state is determined by the balance at each wavenumber between the Lighthill driving and the damping due to particle acceleration. The coupling between the wave and particle spectra, enhanced through the cyclotron resonant condition

(cf. equations 10 and 12), leads to a feedback situation. One would expect that, from an arbitrary initial situation, this coupling would drive the wave and particle spectra towards a state of balance. In this asymptotic state, one would expect both the wave and particle spectra to adjust so as to keep the ratio of particle acceleration and loss rates independent of energy; and also that the overall energy gains and losses would be comparable, thus maintaining a quasi-steady state.

Eilek and Henriksen found a particular analytic example of this balance. They assumed Lighthill driving from a fluid turbulent spectrum of the form $W_f(k) \propto k^{-m}$, with $m = 3/2$ (Kraichnan spectrum), 5/3 (Kolmogorov spectrum) or possibly steeper (say, $m = 2$ for young turbulence, before the cascade is fully established). They found a self similar solution in the presence of synchrotron losses in which the A wave spectrum obeys $W_A(k) \propto k^{-3}$, and in which the particles obey $f(p) \propto p^{-s}$, with $s = 6 - s_t$ and $s_t = 3(m-1)/(3-m)$. This solution thus predicts that the particle spectrum will evolve asymptotically towards a power law with exponent s in the range $4 < s < 5$.

WHAT NEXT?

At the microphysical level, particle acceleration theory in radio galaxies seems to be in good shape. Two mechanisms -- acceleration by shocks and by MHD turbulence -- have been proposed and have been investigated in some detail by several authors. Given the caveat that only low intensity turbulence (including that necessary for shock acceleration) can be modelled by current linear theories without numerical simulation, good progress has been made towards understanding the basic physics of each model. In particular, the details of the wave-particle interactions seem fairly well understood. From recent work, intelligent estimates can now be made of the output particle spectra, energy ranges affected, efficiency and effect of losses for each process. It is comforting that all three models (considering Alfven and MS wave acceleration separately) turn out to give the observed power law particle spectra when operating in some part or other of parameter space.

It is worth noting here that other microphysical mechanisms may also be relevant. Plasma heating and/or superthermal particle acceleration by high frequency plasma waves is known to occur in the solar and magnetosphere environments, as is magnetic reconnection which also energizes the local plasma. While this author is not aware of any work on these processes in the context of radio galaxies, she suspects that they may also be part of the answer.

It is also worth noting that all three processes reviewed here, as well as the others mentioned above, are no doubt relevant to the radio source problem. Particle acceleration will occur locally at sites (such as strong shocks or strong "bursts" of turbulence, cf. Cantwell, 1981) where the acceleration rate exceeds all loss processes. This will give rise to local areas with high particle energy density and flatter particle spectra. As particles flow or diffuse away from these sites, loss

processes will become important; synchrotron losses in particular may lead to the balanced, self-similar spectrum found by Eilek and Henriksen (1984). This will lead to spatial evolution of the photon spectral index on scales on the order of the radiative lifetime times the diffusion speed (cf. Henriksen, 1983).

The next important questions for radio source acceleration problem may be those involving the macrophysics of the source. For instance, consider a general picture of the energy flow within the source, as follows.

a) The luminosity of the extended radio source plasma is being supplied from some initial source, usually considered to be the total (kinetic plus internal) convected energy of the outflowing plasma.

b) By some means this outflowing plasma must make local, internal particle accelerators. These may include shocks, MHD turbulence, high frequency turbulence or other mechanisms. The coupling between the outflow energy and these accelerators probably occurs when the (initially laminar?) outflow shocks and/or becomes turbulent.

c) These accelerators will transfer energy from the flow (or other source) to the relativistic particles ("acceleration") to the cool, inertial gas ("heating") and perhaps to the ambient extragalactic medium.

d) This chain of events will have a profound effect on the structure and evolution of the source, and perhaps on its surroundings as well, through heating and disruption of the soume and through the slow energy depletion.

It may be the time for this sort of global picture to be investigated in more detail. Some parts of the picture, in particular the macro/microphysical coupling as in part (b), are inherently nonlinear, and thus must await further progress in laboratory or numerical simulation. Other parts of the picture may be addressable with current techniques and data. For instance, several morphological or dynamical properties of the sources appear at present to correlate with the radio power of the source (e.g., Bridle, 1984).

-- High power sources tend to be "edge brightened", in the sense of Fanaroff and Riley's (1974) class II, with sharp boundaries and well defined hot spots at their leading edges. Lower power sources tend to be "edge darkened", (FR class I), with rapidly spreading jets and with surface brightness declining steadily away from the nucleus as the flow becomes increasingly flocculent and disrupted.

-- There seems to be a trend for higher power radio galaxies to have jets with lower relative luminosities compared to the lobes (although this trend may not continue for the quasar jets; cf. Owen and Puschell, 1984).

-- The "sidedness" of the jets, the ratio of the surface brightness on the two sides, is clearly related to the source power, in that the more

powerful sources tend to be one sided.

-- The magnetic field may be increasingly important dynamically as the source power increases. Lower power sources appear to be confined by the external cluster gas pressure; the (projected) field is at right angles to the jet, consistent with an internal helical field, and also with a field which responds passively to the flow and expansion of the source, rather than being dynamically dominant. Higher power sources, on the other hand, show overpressure, and may require magnetic self-pinch confinement; the projected field in these sources is along the jet axis, thus requiring the confining azimuthal field to be external to the jet.

These morphological and dynamical correlations should be related to the energy flow considerations listed above, and especially to the creation and side effects of the turbulence and/or shocks which couple the flow energy to the radio luminosity. For instance, the strength and rate of development of large scale turbulence may depend on the source power (modulated by the flow Mach number, for instance), thus relating the "leakiness" of the low energy jets and their edge-darkened morphology to their internal physics, in particular to the onset of fluid turbulence which will both brighten and disrupt the flow. On the other hand, magnetic and electrodynamic effects may be more important in high power sources, so that jet brightening and confinement (by external azimuthal fields) may occur through current driven turbulence and reconnection effects. (Note that the confining field can penetrate the surrounding plasma only if the conductivity of that plasma is anomalously low, as in the presence of microturbulence.)

Such statements as these are no more than unbridled speculation until backed up by calculations and self-consistent models; this author believes the observational situation is now good enough to warrant such efforts.

REFERENCES

Achterberg, A., 1979, Ast. Ap. 76, 276.
Axford, W. I., Leer, E. and McKenzie, J. F., 1982, Ast. Ap. 111, 317.
Barnes, A. and Scargle, J. D., 1973, Ap. J. 184, 251.
Bicknell, G. V. and Melrose, D. B., 1982, Ap. J. 262, 511.
Biretta, J., Owen, F. N. and Hardee, P. E., 1983, Ap. J. Lett. 274, 127.
Bell, A. R., 1978, M.N.R.A.S. 182, 147.
Blandford, R. D. and Ostriker, J. P., 1978, Ap. J. Lett. 221, L29.
Bridle, A. H., 1984, preprint.
Burn, B. J., 1975, Ast. Ap. 45, 435.
Cantwell, B. J., 1981, Ann. Rev. Fluid Mech 13, 457.
Eilek, J. A., 1979, Ap. J. 230, 373.
Eilek, J. A. and Henriksen, R. N., 1984, Ap.J. 227, 820.
Fanaroff, B. L. and Riley, J. M., 1974, M.N.R.A.S., 167, 31p.
Fermi, E., 1949, Phys. Rev. 75, 1169.
Grappin, R., Pouquet, A. and Leorat, J., 1983, Ast. Ap. 126, 51.
Henriksen, R. N. Bridle, A. H. and Chan, K. L., 1982, Ap. J. 257, 63.
Henriksen, R. N., 1983, IAU Symposium 107, in press.

Jokipii, J. R., 1979, in Particle Acceleration Mechanisms in Astrophysics, AIP Proc. 56, p. 1.
Kolmogorov, A. N., 1941, Compt. Rend. Acad. Sci. U.R.S.S., 30, 301; 32, 16.
Kraichnan, R. H., 1965, Phys. Fluids, 8, 1835.
Kulsrud, R. M. and Ferrari, A., 1971, Ap. Space Sci. 12, 302.
Lacombe, C., 1977, Astr. Ap. 54, 1; 1979, Astr. Ap. 71, 169.
Legage, P. O. and Cesasky, C. J., 1982, Astr. Ap. 118, 223.
McKenzie, J. F. and Volk, H. J., 1982, Ast. Ap. 116, 191.
Norman, M. L., Smarr, L. L., Winkler, K.-H. A. and Smith, M. D., Astr. Ap. 113, 285.
Owen, F. N. and Puschell, J. J., 1984, preprint.
Priest, E. R., 1982, Solar Magnetohydrodynamics (Holland:Reidel).
Smith, D. F., 1979, in Particle Acceleration Mechanisms in Astrophysics.
Spangler, S. R., 1982, Ap. J. 261, 310.
Wentzel, D. G., 1969, Ap. J. 157, 545.

THE RELATIONSHIP BETWEEN LABORATORY AND ASTROPHYSICAL JETS

G.V.BICKNELL
Mount Stromlo and Siding Spring Observatories
Research School of Physical Sciences
Australian National University

I Introduction

There are two major problems in understanding the physics of low luminosity extragalactic radio sources. These are: (1) Why do the jets in such sources expand with such a wide cone angle (typically about $15 - 20°$)? (2) What causes the usually slow decrease in surface brightness of the jets? Laminar supersonic models of the jet flow are unable to account for the large cone angles unless they are considerably heated by dissipation. Dissipation of turbulence by particle acceleration has often been invoked to account for the surface brightness but no satisfactory model has emerged. Here I wish to present a completely different view, first suggested by Fanti et al. (1982) that the slow surface brightness decline observed in a number of jets is due to adiabatic processes associated with entrainment. I shall present arguments that the jets in the edge–darkened (Fanaroff–Riley Class I) sources are of low Mach number along a large fraction of their lengths, that they are largely non–dissipative (except near the cores), and that their morphology and surface brightness is governed by turbulent processes. Before considering astrophysical jets in detail, however, I shall review the features of laboratory jets which seem to be pertinent to low luminosity sources.

II Turbulent Laboratory Jets and Shear Layers

There are two types of laboratory experiments which are relevant: These are the experiments on plane two–dimensional shear layers and axisymmetric jets, represented schematically in figure 1. The important parameters in these experiments are the velocity ratios, density ratios, temperature ratios, and Mach numbers of the mixing fluids. The temperature and density ratios are not independent (for fluids of given composition) since (except in regions where there are shocks) the pressure is approximately constant across the mixing region. There does not seem to be a great difference between flows in which density differences are introduced by a composition variation (e.g. an Hydrogen–Air jet) rather than a temperature variation.

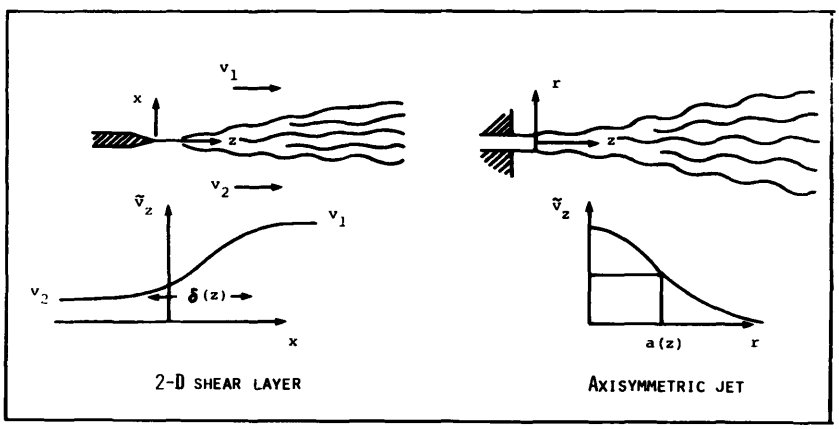

Figure 1. A schematic illustration of the laboratory experiments on 2–D shear layers and axisymmetric jets. The shear layer thickness δ is often taken to be the distance between points whose mean velocities differ from the free–stream values by ten percent. The jet radius a is usually taken to be the radius at the half–maximum velocity point.

Let us consider 2–D shear layers first. Because of the Kelvin–Helmholtz instability the interface between differentially moving fluids is unstable and 2–D shear layers rapidly develop a turbulent mixing region which spreads at a constant rate. When one of the fluids is stationary (say $v_2 = 0$), for constant density flows, the spreading rate of the shear layer thickness (δ) with distance (z) is given by $d\delta/dz \approx 0.12$. Brown and Roshko (1974), in a classic paper, showed that this spreading rate is modified somewhat by the density ratio of the mixing fluids but that this is not nearly as important as the effect of Mach number. Bradshaw (1981) in a recent review shows that the spreading rate of shear layers decreases suddenly from about 0.12 at $M = 1$ to about 0.05 at $M = 3$ and is possibly constant at this value for $M > 3$. There are three important points here for the extragalactic fluid dynamicist: (1) The Mach number dependence of the spreading rate is so dramatic that any modelling of the spreading rate of supersonic extragalactic jets needs to be able to explain it in order to be taken seriously. (Incidentally, there has been no consistent explanation for the laboratory data since 1972 when the Mach number effect was apparent. See Birch and Eggers 1972). (2) The decrease of spreading rate with Mach number means that it is more difficult for a supersonic jet to become fully turbulent. Nevertheless, Lau's (1981) work on axisymmetric jets shows that the rate of spread of annular turbulent boundary layers towards the centre of an axisymmetric jet is about 3 times greater than that which would be inferred from the 2–D shear layer results. (See further discussion below). (3) Here we have some indication as to why the spreading rates of jets decrease with the luminosity of the source (Bridle 1984) if, as might be reasonably expected, the source power increases with jet Mach number.

The laboratory experiments on axisymmetric jets are of more direct relevance to astrophysical jets. The situation with subsonic jets is as follows (see figure 2(A)). When an initially laminar jet emerges from a nozzle it quickly becomes Kelvin–Helmhotz unstable and an annular turbulent boundary layer propagates towards the middle of the jet enveloping it entirely. The term, "potential core", is often used to refer to the region of the jet between the nozzle and the point where fully developed turbulence occurs. In the fully turbulent region the jet spreads due to the transport of momentum out of the centre of the jet by turbulent processes. This process of "turbulent diffusion" causes mixing with the surrounding fluid which is swept into the jet causing an entrainment flow from an extended region surrounding it. The velocity profile in such a jet is strongly sheared and a balance results between the production of turbulence by the shear and the decrease of the shear by the turbulent transport. The diffusion of momentum from the centre of the jet causes it to decelerate.

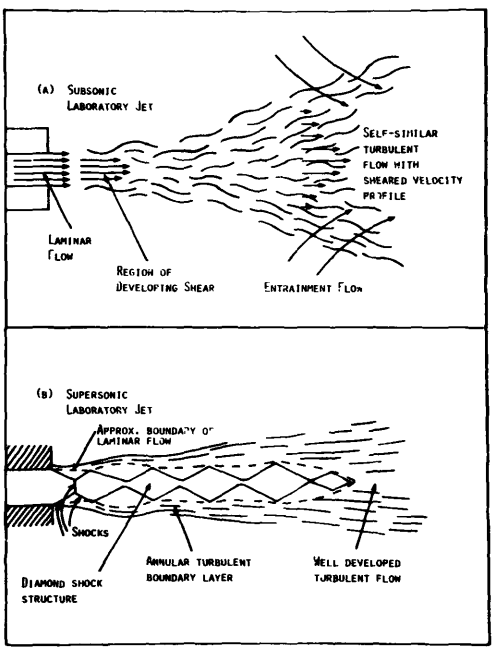

Figure 2. A schematic indication of the behaviour of subsonic and supersonic laboratory jets. The former is based upon Schetz's review; the latter is based upon the work of Love et al., Lau, Morris , and Troutt and McLaughlin .

For a constant density, incompressible jet the asymptotic rate of decay of the jet centreline velocity goes as z^{-1}. Jets which are hotter (and consequently lighter) than the surroundings decelerate more rapidly although there may be no laboratory jets that are as relatively hot or light with respect to their environment as extragalactic jets. Another important feature of the laboratory flows is that lighter jets spread more rapidly. For instance, an Air–Air jet spreads at a cone angle (based upon the HWHM of the velocity profile) of about 10° whereas an H_2–Air jet spreads with a cone angle of about 14° (Era and Saima 1977).

The process of turbulent diffusion also leads to the lateral transport of specific enthalpy (in hot jets) and species concentration (in jets of varying composition) at a slightly greater rate than the velocity. This situation is often summarized by saying that the turbulent Prandtl number (for turbulent heat flux) and the turbulent Schmidt number (for turbulent concentration flux) are slightly less than unity. In the laboratory case the the concentration may be, for instance, the concentration of H_2 in an H_2 –Air jet. In our context it refers to the relative number density of relativistic and thermal particles. The significance of these results to subsonic or transonic extragalactic jets is that a lateral diffusion of momentum should be accompanied by diffusion at a similar rate of the magnetic field and the concentration of relativistic particles (see §VI and §VII).

The dynamics of turbulent supersonic flow are considerably more complex (see figure 2(B)) and a qualitative description is as follows. When a supersonic underexpanded (jet pressure > receiver pressure) or overexpanded (jet pressure< receiver pressure) jet emerges from a nozzle a characteristic pattern of shock diamonds and/or Mach discs arises. The exact pattern produced depends upon the Mach number and pressure ratios. Photographs and analyses of such jets are given in Love et al. (1959). As in the subsonic case a turbulent annular boundary layer propagates into the middle of the jet and after a few nozzle diameters they become fully turbulent *and subsonic*. The shock structure then disappears. The Love et al. jets are cool and dense and may not be directly relevant to extragalactic jets. Nevertheless, more recent experiments (Troutt and McLaughlin 1981, and Lau 1981) on jets of varying temperature and density ratios (including some which are lighter than the surroundings) typically show a potential core region followed by a region of subsonic flow. A Mach 3 jet, for instance, becomes subsonic in about 15 nozzle diameters (Bradshaw 1984). The length of the potential core region is much shorter than that which would be inferred from the spreading rate of 2–D shear layers. Lau attributes the rapid transition to subsonic flow to geometrical effects but the disruptive effects of Mach discs could also be important (Norman et al. 1984). *The importance of these laboratory results can not be underestimated.* They strongly suggest that extragalactic jets of low (but supersonic) Mach number will become subsonic or at least transonic. This will be especially the case if Mach discs occur at the base of the jet near the core. In fact, I have suggested that an initially confined jet could "turn on" due to expansion induced shocks (see Bicknell 1984a; hereafter B84). Sanders' (1983) mechanism for producing shocks in an initially free jet could also be relevant near the core.

In all of the jet flows discussed above the effects of pressure gradients have been negligible. However, the studies of buoyant laboratory jets are also relevant to radio sources. A vertical light laboratory jet has the following characteristics: Near the exit the jet behaves in a similar fashion to the above types of forced jets. As a buoyant jet decelerates the buoyancy force becomes more important than the inertia of the jet and the rate of velocity decrease is different. (For subsonic buoyant jets in a constant gravitational field the velocity makes a transition from a z^{-1} dependence to a $z^{-1/3}$ dependence (see Chen and Rodi 1980)). In the buoyancy dominated regime such a jet is called a *plume*. Because of their slow velocities plumes are sensitive to lateral forces and this is responsible for their often observed meandering motions. The relevance of plume type behaviour to the outer parts of sources such as 3C31 (Fomalont et al. 1980, Strom et al. 1983), 3C449 (Perley, Willis and Scott 1979) and to edge–darkened radio sources in general seems fairly obvious.

In the above summary of the laboratory data I have indicated various points of relevance to extragalactic jets. The most important points suggested by the lab data seem to me to be the following: (1) In low luminosity sources the jets are possibly subsonic or transonic over a large portion of their entire length. This is indicated by the initial cone angles of jets such as 3C31 (Bridle et al. 1980, Coneangle = 17°)

and NGC315 (Willis et al 1981, Coneangle = 19°), suggestive of turbulent expansion of a light, low Mach number, possibly subsonic jet. (2) The morphology of the edge–darkened, Fanaroff–Riley Class I sources, in particular the general absence of hot spots in the lobes and the oscillations of jets before they enter the lobes, suggests that the jets in these sources are decelerated by entrainment. (3) Initially supersonic jets may become subsonic through a combination of shocks and entrainment. This can happen close to an optical core radius. (4) Jets which are initially hypersonic may remain so because of the decreased spreading rate of turbulent boundary layers at high Mach numbers and because of the importance of the non–disruptive reflective modes at low density ratios (Norman et al. 1982, Norman, these proceedings).

In view of the above, in particular points (1)–(3), I shall concentrate almost exclusively on the propagation of transonic or subsonic jets through the atmosphere of a giant elliptical galaxy. The major point that I wish to show is that the surface brightness variations of jets in low luminosity sources can be understood as being due principally to adiabatic effects associated with entrainment. This gives addded weight to the supposition that the morphology of these sources is due to turbulent processes. The following treatment basically follows that of B84 with a few embellishments (notably the use of concentration variables in §VI).

III Favre's Formalism for Compressible Turbulent Flow.

A useful formalism for dealing with compressible turbulent flow was given by Favre (1969). Briefly, Favre decomposes the flow into mean and turbulent components as follows. For the density,

$$\rho = \bar{\rho} + \rho' \quad \text{where} \quad \langle \rho' \rangle = 0 \tag{3·1}$$

and the angular brackets denote an ensemble average. For the velocity components

$$v_\alpha = \tilde{v}_\alpha + v'_\alpha \quad \text{where} \quad \langle \rho v'_\alpha \rangle = 0 \tag{3·2}$$

That is, the veloctity components are mass–averaged. In general, intensive quantities are mass averaged and extensive quantities are averaged in the same way as the density. This procedure leads to a decomposition of the Navier–Stokes equations in which the physical significance of the turbulent terms are readily understood. Favre's equations are equations for the *mean* (ensemble–averaged) flow. In comparing predictions for the mean flow with snapshots of a particular jet departures of the data from the mean are to be expected. Figure 3 illustrates the nature of turbulent jet flow and the process of averaging (in this case a time average). The jet in this case comes from a pressure cooker. The left hand photograph (a 1/125 sec. exposure) clearly shows the turbulent nature of the flow and the spreading of the jet as it exits from the nozzle. The Mach number of the jet in this case is of order 10^{-2} so that the expansion of the jet is definitely not due to expansion of a supersonic jet in an atmosphere of decreasing pressure. The right hand photograph shows the effect of averaging the flow over 8 seconds. This mean flow spreads due to the turbulent transport of momentum evident in the left hand photograph.

In analyzing the mean flow it is useful to keep track of the orders of magnitude of various quantities and in order to do so I take $a = HWHM$ of velocity profile, v_c = central jet velocity, L = length scale of variation of jet velocity, v' = turbulent velocity. The coordinates are the usual cylindrical coordinates (r, ϕ, z) with the jet propagating in the the z–direction.

Mass conservation

$$\frac{\partial}{\partial z}(\bar{\rho}\tilde{v}_z) + \frac{1}{r}\frac{\partial}{\partial r}(\bar{\rho} r \tilde{v}_r) = 0 \tag{3·3}$$

This implies that $\tilde{v}_r \sim a/L\, \tilde{v}_z$

Axial momentum

$$\frac{\partial}{\partial z}(\bar{\rho}\tilde{v}_z^2) + \frac{1}{r}\frac{\partial}{\partial r}(r\bar{\rho}\tilde{v}_r\tilde{v}_z) = -\frac{1}{r}\frac{\partial}{\partial r}\left(r\langle \rho v'_r v'_z \rangle\right) - \frac{\partial \bar{P}}{\partial z} + \bar{\rho} X_z \tag{3·4}$$

The quantity $\langle \rho v'_r v'_z \rangle$ is the turbulent shear stress which gives the transport of z–momentum in the r–direction; X_z is the gravitational field. When the gradients of the turbulent stresses are more important than the pressure gradient this equation leads to the estimate $v'^2 \sim a/L\, v_c^2$ for the turbulent velocity. Thus a modest amount of turbulent kinetic energy (about 10–20% of the mean flow kinetic energy) can be responsible for a spreading cone angle of about $10 - 20°$.

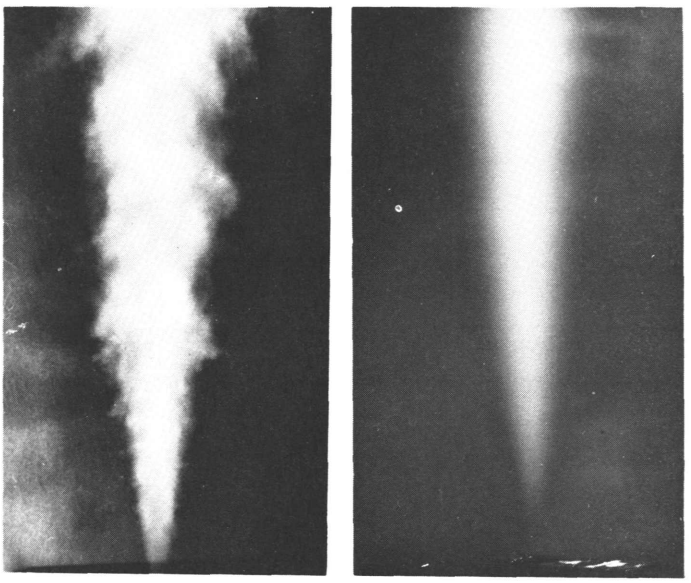

Figure 3. The Stromlo Jet. The two photographs are of jets emerging from a pressure cooker. The left hand photograph is a short exposure, whereas the right hand photograph is a long exposure, illustrating the effect of averaging turbulent flow. These (subsonic) jets expand due to the influence of turbulent diffusion of velocity from the centre of the jet.

Lateral momentum

$$\frac{\partial}{\partial z}(\bar{\rho}\tilde{v}_r\tilde{v}_z) + \frac{\partial}{\partial r}\left(\bar{P} + \langle\rho v_r'^2\rangle\right) + \frac{\langle\rho v_r'^2\rangle - \langle\rho v_\phi'^2\rangle}{r} = 0 \qquad (3\cdot5)$$

With the above expressions for v' and $\tilde{v}_r$, it is easily shown, for $M^2 \sim 1$, that this equation implies

$$\bar{P}(r,z) \approx \bar{P}(z) \qquad (3\cdot6)$$

That is, these jets are in pressure equilibrium with the surroundings in contrast to high Mach number jets in which local over–pressure ratios of order M^2 can occur (Norman et al. 1984).

IV Standard Analyses of Turbulent Flow

A major problem in analyzing turbulent flow are the so–called turbulent closure relations, in particular how does one model the shear stress $\langle\rho v_r' v_z'\rangle$? Here I shall give a brief overview of the various approaches to modeling jets and shear layers which is based upon the more extensive reviews of Schetz (1980, hereafter S80) and Launder et al. (1973).

Taylor's turbulent viscosity

Taylor, in 1932, (see S80, p53) proposed that the turbulent motion of fluid elements gives rise to a *turbulent viscosity* ν_t similar to a molecular viscosity but much larger. He took

$$\langle\rho v_r' v_z'\rangle = \nu_t\bar{\rho}\tilde{v}_{z,r} \quad \text{and} \quad \nu_t = l_m^2\tilde{v}_{z,r} \qquad (4\cdot1)$$

where the *mixing length* l_m is of order the jet width.

Prandtl's turbulent viscosity

Arguing similarly to Taylor, Prandtl in 1926, (see S80, p53) took

$$\nu_t = \kappa b v_c \qquad (4\cdot2)$$

where $\kappa \approx 0.25$, b = jet "width" and v_c =central jet velocity.

Although the Taylor and Prandtl models seem analytically quite different, in practice they give quite similar results. They work well for incompressible constant density flows but are unsatisfactory for detailed models of variable density flows. Nevertheless, order of magnitude estimates based upon the above formulae are useful.

Prandtl, Kolmogorov TKE approach

Prandtl and Kolmogorov (see S80, p64) tried to overcome the problems of the above closure schemes by taking

$$\nu_t = \langle \frac{1}{2} v'^2 \rangle^{1/2} l \qquad (4 \cdot 3)$$

where l again is a suitably chosen jet "width", and $\langle \frac{1}{2} v'^2 \rangle$ is the turbulent kinetic energy per unit mass (TKE). This expression for the turbulent viscosity is supplemented by an equation for the TKE but the approach is not a significant improvement over the Taylor and Prandtl approaches.

$k - \epsilon$ models

In these models (see Launder et al. 1973) two equations are involved, one for $k = \langle v'^2/2$ and ϵ, the rate of dissipation. One then takes $\nu_t = Ck^2/\epsilon$ where C is a constant. The models of which there are two variants, $k - \epsilon 1$ and $k - \epsilon 2$, provide good results for incompressible flows in which there is some density variation. The agreement with experimental data on flows with large density variations is reasonable but not outstanding.

Reynolds Stress models

These are the most sophisticated of the present turbulent closure models. The concept of turbulent viscosity disappears and the shear stress is determined directly from a partial differential equation. These models are at an advanced stage of development (see Reynolds and Cebeci 1976, Launder 1979, Launder and Morse 1979) and predict a number of jet and shear layer flows with reasonable success.

The above turbulent models are mean flow models. Much work has also been done on more direct modelling of the flow. The two main approaches are:

Large scale eddy simulations

The large scale eddy structure in the flow is modelled using a three–dimensional hydrodynamic code. The small scale structures are modelled using turbulent closure schemes similar to the above. Typically such codes take a few hours of Cray–1 time.

Direct simulation

The full 3–D Navier–Stokes equations are used to model the flow over the complete range of scales, from the large, energy containing scales, to the small dissipative scales. This approach is limited to flows of low Reynold's number since the dissipative wave number increases with Reynold's number. For unbounded flows the Reynold's number restriction may not be important. At present, direct simulations involve a large amount of CPU time but one of their uses is to test turbulent closure schemes used in the large eddy simulations.

A recent review of 3–D simulation of incompressible turbulent flows is given by Rogallo and Moin (1984).

I think a number of points should be evident from the above brief review. Firstly, in order to construct detailed models of fully turbulent extragalactic jets complex turbulent modelling is required in order to take acount of the range of densities and Mach numbers involved. Such modelling should involve reasonably sophisticated turbulent closure schemes or detailed 3–D hydrodynamic codes. Secondly, the α–law turbulent viscosity used in accretion disc theory is not relevant to jets. The basic reason for this is that the turbulent kinetic energy is produced by the shear and can not simply be proportional to the jet pressure. Thirdly, none of the turbulent closure schemes for laboratory flows can cope with the Mach number dependence of the turbulent stress. This is of course important to the modelling of supersonic jets. Possibly, a comprehensive theory of extragalactic jets may shed some light on the Mach number dependence of the laboratory results but at present the application of laboratory analyses to supersonic turbulent extragalactic jets is limited. A fourth point is that in the extragalactic context the turbulent stresses are possibly sensitive to the scale height of the atmosphere. For instance, a jet may not become

as fully turbulent as its laboratory counterpart if a sound wave can not propagate across it in a scale height.

So what hope is there for the extragalactic jet theorist? Is it possible to construct some sort of simple analysis of turbulent jet flows which addresses the crucial observations of spreading rate and surface brightness? In the remainder of this paper I shall give an account of one attempt at such an analysis. It is based on the notion that the spreading rate, velocity variation, and dissipation rate of a jet are all related and that one can determine the second and third quantities from the first. Thus, if one temporarily abandons the goal of determining *both* spreading rate and surface brightness from a jet model one can use the first to infer the second. The procedure is analogous to the inference of the surface brightness of a laminar adiabatic jet from the spreading rate. (This gives the well known relation $I_\nu \propto \Phi^{-3.4}$ for the perpendicular field region of such a jet with a spectral index of $0 \cdot 6$.)

A notable omission from the above discussion is the effect of magnetic fields on the turbulent dynamics of jets. In the following the magnetic pressure is neglected compared to the particle pressure. This is certainly a reasonable initial approximation. It is also my opinion that there is no compelling evidence that magnetic fields are dynamically important. There is of course the argument that the collimation of jets like NGC315 and 3C31 is due to magnetic confinement. I shall present arguments that this collimation can be understood if the possibility of subsonic jets is admitted.

V An Integral Approach

In order to infer the surface brightness from the spreading rate it is useful to consider integral relations deduced from the Favre–averaged turbulent equations. These are used to infer the central values of various quantities (denoted by a subscript c). Transverse profiles of variables have to be asumed but the results are generally insensitive to these. Integrating $(3 \cdot 4)$, the equation for the z–momentum, across the jet gives

$$\frac{d}{dz}\int_0^\infty \bar{\rho}\tilde{v}_z^2 r\, dr = \frac{dP}{dz}\int_0^\infty \frac{\bar{\rho}-\rho_{ext}}{\rho_{ext}} r\, dr \qquad (5 \cdot 1)$$

where ρ_{ext} is the density of material external to the jet. The buoyancy force on the right hand side of this equation arises from the assumption of an hydrostatic atmosphere (with $dP/dz = \rho_{ext} X_z$) and elimination of the gravitational field in $(3 \cdot 4)$ in favour of the pressure gradient and ρ_{ext}.

For constant density jets in a uniform pressure the momentum equation gives the well known result that the jet centreline velocity v_c is proportional to z^{-1} (see Landau and Lifshitz 1975). However, in our context there are variations in jet density (both across and along the jet) and the jets are driven by the pressure gradient of the galactic atmosphere. An equation for the specific enthalpy (given below) can actually be used to derive an approximate equation for the jet velocity. However, I shall first give a simple derivation of this velocity law followed by a more complicated one which shows more clearly the assumptions upon which it depends.

Let us assume that the jet pressure is dominated by relativistic particles and that the dissipation of turbulent energy is negligible. Then the jet pressure

$$P \propto n_{rel}^{4/3} \qquad (5 \cdot 2)$$

where n_{rel} is the number density of relativistic particles. Since there is no entrainment of relativistic particles then

$$n_{rel}\, v_c\, a^2 \approx constant \qquad (5 \cdot 3)$$

Combining these two equations implies

$$v_c \propto a^{-2}\, P^{-3/4} \qquad (5 \cdot 4)$$

Now the more complicated derivation. A useful equation for the specific enthalpy can be derived from the first law of thermodynamics which in non–averaged form can be written

$$\rho\frac{dh}{dt} - \frac{dP}{dt} = \rho\mathbf{A} \qquad (5 \cdot 5)$$

where h is the specific enthalpy and A is the rate of turbulent dissipation per unit mass. Favre averaging and specializing to axisymmetric, stationary flow gives

$$\frac{\partial}{\partial z}(\bar{\rho}\tilde{h}\tilde{v}_z) + \frac{1}{r}\frac{\partial}{\partial r}(r\bar{\rho}\tilde{h}\tilde{v}_r) = -\frac{1}{r}\frac{\partial}{\partial r}(r\langle\rho h' v_r'\rangle) + \tilde{v}_z\frac{dP}{dz} + \bar{\rho}\tilde{\Lambda} + \langle v_\alpha'\frac{\partial P}{\partial x^\alpha}\rangle \qquad (5\cdot 6)$$

In this equation the left hand side represents the advection of enthalpy, the first term on the right represents turbulent diffusion of enthalpy, the second term adiabatic cooling, the third term dissipative processes, and the fourth term the work done on the turbulent fluctuations by the pressure. The turbulent dissipation in the jet is of order $\rho v'^3/a$ Landau and Lifshitz (1975) as is the term $\langle v_\alpha'\partial P/\partial x^\alpha\rangle$ (Wygmanski and Fiedler 1969). The previous estimate of the turbulent velocity ($v' \sim (a/L)^{1/2} v_c$) can be used to show that dissipation is unimportant in jets with Mach numbers of order unity, at least in the first approximation. Specifically, it can be shown from equation $(5\cdot 6)$ that the length scale for change in the enthalpy flux due to dissipation is

$$L_h \sim \frac{4P}{\rho v_c^2}\left(\frac{a}{L}\right)^{-3/2} a = 3M_c^{-2}\left(\frac{a}{L}\right)^{-1/2} L \qquad (5\cdot 7)$$

where M_c is the central Mach number. Thus for $M_c \sim 1$, L_h is about an order of magnitude greater than L, the length scale for the change of the velocity. Moreover, this estimate of the length scale L_h is an underestimate because the integration of quantities like dissipation across the jet generally leads to lower estimates than that indicated by the peak values.

Neglecting dissipation, the following integral equation for the enthalpy flux can be constructed, again by integrating across the jet

$$\frac{d}{dz}\int_0^\infty \bar{\rho}\left(\tilde{h} - \tilde{h}_{ism}\right)\tilde{v}_z r\,dr - \frac{dP}{dz}\int_0^\infty \tilde{v}_z r\,dr = -\frac{d}{dz}\tilde{h}_{ism}(z)\int_0^\infty \bar{\rho}\tilde{v}_z r\,dr \qquad (5\cdot 8)$$

where $\tilde{h}_{ism} = 5kT_{ism}/m_p$ is the specific enthalpy of the interstellar medium with temperature T_{ism}. This equation tells us how the flux of the enthalpy difference (between the jet and the surrounding ISM) varies with distance along the jet due to adiabatic losses and entrainment. Some useful approximations can be made here. Firstly, the rate of change of $\tilde{h}_{ism}$ is exactly zero in an isothermal atmosphere and generally small in the inner regions of a cooling flow so that the right hand side can be neglected. Secondly, if the jet is much hotter (and consequently lighter) than the surroundings ($\tilde{h}(0,z) \gg \tilde{h}_{ism}$) then h_{ism} can be neglected in the integral on the left hand side. The interior of the jet consists of a mixture of relativistic and thermal material so that

$$\bar{\rho}\tilde{h} = 4P(z)\left(1 - \frac{3P_{th}}{8P}\right) \qquad (5\cdot 9)$$

where P_{th} is the thermal pressure. The ratio P_{th}/P increases towards the edge of the jet and at this point the bracketed factor in $(5\cdot 9)$ decreases the integrand in the first term of $(5\cdot 8)$ by about 40%. However, this is in a region of the jet where the velocity is decreasing to zero (I generally take the velocity profile to be Gaussian) and so there is not much lost by neglecting the correction due to the thermal pressure so that

$$\frac{d}{dz}\left[4\bar{P}(z)a^2 v_c\int_0^\infty\left(\frac{v_z}{v_c}\right)\xi\,d\xi\right] - \frac{dP}{dz}v_c a^2\int_0^\infty\left(\frac{v_z}{v_c}\right)\xi\,d\xi \approx 0 \qquad (5\cdot 10)$$

where $\xi = r/a(z)$ is a normalized radius. If the velocity is self-similar then $I_1 = \int_0^\infty v_z/v_c\ \xi\,d\xi$ is constant. If the velocity is not self similar then we assume that I_1 varies slowly with respect to the other quantities. Equation $(5\cdot 10)$ then yields $(5\cdot 4)$. The above derivation shows the assumptions under which this velocity law is valid. The most important assumption is that the jet is both much hotter and lighter than the surounding medium. This assumption is justified by the upper limits on jet density obtained from the absence of depolarization (provided there are not too many field reversals along the line of sight). Insertion of a reasonable pressure gradient and observed spreading rate into $(5\cdot 4)$ generally leads to an inferred velocity decrease. Knowing the rate of change of the velocity one can infer the density variation

from (5·1), the equation for the momentum flux. Usually, this leads to an approximately constant density or one which decreases much more slowly than the density of the corresponding laminar jet (see B84).

VI The Electron Distribution Function

As is known from Fanti et al. (1982) and Perley, Bridle and Willis (1983) deceleration of a jet can have a marked effect upon the electron distribution function and the magnetic field. The purpose of the following two sections is to clearly define the relevant physics.

Let us first consider the relativistic number density which satisfies the non–averaged conservation law

$$\frac{\partial n_{rel}}{\partial t} + \frac{\partial}{\partial x^\alpha}\left(n_{rel} v^\alpha\right) = 0 \qquad (6\cdot 1)$$

The "concentration" of relativistic particles $c = n_{rel}/\rho$ is determined by the (averaged) equation

$$\frac{\partial}{\partial z}\left(\bar{\rho}\tilde{c}\tilde{v}_z\right) + \frac{1}{r}\frac{\partial}{\partial r}\left(\bar{\rho}\tilde{c}\tilde{v}_r\right) = -\frac{1}{r}\frac{\partial}{\partial r}\left(r\langle\rho c' v_r'\rangle\right) \qquad (6\cdot 2)$$

This is a diffusion equation for the mean concentration $\tilde{c}$, the term on the right representing the turbulent diffusion of concentration. Usually, in laboratory jets the concentration profile has the same shape as the enthalpy profile and both tend to be wider than the velocity profile. The important deduction for extragalactic jets is that the visible tracers of the jet flow, the relativistic particles, diffuse at approximately the same rate as the velocity. Integration of the concentration equation across the jet, gives for the central relativistic number density n_c

$$n_c v_c a^2 = constant \qquad (6\cdot 3)$$

showing the longitudinal compression of the particle density by the deceleration of the jet.

Now let us consider the evolution of the phase space distribution function $f(p, x^\alpha, t)$ of the relativistic electrons. This evolves according to

$$\frac{\partial f}{\partial t} + v^\alpha \frac{\partial f}{\partial x^\alpha} - \frac{1}{3}\frac{\partial v^\alpha}{\partial x^\alpha} p \frac{\partial f}{\partial p} = Dissipation\ term + \frac{\alpha}{p^2}\frac{\partial}{\partial p}\left(p^4 f\right) \qquad (6\cdot 4)$$

where $\alpha = 4r_0^2 B^2/9m_e^2 c^2 = 4\cdot 7 \times 10^{-5} B_{-6}^2$ and B is the magnetic field. The last term represents the effect of synchrotron losses which are unimportant for energies below the synchrotron cut–off. The "dissipation term" is the particle acceleration term which is the end result of turbulent dissipation. What one puts here depends upon what is one's favourite theory of particle acceleration. Bicknell and Melrose (1982) showed that Fermi acceleration and weak shock acceleration are promising candidates and are more important than resonant acceleration, for instance. However, when dissipation is an unimportant source of energy, it fortunately does not matter what we put for the particle acceleration term and from now on I shall ignore it.

We can treat this equation in the following way. Take

$$f(p, x^\alpha, t) = n_{rel}^{s/3-1}\, \rho\, q(x^\alpha, t) p^{-s} \qquad (6\cdot 5)$$

The factor $n_{rel}^{s/3-1}$ copes with the awkward factor involving $\partial v^\alpha/\partial x^\alpha$ in (6·4), q is a phase space concentration and the factor p^{-s} means, of course, that we are assuming a power law. Generally $s \geq 4$. (Note that the function q defined here differs from that in B84 by a factor of ρ). The result of this substitution is a conservation law for ρq which on Favre–averaging leads to

$$\frac{\partial}{\partial z}\left(\bar{\rho}\tilde{q}\tilde{v}_z\right) + \frac{1}{r}\frac{\partial}{\partial r}\left(\bar{\rho}\tilde{q}\tilde{v}_r\right) = -\frac{1}{r}\frac{\partial}{\partial r}\left(r\langle\rho q' v_r'\rangle\right) \qquad (6\cdot 6)$$

Again the term on the right represents the turbulent diffusion of the phase–space concentration q and one expects that the profile of this quantity will be the same as the concentration of relativistic particles.

Integrating this equation across the jet and assuming that profile integral varies slowly gives $\rho_c q_c v_c a^2 \approx$ *constant*, so that, from $(6 \cdot 4)$ and $(6 \cdot 5)$,

$$f_c \propto \left(v_c a^2\right)^{-s/3} p^{-s} \qquad (6 \cdot 7)$$

This equation is equivalent to similar equations derived by Fanti et al. (1982) and Perley, Bridle and Willis (1983). The point I wish to bring out here is that it depends upon the turbulent diffusion of the concentration of relativistic particles at a rate proportional to that of the velocity. The variation of f implied by $(6 \cdot 7)$ is independent of whatever relation is taken for the velocity.

VII The Magnetic Field

The treatment of *scalars* such as enthalpy and concentration in a turbulent flow is complex enough but the problem becomes an order of magnitude more difficult when one wishes to treat the the turbulent diffusion (and possibly amplification) of a *vector* such as the magnetic field. However, some simply derived relationships are possible if one limits consideration to a field which is intrinsic to the jet and which has two components, one parallel to the velocity and one toroidal. This is not to imply that the field exists in continuous loops wound around the jet. The field can exist in the form of closed loops with parallel and toroidal components predominating. For such a field configuration,

$$B_z \propto \frac{1}{a^2} \qquad (7 \cdot 1)$$

and

$$B_\phi \propto \frac{1}{v_c a} \qquad (7 \cdot 2)$$

These relations are derived from similar turbulent equations and integral averages to those described above. However, there is not enough space here to go into much detail. A complete treatment is given in B84. The appearance of the factor v_c^{-1} in $(7 \cdot 2)$ reflects the compression of magnetic field by the deceleration of the jet. If there is a significant component of radial field in the jet it will be subject to a similar compressive process as the toroidal field. However, this component will also be sheared and so the exact evolution of such a component is uncertain. For the present, I assume that $B_r \propto v_c^{-1} a^{-1}$ but this remains to be justified.

It is often said that jets can not be very turbulent because of the high degree of polarization. However, the turbulent magnetic field $B' \sim (a/L)^{1/2} \bar{B}$ and is quite consistent with the observed degree of polarization.

VIII Modelling the Surface Brightness of 3C31 and NGC315

I take the peak surface brightness of a jet

$$I_\nu \propto f_c \, a \, B^{(s-1)/2} \qquad (8 \cdot 1)$$

where f_c is given by $(6 \cdot 7)$, the components of B are given by $(7 \cdot 1)$ and $(7 \cdot 2)$ and the velocity is given by the hot jet approximation $(5 \cdot 4)$. The velocity *HWHM*, a, is taken to be proportional to the surface brightness *FWHM*, Φ, an ansatz which is justified by the similar rates of diffusion of all quantities due to the turbulence. All quantities are normalized by their values at the field turnover point and the normalized variables are evaluated in each direction away from this point since that is where $B_\perp / B_z \approx 1$. A spline fit to the FWHM data is used to determine $\Phi(\Theta)$, where Θ is the angular distance from the core.

In order to determine the velocity, a model for the pressure of the galactic atmosphere is used, which is either a power–law or derived from an isothermal, hydrostatic atmosphere sitting in the potential well of a King model galaxy . The King model atmospheres are parametrized by the (optical) core radius r_c and the ratio T/T_* of the temperature of the atmosphere to the stellar kinetic temperature

$$T_* = \frac{\mu m_p}{k} \sigma_p^2 = 6 \cdot 6 \times 10^6 \left(\frac{\sigma_p}{300 \, km \, s^{-1}}\right)^2 K \qquad (8 \cdot 2)$$

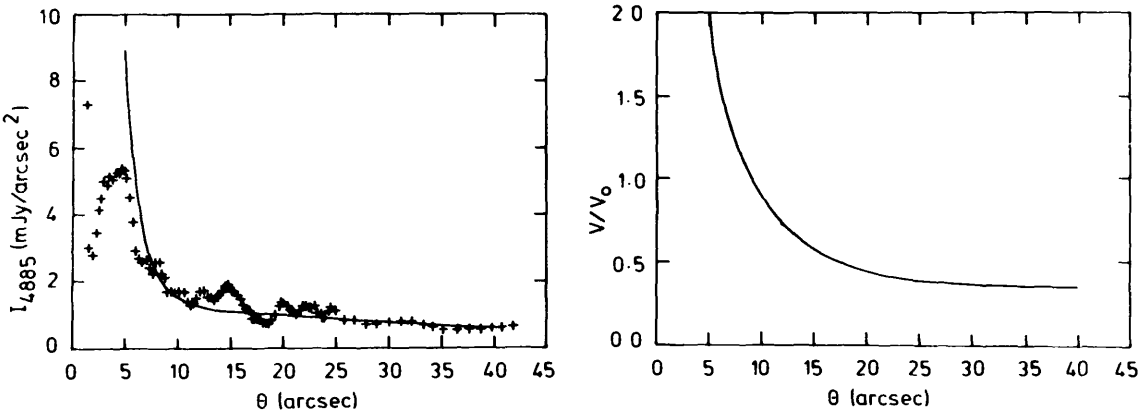

Figure 4. The left hand panel shows a fit to the surface brightness data of Fomalont et al. (1980) on the northern 3C31 jet. The right hand panel shows the inferred velocity variation.

where $\mu \approx 0 \cdot 6$ is the mean molecular weight and σ_p is the projected central velocity dispersion. King models are inapropriate for the outer regions of some (but not all) giant ellipticals which seem to be dominated by massive haloes. Nevertheless, substantial regions of a number of giant ellipticals are well fit by King models (King 1978, Smith and Bicknell 1984, Killeen, Bicknell and Carter 1984), so that the King potential is a good first approximation. In the case of 3C31 (NGC383), an effective radius ($R_e = 23 \cdot 8\ arcsec$) is known from RC2 (deVaucouleurs, de Vaucouleurs and Corwin 1976) implying a core radius, $r_c \approx 2.2\ arcsec$ (see Mihalas and Binney 1981).

The left hand panel of figure 4 shows a model fit to the northern 3C31 jet surface brightness data (Fomalont et al. 1980) with $r_c sin i = 2 \cdot 2 arcsec$ (i = inclination of jet to line of sight) and $T/T_* = 1 \cdot 8$, implying a temperature of $1 \cdot 2 \times 10^7 \left(\sigma_p / 300\ km\ s^{-1}\right)^2 K$. The fit is quite reasonable for $\Theta \geq 5 \cdot 5 arcsec$ but clearly overestimates the data for $\Theta \leq 5 \cdot 5$. It seems reasonably clear that the rise in surface brightness for $\Theta \leq 5 \cdot 5 arcsec$ is due to shock dissipation in view of the disvovery by Butcher, van Breugel and Miley (1980) of knots emitting optical synchrotron in this region. The right hand panel of figure 4 shows the inferred velocity variation of this jet.

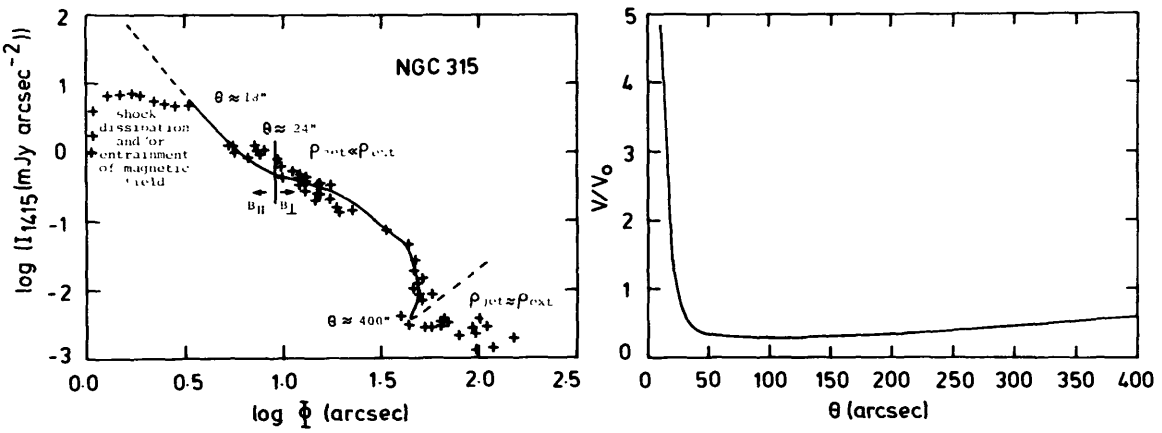

Figure 5.The left hand panel shows a model fit to the NGC315 surface brightness vs FWHM data of Bridle, Fomalont and Henriksen (1984). The right hand panel shows the inferred velocity variation up to 400 arcsec from the core.

The left hand panel of figure 5 shows a similar fit to the NGC315 $I_\nu - \Phi$ data (Bridle, Fomalont and Henriksen 1984). The parameters of this fit are: $T/T_* = 0 \cdot 7$ and $r_c sini = 2 \cdot 0$. This represents quite a plausible temperature for this atmosphere and although there are no published core or effective radii for NGC315 a 2 *arcsec* core radius is reasonable for a galaxy at its redshift. One caveat needs to be made here and that is that NGC315 is an E3 galaxy rather than an E0 and one needs to interpret the value of $r_c = 2 \cdot 0$ as a minor axis core radius and assume that the King model gives a reasonable approximation to the potential on ellipses of constant (optical) surface brightness. The fit shown in figure 5 is not the only fit that can be obtained. As one increases (decreases) the parameter $r_c sini$ the parameter T/T_* increases (decreases) in order that a fit be obtained.

Perhaps two of the outstanding features on the model fit to the NGC315 data are the regions $\Theta < 18$ *arcsec* and $\Theta > 400$ *arcsec* which are *not* fit by the model. As with the 3C31 jet dissipation is required for it to turn on and this may explain the rising then flat surface brightness profile less than 18 *arcsec* from the core. The entrainment of magnetic field may also be important here. The unsatisfactory fit at greater than 400 *arcsec* from the core may be due to one of two causes. Firstly, the King model atmosphere flattens out in this region to a constant pressure. This is the pressure that is required to keep the atmosphere hydrostatic. It would be more reasonable for the pressure in this region to be determined by the gravitational field of the NGC315 group. Secondly, the model described has to break down eventually since the jet density will not stay less than the decreasing background density forever. Thus it is possible that the sudden change in slope of the $I_\nu - \Phi$ relation at $\Theta \approx 400$ represents the point at which $\rho_{jet} \approx \rho_{igm}$. If this is the case, then calculations of the density variation in the jet show that the ratio ρ_{jet}/ρ_{ism} would be approximately 10^{-2} at the field turnover point. The minimum number density required to confine the jet is $\approx 5 \times 10^{-3}$ at this point 24 *arcsec* from the core implying a jet number density of at least 5×10^{-5}. For reasons which are apparent below I favour this explanation for the surface brightness behaviour for $\Theta > 400$.

The inferred velocity in this jet is also shown in the right hand panel of figure 5. The velocity decreases quite rapidly for $\Theta < 50$ but increases slowly thereafter in the "collimation plateau" of this jet (see figure 6). I shall now discuss the implications of this behaviour.

IX The $\Phi - \Theta$ Relation and Turbulent Jet Dynamics–Buoyant Collimation

Although the major thrust of this paper has been to describe the derivation of surface brightness variations from observed spreading rates it is possible to make some semi–quantitative statements about the observed $\Phi - \Theta$ behaviour. The $\Phi - \Theta$ data for both the 3C31 (Bridle et al. 1980), and NGC315 (Willis et al., 1981, Bridle 1982) jets are shown in figure 6. Neither jet shows the *constant* spreading rate of laboratory jets. NGC315, in particular, presents some paradoxes for the model presented here. Why does the jet collimate at about $100 - 400$ *arcsec* from the core if its initial expansion is due to turbulence; why does it reexpand after $\Theta \approx 400$ and why does its velocity slowly increase in the collimated region? I believe the following considerations are important in answering these questions.

Consider the two following equations for the mean velocity components $\tilde{v}_z$ and $\tilde{v}_r$.

$$\tilde{v}_z \frac{\partial \tilde{v}_z}{\partial z} + \tilde{v}_r \frac{\partial \tilde{v}_z}{\partial r} = -\frac{1}{\bar{\rho}} \left(1 - \frac{\bar{p}}{\rho_{ext}}\right) \frac{dP}{dz} - \frac{1}{\bar{\rho} r} \frac{\partial}{\partial r} \left(r \langle \rho v_r' v_z' \rangle\right) \qquad (9 \cdot 1)$$

$$\frac{\partial}{\partial r}\left(\frac{r\tilde{v}_r}{\tilde{v}_z}\right) = \frac{r}{\bar{\rho}\tilde{v}_z^2} \frac{dP}{dz} \left(1 - \frac{\bar{p}}{\rho_{ext}} - M^2\right) + \textit{turbulent terms} \qquad (9 \cdot 2)$$

Two points are apparent from these equations. Firstly, from $(9 \cdot 1)$, the equation for $\tilde{v}_z$, it is evident that in a light jet propagating through a steep pressure gradient, the buoyancy term (the first term on the right) may be able to counteract the velocity decreasing effect of the second term (the turbulent diffusion term). Using Prandtl's turbulent viscosity to estimate the shear stress to order of magnitude, it is easy to show that there is a critical velocity, given by

$$v_{crit}^2 \sim 4 \left(\frac{a}{H}\right) \left(\frac{P}{\rho_{jet}}\right) \left(1 - \frac{\rho_{jet}}{\rho_{ext}}\right) \qquad (9 \cdot 3)$$

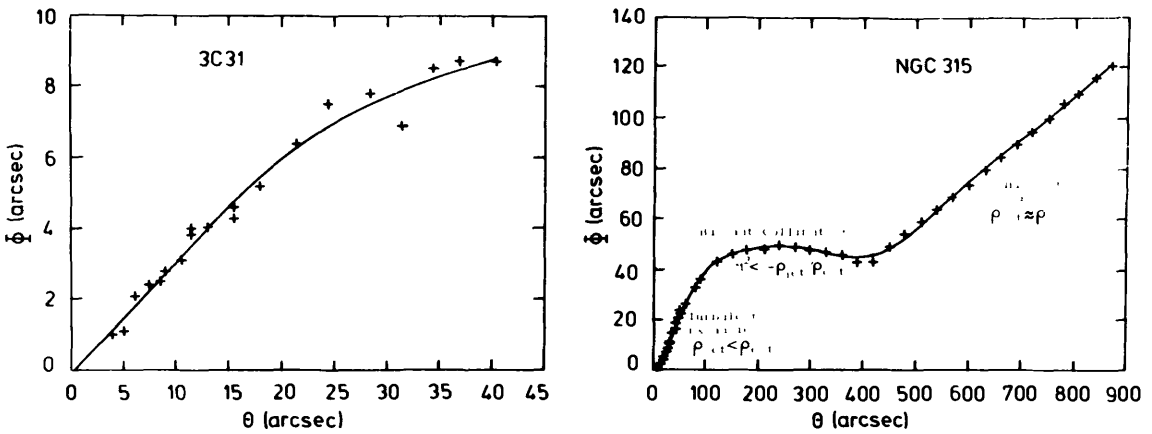

Figure 6. The FWHM data for the 3C31 and NGC315 jets. Neither jet spreads at a constant rate. This is possibly due to the jets becoming subsonic and being collimated by the effect of the pressure gradient. The smooth curves are the spline fits to the data used in the surface brightness models.

(H =scale height), at which the two terms balance. The velocity v_{crit} is likely to be subsonic. This situation would also be favoured if there is some reduction in the turbulent stress due to the pressure gradient. Note that the jet is only accelerated so long as it is light ($\rho_{jet} < \rho_{ext}$) and this is consistent with the surface brightness model described above. Secondly, referring to equation $(9 \cdot 2)$ for $\tilde{v}_r/\tilde{v}_z = dr/dz$ where $r(z)$ is a mean streamline, it can be seen that there are two groups of terms, the first proportional to the pressure gradient, and the second group which have been lumped into "turbulent terms". It is this second group which, in the context of laboratory jets, make dr/dz large in the region "outside" the jet (the entrainment region) but which make dr/dz small (of order (a/L)) in the "interior" of the jet. However, when a substantial pressure gradient is involved, and when

$$M^2 < 1 - \frac{\bar{\rho}}{\rho_{ext}} \qquad (9 \cdot 4)$$

that is, when the jet is both subsonic and light, there is an important collimating force on the jet, due to the first term. Again, this term can overcome the effect of turbulent expansion when the velocity is below v_{crit}. The tendency of subsonic laminar jets to collimate is of course well known from the theory of the deLaval nozzle (Landau and Lifshitz 1975, Blandford and Rees 1974) and what I have described here is the turbulent analogue. An important difference is that it is unlikely that such a "turbulent deLaval nozzle" would lead to supersonic flow. The jet continues to entrain during the collimation region and eventually reaches the state where it is approximately the same density as the surrounding medium. It then has no choice but to expand and decelerate again. This is why I think the outer expanding region of the NGC315 jet which is also slowly declining in surface brightness (indicative of deceleration) corresponds to where $\rho_{jet} \approx \rho_{igm}$. So here we have another indication that jets which initially expand at a wide cone angle are indeed subsonic over a significant fraction of their entire lengths. I think that this process of "buoyant collimation" is more appealing than magnetic confinement because of the well-known instability of the latter.

X Implications of the Global Energy Balance

Some further questions arise about the viability of low Mach number models for jets. Can they supply the necessary energy to power the lobes? Is the estimate of a low Mach number consistent with estimates of the sound speed? Consider the total energy flux across a given jet cross section

$$F_E = 2\pi \int_0^\infty \left(\bar{\rho}\tilde{h}\tilde{v}_z + \frac{1}{2}\bar{\rho}\tilde{v}_z^3 \right) r\, dr \qquad (10 \cdot 1)$$

where the Poynting flux has been neglected because of the weak magnetic field. (Incidentally the magnetic field generally stays weak). The first term in the above integrand (the heat flux) dominates for $M^2 < 6$. Furthermore, when integrated across the jet, the dominance of the first term is even greater. Thus for low Mach number jets the first term is the only important one. With $\tilde{\rho h} \approx 4\bar{P}$, taking a gaussian profile for $\tilde{v}_z$ with the $HWHM$, $a = \Phi/2$ gives

$$F_E \approx 4.4 \times 10^{41}\, P_{-10} v_8 \left(\frac{\Phi}{Kpc}\right)^2 \qquad (10 \cdot 2)$$

(An almost identical relation arises when the velocity profile is a top–hat). An important corollary of the dominance of the energy flux by the heat flux is that, assuming (conventionally) that a large amount of the internal energy is in the form of relativistic electrons, the energy is in a form which is easily radiated. Thus the synchrotron plus inverse Compton luminosity in the lobes is a substantial fraction (η) of the energy flux through the jet. Adiabatic losses in the lobes need to be considered but it seems that a reasonable fiducial value of η is $0 \cdot 25$ (see Bicknell 1984b). Thus an estimate for the jet central velocity at any point in the jet (but most usefully the field turnover point since the surface brightness model has been normalized in terms of values at that point) is

$$v_8 = 0 \cdot 9 \left(\frac{\eta}{0 \cdot 25}\right)^{-1} \left(\frac{L_S + L_{IC}}{10^{41} erg\, s^{-1}}\right) \left(\frac{P}{P_{min}}\right)^{-1} P_{min,-10}^{-1} \qquad (10 \cdot 3)$$

Estimating L_{IC} from the minimum energy magnetic fields in the lobes and the synchrotron luminosity L_S I obtain for the velocities of the 3C31 and NGC315 jets at the field turnover points, $v_8 = 4 \cdot 9(P/P_{min})^{-1}(\eta/0 \cdot 25)^{-1}$ and $v_8 = 4 \cdot 6(P/P_{min})^{-1}(\eta/0 \cdot 25)^{-1}$ respectively. The sound speeds at the turnover points in the two jets ($v_s = (4P/3\rho)^{1/2}$) are $v_{s,8} = 5 \cdot 1(P/P_{min})^{1/2} n_{-4}^{-1/2}$ for 3C31 and $v_{s,8} = 2 \cdot 4(P/Pmin)^{1/2} n_{-4}^{-1/2}$ for NGC315. Thus, for pressures a little higher than the minimum pressures, and number densities around $10^{-4} cm^{-3}$, the jet Mach numbers are about unity. The inference that the jet pressure is somewhat higher than the minimum pressure is consistent with the neglect of the dynamical effect of magnetic fields. A thermal number density around $10^{-4} cm^{-3}$ is consistent with the assumption of a light jet.

XI Summary

There are good reasons for thinking that the Mach numbers of jets in low luminosity sources are of order unity and in some cases less than unity for a significant fraction of the jet length. These are the following: (1) Supersonic laboratory jets can become subsonic within a few nozzle diameters. (2)The surface brightness variations of two jets can be understood in terms of deceleration of low Mach number non–dissipative jets (3) The $\Phi - \Theta$ behaviour of the NGC315 jet is plausibly due to the combined effect of turbulent processes and the buoyancy force acting on a light subsonic jet. For some time there has been a consensus that subsonic jets are creatures of somewhat dubious respectability. After all, aren't subsonic jets bent easily and aren't they subject to severe disruption by the Kelvin–Helmholtz instability? However, as Jones and Owen (1979) pointed out the atmosphere of a giant elliptical can shield it from the ram pressure of the IGM and shielded jets are bent much less than naked jets. Furthermore, the radius of curvature is inversely proportional to the square of the galaxy's velocity and this is often quite small. The Kelvin–Helmholtz instability is a virtue rather than a vice. It is that which leads to the development of turbulence which, as we have seen, can modify the jet dynamics considerably and lead to the observed slow surface brightness variations. Subsonic, of course, does not imply slow if the jet number density is low enough. This quantity is notoriously difficult to estimate (see Laing, these proceedings). However, the values used here are consistent with lack of depolarization and not too many field reversals. One of the limitations of the model I have described here is that it depends upon the jet being much lighter than the surroundings. Because of entrainment and the decreasing density of ther background this will not always be the case and as we have seen the model for NGC315 eventually "blows up". However, models to treat jets of arbitrary density ratio are currently being developed and should be aplicable to the outer plume–like regions of radio sources as well as being applicable to the outer regions of NGC315.

Another important point about light, subsonic, extragalactic jets is that they survive for a longer distance than their laboratory counterparts. This is due to the buoyant driving force associated with the pressure gradient which leads to a slower rate of decline of velocity. An interesting comparison can be made between the two radio sources dealt with here. 3C31 and NGC315 have similar total luminosities but NGC315 is a much larger source. I think that the difference is due to the fact that the pressure gradient in NGC315 required to fit the surface brightness of the jet is much steeper than that of 3C31. Approximately, $P \propto z^{-2.5}$ for the former, whereas $P \propto z^{-1.1}$ for the latter.

Acknowledgements.

The pressure cooker belongs to Bob Gingold who collaborated in taking the photographs. I have benefited greatly from correspondence with Professor P. Bradshaw of Imperial College London and from collaboration with Neil Killeen.

References

Bicknell G.V., 1984a, *Ap.J.*, in press, Nov 1
Bicknell G.V., 1984b, *In preparation.*
Bicknell G.V. and Melrose D.B., 1982, *Ap.J.*, **262**, 511
Birch S.F. and Eggers J.M., 1972, in *Free Turbulent Shear Flows, NASA SP-321*, 11
Blandford R.D. and Rees M.J., 1974, *Mon. Not. R. Astr. Soc.*, **169**, 395
Bradshaw P., 1981, in *The 1980-1981 AFOSR-HTTM Conference on Complex Turbulent Flows*, Thermosciences Division, Mechanical Engineering Department, Stanford University, Stanford, California
Bradshaw P., 1984, *Private Communication.*
Bridle A.H., 1982, in *Extragalactic Radio Sources, IAU Symposium No. 97*, ed Heeschen D.S. and Wade C.M., D. Reidel, Dordrecht, Holland.
Bridle A.H., 1984, *A.J.*, **89**, 979
Bridle A.H., Fomalont E.B., and Henriksen R.N., 1984, *In preparation.*
Bridle A.H., Henriksen R.N., Chan K.L., Fomalont E.B., Willis A.G., and Perley R.A., 1980, *Ap.J.(Lett.)*, **241**, L145
Brown G.L. and Roshko A., 1974, *J. Fluid Mech.*, **64**, 774
Butcher H., van Breugel W., and Miley G.K., 1980, *Ap.J.*, **235**, 749
de Vaucouleurs G., deVaucouleurs A., and Corwin H.G., 1976, *The Second Reference Catalogue of Bright Galaxies*, University of Texas Press, Austin
Chen C.J. and Rodi W., 1980, *Vertical Turbulent Buoyant Jets* , Pergamon Press, Oxford
Era Y. and Saima A., 1977, *Bulletin JSME*, **20**, 63
Fanti R., Lari C., Parma P., Bridle A.H., Ekers R.D., and Fomalont E.B., 1982, *Astron. Astrophys.*, **110**, 169
Favre A., 1969, in *Problems of Hydrodynamics and Continuum Mechanics*, Soc. for Ind. and App. Math., Philadelphia, Pennsylvania.
Fomalont E.B., Bridle A.H., Willis A.G. and Perley R.A., 1980, *Ap. J.*, **237**, 418
Jones T.W. and Owen F.N., 1979, *Ap.J.*, **234**, 818
Killeen N.E.B., Bicknell G.V. and Carter D., 1984, *Ap.J.*, submitted.
King I.R., 1978, *Ap.J.*, **222**, 1
Landau L. and Lifshitz E.M., 1975, *Fluid Mechanics*, Pergamon Press, Oxford
Lau J.C., 1981, *J. Fluid Mech.*, **105**, 193
Launder B.E., 1979, in *Turbulent Shear Flows I*, 259, ed. Durst F. et al., Springer Verlag, Berlin.
Launder B.E. and Morse A., 1979, in *Turbulent Shear Flows I*, 279
Launder B.E., Morse A., Rodi W. and Spalding D.B., 1973, in *Free Turbulent Shear Flows, NASA SP-321.*
Love E.S., Grigsby C.E., Lee L.P. and Woodling M.E., 1959, *NASA TR R-6.*
Mihalas D. and Binney J., 1981, *Galactic Astronomy* , 2nd edition, Freeman, San Francisco.
Morris P.J., 1976, *AIAA Journal*, **14**, 1468
Norman M.L., Smarr L., Winkler K.-H.A. and Smith M.D., 1982, *Astron. Astrophys.*, **113**, 285
Norman M.L., Smarr L., and Winkler K.-H.A., 1984, *Preprint.*

Perley R.A., Bridle A.H. and Willis A.G., 1984, *Ap.J.Suppl.Ser*, **54**, 291
Perley R.A., Willis A.G. and Scott J.S., 1979, *Nature*, **281**, 437
Reynolds W.C. and Cebeci T., 1976, in *Turbulence*, ed. Bradshaw P., Springer Verlag, Heidelberg.
Rogallo R.S. and Moin P., 1984, in *Ann. Rev. Fluid Mech.* , **16**, 99
Sanders R.H., 1983, *Ap.J.*, **266**, 73
Schetz J.A., 1980, *Injection and Mixing in Turbulent Flow*, American Institute of Aeronautics and Astronautics, New York.
Smith R.M. and Bicknell G.V., 1984, *Ap.J.*, submitted
Troutt T.R. and Mclaughlin D.K., 1982, *J. Fluid Mech*, **116**, 123
Willis A.G., Strom R.G., Bridle A.H. and Fomalont E.B., 1981, *Astron. Astrophys.*, **95**, 250
Wygmanski I. and Fiedler H.E., 1969, *J. Fluid Mech.*, **38**, 577

DISCUSSION

Chris O'Dea. You may have trouble applying your model to NGC1265. The continuity equation, nr^2v =const., can be combined with Euler's equation to give the bending scale length as a function of beam velocity and radius. The observed gradual bending of the beam constrains the deceleration of the beam to be significantly less than that required to account for the brightness evolution using *only* adiabatic compression. Thus, *in situ* dissipation of the beam kinetic energy seems required to power the radio emission.

Geoff Bicknell. In higher powered sources than the ones I have considered here I think it is highly likely that the surface brightness is due to a combination of particle acceleration by shocks and adiabatic deceleration. Incidentally, the "n" I was referring to is the relativistic number density; the flux of *relativistic* particles is being conserved when I write na^2v =const. I did not mean to imply that the flux of thermal particles is constant, which of course it is not in an entraining jet.

Jack Burns. There has been much discussion in this Workshop of applying laboratory results of turbulent flow to extragalactic jets. However, no one has addressed whether or not these lab results really scale. This is questionable since the Reynolds numbers of these two "jets" are very different. Can you comment ?

Geoff Bicknell. I don't think it matters that the Reynolds numbers of the two types of flows are different so long as they are both large. The two most important parameters to take into account when assessing the relevance of laboratory flows are most probably Mach number and density ratio.

Dick Henriksen. Many lab results are sensitive to the details of the apparatus, particularly the development of turbulent structure. Moreover they are often (almost always) in *uniform media.* The very large Reynolds numbers likely in astrophysical jets give a very long expected lifetime for the large scale structure compared to that of the dissipation scale. Large scale *pressure driven flow* is more likely astrophysically.

GLOBAL INVARIANTS OF A MEAN FLUID FLOW AND LOCAL TURBULENT SUBSTRUCTURE

R.N. Henriksen
Canadian Institute for Theoretical Astrophysics
University of Toronto, Toronto, ON M5S 1A1, Canada

Fluid turbulence is presumably fully described by exact solutions of the Navier-Stokes equations which contain a sufficient array of spatial and temporal scales. Unfortunately such solutions are not known and if they were known they would be so complex in general as to be useless in practice. There is one exception to this state of affairs, which is to be the subject of this paper, and that is when the various scales are coupled by a renormalizing constraint such as local self-similarity. Fortunately, the real significance of the discovery of the universality of the Kolmogorov Cascade, is that such coupling does occur, at least asymptotically. More traditionally, various means of 'filtering' the Navier-Stokes equations in time and space have been adopted, which aim at reducing the amount of information to a measurable set. Unfortunately, it is never quite clear which information should be suppressed.

In particular, the classical Reynold's decomposition into fluctuating and mean flow (with 'one point correlations' i.e. Reynold's stresses) fails to include the spatial and temporal phase information that seems to be required in order to understand 'coherent structures' and temporal intermittancy or 'bursting' (e.g. Hussain, 1983). The more relevant treatment in this case describes the turbulence in terms of multi-point, multi-time correlations (e.g. Favre, 1983). These are also essential in principle for understanding how turbulence diffuses throughout the mean volume of the flow from onset. It is unlikely to be volume filling as is usually assumed, but rather to have a fractal dimension. This could effect estimates of spatial and temporal derivatives of the turbulent energy, and hence their coupling to the coherent structures of the mean flow.

Astrophysically it is important that we have some 'a priori' method of describing the structure of turbulence, because it may well occur in a wide range of unfamiliar circumstances, so rendering reasoning by laboratory analogy uncertain. Although characterizing a turbulent flow by its Reynolds number, Mach number, turbulent age, amplitude of disturbances and so on is a useful classification, the initial conditions and the boundary conditions must be the determining factors. With these we include any globally conserved quantities (e.g. linear or angular momentum et cet.) or global parameters (such as those required to prescribe pressure gradients, density distributions, magnetic fields et cet. each of which also defines a global invariant or conserved

quantity) including those associated with the turbulent substructure itself (e.g. initial spectrum, interscale coupling by constant energy transport or angular momentum transport et cet.). Our objective is to find a method of linking the character of the subscale turbulence to these global quantities and hence to the mean flow. In this way we can deal with the possibility of the turbulent acceleration of particles (e.g. HBC≡ Henriksen, Bridle and Chan, 1982; EH≡ Eilek and Henriksen, 1983) in a way which is sensitive to the environment. Moreover, our arguments suggest a way of calculating the mean flow by using an appropriate viscosity due to the turbulent substructure in the Navier-Stokes Equations. Our method has already been used to discuss turbulence in the interstellar medium (Henriksen and Turner, 1984), but we proceed here by first using it to duplicate and extend classical work on two point correlations. Some of these results also have astrophysical interest.

§1 Two Point Correlations and Local Self-Similarity

We define the phase sensitive two point - two time tensor velocity correlations as (up to moments of the third order)

$$R^{i,j} \equiv \langle u^i \acute{u}^j \rangle, \quad R^{ik,j} \equiv \langle u^i u^k \acute{u}^j \rangle, \quad R^{i,kj} \equiv \langle u^i \acute{u}^k \acute{u}^j \rangle \qquad (1)$$

where $\langle\ \rangle$ denotes ensemble average, and $u^i = u^i(\underset{\sim}{x},t)$, $\acute{u}^i = u^i(\underset{\sim}{\acute{x}},\ t+\tau)$.

Since our discussion is mainly to be an illustration of a more general method, we restrict ourselves to stationary, homogenous, isotropic, incompressible turbulence. It is then sufficient to set $\tau = 0$ and to work with the two point correlations in the 'comoving frame' (this requires knowing the 'celerity' of the turbulence, which is not always evident but usually exists, by the Taylor hypothesis). Then with quantities defined in the special comoving coordinate system of fig. 1.

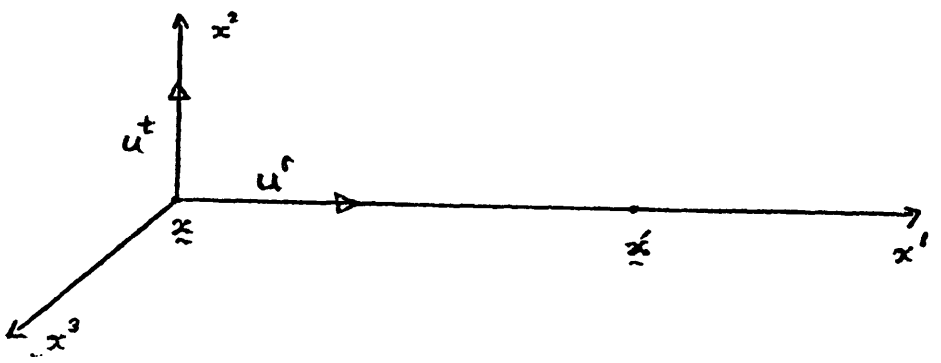

Fig. 1

Von Kármán and Howarth (1938) show that ($r \equiv |\underset{\sim}{x}' - \underset{\sim}{x}|$

$$(1/2)\partial_t R^{r,r} - \frac{\nu}{r}\left[4\frac{\partial R^{r,r}}{\partial r} + r\frac{\partial^2 R^{r,r}}{\partial r^2}\right] + \frac{4R^{r,tt}}{r} + \frac{\partial R^{r,tt}}{\partial r} = 0, \qquad (2)$$

where ν is the true kinematic viscosity.
Now this only relates the second order moment to the third order moment, reflecting the usual closure problem. But we have two powerful results to assist us at this point, one experimental and the other theoretical. Experimentally, once the cascade is established, turbulence in this range has a spatio-temporal scale invariance. That is, turbulent motions do not have independent characteristic lengths and times, but rather the two are coupled in a way which depends on the global parameters (this is usually given as a statement about the velocity scale of the motion, e.g. $V(r) \propto r^{1/3}$ for Kolmogorov range). This constraint can always be written as

$$\xi \equiv r/(V(t)t) \equiv \frac{r^2/t}{rV(t)} \qquad (3)$$

where ξ, the similarity variable or local Reynolds number, is constant in the cascade, and $V(t)$ is a velocity whose functional form depends on the global parameters. The turbulent velocities can only be expressible as $r^{\gamma}u(\xi)$ in order to give the 'scale invariance' associated with the cascade range. It is as though much of the phase information associated with the initial conditions and with the boundary conditions has been 're-normalized' away. We shall refer to this condition variously as self-similar invariance, renormalized or fixed point turbulence or the cascade range.

The theoretical result is argued most clearly by Batchelor (1959) where he shows that the exact probability distribution implied by the infinite expansion in moments of all orders is equivalent to the exact solution of the Navier-Stokes equations plus random initial conditions. Hence since our renormalized turbulence is an 'observed behaviour' of the exact solution, it follows that none of the momements should introduce dependences on r and t other than through ξ. Otherwise they would not produce the cascade range on setting ξ = const.

§2 Application to Decaying or Low Reynolds Number Turbulence

As an example of the power of this realization, let us consider the decay of 'free turbulence', with low local Reynolds number ξ. This has been injected by some disturbance (e.g. an obstacle or a vigorous shear) and is now decaying by viscous damping in the comoving frame of the undisturbed mean flow. Suppose that A is a global invariant which characterizes the initial state of the turbulence. We can always take $[A] \equiv L^p T^q$ (4)

since M can always be removed by using the constant density ρ. Now with A and ν dimensionally independent there is more than one choice for the form of ξ. However, as we are studying the viscous decay of the cascade range, r^2/ν should be the characteristic time for the scale r. Hence we use

$$\xi = r^2/\nu t, \qquad (5)$$

which we expect to have moderately large values initially. It decreases in time as the fluid motion decays.

Moreover, the only possible choices for the functional form of the moments occurring in (2) which depend on A and ν are, by dimensional analysis,

$$R^{r,r} = \frac{A\,\nu^{1-p/2}}{t^{1+q+p/2}}\, f(\xi) \qquad (6)$$

and

$$R^{r,tt} = \frac{\nu}{r}\frac{A\nu^{1-p/2}}{t^{1+q+p/2}}\, h_1(\xi) + \nu\frac{\partial}{\partial r}\left[\frac{A\nu^{1-p/2}}{t^{1+q+p/2}}\, h_2(\xi)\right]$$

Now note that $R^{r,r}$ ($\xi=0$) is simply one third the square of the exact velocity at the reference point (r=0), which scaled value must depend only on ξ in the self-similar cascade. It is reasonable then to expect the exact solution in the cascade to depend only on $f(\xi)$ and its derivatives to all orders for all $\xi\neq 0$ by a Taylor expansion about $\xi=0$. Recalling that the exact solution is also expressed in terms of the moments expansion, this requires all functions h_n to be linearly dependent on f. Consequently $h_1=\alpha_1 f$ and $h_2=\alpha_2 f$ where α_1,α_2 are arbitrary constants. There now follows ($f^1 \equiv df/d\xi$)

$$R^{r,tt} = (\nu/r)\frac{A\nu^{1-p/2}}{t^{1+q+p/2}}\,(\alpha_1 f(\xi) + \alpha_2 \xi f^1(\xi)), \qquad (7)$$

and so closure of equation (2) has now been effected for the cascade range. Equation (2) becomes in fact

$$-(1/2)(\alpha f + \xi f^1) - 10f^1 - 4\xi f^{11} + 3(\alpha_1 f + \alpha_2 \xi f^1)/\xi + 2\frac{d}{d\xi}(\alpha_1 f + \alpha_2 \xi f^1) = 0, \qquad (8)$$

where $\alpha \equiv 1+q+p/2$, which agrees with the rather brilliant deductions of Sedov (1982: eq. 4.50 and eq. 4.42). This yields a hypergeometric function for f which we need only investigate when we wish to follow the evolution away from the fixed point. Useful conclusions regarding the cascade follow simply from the forms of equations (5), (6) and (7). Consider the following examples.

In the first instance suppose [A] are not independent of [ν] (A might be specific angular momentum) so that p=2, q= -1. Then (5) and (6) give immediately

$$R^{r,r} = f(\xi)\ A/t = \nu\xi\ f(\xi)\ A/r^2, \qquad (9)$$

so that $\langle u^2\rangle/3 \equiv R^{r,r}(o) \propto t^{-1}$ describes the decay of the turbulent intensity. If this were to apply say to the free decaying turbulence in a diffuse tail source, then if the mean velocity obeys the law $dx/dt \propto x^{-a}$ we see that $\langle u^2\rangle/3 \propto x^{-(1+a)}$. Eq. (9) also shows that the spectral form of this dying cascade ($\xi=\xi_f$ say) is $E(k) \propto k$, which would not yield any particle acceleration according to EH. The boundary between the persisting inertial range and the damped region is given from $\xi=\xi_f$, that is $r=(\xi_f\nu)^{1/2}t^{1/2}$. Thus the small scales damp first (as ξ declines from ξ_f) and the viscous boundary moves upscale as $t^{1/2}$. Strictly, we must demonstrate from (8) that ξ declining leads to f declining, but the physical result seems clear.

A more elaborate example is furnished by taking the initial turbulence to be a Kolmogorov cascade (in the sense that there is a global parameter $[A]\equiv[K]$ where K is the constant specific energy per unit time exchanged between scales) but at low local Reynolds number (essentially ξ) so that viscosity is important throughout the range. Then p=2 and q=-3 in the preceding arguments yielding

$$R^{r,r} = Ktf(\xi) = (Kr^2/\nu)\ f(\xi)/\xi \qquad (10)$$

Consequently $\langle u^2\rangle/3 \propto t$ until the damping wave at $\xi=\xi_F$ passes over that scale. In the cascade range $\sqrt{R^{r,r}} = \sqrt{(K/\nu)f_F/\xi_F}\ r$ indicating the predominance of undamped large scale correlations or coherent structures. In particular, the consistent turbulent energy spectrum is not Kolmogorov, rather $E(k) \propto k^{-3}$, which is very steep. Such low local Reynolds number turbulence is unlikely to occur astrophysically except on the finest scales, or in the weakest state.

§3 Extention to High Local Reynolds Number Turbulence

At high local Reynolds numbers the true viscosity is dynamically unimportant. Otherwise our approach is the same as that in §2. Here, however, only the global parameter A will be allowed to influence the form of the turbulence. Moreover, if in equation (2) the viscous term is retained, then the viscosity coefficient must be interpreted as being due to the 'subscale turbulence' relative to the scales r,t. Moreover, to within a numerical factor, this too will be determined by the global parameter A. Thus putting these requirements together with the arguments of §2 we find

$$\xi = r/(t\,Y(t)),\quad Y(t) = (A/t^{q+p})^{1/p},$$
$$\nu = \nu_0 r Y(t), \qquad (11)$$
$$R^{r,r} = Y^2 f(\xi),\quad R^{r,tt} = Y^3(\alpha_1 f + \alpha_2 \xi f^1)$$

where ν_0 is another arbitrary number. In fact this number will generally be less than 1 and may on occasion even be negative, if the subscales are transferring energy to the larger scales. Equation (2) becomes now

$$-(1/2)(-2(1+q/p)f+(q/p)\xi f^1)-4\nu_0 f^1-\nu_0\xi f^{11}+4(\alpha_1 f+\alpha_2\xi f^1)\xi^{-1}$$
$$+\frac{d(\alpha_1 f+\alpha\xi f^1)}{d\xi}=0, \qquad (12)$$

which has the same general form as (8). This must be solved as before if the details of the decay of the cascade are required. We proceed rather to discover some applications of equation (11).

The high local Reynolds number Kolmogorov cascade follows by setting [A] = [K] so that p= 2 and q = -3. This yields

$$V(t) = (At)^{1/2} \quad \xi = r/(A^{1/2}t^{3/2}), \qquad (13)$$
$$R^{r,r} = At\, f(\xi) = (Ar)^{2/3}\quad f\xi^{-2/3}$$

where in the cascade range $\sqrt{R^{r,r}} \propto r^{1/3}$, $\langle u^2\rangle/3 \propto t$ and $E(k) \propto k^{-5/3}$ as usual. What we gain by this method is the ability to study the detailed decay on a given scale as $\xi = \xi_F$ passes through it, using equation (12). Equation (13) assures us that the evolution proceeds fastest at the smallest scales.

Another example is afforded by Kraichnan (1965) turbulence. Here a magnetic field is coupled to a conducting fluid. The appropriate global parameter is $V_A K$, where V_A is the mean Alfvén speed. Taking [A] to be not independent of this quantity gives p=3 and q=-4. Hence there follows

$$V(t) = (At)^{1/3}\ ,\ \xi = r/(A^{1/3}t^{4/3}), \qquad (14)$$
$$R^{r,r} = (At)^{2/3} f = (Ar)^{1/2}\ f\xi^{-1/2},$$

which as above yields $\sqrt{R^{r,r}} \propto r^{1/4}$, $E(k) \propto k^{-3/2}$ in the cascade. The evolution proceeds fastest on the smallest scales, so that a field that is not in equipartition for $\xi=\xi_F$ can be expected to evolve towards this first at small scales, creating an inverse cascade of magnetic energy.

§4 Extention to General Flow Conditions Including Compressibility

The preceding sections have motivated the notions of local self-similarity or local Reynolds number invariance, and that of the cascade (renormalized or fixed point turbulence) by making contact with classical results. However

we have also observed that the exact instantaneous solution of the Navier-Stokes equations should reflect these same characteristics. This is a significant step because we can now take our most general equations (e.g. Self gravitating, MHD, Navier-Stokes if desired) and concentrate on their self-similar symmetries. If we imagine a hierarchy of randomly cast domains (none of which need be homogeneous, stationary, isotropic or incompressible) each characterized by scales r,t and together covering the turbulent region, then we link the solutions in the various domains together solely by requiring them to have the same local Reynolds number (ξ_F) in the renormalized turbulence or cascade. Moreover, corresponding angular 'phases' in each separate domain can be given the same angular coordinates Θ_F,ϕ_F in the cascade, because of the freedom we have of rotating axes independently in each domain. Henriksen and Turner (1984) present a fuller discussion of this technique. Here we merely summarize it for the purpose of passing below to a consideration of the mean flow consistent with a given cascade.

In general there must be two global parameters with independent dimensions say

$$A \;\rightarrow\; [A] = L^{p}T^{q}M^{n} \text{ and } B \;\rightarrow\; [B] = L^{p'}T^{q'}M^{n'} \qquad (15)$$

In order to allow M to be eliminated and a local Reynolds number ξ to be formed. In the incompressible case $B\equiv\rho$ and essentially only a combination of A and ρ occurs in what we called A above. The self-similar symmetry always takes the form (V(A,B;t) and ρ_o(A,B;t,r) are functions known from dimensionless analysis based on (15))

$$\begin{aligned}
\xi &= r/(tV(t)) \;;\; V = V(A,B;t,r) \\
\underset{\sim}{u} &= V(t)\ \underset{\sim}{u}(\xi,\Theta,\phi) \\
\rho &= \rho_o(A,B;t,r)\ \rho(\xi,\Theta,\phi) \\
p &= \rho_o V^2\ p(\xi,\Theta,\phi) \\
\nu &= \nu_o\ rV(t),
\end{aligned} \qquad (16)$$

plus similar expressions for supplementary quantities such as gravitational potential or magnetic field. The cascade is found with $\xi=\xi_F$, $\Theta=\Theta_F$ and $\phi=\phi_F$. Otherwise, $\nu_o=\nu_o(\Theta,\phi)$.

Some examples of this approach are given in Henriksen and Turner (1984). Moreover it is not difficult to retrieve the Kolmogorov or Kraichnan cascades following the above principles by taking $B\equiv\rho$ and A the appropriate quantity (K or KV_A). The evolutionary details are harder to come by in this case because the self-similar constraint on r and t still leaves functions of ξ,Θ,ϕ to be found, in the absence of other symmetries.

Another example of some potential importance is that of turbulence in the presence of a uniform background shear.

For definiteness imagine a jet going around a bend as is sketched for the central plane in fig. 2.

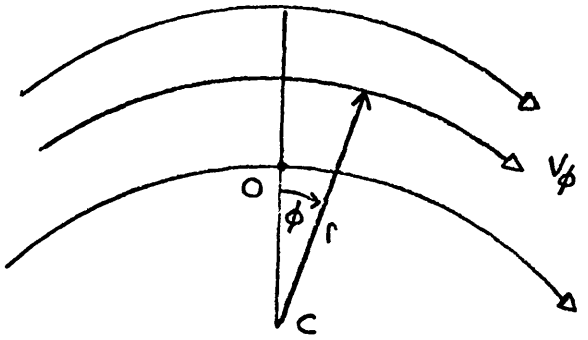

Fig. 2

Let $\omega \equiv \partial V\phi/\partial r = B$ and assume that the internal turbulence has the usual Kolmogorov coupling ($K \equiv \rho u^3/r$) so that with $A = K$, $[A] = MT^{-3}L^{-1}$. Then we see that (16) in this case takes the form

$$\begin{aligned} \xi &= (\omega t)^{-1}, \quad V = \omega r \\ \underset{\sim}{u} &= \omega r\, \underset{\sim}{u}(\xi,\Theta,\phi) \qquad (17) \\ \rho &= (A/\omega^3)\, r^{-2}\, \rho(\xi,\Theta,\phi) \\ p &= (A/\omega)\, p(\xi,\Theta,\phi) \\ \nu &= \nu_o\, \omega r^2 \end{aligned}$$

The cascade is found as usual from $\xi=\xi_F$, $\Theta=\Theta_F$, $\phi=\phi_F$ and we observe that it maintains its form in time because of the separated form of ξ. The interesting point is to note how the linear variation of the global or mean flow is communicated to the subscale turbulence, or vice versa (causality is always difficult to establish because the equations of turbulence are not hyperbolic). Since there is no pressure gradient transverse to the motion (eq. (17)), it is the turbulent viscous stress which provides the centripetal acceleration. This suggests a quite new method of bending a jet and the implications will be discussed elsewhere (Henriksen, in preparation).

§5 Mean Flow

In general there is no reason to expect the mean flow to have the self-similar symmetry (r,Θ,ϕ are taken as macroscopic or external scales in (16) above) when it is subject to many complex influences. In that case the simplest recourse is to solve the Navier-Stokes equations with a turbulent sub-scale viscosity (e.g. Smagorinsky, 1963; HBC, Krautter, 1984). However, when the number of global parameters does not over determine the problem (generally an asymptotic

condition) it is possible to have a self-consistent mean flow and cascade (in the sense of the same self-similar or renormalized scaling), just as in the example (17) above. If a cascade parameter is used in the scaling (e.g. K above) however, we are assuming the internal turbulence to be dynamically important to the mean flow. Otherwise we should use wholly external parameters in the scaling.

As an example when the cascade is important consider a pressure driven subsonic jet whose internal turbulence is constantly being driven by interaction with the surroundings. We use spherical polar coordinates centered on the nucleus with the jet axis as polar axis. A constant opening angle is required so that there is no length scale independent of r. Suppose the external pressure to have the form $p_e = Ar^{-p}$, so that $[A] = MT^{-2} L^{p-1}$, and let the second parameter, B, be the Kolmogorov cascade constant K, $[K] = ML^{-1}T^{-3}$. Then the appropriate form of (16) is defined by

$$\xi = (A/B)\, r^{-p}t^{-1},\quad V = (B/A)r^{p+1} \qquad (18)$$
$$\rho_o = (A^3/B^2)r^{-3p-2}$$

Thus the flow is intrinsically time dependent. In the frame with $\xi=\xi_F$ a constant, (18) gives the appropriate scaling for both the mean flow and the subscale turbulence. The velocities increase but the kinetic energy density decreases. The intermittancy or time dependence at a fixed r must be found from the scaled Navier-Stokes equations.

When the internal cascade is assumed to be decoupled from the mean dynamics, the self-similarity of the mean flow depends entirely on the choice of globally conserved quantities. Thus if in addition to the pressure law above, we suppose that the turbulent viscosity is conserved along the jet ($Re \equiv r\rho V_r/\eta$ is constant by Reynolds self-similarity so that η constant gives a constant entrained mass per unit length). We have $[B] = [\eta] = M\, L^{-1}\, T^{-1}$. The appropriate version of (16) now becomes

$$\xi = (B/A)\, r^p/t,\quad V = (A/B)r^{1-p} \qquad (19)$$
$$\rho_o = (B^2/A)r^{p-2}$$

and again there is intrinsic time dependence. The scaling in the frame $\xi=\xi_F$ is of some interest. We observe that the momentum flux in thejet $F \propto r^{2-p}$, the mass flux $\propto r$ and the self consistent magnetic field $B \propto r^{-p/2}$. From Henriksen (1983) and the adiabatic assumption about the distribution of relativistic particles (Fanti et al., 1982) we easily find the corresponding synchrotron brightness variation as

$$I_\nu \propto r^{(-2(\alpha+1) + p/2\ (1+\alpha/3))} \qquad (20)$$

where α is the observed spectral index. When α=0.6 and p=2, this gives $I_\nu \propto r^{-2}$. In general p is determined by an observation of the brightness index and of α, whence the solution is determined consistantly. Of course, we do not have a unique solution because the requirement η=constant is only justified by analogy with the incompressible examples. Any other choice can be readily explored however. We note here that if the brightness index is to be much less than 2 for $\alpha > 0.5$, then $p > 2$. This corresponds to a jet that is decelerating so rapidly longitudinally that the internal density increases.

Finally, the 'jolly green jet' of lore and legend (these proceedings) can be described by taking A=g in the scaling of eq. (6). Assuming that viscous decay dominates asympotically rather than free fall, then $\xi=\nu^{-1}r^2/t$ and $V_l \propto r^{1/2}$, $\Delta\rho \propto r^{-3/2}$, where r is the increasing longitudinal or transverse scale, $\Delta\rho$ is the density difference between the jet and the reservoir. The negative buoyancy therefore declines as $g\Delta\rho \propto r^{-3/2}$. I have not yet discovered the experimental verdict.

References;

Batchelor, G.K., 1959, "The Theory of Homogeneous Turbulence", Cambridge University Press, Cambridge.

Eilek, J.A., and Henriksen, R.N., 1984, Ap. J., 277, 820.

Fanti, R. et al., 1982, Astron. Astrophys., 110, 169.

Favre, A., 1983, Phys. Fluids, 26, 2851.

Henriksen, R.N., Bridle, A.H., Chan, K.L., 1982, Ap. J., 257, 63.

Henriksen, R.N., 1983, Proc. IAU Symposium #107, Reidel, in press.

Henriksen, R.N., and Turner, B.E., 1984, Ap. J., in press.

Hussain, A.K.M.F., 1983, Phys. Fluids, 26, 2816.

Karman, Th. von, and Howarth, L., 1938, Proc. Roy. Soc., London, 164A, 192.

Kraichnan, R.H., 1965, Phys. Fluids, 8, 1385.

Krautter, A., 1984, Ph.D. Thesis, Queen's University at Kingston.

Sedov, L.I., 1982, "Similarity and Dimensional Methods in Mechanics", MIR Publishers, Moscow.

Smagorinsky, J., 1963, Mon. Weather Rev., 91, 99.

SIDEWISE SHOCKS IN THE CENTAURUS A RADIO JET

J.O. Burns and D. Clarke
University of New Mexico

E.D. Feigelson
Pennsylvania State University

E.J. Schreier
Space Telescope Science Institute

ABSTRACT. New high resolution (1"x0"3), high dynamic range (13,000:1) observations at 2 and 6 cm of Cen A have revealed the presence of side-to-side limb brightening in the inner 700 pc of the radio jet. This edge brightening combined with the magnetic field orientation, the spectral index, and the internal pressure of the knots suggest the presence of transverse shocks in the jet.

1. NEW OBSERVATIONS

As the closest active galaxy at a distance of ≈5 Mpc (1"=24 pc), Centaurus A continues to be a source of new insight into the physics of radio galaxies. Previous radio observations of Cen A (Schreier et al. 1981; Burns et al. 1983) did not exhaust the full capabilities of the VLA. Further, higher resolution observations were possible in the longer spacing A and B configurations at 6 and 2 cm. During the past few months, we have undertaken new VLA observations which improve the resolution of the jet by a factor of three over that reported in Burns et al. (1983). Preliminary analysis of A-array data at 6-cm and matching B-array data at 2-cm will be described here. The beam size is 1"x0"3 corresponding to a linear point response of 24pc x 7pc. The maps were self-calibrated to a dynamic range of ≈13,000 to 1. Correlator (i.e., closure errors) were ultimately responsible for the noise limitations on the maps (RMS noise ≈0.6 mJy) and the low-level radio artifacts to the north and south of the nucleus. A 6-cm grey-scale map is shown in Figure 1 and a 6-cm contour map is shown in Figure 2.

2. NEW STRUCTURAL FEATURES

It is worth noting that the entire jet structure seen in Figures 1 and 2 is only 700 pc in length. This is well within the unresolved nuclear core of radio galaxies and quasars at redshifts of z>0.1 viewed with the highest VLA resolution at 6-cm. Thus, the structure in Cen A may be present in many other active nuclei but unobservable at these dynamic ranges with current instruments.

Three new features appear on these maps. First, the radio jet is clearly limb brightened on alternating sides. Knot(s) A1 lie to the southeast of the jet major axis, the banana-shaped knot A2 is to the northwest, and A3-A4 is edge-brightened on the southeast side. This side-to-side alternation of surface brightness is striking and distinctly different from the centered-brightened structure further down the Cen A jet and in the jet of the next closest active galaxy, M87 (Biretta et al.

Figure 1: Grey-scale map of the inner 700 pc jet in Cen A.

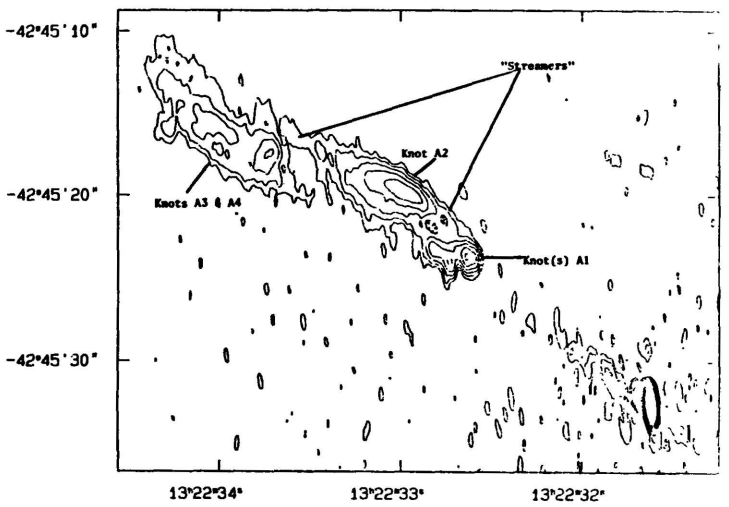

Figure 2: 6-cm contour map corresponding to Figure 1. Levels are -1, 1, 2, 4, 8 16, 32, 64 times 1.5 mJy; peak is 6.92 Jy.

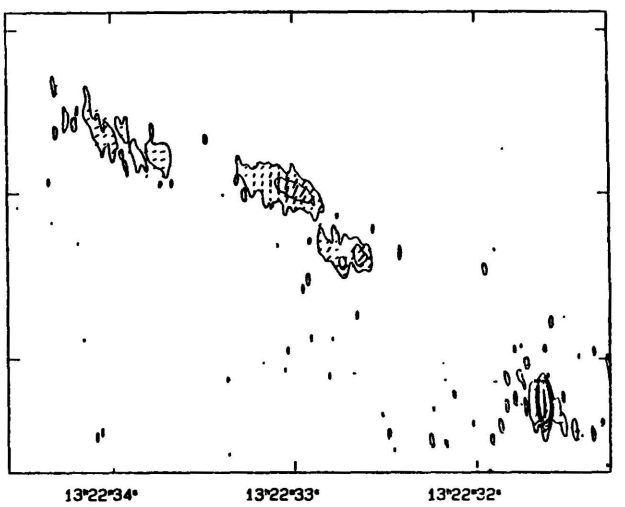

Figure 3: 2-cm total intensity contours with superposed polarization E-vectors. Levels are -1, 1, 4, 16, 64 times 2.5 mJy; peak is 8.94 Jy. Resolution is the same as Fig. 2.

1984). Second, thin filaments of radio emission which we call "streamers" appear to emanate from each of the knots pointing in a direction downstream in the jet. Each streamer begins in a knot and seems to terminate near the next knot. Streamers connecting knots A1 to A2 are at a level of 10σ above the noise, whereas the streamer pointing away from A2 is at a level of 4σ. Third, there are suggestions of an inner jet and faint counter-jet on both the 2 and 6 cm maps. The inner, ~125 pc jet may correspond to the marginally resolved structure N1 noted on the lower resolution maps of Burns et al. (1983). The "counter-jet" would be a completely new structure with obvious significance for flip-flop models. However, we are hesitant to call these "jet" structures real at present since the dynamic range near the map center is the worst on the map. The u-v coverage of Cen A with only 3.5 hrs of data is poor and atmospheric attenuation near the horizon is high. These effects could combine to produce visibility amplitude errors that may stretch along the jet major axis. Higher dynamic range will be required to test the reality of these inner jets.

3. EVIDENCE FOR SIDEWISE SHOCKS

One obvious interpretation of the limb-brightened structure in knots A1 and A4 is that sections of the jet are being illuminated by sidewise moving external or internal shocks. Such shocks probably reaccelerate electrons to produce a bright but clumpy radio jet and possibly the clumpy x-ray jet seen by Einstein. It is interesting to note that Feigelson et al. (1981) saw weak evidence for an offset in the centroid of the innermost x-ray knot in the same direction as the brightest radio knot A2.

We present four pieces of evidence for a sidewise shock system in the Cen A jet. First, the limb brightening and sharp drop off of radio emission in knot A2 is precisely like that expected in such a shock system. The transverse profile of emission through A2 is clearly skewed with a sharp edge to the northwest; the compression of contours in Figure 2 illustrates this fact. There is some resemblence in the structure of A2 with that of the leading edge of many classical double lobes.

Second, the magnetic field orientation at 2-cm is parallel to the jet major axis as is expected from sideways shock compression of the B-field. The polarization E-vectors demonstrate this $B_{\parallel}$ structure in Figure 3. However, one must note that the polarization structure becomes much more complex at 6-cm. There are multiple 90° flips in the E-vector angle across A2 at 6-cm. The rotation measure between 2 and 6 cm at the peak of A2 is ≥ 390 rad/m^2. Strong depolarization occurs between 2 and 20 cm where $m_2 = 42\pm5\%$, $m_6 = 15\pm2\%$, and $m_{20} < 1\%$ (from lower resolution data). This 700 pc part of the jet is embedded well within the prominent dust lane of NGC5128. Some portion of the E-vector rotation and depolarization could be due to a foreground screen in NGC5128, but the correlation of depolarization with total intensity structure also suggests some internal Faraday effects in the jet itself. If the E-vector rotation follows a λ^2 law, then the polarization angles at 2-cm in Figure 3 are within 7° of that extrapolated to zero wavelength. Therefore, we think that the 2-cm polarization data most likely reflects the true orientation of the B-field.

Third, the distribution of spectral index may not be inconsistent with Fermi acceleration of electrons within shocks in the knots. The average spectral index ($S_\nu \propto \nu^{-\alpha}$) between 6 and 20 cm (at 3"x1" resolution) for the knots is 0.6±0.1. However, this steepens to 0.8 ±0.1 between 2 and 6 cm (at 1"x0"3 resolution). Such a break in the spectrum at centimeter wavelengths is not necessarily expected theoretically for a simple shock model, but it is consistent with the spectral index between 6 cm and 2 keV (≈0.8). There is also tentative evidence for steepening in α_2^6 away from a presumed shock front in A2 with $\alpha_2^6 = 0.82\pm0.05$ at the peak of A2 and $\alpha_2^6 = 1.2\pm 0.2$ about 1"2 southeast of the peak.

Fourth, the internal relativistic particle plus magnetic field pressure is consistent with transverse ram pressure confinement. The internal pressure of A2 is $P_{min} \sim 7\times10^{-10}$ dyn cm^{-2}. The external thermal pressure is $nkT \sim 10^{-10}$ dyn cm^{-2} computed from the x-ray IPC emission of NGC5128 and an $r^{-1.8}$ density law (Feigelson et al., 1981) where $n_{ISM} \sim 0.1$ cm^{-3} and $T_{ISM} \sim 10^7$ K. Given the errors in this calculation, the jet could be thermally confined by a hot ISM. However, it is equally plausible that the jet is ram pressure confined in the transverse direction. If we assume that this dynamic pressure is greater than or equal to P_{min}, then the Mach number of the transverse motion relative to the ISM is

$$M \geq \left[\frac{P_{min}}{\gamma\ nkT}\right]^{1/2} \geq 2$$

This, of course, suggests that the transverse velocity of the knot A2 is at least mildly supersonic.

4. NATURE OF THE SHOCKS

There are two possible origins for the shock structure in the knots of Cen A. We classify these possibilities as external or internal shocks.

External shocks could be produced by a sideways moving, large wavelength instability mode in the jet. Boundary shocks are produced wherever the transverse velocity exceeds the external sound speed of the ISM as originally suggested by Benford (1981). This wave mode could either be a strictly two-dimensional sinusoidal structure as in the Benford (1981) model or an n = 1 twisted helix mode as described by Hardee (1984a) and Ferrari et al. (1981). If it is a helix, it must have an elliptical cross section to prevent uniform limb brightening all along the jet. This external shock structure is also interesting from the stability aspect of the Cen A jet. Benford (1981) argued that transverse ram pressure combined with adiabatic expansion of the jet (see e.g., Hardee 1984a,b) can surpress exponential growth of Kelvin-Helmholtz or Firehose instabilities. Indeed, such supression is needed since any wiggles in the Cen A jet beyond knots A are difficult to trace (see Burns et al., 1983); the growth in amplitude of these wave modes beyond knots A cannot be any greater than algebraic.

A second possibility involves internal shocks. Recent 2-D hydrodynamic computer calculations by Norman et al. (1984) and Woodward (1984) indicate that sideways moving (e.g., Kelvin-Helmholtz) perturbations in a jet can set up oblique internal shock waves in regions of high curvature. Unlike the case des-

cribed by Benford (1981), these oblique shocks lie internal to the jet boundary and could potentially be more efficient in re-energizing radio and x-ray emitting electrons.

5. REMAINING QUESTIONS

Since these observations are still quite new, several interesting questions come to mind but have yet to be addressd. We offer here some suggestions for further study.

What is the origin of the "streamers" which appear to emanate out of the knots in the 700 pc jet of Cen A? These structures have not been seen in any other radio jet, but few other jets have been examined with this resolution and dynamic range. One possibility is seen in the plots of the distribution of internal pressure and density of the sinusoidally perturbed jet in the Norman et al. (1984) calculations. The oblique shocks are strongest in regions of high curvature but they do extend all the way across the jet to the next bend on the opposite side of the jet. Could these streamers be the weak part of a shock or newly accelerated electrons sheared from the main shock wave and propagated downstream? Tentatively, the streamers have $\alpha_2^6 > 1$ suggesting some aging of electrons away from the knots.

Is there a transition in modes of acceleration from knots A to the more uniform structure in the downstream jet? Initially, electrons appear to be shock accelerated in knots A, with shock wave growth stimulated by a moderate wavelength Kelvin-Helmholtz or Firehose instability (i.e., limb brightening). At knot B (see Burns et al., 1983), the jet becomes centered-filled and α_6^{20} shows signs of steepening, both of which are expected in large volume turbulent acceleration schemes (e.g., Bicknell and Melrose, 1982). Could we be seeing a cascade from a macroinstability (with shock acceleration) to microinstabilities (e.g., the damping of resonant Alfvén waves by nonthermal particles) as expected in some models (e.g., Eilek and Henriksen, 1984)?

REFERENCES

Benford, G., 1981, Ap.J., 247, 792.
Bicknell, G.V. and Melrose, D.B., 1982, Ap.J., 262, 511.
Biretta, J.A., Owen, F.N., and Hardee, P.E., 1983, Ap.J. (Letters), 274, L27.
Burns, J.O., Feigelson, E.D., and Schreier, E.J., 1983, Ap.J, 273, 128.
Eilek, J.A., and Henrikson, R.M., 1984, Ap.J., 277, 820.
Feigelson, E.D., Schreier, E.J., Delvaille, J.P., Giacconi, R., Grindlay, J.E., and Lightman, A.P., 1981, Ap.J., 273, 128.
Ferrari, A. Trussoni, E., and Zaninetti, L., 1981, M.N.R.A.S., 196, 1051.
Hardee, P.E., 1984a, Ap.J., 277, 106.
Hardee, P.E., 1984b, this workshop.
Norman, M. et al., 1984, preprint.
Schreier, E.J., Burns, J.O., and Feigelsson, E.D., 1981, Ap.J., 251, 523.
Woodward, P., 1984, preprint.

MAGNETIC ENERGY DISSIPATION AS THE SOURCE OF SYNCHROTRON EMISSION IN JETS

Arieh Königl
Department of Astronomy and Astrophysics, The University of Chicago
5640 South Ellis Avenue, Chicago, IL 60637

ABSTRACT. It is proposed that the dissipation of internal magnetic energy, rather than of bulk kinetic energy, could be the main source of power for the synchrotron emission in certain radio jets. This possibility arises naturally in the context of the force-free model of magnetized jets from the requirement that the outward-convected field adjust continuously to maintain a minimum-energy configuration. The rate of energy dissipation calculated from this model is shown to depend only on the nonaxisymmetric component of the magnetic field. A rough estimate of this rate in the inner jet of NGC 6251 is found to be consistent with the observations.

1. INTRODUCTION

It is now widely recognized that, in many cases, the synchrotron emission from jets must be induced by in situ particle acceleration and magnetic field amplification. Traditionally, the ultimate source of energy for the radiation has been taken to be the bulk kinetic energy of the jet, which for a supersonic flow constitutes the main pool of free energy. Specifically, it was proposed (e.g., Ferrari, Trussoni, and Zaninetti 1979) that the flow kinetic energy is tapped through the Kelvin-Helmholtz instability which is excited at the boundary between the jet and the confining external medium. The instability was envisioned to create MHD turbulence which could then lead to particle acceleration either by resonant interactions (e.g., Eilek 1979) or by the Fermi mechanism (e.g., Bicknell and Melrose 1982).

Here I point out the possibility that the immediate source of energy for the radiation could be the internal *magnetic* energy in the jet. The ultimate source would still be the fluid motions which braid and twist the magnetic field lines near the origin of the jet. However, the stored magnetic energy is released only after the jet becomes magnetic-pressure dominated and force-free, and then still only at the rate allowed by the topological constraints on the field lines. A simple demonstration of this process can be given in the context of the force-free jet model described earlier in this Workshop, and is presented in § 2. In § 3 I briefly comment on the apparent analogy between this scenario and the energy dissipation mechanisms that are thought to operate in the solar corona.

2. MAGNETIC ENERGY DISSIPATION IN THE FORCE-FREE JET MODEL

The strongest topological constraint that may be expected to apply to a highly conducting (high magnetic Reynolds number) jet is the conservation of the total magnetic helicity, i.e., the volume integral of $\boldsymbol{A}\cdot\boldsymbol{B}$, where $\boldsymbol{A}$ is the

vector potential and $\boldsymbol{B}$ is the magnetic field vector. The magnetic helicity (defined for a volume enclosed by magnetic surfaces) is a measure of the twist and knottedness of the magnetic field lines (e.g., Berger and Field 1984). Although other constraints may also apply, they should all be weaker if the plasma is somewhat dissipative (e.g., Taylor 1974). The force-free jet model is based on the simplifying assumption that the conservation of the global helicity is the only relevant constraint in a jet which is magnetic-pressure dominated. Under this condition, the minimum-energy magnetic field configuration satisfies the force-free equation $\nabla \times \boldsymbol{B} = \mu \boldsymbol{B}$, with μ locally a constant. As I discussed earlier in this Workshop, the minimum-energy solution in a locally cylindrical geometry is in general a linear superposition of an axisymmetric ($m = 0$) mode and a nonaxisymmetric ($m = 1$) mode.

In a super-Alfvénic jet characterized by a uniform rate of helicity injection at the origin, it is convenient to discuss the magnetic helicity per unit length, $\tilde{K}$, instead of the total helicity. In such a jet, both $\tilde{K}$ and the axial magnetic flux Ψ will be conserved along the jet, although the radius R and the parameter μ will vary with the confining external pressure p_e. The variation of the minimum magnetic energy per unit length, $\tilde{W}$, in this case is shown in Figure 1. For sufficiently high values of p_e, the minimum-energy configuration corresponds to the $m = 0$ mode (dashed curve). However, when the pressure decreases below a certain critical value p_c, given by

$$p_c = 2.7 \times 10^3 \tilde{K}^4 \Psi^{-6}, \tag{1}$$

then the $m = 1$ mode becomes energetically favorable and thereafter increases in amplitude relative to the $m = 0$ mode (solid curve). For a jet which everywhere maintains a minimum-energy configuration, one can imagine that any given fluid element which travels out to regions of lower pressure follows first the $m = 0$ curve in the Figure, and then (at the bifurcation point c) switches over to the $(m = 0) + (m = 1)$ curve, as indicated by the arrows. As the fluid element expands on its way out, it does $p\,dV$ work against the external pressure. Is the accompanying reduction in the internal (magnetic) energy sufficient to keep it on the minimum-energy curve? It turns out that, as long as it "travels" on the $m = 0$ curve, this energy loss is indeed sufficient. However, beyond the bifurcation point, additional energy must be dissipated if the jet is to maintain a minimum-energy configuration.

It is thus seen that the need for magnetic energy dissipation arises naturally in this model. The amount of energy that can be dissipated is limited by the conservation-of-helicity constraint which determines the minimum-energy configuration at each location along the jet. The rate of dissipation , in turn, depends on the external pressure variation (which determines dR/dz, the change of R with distance along the jet) and the velocity v_j of the jet. It also depends on the amplitude B_1 of the $m = 1$ field component (but is independent of the $m = 0$ field). Numerically, the dissipation rate per unit length is found to be

$$\tilde{P}_m = 3.3 \times 10^{-3}\, B_1^2\, v_j\, R\, \frac{dR}{dz} \tag{2}$$

(Königl and Choudhuri 1985). The quantities appearing in equation (2) can, in principle, be estimated from radio observations of jets. In the case of the extended jet in NGC 6251, whose various apparent nonaxisymmetric features are well described by the force-free model, one obtains for the inner

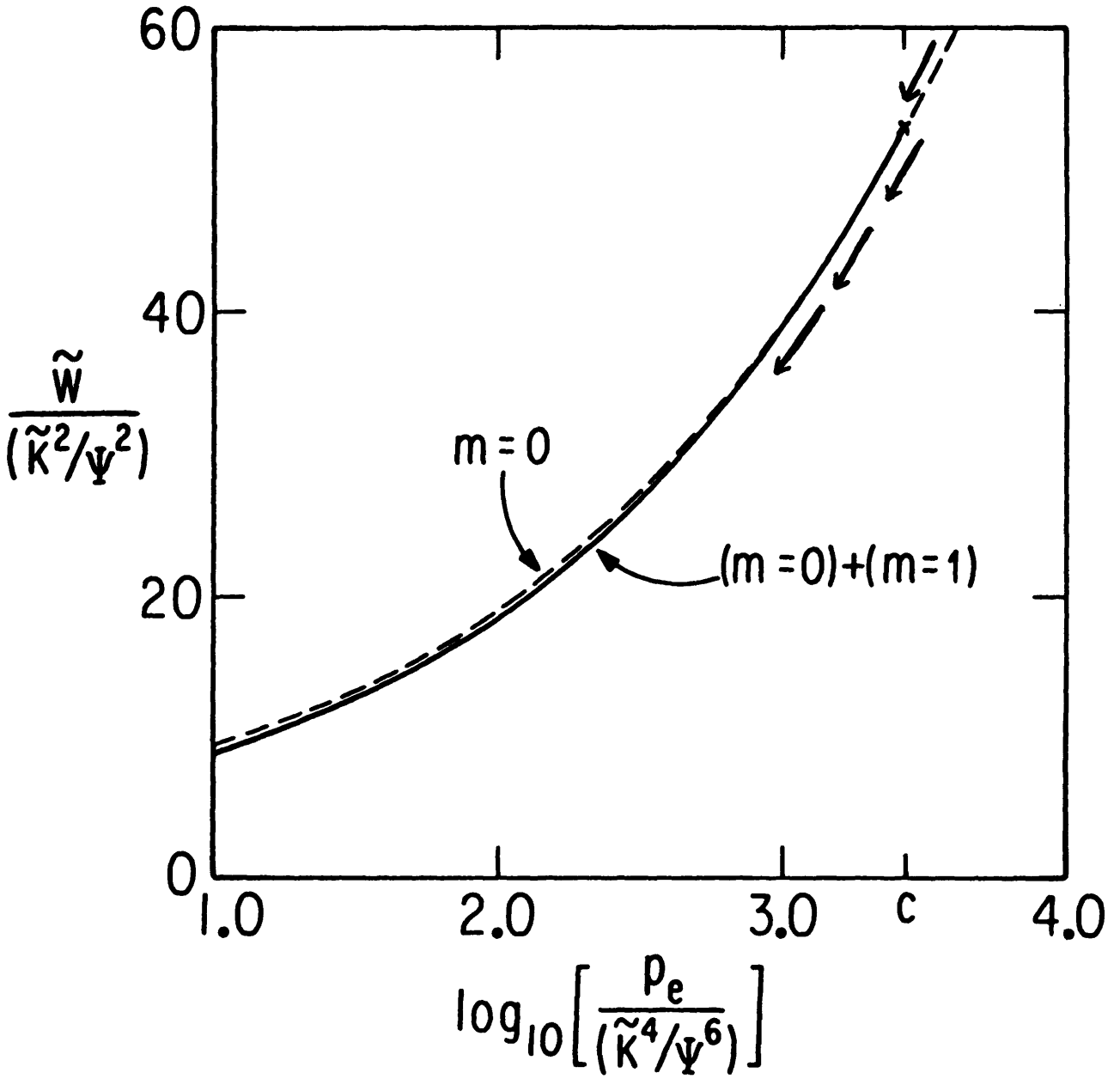
60
40
20
0
$\frac{\tilde{W}}{(\tilde{K}^2/\Psi^2)}$
m = 0
(m = 0)+(m = 1)
1.0
2.0
3.0
c
4.0
$\log_{10}\left[\frac{p_e}{(\tilde{K}^4/\Psi^6)}\right]$

Figure 1

($< 120''$) region $\tilde{P}_m \approx 2 \times 10^{17}$ *erg* s^{-1} cm^{-1} (with $B_\perp$ estimated from the equipartition field). This is remarkably close to the radio luminosity per unit length measured in this region (Perley, Bridle, and Willis 1984). Although the above estimate and the radio luminosity represent lower limits to the magnetic energy dissipation rate and the total synchrotron power, respectively, the close agreement is nevertheless suggestive of the possibility that most of the dissipated power is carried away in the form of synchrotron radiation. Conversely, one can argue from this result that magnetic energy dissipation could be the main source of power for the observed synchrotron emission in this jet.

3. DISCUSSION

The possibility that synchrotron radiation is the main dissipation mechanism in jets has been suggested already in the context of the shear-powered, turbulent jet models mentioned in § 1 (e.g., Henriksen, Bridle, and Chan 1982). In this connection, it is worth pointing out that the equilibrium force-free model discussed here also has a natural interpretation in terms of MHD turbulence (see Turner 1983). It is, however, also worth noting that the field rearrangement processes envisioned in this model bear interesting similarities to the processes that are believed to be responsible for the heating of the solar corona and the production of solar flares (e.g., Parker 1979). In both instances, it is the release of magnetic energy stored in twisted and braided magnetic field lines which is the immediate source of power for the emitted radiation, and in both cases the minimum accessible energy state may correspond to a force-free field with a constant μ (e.g., Norman and Heyvaerts 1983). It is therefore plausible to expect that the experience gained from solar studies may provide useful guidelines for a further development of the magnetic dissipation scenario for jets. In particular, one might gain helpful insight from an analysis of solar flares, which are known to be efficient in accelerating relativistic particles (e.g., Heyvaerts 1981). For example, it has been argued that the resistive tearing mode instability plays an important role in the energy dissipation process in the solar corona (e.g., Van Hoven 1981), and that it may even lead to direct acceleration of particles (through induced DC electric fields). This may well apply also to force-free jets, since it turns out (Gibson and Whiteman 1968) that the minimum-energy field configuration becomes unstable to resistive tearing precisely at the branching point of the mixed-mode state (see Fig. 1). The continued expansion of the jet beyond that point would tend to excite the instability, and this, in turn, could trigger the reconnection processes that might restore the field to the minimum-energy state.

REFERENCES

Berger, M.A., and Field, G.B. 1984, *J. Fluid Mech.*, in press.
Bicknell, G.V., and Melrose, D.B. 1982, *Ap. J.*, **262**, 511.
Eilek, J.A. 1979, *Ap. J.*, **230**, 373.
Ferrari, A., Trussoni, E., and Zaninetti, L. 1979, *Astr. Ap.*, **79**, 190.
Gibson, R.D., and Whiteman, K.J. 1968, *Plasma Phys.*, **10**, 1101.
Henriksen, R.N., Bridle, A.H., and Chan, K.L. 1982, *Ap. J.*, **257**, 63.
Heyverts, J. 1981, in *Solar Flare Magnetohydrodynamics*, ed. E.R. Priest

(New York: Gordon and Breach), p. 429.
Königl, A., and Choudhuri, A.R. 1985, *Ap. J.*, February 1 issue.
Norman, C.A., and Heyvaerts, J. 1983, *Astr. Ap.*, **124**, L1.
Parker, E.N. 1979, *Cosmical Magnetic Fields* (Oxford: Clarendon Press), chap. 21.
Perley, R.A., Bridle, A.H., and Willis, A.G. 1984, *Ap. J. Suppl.*, **54**, 291.
Taylor, J.B. 1974, *Phys. Rev. Lett.*, **33**, 1139.
Turner, L. 1983, *Ann. Phys.*, **149**, 58.
Van Hoven, G. 1981, in *Solar Flare Magnetohydrodynamics*, ed. E.R. Priest (New York: Gordon and Breach), p. 217.

LABORATORY ELECTRON BEAM SIMULATION OF COSMIC RADIO JETS*

Robert G. Spulak, Jr.
Sandia National Laboratories
Albuquerque, NM 87185

Jack O. Burns
University of New Mexico
Albuquerque, NM 87131

ABSTRACT. Astrophysical jets are injections of particles, magnetic fields, and possibly large-scale currents into a background plasma, the intergalactic medium. In principle, they are therefore somewhat similar to the laboratory injection of an electron beam into a plasma. We consider scaling between the astrophysical and laboratory cases and discuss the similarities and differences between them. We discuss what aspects of the physics of astrophysical jets might be investigated with electron beam experiments; in general, the laboratory will be most useful to study purely electrodynamic effects.

1. INTRODUCTION

There are many potential benefits of performing laboratory experiments to mimic cosmic radio jets. Among these are the study of the basic physics assumed when interpreting radio observations. This includes equipartition, synchrotron emission, formation of hot spots, and the interaction with the surrounding medium. In addition, the transport and stability of jets could be observed and compared to numerical studies. Experiments are three-dimensional and fully non-linear, unlike the computations to date. Finally, particle beam experiments would provide an opportunity to investigate electrodynamic effects, which may have not yet been fully incorporated into our understanding of the behavior of radio jets. Some of these effects are magnetic self-confinement, "return currents", electromagnetic instabilities, and the formation of jets by electrodynamic processes.

Of course, scaling a radio jet to the laboratory in order to make meaningful interpretations of laboratory measurements

*This work performed at Sandia National Laboratories and supported by the US Department of Energy under contract number DE AC04-76DP00789.

is the major stumbling block to implementing all of the above. This paper addresses the scaling between electron beams in the laboratory and radio jets. We discuss the aspects of astrophysical jets that will be most easily studied. We describe experiments which will utilize the electron-beam/pulsed-power technology that exists at several universities and laboratories throughout the world.

2. OVERALL SCALING BETWEEN RADIO JETS AND THE LABORATORY

The characteristic quantities of a plasma are frequencies, velocities, lengths, and energy densities (Landshoff 1957). The relationships between these quantities that result in scaling between the cosmos and the laboratory are the subject of this section (see also Elsasser, 1954, and Podgornyi and Sagdeev, 1970). Table 1 gives representative values of fundamental quantities for a specific radio jet (Burns, et al., 1983) and a specific laboratory electron beam experiment (Ekdahl, et al., 1974).

Most scaling laws or parameters consist of dimensionless numbers, the most familiar being the Reynolds number for viscous fluid flow. These dimensionless parameters do not need to be identical in all cases for the physical phenomena of astrophysical jets and laboratory experiments to be the same. This is because the dimensionless numbers represent ratios of terms in the equations that describe the system (energy balance, equations of motion, etc.) and the ratios can be much greater or less than unity. Following is a description of each of the major scaling parameters for ionized flows with magnetic fields.

The magnetic Reynolds number is

$$Re_m = \frac{4\pi\sigma L u}{c^2} \quad , \tag{1}$$

where σ is the conductivity (s^{-1}), L is the length scale of interest (cm), u is the characteristic flow velocity (cm/s), and c is the speed of light. Re_m can be interpreted as the ratio of the decay time of an irregular magnetic field to the hydrodynamic time. Re_m is thus a measure of the extent to which the magnetic field lines are frozen to the flow.

The Mach number, M, is the ratio of the flow velocity to the velocity of propagation of a disturbance in the medium ($M = u/v_{ac}$). For waves that propagate parallel to the magnetic field, the appropriate disturbance speed is the Alfven speed. For waves that propagate perpendicular to the magnetic field, the appropriate speed is the magnetosonic speed.

The Larmor ratio is the ratio of an appropriate gyroradius for particles to the length scale of the region. Alfven

(1939) showed that there is a limiting current which limits the flux of charged particles in a particular direction

TABLE 1. EXAMPLES OF FUNDAMENTAL QUANTITIES FOR A SPECIFIC RADIO JET AND LABORATORY ELECTRON BEAM

	Value	
Quantity	Centaurus A Jet	Plasma Heating Experiment
$n_j(cm^{-3})$	10^{-2}	3×10^{11}*
$n_{bk}(cm^{-3})$	3×10^{-3}	$10^{12} - 6 \times 10^{13}$
u(cm/s)	5×10^{8}	3×10^{10}
$B_z(G)$	5×10^{-5}	2.6×10^{3} (applied)
$B_\theta(G)$	5×10^{-5}	1.8×10^{3}*
$T_j(K)$	1.5×10^{8}#	10^{10}##
$T_{bk}(K)$	2×10^{7}	$10^{7} - 10^{9}$**
r(cm)	1.5×10^{18}	3 - 6
L(cm)	4.5×10^{21}	40 - 180 (1800***)
I_z(statamp)	10^{24}	1.4×10^{14}
J_z(statamp/cm^2)	1.4×10^{-13}	4×10^{12}

---

n_j: number density in jet/beam.

n_{bk}: number density of background.

u: flow velocity of jet/beam.

B_z: longitudinal magnetic field.

B_θ: azimuthal magnetic field.

T_j: temperature of jet/beam.

T_{bk}: temperature of background.

r: radius of jet/beam.

L: length of jet/beam.

I_z: longitudinal current implied from B_θ.

J_z: longitudinal current density.

*Based on a beam current of 45 kA.

**Based on 1-100 keV transferred to background electrons and ions.

***Based on a pulse length of 60 ns.

#Based on thermal pressure 2×10^{-10} dyne/cm^2.

##Based on Bennett pinch condition.

in space. This is because the azimuthal magnetic field produced by this current can reverse the trajectories of the particles. The length scale is the Larmor radius at the Alfven current when the electron trajectories have been reversed across the diameter of the jet (or beam). The Larmor ratio for the jet/beam is then the ratio of the Alfven current to the actual current:

$$(r_L/r)_j \simeq I_A/I \ , \qquad (2)$$

where (Miller 1982, Ch. 4)

$$I_A = \beta\gamma m_e c^3/e \text{ statamp}, \qquad (3)$$

where $\beta = v_e/c$, $\gamma = (1 - \beta^2)^{-1/2}$, v_e is the velocity of the electron (cm/s), m_e is the mass of the electron (g), and e is the charge of the electron (esu). The current, I, is found from the observed azimuthal field. The Larmor ratio for the background is defined using the Larmor radius of the thermal electrons.

The plasma "β" is the ratio of thermal pressure to magnetic pressure. Because of the equipartition assumption for the radio jet (see, for example, Miley 1980), $\beta = 1$ if the relativistic electrons supply the thermal pressure and $\beta > 1$ if the relativistic electrons have only a fraction of the thermal energy. For electron beams, an equilibrium pinch configuration has $\beta = 1$ since the transverse pressure balances the azimuthal field (Lawson 1977, Ch. 4).

The two most fundamental oscillations in a plasma are the plasma oscillation and particle gyrations around a magnetic field. The plasma frequency, ω_p, gives the rate at which the plasma adjusts to an electric field. The cyclotron frequency, ω_c, gives the rate at which the particles sample conditions at locations around their Larmor orbits. What modes of the plasma are excited depends on the plasma frequency and on whether conditions can be averaged over the Larmor orbits. Thus, the ratio of plasma frequency to cyclotron frequency (ω_p/ω_c) is of fundamental interest.

For the jet/beam to behave strictly as a plasma, it must exhibit quasineutrality and collective effects. This means that the Debye shielding length, λ_D, should be small compared to the region of interest (thus defining the Debye ratio, λ_D/r) and the plasma parameter, g, the inverse of the number of particles in a sphere with radius λ_D, should be extremely small. These conditions hold for an astrophysical jet if it is electrostatically neutral. However, charged particle beams are not neutral. Space charge effects can be extremely important (Miller 1982, Ch. 3) but long range

Coulomb interactions dominate particle-particle collisions. Thus, although quasineutrality is violated, a charged particle beam still exhibits collective effects.

Table 2 gives the values of the important scaling parameters for the jet and beam of Table 1. Note that the magnetic Reynolds number indicates that the magnetic field lines are frozen to the flow in both cases. Also the Mach numbers, plasma "ß", Larmor and Debye ratios for the background, and ω_p/ω_c for electrons can easily be made consistent. However, the Larmor ratio (and Debye ratio) of the jet/beam plasma cannot be made to scale.

TABLE 2. SCALING PARAMETER VALUES FOR THE SPECIFIC EXAMPLES OF TABLE 1.

	Value	
Parameter	Centaurus A Jet	Plasma Heating Experiment
Re_m*	10^{11}	5×10^4
M_j**	3	10
M_{bk}	9	20
$(r_L/r)_j$	8×10^{-13}	1
$(r_L/r)_{bk}$	10^{-12}	5×10^{-3}
"ß"	1	1
$(\omega_p/\omega_c)_j$	6	0.6
$(\omega_p/\omega_c)_{bk}$	3	3
$(\lambda_D/r)_j$	6×10^{-13}	0.4
$(\lambda_D/r)_{bk}$	4×10^{-13}	2×10^{-3}

*For the laboratory, $\sigma \sim 2 \times 10^{13}$ s^{-1}; for the astrophysical jet, $\sigma \sim \omega_{pe} \sim 6 \times 10^3$ s^{-1}.
**Subscript j refers to jet/beam plasma; subscript bk refers to the background.

This simply indicates that the electron beam is a beam and the astrophysical jet is not, i.e., in a radio jet, the particles are not streaming in a direction generally parallel to the overall flow. The currents implied from the observed azimuthal fields in the jet are much greater than the limiting Alfven current. In addition, in a typical electron beam experiment, the beam interpenetrates the background while it appears that radio jets displace the intergalactic medium. Thus, the radio jet should behave much like a fluid and the laboratory beam would not be directly applicable to the study of flow and instabilities.

3. ELECTRODYNAMIC EFFECTS

Both the radio jet and the electron beam represent the injection of magnetic field into a background plasma. Because the Larmor ratio in the jet/beam does not scale, it appears that the appropriate areas to study in the laboratory are the purely electrodynamic effects and interactions. As mentioned above, these include "return" (induced) currents in the intergalactic medium or cocoon and magnetic self-confinement.

When the radio jet advances into the intergalactic medium, the high conductivity of the background implies that the magnetic fields are frozen out of the background. Thus, there cannot (initially) be any induced current far from the jet since the background cannot see the changing magnetic field. As the jet pushes aside the background as it advances, the currents induced by the advancing magnetic field will be confined to the surface at the interface between the jet and background.

The surface currents are entirely analogous to those induced in a Tokamak during the startup phase (e.g., Kuznetsov, et al., 1980). There, an induction coil linked with the toroidal plasma produces a changing magnetic field that cannot initially penetrate the high conductivity plasma, and currents are produced initially only on the surface. The high current density at the surface (of a jet or Tokamak) implies a high electron drift velocity. As the electron velocities exceed the velocities of modes of plasma turbulence, these modes can be excited, taking energy from the epithermal electrons (Kaplan and Tsytovich, 1973, Ch. I, §4). This results in an anomalous resistivity that allows the current to penetrate the plasma (e.g., Dnestrovskij and Pereverzev, 1983).

As we hinted by drawing the analogy with a Tokamak, these effects should be observable in the laboratory. The objective is then to scale the background media so that 1) the induced currents will be excluded from the electron beam volume (to simulate the displacement of the intergalactic medium by the radio jet), 2) the induced currents will initially be confined to the surface between the beam and background, and 3) the modes of plasma turbulence excited will be similar. These can be satisfied in the laboratory by making the background conductivity high and the ratio of electron plasma to cyclotron frequencies similar.

Electrons in the background plasma will be pushed aside by the advancing beam pulse (Miller 1982, Ch. 4). This will produce fluid-like motions in the background plasma. In this sense, then, the electron beam may act like a fluid jet in its interaction with the surrounding medium at the head of the beam pulse. Therefore, it may be of interest to consider the Mach numbers of the jet and beam, also.

4. POSSIBLE EXPERIMENTS

A topic that we might address with an electron beam experiment is the geometry of the induced currents in the background. We wish to discover to what extent the anomalous resistivity allows current penetration. A "cocoon" around the jet may be formed by purely electrodynamic effects. We can address these issues by physically measuring the induced currents.

The plasma turbulence leading to anomalous resistivity is itself of interest. Relativistic electrons which produce the observed synchrotron radiation are thought to be accelerated by plasma turbulence. The spectrum of this turbulence can be studied in the laboratory.

Finally, electrodynamic schemes have been proposed as mechanisms for the acceleration of non-thermal particles to form jets (e.g., Lovelace, 1976). We might hope to mimic the dynamo and collective acceleration in those schemes.

In summary, we have shown that a laboratory electron beam and background plasma can be used to perform useful investigations of cosmic radio jets. Simulating the electrodynamic effects of the interaction between the jet and intergalactic medium seems feasible. We propose to initiate such an experiment at Sandia National Laboratories within the next year.

The authors gratefully acknowledge significant discussions of this topic with John Brandenburg, Jean Eilek, Carl Ekdahl, Bruce Miller, and Richard Nebel.

REFERENCES

Alfven, H., 1939, Phys. Rev., 55, 425.
Burns, J. O., Feigelson, E. D., and Schreier, E. J., 1983, Ap. J., 273, 128.
Dnestrovskij, Yu. N., and Pereverzev, G. V., 1983, Nucl. Fusion, 23, 633.
Ekdahl, C., Greenspan, M., Kribel, R. E., Sethian, J., and Wharton, C. B., 1974, Phys. Rev. Lett., 33, 346.
Elsasser, W. M., 1954, Phys. Rev., 95, 1.
Kaplan, S. A., and Tsytovich, V. N., 1973, Plasma Astrophysics, Pergamon Press, Oxford, England.
Kuznetsov, Yu. K., Lebed', S. A., and Pavlichenko, O. S., 1980, Nucl. Fusion, 20, 123.
Landshoff, R. K. M., 1957, Magnetohydrodynamics, p. 69, Stanford University Press, Stanford, CA.
Lawson, J. D., 1977, The Physics of Charged-Particle Beams, Clarendon Press, Oxford, England.
Lovelace, R. V. E., 1976, Nature, 262, 649.
Miley, G., 1980, Ann. Rev. Astron. Astrophys., 18, 165.
Miller, R. B., 1982, An Introduction to the Physics of Intense Charged Particle Beams, Plenum Press, New York, NY.
Podgornyi, I. M., and Sagdeev, R. Z., 1970, Sov. Phys.-Uspekhi, 98, 445.

AN OBSERVER'S PERSPECTIVE – I

PETER N. WILKINSON

Jodrell Bank

At the end of an intense meeting like this, it is good to remind ourselves that progress has been rapid since, for example, the I.A.U. Symposium on *Extragalactic Radio Sources* in Albuquerque in 1981. This is largely because the full VLA has come on stream. It has revealed lots of beautiful flowers in the extragalactic garden; flowers with subtle forms (and colors and stripes !) all of which are crying out for interpretation; but our ignorance remains profound - we are *still* arguing about whether the velocities of the (extended) jets are relativistic or sub-relativistic. The observational aspects of the VLA results will be summarized by Robert Laing in the next talk. I want to stress that the observations of finer-scale structure are also improving steadily, as we learn how to use our existing VLBI Networks effectively, and that VLA-quality results on some small-scale jets should be with us quite soon. Improved data are clearly needed for I have heard nothing this week to change my mind about the inherent power of the observations to lead this very complicated subject !

1. WHERE IS VLBI GOING ?

Until recently the "only" results from VLBI were superluminal motion (rather important !); the alignments of the parsec and kiloparsec scales jets in the big doubles; and the misalignments in the compact sources. We all know that we need to do much, much better than this to get anywhere in the jet physics. Arieh Königl remarked that when he saw the complicated VLA map of the jet in NGC6251, he felt impelled to try to interpret it. To get the same reaction for the parsec-scale jets we need the milli-arcsecond (mas) equivalents of those on the NGC6251 jet. This is a feasible goal for this decade - all we need is 20 or more VLBI telescopes working simultaneously, which should be easy when the VLBA comes on stream - and some improvements in image processing such as "broad-band" mapping - which are now being developed. Even now arrays of about this size (see below) can fruitfully be used at moderate frequencies (e.g., 1.6 GHz) where small telescopes are still useful and calibration is relatively easy. However with Earth baselines we are never going to get very close to the energy source in quasars and radio galaxies. To approach the "monster" itself we shall need to push VLBI into space. Our first step in this direction, QUASAT, may be launched in the early 1990's.

2. SUPERLUMINAL MOTION

We did hear this week some new clues about superluminal motion from John Biretta in the case of 3C345, and Craig Walker for 3C120. At present we see the effect on scales from roughly one to ten parsecs. I want to stress that the scale over which we "need" superluminal motion in the "All-singing, All-dancing Dream Model" is set by observational limits only. It is by no means clear that superluminal motion stops at

10 parsecs - this is just where the fading blobs fall prey to the rather limited dynamic range in the present maps.

Nevertheless, some interesting new effects are now being seen as a result of persistent monitoring, a steady improvement in dynamic range and, tellingly, from doubling the resolution by observing at 22 GHz. Individual components almost certainly do not proceed in straight lines (unless the C4 component in 3C345 proceeds on a straight line that misses the core); the velocities of components appearing at different times can be different; and the velocities of individual components (certainly in 3C345 and possibly in 3C120) seem to accelerate with time. We also saw John Wardle's exciting new result, just the tip of the iceberg we hope, that the outer components in 3C345 are highly polarized; the amount of thermal material there is low; and we see both parallel and perpendicular magnetic fields.

We conclude that *something* is moving with $\beta \approx 1$, at least on the milli-arcsecond scale, but although the observations are getting more complicated the data do not yet justify more detailed modeling. Thus, to summarise, 13 years after the first realisation that there was a "phenomenon" to explain on parsec scales we are now beginning to see second order effects. We still don't have any real physical understanding of what is going on but at least the superluminal sources are no longer simple and there is something to get our teeth into!

We undoubtedly need the VLBA to elucidate the details of superluminal motion. In particular, the present arrays are not good enough at the higher frequencies where we can get the resolution to look closer to the nucleus. Also, with the dedicated VLBA we will be able to see "movies" of nearby objects such as 3C120 and BL Lac where things are changing quickly, and we will be able to measure the detailed polarization distributions over a range of frequencies. Highly detailed maps are also needed to constrain directly the Lind/Blandford idea that relativistic shocks may cause the beaming may be much broader than the $1/\gamma$ radians we have generally been assuming.

In the meantime, however, there is something we can do with our present networks. We should be able to measure component proper motions out to about 100 parsecs, rather than 10 parsecs as now. As I said before this demands much better maps, so in April this year a group of us organised an experiment (at 1.6 GHz) involving 18 telescopes around the world. Amazingly enough, all of them worked and we are going to combine the VLBI data with data from MERLIN and from the phased VLA hopefully to produce maps with a few mas resolution over several tenths of an arcsec, and with lower resolutions on even larger scales. One of the objects we observed, 3C120 (principal investigators Craig Walker, John Benson and Roy Booth), is close enough and strong enough that, if the superluminal velocity is the same > 100 mas along the jet, motions should be detectable in about another two years. Quite good maps already exist showing a bright knot ≈ 50 mas ($\approx 25/h$ pc for $H_0 = 100h$ km/s/Mpc) away from the nucleus and this should have moved by about a beam diameter (3 mas) if it is moving at the same speed as the innermost knots. Thus evidence for or against the beams "pooping out" (to quote Alan Bridle) on 10 parsec scales should soon be coming in. Watch this space - or at least Walker and Benson !

3. SIDEDNESS

Not all VLBI work is on known superluminal sources ! A wide variety of objects now receive attention but there are still no unequivocal detections of any two-sided jets on parsec to 10 parsec scales. The best maps show very one-sided structure, even in the nuclei of steep spectrum sources. For example the classic jet source NGC6251 was recently mapped by Dayton Jones *et al.* using data from 11 VLBI stations. The resulting 1300:1 dynamic range map shows no nuclear counter-jet; the intensity ratio between the VLBI jet and the counter-jet on this scale is >80:1, while the ratio between the extended jet and its counterjet varies with distance from the core, from about 40:1 to $\geq$200:1. The best VLBI sidedness ratio so far is for 3C309.1 (see Wilkinson *et al.* in this Workshop), which taught me the salutary lesson that you have to be very careful indeed if you want to say that things are two-sided. You need *multifrequency* maps to find out where the flat spectrum component is. I obtained these observations on the pretext that this was the first two-sided VLBI jet, interpreting the brightest feature from a single frequency map as the nucleus. It turned out that the northernmost feature is the nucleus, and that the jet is extremely one-sided ! The limits are just beginning to get interesting in relation to whether or not the sidedness can be due to Doppler beaming – the limit on the peak brightness ratio is about 100:1. It should be straightforward to improve this limit by another order of magnitude using Mark III VLB equipment, better receivers, and even more careful calibration.

4. CENTRAL COMPONENTS OF DOUBLE SOURCES

Information here is still scanty, because the sources are weak. The central components are aligned with the "VLA" jets to within about 5°, and the parsec scale jet is in the same direction as the brighter "VLA" jet, without exception. The sidedness mechanism on the parsec scales must therefore be intimately related to that on the kiloparsec scale, whatever either of them is. We haven't yet caught a "flip-flop" in action, but perhaps that is not very surprising. It is not going to be easy to get statistics on the alignments and limits on superluminal motion for large samples of big doubles, but the more sensitive Mark III VLBI equipment is becoming the norm around the world, and the first epoch measurements for quite a few sources have been done. In this area I think it will be several more years before we can expect qualitatively new results – but I hope that observers will prove this prediction to have been pessimistic !

5. VELOCITIES ON KILOPARSEC SCALES ?

As the VLBI technique improves we can see prospects for getting measurements of velocities in kiloparsec scale jets in the not too distant future. The best candidates, due to their closeness, are M87 and 3C120. Sadly, Centaurus A, which would otherwise be the best candidate, is below the ground for many VLBI telescopes. The 15 GHz map of M87 shows the first good evidence of a jet with a shock, and there are other bright bits of the jet closer to the nucleus which we can hope to "key on" to measure proper motions. This is one of four sources observed in the recent 18-element "World Array" observations (principal investigators for M87, Mark Reid and Ralph Spencer), so we now have first-epoch observations for an experiment which should give us some useful velocity information by the end of this decade. My guess is that the current "World

Array" data will allow us to map the narrow M87 jet with < 5 mas resolution over the inner arcsecond, and with < 50 mas resolution out to Knot A. A velocity of 20,000 km/s (Frazer Owen's estimate) corresponds to a proper motion of ≈ 1 mas in 4 or 5 years. This measurement is clearly "do-able" close to the nucleus and, especially if the VLBA is built, is feasible on knot A within 10 years.

One of my previous worries about this whole line of attack on the physics of jets was that we may not see anything moving – and that this would not enable us to say anything because the knots could be slow-moving shocks in a much faster flow. What I have heard this week from the theorists gives me more hope that most shocks will be moving quite close to the bulk flow velocity and thus that these large, and therefore hard-to-organise and hard-to-reduce, VLBI observations will be worth the effort. However it is worthwhile repeating Rees's stricture that failure to detect proper motions cannot be taken as unequivocal evidence for slow beams. These proper motion experiments will only ever give us lower limits to the beam velocity. It would simplify matters for everyone if it turns out that the knot velocities are high!

6. MAN-MADE LIMITATIONS

I cannot end this talk without stressing how important it is for the continued progress of the subject that the VLBA, which is presently in a metastable state of funding, goes ahead. So if anyone asks you whether it should still be supported then your answer should be a resounding – *"yes"* ! However, the VLBA won't be finished until 1989 and until then there is much to be done with the large number of existing telescopes. The obstacles in our way are now the size of the VLBI correlators (tiny) and the computing power needed to handle the data from VLBI/MERLIN/VLA arrays (large); to make the combined maps we shall sometimes need images with $> 20{,}000$ pixels on one of the sides. I emphasise that *existing* telescopes would allow us to do this on some jets – M87 for example – if we observed at many different frequencies in the L band. But the processing would be horrendous and then one could never get enough VAX time to make the maps. Thus the science is being limited by relatively cheap digital hardware and not by expensive observatories (in which the investment has already been made).

Even our best current tool, the VLA, is not being fully utilised on these problems. It's rather amusing that the results that Craig Walker showed on 3C120 and the best VLA results on the counterjet in NGC6251 have come by the "back door", as the result of phased array observations intended for VLBI experiments. As an example, the VLA map of NGC6251 with 28 hours of data (principal investigators Rick Perley, Alan Bridle, Dayton Jones and Tony Readhead) clearly reveals the counterjet, which shows that full (in this case very full !) syntheses on the VLA can bring us new science. The seductive speed of the VLA has led us to overemphasise the idea that unless you can get astrophysical results in a few minutes or an hour or two, then it isn't worth doing.

AN OBSERVER'S PERSPECTIVE – II

ROBERT A. LAING

Royal Greenwich Observatory

Peter Wilkinson has dealt with what we should do next, leaving me to summarise what we have done so far ! I will begin with a personal selection of the observations presented at this meeting which showed where we have learned a lot recently.

1. IMPORTANT NEW OBSERVATIONS

Continuity from parsec to kiloparsec scales. Craig Walker's maps of 3C120 traced a jet all the way from superluminally expanding knots to 100-kiloparsec scales, bending continuously as it goes, with a wavelength increasing with distance from the nucleus. These are beautiful observations, and we need more like them !

Relativistic effects. There was indirect evidence against large scale jets with velocities approaching c in the powerful sources – there are too many quasar jets, and the bent jets in quasars are not brightening as they turn. However, there is the very important work presented by Lind and Blandford showing that the beaming cone may be bigger than we thought it was. The dust lane data that I presented show that low power sources have brightness asymmetries at their bases on the kiloparsec scale even in jets that are near the plane of the sky.

Hot spots. The energetics of hot spots are driving us to a picture of powerful sources where the jets are light and fast, but not necessarily relativistic. Their morphologies show very small (100-parsec) components rather frequently, and a rather remarkable lack of axial symmetry but otherwise good agreement with the simulations.

Bent sources. Chris O'Dea and Frazer Owen analyzed these in considerable detail, going systematically through the models, eliminating the ones that don't work and looking at the parameters of the ones that do.

Individual sources. M87 and Cygnus A, the brightest and the closest, are the sources that are telling us most, as usual. In M87, there is good evidence for a shock in the jet from data with many beamwidths across the source and at many different wavelengths. There are also the polarized filaments in the lobes[1]. In Cygnus A, John Dreher and Rick Perley have discovered a whole new series of features in the lobes – the filamentary structure, and a very weak jet in terms of fractional flux density. Rick Perley, Peter Scheuer and I also mapped the hot spots in extreme detail at 0.1″ resolution[2].

VLBI cores. John Biretta showed that superluminal motion is more complicated than we thought and John Wardle found that there is lots of polarization down there.

[1] Reported at the Workshop by Frazer Owen, but not contributed to these Proceedings – Eds.

[2] See the cover of these Proceedings – Eds.

2. Diagnostics – Problems of Interpretation

The theorists, of course, are all frustrated. They would like us to say "here is a jet, with a density of *something*, a magnetic field of *this*, and a velocity of *that*, and please would you calculate it ?". We're not actually helping very much along those lines, so the next important thing to think about is how we are going to measure such numbers. We have made various attempts which have not been very convincing so far.

Density. We have to understand the interpretation of Faraday rotation and depolarization in a much more sophisticated way than we have done so far. I delivered my polemic on this earlier! We have to be more careful about estimates of the jet densities, taking out the local complicating factors, such as foreground screens (which in fact are interesting in themselves). We need to study the effects of the broad and narrow optical emission line regions, of halo gas, of the intracluster media, and of the galactic foreground, in some detail. To do this, we need more of the sort of multifrequency scaled-array experiments that we saw here for example from Tim Cornwell for 3C449 and which Alan Bridle and Rick Perley did for NGC6251. We need many frequencies to sort out exactly where the material in the Faraday screens is and how dense it is before the polarization diagnostics can be used again with more certainty. We should also look for "clean" cases of jets without much foreground matter.

Magnetic field strength. I suspect that we will have to wait for an X-ray satellite to measure this properly, by looking for inverse Compton emission. We might also be able to do low frequency VLBI at the turnover frequency in some cases.

Particle acceleration. I suspect that most progress on this topic will come in the optical band in the near future. We need to know the limits of the particle energy spectrum. The shock acceleration models require the upper limit, so we must try to trace the knots up in frequency as far as we can through the millimetre and infrared bands into the optical and even to X-ray bands (if we can prove they are synchrotron radiation). Do the optical and radio emissions come from the same volume ? The optical work is do-able, the X-rays will have to wait a while, perhaps for *AXAF*.

Loss processes and ageing. We heard very little about these, which used to be quite a heavy industry when I was doing my Ph.D. a few years ago. I want to mention them in case we've forgotten them ! The interpretation of spectral indices and spectral curvature as a diagnostic is something we should *return* to, as we can now image sources over a factor of 100 in frequency. We can use MERLIN at 151 MHz and work up through various VLA configurations to 15 GHz to get information on the spectral curvature at each point in a source as well as on the spectral gradients across it. It's time to re-evaluate the use of spectral diagnostics, which can tell us about particle lifetimes and expansion speeds.

Pressure. I was appalled to hear Greg Benford talk yesterday about collective processes and other ways in which we can go wrong – that's very much a theoretical problem. We must also understand how to use minimum energy arguments to get p_{min} more reliably.

3. Critical New Observations

At the VLA, we need more "multi-everything" studies ! We must look at the closest and brightest sources with everything we've got, for as long as we can ! Radio

astronomy has learned a great deal by using its best instruments to map the Crab, Cas A, Cyg A, Virgo A and Cen A – the brightest and the nearest sources, which we can study in the greatest detail. Peter Wilkinson emphasised the importance of direct velocity measurements, and we must push that as hard as we can with *both* the VLA and VLBI. It is also extremely important to look at the one-sided quasar jets with as high sensitivity and dynamic range as possible, to improve the limits on, or actually show, the counterjets and thus to push the relativistic jet models harder.

We should also pursue orientation indicators harder – that's primarily an optical chore, using emission lines, dust lanes, and so on. We should look at whether LF variability is indeed due to interstellar scintillation, as that will remove one of the arguments favoring relativistic motions on parsec scales.

We should find out whether the VLBI cores in low-power sources with symmetric jets are also one-sided. We also need more resolution in a few areas which Peter Wilkinson didn't mention, e.g. the hot spots, where the VLA's maximum resolution of 0.065″ is not quite enough for work on compact quasar hot spots. We must find out what the values of u_{min} in these compact hot spots actually are, as they are going up way above what one would naively expect to balance by ram pressure. There are ways out of this, as Greg Benford and Geoff Bicknell have suggested, but we must look at this closely to see if there is a physical contradiction with interpreting them as beam caps.

In the context of confinement and collimation, we don't know enough about the opening angles of quasar jets, and that's another field where more modest resolution, perhaps 0.1″ , would tell us a lot more. In the context of magnetic confinement, it is important to look for the circumferential magnetic field components B_ϕ. As Geoff Bicknell indicated, we must also find out more about the potential and gas distribution in and around galaxies, from surface photometry, galaxy dynamics and X-ray brightness distributions. We may as well get that right, because we can, and it will remove some of the uncertainties.

4. Theoretical Questions

Fast jets. We have seen considerable progress on the physics of fast, high Mach number, low density fluid jets, primarily from the simulations, but I am also impressed by the way in which the simulations and the linear stability theory appear to be coming together by using the linear theory to understand the results from the simulations. That's obviously a front which is making rapid progress, so I want a bit *more* out of it ! Can we have some simulations of very high Mach number, very low density beams, which are probably most relevant to the powerful sources ? Can we extend the simulations to three dimensions, look at relativistic flows, and put in the correct radiation mechanisms and radiative transport ? The other thing we must do, and I'm sure Mike Norman has this on his list, is to understand how much we can believe generally from the simulations that applies to the observations and how much is a property of the individual simulation. In particular, can we set a hard limit on the density contrast from the size of the cocoon ? Can we guide the interpretation of u_{min} in post-shock regions ?

Slow jets. In the case of subsonic or transonic turbulent jets, I found myself rather confused. I would like to find out from the theorists in this area how general are their

models, especially the self-similar models, and how far we have really got with the closure relations in the equations ? Then, when we see a plot of collimation against surface brightness, to what extent is it *the* model and to what extent is it *a* model ? There's obviously *something* in these models, but I am not sure what !

Relativistic jets. Kevin Lind reported some extremely important results showing that the beaming angle may be larger than we thought it was. It is important to follow this up for realistic brightness distributions. Another extremely important point seems to be the subject of controversy – whether relativistic jets can be decelerated between parsec and kiloparsec scales. Dave De Young said "no", Dick Henriksen said "maybe" (if you sweep stuff up) and Mitch Begelman has said "yes" (if the Mach number is near unity). It's an extremely important question, and I hope it will soon be possible to get agreement on the answer.

Particle acceleration. We need a way of discriminating among the three front-running models: shocks, turbulence and field reconnection (which has been rather orphaned at this meeting, and I would like to hear more about it). How will we distinguish between these mechanisms observationally ?

"Flip flops". Can anybody calculate a mechanism by which a jet can change sides, telling us how and when it will happen, and for how long ? We need physics and time scales here. Also, could a jet dissipate preferentially on one side of the nucleus ?

5. The Velocity Problem

I want to emphasise the *consensus* that extended jets in low power radio sources are slow, from the evidence on brightness and bending, the prevalence of two-sided structure, and from the dust lane data. There was also a fair amount of agreement that the jets in extended higher power sources are fast, but not necessarily relativistic (i.e., we may not need $\beta > 0.2$), and that things are much easier if the motions in the cores are relativistic, though nagging doubts may remain. It is difficult, but not impossible, to come up with explanations of superluminal motion that do not involve bulk relativistic motions. But the high-γ_j flows *do* explain superluminal motions, one-sided VLB jets, the inverse Compton problem and rapid variability (at least at high frequencies).

We must focus our attention on the conflicting evidence from high power extended jets. The direct evidence for velocities close to c there is zero, though the energetic arguments John Dreher presented are suggestive and I think they are probably made stronger by adjustments required by the numerical simulations. Arguments against velocities this high are the sizes of the extended structures around superluminal sources, the lack of brightness changes at bends in quasar jets, the fact that there are too many quasar jets and the one-sidedness of the VLBI jets in the cores of low power sources.

How do we get out of this ? I can see no really nice solution, though there are a number of possibilities, depending on the outcome of the observations I suggested earlier. Although the "Observers' Have-it-all Model" will undoubtedly stimulate discussion, I doubt that it is really the right way to tackle the question.

DISCUSSION AFTER OBSERVERS' REVIEWS

John Dreher. It's not only the long syntheses, but also the multiple array (A,B,C) observations that are very time consuming. Typically, it's been necessary to spend *years* getting the data together, because it's been difficult to convince the VLA reviewers that there are important things that can't be done in an hour of observing.

Frazer Owen. My M87 map was only about three hours of data.

John Dreher. Think how much better it would have been with thirty-six hours !

Larry Rudnick. The VLA referees having been suitably chastised, I would like to take the Chaircreature's prerogative to emphasize one thing that has been ignored on the observational side throughout the meeting, and that is that we *have* measured velocities associated with jets and hot spots, through the optical emission lines measured by van Breugel, Heckman and others.

Robert Laing. No, we haven't.

Larry Rudnick. They are *associated* velocities. The problem is an interpretational one – we have no idea what they are measuring. *(Laughter).* There is information there, which is really not being analysed as it should be, perhaps because we're not ready. We have measured things that are interacting with radio emission. I showed one example of that also in a quasar but it's not with anywhere near the resolution with which we see it in these galaxies ...

Robert Laing. The reason I didn't mention it is that it *is* a question of interpretation, and I don't understand what it means !

Larry Rudnick. That's fine, but it's a real diagnostic that needs some work.

Frazer Owen. It's not at all clear. If you take the simplest interpretation, as Dave[1] does, that we're looking at entrained material, then it's not very useful. It's interesting to his calculation, but not to this problem at all.

Larry Rudnick. I don't understand that. If you can learn something about how material got entrained, it tells you something about the jet velocity.

Frazer Owen. But it's stuff on the boundary – it's somewhere close to the velocity of the ambient medium, that's all it tells you.

Dick Henriken. But if you could predict the profile ...

Dave De Young. If you could model that, you could maybe get some handle on it, depending on your model.

Frazer Owen. But that takes several steps. The statistical way is much more productive.

Alan Bridle. If it's stuff that has been pushed aside by the flow rather than entrained into it, you've got quite different relationships to the jet velocity. I think that's the problem at the moment. It looks more like it's stuff that's been pushed aside.

[1] De Young

Larry Rudnick. But then you know how much mass has been pushed aside, and things like that. There's some real information in there.

Alan Bridle. But it's hard to get at it.

Geoff Bicknell. Surely this is amenable to some good 3-D modeling.

Greg Benford. Speaking of velocity, did we hear anything at all about Sco X-1 ?

John Dreher. No.

Greg Benford. Is there anything ?

(Unidentified Voice). Yes. *(Laughter).*

Robert Laing. The high energy density hot spot is moving at less than 30 kilometers per second.

Greg Benford. And people are still tracking ?

Robert Laing. I've heard no really acceptable solution. It's just within the bounds of possibility that a very high speed, very light jet could do it. There's the pinch model. I've no feeling for whether that's realistic or not.

Peter Wilkinson. No, *tracking.*

Robert Laing. If you look at it for another five years and it's still not moving, then there's a certain smell of rat about it all. It's interesting that the other hot spot is at a similar distance. *(Overlapping discussion).*

Frazer Owen. It wouldn't have been picked out if it wasn't at a similar distance.

Robert Laing. That's true.

Larry Rudnick. John wants to leave us something before coffee.

John Dreher. I, like Robert, am a bit confused by the models, probably even more confused. This is *why* I'm confused – it's a summary of the choices we have to make about the models, the basic decision tree. We have to decide between high and low Mach numbers, relativistic and nonrelativistic flows, high and low density contrasts between the jet and the medium, magnetic versus thermal confinement, and laminar versus turbulent flows. Altogether there are thirty-two basic choices ! *(Laughter).* Just as a formal exercise, without doing any physics, just pure logic ! *(Laughter).* The question I want to leave you is – could you first remove the ones that are not physical, the inconsistent choices (I'm sure there are some rather ridiculous models here), and then see which ones are not allowed by observations ? Then, for theorists only (or any observers I suppose if you *really* want to), would those of you who have presented a theory indicate where it lies on this tree ? I'd like to collect these back and see if there are any nodes that are generally considered to be viable but have not yet been explored theoretically, and vice versa.

Greg Benford. There must be, we don't have thirty-two theorists.

Alan Bridle. Come on, since when have we had only one theory per theorist ? *(Laughter).*

Geoff Bicknell. I'd like to make a point to Robert about subsonic turbulence. I think the stage it's at at the moment is that it has been shown that making two crucial assumptions, i.e. that the jet is much lighter than the surrounding medium and that the jet is turbulently spreading, gives a reasonable account of the surface brightness variation. So far as the turbulent closure relations are concerned, in the future modeling these will give more handles on the parameters. For a turbulent subsonic jet, the main thing which is going to determine the spreading is the density ratio, and if the turbulent closure relations can be modeled we'll have some more constraints on the theory.

The second point I want to make, and I'm glad you brought it up, is that surface photometry and galaxy dynamics are important. It's frustrating that even for very well known radio sources there is so little photometry and velocity dispersion information in the literature. That even now forms an important constraint on the models because we want to know the sort of gravitational field into which we're dumping the gas which confines the low Mach number jets. That's information, I guess of a fairly mundane nature, that should be easy to get, and I'd appreciate it if there was more effort.

Frazer Owen. The biggest problem I have with the models that you presented, which is not necessarily a *flaw* but a lack of exploring parameter space, is that you have dealt mainly with straight jets, but the bending arguments tend to force you to lower velocities. You don't have a constraint on the upper range of velocities you've allowed, especially if you want to increase the brightness by slowing the jet down. But if you're constrained by a bend, that forces you to an upper limit that's much lower for the maximum velocity. That's a critical thing to be added.

Geoff Bicknell. That's one thing on the program to be considered – the bending of turbulent subsonic jets. Clearly it's going to be somewhat different in that the bending is going to vary as you go along the jet. It's important to fit that to the model.

Frazer Owen. My other point is that I agree we'd like to have all this surface photometry, and especially the velocity dispersions, but I think the surface photometry is somewhat dangerous based on the run the arguments are taking right now about missing mass. We weren't in a position to get into this much here, but it really argues strongly that the mass doesn't go like the surface brightness in these types of galaxies. I'd much rather have the X-ray information, for example. One needs to be careful using surface surface photometry.

Geoff Bicknell. Oh yes, I quite agree. The missing mass I suggest is still a controversial area, but some data is better than no data. There is some existing X-ray data for these galaxies, and in the future with *AXAF* there should be much better X-ray data. I think there is still quite a lot of point getting the surface photometry now, though. And so far as velocity measurements are concerned, it appears that the rotation of radio galaxies is an important clue as well, and to get that data you need velocity measurements in about three position angles to pin down the rotation axis. I would like to see more work along those lines, as well.

Arieh Königl. I want to get back to Robert's question about turbulence and I want to amplify something that I overheard Alan Bridle say yesterday after Geoff's talk. We have to distinguish between two things – the specific turbulence model (what is the

turbulent velocity law ?) and something that is largely model independent which is a general "plus" (the point that comes from just Bernoulli's law and mass conservation). When you have a certain pressure law and a certain velocity, that gives you the density. If we can say what the velocity does, if we know that it decelerates, that's enough to tell us that the density increases correspondingly and we can solve or ameliorate the surface brightness problem. We don't have to have a particular model for the deceleration, it's enough for us to know that it decelerates.

Peter Wilkinson. Does Alan agree that he was saying that ?

Alan Bridle. Maybe I should remake the point that Arieh has just amplified ! The main goodness of fit that Geoff showed you for his model to our data on NGC315 comes from the adiabatic compression and the velocity variation. It has very little to do with the turbulence or the particle acceleration model *explicitly.* If the jet is slowing down, and you put in the right adiabat, the slowdown alone gives you a good fit to the data. What Geoff had in two or three *lines* on the blackboard here, not in his talk, showed you how he had derived the velocity slowdown from the pressure variation. Adiabatic compression is a very *simple* way to account for the brightness variation where the magnetic field is perpendicular, and a lot of the sound and fury about the turbulent models yesterday did not have a great deal to do with the fit to the data on NGC315 !

Dick Henriksen. I'd like to have a chance to speak to this also, because I really think I can clarify the issue. What Arieh just said is in fact what I have been trying to say, but unfortunately I didn't have time to get to the bottom line yesterday. I don't disagree with Geoff's models, because I think these models are very simple. My point is that they are dictated by your global assumptions. The global assumptions I was trying to show by using laminar flow models which conserve momentum and energy, and so on. That's my whole point, the global parameters are these self similar parameters. When I apply my ideas to those mean flows I conclude that if the external pressure just for example has a parameter which tells you that $p_e = Ar^{-p}$ then the corresponding velocity is $v_z = kr^{1-p}$, and that's *all you need* to put into the adiabatic laws. It's *as simple as that.*

Geoff Bicknell. I disagree entirely.

Dick Henriksen. Well, just let me finish. Suppose we take $p = 12/7$. I've used different assumptions, I've used Reynolds number invariance as well as $T_{\theta\theta} = constant$, which is where I get this global invariant of pressure balance. These assumptions are the things that give you the variety of possibilities. If you assume pressure balance (which isn't always going to be the case), you take this r^{-p} pressure law, you use self similarity (and for $p = 12/7$ it corresponds to your case), it conserves relativistic particles (the other assumption you put in which I don't). I say that this is what is really fundamental.

Arieh Königl. The self similarity isn't required.

Dick Henriksen. Well, it's a simple way of getting the result. But there shouldn't be any confusion on these points.

Geoff Bicknell. Well, I think you *have* introduced a confusing point, because I just couldn't agree with that model.

Frazer Owen. I think the other thing that is happening is that in the powerful jets it looks like we are in a high velocity supersonic case so maybe the external medium interacts much less. To some extent the types of model that Mike Norman and other people have presented can address these problems directly. But these low velocity jets interact strongly with the environment, and to some extent these are nicer in the sense that they tie us back more to the rest of astrophysics. We are going to have to understand the structures of the galaxies, the mass distributions, things relating back to galaxy formation, and so on, to understand these sources. Maybe some of the arguments here are because we *can* get closer to the details of these parameters !

Geoff Bicknell. There's one important point you've raised. Mike is working at the high Mach number end and I'm working at the low Mach number end. There's going to be a meeting ground in between which is only going to be addressed correctly by fully 3-D models.

John Wardle. Can I change the subject ?

Larry Rudnick. Let's break for coffee, and have a longer discussion after the theoretical talks.

A THEORIST'S PERSPECTIVE – I

PAUL J. WIITA

Department of Astronomy and Astrophysics, University of Pennsylvania

Let us start with a very brief history of extragalactic radio astronomy, subtitled "The Theorist's Lament" (see Figure 1). We have Mr. or Ms. O, the observer, at the left, and on the right Mr. or Ms. T, the theorist. The observer is continually saying "take a look at this stuff", and we theorists can always come up with an explanation. A few people may take ten seconds to do so and other people may need a couple of days, but a theorist will always come up with a model.

First, the observers asked us to explain two radio emitting blobs in the sky, and while we had some blobby models, most of us liked the twin beam models better. Then the observers found "head tail" and WAT sources. It didn't take us too long to figure out at least the basic physics of these things. (However, as we learn more about them it's getting harder to fit a simple model, as Chris O'Dea has reminded us). Then people found sources that are expanding too fast for anyone who likes Einstein, but among many possibilities, most of us settled on a reasonable model using relativistic jets near the line of sight.

Then observational resolution improved and we started seeing jets with lots of knots. There are plenty of models for this, but a train of shocks fits some of the observations quite well. But then Frazer Owen goes and finds things like 3C75[1] ! So far my reaction to this double-double is that of Mr. T. in the last panel of Figure 1.

I have coordinated my review with Arieh Königl, but not with Peter Wilkinson or with Robert Laing, and it turns out there is some overlap. Perhaps this will show that a theorist can agree with the observers about which of their new results are exciting !

1. SOME EXCITING OBSERVATIONS

The continuity in 3C120 shown with incredible dynamic range by Craig Walker means that we should be able to get information on other sources in the 10 pc to 100 pc scale "gap". It's very important to look for relativistic motions on the 100 parsec scale since if they are seen rapid slowing of jets may not be necessary, at least in some cases. To me, the strongest evidence against relativistic jets is in the sharp bends we see on that sort of scale. But if the jets have to be slowed down on that scale, where does the energy go ? Can the jets help drive galactic winds, or could their energy be pumped into additional compression of the interstellar medium, perhaps driving more star formation ? We should note the correlations between Seyfert galaxies, where we have a powerful nuclear source and often jets (e.g. Wilson and Ulvestad 1982), and

[1] Detailed maps of the double-jet system associated with the two nuclei of 3C75 were included in Dr. Owen's presentation on "Wide Angle Tail Radio Galaxies", but were not contributed to these Proceedings – Eds.

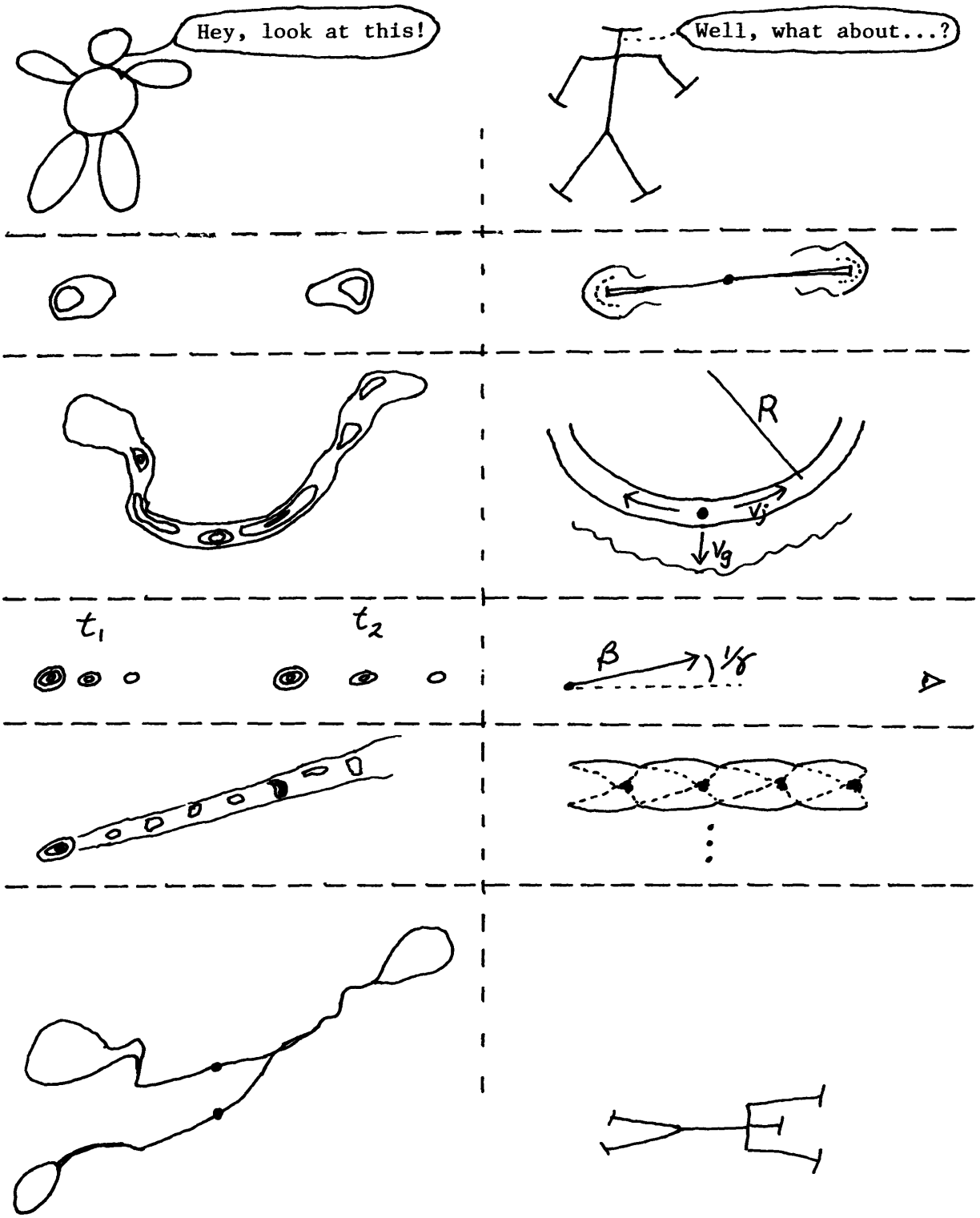

Figure 1

galaxies with a lot of current star formation – the so-called "starburst" galaxies (e.g. Weedman *et al.* 1981).

The next set of interesting results I'd like to stress is the tentative observation by Jack Burns that classical double radio galaxies with strong cores may have jets about as often as QSRs, and that the more powerful jets are clumpier. The first conclusion fits my preconceptions rather well, but the second is something of an embarrassment to the kinds of hydro models (like my own) where you get breakup into blobs at the lower luminosities, yet it's the more powerful jets that seem to be less regular. In terms of the models that were presented here, the more powerful jets do survive, and have oblique shocks, but in the weaker ones we are seeing the dominance of turbulence, making them smoother. Breaking off into blobs may then actually be irrelevant or rarely seen in the fainter jets.

Another important observation is that the "gaps" that looked to be a big problem are filling in with high dynamic range (e.g. 3C449 – Tim Cornwell, M87 – Frazer Owen). Looking for counterjets in large scale classical doubles by using the improved dynamic range now possible is necessary to distinguish between the intrinsic asymmetry, flip-flop, and Doppler boost models (cf. Cygnus A – John Dreher).

The agreement between the exciting new observations of the small scale structure of hot spots (Robert Laing, John Dreher) and Mike Norman's simulations is extremely nice, considering that he was just showing us one jet at six different times[2]. It's important that they got such a good fit to a wide array of different hot spot morphologies. On the other hand, many of the morphologies are nonaxisymmetric and this modelling is going to have to be taken somewhat further. The fact that we now see some double hot spots where the jet is leading into one and there's another strong one off to the side, seems to imply a light, fast long-lived jet that has been bent. The thrust and power arguments used by John Dreher for the powerful sources also suggest that the jet is at least mildly relativistic out to large distances, but this has to be analyzed very carefully. Thus there may be evidence for relativistic motions on the 100 kpc scale.

2. THEORETICAL TRENDS

Now I'd like to talk about theoretical trends, or at least, theoretical fashions. I define here another R_e, that's R_{el} for relevance ! I'd like to look at which of the basic theories have $dR_{el}/dt > 0$.

From what we've heard here (Geoff Bicknell, Dave De Young, Jean Eilek, Dick Henriksen), turbulence is present at some level, is probably very important in low power beams and is necessary for *in situ* acceleration. This growing consensus is going to drive me and many others back to our books on turbulence to try to understand better what's going on. On the other hand, I want to reiterate the point that we have to be extremely careful when going from the laboratory to the astrophysical case when we

[2] Dr. Norman showed results of hydrodynamic simulations of the radio surface brightness distributions of the beam cap of an axisymmetric supersonic jet ramming through its confining medium, in a presentation not separately contributed to these Proceedings. For details, see M.D.Smith, M.L.Norman, K.-H. A. Winkler, and L.L.Smarr, *Hot spots in radio galaxies: a comparison with hydrodynamic simulations*, submitted to *Monthly Notices of the Royal Astronomical Society* (available as a preprint from the authors) – Eds.

try to compare simulations with observations. I'm not convinced that when you change Reynolds numbers from around 10^3 to more than 10^6 that nothing changes.

Another area where R_{el} is still increasing is that of magnetic fields, in the sense that they can have dynamical importance and may have a big role in confining some jets (Siah and Wiita). Here we saw a beautiful theory by Arieh Kõnigl and to me the first question is: is this force free limit really valid in many cases ? There are also questions concerning the conductivity and the interaction with the external medium. We have to worry about how the magnetic fields connect with the cocoon and how the current returns around the jet (Greg Benford, Jack Burns, Jean Eilek). All of these topics are not settled, and all require more investigation before we can be sure of their relevance.

Another theoretical trend I was very happy to see is that there is some agreement between what Phil Hardee has done and what Birkinshaw (1984) has done (despite what Birkinshaw says) in the linear stability analyses. These linear analyses are important and so far are our only handle on nonaxisymmetry. Finally, Kevin Lind demonstrated the possibility of wider beams being present. In terms of trying to hold on to some kind of unified model, we may need to consider some difference in the beaming in the radio and in the optical.

3. WHERE NEXT ?

To some extent the simplest things to push, and probably also the most relevant, are the numerical experiments. The first thing to do is more 2-D hydro. Mike Norman has reported on twelve models that cover a lot of parameter space and we saw one picture of a slab calculation as well as the cylindrical evolutions. I want to make an advertisement here for some work that Paul Woodward (1984) has done. In Figure 2a we see a supersonic ($M_j = 2$) flow through a 2-D slab geometry, showing a firehose instability (what Woodward calls the fundamental odd mode) growing rather rapidly; shocks form and quickly distort the beam. The development of the pinching, or fundamental even, mode is shown in Figure 2b. This grows very fast but does not not disrupt the beam as much; the beam as a whole tends to last a little longer as it slowly widens. There is no magnetic field in any of the 2-D models presented so far.

It will be very important to use realistic galactic potentials and gas cloud parameters in future work. So far I have been guilty of not doing that but I'm glad to see that people like Dean Sumi have been including these to a degree. We do know some details about some galaxies. Granted we don't know enough, and there's the missing mass problem and many uncertainties, but we should be able to come up with more realistic models, shifting from the logarithmic potentials to power laws further out.

Relativistic flows also have to be treated in more detail. Some of the 2-D codes are being modified to include special relativity, and those codes have to be tested and run. A very interesting question for the flip-flop picture is: what happens if we shut off the source ? I think Mike Norman has a pretty good idea what will happen, but it must be carefully examined.

The next step is to add magnetic fields to 2-D codes. Another advance requires making a bunch of assumptions (it would be very nice to have radiation losses included), so that we can continue as Dave De Young has been doing with entrainment calculations and try to understand what happens if the jet does hit an obstacle (cf. Wayne

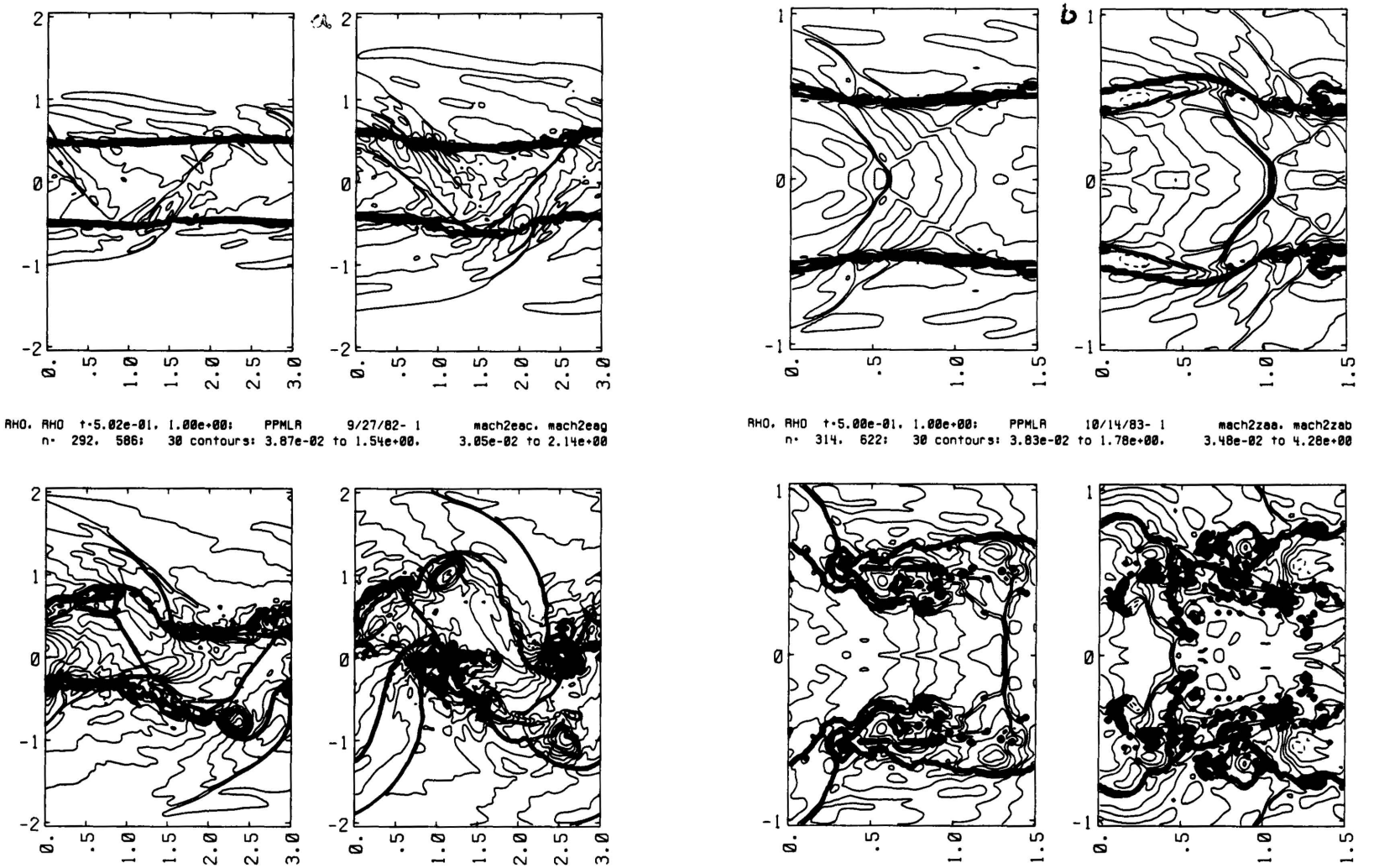

Figure 2. (a) The growth of the lowest "firehose" mode for a M=2, light, pressure equilibrated jet in a slab geometry. Thirty logarithmic density contours are shown at four equally spaced times. (b) As in (a) for the lowest "pinching" mode (Woodward 1984).

Christiansen, Dick Henriksen). Then in order to make a real comparison with the linear analyses which indicate that nonaxisymmetric modes dominate we have to go to 3-D numerical models. Finally, the Holy Grail is a 3-D magnetohydro code; Frits Eulderink here indicates that that may be possible in the not too distant future on a Cyber 205 using new advanced mathematical techniques.

The other environmental effects also have to be investigated. We see that there are problems with the simplest models of the wide angle tails, and we have to come up with a proper explanation. Also, while it is very easy to come up with a flip-flop "explanation" on the back of a napkin, it is not easy to get one to work with the requisite time scales. Finally, we have to tie beams into the power house. We have been talking about energy transport, but where does that energy come from ?

4. THE POWER HOUSE

To mangle an overworked quote, there are more things here than we have dreamed of – particularly, there are more parameters ! The situation is analogous to dining at a Chinese restaurant where there is a wide menu of choices. In particular, we're a family here so we can take several from every column.

In Column A we have the central engine: the minimal parameters are the mass of the central object and the accretion rate (which of course is tied back into the environment); perhaps the magnetic field is an independent parameter too. Maybe some genius will tie everything up self consistently, but I wouldn't want to bet on that. At this point we have the standard model, namely the "Black Hole Plus". Spherical accretion may occur but it's not going to give any collimation at all, so let's forget that. We can have a thin accretion disk, with a wind or a corona, or maybe both, starting off the beams. Whether that disk has important magnetic fields in it is a very interesting question and only very preliminary work has been done, but the mathematical formalism is now available (Thorne and Macdonald 1982). Another possibility that may be relevant for QSRs but is less so for radio galaxies is a thick radiation supported disk. Even though I'm one of the originators of this idea, right now I must say that dR_{el}/dt seems to be negative for this picture, mainly because such disks may be dynamically unstable (Papaloizou and Pringle 1984). Another possibility is the thick, two temperature ion-supported disk (Rees *et al.* 1982); in this case the magnetic field is absolutely essential. Although the physics is very complex here, dR_{el}/dt does look positive for these models.

Some sources may not just have another Black Hole, but a probably transitory powerhouse could still be there – something like a spinar, which after all is not too different from a black hole with a big disk around it, or a relativistic star cluster. We still have to look at those models carefully to see if they are viable.

In Column B is the environment. First comes the inner environment: the mass of stars in the galactic nucleus, the scale height of the galaxy, plus all of the structural factors. We must clarify how a jet interacts with the broad line region and the narrow line region. I want to stress that people are finding broad narrow lines – it's really a continuum between these regions from 0.1 pc out to a kiloparsec. The next question concerns the intermediate scale. Is the galaxy a spiral or an elliptical; is it a merger product (there are plenty of these around) ? These "parameters" must help determine

the type of active galaxy we see. Then, the outer environment must be chosen – is the galaxy in a cluster, a small group, a pair, or is it isolated ?

Finally, in Column C we come to the viewing angle to any jets and the intervening junk. The problems intervening material gives us with interpreting polarization have been stressed here (Robert Laing). But the possibility of gravitational lensing confusing us even more also has to be borne in mind.

There are many parameters that have to have some relevance, and I don't think we know enough to rule out many of them now. The "Observers' singing, dancing dream model" (Alan Bridle) will have to incorporate most of these things to yield a wide variety of different kinds of jets – relativistic, nonrelativistic, turbulent, stable, unstable, etc., etc. We won't be able to get away with a very simple model, but some form of unification will probably eventually emerge.

I thank Paul Woodward for permission to reproduce Figure 2 before publication. This work was supported in part by NSF grant AST82-11065.

N.B. Many of the papers presented at this Workshop were implicitly cited in the body of this review when the name of the author(s) was mentioned. Only references to other works are given below.

REFERENCES

Birkinshaw, M. (1984). M.N.R.A.S. **208**, 887.

Papaloizou,J.C.B. and Pringle,J.E. (1984). M.N.R.A.S. **208**, 721.

Rees,M.J., Begelman,M.CF., Blandford,R.D. and Phinney,E.S. (1982). Nature **295**, 17.

Thorne,K.S. and Macdonald,D. (1982). M.N.R.A.S. **198**, 339.

Weedman,D.W., Feldman,F.R., Balzano,V.A., Ramsey,L.W., Sramek,R.A. and Wu,C-C. (1981). Ap.J. **248**, 105.

Wilson,A.S. and Ulvestad,J.S. (1982). Ap.J. **260**, 56.

Woodward,P.R. (1984). To appear in *Astrophysical Radiation Hydrodynamics* (ed. K.-H.A.Winkler and M.L.Norman) Boston: Reidel.

A THEORIST'S PERSPECTIVE – II

ARIEH KÖNIGL

The University of Chicago

Three qualitatively new approaches to the modeling of energy transport in jets came out in this Meeting, and I will organize my talk around them.

1. NOT ALL JETS ARE EVERYWHERE SUPERSONIC

Since the original twin-beam de Laval nozzle model, we have been accustomed to thinking that the jets are supersonic between the nozzle and the lobes, and generally are becoming more and more supersonic. The new idea, which Geoff Bicknell has drawn our attention to here, is that the jets in low-power sources may have low Mach numbers and be transformed into subsonic jets. Subsonic hydrodyamics differs qualitatively from supersonic hydrodynamics in several ways. First, just from Bernoulli's equation for a laminar, ideal flow, a one dimensional channel that goes into a lower pressure region contracts rather than expands. That idea was applied by Geoff in his discussion of buoyant collimation. Second, disturbances in the flow do not propagate only downstream as they would in a supersonic jet, with the implication that no shocks are formed. This is essentially the difference between elliptic and hyperbolic equations that describe these two types of flow. Third, subsonic jets are more susceptible to Kelvin-Helmholtz instabilities. We invoked supersonic flows to alleviate some of these stability problems. Now we may be going the other way, in fact; because subsonic flows *are* more susceptible to the instabilities, they may naturally and rapidly lead to turbulence. Coupled with turbulence is the possibility of efficient entrainment, and the consequences that this may have.

What are the implications of this ? The main qualitative implication is that one can allow for the deceleration of jets on the way out rather than assume a nearly constant velocity as in our earlier models. Deceleration allows a slower decrease of surface brightness on quite general grounds, by giving rise to higher densities (perhaps constrained by the observations of Faraday rotation and depolarization) and higher magnetic fields than in a constant-velocity jet.

The caveats that we should bear in mind are the following: The intuition that we have developed about turbulence and entrainment comes mainly from analytic solutions and some experiments which deal with subsonic flows. It also comes from experiments that have relatively low Reynolds numbers, although some experiments were mentioned that have nominal Reynolds numbers approaching 10^6. In the jets we expect that either the initial portions, or some portions, may still be supersonic, and we infer very large Reynolds numbers ($> 10^9$?), though we really don't know. It was mentioned this morning that, once the Reynolds number is much larger than unity it might as well be infinity, but I'm not sure that such an extrapolation over several orders of magnitude is really justified.

What do we need in order to address some of these issues ? One topic is the physics of entrainment into supersonic flows. We heard two different points of view. One was the numerical work of Dave De Young, where it appeared that supersonic entrainment was mostly the result of vortices induced at the working surface. On the other hand, we heard the work of Dick Henriksen relating to the Landau-Squires solution where the entrainment occurs all along a supersonic jet essentially by viscous coupling. The other aspect that has to be clarified is the nature of the turbulence. We are not completely clear whether we are talking mainly about collisionless processes or whether we are using microturbulence implicitly to assume that we actually have a large-scale fluid description of the turbulence (perhaps an MHD description ?). We discussed the possibility of observational constraints on such things as the number, size, and location of large-scale turbulent cells. We should start using the models to actually predict brightness and polarization profiles across the jet, and then impose the available observational constraints, such as the absence of limb brightening.

2. Oblique Shocks

We have rediscovered that shocks can be oblique ! Again, there are qualitative differences from what we have been used to thinking. In an oblique shock, only a fraction of the kinetic energy is dissipated rather than most of it, and there is the possibility that the post-shock flow is supersonic so that it can further shock. This was applied in three different contexts.

One is the interpretation of knots. There was a happy marriage (or at least the beginning of one) between the linear analytic work of people such as Cohn, Ferrari and Hardee and the nonlinear numerical work of Norman *et al.* It was suggested that the linear theories' distinction between ordinary and reflection pinching modes translates itself in the nonlinear regime into a distinction between dissipative Mach disks and oblique X-shocks which can be convected out and which do not necessarily disrupt the jet. Further work needs to be done on the the influence of the waves that are transmitted into the ambient medium; these were discussed in connection with reflection modes, and are interesting in the general context of the influence of the jet on the surrounding medium and the process of entrainment. Another natural extension is from the $m = 0$ pinching mode to the $m = 1$ helical mode; for example, what is the nonlinear development of the reflected and the transmitted helical modes ? This may relate to the question of internal versus external shocks when the beam is kinked. We heard some discussion of this possibility from Jack Burns in connection with the knots in Centaurus A.

The third suggestion for future work arises from the need to add realistic density and pressure distributions to these treatments. One possibility, in the same vein as the idea that the transition from supersonic to subsonic flow is induced by variations in the external pressure, is suggested by the laboratory observation that a supersonic jet which emerges from a rigid nozzle into a lower-pressure region forms shocks that are stationary in the frame of the observer rather than moving with the flow. Is there anything analogous that a realistic pressure law could induce – features that are similar to Kelvin-Helmholtz pinches, but which are stationary, rather than convected, shocks ?

The other area where oblique shocks have been applied is the interpretation of hot spots, as we heard from both Robert Laing and John Dreher. There is some evidence for spot wandering, both around the lobe and from side to side. Is the wandering from side to side due to some kind of a "flip-flopping machine gun", as previously discussed by Peter Scheuer, or is it a local effect induced perhaps by a Kelvin-Helmholtz instability in the lobe itself, as Mike Norman has started to think about ? What we need are observations to look at symmetries from lobe to lobe, as in Cygnus A, and at spectral index evolution; also, numerical experiments which can handle nonaxisymmetric conditions.

The third context where oblique shocks are relevant is the question of wide-angle bends. Here I lump the wide-angle tails discussed by Frazer Owen and by Peter Wilkinson with the dogleg quasars discussed by Wayne Christiansen, perhaps somewhat presumptuously given the fact that they actually tried to separate these two effects ! Perhaps one may attribute bends to obstacles in low-Mach-number jets in the WATs versus high-Mach-number jets in the dogleg quasars. The main requirement here is the observational test, whether one can detect strong evidence for an obstacle. But we should bear in mind that for a sufficiently low-Mach-number flow we might not be able to detect a hot spot in the region of bending even if an oblique shock associated with an obstacle were present there.

3. Magnetic Effects

Just as we have discovered that it may be necessary to generalize our ideal-hydrodynamics models to include turbulence and dissipation, we now realize that modeling magnetic effects using perfect MHD may not give us the whole story. Interesting effects require localized deviations from perfect conductivity, as was emphasized by Greg Benford. The other new aspect that was pointed out is the importance of the conservation of magnetic helicity, and not only of flux, in magnetic-pressure-dominated flows, and the possibility of nonaxisymmnetric equilibria whose characteristic wavelength comes out be about 5 times the radius of the jet.

The implications are that nonaxisymmetry does not always imply instability; knots and apparent narrowing do not necessarily imply compression; the polarization P.A. rotation in BL Lac objects; and the possibility that magnetic energy dissipation is the source of the observed synchrotron emission. In a more general vein, the possibility exists that electromagnetic effects may be important all along a jet, and that they may play a role in production, collimation, internal field geometry and perhaps even lobe structure.

The questions which should still be settled concern, first of all, the differences between the particle-beam picture and the fluid (MHD) picture for these jets. Secondly, do jets really get to be magnetically dominated ? One way of checking this is to examine whether the predictions of the force-free models are borne out observationally. Thirdly, what is the relation between the accretion-disk magnetic field which figures in various jet production mechanisms and the field detected at large distances from the origin ? For instance, does the magnetic flux in the jet originate in the central source or is it entrained along the way ? Finally, what can we learn from observations of solar flares, pulsars, etc. about the electromagnetic effects taking place in extragalactic jets ?

4. OTHER GENERAL QUESTIONS

One general question is the connection between relativistic and nonrelativistic flow. We have been beating this bush for the whole week. Does the relativistic flow inferred on the VLBI scales persist until the lobes ? If the answer is "yes", then there is a problem with the large-scale QSR jets which John Wardle presented. One possible resolution (suggested by Robert Laing) is that the parent population be increased to include the powerful classical doubles. But this possibility may be constrained if jets continue to be detected in classical doubles, as reported here by Jack Burns.

If the answer is "no" – then we have the problem of dissipating the kinetic power in the jet, which has to be decreased to v_j/c times the relativistic power. Can this be done gradually by turbulent entrainment ? Is it compatible with QSR jet morphology, which seems to indicate that the jets are quite straight and powerful, and perhaps do not undergo much entrainment ?

A third answer which came out here at Green Bank is "yes and no", a hybrid model[1] in which both of these flows coexist and the relativistic flow fades away. Is this coexistence compatible with the rotation-measure constraints ? It seems to me that this is marginally so. What is the theoretical justification for this scenario and how does it depend on the parent populations ? Does it apply only in QSRs or also in the elliptical galaxies, etc. ?

Another main question that we discussed was about flip-flop activity. We heard some suggestive evidence from the asymmetries that Larry Rudnick presented. The evidence from Alan Bridle that the inner 10% or so of straight jets are "one-sided" (using his operational definition) could indicate a characteristic flip-flop time scale. In addition, the hot spot evidence of Robert Laing is consistent with the jet pointing successively at opposite lobes.

The question I still have is – is it actually a flip-flop, or only an asymmetric non-steady ejection ? Is the ejection continuous until it flips over to the other side, or is it intermittent also on any given side ? Can the same source exhibit both one-sided and two sided activity at different times ? Before we proceed to model anything, we have to be sure what it is that we want to model ! Also, are the flip-flop time scales longer in QSRs as the "Green Bank" model suggests, or is it simply that the ejection velocities are larger in these sources ? (If the velocities are relativistic, then there is, of course, an alternative explanation of the absence of detectable counterjets – namely, that they are beamed away.)

In the remaining negative minute[2], I will make some "positive" remarks. Regarding the observations, we are now focusing on both the innermost and the outermost parts of the source in some detail. Studying the first 100 pc and extending the VLBI scale to see the connections between it and the VLA scale (as Peter Wilkinson discussed) could possibly answer the question about the relativistic/nonrelativistic transition. There is even the possibility that optical interferometry will tell us something about the sub-VLBI scale some time in the future. We are also looking now at lobe structure in more

[1] The "Observer's Dream Model" (Bridle, these Proceedings) – Eds.

[2] At this point the Chairman began approaching the speaker – Eds.

detail. We found out that there are filaments in both polarized flux and intensity-gradient maps – what are they ? Are they vortex rings, or magnetic loops ? We also need more numerical experiments and both particle-beam and wind-tunnel experiments. Until now, a major problem with wind-tunnel experiments on jets was that we wanted them to generate huge Mach numbers. Perhaps now we realize that these are not necessarily required, so that experiments with Mach numbers not much greater than unity could still give us relevant information about such issues as the interaction with obstacles, pressure gradients and buoyancy effects.

DISCUSSION AFTER THEORISTS' REVIEWS

Larry Rudnick. I think we are all very appreciative of our four reviewers for their thoughts on where things are going. Before we start the discussion, I think we should also extend our appreciation to Wally Oref, who has made this a very easy thing for us by keeping everything flowing smoothly and by sitting through our talks for the whole week. He's put up with us for a long time. Thank you, Wally. *(Applause).*

Let me say one other thing. I don't know what Alan thought was going to happen when he asked me to chair this discussion, but I would like to try an experiment in the last ten minutes. I would like to go around the room once. There are some people who don't speak up when they've got to break into the discussion and I would like to suggest that everybody think what they would say if they had fifteen seconds to talk – what *one* point would you make ? You needn't take it, but I would like to give everybody the opportunity to take that time at the end. Otherwise I won't call on people, so long as they're self-regulating !

OK, before John Dreher bursts, we should let him make his comment, then John Wardle, who I cut off before coffee. Dr. Dreher, do you want to comment ?

John Dreher. No. *(Laughter).*

John Wardle. If we are going to take the "flip flop" model seriously, then we had better find some jets which are in the act of flip-flopping. Now there are plenty of jets where we see just fragments, either only near the lobe or only near the quasar, and I'd like to ask "how can we tell whether these are just fluctuations in brightness ?", or "what is the signature of a real jet turning on and off ?" That ties in with a plea to the numerical modelers to turn their jets on and off. We've got to find these things if that's what's happening.

Robert Laing. Can I put on my other hat for a moment and say there are a number of things we haven't addressed at all ? One absolutely fundamental fact has been known for years. Why are the double sources primarily, perhaps *exclusively*, in elliptical or eliiptical-like systems ? It's an extremely important point and an extremely clean result. Every galaxy that we know of that is a double radio source is an elliptical ...

Frazer Owen. That's no longer true.

Robert Laing. Which one isn't ?

Frazer Owen. There's been a nice example found by the *IRAS* surveys – a powerful galaxy that's got Seyfert characteristics and a beautiful double radio source ...

Robert Laing. OK, one example, but that doesn't ...

Frazer Owen. And some others that people have argued about.

John Dreher. But over 99% of them are ellipticals ...

(Overlapping discussion).

Arieh Königl. This was addressed by Sparke and Shu.[1]

Robert Laing. Do we *agree* with that model ? I've heard no discussion of it.

Arieh Königl. It's at least reasonable. If the jet finds it difficult to escape from the surrounding gas ...

Geoff Bicknell. Then the problem spreads into the Seyferts. Why does so much of the power of the source go into optical emission rather than radio radiation ?

Dave De Young. By interacting with the surrounding gas. It follows from the interaction if there's lots of gas in Seyferts ...

Robert Laing. From what we know about the gas rotation in low power sources as opposed to high power sources, the gas in the high power sources appears to be rotating *more*, rather than less, which is the wrong way round. The gas is what they are using to do the collimation.

Dave De Young. Are you talking about theoretical gas or observed gas ?

Robert Laing. I'm talking about *observed* gas !

John Dreher. I have a plea in a different light. If we're really going to get coherent plasma processes radiating in disguise as synchrotron, we've got to settle that very quickly, because it has a *drastic* effect on our interpretation. We've got to *kill* that very quickly ! *(Laughter).*

Larry Rudnick. That's easier said than done. It's easier to *find* it than to kill it. Finding it may be impossible, so killing it would be worse !

John Dreher. Let's not just ignore it. Please let's sort this out.

Wayne Christiansen. I'd like to try to kill it ! I think it suffers from the same problems in some senses as the relativistic interpretations of extended sources do, namely you have to be viewing it *along* the beam in order to see your tremendous enhancement in the surface brightness. Isn't that right ?

Greg Benford. No you don't, because the beam ...

Wayne Christiansen. What would coherent plasma oscillations of a beam look like if you viewed the beam transversely ?

Greg Benford. If you looked transverse to a *beam* you'd be out of the $1/\gamma$ cone, *but* the problem is ... who says that in a lobe or a hot spot it's all that beamed ? The whole process is turbulent and it may get turned in the right direction. All that's necessary is that it's a stream of plasma, not that it be ...

(Overlapping discussion).

Dave De Young. Yes, but since this is a streaming process, then you've got to arrange for the relativistic electrons to be moving *isotropically* through the plasma ...

Greg Benford. Which is the assumption you make for synchrotron radiation.

---

[1]L.S.Sparke and F.H.Shu, "Why extended radio doubles are found in elliptical galaxies", *Astrophysical Journal Letters*, vol. 241, pp. L65-L68 (1979); also L.S.Sparke, "Galactic gas and the shapes of radio sources", *Astrophysical Journal*, vol. 254, pp. 456-464 (1982) – Eds.

Dave De Young. Except that this is a streaming problem ...

(Overlapping discussion).

Greg Benford. So you have to have two components ...

(Overlapping discussion).

Phil Hardee. ... and that might be difficult to arrange.

Dave De Young. Hard to build.

Greg Benford. But what is a shock ? Shocks are hard to build, too.

Wayne Christiansen. Your proposal in a sense is to eliminate a turbulent magnetic field in which you see beaming from individual electrons and put in a turbulent plasma wave field from which you see beaming from little clumps of electrons.

Greg Benford. Right.

John Dreher. I just pleaded to get this settled, not to settle it *here* !

Larry Rudnick. Well, I've been talking to Greg about a way to settle this, also. I think there's a straightforward way. but it depends very sensitively on how many independent coherent regions there are in one ...

John Dreher. I'd just like to see an in-print figure of just what the mechanism *is* and what its time scales are, and its surface brightness, and things like that, so that we can think of ways of testing it ...

Greg Benford. I'll put it in the Proceedings. I might mention that in our experiments the number of radiators is probably no more than about 10^4, and it's very easy to see the coherence factor from the individual radiators. When you get up to a very large number of radiators, it becomes more difficult, but I think it should be do-able if there are no more than a million. It goes like $\sqrt{N}$. One part in a thousand is not hard to see.

Frazer Owen. What would it look like ?

Greg Benford. You'd see a coherence factor as a self-correlation in the signal that would be quite long, but you'd have to have a small number of radiators.

Frazer Owen. There might be other things in radio sources that would have that sort of property.

Greg Benford. Well, incoherent synchrotron radiation won't do that !

Larry Rudnick. But that in itself would be interesting. If we were to see *any* sign of a coherent process, independent of how you interpret it. Right now everything is supposed to be incoherent.

Greg Benford. I think the best place to look is Sco X-1, it's small and close.

John Dreher. It's also irrelevant to extragalactic radio sources ! *(Laughter).*

Alan Bridle. But the *mechanism* isn't irrelevant !

Greg Benford. That's another tendency – every time you find a *local* jet, in the Galaxy, you *immediately* disclaim that it has anything to do with extragalactic sources !

(Various). No. No, we don't.

Greg Benford. But look at the number of people who've said "should we even mention SS433 ?". And you say – "yes, it's the only known jet in which we have a velocity, so throw it out !"

Alan Bridle. I don't think we're doing that at all, it's just that the *details* may not scale up.

Mike Norman. I'd like to address a question to both Kõnigl and Wiita. They both said that there's an increasing relevance of magnetic fields in the dynamics of jets. But when I looked over my notes, I couldn't really see what the observational bases for those statements were. Can someone summarise those again for me ?

Arieh Kõnigl. Maybe you should look at *yesterday's* notes !

Mike Norman. Aside from your model, which reproduces the knot and polarization structures in NGC6251 very nicely ! Do we have anything more than that which is really convincing ?

Frazer Owen. The apparent overpressures relative to the thermal background from the X-ray observations, but you can argue about that if you like.

Mike Norman. But that's less than an order of magnitude, isn't it ?

Phil Hardee. It's up to more than an order of magnitude, and it's a *minimum* pressure in the jet.

Arieh Kõnigl. But how does it compare with the thermal pressure, in the jet ?

Frazer Owen. It's an *extreme* minimum pressure. It could be much worse, in fact. We don't know how bad it is.

Alan Bridle. It's also worse for the powerful quasar jets in some cases. But it matters whether the overpressure is just in the knots, at shocks, or all the way along the jet – in some cases it's all along, in between the bright knots, too.

Mike Norman. Let me ask a follow-up question. There's also this u_{min} problem associated with hot spots, that both Dreher and Laing mentioned. Could this be explained in terms of magnetic effects ?

Arieh Kõnigl. But this we believe to be due to *shocks*, and that's a somewhat different question. In a shock you have essentially translated directed motion, and then these are transitory effects. I think that is the most natural way to explain them, in terms of ends of the directed motion.

Frazer Owen. We could argue about John's correlations, but you saw the types of argument he was using ...

Mike Norman. It's going to be a problem, and if you can explain it by just going to lower densities ...

John Dreher. It's not a *problem* so much as just evidence for mildly relativistic motion in some jets.

Frazer Owen. But if you believe your full analyses, you had to perturb the parameters dramatically even to get *down* to mildly relativistic velocities.

John Dreher. But I directed that analysis entirely to see whether jets were moving with β greater than, say 0.2. There are some loopholes to get out of the energy problems. but you grant that ...

Arieh Königl. But the very fact that you *see* them presumably tells us that we have a shock here in the supersonic motion ...

Frazer Owen. I'm not saying that there's a shock, Arieh, that's a leap of faith. It may look pretty good, but if you have a major problem with the observations ... It also looked pretty good that the jets were relativistic because of their one-sidedness, but now that's gone away. We have to be a little careful about believing these statements about the data. *(Laughter).*

Robert Laing. Can I say something about the hot spot ram pressure confinement ? The problem is primarily in quasar hot spots at high redshift with very high energy densities, by naively trying to equate u_{min} to ρv^2 in the external medium with a plausible ρ, and v set by the separation ratio. Am I correct in saying that we may be *incorrect* if we naïvely interpret u_{min} behind the shock as a static pressure ? That's where the shock comes in.

John Dreher. "Does it really stagnate there ?" is the question.

Robert Laing. In the 3-D model, it won't stagnate, for a start. And as Arieh just said, and Geoff pointed out earlier, it is a transient thing behind the shock that converts itself into forward kinetic energy.

John Dreher. It seems to me though that that's basically avoiding the main problem for the energetic argument, because ...

Robert Laing. It's *nothing to do* with the energetic argument ! This is a separate argument. We've been saying that if a hot spot came to a stop and formed this very high pressure region, and the only way we had of keeping it in was the ram pressure of the source moving out through the IGM, then we know it can't do the job ...

Arieh Königl. It has to be a minimum value, of course. If it's oblique, it has to be even more. What you would infer from u_{min} would be the minimum you would have to have there if you wanted to confine it.

Robert Laing. Oh yes, that's certainly a lower limit.

John Dreher. If the hot spots were really *very* oblique, clearly this would help a lot, but in fact you seem to see bends of 90° ...

Robert Laing. You're only changing the momentum transfer presumably by factors of two or three. But that's not the point that Geoff was making, is it ?

Geoff Bicknell. The point I was making was specific to knots in jets rather than hot spots.

Robert Laing. But if we go to the 3-D "glance" model for these, and *all* of these things in quasars *are* recessed hot spots, then shouldn't we be treating them more as jet knots than as the stagnant cap on a beam ?

Geoff Bicknell. Certainly treating it as an oblique shock changes your estimates of the energy balance, and so on, by factors of two or three or so. I'm not very familiar in

detail with the sort of numbers you've been getting for hot spots, so I can't say whether that's significant or not.

Robert Laing. What we should try to do is to work out whether there is still a problem, taking these things into account. I think we can probably do that pretty soon.

Geoff Bicknell. What you *should* do is take the relations for oblique MHD shocks that are given in Bazer and Ericson in *Ap.J.* '59[2]. They give all the relations you require for this.

Larry Rudnick. I would like to make another pitch to the theorists, and that is to follow up the point that Arieh made, and a few of us were discussing at breakfast, about the structures in the lobes. All of these pretty structures are starting to come out from the image processing and from the long syntheses. I look at that and see these things as vortex rings, and if Tom Jones is able to do it, we'll put some physics in there ! *(Laughter).* But it would be nice to have some guidance about what sorts of things to look for. What would you like to know about the filaments ? There's the question about the filling factor, for example. What are the most important things, the critical parameters ? There's so much information coming here, and we'll do some things on it anyway, but what are the most intelligent, the most useful, things ?

John Dreher. Can I say just one word on that ? Arieh seemed uncertain about the intensity gradients. They really are in I.

Larry Rudnick. You may need to make a gradient map to see them, but they really are gradients in I.

Arieh Königl. But Jean Eilek said she didn't see them in total power in some of the sources.

Jean Eilek. In some sources you do, in some sources you don't. It depends on I and P.

Larry Rudnick. OK, it is true that when you look at some of these things on a screen, like that "piece of a jet" I was looking at, you can see there are transition regions. There are regions that are very filamentary and then regions that are very smooth, and that's the kind of thing that gradient maps show up.

Arieh Königl. Why that may perhaps be relevant is that the physical question is whether or not the filaments dominate the dynamics of the total lobe. Is it just that we distinguish them as features because there are large gradients there, but they may not necessarily be where all the action is ? For example, they could be smoke rings that maintain some coherence on their own, or because of flux loops, but not necessarily because they dominate the dynamics.

John Dreher. You can decide that easily by looking at an I map.

Frazer Owen. Let me say one thing about the M87 filaments that is probably very important. The dynamic range that we have on the lobes right now, because of the problems of doing image restoration, is pretty low. If you try to calculate limits on whether these filaments could actually be slightly denser regions of coherent field, it is

[2] J.Bazer and W.B.Ericson, "Hydromagnetic Shocks", *Astrophysical Journal*, vol. 129, pp. 758 - 785 (1959) – Eds.

hard to rule that out. Whether we will be able ultimately to see them in the *I* maps is not settled, because we certainly don't have the dynamic range that you do in Cygnus A.

John Dreher. I *told* you you needed more data !

Geoff Bicknell. I think one of the interesting things about these filaments, as I pointed out to John Dreher earlier, is that they look very similar to the sort of filaments that you see in contrast enhanced pictures of HII regions produced by Dave Malin at the *AAT*. Presumably those sort of filaments are due to thermal instabilities and so on, operating on this sort of gas with magnetic field threading through it. One of the standard theoretical waffles about that is that the electron conduction is suppressed perpendicular to the magnetic field but it can operate *along* the magnetic field, so this tends to make the filaments collapse – to make the gas collapse in a thermally unstable fashion and follow the field lines. I would think that very similar physics is possibly operating in this context.

Dave De Young. Almost twenty years ago, Mike Simon and Ian Axford proposed a similar thing for a *synchrotron* instability which gives you filaments in synchrotron sources. That's been buried in the literature since about 1966[3].

Arieh Königl. That was really the original. That was for the Crab Nebula. Again, there's a question of whether these are thermal instabilities, in which case you would be somewhat puzzled why they are so bent, or whether the bent structure already came from having magnetic fields there in the first place.

John Dreher. I don't think I would buy your HII region thing anyway, because the thermal energy is two orders of magnitude greater than the magnetic energy in an HII region.

Geoff Bicknell. But the magnetic field can be important even though it's not dynamically dominant. It doesn't have to be dynamically important to be able to suppress the electron conduction. That's an argument that's been around for a long, long time, in fact it's been one of the arguments which has justified fluid dynamical treatments of jets. You don't have to have a dynamically important magnetic field for that to be important.

Larry Rudnick. Greg is going to intentionally change the subject.

Greg Benford. The observers, I think quite rightly, may object to some theorists who have in the last few years said that maybe what we are all studying out here is the "weather", and that the "real point" is the galactic engine. One way to offset that is to point out that we should always try to elicit the properties of the jet which directly connect to the engine, and are not just the weather. You can learn a lot about the weather, and that's fine, but there are some quantities that will be conserved. The obvious one is **J**, in fact. It's very hard to entrain **J**. If there's a net **J**, then you find out something about it. *(Laughter).* You can entrain lots of stuff, but not currents – Maxwell doesn't like it. And there are other things about the jet – the early Mach

[3] M.Simon and W.I.Axford, "Thermal instability resulting from synchrotron radiation", *Astrophysical Journal*, vol. 150, pp. 105-113 (1967) – Eds.

number and things like that. It's really worth doing all the simulations, etc. to find out what is absolutely *needed* as far down as possible. Always keep in mind that we should be working backwards towards the core, not because that's the whole point of it, but rather because that is the *biggest* mystery. Theoretically, it's getting tougher on those models. As Paul Wiita pointed out[4], dR_{el}/dt is *negative* for some of the models. I thought it was very brave of him to say that of one of his own models. We should always be trying to give those modelers much more constraints than they have now, to avoid the "tennis with the net down" problem. *(Laughter).*

Mike Norman. I'd like to follow up on that by saying that I've always disagreed with the Cambridge school on this "weather" issue, in that these jets are commonly assumed to be supersonic. We know that supersonic flows have coherent nonlinear structures which we know *are* a probe of the flow conditions, whereas we know weather is subsonic. *(Laughter).*

Peter Wilkinson. Usually.

Arieh Königl. That's the whole point, Peter.

Mike Norman. I'd like to augment a point that Paul Wiita made in his review – that is, not only do the linear stability analyses of the Kelvin Helmholtz modes appear to be converging, but they also seem to be converging with the nonlinear studies. Not only for the pinching instabilities that I've investigated, but also for the kink type instabilities that Paul Woodward has illustrated. My second point is that we should highlight in this meeting the theoretical problems that have gradually *disappeared* over the last few years.

Greg Benford. And the theorists ! *(Laughter).*

Mike Norman. One of these, in my opinion, is the problem of jet stability. It appears now that if we believe that the important pinch instability in high Mach number jets is the reflecting mode, my work has shown that this is not disruptive. If we believe that the most important kink mode is the lowest order reflecting mode, which I believe is the case on the basis of Woodward's calculations, then it's possible to get great distances without disruption by simply cranking up the Mach number. That's point number two.

Point number three is that if there is a single mode that *always dominates* in either the pinch or the kink case, then that gives us a tracer of the underlying flow. In the case of the pinch instability, which I'm more familiar with, it appears that there is a characteristic wavelength that is a few times the jet diameter, where *knots* appear and these should be moving with more or less the beam velocity. That's an important tracer of the flow.

Dick Henriksen. I think one of the important problems we really need to do in a general way is the extent to which motions on the smaller scale cascade up to the larger scales. If you think about it, that would impinge on a lot of the things we've been worrying about. Can supersonic jet haloes grow to the size we've been worrying about ? Can you entrain large eddies ? It's the old question about what we actually *see* being perhaps

[4] In his review talk – Eds.

the whole story or only just the tip of the iceberg. It may be that as the dynamic range improves and the flow visualisation techniques improve we'll see a lot of this other stuff.

My second comment is on this "shock" point that Robert raised. I think there's some confusion there. Basically, it's a question of whether the flow continues or not. If we're going to say that the spot is confined statically, then there's no escape !

Robert Laing. That was my point – that the only hot spots showing this problem are the recessed ones where we can say that the flow is deflected but continues in the basically forward direction.

Dick Henriksen. Then there isn't any problem.

Robert Laing. Well, you've still got to balance momentum transfer sideways, where it bounces off the wall, but that's less of a problem.

Dick Henriksen. The actual pressure you require in order to *deflect* the flow goes like $\sin^2$ of the angle of the shock.

Wayne Christiansen. In the case of the quasars, are you talking explicitly about deflected hot spots ? I wasn't here when you mentioned this.

Robert Laing. No. What I'm talking about are regions of high u_{min}, particularly the ones that Colin Lonsdale and Peter Barthel[5] have studied using VLBI. If you consider them as confined by forward ram pressure, you've got yourself in something of a muddle.

Arieh Königl. I have some questions now to different people. First, for Jack Burns. Do you think the structure that you see in Knot A2 in Cen A when you observe the Cen A jet at 6cm, has any resemblance to the filamentary structures in the polarization maps of Cyg A lobes ?

Jack Burns. That's hard to say. For one thing, the polarization situation is still very confusing, and I haven't sorted it out. Also, the resolution is such that we still have only two or three beamwidths across the jet. We have some more data that will improve that by a factor of three ... *(inaudible)* ... so maybe in a few months I'll be able to answer that more clearly.

Arieh Königl. A question to Mike Norman – do you think you could test whether you would get different types of pinches or shock modes if you used a more realistic pressure law, say a gradient in the pressure that has a scale larger than the scale for development of such modes ?

Mike Norman. I think there are two regimes. One is when the spreading rate is small, in the sense of Phil Hardee's analysis, in which case I would expect the shock wavelength would probably scale with the local jet radius. In the case of rapid jet spreading, I would expect things to be considerably different.

Arieh Königl. My last question is about flip flops. I still don't quite understand from the observers whether there is evidence for things shooting out first on one side then the other, or can you shoot in both directions at the same time ? If it is stochastic, just

[5] See C.J.Lonsdale and P.D.Barthel, "High resolution dual frequency observations of 3C205", *Astronomy and Astrophysics*, vol. 135, pp. 45-52 (1984), and references therein – Eds.

what is it that we have to explain ? There's no point in *thinking* about it if we don't know.

Larry Rudnick. The evidence so far as I'm concerned is still suggestive that the sources are different on the two sides, but there is nothing that you are *forced* to explain. As far as what *suggestive* evidence I can see, it is not a *regular* back and forth. It is as if you shot on one side, turned off, and then shot again on a random side. I am working very hard to develop refined tests to sort this out, but there's no corner that you're forced into yet.

Wayne Christiansen. One of the reasons this is confusing is that the strict behavior of needing to go from one side to the other is because of the "gaps", or "brightness contrast", or whatever. That goes away somewhat if the lengths of the two sides are different, because even if you throw things out simultaneously, the events at the ends of the channel occur at different times and you can see different structures, which you might infer are flip flop structures. But if you want to do things on the two sides simultaneously, in order to have that kind of *opposition* on the two sides you need different channel lengths so that the lighting up of the two lobes, or such things as splashbacks, take place at different times.

Dave De Young. You need a pre-existing channel for that.

Wayne Christiansen. Yes, I understand that !

Larry Rudnick. One of the things Wayne is saying that people may not appreciate about the splashback model is that some of the stuff we would normally interpret as being out along the way, you would interpret as being on its way back.

Arieh Königl. Even from distances of kiloparsecs ?

Wayne Christiansen. Yes. I'd like to make a plea to Mike Norman in connection with his models – we were talking about this at coffee. Splashbacks can occur from crashing phenomena, but I think what looks like a splashback can also occur if you turn off the beam. The basic point is – in a lot of Norman's models, you see these beautiful little valleys at the ends of the jet which are Rayleigh-Taylor instabilities. These valleys do not grow and propagate all the way down the axis for a very good reason – there's a jet pressure impinging on them. If you shut off that pressure I believe the valleys will probably pass back down the center of the jet, perhaps entraining material and making a splashback.

Dave De Young. That's a calculation that has got to be done.

Wayne Christiansen. Absolutely, that's why I said this is a *plea* to Mike !

Mike Norman. We discussed it, and it's plausible.

Larry Rudnick. Ladies and gentlemen, we are all in a sense experimentalists, and I would like to experiment with our "final statement" scenario. Do you have any final words for this captive audience ? [6]

[6] Larry then called on everyone present in order of their seating in the room. Not everyone took advantage of the opportunity, and some were audible on the tape, but we reproduce as many of these remarks as we can. – Eds.

Peter Wilkinson. There is a possibility of tying things down directly – we seem to be thrashing around, so *my* hope is to measure jet velocities directly very soon.

Arieh Königl. I can only say "thank you" to my volleyball team ! *(Laughter and Applause).*

Greg Benford. Try to find out whatever we can about the central source by studying the flow as far back as we possibly can. Look for the invariants.

Dick Henriksen. Are you going to measure your "Jolly Green Jet" ? I want some experiments on the Green Jet[7] !

Dave De Young. I would be in favor of more calculation, and less speculation.

Craig Walker. We should remember that these jets go on over four orders of magnitude in distance. A lot of the calculations are only over one order of magnitude.

Mike Norman. That's a problem of *numerical* dynamic range !

Phil Hardee. Well, I just hope that what we see in the *radiation* patterns is really telling us what's there ! *(Laughter).*

(Unidentified voice). If it's not, we can all give up.

Wayne Christiansen. One thing that slightly came out that might be important is that we should look at radiative processes – the synchrotron instability was mentioned, and it was also mentioned that radiative losses are sort of balanced in terms of the reconnection rate. I think these ideas could be important.

George Seielstad. I would sound a cautionary note that there's a lot of parameter space that astronomers could focus on, and maybe we've picked a very small subset here. It's kind of a "forest versus trees" argument. We could be starting to focus on microdetail that's of no interest to anybody ! *(Laughter).*

Frazer Owen. I'll just say that I disagree with George ! *(Laughter and Applause).*

Tim Cornwell. I haven't heard anything about equipartition and how it's maintained.

Mike Norman. I've got a long list of jet calculations to do that will keep me busy for another five years, but I still need input from observers – put me on your mailing lists !

Paul Wiita. Aside from my last viewgraph, which I hope you will all remember – just as observers now want the *VLBA* and space based interferometry, I think more of the theorists deserve what Mike's got, and should have supercomputers !

Dean Sumi. We shouldn't *forget* all the elliptical galaxies that don't have any radio emission.

Jack Burns. Just to reiterate that we have some difficult, but do-able, experiments with the VLA – for example, looking for jets with cocoons, looking for counterjets – that require long detailed VLA observations. These should be done, despite the limitations in computing power.

Kevin Lind. I think one thing we need to get more serious about is really convolving theoretical models with radiation processes and observational constraints so we can see what these things would look like hot off the 'scope.

---

[7] See the description by Larry Rudnick earlier in these Proceedings – Eds.

John Biretta. A lot of the information we have right now is single images. If we had time evolution data for some of these sources, as we might have a few years from now for the nearby jets, this would help.

Robert Laing. I just wish ... *(inaudible)* ... could come up with a hard number for velocity, pressure, density or some other number that is what the input to a hydrodynamic model should actually be.

Frits Eulderink. I'd like to thank everybody present for all the things I've learned at this conference.

Geoff Bicknell. Well, one *scientific* comment. *(Laughter).*

Larry Rudnick. It had better be short !

Geoff Bicknell. As far as mapping out parameter space is concerned, I think the diagram introduced by Mike Norman of density ratio against Mach number is going to play a large role in simulations. We're all mapping different regions of Mach number space.

The *personal* comment I'd like to make is that I've found this an intensely stimulating week and it's certainly given me food for thought for the next ten years before I make another appearance on this continent !

Chris O'Dea. More work needs to be done on *bent jets*, for three reasons. One is that this will keep *me* employed ! Another is that bent jets pose special problems for stability. Also, bent jets give you a good constraint on the momentum flux, and that ties things down a lot better.

Also, in NGC1265 you have an example of a cocoon that is not associated with backflow from a working surface – keep in mind that not all cocoons can be generated by backflow from working surfaces !

Alan Bridle. We've had an enjoyable week, and I don't want us to forget all the people who we couldn't invite in order that *we* have such a small, participatory meeting. Please – put your best thoughts down in the Proceedings, so we can get them out to all those other people who ought to have been here too, but who we couldn't invite and still keep the meeting small and informal.

Larry Rudnick. Wally - would you like to say anything ?

Wally Oref. Lunch is in two minutes !

Larry Rudnick. The Chaircreature reserves the last comment, which is that so far as I'm concerned this is a *good* part of the way science is done – with discussion and dissension. We understand that, but our students, especially undergraduates, don't. Even more important, the public, who fund us, doesn't understand that. Make sure that, when you have contact with the public in various ways, you show them the nature of the way that science is done. And thank you all !

QUOTES WITHOUT COMMENT

Craig Walker This thing looks very lobish.

John Wardle Where does 90 per cent come from ?
Dave De Young Off the top of my head.

Robert Laing I'll be fairly brief.
Larry Rudnick That was good, Robert !

Robert Laing I don't want to get into that kettle of red herrings.

Greg Benford These aren't really models, they're expressions of concern.

Larry Rudnick, to Robert Laing I'm not sure which way is "up" in your terminology.
Alan Bridle To someone from Cambridge, the direction away from the observer is always "down".

Greg Benford This occurred to me more or less *in vacuo.*

Larry Rudnick What you see is not always what's going on.

Larry Rudnick I think we can get around that, but let's talk about it later.
Robert Laing I don't.
Larry Rudnick That's why we should talk about it later.

John Dreher Should we expect to see the large scale eddies ?
A. Theorist It depends on your flow visualisation technique.
A.N.Observer We call ours "radio astronomy".

Dave De Young You can collapse and make stars on the back of an envelope.

Geoff Bicknell The orifice was a pressure cooker in the Mount Stromlo kitchen. We lowered the velocity by turning down the heat.
A.N.Observer Is this one of those precisely machined orifices we've been talking about ?

A. Theorist These are the full equations.
Larry Rudnick This is incomprehensible flow.

Geoff Bicknell To get involved in turbulent modeling, you need to be some kind of masochist.

A. Theorist The notation is consistent, it's just that R doesn't mean the same as it did before.

A.Kõnigl How does the current return ?
Greg Benford It hits the wall and runs back to Mother.

A. Theorist It's in *Landau and Lifshitz.*
A. Theorist It's done as a problem in *Landau and Lifshitz.*
A. Theorist This is straight out of *Landau and Lifshitz.*
A. Theorist It's in *Landau and Lifshitz,* but I'm not going to tell you where !

Greg Benford In astrophysics, everything is small except the size of the objects.

Jack Burns I don't want to say whether this is real. Dynamic range is a strong function of position on a map. *(Silence)*
Jean Eilek Oh ... God !

A.Theorist Helicity is a relatively conserved quantity.
Greg Benford Being "relatively conserved" is like being "half pregnant".

Greg Benford You have one particle carrying the current, then a whole lot of relatives living off this particle, being confined by it.

AUTHOR INDEX

Benford, G. 185
Bicknell, G. V. 63, 229
Biretta, J. A. 120
Blandford, R. D. 121
Bridle, A. H. 1, 135
Burns, J. O. 25, 83, 255, 265
Christiansen, W. A. 83, 129
Clarke, D. 255
Cornwell, T. J. 39, 76
Cowan, J. N. 57
De Young, D. S. 100, 202
Dreher, J. W. 57, 109
Eilek, J. A. 216
Feigelson, E. D. 255
Hardee, P. E. 144
Henriksen, R. N. 122, 211, 245
Königl, A. 200, 260, 292
Kus, A. J. 76
Laing, R. A. 90, 119, 128, 276
Lind, K. R. 121
Norman, M. L. 150
O'Dea, C. P. 47, 64
Owen, F. N. 47, 89
Pearson, T. J. 76
Perley, R. A. 39, 57
Potash, R. I. 30
Readhead, A. C. S. 76
Roberts, D. H. 99
Rudnick, L. 35, 114, 133, 182
Schreier, E. J. 255
Siah, J. 193
Smarr, L. L. 150, 168
Spulak, R. G. Jr 265
Stocke, J. T. 83
Sumi, D. M. 168
Walker, R. C. 20
Wardle, J. F. C. 30, 99
Wiita, P. J. 193, 285
Wilkinson, P. N. 76, 272
Winkler, K.-H. A. 150

SUBJECT INDEX

(New data, or major discussions, are referenced **in bold type**).

Coherent plasma emission **190–192**,277,298,299
"Core" radio sources
  Correlation with jets 28,105,138,274
  Steep-spectrum cores 77
  Relative prominence of 7,25,136
  Variability 104,108,120,201,278,279
  X-ray emission 105
Faraday effects **90–98**
  Depolarization 16,39,40,54,91,93–98,236,242,257,277
  Foreground screens 91,94–98,257,277,291
  Mixed geometries 91–93,96
  Rotation 17–18,48,52–56,200,277
"Flip Flop" Model 8,29,33,**38–38**,129,140–143,274,279,290,295,297,305,306
Galaxy atmospheres
  Bending of radio sources 85–87,282
  Cooling inflows 174,175,177–180
  Faraday rotation 94–96,277
  Jet propagation in 44,160,**168–181**,194–199,232,234,235,238,239,242,253,278,282–284,288, 290,297,298
  Winds 174,175,177–180
  X-ray halo emission 10,11,28,29,40,174,193,278,282
Hot Spots 2,60,61,**109–113**,**128**,232,276,287,294,300,301
  Magnetic configurations 9,128,210
  Magnetic field strengths 110,277
  Optical emission 114,**116**,280
  Pressures in 110–112,278,287,300,301,305
  Sizes of 10,110–112,276,278
  Spectra 128,141
  Symmetries 29,61,107,128,131,141,276,287,294
  Velocities of advance 113,141,301
Jets
  Adiabats for 14,44,234,237,238,253
  Asymmetries (sidedness) 3,7,28,30,33,35,46,58,60,77,80,102,106,107,114,118,119,128,131,138–142, 214,215,226,274–276,278,279,287,295,307
  Cocoons around **5**,13,28,55,157,163,304,307,308
  Collimation properties 5,9,10,40,43,58,120,137,189,194–199,214,215,229,231,232,235,240–242, 278,279
  Confinement, buoyant 241,242,292
  Confinement, thermal 10,12,28,29,44,63,**168-181**,227,258
  Confinement, magnetic 11,12,25,28,147,188,193,197–199,227,270,278,288,294
  Confinement, viscous **213–215**
  Currents in 89,147,**185–192**,227,267,270,288,303
  Curvature 4,9,22–24,**64–75**,89,104,135,242,244,274,276
  Deceleration of 16,38,44,75,89,105–107,137,141,143,155,159,169,173,206,211,229–232,239, 242,244,254,279,282,283,285,292,295
  Definition of **4**,32
  Deflections 3,9,**64–75**,**76–82**,**83–88**,**89**,102,104,**122–127**,188,244,252,276,282,285, 287,288,293,294,301,305,308
  Densities in 39,40,45,54,66,67,68,73,94,99,236,242,254,267,277,283,292
  Depolarization 16,39,40,54,91,93–96,236,242,257

Jets, continued
Disruption of 152–154,159,193,195–199,293,304
Fractional luminosity in 28,29,58,226,227,276
Elliptical cross-section 15
Energy flux 65,109,111,241,242
Enthalpy flux 235,236
Entrainment by 16,44,75,89,104,137,153,154,159,169,173,182,184,**203–207**,**211–215**,229–232, 235,240,241,280,292,293,295
Faraday depths of 16,17,54,99,200,295
Formation of 101,143,188-190,**193–199**,**211–215**,290,294
"Gaps" in 15,24,35,129,142,216,287,306
Incidence of 5,7,25,103,138,287,295
Intensity-radius variations 14,15,40,43,44,216,238–240,253,254,279,283,292
Knots in 4,9,10,11,13,14,16,22,24,26,32,77,99,102,129,154–156,160,179,185,200,201, **255–259**,275,276,285,287,293,300,305
Laboratory examples **133**,153,159,160,**182–184**,185–187,190,191,203,204,**229–233**,244,**265–271**, 287,288,292,296
Linear polarization of 13,17,40,48,50,51,**99**,256,257,300
Mach number estimates 242,269
Magnetic configuration 8,9,16,28,40,48,52,137,185–189,194–195,**200**,**201**,212–214,238,257,260–264, 278,288,294
Magnetic field strengths 14,54,58,208,212–214,238,267,277
Mass flux 73,211–214
Momentum flux 12,64,109,111,211–214,308
Orientation (inclination) 32,105,119,120,135,136,276,278
Optical continuum emission 13,239,277
Particle acceleration by 67,68,73,109,112,219
Particle acceleration in 14,65,**129–132**,143,**216–228**,237,244,260–264,271,277,279,287
"Pieces of" 8,**35–38**,141,302,306
Precession 80,83,102
Pressures in 10,11,12,28,42,66,80,158,160,208,235,236,242,258,260–263,268,300
Reynolds numbers of 133,182,183,202,203,217,244,245,247–254,260,266,269,283,288,292
Self-Compton X-rays 14,77,120,279
Shocks in 2–4,9,11,16,44,63,77,102,121,122–127,137,154–160,164–167,169–173,176–180, 201,220,230,231,257–259,273,274,276,285,286,288,289,292,293,300,305
Spectral indices 13,24,37,38,63,120,258,277
Stability of 45,133,**144–149**,**150–167**,**168–181**,187,188,193,194,196,197,199,200,201, 242,278,287,294,304,308
Star formation in 207
Stellar 2,108,300
Symmetry, C type 9,**64–75**,83,136 (see also *Radio trail sources*)
Symmetry, S type 61,83
Velocity estimates 3,39,45,67,68,72,73,77,**100–108**,**109–113**,**114-118**,**135–143**,267,274–276, 278–282,287,301
Viscous effects in 66,182,**211–215**,252
Kelvin-Helmholtz instabilities **144–149**,**150–167**,**168–181**,193,277,288,292,304
Conical jet 146,230,242,305
Cylindrical jet 145,150–167
Effect of magnetic fields 146,147,197,199,200,201
Effect of velocity shear 147,148
Fastest growing wavelength 146,147,158

Kelvin-Helmholtz instabilities, continued
Growth rates 145,151
Helical (twist) instability 144–146,148,169,182,200,258,293,304
Pinch instability 144,145,147,148,**150–167**,169,293,304
Reflection modes 144–148,151,154–157,169,293
Vortex growth 182–184,204–206,230–231
Lobes
Depolarization 40,60
Filaments in 57,60,182,276,296,302,303,305
Intensity asymmetries 33,60,61,103,**129-132**,140
Magnetic fields in 52,207,276,277,303
Rings in 60,182,296,302
Rotation measures 40,60,95
Shocks in 60,124,205,294
Spectral index gradients 45,60,277
Thermal instability 303,307
Velocities of advance 61,111
Magnetic Fields
Energy dissipation **260–264**,294
Helicity 200–201,209,260,261,294
Hot spots 9,110,128
Instabilities in lobes 303
Jet dynamics 146,147,**185–190**,**193–199**,**200**,**201**,288,294
Jets, collimation of 11,12,25,28,147,188,193,278,288,294
Jets, configuration in 8,9,16,28,40,48,52,137,185–189,200,201,238,260–263,278,288,294
Origin of 188–189, **207–209**,294
Reconnection 225,263,279,307
Strengths of 14,40,52,54,58,110,207,208,212–214,238,267,277
Numerical simulations **150–167**,**168–181**,**194–199**,278,287,**288**,**289**,294,297,304
Backflows 5,306
Cocoons 152–154,162–163,278
Entrainment 153,154,159,**204–206**,288
Firehose instability 288,289
Hot spots 128,287,294
Pinch instability **150-167**,169,288,289,304,305
Shocks in jets 151,154–160,165–167,169–173,278,288,289,293,304,305
Turbulence 234
Optical Emission Line Gas
Bending of radio sources 77
Effect on radio polarization 94,276
Excitation 3,103,104,114,118,203,**206**,**207**
Origin 3,103,118,**206**,**207**
Peculiar velocities 3,103,104,**114–118**,280,281
Symmetries 3,118,138
Particle acceleration, see *Jets, Shocks, Turbulence*
Plasmoid (plasmon) models 69,70,85–87,306
Plumes 5,44,61,101,102,160,179,180,**231**
Radio trail sources ("head-tails")
Bending models **64–75**,89,276,285
Narrow angle trails **47–56**,**64–75**,89,136
Spectral gradients in 216,277
Wide angle trails **89**,160,179,285,290,294

Relativistic effects (see also *Superluminal motions*)
- Aberration 201
- Doppler beaming/boosting 12,29,32,33,46,71,103,118,119,121,130,135–139,273,274,276,279,288,295
- Time delay asymmetry 61,103,107,113

Shocks
- Jet bending 3,85,86,102,**122-127**,257–259,294,301,305
- Jet knots 2,102,121,154–160,165–167,201,257–259,274–276,285,287,293,300,301,304
- Oblique 9,16,113,121,**122–127**,128,138,151,154–159,165–167,169,170,172,173, 177–180,231,258,259,287,293,294,301,302,305
- Origins of 11,44,63,102,151,154–159,169–174,177–180,231,258,259,293
- Particle acceleration by **217–221,225–227**,237,259,277,279
- Pattern speeds 4,121,158,160,201,275,293,304

Size distribution of sources 32,136,279

Solar flares 218,263,294

Superluminal motions 20,105,106,120,121,125,126,135,139–142,272–274,276,279

Turbulence **202–210**,217–218,221–225,**229–244,245-254**,278,279,292
- Closure relations 233–235,279,282,283
- Decay of 247–249
- Entrainment 104,153,154,159,182,184,**203–207,211–215**,230,292,293
- Favre formalism 232,233,235,237
- Field amplification by **208,209**
- Global invariants **245–254**,283
- Scales of 203,217,218,247,293,304
- Spectrum of 210,217,218,224,225,247,249,250
- Spreading rates 152–154,230,231,282
- Particle acceleration by 16,38,63,73,203,207,209,216–218,**221–227**,237,259,263,271,279,287
- Production of 153,154,**202–210**,217,218,230,231,242,271,292,293

VLBI
- In space (QUASAT) 272
- Intensity mapping 76–82,120,272,273,277,295
- Knot brightness changes 120,273
- Polarization mapping 94,**99**,142,189,273,276
- Proper motions 2–4,20,120,137,139,142,273,274,285,295,307
- VLBA 272,273,275

"Weather" 188,303,304

OBJECT INDEX

(New data, or major discussions, are referenced **in bold type**).

BL Lac 273
Cen A (NGC5128) 8,9,11,13,103,139,206,207,220,**255–259**,267,274,278,293,305
Crab Nebula 187,278,303
Cygnus A (3C405) 7,28,29,**57–62**,96,110,139,141,182,276,278,287,294,303,305
Fornax A 13
Hercules A 60,182
IC708 7
IC4296 11,13,38,44,**63**
M84 5,9,13,94,**95**,96–98,139,141
M87 (Virgo A) 2,4,8,9,11,13,14,139,169,174,179,220,255,274–276,278,280,287,302
NGC315 10,11,13,15,16,35,139,168,179,232,**239**,240,242,243,283
NGC1265 5,8,9,**47–56**,65,69,73,89,102,202,244,308
NGC3078 8
NGC6146 8
NGC6251 4,9,11,13,15,35,39,58,96,104,139,169,179,200,260,261,272,274,275,300
NRAO140 105
NRAO512 4
Sco X-1 185,192,281,299
SS433 2,108,300
0007+33 30,**31**
0039+211 72
0110+297 **26**,30,**31**
0130+24 30,**31**
0727-115 201
0812+02 **114–118**,138
0907-091 73
0938+39 5,30,**31**
0957+56 139
1001+22 30,**31**
1108+411 72
1132+492 72
1244+699 73
1321+31 (NGC5127) 5,10,16
1512+37 30
1619+428 72
1705+786 73
1919+479 (4C47.51) 101,179,202
2244+366 110
2325+29 30,**31**
2354+47 5,10
3C31 5,9,13,15,141,231,239,240,242,243
3C33 106,110
3C33.1 12,35,**36**,38
3C48 77,80
3C61.1 110,113
3C66B 11,13
3C75 285,286
3C78 139
3C84 (NGC1275) 139,174,179
3C98 110

3C111	12,58,110,139,169
3C120	4,**20–24**,106,139,142,272–274,276,285
3C129	7,89,137
3C147	5,136,139
3C179	4,139
3C192	110
3C200	26,**27**,29
3C204	**27**
3C205	305
3C219	5,**6**,8,12,58,60
3C220.1	**27**
3C234	110
3C249.1	**27**
3C270.1	87
3C273	13,29,139
3C275.1	**84**
3C277.3	3,13,14,17,138,206,207
3C279	13,139
3C309.1	**77–80**,139,274
3C310	60,182
3C321	110
3C341	5, **6**
3C345	4,9,**99**,**120**,139,272,273
3C351	138
3C371	139
3C380	**80–82**
3C382	110
3C388	17
3C390.3	110
3C401	35
3C418	9,80,139
3C438	8
3C445	8
3C449	5,10,27,**39–46**,58,94–98,101,202,231,287
3C452	110
3C454.3	139
3C465	89,101
4C25.01	87
4C29.30	206
4C26.42	179
4C32.69	5,13,30,58,137,138,187
4C39.25	3
4C49.22	137